Longitudinal blood based biomarkers of Alzheimer's disease pathology in healthy elderly individuals

Westwood, Sarah Elisabeth

Awarding institution:
King's College London

LONGITUDINAL BLOOD BASED BIOMARKERS OF ALZHEIMER'S DISEASE PATHOLOGY IN HEALTHY ELDERLY INDIVIDUALS

Sarah Elisabeth Westwood

Submitted to King's College London University in fulfilment of the requirements for the degree of Doctor of Philosophy

2014

Abstract

There is an urgent need for Alzheimer´s disease (AD) biomarkers that can detect the disease at the early pre-symptomatic stages. Case versus control study designs often ignore clinical heterogeneity in patients and neuropathology in controls resulting in markers with doubtful clinical utility. Using markers of in vivo β-amyloid deposition (e.g. ^{11}C-PiB) combined with positron emission tomography (PET) or MRI to derive biologically relevant biomarkers associated with established endophenotypes of disease pathology is a better approach. Neuropathological hallmarks of AD (β-amyloid plaques and neurofibrillary tangles) are commonly reported in post-mortem brains of non-demented elderly individuals, suggesting these cases might represent preclinical AD and may be a good population in which to detect early AD biomarkers. Here we aimed to identify plasma biomarkers associated with AD endophenotypes of brain amyloid burden or brain atrophy in non-demented older individuals using two complimentary longitudinal discovery-phase proteomic analyses.

Two-dimensional gel electrophoresis coupled with mass spectrometry was performed on longitudinal plasma samples from non-demented older individuals exhibiting a range of ^{11}C-PiB PET measures of amyloid load. The relationship between protein levels and measures of brain atrophy, cognitive decline, and amyloid load were examined. A label-free LC-MS/MS approach targeted at low molecular weight proteins (<30kDa) was also performed on a subset of these subjects to enhance coverage of the plasma proteome. Validation of candidate biomarkers was performed in an independent cohort using quantitative immunoassays and aptamer-based arrays.

We have identified 15 plasma proteins associated with brain amyloid load, brain atrophy and cognitive scores. Our longitudinal study design allowed us to explore dynamic changes in concentrations of plasma protein profiles in relation to rates of change in both measures of AD pathology and cognition. Validation experiments determined whether these candidate biomarkers of pathology performed in an AD cohort.

Table of Contents

Page

Table of Figures

Page

Chapter 4: Discovering low molecular weight proteins as longitudinal biomarkers of early Alzheimer's disease pathology and cognitive decline using liquid chromatography-tandem mass spectrometry

Chapter 5: Validation of candidate biomarkers of Alzheimer's disease pathology and cognitive decline

Table of Tables

Page

Chapter 2: Aims and Methods

Chapter 3: Longitudinal blood based biomarker discovery of early Alzheimer's disease pathology and cognitive decline using two-dimensional gel electrophoresis

Chapter 4: Discovering low molecular weight proteins as longitudinal biomarkers of early Alzheimer's disease pathology and cognitive decline using liquid chromatography-tandem mass spectrometry

Chapter 5: Validation of candidate biomarkers of Alzheimer's disease pathology and cognitive decline

Abbreviations

2DGE	Two dimensional gel electrophoresis
A1M	Alpha-1-microglobulin
AAT	Alpha-1-antitrypsin
ABGP	Alpha 1β glycoprotein
ACN	Acetronitrile
AD	Alzheimer's Disease
ADAS-Cog	Alzheimer’s Disease Assessment Scale
ADRDA	Alzheimer’s Disease and Related Disorders Association
AGP	Alpha 1 acid glycoprotein
AIII	Antithrombin-III
AL	Light chain amyloidosis
Ambic	Ammonium Bicarbonate
AMBP	Alpha-1-microglobulin/bikunin precursor
ANCOVA	One-way analysis of co-variance
ANIMAL	Automated Non-linear Image Matching and Anatomical Labelling
ANOVA	Analysis of variance
ApoA-IV	Apolipoprotein A-IV

APOE ε4	Apolipoprotein E epsilon 4 gene
APP	Amyloid precursor protein
APS	Ammonium persulphate
ARUK	Alzheimer's Research UK
AUC	Area under the curve
Aβ	Beta-amyloid
B2M	Beta 2 microglobulin
BACE1	Beta-secretase
BBB	Blood-brain-barrier
BLSA	Baltimore Longitudinal Study of Aging
BMI	Body mass index
BRB	Blood-retinal-barrier
BSA	Bovine serum albumin
CAMDEX	Cambridge Mental Disorders of the Elderly Examination
CDR	Clinical Dementia Rating scale
CERAD	Consortium to Establish a Registry for Alzheimer's Disease
CES-D	Centre for Epidemiologic Studies Depression Scale
CID	Collision-induced dissociation

CLASP	Constrained Laplacian anatomic segmentation
CNS	Central nervous system
CSF	Cerebrospinal fluid
CV	Coefficient of variation
Da	Dalton
DAF	Decay accelerating factor
DCR	Dementia Case Register
ddH20	Double distilled H_20
DLB	Dementia with Lewy bodies
DNA	Deoxyribonucleic acid
DSM-IV	Diagnostic and Statistical Manual of Mental Disorders-IV
DTT	Dithiothreitol
DV	Dependant variable
DVR	Distribution volume ratio
EDTA	Ethylenediaminetetraacetic acid
EFPIA	European Federation for Pharmaceutical Industries and Associations
ELISA	Enzyme linked immunosorbent assay

FAD	Familial AD
FDA	US Food and Drug Administration
FDG	Fluorodeoxyglucose
FDR	False discovery rate
FTMS	Fourier transform mass spectrometry
GWAS	Genomewide association studies
HCl	Hydrochloric acid
HDL	High density lipoproteins
IAA	Iodoacetamide
IEF	Isoelectric focussing
IgG	Immunoglobulin
IGKC	Ig kappa chain C region
InnoMed	Innovative Medicines in Europe
kDa	Kilodalton
LC	Immunoglobulin light chain
LC-MS/MS	Liquid chromatography-tandem mass spectrometry
LDL	Low density lipoproteins
LMTX	Methylthioninium

LMW	Low molecular weight
LRG1	Leucine rich alpha 2 glycoprotein 1
LTQ	Linear trap quadrupole
MBL	Mannose-binding lectin
MCI	Mild cognitive impairment
mCi	Millicurie
MHC	Major histocompatibility complex
MMSE	Mini Mental State Examination
MP-RAGE	Magnetization-prepared 180 degrees radio-frequency pulses and rapid gradient-echo
MRI	Magnetic resonance imaging
MRM	Mixed-effect regression model
MS	Mass spectrometry
MW	Molecular weight
MWCO	Molecular weight cut off
N	Number
NINCDS	National Institute of Neurological and Communicative Disorders and Stroke
nm	Nanometer

NMDA	N-methyl-D-aspartate
℃	Degrees Celsius
OD	Odds Ratio
PDA	Piperazine diacrylamide
PET	Positron emission tomography
PiB	Pittsburgh compound B
PMA	Primary Mental Abilities
PON1	Serum paraoxonase/arylesterase
ppm	Parts per million
PSM	Peptide spectral matches
p-tau	Phosphorylated tau
PTM	Post-translational modification
ROI	Region of interest
rpm	Revolutions per minute
RT	Repetition time
SDS	Sodium dodecyl sulfate
SDS-PAGE	Sodium dodecyl sulfate polyacrylamide gel electrophoresis
sMRI	Structural MRI

SOMA	Slow Off-rate Modified Aptamer
SPGR	Spoiled grass
SRC	Spearman’s Rank Correlation
STAND	STructural Abnormality iNDex
T3PQ	Top 3 protein quantification
TE	Echo time
TEMED	Tetramethylethylenediamine
TFA	Trifluoroacetic acid
TIFF	Tagged Image File Format
TMT	Tandem Mass Tagging
TREM2	Triggering receptor expressed on myeloid cells 2
t-tau	Total-tau
TTR	Transthyretin
T6	Time point 6 years after baseline
T12	Time point 12 years after baseline
x g	Acceleration due to gravity
ZAG	Zinc-alpha-2-glycoprotein
α2M	Alpha-2-macroglobulin

µg	Microgram
µl	Microlitre

Acknowledgements

Firstly I would like to express great appreciation and thanks to my supervisor Professor Simon Lovestone for the opportunity to conduct this research, and for his guidance and encouragement over the course of my PhD. I would also like to thank my two other supervisors Dr Angela Hodges, and Dr Madhav Thambisetty, for their support and advice.

Further thanks must go to Dr Chantal Bazenet for her constant support, advice and project management and to Dr Abdul Hye for expert technical guidance and being a continued source of advice.

Thanks to all of my colleagues in the biomarker group for a supportive and friendly environment, with special thanks to Dr Emanuela Leoni for her help with the two dimensional gel electrophoresis experiments, involving many long days and late nights!

Lastly I would like to say a special thanks to my mum, Mark, Nain, and Tommy, for their continued support, patience, and encouragement throughout my PhD.

Chapter 1. Introduction

Dementia is a broad term used to describe disorders which cause decline in various cognitive functions, including; memory, executive function, language, behaviour, and the ability to perform everyday activities. Different types of dementia include; Alzheimer's disease, frontal temporal dementia, dementia with lewy bodies (DLB), and vascular dementia, with each type having different symptom patterns and brain abnormalities.

Dementia prevalence rates are increasing rapidly. In 2010 35.6 million people worldwide (around 0.5% of the world's population) were reported to be living with dementia. By 2030 it is estimated that this figure will almost double to 65.7 million people, and further double again to 115.4 million by 2050[1]. The single greatest risk factor for dementia is age, affecting approximately 1/100 of those aged 65-69, increasing to 1/3 at age 90 or older[2]. These numbers are not only alarming on an individual level, but they are also unsustainable for our economy. Dementia costs the global economy US$604 billion, and like prevalence rates this figure is also set to increase with an 85% rise in costs estimated by the year 2030[3].

All of these figures can be revised if interventions are found to delay or prevent the onset of dementia. The most common form of dementia is Alzheimer's disease (AD), accounting for around 60-80% of cases and this is the main contributor to the steep increase of dementia prevalence with age[2].

1.1 Alzheimer's Disease (AD)

Alzheimer's disease (AD) was first identified in 1907 by Alois Alzheimer[4]. Although age is the greatest risk factor it is not entirely restricted to the elderly with over 16,000 people under the age of 65 with dementia in the UK[5]. According to the Diagnostic and Statistical Manual of Mental Disorders-IV-TR[6] AD is characterised by multiple cognitive deficits, including a memory deficit, which cause significant impairment to social or occupational functioning. The disease is also characterised by a gradual onset followed by continuing cognitive decline, with a mean duration of approximately 8.5 years from the onset of clinical symptoms to the death of the patient[7]. AD is diagnosed through a combination of patient history, clinical

symptoms, and neuropsychological tests (e.g. Clinical Dementia Rating scale (CDR) and the Mini Mental State Examination (MMSE)), and is also largely based on the exclusion of other dementias. Currently a definitive diagnosis of AD can only be given by examination of post-mortem brain tissue, consequently the clinical diagnosis is presently inaccurate in around 10-15% of patients[8].

1.2 Alzheimer's Disease Pathology

Alzheimer's disease neuropathology is characterised by two key hallmarks; extracellular deposits of senile plaques and intracellular deposits of neurofibrillary tangles in the brain at autopsy[6]. The central component of senile plaques is the protein beta-amyloid (Aβ), generated by the cleavage of its precursor amyloid precursor protein (APP). The deposition of Aβ in the brain has been proposed as a central event in AD by the 'amyloid cascade hypothesis', a hypothesis which has dominated AD research for the past twenty years. This hypothesis proposes that APP mismetabolism and Aβ deposition are the primary events in AD neuropathology, initiating a cascade eventually leading to neuronal death[11].

Neurofibrillary tangles consist of abnormally hyper-phosphorylated tau which self-associates, winding into paired helical filaments and accumulating intracellularly. Tau is a microtubule associated protein, which promotes microtubule assembly and stabilisation when functioning correctly[9]. The density and distribution of neurofibrillary tangles is known to increase with AD severity[10]. Although the amyloid cascade hypothesis is the dominant model of AD pathogenesis, some scientists (sometimes called tauists) believe that changes to tau and the formation of neurofibrillary tangles are instead the key event in AD leading to neurodegeneration. It is also possible that a third event, common to both plaques and tangles, is instead crucial for the initiation of neurodegeneration in AD[11].

Post-mortem analyses have identified the hippocampus and the entorhinal cortex as the first brain areas to be affected by plaques and tangles in AD with cortical association areas becoming increasingly affected as the disease progresses[12]. Overall the temporal lobe cortex and hippocampus are found to be the areas most severely affected by neurofibrillary tangle formation in AD[13], which is unsurprising as these areas are well known for their involvement in cognitive

function, particularly memory. Although post-mortem analysis is currently our sole method of a 100% accurate AD diagnosis, there are other signs of AD that we can look for in vivo. The pattern of brain atrophy characteristic of AD is a decrease in volume of the temporal lobes, hippocampus, and the thalamus, with a significant increase in the size of the lateral ventricles and an expansion of the circular sulcus of the insula[14]. AD patients also have regions of abnormal metabolic brain function, most notably in neocortical association areas such as the posterior cingulate, precuneus, temporoparietal and frontal multimodal association regions[15].

There are many other features seen in AD, such as cerebral amyloid angiopathy, neuroinflammation and vascular disease, which on top of the presence of plaques, tangles, and brain atrophy, are likely to significantly contribute to disease progression[16].

1.3 Genetic Risk Factors

There are two subtypes of AD; early onset (familial) and late onset, both types have a genetic component. Familial AD (FAD) is rare, representing approximately 5% of AD cases, and onset normally occurs aged 30-60. All cases of FAD are inherited and caused by a genetic mutation. Three main known genetic mutations causing FAD are; amyloid precursor protein (APP)[17-19], and presenilin 1 and 2[20-22].

The majority of AD cases are sporadic, developing at an older age. The known genetic components of sporadic AD are not causal, but do increase the risk of developing the disease. The risk gene with the strongest influence is Apolipoprotein E, with the epsilon 4 allele (*APOE* ε4) considered a potent risk factor for AD. The risk associated with *APOE* ε4 varies between studies, but the majority of clinically diagnosed AD cases are normally found to carry at least one ε4 allele[23-24]. *APOE* ε4 has been found to not only increase the risk of AD, but to also significantly reduce the age of onset[24-25] and has also been shown to increase the rate of cognitive decline[26-28]. The risk factor linked to *APOE* ε4 has also been found to be stronger in women than men[29]. Although *APOE* ε4 increases the risk of AD it is not necessary or sufficient for AD pathology development[26], and therefore the sensitivity and specificity of *APOE* genotyping for AD is low. However *APOE* ε4

status is still relevant for biomarkers as it may influence biomarker activity or expression, and so is commonly included as a covariate in biomarker research.

TREM2 is another genetic risk factor for AD; heterozygous rare variants of *TREM2* have been associated with an increased risk of AD and the expression of *TREM2* has been shown to rise in parallel with an increase in cortical levels of Aβ[30]. One of the known roles of *TREM2* is to regulate inflammation and the discovery of this genetic link to AD confirmed the inflammation element of the disease[31]. Genomewide association studies (GWAS) have recently identified many other genes as low-risk factors for sporadic AD, including; *CLU*, *PICALM*, *CR1*, *BIN1*, *MS4A*, *CD2AP*, *CD33*, *ABCA7,* and *EPHA1*[32-34]. Pathway analysis of susceptibility genes for AD can pinpoint biological pathways involved in disease development and hence provide targets for intervention strategies. This analysis approach has so far highlighted pathways such as inflammation and complement biology[35-36].

1.4 Therapeutic interventions

1.4.1 Symptomatic Treatments

There is currently no cure or preventative for AD, however there are drug treatments that help with the cognitive and behavioural symptoms. There are two main groups of treatments for AD; cholinesterase inhibitors and NMDA receptor antagonists. Cholinesterase inhibitor drug therapies inhibit acetylcholinesterase; increasing the concentration of acetylcholine in the brain to replenish acetylcholine lost by cholinergic neuron death. This is based on the cholinergic hypothesis that states that the degeneration of cholinergic neurons and consequently the loss of cholinergic neurotransmission in certain brain areas contribute significantly to the deterioration in cognitive function observed in AD[7]. Therefore if drugs improve cholinergic neurotransmission, the patient's cognitive function is also expected to improve. NMDA receptor antagonists work by blocking the activity of the neurotransmitter glutamate, which is released in excess quantities by damaged cells in AD brains. High levels of glutamate results in neurotoxicity, so NMDA receptor antagonists work to normalise the glutamatergic system and improve cognitive deficits[37]. However benefits of both types of drugs are modest, temporary, and do not affect

disease progression[38]. In fact there are no drugs currently in clinical use that can successfully alter AD progression.

1.4.2 Disease Modifying Treatments

At present the search for disease-modifying interventions is largely focused upon targeting the Aβ pathway. Based on the amyloid cascade hypothesis intervention strategies may focus upon inhibition of the formation of amyloid plaques or the alleviation of abnormal APP activity to successfully halt or slow the progression of the disease[39]. One example of this is both passive and active immunotherapy research that attempts immune-mediated Aβ reduction in the brain of AD patients, with the aim of consequently increasing their cognitive performance or at least slowing decline[38]. Active immunotherapy involves combining Aβ with an adjuvant to stimulate an immune response producing anti-Aβ antibodies, whilst passive immunotherapy involves directly injecting anti-Aβ antibodies[40]. Recent clinical trials in humans have shown promise but have also displayed serious complications. For example, a phase II clinical trial of AN1792 immunization successfully resulted in clearance of amyloid plaques whilst also showing CSF tau level reductions and minor cognitive benefits, however the trial was halted as 6% of patients developed meningoencephalitis, a life-threatening inflammation of the brain and meninges[41]. Although this trial was halted it does show encouraging signs that Aβ immunotherapy may be useful for AD. However this trial did not prevent progressive neurodegeneration or show long term cognitive benefits[42]. Clearly further developments are needed and improvements in disease models and biomarkers are essential for the advancement of such interventions.

Beta-secretase (BACE1) and gamma secretase inhibitors are two other intervention strategies based upon the amyloid cascade hypothesis of AD. BACE1 and gamma secretase are APP cleaving enzymes, initiating the production of Aβ that is subsequently deposited in plaques. Inhibiting these enzymes is therefore expected to interrupt the formation of Aβ plaques and prevent neurodegeneration and so has been the target aim of many intervention strategies[43-44]. During the past few years much progress had been made on the development of BACE1 inhibitors, which have been shown to have positive effects in experimental animal models. For example the

BACE1 inhibitor GRL-8234 was shown to rescue age-related cognitive decline in transgenic APP mice (Tg2576)[45]. There are now several BACE1 inhibitors currently in the first stages of human clinical trials[46-47]. Unfortunately clinical trials of gamma-secretase inhibitors have so far encountered complications [48], thought to be mainly due to a disruption of Notch signalling, but if future developments can avoid this then the intervention has great potential.

Another potential therapeutic strategy distinct from Aβ-based interventions is the inhibition or reversal of tau aggregation, and treatments targeting neurofibrillary tangles are currently in development. The first tau-based phase 3 clinical trial is currently underway, testing methylthioninium (LMTX) a tau aggregation inhibitor[49]. It is hoped that more success is found with tau based treatments than achieved so far with Aβ based interventions.

Although there has been great advancements in our understanding of dementias the results of clinical trials has so far been disappointing. Only a handful of drugs have been approved to treat dementia, including Razadyne, Exelon, and Aricept, and such drugs only temporarily treat symptoms and are not disease modifying. This lack of current clinical trial success together with laboratory research results indicates that earlier interventions may have a better success rate. Because of this, attention is now being directed towards prevention strategies. To do this we will need to identify individuals in the preclinical phase of the disorder; during the early stages of neuropathology development but prior to the onset of clinical manifestations. Certain Aβ antibodies which proved disappointing in immunotherapy clinical trials of AD patients are being re-considered for their utility as preventative treatments. For example a clinical trial of Solanezumab is planned to commence in 2014 aiming to test this drug in 1000 cognitively normal volunteers, aged 65-86, who are showing signs of AD pathology (Aβ plaques, as identified by a positron emission tomography (PET) brain scan)[50]. It is hoped trials like this will show that Aβ plaque removal or neurofibrillary tangle reduction at this early stage could prevent subsequent neurodegeneration and eventual cognitive decline. Successful recruitment of preclinical AD individuals will be a key factor for these preventative clinical trials. Subject selection using expensive imaging methods to detect AD pathology in cognitively healthy individuals will substantially increase the cost of these trials. A

more practical alternative would be to use a blood based biomarker of AD pathology. Using a blood test as a trial entry criterion would be minimally invasive and easy to implement, and could also be used to help triage subjects to further testing using imaging methods.

1.5 Timeline of AD pathology and clinical symptom development

The clinical presentation of Alzheimer's disease is thought to be the end product of many years of silent gradual changes in various pathological processes. The timeline of AD development can be thought of in three stages; preclinical, prodromal (mild cognitive impairment (MCI)), and dementia, with each stage having its own continuum of severity. The timeline of AD pathology and clinical symptom development from the preclinical stages through to severe dementia can be investigated by looking at the behaviour of well established AD biomarkers throughout these stages, for example; PiB PET, CSF $A\beta_{1-42}$, t-tau and p-tau, FDG PET, MRI, and cognitive measures.

A comparison of cross sectional values of both global cortical PiB PET and hippocampal volumes for control, MCI, and AD individuals reveals that approximately 20% of healthy control individuals showed amyloid load levels comparable to that identified in AD individuals, whereas minimal overlap between the two groups was identified when measuring hippocampal volumes[51]. This suggests that significant plaque deposition occurs prior to neurodegeneration and clinical decline, with fairly high amyloid load already observed in presymptomatic individuals. This is further supported by CSF $A\beta_{1-42}$ measurements that have been found to be reduced in some healthy individuals[52], thought to reflect the retention of Aβ in plaques.

Longitudinal research measuring annual change in these markers revealed further information. Rates of change for PiB PET values are comparable across all three control, MCI and AD groups, with MCI showing the greatest variability. However rates of change in ventricular volume are shown to increase from control to MCI to AD [53]. This implies that longitudinal changes in cognition are closely coupled to the rate of neurodegenerative progression, not to the rate of amyloid deposition. This also supports the theory of brain amyloid deposition as an early initiating event, with

rates of accumulation then remaining fairly constant over time, from preclinical through to severe AD.

Both CSF t-tau and p-tau have been shown to be elevated in cognitively healthy individuals and in those with mild cognitive impairments[52, 54], though changes are less pronounced than seen for CSF $A\beta_{1-42}$. It is often assumed that accelerated neurofibrillary tangle formation occurs alongside an increased release of tau protein into CSF[54-55]. Based upon this assumption this data suggests that prior to presentation of clinical symptoms, amyloid deposition in cognitively healthy individuals is subsequently followed by an elevation of tau.

Both individuals with very early Alzheimer's disease, and cognitively healthy individuals who progress to MCI/dementia have shown marked brain metabolic reduction, as measured using FDG PET[56-59]. This shows that brain metabolic reductions are also initiated at an early, preclinical stage of AD. Regions showing early metabolic reductions have been reported to often overlap with the regions of greatest tangle pathology and also correlate with early increased CSF tau protein levels[54, 60-61].

Both PiB PET and CSF $A\beta_{1-42}$ show mild correlations with volume measurements of various brain regions in cognitively healthy individuals, which suggest that subtle brain atrophy also begins to occur at a preclinical stage[62-64]. CSF p-tau has been shown to correlate mildly with cognition in the early preclinical stages, however once individuals are clinically impaired MRI has a much stronger correlation with cognitive ability and retains this strong relationship with cognitive performance throughout the mid and late clinically symptomatic stages[65]. MRI is also able to predict future clinical function and conversion to MCI/AD better than CSF measures[65]. This relationship between MRI and cognition appears to be non-linear; with small amounts of brain atrophy reported preclinically and subsequent acceleration of atrophy once clinical symptoms manifest[66].

Additionally very subtle cognitive changes which predict subsequent development of AD can be detected years before even reaching a diagnosis of mild cognitive

impairment[67]. These impairments are found in specific cognitive measures such as episodic and semantic memory and executive function tasks[67-69].

These studies reveal that AD biomarker abnormalities precede clinical symptoms and that different biomarkers change in an ordered manner over time. Amyloid accumulation (as measured by PiB PET and CSF $A\beta_{1-42}$) becomes abnormal first, followed by changes in FDG PET and CSF t-tau and p-tau biomarkers, representing the subsequent development of neurofibrillary tangles. Following this small MRI changes are apparent prior to the onset of very mild cognitive impairments. All of these changes occur before conversion to a prodromal stage. The biomarkers will then increase in severity throughout the prodromal stage through to dementia, though each biomarker will show different rates of change and saturation points. It is also likely that changes in these biomarkers are non-linear when measured over long periods of time. Based upon similar conclusions Jack et al (2010, revised in 2013) proposed a time-dependent ordered model of well validated AD biomarkers and their relationships to the clinical symptoms (see Figure 1-1)[70-71]. This model is now well accepted as a good, simplified reflection of a typical AD time line. One hypothesis of this model is that a clinically asymptomatic individual with underlying pathological changes indicative of AD would ultimately develop the disease if they lived long enough. Additionally this model suggests that AD risk factors such as genetic risk alleles, low cognitive reserve, and other comorbidities can shift the onset of cognitive impairment to an earlier stage.

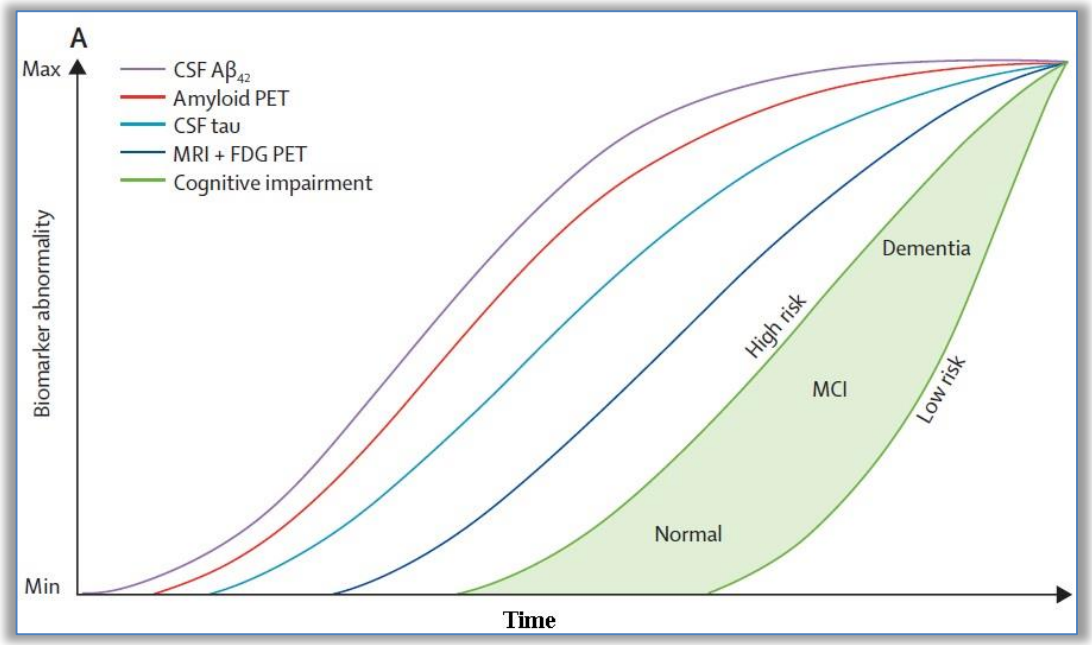

Figure 1-1: Model of AD timeline as taken from Jack et al, (2013). Cognitive impairment can be shifter earlier or later, as represented by the large green area, dependent on AD risk factors.

1.6 Mild Cognitive Impairment (MCI)

Individuals with MCI have regularly been included in AD research aiming to investigate the earlier stages of the disease, with the hypothesis that these individuals are prodromal AD. MCI individuals are known to have an increased risk of developing dementia, however a meta-analysis of 41 cohort studies where conversion to Alzheimer's was documented revealed that only 30-34% of MCI individuals progressed to AD within 10 years[72]. Therefore although this is currently the best known population for studying prodromal AD, there is clearly large clinical heterogeneity in this group of individuals, and the majority of individuals with MCI will not progress to AD. Contributing to this heterogeneity is a lack of firm and appropriate clinical criteria for MCI diagnosis. Different researchers stress the importance of different symptoms and memory tests for which they base their inclusion and exclusion criteria on, impeding the comparison of results between studies. The large variability found in conversion rates of MCI patients to AD may be due to an inconsistency of criteria used across studies. Standardising these criteria, as well as including prognostic biomarkers, will increase accuracy and reduce variability in MCI diagnosis.

Research focusing on the differences between MCI individuals who convert to AD compared to those who remain stable can reveal information about the prodromal stages of AD. Unsurprisingly MCI convertors have been found to have a very similar pattern of brain atrophic changes to AD individuals, with neurodegeneration of medial temporal structures being the best indicator of AD conversion[73]. Neurodegeneration has been repeatedly reported as a reliable short-term prognosis of progression to AD. CSF biomarkers of brain amyloid show longer-term prognosis of progression to AD[74], which corresponds with the time line of AD development presented above. Differences in plasma proteins have also been reported in MCI individuals[75-77], these proteins reflect many different mechanisms but inflammatory proteins are frequently reported suggesting inflammation occurs early and significantly contributes to disease progression.

Although individuals with MCI present an interesting population to study early AD, it is likely that to effectively treat or prevent the development of AD individuals in the preclinical stages of the disease need to be identified and targeted. As previously mentioned, it is known that AD pathology develops silently for many years in cognitively healthy individuals. Perhaps during this phase plasticity and compensatory mechanisms of the brain allow normal functioning to continue up until a damage threshold is reached. This preclinical phase allows a critical but challenging opportunity for therapeutic intervention. Intervention at this stage is likely to maximise treatment benefits, though identifying seemingly healthy individuals who will later develop clinical signs of dementia is difficult.

Some preclinical studies have focused on cognitively healthy individuals at higher risk of AD development due to genetic risk factors, family history or other comorbidities known to increase the risk of AD. Other studies have used biomarkers of AD pathology to identify healthy control subjects with underlying AD pathology, classifying them as preclinical AD. However some elderly individuals displaying AD pathology do not ever progress to the clinical stages of MCI or dementia within their lifetimes. It is possible that some individuals are resistant to clinical decline due to various factors such as cognitive reserve, protective genetic factors, or environmental influences. Such influences may also just be extending the preclinical phase and if

they were to live longer it is thought that these individuals may still go on to develop dementia.

More research is needed for preclinical AD. Biomarkers that can accurately identify individuals in a preclinical AD stage will benefit clinical trial recruitment and monitoring, and may also reveal therapeutic targets. AD-related changes detected at this early stage are likely to be very subtle and therefore longitudinal measures over time will be more sensitive than any one-time measure and so should be prioritised for preclinical AD research. Recently preclinical AD diagnostic criteria has been outlined by the NIA to aid research into this stage of the disease, the criteria includes biomarkers of brain changes including neuroimaging and CSF measures.[78-79].

1.6.1 Ethical implications for pre-symptomatic testing of AD

Although research into a biomarker screening tool for preclinical AD is in its infancy, it is important to consider the ethical, social, and legal implications such tool may have. If 'clinically healthy' individuals are given knowledge that they have preclinical AD, particularly prior to the development on disease modifying interventions, then this knowledge may lead to increased stress which could potentially accelerate the disease and reduce quality of life for their remaining years. Other personal and psychosocial considerations include; education, employment, marriage, family planning, and insurance.

The appropriate use of this information is much debated, and while there are no disease modifying treatments an AD screening tool appears to have limited benefits to the individual affected. Therefore some argue that preclinical testing should remain within research protocols, and the results should not be shared with subjects until treatments become available. Though others argue that this disrespects the subject's autonomy and that a few benefits to knowing do exist [347]. Firstly, preclinical screening can help relieve uncertainty in individuals who worry they may have inherited increased risk of AD. For some individuals the stress of uncertainty may be more considerable than the stress of knowing. Secondly, an early diagnosis will help individuals to plan, whether this obtaining relevant insurance or care packages, altering educational/career or family plans, or ensuring lifelong ambitions are achieved quickly.

Similar implications have been extensively discussed in relation to genetic testing for increased risk of AD, a much more established area of research (see 348 & 349 for good discussions). While it is clear that identifying individuals in the preclinical stage of the disease will hugely benefit AD research and clinical trials, it is imperative for the individuals involved in this research that informed consent is obtained, appropriate support and advice is available, and safeguards and legislation follow the results.

1.7 Approaches of AD Biomarker Studies

A biomarker is a measureable biological characteristic that correlates with normal or pathogenic processes in the body. Biomarkers can be used as indicators of disease presence, pathology, and progression, and they are implemented in drug development and clinical trials as surrogate endpoints, markers of efficacy or toxicity, and are also used for patient stratification and cohort enrichment.

In many medical areas biomarkers are already having a powerful influence on patient treatment and drug development. Biomarkers are being implemented to help clinicians diagnose syndromes, monitor treatment effects, optimise treatments, and track progression. However for dementia the clinical use of biomarkers is relatively new, especially in the early stages, and their development and validity is still a work in progress. In 1998 the Alzheimer's Association and the National Institute on Aging proposed criteria that an ideal AD biomarker should fullfill[348]. These requirements include; the ability to detect a fundamental feature of disease pathology, well validated in neuropathologically-confirmed cases, both a sensitivity and specificity of >80%, reliable, non-invasive, simple to perform and inexpensive. These criteria are excellent guidelines to use for biomarker discovery, however it is important to consider that for different uses of biomarkers the importance of each of these criteria may change. For example; biomarkers for AD drug development would place emphasis their ability to indirectly measure disease severity, though high specificity is not a necessity for this biomarker use.

Current AD diagnosis criteria (e.g. DSM-IV) are primarily exclusion criteria, poorly specific of the pathology, and lacking sensitivity in early stages. Biomarkers may help to improve the current level of accuracy of AD diagnosis. Tabaraud et al (2011)

found that the inclusion of CSF biomarkers in neurological daily practice improved AD diagnosis[80]. There are numerous other reasons as to why AD biomarkers are important. Most obviously biomarkers will allow us to predict who will develop AD, which is important for early treatment of the disease. Additionally biomarkers may also be used as indirect measures of disease severity [5]. More sensitive and specific markers of early AD progression will help monitor the effectiveness of new treatments, and lessen the time and cost of clinical trials. Current approaches to biomarker discovery for AD include neuroimaging and testing of body fluids such as cerebrospinal fluid (CSF) and blood (plasma).

1.7.1 Neuroimaging biomarkers

Currently, our best biomarkers for preclinical, prodromal and clinical AD are neuroimaging approaches. A variety of imaging techniques have been used as AD biomarkers with magnetic resonance imaging (MRI) and positron emission tomography (PET) as the most frequently employed. Although neuroimaging methods show very promising results these approaches are expensive and sometimes mildly invasive, whilst scanner availability and consistency limits widespread use and study comparisons.

Amyloid imaging with positron emission tomography (PET) imaging agent Pittsburgh compound-B (PiB)

PiB PET was developed to enable detection of amyloid plaques in vivo and is now established as a valid biomarker of fibrillar Aβ brain amyloid load. Compared to controls PiB PET scans of AD patients show higher PiB retention in areas known to contain large amounts of amyloid plaques post mortem (e.g. frontal cortex)[81-82] and comparisons with post mortem brain tissue show excellent concordance with anti-mortem amyloid load as measured by PiB PET[83]. PiB PET has been found to have around 90% accuracy for AD diagnosis detection[84] and can indicate preclinical AD individuals by detecting AD pathology in healthy controls[85-86]. Additionally through repeated PiB PET scans pathology progression can be monitored throughout the disease course. Similarly novel disease-modifying therapies for AD which aim to remove Aβ deposits from the brain now have an in-vivo monitoring tool of the effectiveness of their drug outcome.

One of the problems with PiB is the short half-life of ^{11}C (20 minutes). This means that a cyclotron has to be available on site for isotope production, increasing costs and severely limiting its widespread use. Alternatives to PiB are being developed and currently three ^{18}F labelled tracers (110 minute half-life) for Aβ are in or have completed clinical trial stage. All of these tracers have so far shown promising results, for example flutemetamol has been found to have both a sensitivity and specificity of 93% for discriminating AD patients from controls[87]. In the USA flutemetamol has recently been approved by the US Food and Drug Administration (FDA) for the evaluation of amyloid in the brains of individuals with possible Alzheimer's disease. Comparisons of PiB and flutemetamol have revealed that the results of the two tracers are highly correlated[88-89].

Tau neurofibrillary tangle imaging with positron emission tomography (PET)

Some researchers argue that a successful technique to image tau pathology in the human brain would be a significant step forwards from Aβ plaque imaging as, unlike Aβ, neurofibrillary tangles have been found to reliably correlate with neurodegeneration and cognitive impairment[90]. There is currently no well established method for imaging neurofibrillary tangles, however there are radiotracers such as ^{18}F-THK523 under development which look promising, especially for AD research[90]. ^{18}F-THK523 has been shown to have high affinity and selectivity for tau neurofibrillary tangles in preference to Aβ or α-synuclein deposits, and it appears to selectively bind to tau lesions in AD brains but not in other non-AD tauopathies[91-92].

Magnetic resonance imaging (MRI)

Brain atrophy measured by structural MRI is repeatedly reported as a robust AD biomarker. In particular decreased hippocampal and entorhinal cortex volume is a distinguishing feature of an AD brain[93-94]. These regions have also been shown to be effected early on in the disease, with hippocampal volumes and cortical volumes in the right medial temporal, left lateral temporal, and the right posterior cingulate, able to predict the likelihood of progression from normal to MCI and also from MCI to AD[73, 94-96]. As expected, MRI measures strongly correlate with cognition, especially during the mid to late clinically symptomatic stages of AD, and are also good predictors of future cognitive decline[65].

Serial MRI measures taken from subjects followed from a preclinical stage through to moderately severe dementia show a non-linear relationship between cognition and brain atrophy, with the rate of atrophy increasing with disease severity[66]. This demonstrates that although MRI has biomarker ability preclinically its strength lies after the onset of clinical symptoms. These findings also indicate that early interventions are needed before the subsequent acceleration of brain atrophy.

MRI has also been used as an indirect measure of neurofibrillary tangle pathology[97]. As neurofibrillary tangles are distributed in a fairly consistent pattern of progression in AD a staging system for neurofibrillary tangles was proposed by Braak and Braak[98]. This six-stage system is now well established for pathological AD severity staging. Although this progression cannot currently be imaged in-vivo directly an approximate measure of pathological staging can be obtained using information from MRI scans. For example, Vemuri et al (2011) demonstrated that optimally extracted atrophy information from MRI scans can be converted into an abnormality score (STructural Abnormality iNDex (STAND)) which shows good correlation with Braak staging post mortem[97].

18F Fluorodeoxyglucose-PET (FDG-PET)

FDG PET scans measure brain glucose metabolism and investigations have shown that in AD a decline in glucose utilisation is progressive, correlates with AD severity and can also predict a diagnosis of AD post-mortem[8, 99]. Such studies have typically revealed metabolic reductions in the posterior cingulate, parietal, temporal, and prefrontal cortex to be correlated with AD severity and progression[100]. Glucose metabolism abnormalities identified using FDG-PET scans has also been found to successfully predict conversion from MCI to AD[101-102] with very early metabolic deficits reported in the medial parietal cortex[103]. Regions showing early metabolic reductions have been reported to often overlap with the regions of greatest tangle pathology and also correlate with early increased CSF tau protein levels[54, 60-61].

1.7.2 Cerebralspinal fluid (CSF) biomarkers

CSF is in direct contact with the extracellular space of the brain. Therefore biochemical changes in the brain are often reflected in the CSF, providing a good

source of biomarkers for such changes. In comparison with blood CSF has relatively low protein content and is therefore much less complex to analyse, though blood-brain-barrier (BBB) disruption does increase the total amount of protein present in the CSF. For example, increasing levels of albumin are observed with increasing BBB impairment[104]. Along with neuroimaging certain CSF protein measurements are currently our best AD biomarkers. In particular CSF quantification of $A\beta_{1-42}$, phosphorylated tau (P-tau) and total-tau (T-tau) have shown great biomarker abilities for AD, and are thought to reflect the core pathologic features of AD; amyloid plaques, neurofibrillary tangles and neuronal loss, respectively. These biomarkers have recently been included in AD diagnostic guidelines to help increase the accuracy of an early preclinical or prodromal AD diagnosis for research purposes by indicating pathology presence and severity in these early stages[78]. These three biomarkers are discussed in more detail below, though it is important to note that there have been many other promising CSF biomarkers also discovered, for example; BACE1[105-108], sAPPα/sAPPβ[109-112], and Aβ oligomers[113-115], see [116-118] for good reviews of CSF biomarkers.

CSF $A\beta_{1-42}$

CSF $A\beta_{1-42}$ concentrations are consistently reported as reduced in AD patients compared to controls[119-120], thought to reflect the retention of Aβ in brain amyloid plaques. There is a clear inverse relationship between CSF $A\beta_{1-42}$ and cortical PiB binding, suggesting this CSF measurement is a strong surrogate marker for in-vivo brain amyloid burden[52, 99, 121-122]. Also supporting this, low concentrations of CSF $A\beta_{1-42}$ are correlated with brain Aβ neuropathology at autopsy[123]. Reductions in CSF $A\beta_{1-42}$ have been reported preclinically indicating this biomarkers predictive ability for subsequent conversion to dementia[124]. Additionally there is also a mild, but significant, positive relationship between CSF $A\beta_{1-42}$ and brain volume[62].

CSF total-tau (t-tau) and phosphorylated tau (p-tau)

Increases in CSF p-tau and t-tau have been associated with neocortical neurofibrillary pathology, cognition, and temporal lobe hypometabolism. Total tau has often been reported as increased in CSF of AD patients, with increases of 50-300% reported compared to controls[125-127], and has also been found to have a

strong correlation with episodic memory[122]. P-tau is the main component of paired helical filaments that form neurofibrillary tau tangles, and so CSF p-tau is thought to reflect neuronal degeneration more accurately than t-tau. Like t-tau, p-tau can be used as a diagnostic biomarker for AD, with a sensitivity for AD of 85% reported[128]. Both t-tau and p-tau have also shown a significant correlation with cortical PiB binding in healthy individuals[52], though this correlation is much weaker than the previously mentioned relationship between CSF $A\beta_{1-42}$ and cortical PiB binding. Abnormal CSF concentrations of t-tau and p-tau have been reported before the clinical onset of dementia, indicating their predictive ability of future conversion to dementia[124].

CSF protein ratios

Ratios of the above mentioned CSF markers have also been identified as useful AD biomarkers. CSF $A\beta_{1-42}$/t-tau has been identified as a good predictive marker of future conversion from MCI to AD[65] and also of future cognitive decline in nondemented older adults[129]. CSF $A\beta_{1-42}$/p-tau has also been reported as a biomarker; De Meyer et al (2010) identified a CSF $A\beta_{1-42}$ and p-tau mixture as a biomarker of AD which was present in 90%, 72%, and 36% of patients in AD, MCI and normal groups, respectively [130]. These results were autopsy confirmed where the biomarker was 94% successful in predicting diagnosis, additionally MCI patients found to possess this biomarker all progressed to AD within 5 years. As this biomarker was also present in more than one-third of their control participants it may also be able to detect AD pathology at a preclinical stage. CSF $A\beta_{1-42}$ and p-tau ratio has also been found to reflect disrupted default mode network functional connectivity in AD patients, particularly in the left precuneus/cuneus[131].

While these CSF markers show interesting research results, their clinical utility is limited by the invasive nature of obtaining CSF (lumbar puncture), particularly from elderly individuals. This mainly restricts longitudinal studies or clinical progression monitoring where repeated CSF measures are needed. Therefore a CSF biomarker would have to have a considerably increased predictive ability over alternative methods to justify its addition to standard clinical procedures. However CSF acquisition is cheaper than some neuroimaging approaches, and compared to plasma based approaches CSF may be able to generate biomarkers that more accurately

reflect disease biology. For these reasons CSF biomarkers have high potential, but a more practical alternative would be preferential especially for longitudinal studies.

1.7.3 Blood based biomarkers

All of the biomarker approaches mentioned above have yielded promising results. However availability and cost of neuroimaging approaches and the moderately invasive nature of CSF lumbar puncture limits their usage and restricts longitudinal repeated measures studies. On the contrary blood/plasma based biomarker approaches are practical and minimally invasive, allowing repeated sampling in large cohorts.

Various substances formed by the nervous system during its metabolic activity diffuse into the CSF. CSF is renewed four or five times daily and as it is renewed old CSF is absorbed into the bloodstream. As CSF is absorbed, products reflecting the condition of the brain are also passed into the blood. Additionally the blood-brain-barrier is often compromised in neurodegenerative conditions such as AD which allows more analytes to pass into the blood stream[132]. Blood has therefore been the focus of much research into AD biomarkers, with the aim to develop a blood test for AD. A blood test would be practical to implement, relatively cheap, and minimally invasive and therefore has significant advantages over other biomarker modalities. Initially there was some speculation as to whether an AD signal can pass through the BBB from CSF into the blood, and if so whether this signal can be detected. Recent evidence suggests that there is detectable peripheral signal in the blood which reflects neuropathological features of AD and that this may be sensitive to both disease severity and progression.

Comparisons between CSF and plasma research show that some AD biomarker signals known to be present in CSF are also present in plasma. For example; CSF transthyretin (TTR) has been reported to protect against brain Aβ deposition, and lower levels of CSF TTR are often related to AD diagnosis and severity[133-134]; this biomarker ability of TTR has been replicated in plasma[135-136].

Many other proteins have been identified as plasma based biomarkers of AD. One of the most promising is clusterin. High levels of clusterin have been found to be

associated with brain atrophy and a more rapid rate of cognitive decline in AD patients[137]. Furthering this, increased clusterin concentration has been found to be an antecedent marker of pathology in normal elderly individuals; baseline plasma clusterin concentrations predicted subsequent development of in vivo fibrillar amyloid burden ten years later[137]. Other work has identified clusterin as having roles in amyloid clearance, complement inhibition and apoptosis, and also peripheral concentrations of clusterin have been found to accurately reflect its concentration within brain regions known to be vulnerable to AD pathology[138]. Results from clusterin, and many other plasma proteins, show that plasma biomarkers, can reflect disease status and AD pathology, including in nondemented elderly individuals years before a clinical diagnosis can be made.

It is unlikely that any one plasma protein will have sufficient power to be solely used as an AD biomarker. Their true strength is likely to instead lie as a biomarker panel of multiple proteins, each reflecting different aspects and mechanisms involved in the disease[76]. AD biomarker panels have been successfully identified and tested several times[76, 139-142]. Hye et al (2006) used a 2DGE proteomics approach and identified a panel of protein spots that together could discriminate between AD patients, normal controls, and other neurodegenerative diseases with 56% sensitivity and 80% specificity[142]. A panel of 18 plasma proteins identified by Ray et al (2007) could also categorise patients, and additionally predict MCI patients who would convert to AD within 5 years with nearly 90% accuracy[76]. Recently a panel of ten proteins strongly associated with disease severity and progression were found to be able to predict MCI progression to AD with 87% accuracy[75], showing that such biomarker panels could be used to enhance diagnostic specificity to identify MCI individuals in a prodromal AD stage.

Recently considerable progress has been made into the investigation of biomarkers for AD. However further research is still required to clarify the transitional period from healthy aging to the first manifestations of AD. Different biomarkers may have individual strengths and therefore contribute differently to our understanding of this transitional period, but those that have high reliability and are easy to implement will be the most useful. The combination of plasma proteomics with in vivo brain

imaging will provide us with biologically relevant, clinically useful, peripheral markers of Alzheimer's pathology.

1.8 Detection and measurement of blood-based markers

Whilst there are many advantages for using blood as an AD biomarker its use is still limited due its complex composition and therefore the technical difficulties it poses. Changes within the blood are often very small and reflect a wide range of both peripheral and central processes so pinpointing AD specific changes can be challenging. Separated by the blood-brain-barrier (BBB) the relationship between analytes found in the blood and changes in the brain is still uncertain. Yet in AD the BBB is known to be disrupted resulting in increased permeability [143], and this disruption should only strengthen the relationship between blood and brain. Nevertheless concentrations of most known potential biomarkers are several times lower in the blood than reported in CSF (e.g. Abeta peptide concentration is 100-fold lower in blood [144]). Additionally highly abundant plasma proteins such as albumin and IgG may repress signals from potential biomarkers, consequently increased sensitivity and power is needed for this research.

Among the many technological platforms used to investigate AD blood biomarkers, proteomics is currently the most frequently employed. Detailed characterisation of proteins including changes in quantification, location, interactions, isoforms and post-translational modifications (PTMs) can help further our understanding of different biological states. The identification of these features is challenging as proteins need to be identified from within a matrix of cells, tissues, fluids, and other proteins of varying concentrations. Additionally the dynamic range of proteins in a blood sample is large, with those in a plasma sample spanning up to 12 orders of magnitude [145]. This complexity is reflected in the limitations of the different proteomic techniques.

There are many analytical techniques available for biomarker discovery, each has its pros and cons meaning often a compromise will need to be taken. A wider understanding of many of the techniques available may facilitate biomarker research. Moreover, combining complimentary aspects of different techniques and adding other parameters such as neuroimaging data should increase our accuracy. For

example, two-dimensional gel electrophoresis (2DGE) and mass spectrometry (MS) are both highly useful techniques for AD blood biomarker discovery research in their own right. However the two methods have also been found to provide different but complementary information about proteins [146-147], suggesting that these two methods could be used in compliment to one another to improve discovery approaches.

To get the best out of our currently available technologies we must ensure that we have an optimal experimental design and accurate interpretations. A common limitation of biomarker studies is that they rely on a case versus control study design, a design that ignores clinical heterogeneity in patients and neuropathology in controls. Therefore biomarkers identified may instead reflect secondary changes specific to the cohort used rather than the disease biology. Using markers of in vivo β-amyloid deposition (e.g. ^{11}C-PiB) combined with positron emission tomography (PET) or structural MRI (sMRI) to derive biologically relevant biomarkers associated with established endophenotypes of disease pathology is a better approach. A marker found through this approach should be more robust and have greater clinical utility. Endophenotype approaches for blood based biomarkers have already successfully been conducted for various Alzheimer's disease pathologies such as brain atrophy[137, 148] and metabolism[149], and amyloid-beta burden[150-151], though much more work is needed especially in the early preclinical stages.

Additionally it is important to consider that surrogate markers of AD for which biomarkers are discovered, need to be well established and accurately reflect disease progression and severity. One area where more focus should be encouraged is measures of cognitive decline. MMSE classification is often used as a reference point to discover biomarkers reflecting cognition, yet we are aware that MMSE itself has an error rate of approximately 20%, is influenced by age and education, and is subject to ceiling and floor effects [152-154]. Without an objective standard to compare to an issue of circularity is introduced when assessing the validity of a potential AD biomarker.

1.9 Conclusion

Biomarker changes in AD are dynamic with disease development, and these changes start at an early preclinical stage. Many biomarkers have been identified but more work is required to identify robust preclinical biomarkers reflecting early AD pathology, and predicting future outcomes. AD-related changes detected at this early stage are likely to be very subtle and therefore longitudinal measures are required to sensitively detect these changes. The most suitable application in biomarker investigation at a preclinical stage is venepuncture for blood analysis; allowing large nondemented populations to be studied and followed longitudinally, and increasing future clinical utility of discovered biomarkers. Due to the complex composition of blood multiple technical platforms may need to be utilised in combination to provide a comprehensive coverage of the proteome for the discovery of biomarkers.

This work will therefore aim to identify and validate longitudinal blood based biomarkers of preclinical Alzheimer's disease pathology, using multiple proteomic platforms to enhance their discovery.

Chapter 2. Aims and Methods

2.1 Aims

Broad Aim: To discover longitudinal blood based protein biomarkers of early Alzheimer's disease pathology in healthy elderly individuals.

Specific aims: 1) To use two complementary longitudinal discovery phase proteomic analyses (2DGE and LC-MS/MS) to investigate plasma proteins related to amyloid load in the brain as measured using Pittsburgh compound B (PiB) PET imaging, brain atrophy as measured using structural MRI (sMRI), and cognitive decline as measured using various cognitive assessments. 2) To select target proteins from the discovery phase proteomic data and validate proteins in an independent cohort using quantitative immunoassays and aptamer-based arrays. 3) To determine whether the identified markers of Alzheimer's disease pathology can also be used as a diagnostic tool for Alzheimer's disease.

2.2 Participants

2.2.1 Discovery cohort: Baltimore Longitudinal Study of Aging (BLSA)

The BLSA was initiated in 1958 as a prospective longitudinal study of healthy human aging[155-158]. The primary objective of the study is to understand the physical and cognitive changes associated with normal aging. Over the past 50 years other issues have also been addressed by the study including the relationship between disease and age related changes. To date the BLSA has recruited over 1,300 healthy volunteers to the cohort ranging from 20 to 90 years old[159-162]. Participants include healthy, community-dwelling, middle to upper-middle class volunteers. Originally the study recruited only men, with the inclusion of women from 1978. Participants aged under 60 are cognitively assessed every 4 years, those aged 60-79 years are assessed every 2 years, and those aged 80 and over are assessed annually.

BLSA neuroimaging substudy

Currently in its 19th year (commenced in 1996) the neuroimaging substudy includes a subset of BLSA volunteers who return annually for imaging and clinical evaluations. The neuroimaging substudy is described in detail by Resnick et al (2003)[163].

Inclusion and exclusion criteria

All BLSA participants were selected for inclusion to the neuroimaging substudy if they were aged between 55-85 years and had prior cognitive and memory assessments. Exclusion criteria at baseline included; central nervous system (CNS) diseases (e.g. epilepsy, stroke, dementia), severe cardiovascular disease (e.g. myocardial infarction coronary artery disease), pulmonary disease or metastatic cancer. Exclusions were minimised to allow a representative sample of the main BLSA cohort and individuals displaying small signs of cognitive impairment (whilst not meeting criteria for dementia) and those with past or current depression were included since these factors may be dementia risk factors.

Consent

Written informed consent was obtained annually from all participants in conjunction with each neuroimaging visit.

MRI image acquisition and analysis

A GE Sigma 1.5 Tesla MRI scanner was utilised to acquire volumetric 'spoiled grass' (SPGR) scans (repetition time (RT) = 35; echo time (TE) = 5; flip angle = 45; field of view = 24; matrix = 256x256; number of excitations = 1; voxel dimensions of 0.94x0.94x1.5mm slice thickness). Head movement was reduced through the use of a custom thermoplastic mask and head-holder, which also aided repositioning for repeated longitudinal assessments.

A semi-automated approach was used to analyse the MRI volumes as described in Goldszal et al (1998)[164]. Briefly, images were firstly reformatted parallel to the anterior and posterior commissures. Extracranial tissue, the cerebellum, and brainstem structures inferior to the mamillary bodies were removed using both a semi-automatic and manual procedure. Remaining tissue was then classified into grey matter, white matter, and CSF. Ventricular CSF was defined by drawing a crude region of interest (ROI) used to then eliminate any non-ventricular CSF. The segmented images are then normalised using an elastic deformation approach[165] within Talairach stereotaxic coordinate space[166]. The number of voxels classified as gray matter, white matter, ventricular CSF, and other ROIs are then extracted for statistical analysis.

PiB PET image acquisition and analysis

Dynamic ^{11}C-PiB PET scans were performed in a GE Advance scanner in 3-dimensional mode, and 37 time frames (90 minutes) were obtained at rest. PET scanning started immediately after an intravenous bolus injection of approximately 15mCi. During the scan participants were fitted with a thermoplastic mask to minimise head movement. Transmission scans in 2-dimensional mode were used for attenuation correction of the emission scans. Dynamic images were reconstructed using filtered backprojection with a ramp filter (image size = 128x128; pixel size = 2x2mm, slice thickness = 4.25mm) yielding a spatial resolution of approximately 4.5mm full width half maximum at the centre of the field of view. Partial volume effect was minimised by excluding edges of tissue in definition of volumes of interest. Parametric images of distribution volume ratios (DVR) were calculated by simultaneous fitting of a reference tissue model using linear regression and spatial constraint (SPM5; Wellcome Department of Imaging Neuroscience, London, UK). The cerebellum was used as a reference region and 15 other regions of interest (ROIs) were defined; caudate, putamen, thalamus, lateral temporal, medial temporal, orbital frontal, prefrontal, occipital, superior frontal, parietal, anterior cingulate, posterior cingulate, pons, midbrain, and white matter. The mean cortical DVR was calculated by averaging values from orbitofrontal, prefrontal, superior frontal, parietal, lateral temporal, occipital, and anterior and posterior cingulate regions. ^{11}C-PiB parametric DVR images were spatially normalised and smoothed using a Gaussian filter of 8, 8, and 8mm in the x,y, and z planes[167].

Cognitive assessment

Various cognitive assessments are conducted annually for memory (California Verbal Learning Test[168] and Benton Retention Test[169]), word knowledge and verbal ability (Primary Mental Abilities Vocabulary[170]), verbal fluency (Letter[171] and Category fluency tests[172]), attention and working memory (Digit Span test of the Wechsler Adult Intelligence Scale-Revised[173]), executive function (Trails Making test A and B[174], and Digits Backward[173]), and visuospatial function (Card Rotations test[175]). Additionally the Mini-Mental State Examination (MMSE)[176] was conducted to assess cognitive impairment and the Centre for Epidemiologic Studies Depression Scale (CES-D)[177] was administered to measure depressive symptoms.

Blood samples

All blood samples were drawn by venipuncture and collected into EDTA glass tubes. Subjects were required to fast overnight prior to collection. Samples were centrifuged at 3000rpm for 30 minutes at 4°C. Plasma was then carefully collected, aliquotted and stored at -80°C until further use.

2.2.2 Validation cohorts: AddNeuroMed, Dementia Case Register (DCR) and Alzheimer's Research UK (ARUK)

AddNeuroMed is part of Innovative Medicines in Europe (InnoMed) program and is a multi-centre European study for the identification of Alzheimer's disease biomarkers funded by the European Union and members of the European Federation for Pharmaceutical Industries and Associations (EFPIA). AD subjects are assessed at three monthly intervals in their first year of assessment, and annually thereafter. MCI and control groups are assessed annually. All subjects are white Europeans recruited from six centres: King's College London, UK; University of Kuopio, Finland; University of Perugia, Italy; Aristotle University of Thessaloniki, Greece; University of Lodz, Poland; and University of Toulouse, France.

The Maudsley and King's Healthcare Partners DCR cohort was designed as a tool aiming to accelerate biomarker discovery, develop new therapies and generate testable hypotheses about the causes and symptoms of the dementia. The ARUK cohort is funded by Alzheimer's Research UK, has parallel aims to the DCR and sample collection and protocols between the two cohorts are identical. All subjects in these two cohorts are white UK citizens with grandparents born in the UK and are assessed annually.

Inclusion and exclusion criteria

Exclusion criteria included other neurological or psychiatric disease, significant unstable systemic illness or organ failure, and alcohol or substance misuse. Alzheimer's disease subjects were included if they met the ADRDA/NINCDS[178] and DSM-IV[179] criteria for probable Alzheimer's disease, had an MMSE score in the range of 12-28, a Clinical Dementia Rating (CDR)[180] scale score of above 0.5, and were aged 65 years or above. Individuals were classed as MCI if their MMSE

score ranged between 24 and 30, were aged 65 years or above, and scored 0.5 on the CDR. Control subjects were included if they scored 0 on the CDR.

Consent

Informed consent was obtained for all subjects according to the Declaration of Helsinki (1991)[181]. In cases where dementia compromised capacity then assent from the patient and consent from a relative, according to local law, was obtained.

MRI image acquisition and analysis

MRI data was obtained from AddNeuroMed subjects only. The AddNeuroMed sMRI protocol is described in detail by Simmons et al (2009)[182]. Briefly, MRI acquisition was completed at all six centres using six different 1.5T MR systems (four General Electric (General Electric Healthcare, Milwaukee, WI); one Siemens (Siemens Medical Solutions, Erlangen, Germany); and one Picker (General Electric Healthcare)). Whole-brain sagittal three-dimensional MP-RAGE images (TR=8.6, TE=3.8, 256x192 acquisition matrix, 180x1.2mm slices, 1.1x1.1x1.2mm voxel size) were acquired. To control quality across the six centres an MRI scan of a phantom was regularly acquired at each centre and assessed using ImageOwl web-based automated quality control system (http://www.imageowl.com/). Additionally two volunteers were scanned at each site and their scans were processed and analysed using the same tools as the cohort images. Structural MRI data analysis consisted of image intensity nonuniformity correction (N3 algorithm), segmentation of brain tissue (grey matter, white matter, CSF, and lesion subtype), regional brain parcellation (Automated Non-linear Image Matching and Anatomical Labelling (ANIMAL)), and cortical thickness measurement (Constrained Laplacian anatomic segmentation (CLASP)).

Cognitive and clinical assessments

The CDR, MMSE, Geriatric Depression Scale, sensory/motor impairment measure, global deterioration scale, and the Consortium to Establish a Registry for Alzheimer's Disease (CERAD)[183] cognitive battery were assessed for each participant. AD subjects were additionally assessed using the Alzheimer's Disease Assessment Scale (ADAS-Cog)[184] and the Cambridge Mental Disorders of the Elderly Examination (CAMDEX)[185].

For the AddNeuoMed cohort MMSE scores were obtained at five visits, three months apart. MMSE scores for ARUK and DCR cohorts were obtained annually over a period of two years (3 visits).

Blood samples

All blood samples were drawn by venipuncture and collected into EDTA glass tubes. Subjects were required to fast for at least 2 hours prior to collection. Both AddNeuroMed and DCR samples were centrifuged at 2000rpm for 10 minutes at 4°C. ARUK samples were centrifuged at 3000rpm for 8 minutes at 4°C. All samples were centrifuged within 2 hours of collection. Plasma supernatant was collected, divided into aliquots, and frozen at -80°C until further use.

2.3 Materials

The following is a list of reagents and the suppliers they were purchased from.

Reagent	Supplier	Catalogue #
Acetic acid, 100% glacial	VWR	20102.32
Acetronitrile (ACN)	Fisher Scientific Ltd	A0627OB17
Acrylamide PAGE, PlusOne, 40%	Fisher Scientific Ltd	17-1303-01
Agarose, low melting point	Sigma	A9414
Alpha-1-Microglobulin/Bikunin Precursor (A1M) ELISA Kit	USCN Life Science	E90217Hu
Amicon Ultrafree-MC centrifugal filter tubes, 0.5ml 3,000 MWCO	Millipore	UFC3LTK00
Ammonium Bicarbonate (Ambic)	Sigma	A6141
Ammonium hydroxide	Sigma	221228
Ammonium persulphate (APS)	Sigma	A3678

Bradford protein assay	Bio-Rad	500-0006
Bromophenol blue	Sigma	B8026
Citric acid	Sigma	C1857
Desalt Spin Column, 0.5mL Zeba	Fisher Scientific Ltd	89882
DeStreak rehydration solution	WVR	17-6003-19
Dithiothreitol (DTT), >98% (TLC), >99% (titration)	Sigma	D0632
Dithiothreitol (DTT), BioXtra, >99% (titration)	Sigma	D5545
Ethanol	VWR	283047K
Formaldehyde solution, 37 wt. % in H_2O	Sigma	252549
Glutaraldehyde solution	Sigma	G6403
Glycerol, for molecular biology, min.99%	Sigma	G5516
Human Zinc-Alpha-2-Glycoprotein (ZAG) ELISA kit	BT Labs	E3056Hu
Hydrochloric acid, 37% (HCl)	VWR	20252.244
Immobiline Drystrip gels, pH 3-11 NL, 18cm	VWR	17-6003-76
Iodoacetamide	Sigma	I1149
IPG Buffer, 3-11 NL	VWR	17-6004-40
Isopropanol	VWR	20839322
Mineral Oil	Sigma	M3516
Nathelene sulphonic acid	Sigma	70240
Piperazine diacrylamide (PDA)	Bio-Rad	161-0202

Proteoprep Immunoaffinity Albumin & IgG Depletion Kit	Sigma	PROTIA-1KT
SDS PAGE Tank Buffer, (10X) Tris-Glycine SDS	Geneflow Ltd	EC-870
SDS, 20 % solution	Sigma	5030
Silver nitrate	VWR	21572.235
Sodium acetate, SigmaUltra, min. 99%	Sigma	S7545
Sodium hydroxide, >=99%	Sigma	S8045
Sodium thiosulphate pentahydrate, SigmaUltra, min. 99.5%	Sigma	S6672
Tetramethylethylenediamine (TEMED)	Sigma	T9281
Tickopur r 30 neutral cleaner	SLS	Z660043
TMD-8, mixed bed resin	Sigma	M8157
Trifluoroacetic acid (TFA)	Merk Millipore	1.08262.0100
Trizma base	Sigma	T6791
Trypsin, Modified Sequencing Grade	Roche	11418025001
Urea, SigmaUltra	Sigma	U0631

2.4 Solutions

All solutions were made up using 18.2MΩcm ultra-pure water (ddH_20) unless specified otherwise.

Stock	Procedure
0.1% Nathelene sulphonic acid solution	2g Nathelene sulphonic acid 2l ddH_20
10% Acrylamide Gel Solution (12 gels)	250ml Acrylamide Stock 187.5ml Resolving Buffer Solution 3.75ml SDS 3ml Sodium thiosulphate (20% in ddH_20) 300ml ddH_20 5ml APS (10% in ddH_20) 500µl TEMED
10% APS Stock	2g APS 18ml ddH_20
100mM Ambic	0.79g Ambic 100ml ddH_20
10mM Dithiothreitol	15mg DTT (BioXtra) 1ml ddH_20 Dilute 10 fold with 100mM Ambic
200mM Iodoacetamide (IAA)	40mg Iodoacetamide

	1ml 100mM Ambic
50mM Ambic	40ml 100mM Ambic 40ml ddH_20
50mM Dithopthreitol	15mg DTT (BioXtra) 1ml 100mM Ambic Dilute 2 fold with 100mM Ambic
55mM Iodoacetamide (IAA)	10mg Iodoacetamide 1ml 100mM Ambic
Acrylamide Stock	750ml Acrylamide 250ml ddH_20 8g PDA 3-4 large scoops TMD-8* *once solution is de-ionised filter out.
Agarose Sealing Gel	0.5g Agarose 100ml SDS Running Buffer 200µl Bromophenol blue (0.002% in ddH_20)
BSA Stock (10mg/ml)	10mg BSA 1ml ddH_20
Developer solution	2ml Citric acid (5% in ddH_20) 5.4ml Formaldehyde 1992ml ddH_20

Displacing Solution	25ml Resolving Buffer 50ml Glycerol 25ml ddH_20 200µl Bromophenol Blue (0.002%)
Resolving Buffer	181.7g Trizma base 750ml ddH_20 pH adjusted to 8.8 with HCl (6M) Solution made to 1l with ddH20
SDS Equilibration Buffers: Equilibration DTT and equilibration IAA solutions	6.7ml Resolving Buffer Solution 72.07g Urea 70ml ddH_20 Let Urea dissolve overnight then add: 60.6ml Glycerol 20ml SDS 400µl Bromophenol blue (0.002% in ddH_20) Solution made to 200ml with ddH_20 Prior to use divide into 2x100ml Add 1g DTT to 1x100ml Add 2.5g Iodoacetamide to the second 100ml.
Silver nitrate solution	Solution A: 16g Silver nitrate

	200ml ddH_20 Solution B: 26.6ml Ammonium hydroxide (14.8M) 4ml Sodium Hydroxide (10M) 1000ml ddH_20 Add solution A to B slowly whilst mixing Add 800ml ddH_20
Sodium acetate-glutaraldehyde solution	84.6g Sodium Acetate 40ml Glutaraldehyde 1960ml ddH_20
Stop solution	100g Trizma base 40ml Glacial acetic acid 1860ml ddH_20
Strong Fix Solution	800ml Ethanol 200ml Glacial acetic acid 1000ml ddH_20
Trypsin 0.1% TFA	250µl 0.1% TFA (5ml ddH_20, 5µl TFA) 25µg Trypsin
Weak Fix Solution	100ml Ethanol 100ml Glacial acetic acid 1800ml ddH_20

2.5 Methods: Discovery 1

2.5.1 Bradford assay

Protein concentrations of plasma samples needed to be determined in order to be able to keep the amount of protein assessed in the various proteomic techniques uniform across subjects, allowing comparisons to be possible. Protein concentrations of each plasma sample were therefore determined according to the method of Bradford[186] using bovine serum albumin (BSA) as a standard. Briefly, BSA standards of 7 concentrations ranging from 2-0.125mg/ml plus a blank sample (0mg/ml) were used to create a standard curve. Plasma sample dilutions were prepared (1:100). 10µl of each standard and sample was added in triplicate to a 96 well plate. Bradford reagent was diluted 1:4 with double distilled H_20 (ddH_20) before adding 190µl to each well. The plate was then incubated at room temperature for 10 minutes before reading absorbance values with a spectrophotmeter at 595nm. Standard curves were then created by plotting the 595nm values (y-axis) versus their concentration in µg/ml (x-axis). The standard curve was used to determine the concentration of each plasma sample, adjusting for the dilution factor used.

2.5.2 Two dimensional gel electrophoresis (2DGE): analytical gel

Global analyses of all proteins present in a sample in combination with cognitive and/or imaging data allows for the discovery of novel biomarkers and confirmation of those previously reported. Two dimensional gel electrophoresis (2DGE) is a well-established proteomic discovery technique for the separation and, when coupled with mass spectrometry, for the identification of large numbers of proteins present on a gel. Here 2DGE was utilised to screen plasma samples for a protein profile of Alzheimer's disease endophenotypes. As shown in Figure 2-1 2DGE comprises 9 steps: (1) sample preparation, (2) separation in the first dimension, (3) second dimension separation, (4) Protein visualisation (staining), (5) image analysis, (6) statistical analysis, (7) preparative gel (8) spot selection and digestion, (9) mass spectrometry identification.

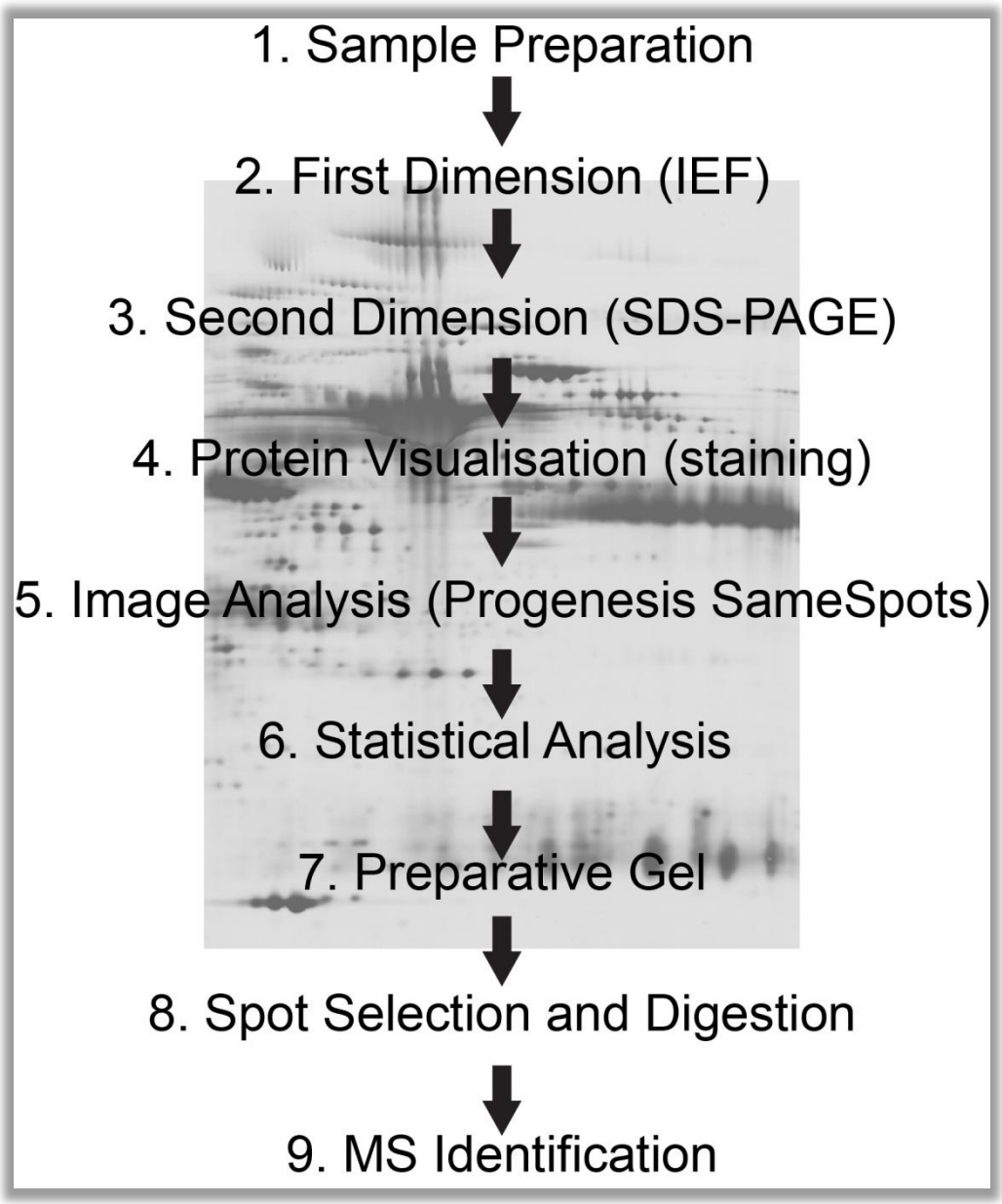

Figure 2-1: 2DGE workflow

Sample preparation

For each plasma sample 1:10 dilutions were prepared. Having previously calculated the protein concentration of each sample the 1:10 dilutions were then aliquotted into two aliquots each containing 50µg of protein (each sample was to be run in duplicate). Each aliquot was then made up to 350µl with DeStreak rehydration solution in which IPG buffer (7-11 NL) had been added just prior to use. Samples were then vortexed, pulse centrifuged and left at room temperature for 15 minutes to solubilise proteins.

First dimension – Rehydration and isoelectric focussing (IEF).

Rehydration buffer/sample solution aliquots were applied to Immobiline DryStrips (pH 3-11, 18cm) placed in strip holders. Using IPGphor™ (Amerham Bioscience) apparatus the strips were then rehydrated for 12 hours and IPG electrofocused for 16 hours using the protocol detailed in Table 2-1 below.

Table 2-1: 2DGE first dimension rehydration and isoelectric focusing experimental settings

Phase	Voltage (V)	Duration (hours)
Rehydration	50 μA/strip	12
1. Hold	500	2
2. Gradient	500-1000	2
3. Hold	1000	2
4. Gradient	1000-8000	2
5. Hold	8000	8

Following electrofocusing the strips were frozen at -80C until required for second dimension.

Second dimension: SDS-PAGE

The second dimension consists of four steps: (1) Gel preparation, (2) IPG strip equilibration, (3) IPG strip electrophoresis preparation (4) electrophoresis.

(1) Gel preparation. Acrylamide gels were prepared using the Ettan Dalt II gel caster system (Amersham Bioscience, UK). A 10% acrylamide solution was prepared and poured into the casting system, followed by a displacing solution. Using a pipette 1ml of isopropanol was then overlaid on top of each gel to minimize exposure to oxygen and to create an even gel surface. The gels were allowed to polymerise for 1 hour before being covered in water and left overnight to fully polymerise.

(2) IPG strip equilibration. Previously rehydrated and IPG electrofocused strips were equilibrated in a two-step process. Firstly strips were equilibrated in an equilibration DTT solution for 15 minutes to reduce disulphide bonds, immediately followed by an equilibration iodoacetamide solution for 15 minutes to prevent the reformation of these bonds.

(3) IPG strip electrophoresis preparation. After equilibration, the IPG gel strips were cut at both extremities to remove sections of salt build up. The strips were then placed on top of the polymerized acrylamide gels, making sure there were no bubbles between the gel and the strip, and then sealed in place with agarose sealing gel.

(4) Electrophoresis. Electrophoresis was performed using the Ettan Dalt ™ II large vertical system (Amersham Bioscience, UK). The electrophoresis was achieved through two phases; resolving and separating. Table 2-2 below details the settings for each of these stages. The Ettan Dalt ™ system was set to maintain a constant temperature of 15°C throughout.

Table 2-2: 2DGE electrophoresis settings

Phase	Power (W)	Duration (hours)
Resolving	5 W/gel	1 h
Separating	Increase to 80 W	6-8hrs/12 gels

Protein Visualisation (silver staining)

After electrophoresis gels were fixed for 1 hour in strong fixing solution in separate staining boxes. They were then transferred to weak fixing solution and left overnight at room temperature. Protein detection was achieved using silver staining according to the Hochstrasser protocol[187]. The gels were fixed and stained using the solutions and incubation steps shown in Table 2-3.

Table 2-3: Hochstrasser silver staining protocol steps

Silver staining step	Time
Strong Fixing Solution	1 h
Weak Fixing Solution	overnight
Wash (ddH_20)	5 min
Sodium acetate-glutaraldehyde solution	1.5 h
Wash (ddH_20)	4x15 min
Nathelene sulphonic acid solution	2x30 min
Wash (ddH_20)	4x15 min
Silver nitrate solution	25 min
Wash (ddH_20)	4x4 min
Develop solution	As required
Stop Solution	As required

Image analysis: Gel pre-processing

The silver stained gels were scanned using a GS-800 calibrated densitometer at medium resolution (72 dpi) and saved as TIFF images for image analysis. Spot detection and analysis was performed using Nonlinear Progenesis SameSpots software version v.3.3.3420.25059 (Nonlinear Dynamics, Newcastle upon Tyne, UK). Scanned gel images were firstly added into the software where quality checks were performed and images were edited (cropped and rotated) if required. One gel image with a clear, representative spot pattern with minimal distortion was selected as a reference image for the other images to be later aligned to. A mask of disinterest was applied to exclude areas around the edge of the gel before manual and then automatic alignment was performed. The reference gel was then automatically matched against all the individual gels to identify spots that could be confidently

matched on every gel across the whole sample cohort. Filtering of these spots was then performed to include only single, well defined spots. A within subject experimental design was then specified and gel images were grouped by time point. The results of this time point comparison allowed individual spots to again be viewed in detail using the spot expression profile and 2D/3D montage view. Using these tools further filtering of spots was performed at this stage by a manual review of every spot, removing any overlapping and less defined spots. Normalised volume values for the remaining spots were exported into an excel spreadsheet for further statistical analysis.

Statistical analyses

As each sample had been run in duplicate the coefficient of variation (CV) was calculated for every duplicate spot using R version 3.0.0 software (R Foundation for Statistical Computing, Austria). If the CV between the duplicates was <40% then an average of the two normalised spot volumes was calculated to be used as the value for further statistical analyses. If the CV was >40% then the spot closest in value to the overall normalised spot volume mean was selected to be used for further analyses. Normality tests (Kolmogorov-Smirnov) were then calculated for every spot. The data was then logged (base 10) to minimise skewness and non-normal spot distributions. The remaining statistical analysis was split into three sections: cross sectional analysis with PiB PET DVR, longitudinal analysis with sMRI volumes, and longitudinal analysis with cognitive scores. Covariates included in statistical tests were; age, gender, education (years), body mass index (BMI), cholesterol, and *APOE* ε4 status. All of these factors have known impacts upon the risk of AD, and were included as covariates to remove their influence and enable any relationship between protein and AD to be identified. Although 6 is a large number of covariates to include, as this study was investigating preclinical AD a blood based biomarker signal is likely to be weak, and therefore it was considered necessary to remove as much additional variance as possible.

Cross sectional analysis with PiB PET DVR

Cross sectional analyses were performed with the aim to identify protein spots at each time point significantly related to PiB PET DVR 12 years later, 6 year later, and concurrently (see Figure 2-2). Using R version 3.0.0 software with package ‘ppcor’ a

partial correlation was performed correlating every spot with PiB PET DVR scores whilst controlling for age, gender, education (years), body mass index (BMI), cholesterol, and *APOE* ε4 status. Spots found to be significantly correlated with PiB PET DVR were then manually assessed to determine whether they could be successfully picked out of the gel for later identification. Spots that were not visually well defined and discrete were discarded. Using R package 'glmnet' the remaining significant spots were entered into a penalised elastic-net regression model with leave-one-out cross validation. To provide an indication of how well the resulting panels of significant spots from each time point could predict PiB PET DVR the spots were entered into a standard linear regression model using SPSS version 20 (IBM Statistics Software, USA).

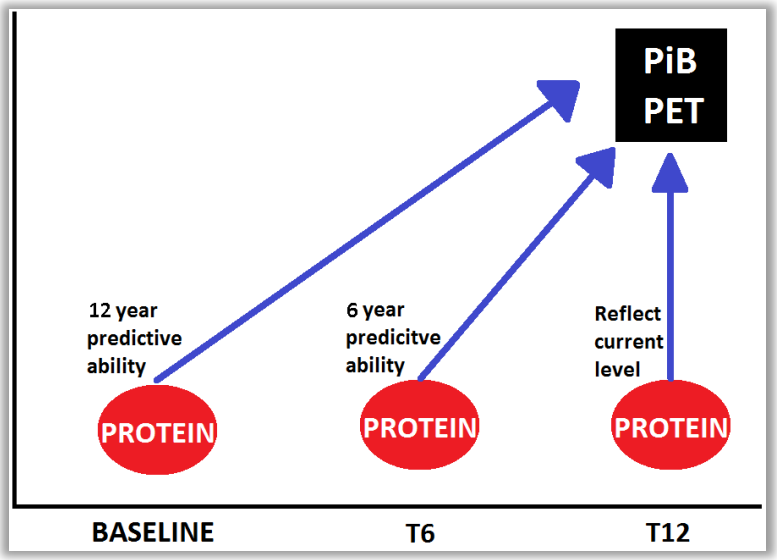

Figure 2-2: Cross sectional analysis; finding 2DGE spots related to PiB PET DVR at each time point.

Longitudinal analysis with MRI volumes

To identify MRI brain volumes that significantly changed over time one-way repeated measures ANOVAs were conducted on all regions using SPSS version 20. Regions that changed non-linearly were discarded as further analysis using regression models used could only model linear change over time. Regions that showed significant atrophy were then ranked based on their percentage change in volume over time. The region with most change was taken forwards and using R version 3.0.0 software mixed-effect regression models were conducted to perform a slope comparison between protein spot normalised volumes and sMRI brain volume

whilst controlling for age, education (years), gender, BMI, cholesterol, and *APOE* ε4 status.

Longitudinal analysis with cognitive scores

To identify cognitive scores that significantly changed over time, one-way repeated measures ANOVAs were conducted on all measures using SPSS version 20. Measures that changed non-linearly were discarded leaving only one remaining significant cognitive measurement. Using R version 3.0.0 software mixed-effect regression models were conducted to perform a slope comparison between protein spot normalised volumes and cognitive score whilst controlling for age, education (years), gender, BMI, cholesterol, and *APOE* ε4 status.

2.5.3 Two dimensional gel electrophoresis (2DGE): preparative gel

To identify proteins present in a given spot using mass spectrometry a 2DGE preparative gel was needed. Protocol was kept the same as for the analytical gel except for the following three amendments; (1) Sample aliquots contained 300-400µg protein (2) sodium-acetate glutaraldehyde solution contained no glutaraldehyde, (3) develop solution had 50% less formaldehyde.

2.5.4 Two-dimensional gel electrophoresis (2DGE): Mass spectrometry protein identification

Spot picking

Protein spots showing a statistically significant relationship between their normalised volumes and Alzheimer's disease pathology were selected as biomarker candidates and taken forward to be identified by mass spectrometry. Spot picking was completed manually. Gels were kept in stop solution throughout. A 1:1 size-matched print-out copy of the scanned gels was created and spots of interest were highlighted to aid with picking. Gels were placed on top of a light box during picking to help view the spots. Pipette tips were cut so that the opening was approximately the size of the spot of interest. Approximately 100µl of water was drawn into the tip before the opening was carefully pressed down on top of the spot into the gel to remove the spot. The picked spot was then transferred to an eppendorf tube by pushing the water out of the tip.

In gel tryptic digestion

Excised gel spots were cut into small $2mm^3$ pieces and transferred back into an eppendorf tube. The gel spots were then washed with 100mM Ambic (added in excess) for 5 minutes then decanted. Next acetonitrile (ACN) was added in excess, decanted, and then the same volume was added again to fully and quickly dehydrate the gel pieces. ACN was then removed and gel spots were dried in a speed vac for 5 minutes. Gel spots were then rehydrated with 10mM dithiothreitol (DTT) and heated at 56°C for 30 minutes. DTT was removed and ACN was again added twice, as in earlier step, to dehydrate before again drying in a speed vacuum for 5 minutes. Next 55mM iodoacetamide (IAA) was added to the gel spots and incubated at ambient temperature for 20 minutes in the dark. The supernatant was discarded and gel spots were washed briefly with 100mM Ambic buffer that was then replaced and spots were washed for a further 5 minutes before the buffer was discarded. Gel spots were dehydrated as before with ACN and dried in a speed vacuum for 5 minutes. 200µl of 50mM Ambic was added to each trypsin 0.1% trifluoroacetic acid (TFA) aliquot (30µl) to give a final trypsin concentration of 13ng/µl. Gel pieces were rehydrated in a minimal volume of this trypsin solution (i.e. enough to cover and rehydrate the gel pieces) at 4°C for 20 minutes. Unabsorbed trypsin was then removed and a minimal volume of 50mM Ambic (10-20µl) was added to cover the gel pieces and keep them wet during enzyme cleavage. Gel spots were incubated at 37°C for 2 hours then overnight at room temperature.

Peptide extraction

Supernatant was decanted from gel pieces and collected into a new eppendorf tube. Using a minimal volume to immerse the gel pieces they were washed with 50mM Ambic for 5 minutes at 37°C, which was then decanted and supernatant pooled into the same eppendorf tube as before. Gel pieces were next dehydrated with ACN for 10 minutes at 37°C, after which the supernatant was again decanted and pooled into the eppendorf tube. The above wash and dehydrate steps were then repeated once. The pooled supernatant was then frozen and dried down to completion whilst avoiding over drying and then stored at -80°C until required.

Mass spectrometry

After digestion and extraction the resulting peptide mixture was loaded into an orbitrap mass spectrometer for protein identification. Samples were firstly reconstituted in 20µl 50mM Ambic, 10µl of which was loaded into an orbitrap loading vial. 8µl of each sample was injected onto a Thermo C18 pre-column, using the Proxeon EASY-nLC II system (Thermo Fisher Scientific Inc, USA). Peptides were resolved by reverse phase chromatography over an increasing gradient of 0.1% formic acid (FA) in ACN through a Thermo C18 analytical column. Mass spectra were acquired on an LTQ Orbitrap Velos Pro (Thermo Fisher Scientific Inc, USA) throughout the chromatographic run (35 minutes) using 20x collision-induced dissociation (CID) scans following each Fourier transform mass spectrometry (FTMS) scan (2x µScans at 30,000 resolving power @ 400 m/z). CID was carried out on 20 of the most intense ions from each FTMS scan. Blank samples were run in between every four samples to avoid protein cross over.

Mass spectrometry data pre-processing

Peak lists were extracted from Xcalibur raw data files using Proteome Discoverer 1.4 that were then searched against the UniProtKB/Swiss-Prot database (uniprot_sprot.fasta, downloaded from http://www.uniprot.org/downloads on 20/02/13) using Mascot 2.2.06 search engine. Taxonomy was set to Homo-sapiens (human). The search was programmed to include tryptic peptides with up to 3 missed cleavages, with variable modifications set as Carbamidomethyl (C), Oxidation (M), and Acetyl (Protein N-term). Precursor mass tolerance was set to 10 ppm and fragment mass tolerance 0.8 Da. A percolator filtered identifications based on a false discovery rate (FDR) of 0.5%, set at the peptide level, based on a target-decoy search approach.

Protein quantification

Several proteins were often identified as present in each gel spot. These were ranked for abundance using three different approaches; peptide spectral matches (PSM), area under the curve (AUC), and unique peptide count. Abundance ranking based on PSMs uses the number of tandem spectra matched to peptides of a certain protein to determine a total spectral count. This count is considered to be positively associated with the abundance of the protein and so can be used as an indicator of relative

abundance. The second approach (AUC) suggests that for each protein identified, the average signal of the three most efficiently ionised peptides directly correlates to the protein abundance. Thirdly, unique peptide count is based upon the fact that proteins within a 2DGE spot have roughly the same weight and charge. This approach therefore assumes that the proteins within a spot will have similar numbers of amino acids, so similar numbers of lysine and arginine frequencies for trypsin to cleave, and therefore roughly the same number of potential peptides. If the number of potential peptides is equivalent and the ionisation efficiency on the mass spectrometer is similar (as proteins within a spot have similar isoelectric points) then the number of unique peptides can be said to represent the relative abundance.

The 'Precursor Ions Area Detector' of Proteome Discoverer 1.4 was utilised to calculate the area AUC of each precursor ion using integration. This information was exported from Proteome Discoverer to Excel along with the number of peptide spectral matches (PSMs) and unique peptide number. Proteins were stringently filtered so that only the most likely candidates survived (rank of peptide match= 1, is bold (match assigned only once) = 1, peptide match score >30, peptide match expectation value <0.01, number of peptide sequences >3). Any keratin or trypsin present in the dataset was removed. Proteins were then ranked on abundance using each of the three approaches. For each method of quantification proteins that were contributing to less than 5% of a spot's total protein quantity were removed from the spot. Out of the remaining proteins those included in 2/3 of the quantification approaches were considered to be abundantly present and were suggested candidates for the statistical signal found from that spot.

2.6 Methods: Discovery 2

2.6.1 Liquid chromatography-tandem mass spectrometry (LC-MS/MS)

LC-MS/MS is a quantitative and sensitive approach for proteomic analyses. It offers superior sensitivity and specificity for low molecular weight analytes compared to 2DGE. Here through prior depletion of abundant and high molecular weight plasma proteins allowing for the extraction of proteins with a low molecular weight (<30ka), LC-MS/MS was performed to provide a complementary evaluation of the proteome

to that already conducted using 2DGE (20-250kDa range). Figure 2-3 displays the workflow used for this discovery phase.

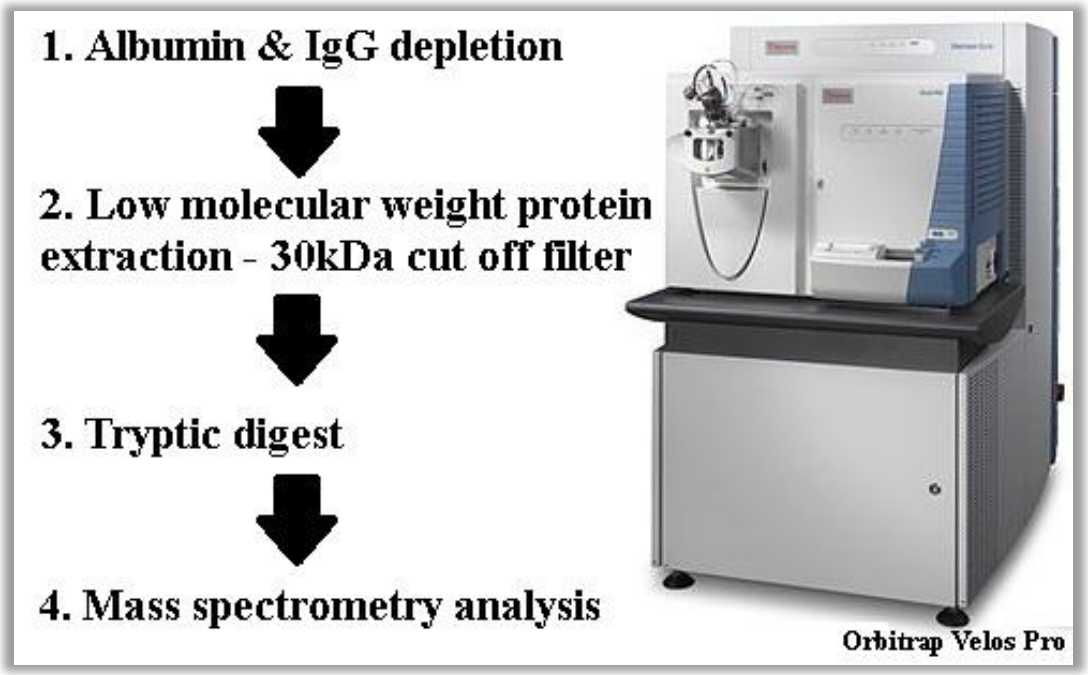

Figure 2-3: Label free LC-MS/MS workflow

Depletion of albumin and IgG from plasma samples

Depletion columns were firstly equilibrated using equilibration buffer provided in the depletion kit. 15mg of protein (~25µl of plasma sample) was then loaded onto the depletion column medium bed and incubated for 10 minutes. Next the column was centrifuged at 8000xg for 1 minute. The eluate in the collection tube was then re-applied to the medium bed and incubated for a further 10 minutes. Next the column was centrifuged again at 8000xg for 1 minute. The twice depleted plasma remained in the collection tube to be combined with the following wash for optimal protein recovery. 125µl of equilibration buffer was added to the medium bed and centrifuged for 60 seconds to wash through any remaining unbound proteins from the spin column.

Removal of remaining large proteins (>30kDa)

Depleted plasma samples were each pipetted into a 30kDa cut off filter cup placed inside a filtrate collection tube. The filter was then centrifuged at 5000xg for 45 minutes. The protein concentration of the filtrate was determined using a NanoDrop

instrument (Thermo Fisher Scientific Inc, USA) before being divided into two 15µg aliquots and stored at -80℃.

In-solution trypsin digest

Samples were reconstituted in 100µl 50mM Ambic. 11µl of 50mM DTT was then added and incubated at 56℃ to reduce cysteine residues. Samples were next alkylated by treatment with 12µl 200mM iodoacetamide in the dark for 20 minutes at ambient temperature. Then samples were digested with 10µl trypsin 0.1% TFA and incubated at 37℃ for 2 hours and then overnight at room temperature. Samples were then frozen and dried down to completion and stored at -80℃ until required.

LC-MS/MS analysis

Samples were reconstituted in 30µl 20% ACN, 0.1% FA. All 30µl was loaded into an orbitrap loading vial whilst avoiding any precipitate. 8µl of each sample was injected onto a Thermo C18 pre-column and mass spectra were acquired as described previously throughout a 35 minute chromatographic run. Samples were run in triplicate and blank samples were run in between every triplicate to avoid cross over between subjects.

LC-MS/MS data pre-processing

Peak lists were extracted and searched as previously described, except for precursor mass tolerance and fragment mass tolerance that were set to 5ppm and 0.5Da respectively. Data was then loaded into Scaffold 4 (Proteome Software Inc, USA) allowing the merging of the triplicate sample injections into one BioSample. Proteins were filtered using the following cut off values; protein threshold = 95%, minimum number of peptides = 2, peptide threshold = 80%. Decoy proteins, keratin and any trypsin were removed. To enable comparisons across samples the Normalised Total Spectra quantitative value was selected. This value is calculated by averaging the spectrum count for all of the BioSamples, then the number of spectra assigned to one protein is multiplied by the ratio of the average spectrum count and the number of spectra in that sample. This data was then exported to Excel for further analysis.

Statistical analysis

Statistical analysis was conducted using R version 3.0.0. For each time point a partial correlation was performed correlating every protein with PiB PET DVR whilst controlling for six co-variables; age, gender, education (years), body mass index (BMI), cholesterol, and *APOE* ε4 status. Additionally mixed-effect regression models were conducted to perform slope comparisons between proteins and sMRI brain volumes and cognitive measures whilst controlling for the same six co-variables as previously stated.

2.7 Methods: Validation

2.7.1 Validation of proteomic data using an aptamer based array (SOMAscan) and enzyme-linked immunosorbent assays (ELISA).

Aptamer based array: SOMAscan (SomaLogic, Inc, Boulder, Colorado)

A Slow Off-rate Modified Aptamer (SOMAscan) array uses chemically modified nucleotides to measure 1,001 different human proteins by transforming their protein signal into a nucleotide signal that can then be quantified using relative florescence on microarrays. SOMAscan is conducted by SomaLogic as a fee-for-service; Figure 2-4 displays the SOMAscan mechanism. Briefly, SOMAmers attached via a linker to streptavidin beads bind to proteins in a sample. The bound proteins are then biotinylated before the SOMAmer-protein complexes are released by photocleaving a linker. Biotinylated proteins are then bound to a second streptavidin bead and the bound SOMAmers are removed from the proteins. These SOMAmers are then collected and denatured before being measured using standard DNA analysis techniques such as microarrays.

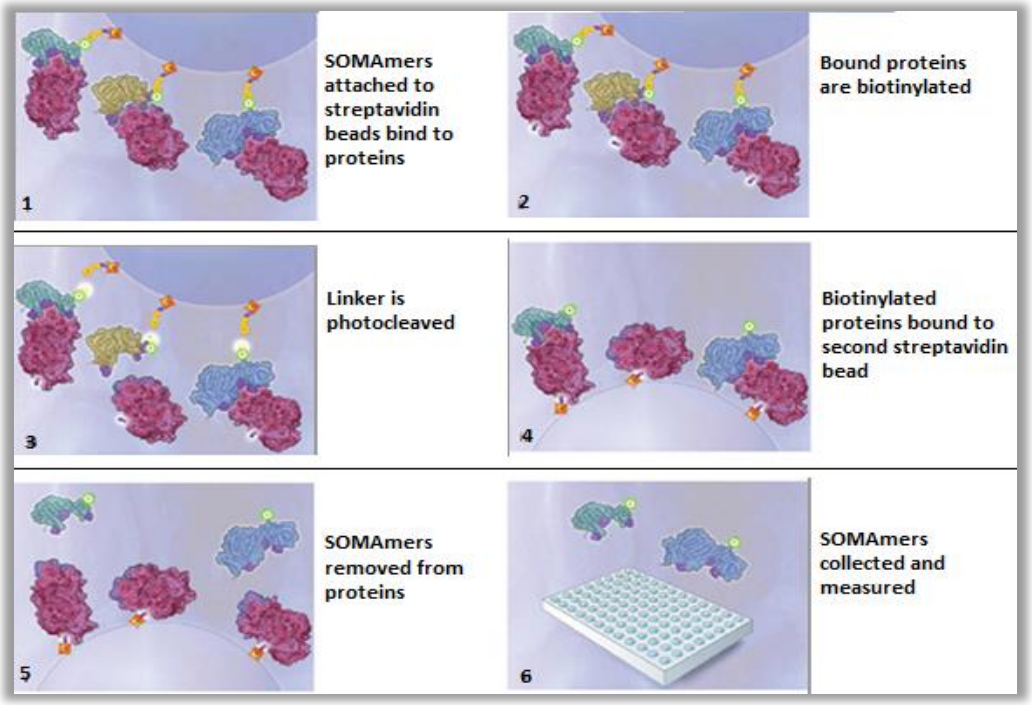

Figure 2-4: Mechanism of SOMAscan assay, adapted from http://somalogic.com/Technology/How-it-works.aspx

SOMAscan statistical analysis

SomaLogic SOMAscan aptamer-based assays were available for a subset of the candidate biomarkers requiring validation. Analysis was conducted as reported in Kiddle et al (2014)[188], but was conducted here only for candidate biomarkers of interest. Using R the candidate proteins were analysed individually for their association with AD phenotypes: AD disease status (AD v control), sMRI volumes (left and right entorhinal volume, left and right hippocampal volume) and rate of cognitive decline (change in MMSE per day; slope coefficient from a linear mixed effect model using longitudinal MMSE scores[188]). Disease status was analysed using logistic regression whilst adjusting for age, gender, *APOE* ε4 status, and research centre. Partial Spearman's Rank Correlation (SRC) was performed to investigate the correlation between sMRI volumes and proteins whilst controlling for age, gender, research centre and *APOE* ε4 status. SRC was also used to investigate the correlation between cognitive decline and proteins. False discovery rate (FDR) multiple testing corrections were applied to the resulting p-values. Both a strict (q-value = 0.05) and less strict (q-value = 0.1) were considered.

Enzyme-linked Immunosorbent Assay (ELISA)

Two candidate biomarkers for which SOMAscan assays were not available were instead analysed using commercially available ELISA assays to provide an independent comparison and validation of the discovery phase experiments.

ELISA for Alpha-1-Microglobulin/Bikunin Precursor (a1M)

This sandwich ELISA was carried out according to the USCN assay instruction. Briefly, all reagents, samples (500 fold dilution) and standards (0-300ng/ml dilution range) were prepared. 100µl of standard, blank, or sample was added in duplicate to the appropriate well and incubated for 2 hours at 37°C. The liquid of each well was then removed by inverting the plate and blotting it against absorbent paper. 100µl of detection reagent A provided was then added to each well and the plate was incubated for 1 hour at 37°C. The plate was then washed 3 times with 300µl of the washing buffer provided before 100µl of detection reagent B was added to each well and incubated for 30 minutes at 37°C. The plate was then washed 5 times with washing buffer before 90µl of substrate solution was added to each well and incubated for 25 minutes at 37°C in the dark. 50µl of stop solution was then added to each well. The plate was immediately read on a microplate reader at 450nm. The plate was also read at 595nm allowing the subtraction of noise. Sample replicates were averaged and standard values were used to create a standard curve in SigmaPlot version 12.5 (Systat Software Inc, USA) from which protein concentrations could be determined.

ELISA for Zinc-Alpha-2-Glycoprotein (ZAG)

This sandwich ELISA was carried out according to the BT Laboratory assay instruction. Briefly, reagents, standards (0-480µg/µl) and samples (neat) were prepared. Blank and standards (50µl) and samples (40µl, plus 10µl ZAG antibodies) were added in duplicate into the appropriate wells and 50µl of streptavidin-HRP was then added and incubated for 60 minutes at 37°C. The plate was then washed 5 times with 300µl of the washing buffer provided before 50µl of chromogen solution A and B was added to each well and incubated for 10 minutes at 37°C in the dark. 50µl of stop solution was next added to each well and the plate was read on a microplate reader at 450nm. The plate was also read at 595nm to allow the subtraction of noise. Sample replicates were averaged and standard values were used to create a standard

curve in SigmaPlot version 12.5 from which protein concentrations could be determined.

ELISA statistical analysis

Protein concentrations were analysed using SPSS. T-tests were used to determine differences in concentrations between AD and control subject groups. Pearsons correlation was performed to identify proteins correlated to brain atrophy and/or cognitive decline.

Chapter 3. Longitudinal blood based biomarker discovery of early Alzheimer's disease pathology and cognitive decline using two-dimensional gel electrophoresis

3.1 Introduction

Two dimensional gel electrophoresis (2DGE) is a well established technique that has been employed for protein separation since 1975[189-190]. 2DGE has so far been extremely useful as an analytical tool for biomarker discovery in many areas of research, and in the past decade has shown its utility for blood-based biomarker research for Alzheimer's disease[142, 151]. 2DGE enables the separation of proteins in a complex sample according to charge (pH/pI) in the first dimension followed by molecular weight (MW) in the second dimension. This technique also allows the separation of different protein isoforms due to naturally occurring protein cleavage and post translational modifications, such as glycosylation and phosphorylation, which affect both charge and mass. Proteins are then visualised by one of many staining techniques available revealing a pattern of proteins present characteristic to the sample type used. Gels can then be scanned and converted to digital images allowing in depth analysis by informatics and statistical software. Following analysis 2DGE spots of interest can be extracted from the gel and identified by liquid chromatography-tandem mass spectrometry (LC-MS/MS), which also enables relative quantification of the proteins present.

In 2010 Thambisetty et al performed a retrospective preclinical AD biomarker study investigating plasma proteins reflecting brain amyloid load 10 years later[151]. Using an elderly healthy cohort (Baltimore Longitudinal Study of Aging) they performed 2DGE and discovered a panel of 18 protein spots that could differentiate between healthy individuals who would have high or low brain amyloid load 10 years later, accounting for 59% of the variance in PiB PET distribution volume ratio (DVR). This confirmed that a peripheral signal of preclinical Alzheimer's pathology could be detected in cognitively healthy individuals. This project aimed to repeat and expand upon this work. Here, using 2DGE, plasma proteins were assessed for their relationship to amyloid load 12 years later (baseline), 6 years later (T6), and concurrently (T12) to the PiB PET scan. Additionally the plasma proteome was

investigated for a correlation with two more indicators of Alzheimer's disease (cognitive decline and brain atrophy) over a longitudinal 12 year period.

3.2 Aims

To identify proteins predictive of amyloid load using 2DGE coupled with LC-MS/MS. To discover the most predictive protein panels at each time point (12 years prior, 6 years prior, and concurrently) using multivariate analyses of proteins against quantitative amyloid imaging measures (^{11}C-PiB PET DVR). Additionally using the same proteomic technique, proteins longitudinally related to brain atrophy and cognitive decline will be identified.

3.3 Results

3.3.1 Demographic characteristics

Individuals (n=68) were selected from the Baltimore Longitudinal Study of Aging (BLSA) neuroimaging cohort previously described (Chapter 2). These individuals must have had serial MRI scans, serial cognitive assessments and serial blood sampling to be included in the study. The majority of these individuals (n=54) also had one PiB PET scan. Plasma samples were drawn at three time points (1.5ml aliquots in EDTA; a total of 204 samples). Time points corresponded to neuroimaging visits ~6 years apart (baseline, T6 = 6+/-2 years, and T12 = 12+/-2 years) (Figure 3-1). The third time point samples (T12) were concurrent to the subjects PiB PET scan. 2DGE analysis of each sample was performed in duplicate, or more if gels of poor quality required repetition.

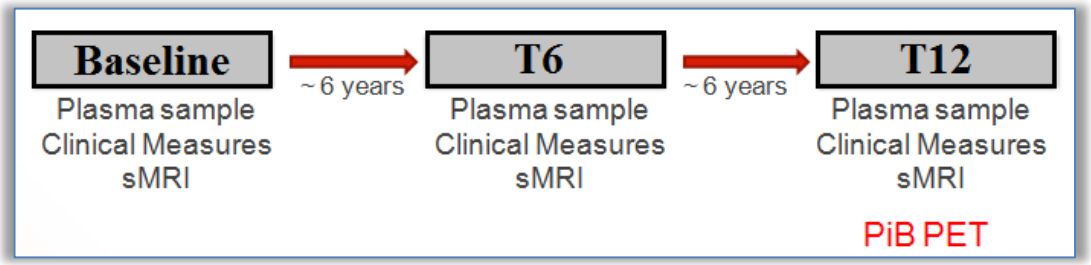

Figure 3-1: Diagram illustrating information available at each time point (baseline, T6, and T12); plasma samples, clinical measurements, structural MRI volumes, and PiB PET DVR

Table 3-1 below summarises the demographic characteristics of the study population at baseline.

Table 3-1: Subject demographics

	N	Mean age at baseline	Std. dev
Female	29	66.34	6.55
Male	39	67.82	5.54
Total	68	67.19	5.99

Table 3-2 below displays the number of these subjects whom had PiB PET scan information available, mean distribution volume ratios (DVR), and when the PiB PET scan was conducted (mean number of years after baseline (baseline)). Figure 3-2 shows the distribution of PiB PET DVR values across these subjects. This histogram displays a wide range of PiB PET DVR values, with approximately half of the subjects forming a cluster at the lower end of the distribution, and the remaining half spread out over higher DVR values.

Table 3-2: Subject PiB PET DVR information

	N	Mean PiB PET DVR	Mean no. years between baseline plasma sample and PiB PET scan
Female	29	1.17	11.39
Male	25	1.13	11.45
Total	54	1.15	11.43

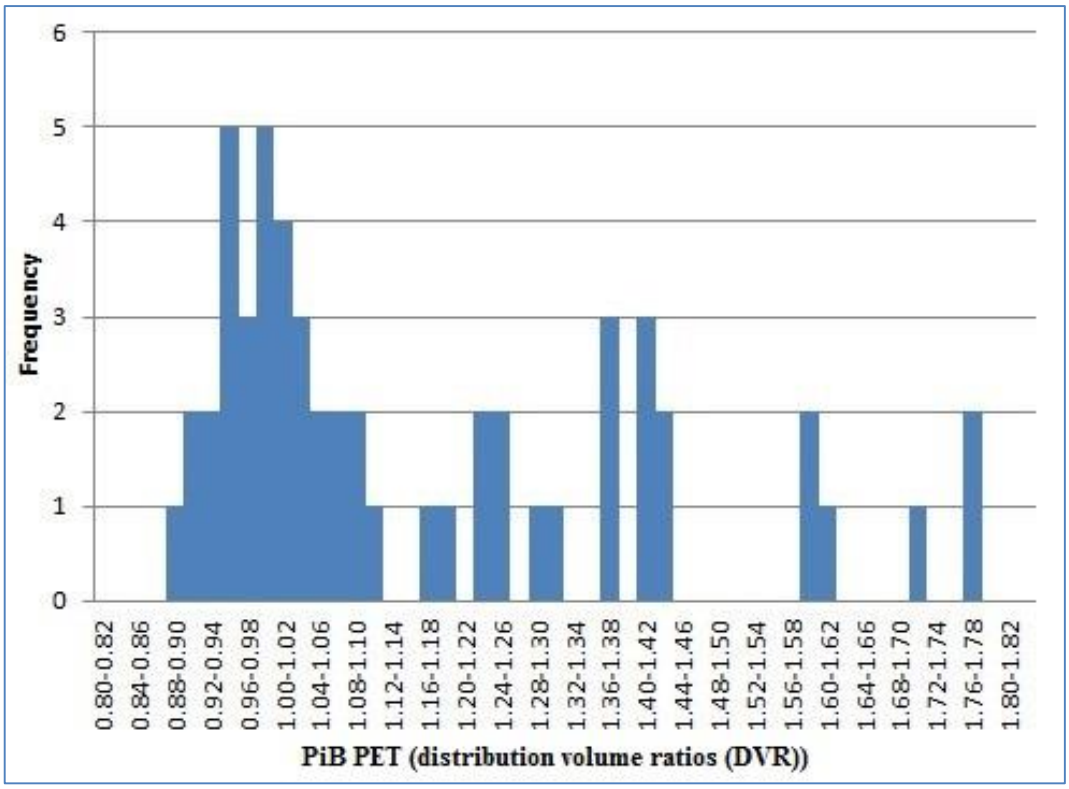

Figure 3-2: Histogram displaying the distribution of PiB PET DVR values across subjects

3.3.2 2DGE gel image pre-processing

In addition to the automatic processes applied by the analysis software a substantial manual review of every spot was completed. 2DGE gel images can be influenced by a number of complex issues including co-migration (2DGE captures large numbers of proteins and so it is likely that some will have similar pI and MW and therefore co-migrate) and spot saturation (highly abundant proteins may stain to saturation resulting in difficulty distinguishing between spots)[191]. Furthermore, heavy tails of abundant protein spots may mask other proteins in the surrounding area and artefacts such as gel cracks and stain binding to non-protein contaminants may challenge the automated spot detection software. Additionally variations in gel casting and polymerisation, buffers and electric field can all contribute to geometrical deformation resulting in difficulty matching spots. Although it is not possible to eliminate all of these issues from an analysis, manual intervention during image preprocessing can help to minimise their influence. Spots were therefore reviewed individually and those that were not well defined, discrete, and present in the

majority of gels were removed. Figure 3-3 displays a comparison between two 2DGE spots; one included and one rejected from further analysis based on a manual review.

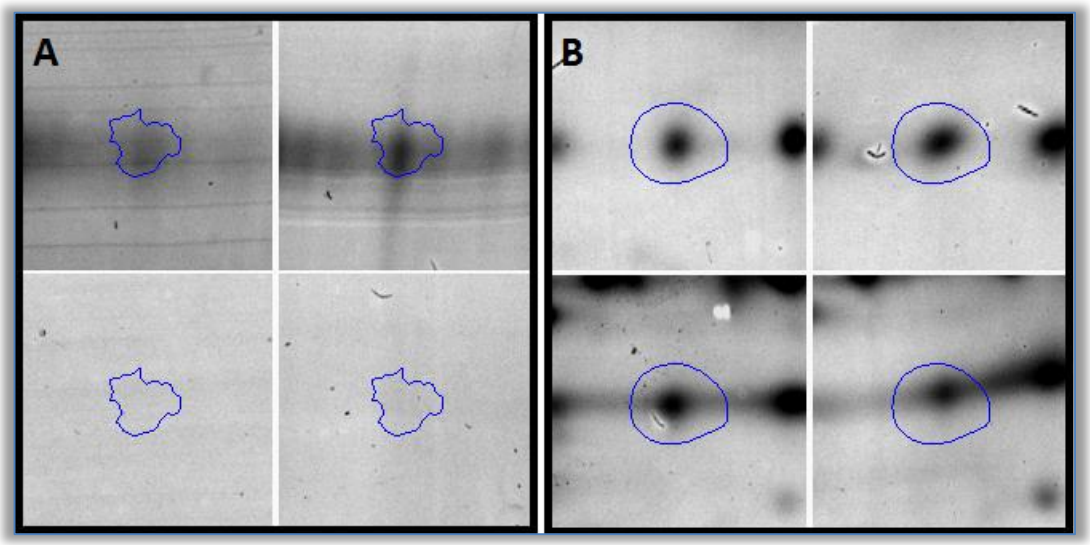

Figure 3-3: A comparison of two 2DGE spots and their presence on four gels. Spot A was not well defined or present in the majority of gels, and so was rejected from further analysis. Spot B was well defined, discrete, and present in the majority of gels, and so was included for further analysis.

1386 spots were selected to be included in statistical analysis; included spots are outlined in Figure 3-4. Volumes for each of these spots were exported for statistical analysis.

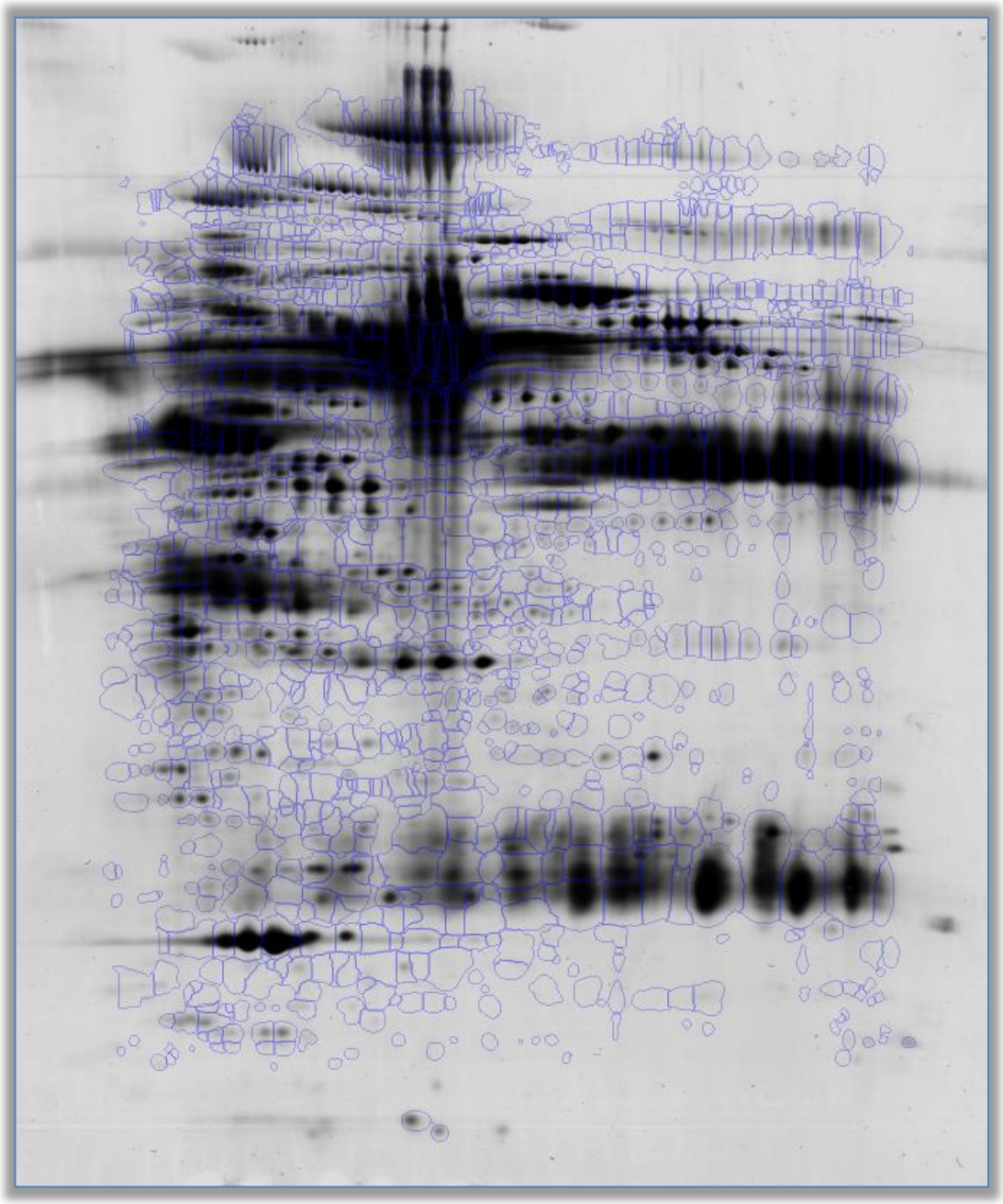

Figure 3-4: 2DGE reference gel highlighting 1386 spots selected for statistical analysis

3.3.3 Coefficient of variation (CV)

For statistical analysis both R version 3.0.0 (R Foundation for Statistical Computing, Austria) and SPSS version 20 software (IBM Statistics Software, USA) were used. As 2DGE had been completed in duplicate for every sample, the coefficient of variation (CV) for every spot volume between duplicate gels was calculated. These CVs were then averaged to obtain an overall experiment within-subject CV of 33.52% (Table 3-3). In addition, to assess whether there was a similar variation

across time points the mean CV per time point was also calculated, these are detailed in Table 3-4 and illustrated in Figure 3-5. The mean CV's at each time point were: baseline = 34.98%; T6 = 33.87%, and T12 = 31.72%.

Table 3-3: Overall experiment mean within subject spot CV

	N (spots)	Minimum	Maximum	Mean	Std. Deviation
CV	4158	11.68	64.41	33.52	7.77

Table 3-4: Mean within subject spot CV's per time point

Time point	N (spots)	Minimum	Maximum	Mean	Std. Deviation
BASELINE	1386	12.80	64.41	34.98	7.83
T6	1386	11.80	62.27	33.87	7.75
T12	1386	11.68	60.47	31.72	7.38

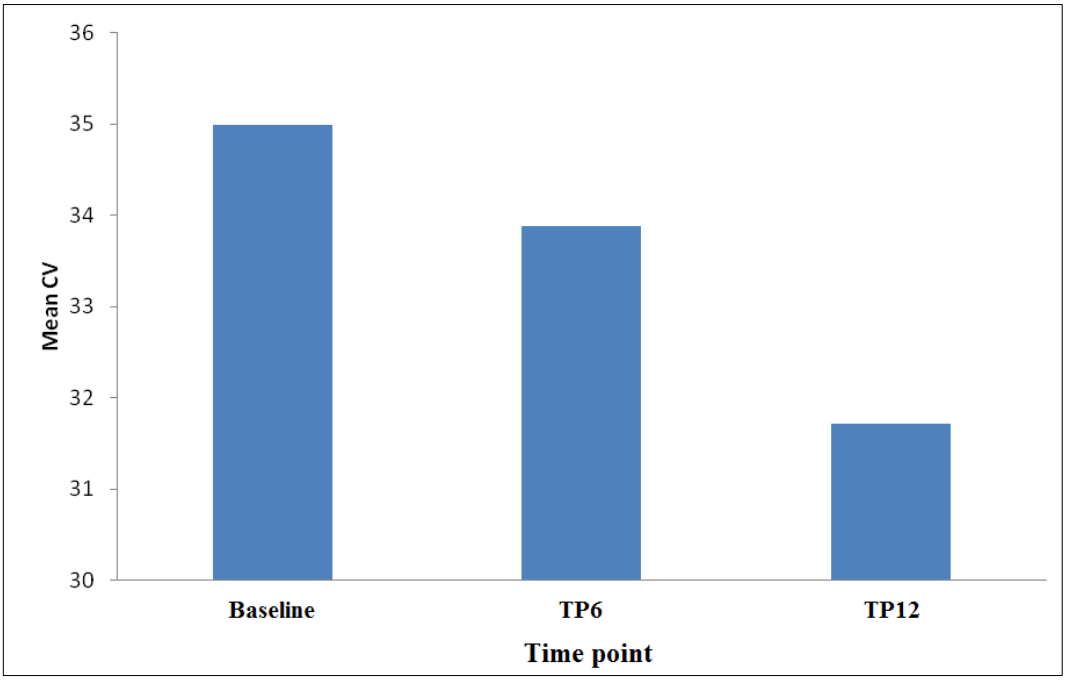

Figure 3-5: Mean within subject CV's per time point

A one-way analysis of variance (ANOVA) was conducted to compare differences between CV's at each time point. This revealed statistically significant differences between mean CV's at each time point ($F(2,4155) = 65.37$, $p<0.001$). Post hoc comparisons using the Bonferroni test indicated that at all three time points the mean CV's were significantly different from each other ($p<0.001$).

As analytical variance normally ranges 16-40% in 2DGE experiments[192-194] a 40% threshold was selected for an acceptable spot CV. Using this threshold of 40%, data from duplicate gels were combined either by averaging the spot volumes (if CV = <40%) or by taking the value closest to the overall spot mean (if CV= >40%) (see Figure 3-6). These values were used for further statistical analysis.

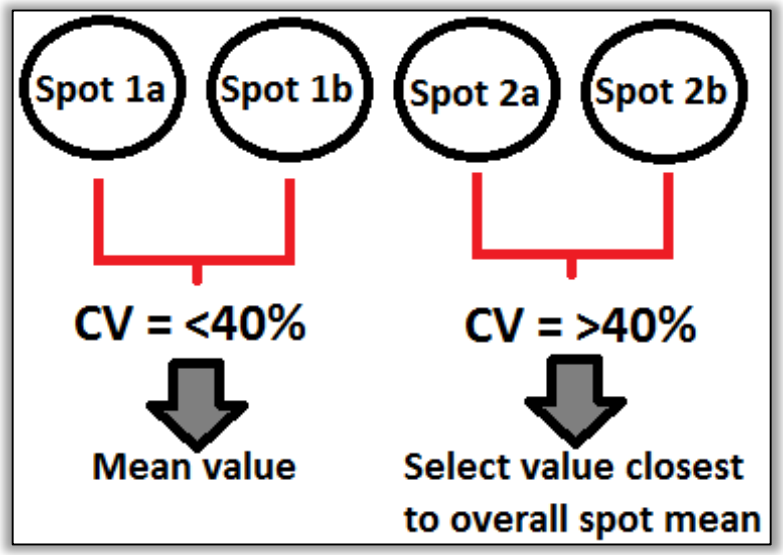

Figure 3-6: Data quality improvement based on the coefficient of variation between duplicate gels

3.3.4 Normality tests

Normality tests were performed to determine the normality of the spot volume distributions. A Kolmogorov-Smirnov test for normality indicated that 34% of the spot distributions were normally distributed ($p<0.05$). Spot data was then logged (base 10) to minimise skewness and non-normal spot volume distributions, and normality tests were repeated. Kolmogorov-Smirnov tests on logged spot data indicated that 80% of the spot distributions were normally distributed ($p<0.05$). Logged data was therefore used for the following statistical analysis.

3.3.5 2DGE analysis of plasma protein spots associated with amyloid load as measured by PiB PET DVR

Partial correlations

Partial correlation was used as a first step to identify spots that have a relationship with amyloid load. Protein spot volumes correlating with ^{11}C-PiB PET DVR at each time point, whilst controlling for age, gender, education (years), body mass index (BMI), cholesterol, and *APOE* ε4 status were identified. Partial correlations at baseline, T6, and T12 revealed 119, 47, and 73 proteins spots, respectively, which significantly correlated with PiB PET DVR 12 years later, 6 years later and concurrently (p<0.05). Significant results are displayed in Table 3-5 for baseline, Table 3-6 for T6, and Table 3-7 for T12. Full results are reported in appendix 1 (baseline) appendix 2 (T6) and appendix 3 (T12).

Table 3-5: Significant baseline partial correlation results for 2DGE spots with PiB PET DVR (p<0.05). Spots ranked in order of significance based on p value.

Spot ID	Correlation coefficient	p-value
X1370	-0.532	0.000
X1310	-0.492	0.000
X1793	-0.484	0.000
X696	0.481	0.001
X749	-0.466	0.001
X1365	-0.451	0.001
X1554	-0.451	0.001
X2279	-0.445	0.002
X1671	-0.427	0.003
X1239	-0.423	0.003
X595	0.419	0.004
X2063	-0.416	0.004
X1258	-0.414	0.004
X632	0.409	0.005
X1295	-0.404	0.005
X529	0.401	0.006
X1331	-0.400	0.006
X1224	-0.399	0.006
X639	0.392	0.007
X716	-0.391	0.007
X758	-0.384	0.009
X1534	-0.383	0.009
X1525	-0.383	0.009
X1056	-0.380	0.009
X1029	0.378	0.010
X2245	0.374	0.011
X938	-0.374	0.011
X393	0.374	0.011
X1260	-0.371	0.012
X1583	-0.369	0.012
X1402	-0.368	0.012
X1432	-0.367	0.013
X1524	-0.365	0.013
X1292	-0.365	0.013
X1400	-0.365	0.013
X697	-0.364	0.014
X1551	0.359	0.015
X1303	-0.359	0.015
X872	0.358	0.015
X825	-0.355	0.016
X1054	-0.353	0.017
X1317	0.352	0.018
X1188	-0.352	0.018
X2026	-0.351	0.018
X1272	-0.351	0.018
X1312	-0.349	0.018
X625	0.349	0.018
X766	0.349	0.019
X1265	-0.348	0.019
X1284	0.348	0.019
X1268	-0.346	0.020
X1314	-0.343	0.021
X1732	0.342	0.021
X1155	-0.342	0.022
X1128	-0.341	0.022
X1297	0.341	0.022
X2048	0.340	0.022
X732	0.340	0.022
X1287	-0.338	0.023
X2143	-0.337	0.024
X1930	0.336	0.024
X1264	-0.336	0.024
X2031	0.335	0.024
X765	0.334	0.025
X1574	-0.333	0.026
X1332	-0.331	0.026
X1283	0.328	0.028

X991	0.328	0.028
X2187	0.328	0.028
X1561	-0.327	0.029
X1357	-0.327	0.029
X2181	-0.326	0.029
X754	-0.326	0.029
X1621	-0.326	0.029
X1313	0.325	0.030
X652	-0.325	0.030
X2105	0.323	0.031
X733	0.322	0.031
X953	0.322	0.031
X1273	0.321	0.032
X740	-0.317	0.035
X1339	-0.316	0.035
X1241	-0.316	0.035
X1237	-0.316	0.035
X1636	-0.316	0.035
X1394	0.313	0.037
X1855	-0.313	0.037
X925	-0.312	0.038
X699	-0.312	0.038
X1792	-0.312	0.038
X1052	-0.311	0.038
X746	-0.311	0.038
X1702	-0.311	0.039
X2182	-0.309	0.040
X1333	0.309	0.040
X1857	-0.308	0.040
X1315	-0.308	0.041
X2103	-0.308	0.041
X1988	0.308	0.041
X624	0.306	0.042
X2020	0.306	0.042
X1730	0.305	0.043
X1361	-0.305	0.043
X1408	-0.304	0.043
X1059	-0.304	0.044
X1110	-0.304	0.044
X1953	0.302	0.045
X653	0.302	0.045
X1410	-0.301	0.046
X680	0.301	0.046
X1508	0.301	0.046
X805	-0.301	0.046
X727	0.300	0.047
X591	0.300	0.047
X1074	-0.299	0.047
X1619	-0.299	0.048
X1966	0.298	0.048
X2157	0.298	0.048
X1189	-0.297	0.049

Table 3-6: Significant T6 partial correlation results for 2DGE spots with PiB PET DVR (p<0.05). Spots ranked in order of significance based on p value

Spot ID	Correlation coefficient	p-value
X558	0.524	0.000
X527	0.494	0.000
X1699	-0.461	0.001
X842	-0.454	0.001
X808	-0.445	0.001
X2063	-0.444	0.001
X1309	-0.422	0.003
X2267	0.383	0.007
X1648	-0.383	0.007
X831	-0.369	0.010
X1054	-0.363	0.012
X2177	0.360	0.012
X1245	-0.360	0.012
X1833	0.356	0.014
X1787	0.353	0.014
X869	-0.351	0.015
X2209	0.348	0.016
X815	0.342	0.018
X875	-0.339	0.019
X2344	-0.335	0.021
X2345	-0.332	0.022
X797	-0.332	0.022
X1770	-0.331	0.023
X1660	-0.330	0.024
X1527	0.327	0.025
X822	-0.324	0.027
X1267	-0.322	0.027
X1941	-0.318	0.029
X1694	-0.314	0.032
X1406	0.314	0.032
X2271	0.312	0.033
X802	-0.312	0.033
X1394	0.311	0.034
X949	0.311	0.034
X1197	-0.311	0.034
X1544	-0.310	0.035
X1917	0.310	0.035
X1334	-0.309	0.035
X1619	-0.306	0.038
X1695	-0.303	0.039
X1409	-0.303	0.039
X1763	-0.302	0.040
X1298	0.300	0.041
X1257	-0.300	0.042
X819	0.298	0.043
X1261	0.298	0.043
X255	0.297	0.044
X1615	0.294	0.046
X1556	-0.294	0.046
X1365	-0.293	0.047
X1015	-0.293	0.047
X791	-0.293	0.047
X1696	0.291	0.049
X1495	-0.290	0.050

Table 3-7: Significant T12 partial correlation results for 2DGE spots with PiB PET DVR (p<0.05). Spots ranked in order of significance based on p value

Spot ID	Correlation coefficient	p-value
X2143	-0.533	0.000
X1309	-0.500	0.000
X630	-0.468	0.000
X635	-0.439	0.001
X1110	0.428	0.002
X598	-0.424	0.002
X1496	0.424	0.002
X966	-0.423	0.002
X1780	0.415	0.002
X899	-0.410	0.003
X381	-0.406	0.003
X1171	-0.398	0.004
X1500	0.392	0.004
X589	-0.391	0.004
X1718	0.390	0.004
X969	-0.389	0.005
X2141	-0.388	0.005
X996	-0.385	0.005
X1549	0.382	0.006
X593	-0.380	0.006
X911	-0.377	0.006
X584	-0.369	0.008
X2177	0.366	0.008
X1015	-0.365	0.009
X596	-0.364	0.009
X1377	0.360	0.010
X1597	0.359	0.010
X1593	0.359	0.010
X1557	0.356	0.011
X386	-0.353	0.011
X641	-0.353	0.011
X642	-0.350	0.012
X1112	0.349	0.012
X1710	-0.342	0.015
X1662	-0.340	0.015
X1303	-0.339	0.015
X587	-0.337	0.016
X685	-0.335	0.017
X629	-0.334	0.017
X272	-0.331	0.019
X1399	0.329	0.019
X2024	-0.329	0.020
X1929	0.328	0.020
X2040	-0.327	0.020
X993	-0.327	0.020
X2235	0.325	0.021
X1129	0.322	0.022
X585	0.321	0.023
X1170	-0.318	0.024
X1580	0.317	0.025
X1738	-0.317	0.025
X705	-0.315	0.026
X1172	-0.312	0.027
X634	-0.311	0.028
X1963	0.310	0.029
X1617	0.309	0.029
X1017	-0.309	0.029
X1299	0.308	0.030
X1078	-0.307	0.031
X1067	-0.303	0.033
X1402	-0.302	0.034
X640	-0.299	0.035
X2214	0.296	0.038
X1966	0.295	0.038
X525	-0.293	0.040
X1762	-0.293	0.040
X971	-0.292	0.041
X905	-0.290	0.042
X1362	0.289	0.043
X906	-0.289	0.043
X1367	0.288	0.044
X1474	0.286	0.045
X669	-0.286	0.045
X1071	0.285	0.046
X654	-0.283	0.047
X281	-0.283	0.048

2DGE protein spots significant in the partial correlation were visually re-assessed to identify those that would be possible to manually 'pick' for later mass spectrometry analysis. Spots that were too small or faint to be accurately located by eye were removed. After these visual inspections the number of spots remaining was: 53 spots for baseline, 6 spots for T6, and 33 spots for T12. These proteins were taken forward for further analysis.

Elastic-net penalised regression model with leave-one-out cross validation

The remaining significant spots were entered into a penalised elastic-net regression model with leave-one-out cross validation. Colinearity is common in 2DGE datasets

perhaps as different forms of the same protein may be present within multiple 2DGE spots. An elastic-net regression model was chosen as it accounts for multi-colinearity between predictors (spots) through encouraging a grouping effect where strongly correlated predictors tend to be in or out of the model together. This type of regression model also performs well when there are a large number of variables, but not a large sample size. For each time point an elastic-net penalised regression model with leave-one-out cross validation was performed on the remaining spots with seven co-variates included; age, gender, BMI, cholesterol, education (years), *APOE* ε4 status, and prediction time (years between plasma sample and PiB PET scan). The elastic-net model with the minimum error was selected as the model of interest.

At baseline the value of lambda which resulted in minimum mean cross validated error was 0.025 (see Figure 3-7). The corresponding regression model included 20 significant protein spots plus two co-variates; age and *APOE* ε4 status. The regression coefficient values for these variables are displayed in Table 3-8.

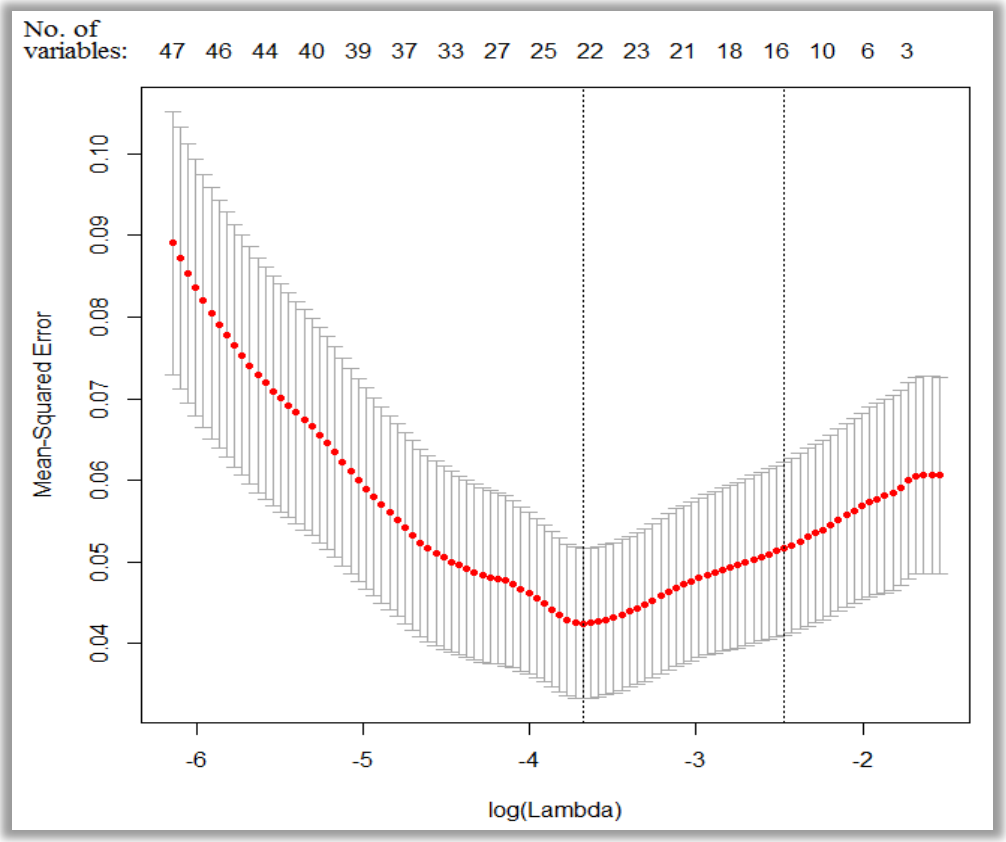

Figure 3-7: Graph illustrating baseline elastic-net leave-one-out cross validation models. The value of lambda that resulted in minimum mean cross validated error = 0.025 (logged value = -3.68)

Table 3-8: Baseline elastic-net regression model coefficient values for variables included in model with minimum error.

Variable	Coefficient
X393	0.073
X529	0.313
X639	0.026
X632	0.101
X740	-0.235
X765	0.007
X1052	-0.065
X1128	-0.048
X1155	-0.132
X1273	0.232
X1287	-0.002
X1400	-0.086
X1702	-0.168
X1730	0.012
X1792	-0.359
X1988	0.005
X2020	0.022
X2026	-0.067
X2048	0.056
X2157	0.231
age	0.007
APOE ε4	0.178
(Intercept)	1.421

At T6 the value of lambda which resulted in minimum mean cross validated error was 0.007 (see Figure 3-8). The corresponding regression model included 5 significant protein spots plus all seven co-variates. The regression coefficient values for these variables are displayed in Table 3-9.

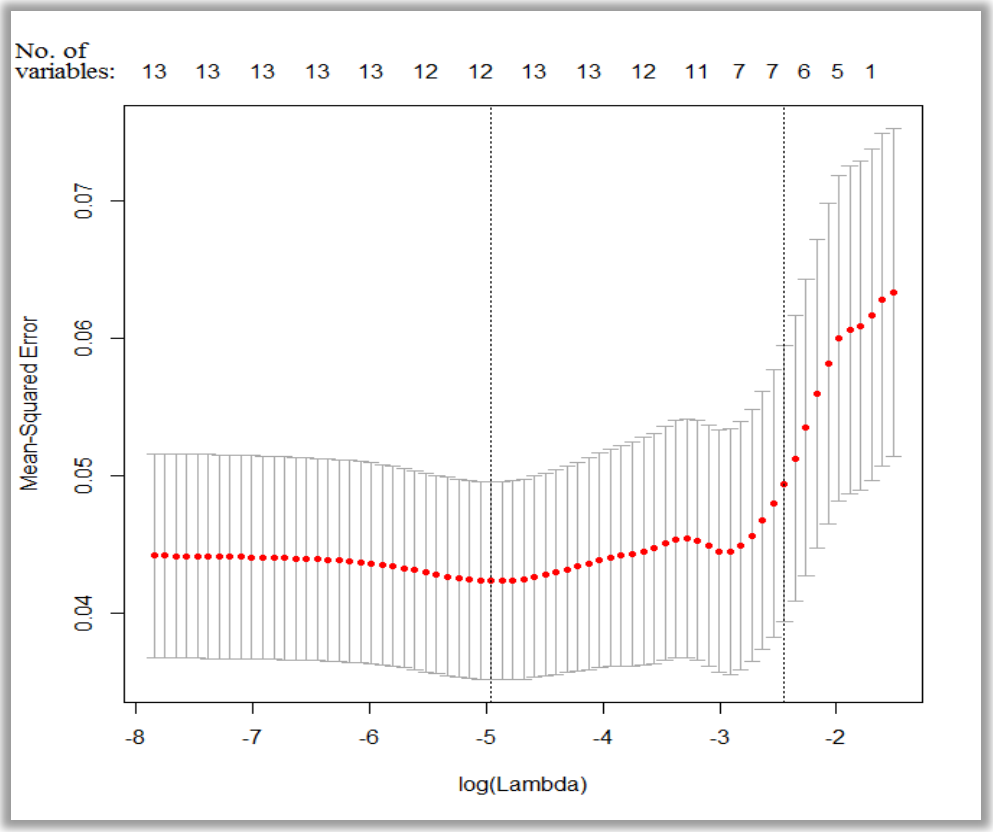

Figure 3-8: Graph illustrating T6 elastic-net leave-one-out cross validation models. The value of lambda that resulted in minimum mean cross validated error = 0.007 (logged value = -4.958)

Table 3-9: T6 elastic-net regression model coefficient values for variables included in model with minimum error.

Variable	Coefficient
X949	0.131
X1309	0.449
X1660	-0.161
X1763	-0.183
X2271	0.371
Gender	-0.086
Age	0.009
Cholesterol	0.001
APOE ε4	0.255
Education	0.013
Prediction years	-0.015
(Intercept)	1.659

At T12 the value of lambda that resulted in minimum mean cross validated error was 0.029 (see Figure 3-9). The corresponding regression model included 14 significant protein spots plus three co-variates; age, *APOE* ε4 status, and prediction years. The regression coefficient values for these variables are displayed in Table 3-10.

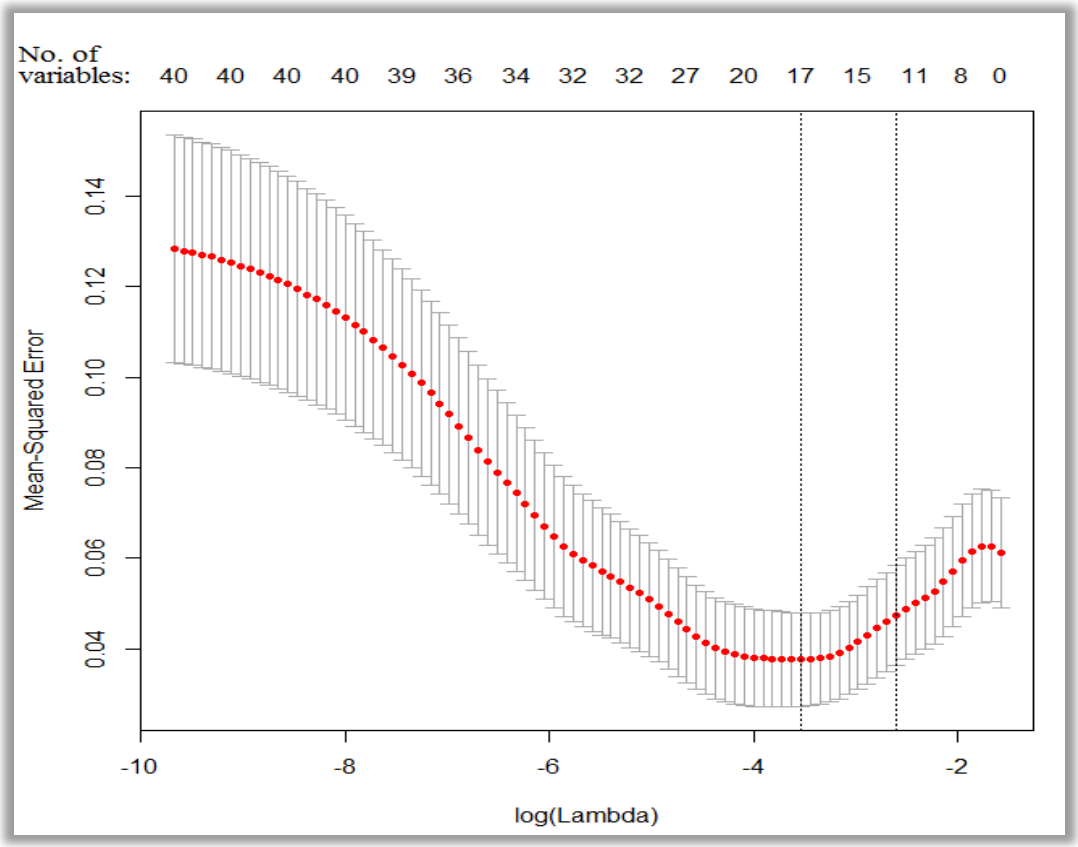

Figure 3-9: Graph illustrating T12 elastic-net leave-one-out cross validation models. The value of lambda that resulted in minimum mean cross validated error = 0.029 (logged value = -3.536)

Table 3-10: T12 elastic-net regression model coefficient values for variables included in model with minimum error.

Variable	Coefficient
X381	-0.051
X386	-0.197
X584	-0.089
X642	-0.103
X1110	0.366
X1172	-0.114
X1170	-0.049
X1303	-0.035
X1309	-0.231
X1377	0.081
X1597	0.291
X1593	0.163
X1710	-0.085
X1762	-0.005
Age	0.004
APOE ε4	0.205
Prediction Years	0.001
(Intercept)	1.396

The proteins included in each elastic-net regression model were selected for identification with mass spectrometry. Figure 3-10, Figure 3-11, and Figure 3-12 show the location of the proteins selected and picked for baseline 1, T6 and T12, respectively.

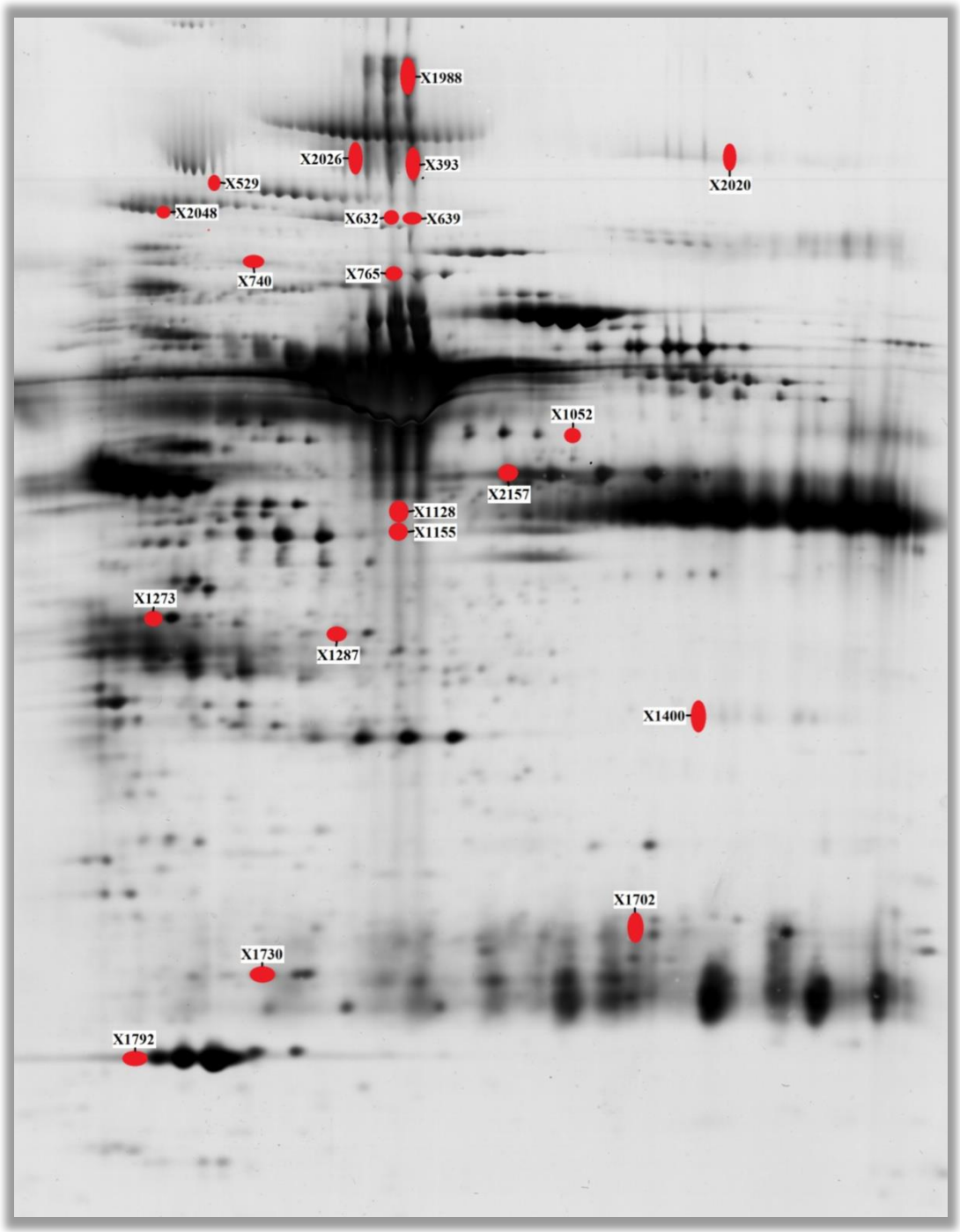

Figure 3-10: Protein spots related to PiB PET DVR selected for mass spectrometry identification at baseline

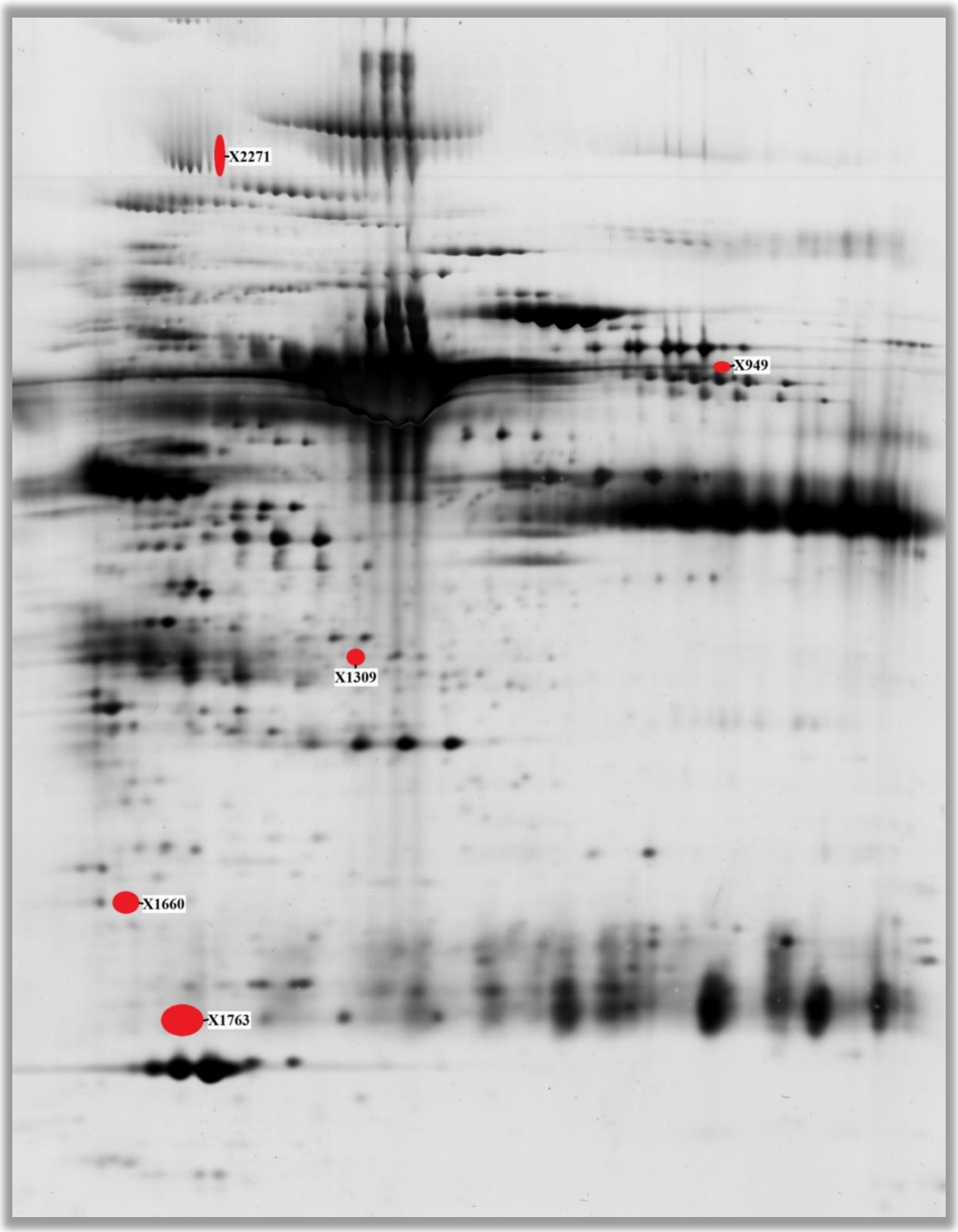

Figure 3-11: Protein spots related to PiB PET DVR selected for mass spectrometry identification at T6

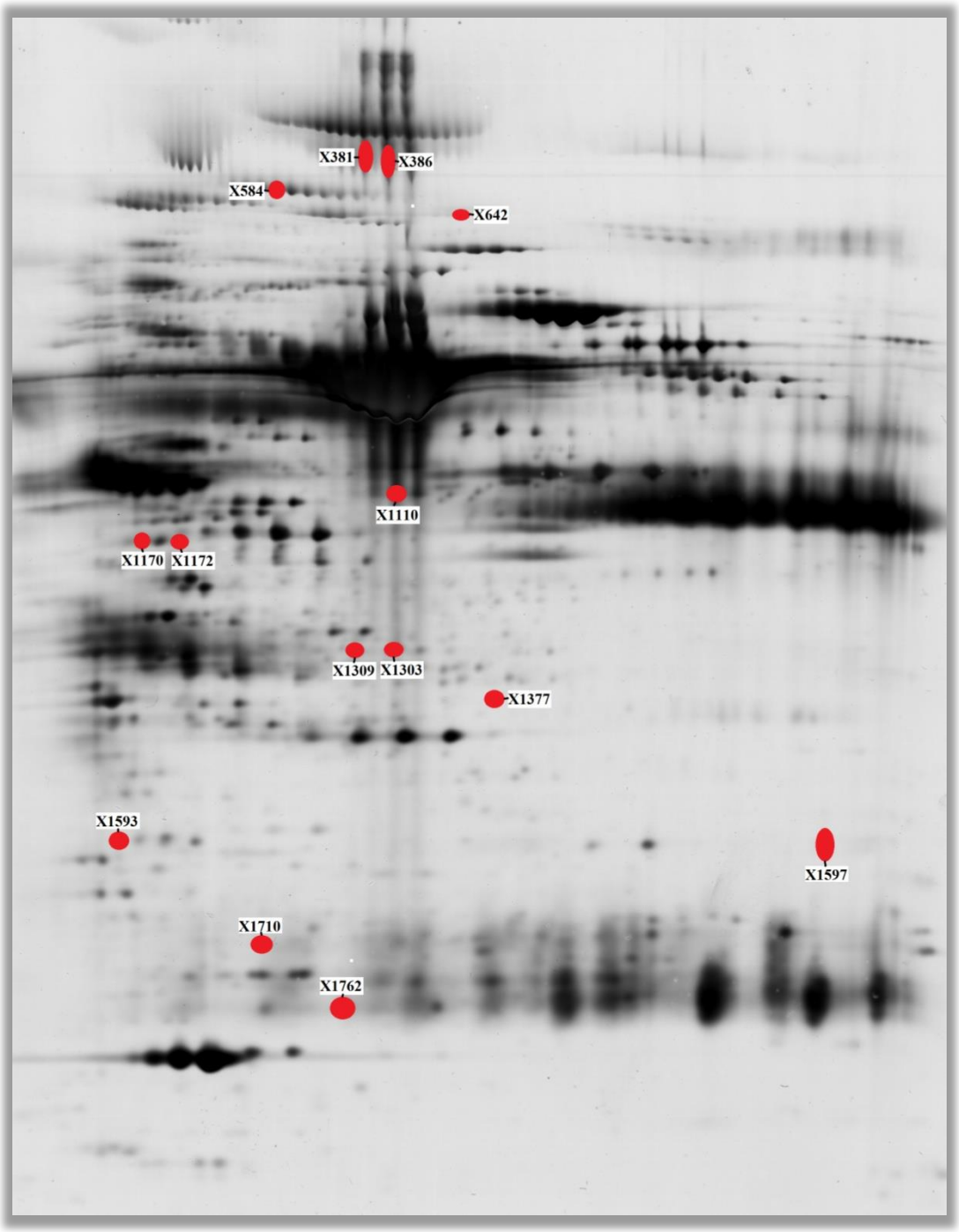

Figure 3-12: Protein spots related to PiB PET DVR selected for mass spectrometry identification at T12

Multiple linear regression

To obtain a measure of how well these protein models can predict PiB PET DVR multiple linear regressions were performed:

At baseline the resulting elastic-net regression model of 20 protein spots and 2 covariates (age and *APOE* ε4 status) were entered into a multiple linear regression

model. Rsquare = 0.828, (F(22,30)=6.575, p<0.001) indicating that this model can explain 83% of the variance in PiB PET DVR levels 12 years later.

At T6 the resulting elastic-net regression model of 5 protein spots and 6 covariates (age, gender, education, *APOE* ε4 status, cholesterol, and prediction years) were entered into a multiple linear regression model. Rsquare = 0.527 (F(12,38)=3.524, p<0.005) indicating that this model can explain 53% of the variance in PiB PET DVR levels 6 years later.

At T12 the resulting elastic-net regression model of 14 protein spots and 3 covariates (age, *APOE* ε4 status, and prediction years) were entered into a multiple linear regression model. Rsquare = 0.898 (F(17,36)=18.728, p<0.001) indicating that this model can explain 90% of the variance in PiB PET DVR levels concurrently.

3.3.6 2DGE analysis of plasma proteins longitudinally associated with brain atrophy

One-way repeated measures ANOVA

Longitudinal volume data was available for 22 sMRI regions. It was important to firstly assess which sMRI regions were significantly changing over time and identify the region most interesting for analysis. One-way repeated measures ANOVAs with Greenhouse-Geisser corrections were conducted for each of the sMRI regions for all 68 subjects to determine whether the regions significantly differed at each time point and so to identify those that significantly changed over time. Parahippocampal gyrus was the only region that did not significantly change over time (p=0.51). The remaining 21 regions were found to significantly change over time (p<0.005) and the results are reported in Table 3-11 below.

Table 3-11: One-way repeated measures ANOVA with a Greenhouse-Geisser correction results for 21 sMRI regions to determine whether volumes significantly changed over time. Post hoc tests using the Bonferonni correction reveal which time points significantly differ.

sMRI region	F value	Degrees of freedom	P value	Significant post hoc comparisons ($p<0.05$, Bonferonni)
White Matter	58.934	1.66,69.78	0.001	BASELINE-T6 ($p<0.001$), T6-T12 ($p<0.001$)
Grey Matter	131.726	1.47,61.61	0.001	BASELINE-T6 ($p<0.001$), BASELINE-T12 ($p<0.001$), T6-T12 ($p<0.001$)
Ventricles	148.477	1.25,52.34	0.001	BASELINE-T6 ($p<0.001$), BASELINE-T12 ($p<0.001$), T6-T12 ($p<0.001$)
Temporal White Matter	83.617	2,84	0.001	BASELINE-T6 ($p<0.001$), BASELINE-T12 ($p<0.001$), T6-T12 ($p<0.001$)
Frontal Grey Matter	96.982	1.55,64.98	0.001	BASELINE-T6 ($p<0.001$), BASELINE-T12 ($p<0.001$), T6-T12 ($p<0.001$)
Temporal Grey Matter	91.206	1.59,67.10	0.001	BASELINE-T6 ($p<0.001$), BASELINE-T12 ($p<0.001$), T6-T12 ($p<0.001$)
Medial Frontal Gyrus	47.953	2,84	0.001	BASELINE-T12 ($p<0.001$), T6-T12 ($p<0.001$)

Orbito Frontal Gyrus	14.002	2,84	0.001	BASELINE-T12 (p<0.001), T6-T12 (p<0.001)
Superior Parietal Lobule	93.355	1.49,62.67	0.001	BASELINE-T6 (p<0.01), BASELINE-T12 (p<0.001), T6-T12 (p<0.001)
Superior Temporal Gyrus	78.622	2,84	0.001	BASELINE-T6 (p<0.01), BASELINE-T12 (p<0.001), T6-T12 (p<0.001)
Middle Temporal Gyrus	73.345	1.68,70.53	0.001	BASELINE-T6 (p<0.001), BASELINE-T12 (p<0.001), T6-T12 (p<0.001)
Hippocampus	7.539	2,84	0.001	BASELINE-T6 (p<0.05), BASELINE-T12 (p<0.01)
Entorhinal Cortex	4.515	1.72,72.13	0.05	BASELINE-T6 (p<0.05)
Inferior Occipital Gyrus	6.653	1.60,67.21	0.01	BASELINE- T6 (p<0.05), BASELINE-T12 (p<0.01)
Cingulate Gyrus	93.053	1.54,64.53	0.001	BASELINE-T6 (p<0.001), BASELINE-T12 (p<0.001), T6-T12 (p<0.001)
Insula	36.766	2,84	0.001	BASELINE-T12 (p<0.001), T6-T12 (p<0.001)
Wholebrain	171.126	1.63,68.53	0.001	BASELINE-T6 (p<0.001), BASELINE-T12 (p<0.001), T6-T12 (p<0.01)

Superior Frontal Gyrus	25.360	2,84	0.001	BASELINE-T12 (p<0.001), T6-T12 (p<0.001)
Middle Frontal Gyrus	70.146	1.65,69.29	0.001	BASELINE-T6 (p<0.001), BASELINE-T12 (p<0.001), T6-T12 (p<0.001)
Superior Occipital Gyrus	23.450	1.66,69.66	0.001	BASELINE-T12 (p<0.001), T6-T12 (p<0.001)
Middle Occipital Gyrus	9.219	1.67,69.96	0.01	BASELINE-T12 (p<0.01), T6-T12 (p<0.05)

Assessing direction and linearity of change

For each region found to significantly change over time, the mean volume at each time point was plotted on a line graph to visually assess direction and linearity of change. This assessment was especially important for smaller regions of interest (ROIs) where volume identification is more difficult and susceptible to measurement error. Five regions had a non-linear change over time; white matter (Figure 3-13), temporal white matter (Figure 3-14), orbito frontal gyrus (Figure 3-15), entorhinal cortex (Figure 3-16), and insula (Figure 3-17). The remaining 16 regions had a linear change over time; grey matter (Figure 3-18), ventricles (Figure 3-19), frontal grey matter (Figure 3-20), temporal grey matter (Figure 3-21), medial frontal gyrus (Figure 3-22), superior parietal lobule (Figure 3-23), superior temporal gyrus (Figure 3-24), middle temporal gyrus (Figure 3-24), hippocampus (Figure 3-26), inferior occipital gyrus (Figure 3-27), cingulate gyrus (Figure 3-28), wholebrain (Figure 3-29), superior frontal gyrus (Figure 3-30), middle frontal gyrus (Figure 3-31), superior occipital gyrus (Figure 3-32), and middle occipital gyrus (Figure 3-33).

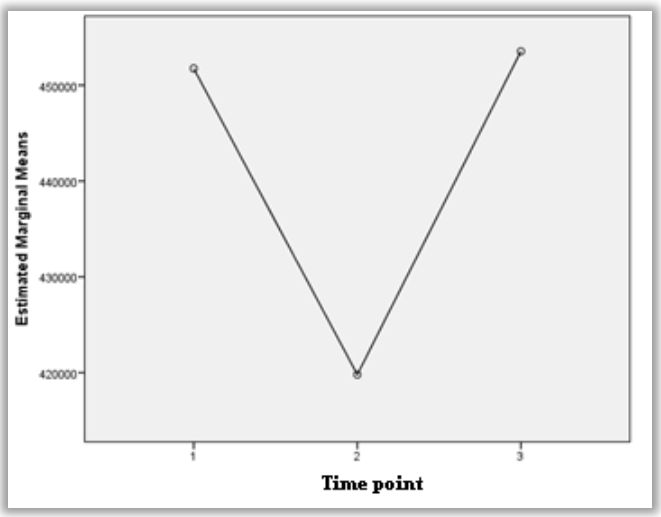

Figure 3-13: White matter mean volumes at each time point (1=baseline, 2=T6, 3=T12)

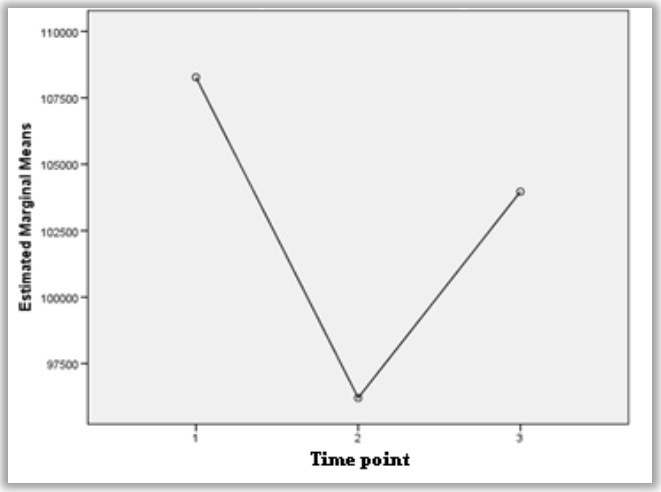

Figure 3-14: Temporal white matter mean volumes at each time point (1=baseline, 2=T6, 3=T12)

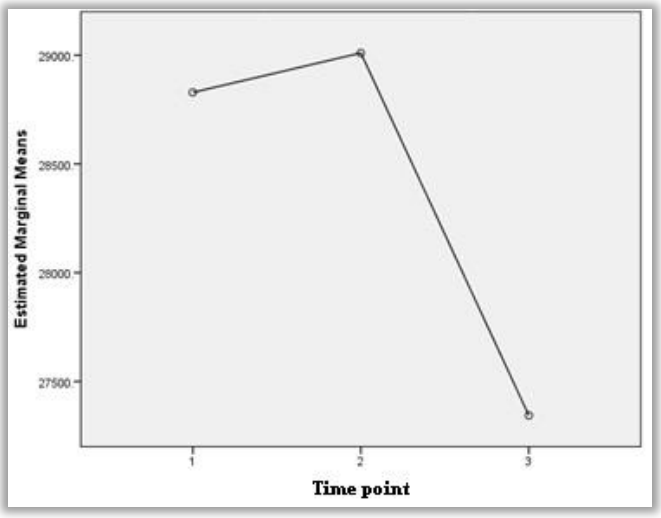

Figure 3-15: Orbito frontal gyrus mean volumes at each time point (1=baseline, 2=T6, 3=T12)

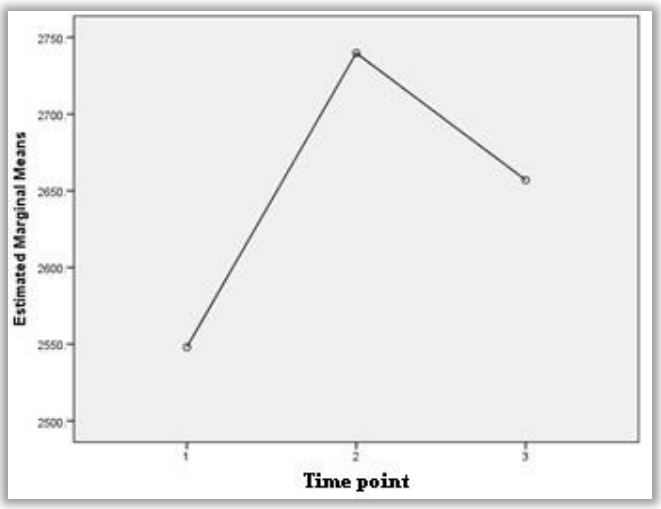

Figure 3-16: Entorhinal cortex mean volumes at each time point (1=baseline, 2=T6, 3=T12)

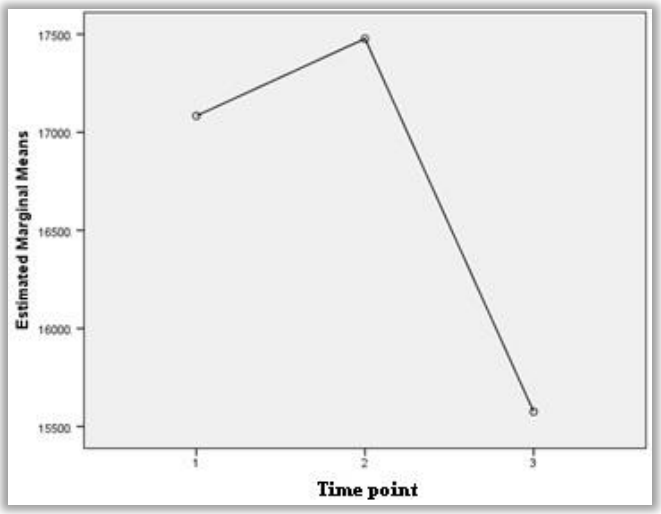

Figure 3-17: Insula mean volumes at each time point (1=baseline, 2=T6, 3=T12)

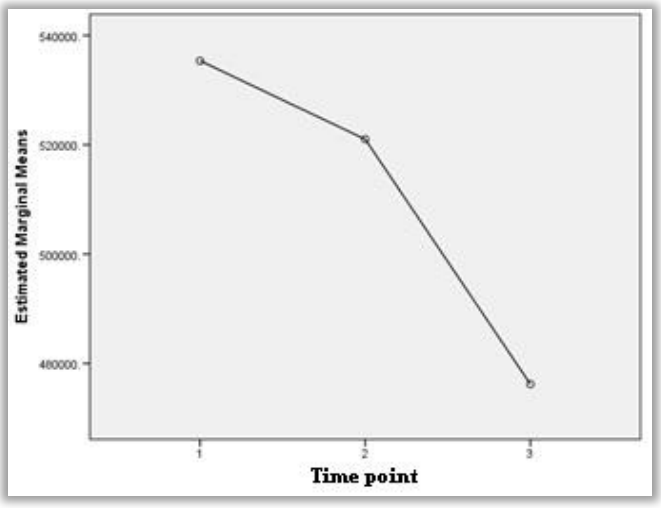

Figure 3-18: Grey matter mean volumes at each time point (1=baseline, 2=T6, 3=T12)

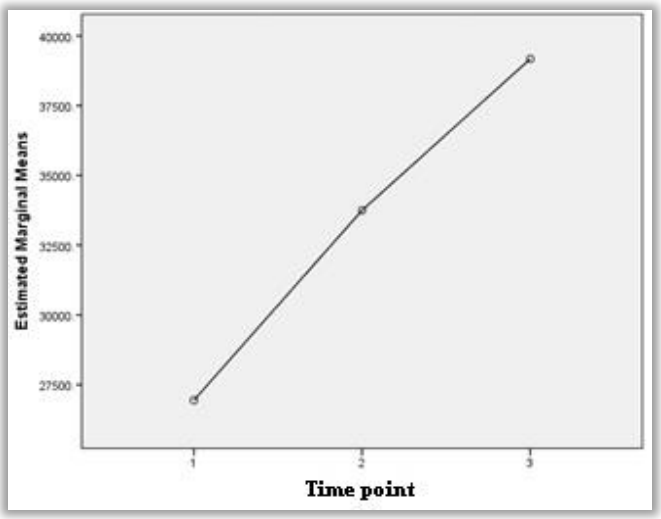

Figure 3-19: Ventricular mean volumes at each time point (1=baseline, 2=T6, 3=T12)

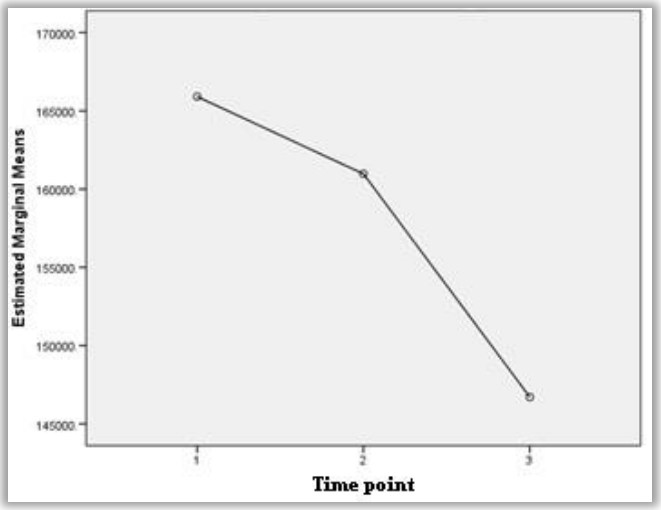

Figure 3-20: Frontal grey matter mean volumes at each time point (1=baseline, 2=T6, 3=T12)

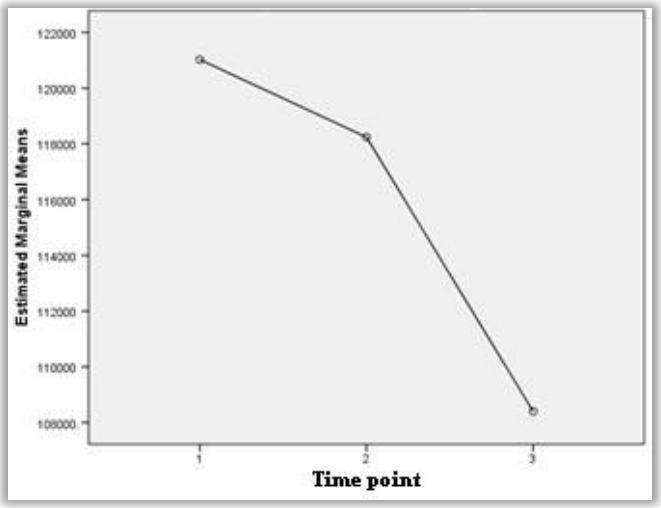

Figure 3-21: Temporal grey matter mean volumes at each time point (1=baseline, 2=T6, 3=T12)

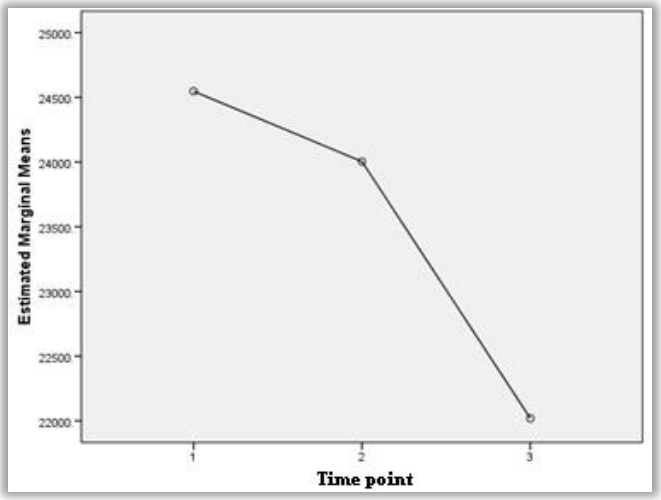

Figure 3-22: Medial frontal gyrus mean volumes at each time point (1=baseline, 2=T6, 3=T12)

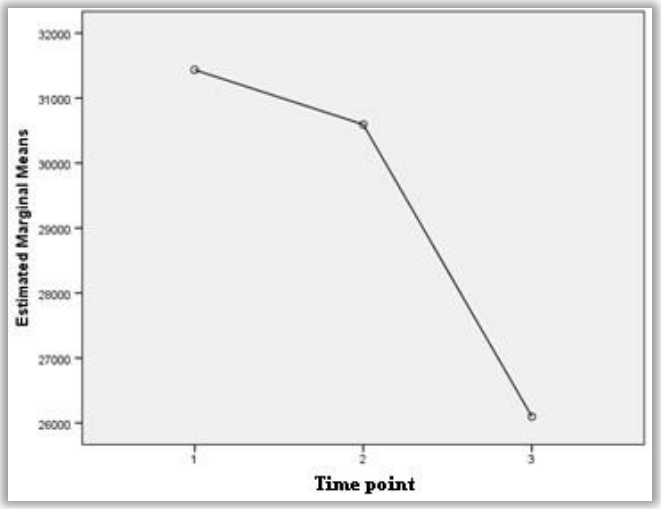

Figure 3-23: Superior parietal lobule mean volumes at each time point (1=baseline, 2=T6, 3=T12)

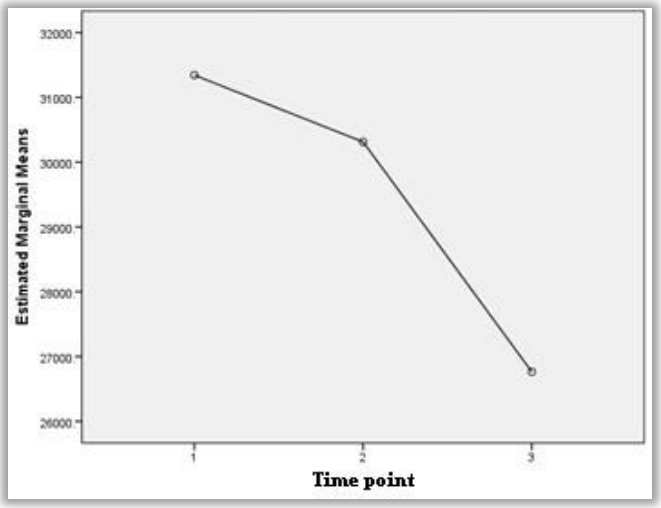

Figure 3-24: Superior temporal gyrus mean volumes at each time point (1=baseline, 2=T6, 3=T12)

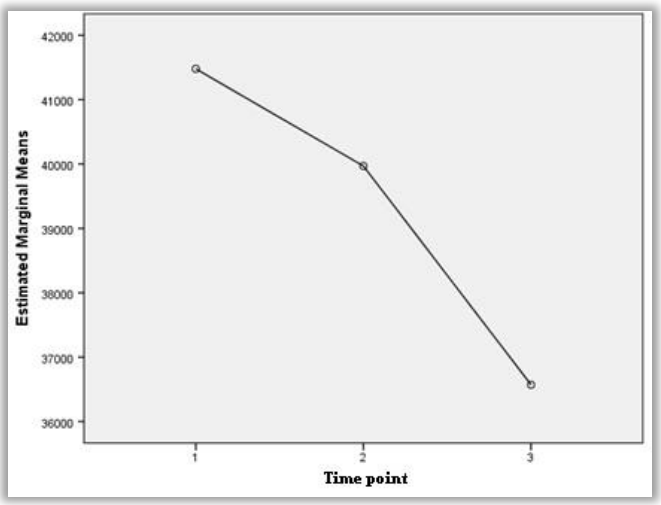

Figure 3-25: Middle temporal gyrus mean volumes at each time point (1=baseline, 2=T6, 3=T12)

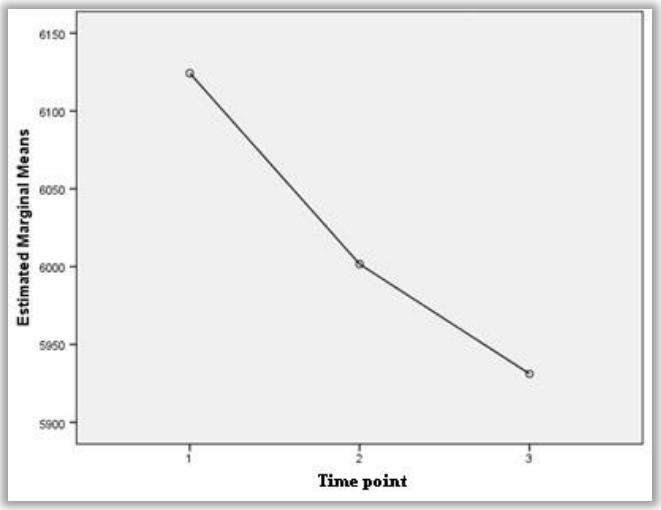

Figure 3-26: Hippocampus mean volumes at each time point (1=baseline, 2=T6, 3=T12)

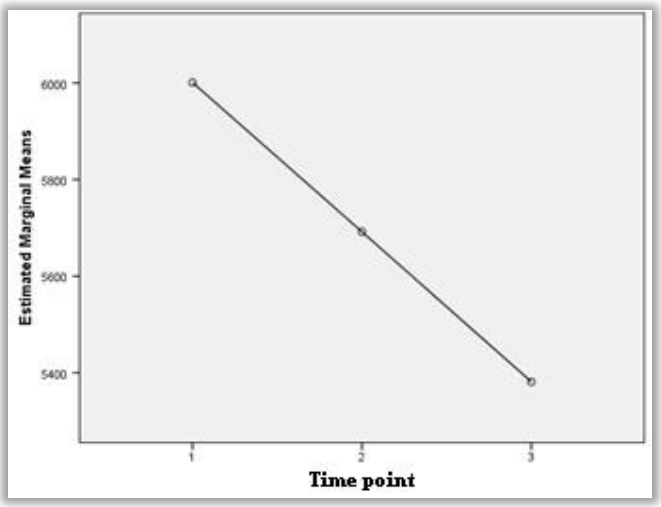

Figure 3-27: Inferior occipital gyrus mean volumes at each time point (1=baseline, 2=T6, 3=T12)

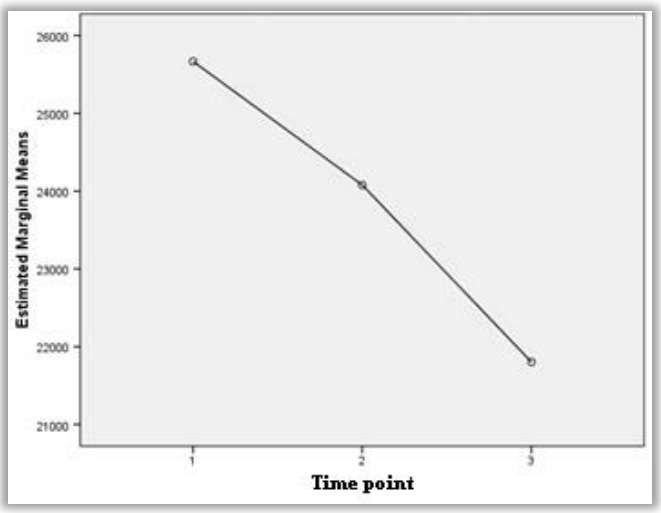

Figure 3-28: Cingulate gyrus mean volumes at each time point (1=baseline, 2=T6, 3=T12)

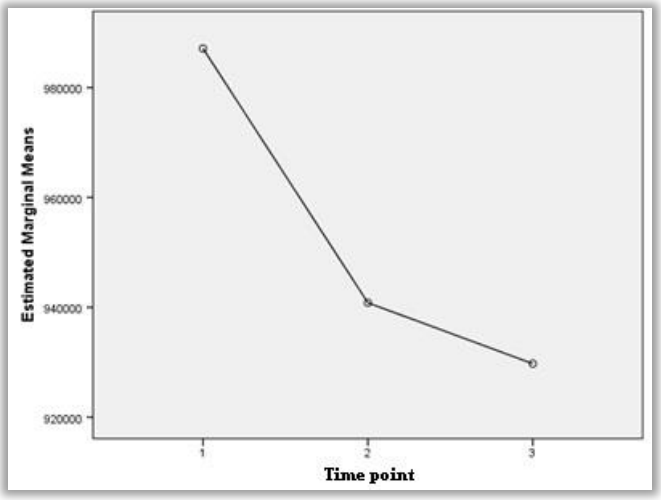

Figure 3-29: Wholebrain mean volumes at each time point (1=baseline, 2=T6, 3=T12)

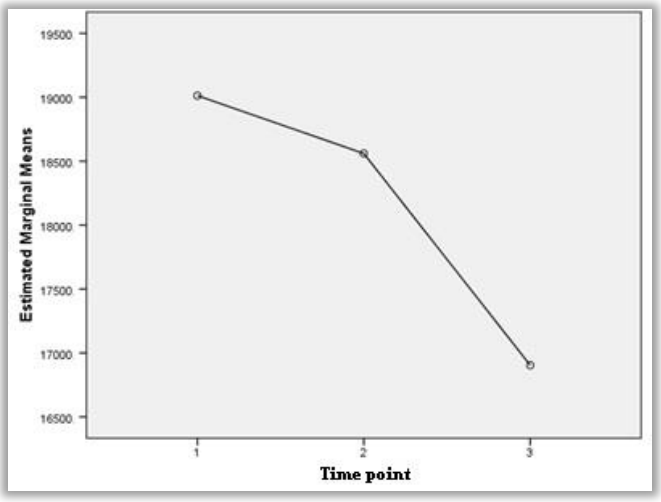

Figure 3-30: Superior frontal gyrus mean volumes at each time point (1=baseline, 2=T6, 3=T12)

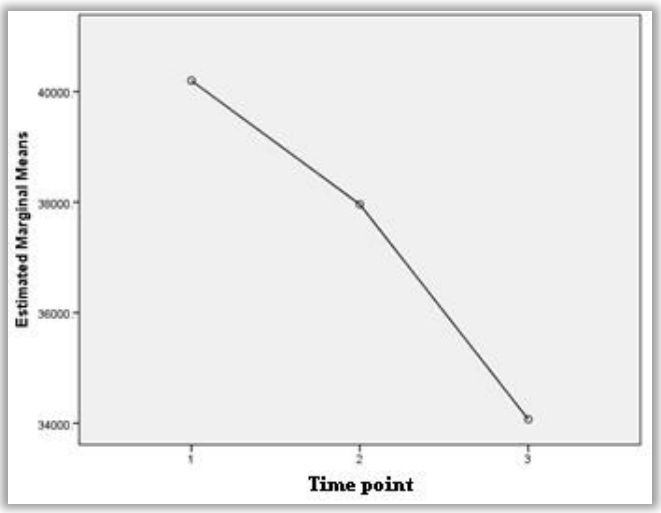

Figure 3-31: Middle frontal gyrus mean volumes at each time point (1=baseline, 2=T6, 3=T12)

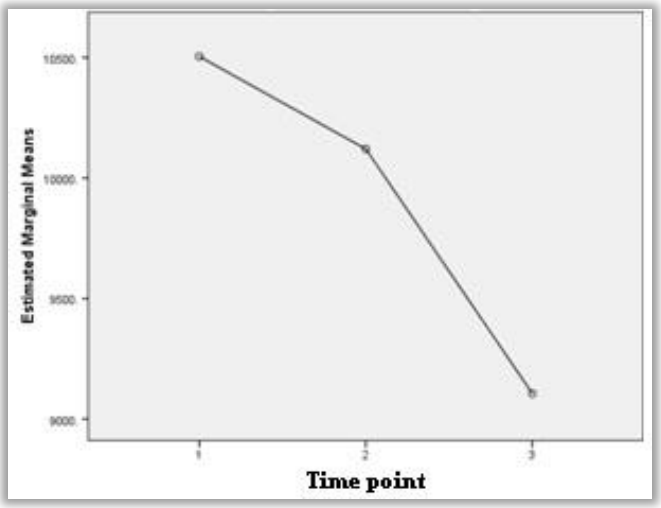

Figure 3-32: Superior occipital gyrus mean volumes at each time point (1=baseline, 2=T6, 3=T12)

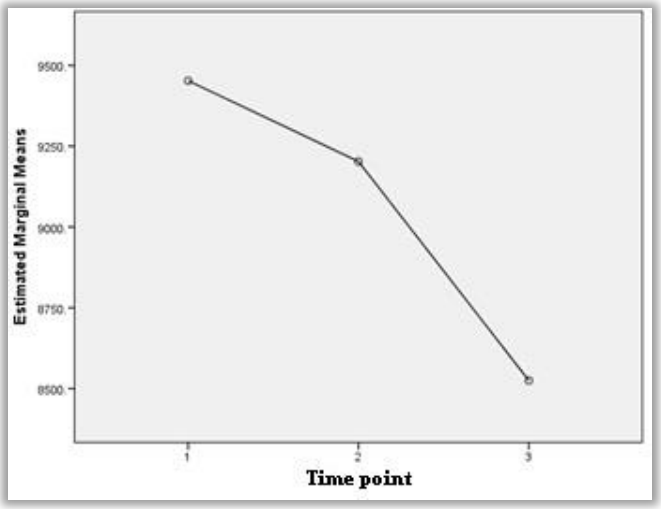

Figure 3-33: Middle occipital gyrus mean volumes at each time point (1=baseline, 2=T6, 3=T12)

Percentage change over time of sMRI brain regions

For the 16 regions known to significantly change over time, percentage change was calculated and the regions were ranked from largest to smallest change (Table 3-12). Ventricles showed the biggest percentage change over time (mean per year = 4.72%), which was also considered a biologically significant change ([195]see discussion for more detail) and therefore this region was selected as the ROI for subsequent sMRI analyses.

Table 3-12: Percentage change over time (per year) for sMRI regions. sMRI regions ranked from largest to smallest percentage change

sMRI region	Mean percentage change over time (% per year)
Ventricles	4.72
Superior parietal lobule	1.61
Cingulate gyrus	1.41
Middle frontal gyrus	1.41
Superior temporal gyrus	1.33
Superior occipital gyrus	1.09
Middle temporal gyrus	1.08
Frontal grey matter	1.07
Grey matter	1.03
Superior frontal gyrus	1.00
Temporal grey matter	0.95
Medial frontal gyrus	0.93
Middle occipital gyrus	0.87
Inferior occipital gyrus	0.80
Wholebrain	0.54
Hippocampus	0.25

Longitudinal analysis: Mixed-effects regression model

Mixed-effect regression models (MRM) enable longitudinal slope comparisons of observations (spot and brain volumes) per individual subject, and then extend these comparisons to the whole sample population whilst considering covariates. Here a

longitudinal slope comparison between protein spot volume and ventricular expansion was conducted per spot (1386) using MRMs with age, gender, education, BMI, cholesterol and *APOE* ε4 status as covariates. MRMs for 35 protein spots reported a significant longitudinal relationship with ventricular expansion. These significant results are reported in Table 3-13 below, for full results see appendix 4.

Table 3-13: Mixed-effects regression model results for the 35 protein spots significantly longitudinally related to ventricular expansion.

Spot ID	Coefficient	*p* value
X1595	-5622.09	0.000543
X1948	-10591.9	0.001269
X1406	-6316.04	0.003753
X767	-4875.01	0.004717
X1068	6049.642	0.00568
X1586	-4200.86	0.006049
X1643	5407.359	0.009337
X1470	-4813.45	0.015904
X1351	4521.493	0.021022
X1412	-3934.76	0.021512
X1590	-3594.51	0.025876
X865	-5258.35	0.025906
X2174	4028.063	0.026012
X988	-4212.2	0.026781
X471	4921.971	0.027109
X2292	4607.122	0.028906
X1435	-3311.15	0.032718
X1837	4719.904	0.033362
X1495	-4054.4	0.033829
X2157	7679.915	0.034074
X1297	5368.935	0.036631
X1284	3836.693	0.038436
X1165	5265.663	0.041349
X933	-4304.7	0.041744
X1624	4594.943	0.044159
X1694	-3550.88	0.045329
X432	4430.796	0.045723
X1550	-6216.19	0.046278
X1689	-3310.46	0.046992
X1050	6968.624	0.047168
X1156	4743.363	0.047843

X1085	7165.327	0.04795
X1501	-3377.37	0.048327

X594	-3201.58	0.049544
X1022	5436.878	0.049806

The 35 proteins with a significant longitudinal relationship with ventricular expansion were then visually inspected to determine whether they could be accurately picked (accurately locate by eye) and identified with mass spectrometry. Based on the visual inspection 22 spots were discarded and 13 were taken forward for identification (Figure 3-34).

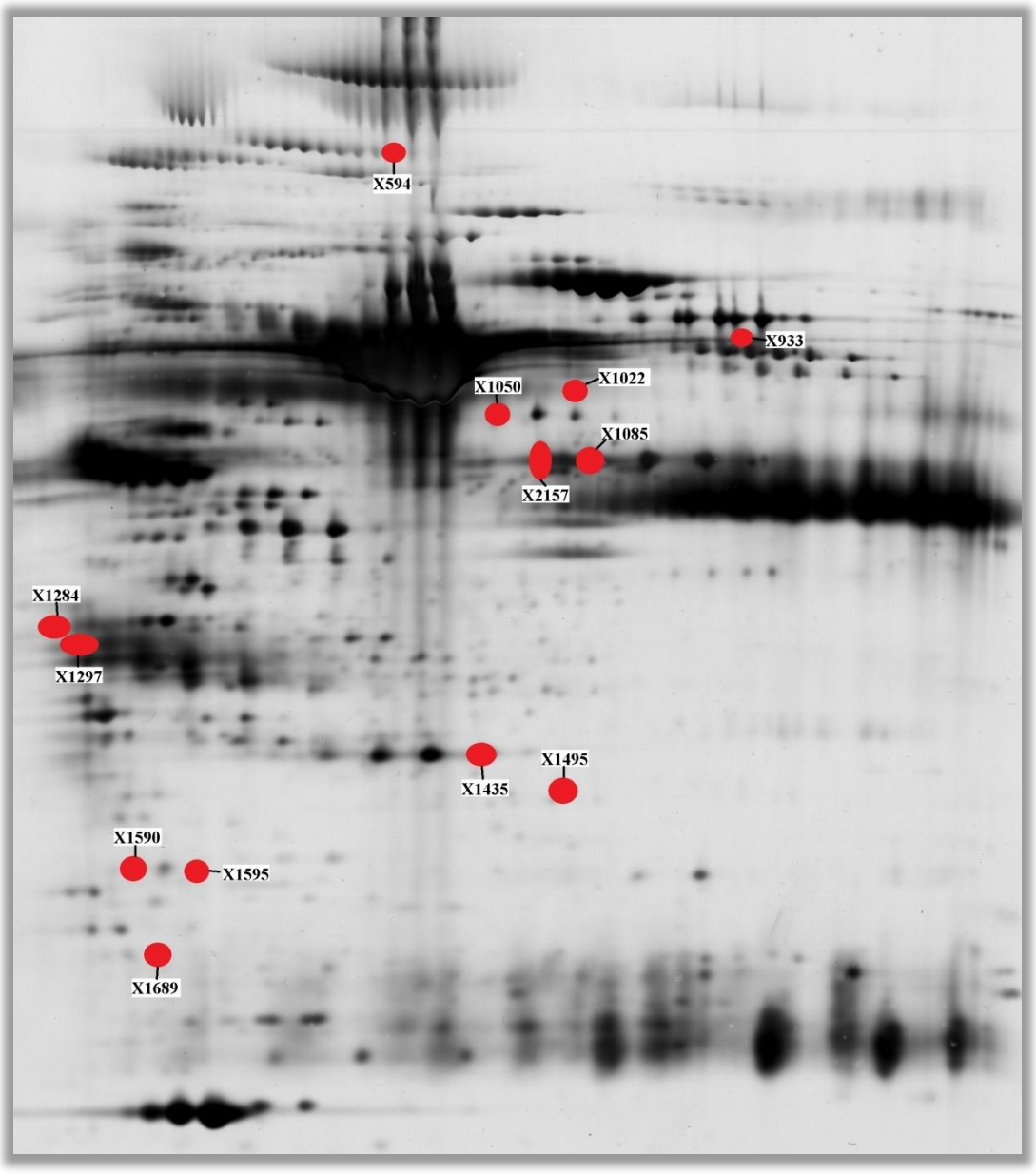

Figure 3-34: 13 protein spots significantly related to ventricular expansion selected for identification with mass spectrometry

3.3.7 2DGE analysis of plasma proteins longitudinally associated with cognitive decline

One-way repeated measures ANOVA

Longitudinal cognitive data was available for 12 cognitive measurements. To identify which measurements significantly and linearly changed over time one-way repeated measures ANOVAs with a Greenhouse-Geisser correction were conducted for each of the measurements for all 68 subjects to determine whether the measurements significantly differed at each time point. 10 cognitive measures did not significantly change over time ($p<0.05$). Two remaining cognitive measures were found to significantly change over time and the results are reported in Table 3-14 below.

Table 3-14: One-way repeated measures ANOVA with a Greenhouse-Geisser correction results for PMA vocabulary and Trails B test. Post hoc tests using the Bonferonni correction reveal which time points significantly differ

Cognitive measure	F value	Degrees of freedom	P value	Significant post hoc comparisons ($p<0.05$, Bonferonni)
PMA vocabulary	3.889	2,122	0.023	
Trails B	10.413	2,120	0.001	BASELINE-T12 ($p<0.001$), T6-T12 ($p<0.01$)

Assessing direction and linearity of change

For the two measures found to significantly change over time the mean cognitive score at each time point was plotted on a line graph to visually assess direction and linearity of change. This assessment was important for cognitive measurements as practice effects may influence results. PMA vocabulary test had a non-linear change over time (Figure 3-35). Trails B had a linear change over time (Figure 3-36). Although all subjects remained cognitive healthy throughout the study, many subjects did change in their Trails B age appropriate percentile membership[196] in a negative direction, supporting significant cognitive decline over time (see discussion

for more detail). Therefore for the combination of these reasons Trails B was selected as the cognitive measure of interest for subsequent analyses.

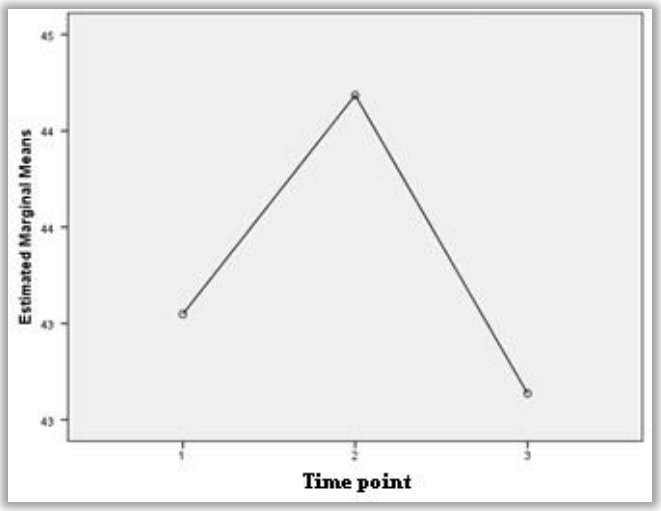

Figure 3-35: PMA vocabulary mean test scores at each time point (1=baseline, 2=T6, 3=T12)

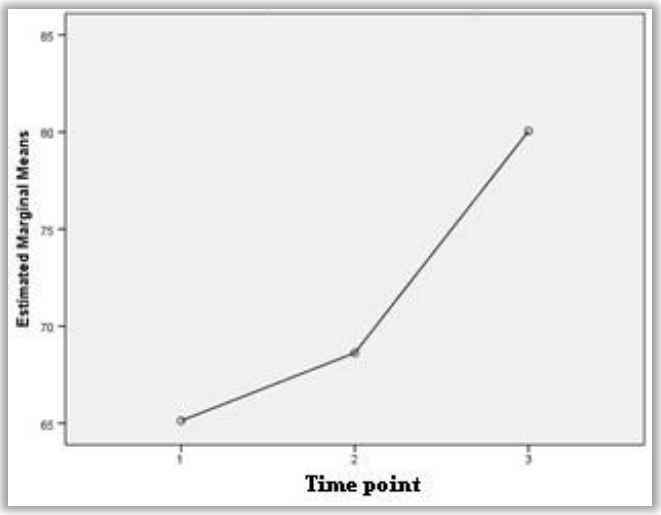

Figure 3-36: Trails B mean score at each time point (1=baseline, 2=T6, 3=T12)

Longitudinal analysis: Mixed-effects regression model

A longitudinal slope comparison between protein spot volume and Trails B score was conducted per spot (total number of spots = 1386) using mixed-effect regression models with age, gender, education, BMI, cholesterol and *APOE* ε4 status as covariates. Mixed-effects regression models for 89 protein spots reported a significant longitudinal relationship with Trails B decline. These significant results are reported in Table 3-15 below, for full results see appendix 5.

Table 3-15: Mixed-effects regression model results for the 89 protein spots significantly longitudinally related to Trails B.

Spot ID	Coefficient	P-value
X779	-38.8492329	0.000129
X1138	-22.6147243	0.001265
X2187	44.18654861	0.0014
X767	-25.8127413	0.001442
X1543	-24.764491	0.002762
X849	-21.3638027	0.00312
X1307	39.64948297	0.003603
X1302	35.67988648	0.004902
X1644	-25.9229164	0.005499
X2184	30.82080343	0.005551
X1656	-23.4113819	0.005726
X1492	-13.7809576	0.006758
X1368	-16.3115874	0.007011
X1228	-15.2270665	0.007089
X1758	34.06306507	0.00758
X1595	-19.2328974	0.008156
X2256	26.91087468	0.008471
X324	21.46611472	0.010289
X865	-29.0653696	0.011975
X1639	-19.9488006	0.012429
X2188	33.83091186	0.01316
X1538	-26.5877435	0.013985
X2142	30.02389939	0.014312
X2111	32.17498689	0.014767
X1879	21.76259571	0.015948
X688	-22.5864682	0.016207
X1095	-25.6577157	0.01682
X1401	-20.7567029	0.016832
X1134	29.60979672	0.01701
X2232	19.88615869	0.017103
X1037	30.89805589	0.017657
X1036	10.48178108	0.017812
X2031	23.28869105	0.017885
X782	-16.1362958	0.01847
X2091	15.10258622	0.018686
X1694	-19.6434596	0.019307
X682	21.61107032	0.020827

X1427	-27.5135054	0.022179
X1755	32.18365359	0.023301
X1297	25.36407848	0.024246
X1359	-16.9147605	0.024872
X1693	-25.2178795	0.024905
X1057	-17.2591557	0.025338
X887	-16.0460346	0.0256
X2274	-16.9932297	0.026973
X1590	-15.6650304	0.027109
X1296	30.42412166	0.027331
X763	-20.2976746	0.027794
X2341	16.15078578	0.028154
X1495	-19.4584054	0.029494
X1347	-22.9767284	0.029749
X1511	-22.0383665	0.029792
X1499	-14.3737404	0.030476
X804	-19.2768316	0.030818
X1431	-16.0895998	0.031042
X1743	16.75944942	0.031338
X661	19.48381126	0.031421

X1785	-20.2840052	0.032761
X1990	16.74274954	0.032982
X1283	25.48531274	0.034231
X1640	-17.5831067	0.034311
X1671	-18.6216857	0.035148
X1463	-17.197246	0.036268
X1196	-12.9554852	0.037104
X1649	-19.6685034	0.037119
X663	15.35375583	0.038327
X758	-20.7793545	0.039644
X1732	27.0881448	0.040093
X1163	-23.3349569	0.040317
X1631	-24.5003442	0.041297
X1153	-22.6541249	0.042028
X931	12.40310856	0.042028
X1271	21.49938078	0.042199
X813	14.51678027	0.042937
X1459	-15.3047626	0.043009
X1367	22.66852487	0.044395
X1022	23.26224815	0.044732

X2255	-18.3771034	0.044869
X2202	-19.0059032	0.046178
X1516	-19.4738434	0.046449
X793	-20.0510331	0.047364
X2210	-21.0433851	0.047386
X1513	-18.3121775	0.047616

X2250	-16.7490082	0.048107
X811	14.1477596	0.049033
X799	-18.3947516	0.049093
X1058	-19.7344176	0.049152
X815	13.96285968	0.049244
X839	-31.5325736	0.049551

These 89 proteins with a significant longitudinal relationship with Trails B decline were then visually inspected to determine whether they could be accurately picked (accurately located by eye) and identified with mass spectrometry. Based on the visual inspection 59 spots were removed and 30 were taken forward for identification (Figure 3-37).

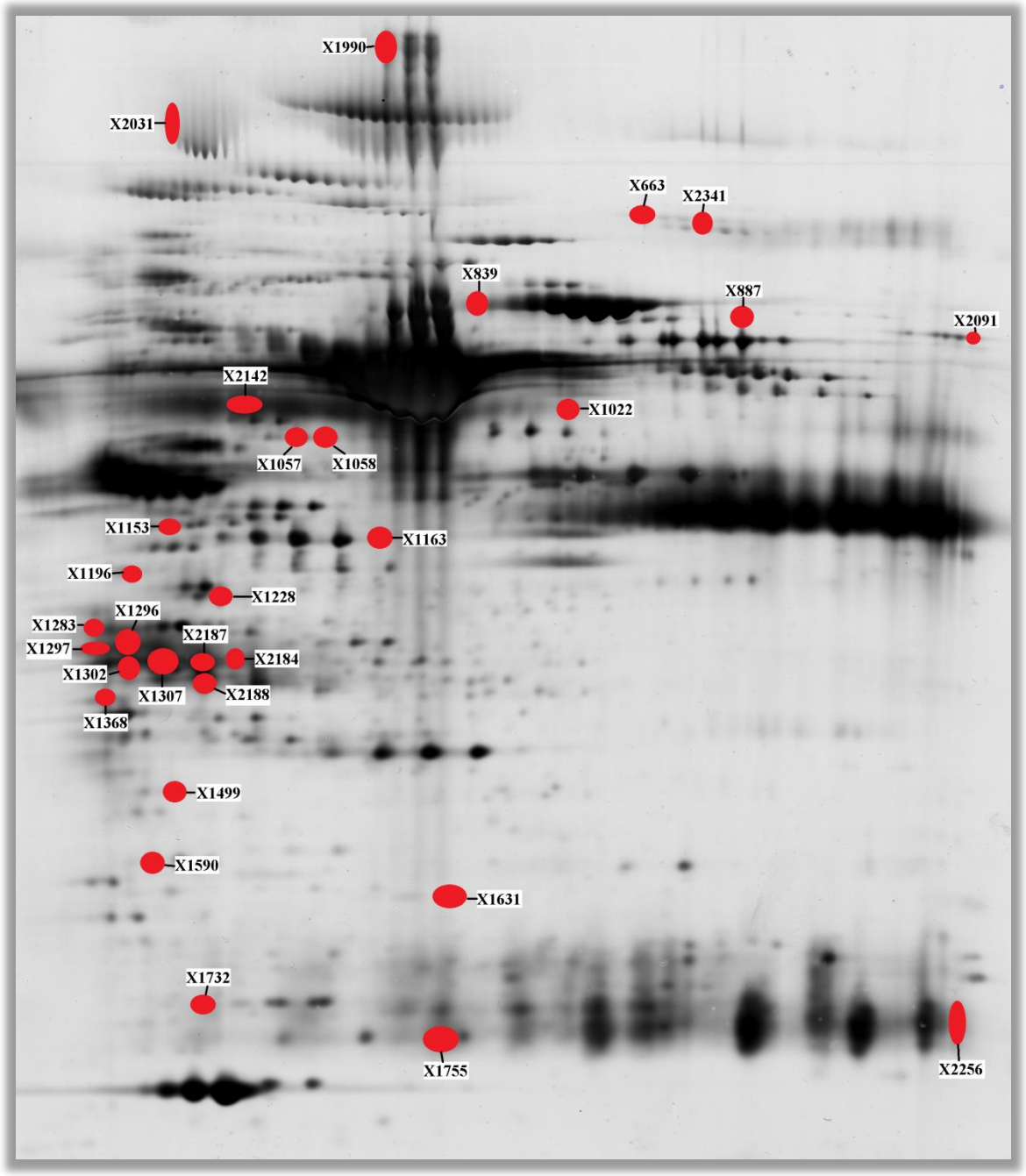

Figure 3-37: 30 protein spots significantly related to Trails B decline selected for identification with mass spectrometry

3.3.8 Mass spectrometry identification and abundance ranking

Manual spot picking of significant spots was performed as described in the methods chapter (chapter 2). The proteins present in a given spot were trypsin digested and the peptides subjected to LC-MS/MS where protein identification relies on identification of the peptide sequence. An orbitrap velos pro (Thermo Fisher Scientific Inc, USA) was used for LC-MS/MS protein identification of picked 2DGE

spots. This mass spectrometer has improved sensitivity and resolution compared to older models (e.g. LTQ) and therefore a greater amount of data was produced from each 2DGE spot. However extracting reliable protein abundance information from the produced data remains challenging. Several proteins were identified as present in each spot. This presented a challenge to determine the most abundant protein(s) and therefore those most likely to be contributing to the statistical signal detected from the spot. There are several different analysis approaches to determine protein abundance from LC-MS/MS data. Here three approaches to protein abundance quantification were considered; peptide spectral matches (PSM, for spectral counting), area under the curve (AUC), and unique peptide count.

Peptide spectral matches (PSM)

PSMs is the most common approach used for protein quantification for label free LC-MS/MS data. This approach uses the number of tandem spectra matched to peptides of a certain protein to determine a total spectral count. This count is considered to be positively associated with the abundance of the protein and can therefore be used as an indicator of relative abundance. Although simple and widely used, there are also issues with this approach to be considered. The acquisition of spectral counts is highly dependent on the mass spectrometer setup, sample type, and complexity[197], and so between study comparisons may be difficult. In addition the individual properties of the proteins measured can influence the acquisition through factors such as MS/MS fragmentation and precursor competition, leading to misestimation of protein abundance. Other factors such as protein load can cause issues with spectral counting with higher protein concentrations suffering from saturation effects. However PSMs is still an important approach to consider as it is quick and simple to employ, also the vast amount of literature utilising this approach allows data comparisons. Further supporting its utility here Tabb et al (2010) found the statistical analysis of PSMs to be more robust when using orbitrap mass spectrometers compared to older LTQ instruments[198].

Area under the curve (AUC)

Top 3 protein quantification (T3PQ) is an AUC approach suggested by Silva et al (2006)[199] and can be automatically calculated in proteome discoverer. This method suggests that for each protein identified the average signal of the three most

efficiently ionised peptides directly correlates to the protein abundance and can therefore be used as an indicator of relative abundance of a protein. Grossman et al (2010) found that precursor signal intensity based methods including T3PQ are the most robust methods of relative quantification and are suitable for complex samples with a large dynamic ranges[200]. In T3PQ proteins with less than 2 peptides identified are either discarded or the ion score needed to pass the acceptance threshold is increased.

Unique peptide count

This is a unique approach to apply to 2DGE spot data. It is an approach that is specifically tailored for a sample that has undergone separation, such as 2DGE spots that have been separated based on their isoelectric point (pI/pH) and their molecular weight. Due to this separation all of the proteins in a 2DGE spot have roughly the same weight and charge. This method assumes that as the proteins are roughly the same weight they also therefore will have similar numbers of amino acids, and therefore similar numbers of lysine and arginine frequencies for trypsin to cleave. Therefore each protein in a 2DGE spot has roughly the same number of potential peptides (Figure 3-38A). As the proteins have similar pIs the ionisation efficiency of these peptides will also be similar; while the mass spectrometer is in the positive charge mode more acidic peptides ionise less efficiently whilst more basic peptides ionise more efficiently. If the number of potential peptides and their ionisation efficiency on the mass spectrometer is equivalent then the difference in number of unique peptides detected can be said to accurately represent the relative abundance of a protein in the gel spot. This is because during within-gel tryptic digest inner sections of a protein may have less chance of being cleaved to form peptides. The higher the abundance of a protein in the gel the increased chance that these inner-sections will be cleaved into peptides, resulting in more unique peptides for that protein (Figure 3-38B). Although unique peptide count has many assumptions the two other approaches for relative abundance detailed above are critically dependent upon the performance of the mass spectrometer whereas this approach is less so and therefore lesser influenced by liquid chromatography biases. It is also the only approach aimed specifically at gel based experiments and so good to consider here. Nevertheless the large number of assumptions on which this approach is based makes it necessary for other, more traditional, approaches to be considered.

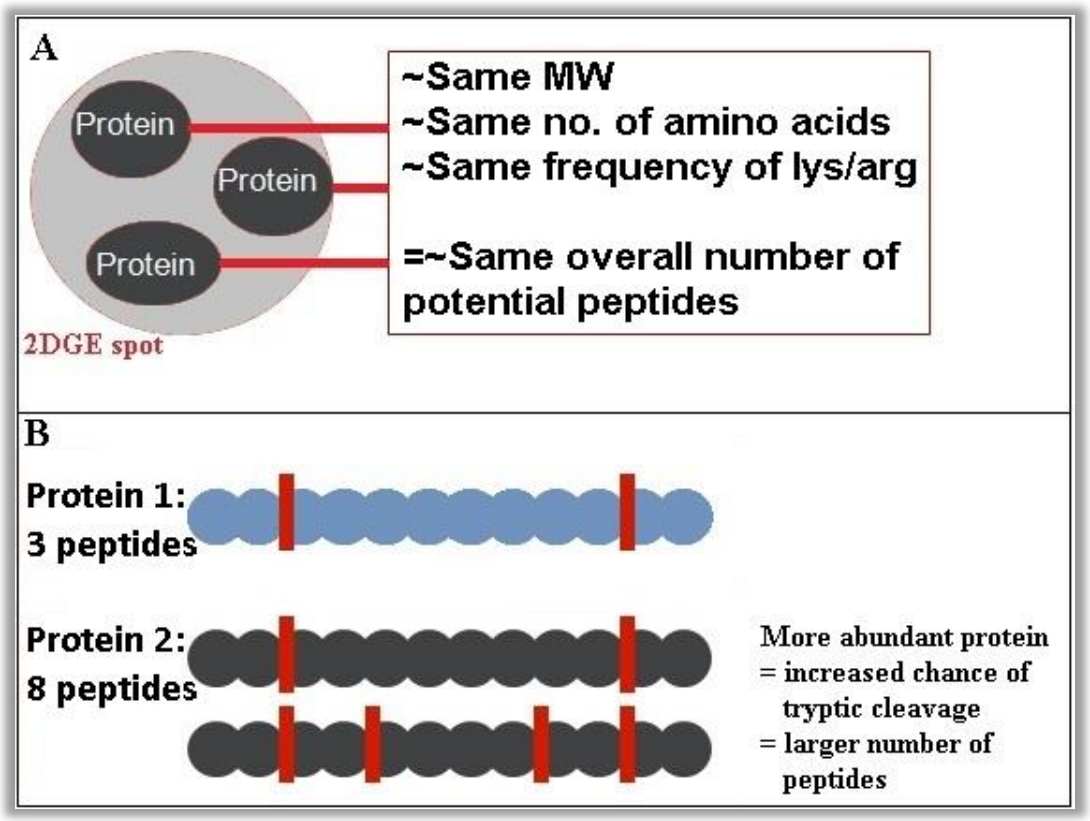

Figure 3-38: Assumptions of the unique peptide approach to relative protein abundance. A) Proteins within a 2DGE spot have same molecular weight (MW), therefore similar numbers of amino acids and so similar frequency of lysine and arginines resulting in same number of potential peptides. B) Highly abundant proteins have increased chance of tryptic cleavage and so produce larger numbers of unique peptides.

Combining approaches

The three approaches outlined above do not make full use of the wealth of information that is provided by the orbitrap mass spectrometer when considered separately, though utilising them in combination may boost efficiency. Here the three analysis methods were considered in combination to determine relative protein abundance, as described in the methods chapter (chapter 2). Firstly, for each approach proteins contributing to less than 5% of a spot's total protein quantity were discarded. This 5% threshold was selected based on the 0.05 statistical threshold commonly adhered to; there was a 95% probability that discarded proteins were not contributing to the statistical signal from the 2DGE spot. Out of the remaining proteins those included in 2/3 of the quantification approaches were considered to be abundantly present and were suggested candidates for the statistical signal found from that spot, as illustrated in Figure 3-39. This 2 out of 3 approach ensured that if

one of the abundance ranking methods was stricter than the others then that one method would not dictate the results.

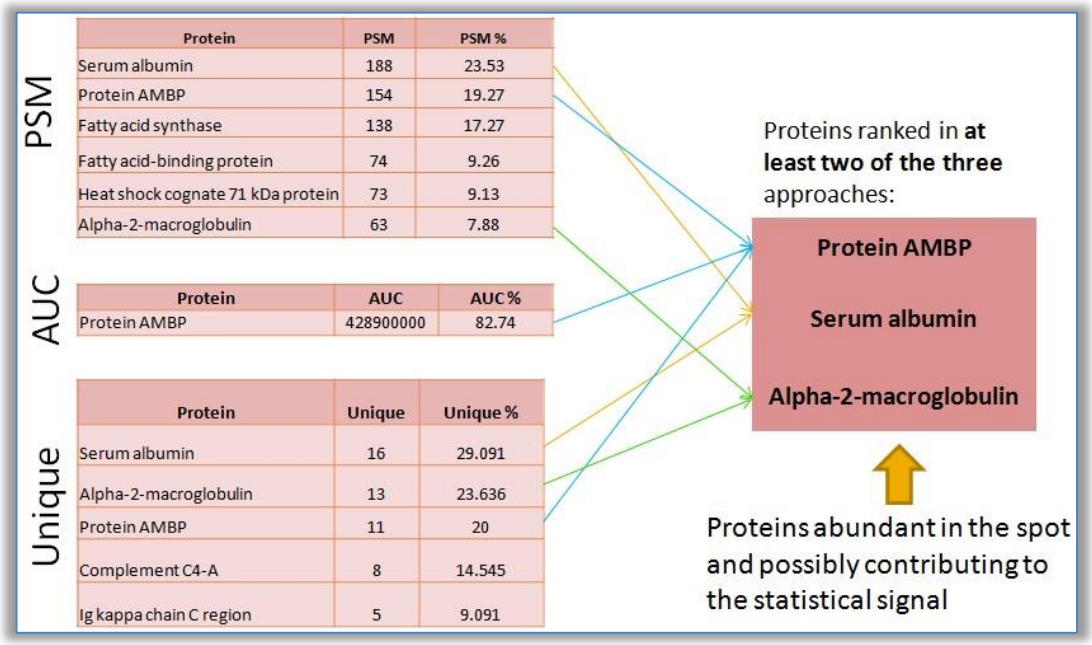

Figure 3-39: '2 out of 3' criteria for proteins ranked as abundantly present within a 2DGE spot. The tables on the left show proteins ranked as abundant for each method; PSM, AUC, and unique peptide count. Proteins ranked as abundant in 2 or more of these methods were included in the final list of proteins considered to be abundantly present within the 2DGE spot.

Based on this 2/3 criteria, the tables below detail the proteins found to be abundantly present in the 2DGE spots significantly related to PiB PET DVR at baseline (Table 3-16), T6 (Table 3-17), and T12 (Table 3-18), and those longitudinally related to ventricular expansion (Table 3-19), and Trails B decline (Table 3-20).

Table 3-16: Most abundant proteins identified in baseline 2DGE spots significantly related to PiB PET DVR

Spot ID	Most abundant proteins identified in 2DGE spot
X1052	Alpha-1-antitrypsin Alpha-2-macroglobulin Beta-2-glycoprotein 1

	Fibrinogen beta chain Ig gamma-1 chain C region
X1128	Fibrinogen gamma chain Serum albumin
X1155	Fibrinogen gamma chain Serum albumin
X1273	Alpha-1-antitrypsin Apolipoprotein A-IV Haptoglobin Inter-alpha-trypsin inhibitor heavy chain H4
X1287	Alpha-2-macroglobulin Haptoglobin Serum albumin
X1400	Alpha-1-antitrypsin Haptoglobin Ig gamma-1 chain C region Ig gamma-2 chain C region Ig kappa chain C region Inter-alpha-trypsin inhibitor heavy chain H4
X1702	Ig kappa chain C region

	Serum albumin
X1730	Ig kappa chain C region Ig lambda-2 chain C regions Immunoglobulin lambda-like polypeptide 5 Serum albumin Serum amyloid P-component
X1792	Apolipoprotein A-I
X1988	Alpha-2-macroglobulin Serum albumin
X2020	Alpha-2-macroglobulin Complement C3 Ig gamma-1 chain C region Ig gamma-2 chain C region Serum albumin
X2026	Alpha-2-macroglobulin Complement C3 Serum albumin
X2048	Alpha-1-antitrypsin Ceruloplasmin Inter-alpha-trypsin inhibitor heavy chain H4

X2157	Beta-2-glycoprotein 1 Fibrinogen beta chain Ig gamma-1 chain C region Ig gamma-2 chain C region Serum albumin
X393	Alpha-2-macroglobulin Serum albumin
X529	Alpha-2-macroglobulin Ceruloplasmin Ig alpha-1 chain C region Serum albumin
X632	Alpha-2-macroglobulin Complement C3 Serum albumin
X639	Alpha-2-macroglobulin Complement C3 Complement component C6 Serum albumin
X740	Alpha-2-macroglobulin Ceruloplasmin

	Complement C1r subcomponent Ig alpha-1 chain C region Serum albumin
X765	Alpha-2-macroglobulin Serum albumin

Table 3-17: Most abundant proteins identified in T6 2DGE spots significantly related to PiB PET DVR

Spot ID	Most abundant proteins identified in 2DGE spot
X1309	Alpha-2-macroglobulin Complement C4-B Haptoglobin Serum albumin
X1660	Alpha-2-macroglobulin Protein AMBP Serum albumin
X1763	Alpha-2-macroglobulin Apolipoprotein A-I Ig kappa chain C region Serum albumin
X2271	Alpha-2-macroglobulin

	Ceruloplasmin Complement factor H Serum albumin
X949	Fibrinogen alpha chain Serum albumin

Table 3-18: Most abundant proteins identified in T12 2DGE spots significantly related to PiB PET DVR

Spot ID	Most abundant proteins identified in 2DGE spot
X1110	Fibrinogen beta chain Fibrinogen gamma chain Ig gamma-1 chain C region Ig gamma-2 chain C region Serum albumin
X1170	Alpha-2-macroglobulin Complement C3 Fibrinogen gamma chain Serum albumin Serum paraoxonase/arylesterase 1
X1172	Alpha-2-macroglobulin Fibrinogen gamma chain

	Serum albumin
X1303	Apolipoprotein L1 Complement C4-A Dermcidin Haptoglobin Serum albumin
x1309	Alpha-2-macroglobulin Complement C4-B Haptoglobin Serum albumin
X1377	Alpha-1-antitrypsin
X1593	Alpha-1-antitrypsin Protein AMBP
X1597	Alpha-1-antitrypsin Alpha-amylase 1 Annexin A1 Complement C4-A Desmoplakin Fibrinogen alpha chain Ig gamma-1 chain C region

	Ig kappa chain C region
X1710	Alpha-1-antitrypsin Alpha-2-macroglobulin Complement C4-A Fibrinogen beta chain Ig gamma-1 chain C region Ig kappa chain C region Ig kappa chain C region Ig lambda-2 chain C regions Serum albumin Serum amyloid P-component
X1762	Alpha-1-antitrypsin Alpha-2-macroglobulin Apolipoprotein A-I Ig kappa chain C region Serum albumin
X381	Alpha-2-macroglobulin Complement C3 Serum albumin
X386	Alpha-2-macroglobulin

	Serum albumin
X584	Alpha-1-antitrypsin Alpha-2-macroglobulin Ig alpha-1 chain C region Serum albumin
X642	Alpha-1-antitrypsin Complement C3 Complement component C6 Serum albumin

Table 3-19: Most abundant proteins identified in each 2DGE spot significantly related to ventricular expansion

Spot ID	Most abundant proteins identified
X1022	Alpha-1-antitrypsin Ig alpha-1 chain C region
X1050	Alpha-1-antitrypsin Alpha-2-macroglobulin Ig alpha-1 chain C region Ig alpha-2 chain C region Serum albumin
X1085	Fibrinogen beta chain

	Ig gamma-1 chain C region
X1284	Alpha-2-macroglobulin Apolipoprotein A-IV Haptoglobin Serum albumin Serum paraoxonase/arylesterase 1
X1297	Apolipoprotein A-IV Haptoglobin Zinc-alpha-2-glycoprotein
X1435	Haptoglobin Haptoglobin-related protein Serum albumin Zinc-alpha-2-glycoprotein
X1495	Alpha-2-macroglobulin Serum albumin
X1590	Complement C4-A Fibrinogen beta chain Haptoglobin Ig gamma-2 chain C region Protein AMBP

	Serum albumin
X1595	Alpha-2-macroglobulin Ceruloplasmin Complement C4-A Serum albumin
X1689	Alpha-2-macroglobulin Serum albumin
X2157	Beta-2-glycoprotein 1 Fibrinogen beta chain Ig gamma-1 chain C region Ig gamma-2 chain C region Serum albumin
X594	Alpha-2-macroglobulin Complement C3 Haptoglobin Ig alpha-1 chain C region Serum albumin
X933	Alpha-2-macroglobulin Complement C3 Fibrinogen alpha chain

	Serum albumin

Table 3-20: Most abundant proteins identified in each 2DGE spot significantly related to Trails B decline

Spot ID	Most abundant proteins identified in 2DGE spot
X1022	Alpha-1-antitrypsin Ig alpha-1 chain C region
X1057	Ig alpha-1 chain C region Haptoglobin Alpha-1-antitrypsin Serum albumin Alpha-2-macroglobulin Antithrombin-III
X1058	Complement C3 Serum albumin Alpha-1-antitrypsin Alpha-2-macroglobulin
X1153	Haptoglobin Serum paraoxonase/arylesterase 1 Fibrinogen gamma chain Serum albumin

	Ig alpha-1 chain C region Alpha-1-antitrypsin
X1163	Fibrinogen gamma chain Haptoglobin Serum albumin Complement C3
X1196	Serum paraoxonase/arylesterase 1 Haptoglobin Ig alpha-1 chain C region Serum albumin Fibrinogen gamma chain Complement C3 Antithrombin-III
X1228	Haptoglobin Plasminogen Sex hormone-binding globulin Complement C3 Complement C4-A Ig gamma-1 chain C region Serum albumin

	Apolipoprotein A-IV
X1283	Haptoglobin Zinc-alpha-2-glycoprotein Serum paraoxonase/arylesterase 1 Apolipoprotein A-IV
X1296	Haptoglobin Ig alpha-1 chain C region Serum albumin
X1297	Apolipoprotein A-IV Zinc-alpha-2-glycoprotein Haptoglobin
X1302	Haptoglobin Zinc-alpha-2-glycoprotein Serum albumin Complement C3
X1307	Haptoglobin Serum albumin Complement C3 Serum paraoxonase/arylesterase 1
X1368	Complement C3

	Clusterin Ig kappa chain C region
X1499	Haptoglobin Inter-alpha-trypsin inhibitor heavy chain H4 Apolipoprotein A-I Clusterin Complement C3 Serum paraoxonase/arylesterase 1 Serum albumin
X1590	Complement C4-A Fibrinogen beta chain Haptoglobin Protein AMBP Ig gamma-2 chain C region Serum albumin
X1631	Haptoglobin Ig kappa chain C region Serum albumin Complement C3
X1732	Ig kappa chain C region

	Serum amyloid P-component Ig kappa chain V-IV region Len Ig kappa chain V-III region SIE Apolipoprotein A-I Serum albumin
X1755	Ig kappa chain C region Serum albumin Apolipoprotein A-I Haptoglobin Fibrinogen gamma chain
X1990	Serum albumin Alpha-2-macroglobulin
X2031	Ceruloplasmin Alpha-2-macroglobulin Serum albumin Inter-alpha-trypsin inhibitor heavy chain H4
X2091	Complement C4-A Serum albumin Complement C3
X2142	Ig alpha-1 chain C region

	Haptoglobin Ig alpha-2 chain C region Serum albumin
X2184	Haptoglobin Serum albumin Complement C4-A
X2187	Haptoglobin
X2188	Haptoglobin Serum albumin Complement C3
X2256	Ig kappa chain C region Apolipoprotein A-I Serum albumin
X2341	Plasminogen Ig gamma-1 chain C region Complement C3 Ig gamma-2 chain C region Haptoglobin Serum albumin
X663	Serum albumin

	Plasminogen Ig gamma-1 chain C region Alpha-2-macroglobulin Serotransferrin
X839	Complement C3 Serum albumin Serotransferrin Alpha-2-macroglobulin Ig mu chain C region
X887	Complement C3 Serum albumin

A summary of the proteins related to PiB PET DVR at baseline, T6, and T12, ventricular expansion, and Trails B decline are summarised in Table 3-21, Table 3-22, Table 3-23, Table 3-24, Table 3-25 below, respectively.

Table 3-21: Summary of proteins related to PiB PET DVR at baseline

Protein	No. of 2DGE spots
Alpha-1-antitrypsin	4
Alpha-2-macroglobulin	11
Apolipoprotein A-I	1
Apolipoprotein A-IV	1
Beta-2-glycoprotein 1	2

Ceruloplasmin	3
Complement C1r subcomponent	1
Complement C3	4
Complement component C6	1
Fibrinogen beta chain	2
Fibrinogen gamma chain	2
Haptoglobin	3
Ig alpha-1 chain C region	2
Ig gamma-1 chain C region	4
Ig gamma-2 chain C region	3
Ig kappa chain C region	4
Ig lambda-2 chain C regions	1
Immunoglobulin lambda-like polypeptide 5	1
Inter-alpha-trypsin inhibitor heavy chain H4	3
Serum albumin	15
Serum amyloid P-component	1

Table 3-22: Summary of proteins related to PiB PET DVR at T6

Protein	No. of 2DGE spots
Alpha-2-macroglobulin	4
Apolipoprotein A-I	1

Ceruloplasmin	1
Complement C4-B	1
Complement factor H	1
Fibrinogen alpha chain	1
Haptoglobin	1
Ig kappa chain C region	1
Protein AMBP	1
Serum albumin	5

Table 3-23: Summary of proteins related to PiB PET DVR at T12

Protein	No. of 2DGE spots
Alpha-1-antitrypsin	7
Alpha-2-macroglobulin	8
Alpha-amylase 1	1
Annexin A1	1
Apolipoprotein A-I	1
Apolipoprotein L1	1
Complement C3	3
Complement C4-A	3
Complement C4-B	1
Complement component C6	1

Dermcidin	1
Desmoplakin	1
Fibrinogen alpha chain	1
Fibrinogen beta chain	2
Fibrinogen gamma chain	3
Haptoglobin	2
Ig alpha-1 chain C region	1
Ig gamma-1 chain C region	3
Ig gamma-2 chain C region	1
Ig kappa chain C region	4
Ig lambda-2 chain C regions	1
Protein AMBP	1
Serum albumin	11
Serum amyloid P-component	1
Serum paraoxonase/arylesterase 1	1

Table 3-24: Summary of proteins related to ventricular expansion

Protein	No. of 2DGE spots
Alpha-1-antitrypsin	2
Alpha-2-macroglobulin	7
Apolipoprotein A-IV	2

Beta-2-glycoprotein 1	1
Ceruloplasmin	1
Complement C3	2
Complement C4-A	2
Fibrinogen alpha chain	1
Fibrinogen beta chain	3
Haptoglobin	5
Haptoglobin-related protein	1
Ig alpha-1 chain C region	3
Ig alpha-2 chain C region	1
Ig gamma-1 chain C region	2
Ig gamma-2 chain C region	2
Protein AMBP	1
Serum albumin	10
Serum paraoxonase/arylesterase 1	1
Zinc-alpha-2-glycoprotein	2

Table 3-25: Summary of proteins related to Trails B decline

Protein	No. of 2DGE spots
Alpha-1-antitrypsin	4
Alpha-2-macroglobulin	6

Antithrombin-III	2
Apolipoprotein A-I	4
Apolipoprotein A-IV	3
Ceruloplasmin	1
Clusterin	2
Complement C3	14
Complement C4-A	4
Fibrinogen beta chain	1
Fibrinogen gamma chain	4
Haptoglobin	19
Ig alpha-1 chain C region	6
Ig alpha-2 chain C region	1
Ig gamma-1 chain C region	3
Ig gamma-2 chain C region	2
Ig kappa chain C region	5
Ig kappa chain V-III region SIE	1
Ig kappa chain V-IV region Len	1
Ig mu chain C region	1
Inter-alpha-trypsin inhibitor heavy chain H4	2
Plasminogen	3

Protein AMBP	1
Serotransferrin	2
Serum albumin	25
Serum amyloid P-component	1
Serum paraoxonase/arylesterase 1	5
Sex hormone-binding globulin	1
Zinc-alpha-2-glycoprotein	3

3.3.9 Assessing dependant variable relationship

There was large overlap in proteins found to be related to all three dependant variables (PiB PET DVR, ventricular expansion, and Trails B decline). Therefore the relationship between the dependant variables was assessed to see whether the protein-DV relationship was reflecting the same pattern for each DV. Pearsons correlation coefficient revealed that there was no correlation between PiB PET DVR and ventricle size or between PiB PET DVR and Trails B at any time point ($p<0.05$). No correlation was also found between rate of decline for Trails B and rate of ventricular expansion. Though when correlating ventricle size and Trails B score at each time point a moderate positive correlation was found at T12 ($r=0.35$, $p<0.05$) (Figure 3-40). No significant correlation was found between ventricle size and Trails B score at baseline or T6 ($p>0.05$).

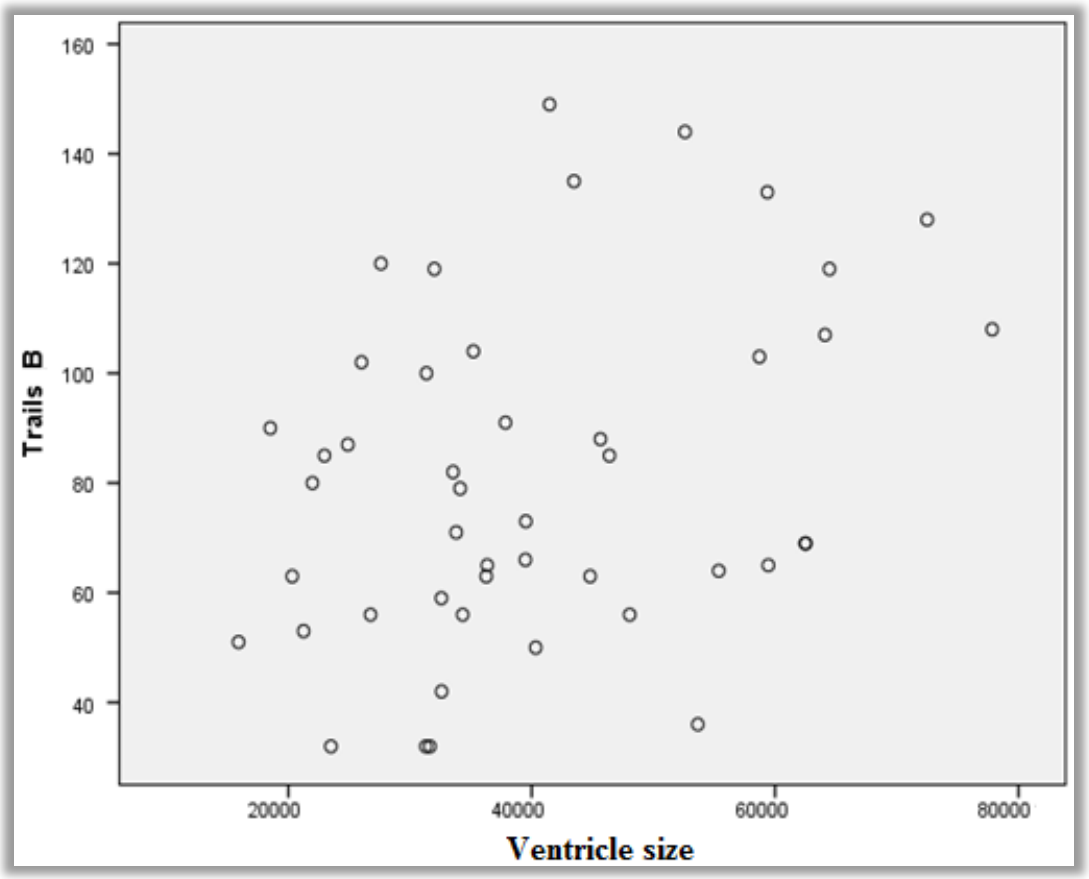

Figure 3-40: Pearsons correlation between ventricle size and Trails B score at T12 (r=0.35, *p*<0.05)

3.4 Discussion

3.4.1 Two dimensional gel electrophoresis experimental performance and analysis

This study utilised a well established proteomic discovery tool; two dimensional gel electrophoresis. It is known that technical variability can be high in 2DGE experiments. For this reason samples were run in duplicate and the coefficient of variation (CV) was determined to indicate the level of analytical variance achieved. The overall CV was 33.5%, this was deemed acceptable as previous reports of 2DGE variance in the literature suggest an approximate normal range to be 16-40%[192-194]. However to further improve the quality of the data a clean-up was conducted to remove individual data points where the CV of duplicates exceeded the 40% 'normal' threshold. Therefore a good level of data quality was achieved and statistical analysis was conducted with confidence.

A comparison of the CV achieved between time points revealed a sample storage effect on the 2DGE technique. 2DGE had increased experimental performance for samples that had been stored for less time, shown by a decreased CV between sample replicates at the most recent time point. This is an interesting point to consider for future experiments, including other proteomic techniques, especially retrospective studies that aim to use samples stored for many years to predict current events such as conversion to disease or rate of decline. This prediction may be influenced by sample age and must be considered. Predictive biomarker abilities are often discovered in stored samples and it may be interesting to compare how these biomarkers perform when obtained from a fresh/recent sample.

2DGE involves many steps for which different protocols or analysis techniques can be used. For example, there are many staining techniques available each with their own strengths and weaknesses. Here 2DGE was conducted using a silver staining protocol. Silver stain has a limited dynamic range, poor stoichiometry, and involves multiple steps during which subtle differences in timing can contribute to between-gel variability. This method does however have high sensitivity, is relatively cheap compared to other methods, and it allows gel scanning using a standard desktop scanner. Silver stain was chosen as the most appropriate staining method for this study due to equipment availability and cost. As samples were completed in duplicate, staining related variability could be monitored and gels were repeated if visual inspection was not satisfactory (e.g. saturation or high background staining). Once stained the gels were scanned and digital gel images were pre-processed for statistical analysis using Progenesis SameSpots. Progenesis SameSpots is one of many commercially available 2DGE analysis software packages. Reports comparing these packages show that Progenesis SameSpots performs well, especially in spot matching accuracy [201-202].

Another step for which there were many options was the analysis of protein abundance within a 2DGE spot. Here a novel approach for determining protein abundance using LC-MS/MS data was presented. This approach combined three current methodologies; peptide spectral matches, area under the curve, and unique peptide count. Proteins that were ranked as highly abundant (>5% contribution to the spot) in at least 2 out of these 3 approaches were considered to be abundant. Using

this 2 out of 3 criteria ensured that the results were not biased towards one method, which may be stricter than the other methods. The three approaches often ranked proteins differently based on abundance, highlighting that 2DGE experiments cannot be compared if this analysis step differs. 'Unique peptide count' was the most relaxed of the ranking methods and resulted in a larger number of abundant proteins per spot. Whereas 'Area under the curve' was the strictest method tending to only rank one or two proteins as abundant per spot. Using the combination of the three approaches allowed their strengths to be combined and individual weaknesses to be diluted. Until a definitive way in which protein abundance can be ranked is determined it is important to consider as much information in your analysis as possible at this stage. The limitation to this approach was that more proteins per spot were considered to be abundant than usually presented in 2DGE experiments. The use of an orbitrap mass spectrometer, with improved sensitivity compared to older models, will have also contributed to this. This presented a problem when determining which abundant protein(s) may be producing the statistical signal detected, and it was decided to consider all abundant proteins in a spot as candidate biomarkers. Although this increases the number of false positive biomarkers found it also ensures true positives remain in contention. As a discovery experiment, ensuring that all true biomarkers are identified is the main concern. Validation experiments are necessary to confirm biomarker utility of the candidates, and discard any false positive findings. Furthermore, lack of false discovery rate (FDR) significance thresholds throughout this study will also increase the number of false positive findings reported. FDRs were not considered here due to the vast amount of statistical tests performed that would result in extremely few 2DGE spots passing an FDR correction. An uncorrected 0.05 *p*-value was considered an acceptable significance level for this discovery stage experiment, with subsequent validation experiments important to confirm true positives and discard false positive findings.

3.4.2 Selecting measures of cognitive decline and brain atrophy

A limitation of 2DGE here was that the number of spots that could be picked for LC-MS/MS protein identification was limited by time and cost. This restricted the amount of analysis that could be completed. Here, data was available for 22 structural MRI regions and 12 cognitive measures, though due to time and cost only

the singular most interesting and relevant sMRI region and cognitive measure were selected to be used for analysis. This was done by identifying which sMRI regions and cognitive measures were significantly changing over time and were therefore most relevant to include in a longitudinal analysis. Linearity of change was also assessed as the statistical tests used only considered linear change.

16 sMRI regions showed significant, and linear, atrophy over the 12 year period measured in these healthy individuals. Of these the ventricles were shown to have the greatest percentage change per year and were therefore selected as the single region of interest for further analysis. Ventricular expansion reflects atrophy of the surrounding brain regions; for example the temporal horn of the ventricles lies next to the hippocampus and so will reflect hippocampal atrophy. Deficits in many functions associated with the surrounding regions (e.g. memory) may therefore be reflected in ventricular expansion. Longitudinally, ventricular expansion has been found as an excellent marker of change over time in cognition, disease status and severity, outperforming other MRI regions including the hippocampus[195, 203-205], although the hippocampus does outperform in cross sectional studies. Perhaps this is due to an increased ability of the ventricles to reflect changes in multiple cognitive domains over time. Additionally with continued cognitive decline ventricular expansion will continue to increase, whereas hippocampal atrophy will plateau. The focus of this investigation was longitudinal measures of change and therefore ventricular expansion was very appropriate. Furthermore along with the hippocampus and the entorhinal cortex, ventricles have been identified as one of the first brain regions affected in dementia and so it is a logical area to investigate in preclinical AD subjects. Higher ventricular expansion has been reported in healthy subjects who converted to MCI or AD compared to those that remain stable[203, 206] showing its utility in preclinical AD studies. Carlson et al, (2008)[195] reported ventricular expansion rates in healthy individuals aged 75-95 vary according to future diagnosis. Individuals who remained stable at follow-up were found to have expansion rates of 3-4.1% per year, 2.4-5.6% for those who converted to MCI over 2.3 years later, and 4.9-8.7% for those who converted to MCI within 2.3 years[195]. In this study ventricular expansion rates ranged from 0.35-13.96% per year, with a mean of 4.72%, although individuals included here were younger (age range = 57-81). Compared to Carlson et al (2008) these rates of ventricular expansion indicate

that the change measured in these individuals is biologically significant. For these reasons the inclusion of ventricles as the measure of brain atrophy was a confident selection, backed up by statistics and previous literature.

Trails B was the only cognitive measure that changed significantly and linearly over time, and was selected as the measure by which cognitive decline would be determined for this study. Trails B is one of two parts of the Trails Making Test, a commonly used clinical tool, and is a measure of executive function [207]. In the Trails B task subjects have to connect-the-dots of 25 targets of alternative numbers and letters in sequence (1, A, 2, B, etc.) (Figure 3-41). The goal is to finish the test as quickly as possible and time taken to complete it is used as the performance measurement.

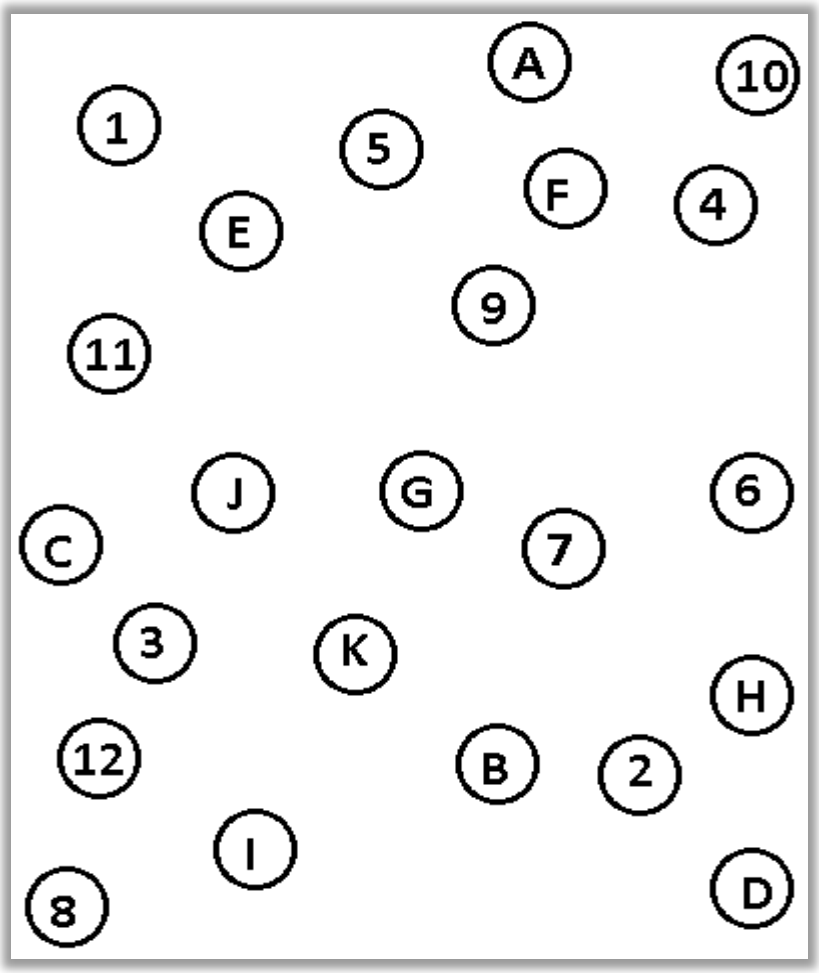

Figure 3-41: Trails B task: subjects have to connect the circles in sequence; 1, A, 2, B, etc.

Tombaugh (2004)[196] present normative percentile data for Trails B performance (time) for community dwelling individuals, stratified for both age (in 5 year increments) and education (<12 years and >12 years in education). For an example see Table 3-26: Trails B percentiles for subjects aged 75-79 years, taken from Tombaugh (2004). Using these norms as a guideline, many individuals in our study remained in the same percentile over time, and even a handful improved showing less than expected cognitive decline with age. However 1/3 of the cohort decreased in their percentile group membership from baseline to T12 (average = 22% decrease). This indicates that in this cohort many individuals showed cognitive decline at a faster rate than you would expect merely from an increase in age.

Table 3-26: Trails B percentiles for subjects aged 75-79 years, taken from Tombaugh (2004)

Percentiles (for individuals aged 75-79)	Education 0-12 years, Trails B time (seconds)	Education 12+ years, Trails B time (seconds)
90	78	57
80	92	59
70	96	66
60	107	73
50	120	87
40	140	106
30	456	126
20	167	141
10	189	178

Executive function is known to be an early indicator of dementia and like memory it is one of the first functions to show deterioration[69, 208]. In particular executive function tasks like Trails B which include set shifting, sequencing, and self-

monitoring are particularly impaired early on in the disease[209]. Trails B has previously been shown to predict group membership of healthy individuals based on cognition and disease outcomes 3 years later[210] indicating its utility as an early preclinical marker. For these reasons, in addition to showing the greatest change over time, Trails B was considered a good cognitive measure to utilise here to find markers of longitudinal cognitive decline in healthy individuals.

3.4.3 Dependent variable relationship

Many of the same proteins were found to be significantly related to all three dependent variables (PiB PET DVR, brain atrophy, and cognitive decline). An analysis, conducted to determine whether the protein-DV relationship was reflecting the same pattern for all three DVs, revealed that there was very minimal correlation between the three DV measures. Only a moderate correlation was found between ventricle size and Trails B at T12, but no other correlations were reported between any DV at any time point. This suggests that either the sensitivity of these measures differ or perhaps different forms of the same protein are related to the three DVs. The latter is supported by the varied gel locations for many proteins, indicating protein modification or cleavage, discussed further below.

The finding that the three DVs are, on the whole, not correlated to one another also provides insights into the onset of AD pathology and cognitive decline in preclinical AD. These results suggest that, at least initially, larger brain atrophy does not significantly reflect poorer cognition, and that their onset and initial developments are independent of one another. Though it is important to consider compensatory mechanisms for cognitive functions may influence these results. Although data for amyloid load was only available at the final time point, the results also suggest that brain atrophy and cognitive decline are independent of increased amyloid deposition, at this assumed preclinical stage. Jack et al, (2010 and 2013) presented a temporal model of AD in which amyloid accumulation occurs first, followed by brain atrophy, and finally cognitive impairment[70-71]. However later in 2013 they also presented evidence showing that approximately half of the individuals measured that were ‘amyloid PET positive’ had evidence of neurodegeneration prior to amyloid positivity, whereas the other half reached amyloid positivity prior to brain

abnormalities[211]. This finding of both amyloid-first and neurodeneration-first profiles in preclinical AD shows that individuals may reach a clinical AD diagnosis via different pathways. Perhaps this explains why hardly any correlation was reported between the three DVs in this study. Nevertheless this finding is still surprising, and likely also reflects heterogeneity within the cohort.

3.4.4 Candidate biomarkers of all three markers of AD

Many candidate biomarkers of AD pathology and cognitive decline were identified here. Of these 14 proteins were found as candidate biomarkers for all three markers of AD. These 14 proteins are therefore very strong biomarker candidates for preclinical AD and are discussed below.

Alpha-2-macroglobulin (α2M)

α2M is a large, major circulating protease inhibitor known to block a wide variety of proteases, regulate the immune response[212], and is released in response to inflammatory stimuli[213]. Here α2M was found to be significantly related to all three markers of AD, including PiB PET DVR at every time point (Table 3-27). Literature shows strong links between α2M and AD; it has been shown to be present in senile plaques in AD[214], binds to beta-amyloid$_{1-42}$[215-216], attenuates fibrillogenesis and neurotoxicity of beta-amyloid[215-216], though has also been found to mediate beta-amyloid degradation and clearance[217-218]. Genetic variation in the *A2M* gene has been linked to an increase in AD risk[219-220] and it has also been suggested that α2M is a sex-specific biomarker strongly correlating with female AD progression but not with males[221]. α2M has also previously been found as an AD biomarker using 2DGE; Hye et al (2006)[142], and Thambisetty et al (2008)[149] reported plasma α2M as a biomarker of disease status and hippocampal metabolism, respectively. Other studies using various proteomic platforms have identified plasma α2M as an AD biomarker. In fact α2M is one of the most reproducible plasma protein markers of AD, associating with AD-related phenotypes in five independent cohorts across 21 studies[188]. With all of these possible links it is likely that α2M is also implicated in the early stages of the disease, as the results here suggest.

Table 3-27: α 2M summary; number of significant 2DGE spots in which α2M was present for each surrogate marker of AD, and their coefficient directions

PiB PET DVR			Longitudinal measures:	
Baseline	**T6**	**T12**	**Trails B**	**Ventricles**
11 ↑ ↓	4 ↑ ↓	8 ↓	6 ↑ ↓	7 ↑ ↓

For each surrogate marker of AD α2M was found in multiple spots and showed both positive and negative relationships with pathology. A similar finding was reported by Zabel et al (2012)[222] who found A2M to have a significant negative relationship with disease status when measured by ELISA, though a significant positive relationship when measured by LC-MS/MS. They explain this as sensitivity differences between the two methods. It is likely that both approaches yield correct results and are measuring different parts or forms of the same protein. Additionally Sui et al (2014)[223] also reported this discrepancy in serum from triple transgenic mice (PS1M146V/APPSwe/TauP301L); certain isoforms of α2M were decreased whilst others were significantly elevated when compared to wild type mice. They suggest that this may be due to differences in post-translational modifications. Visual inspection of the 2DGE gel may allow an insight into this suggestion; significant spots containing α2M were found at various molecular weights and pIs indicating α2M modifications, or fragments, are present (Figure 3-42).

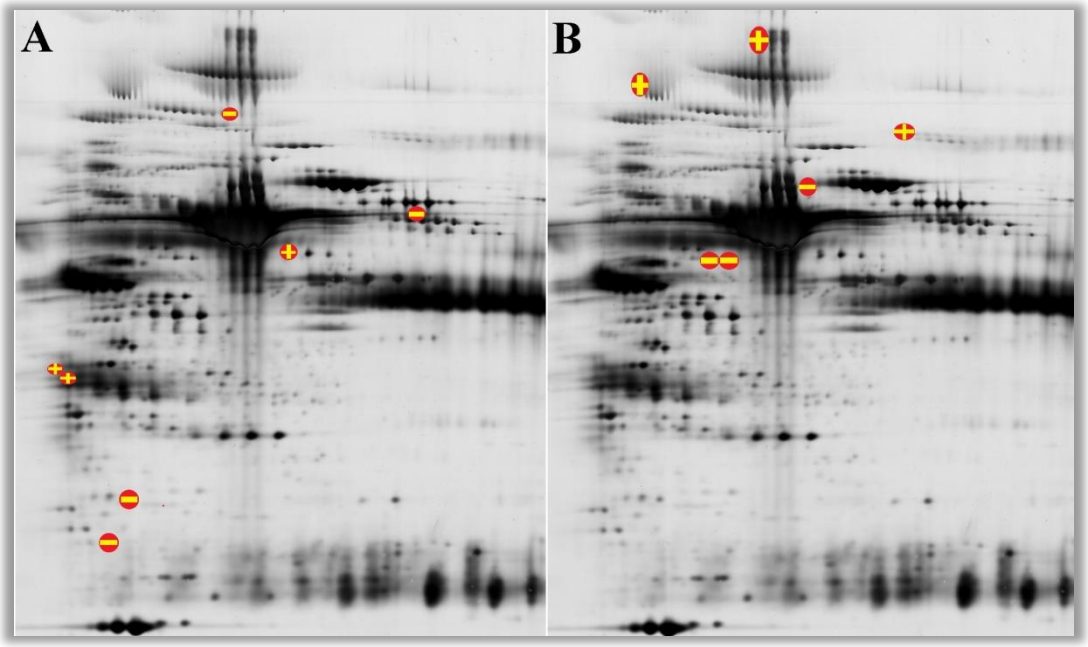

Figure 3-42: 2DGE spots containing α2M which are longitudinally related to: A) Ventricular expansion, B) Cognitive decline (Trails B). Positive and negative signs indicate the direction of the statistical relationship reported.

Opposite coefficient directions between 2DGE spots containing the same protein was not limited to α2M and was found for many proteins discussed below. It is therefore likely that these other results are also a consequence of protein modifications and/or cleavage. Therefore such results may not be conflicting, but instead reflect the strength of the 2DGE technique in detecting and measuring many different forms of a singular protein in one experiment.

Serum albumin

Serum albumin is the most abundant protein in human plasma, and unsurprisingly it was the most commonly identified protein in this study, present in 66 significant spots and related to all three DVS. Serum albumin is known to be involved in many functions including transportation of hormones, fatty acids, drugs, and metabolites, and maintaining oncotic pressure. Serum albumin is also commonly used as a biomarker of blood-brain-barrier (BBB) integrity, with an increase of albumin in CSF reflecting BBB disruption[104]. In AD various protective mechanisms of albumin have been suggested including preventing oxidative damage, binding beta amyloid for clearance, and preventing misfolding and aggregation of proteins such as beta amyloid[224-225]. Serum albumin often appears as a biomarker candidate for AD[142, 151, 226], though due to its high abundance it is difficult to determine its

validity as it is sometimes considered to contaminate findings and mask other biomarkers.

Table 3-28: Serum albumin, summary; number of significant 2DGE spots in which serum albumin was present for each surrogate marker of AD, and their coefficient directions

PiB PET DVR			Longitudinal measures:	
Baseline	**T6**	**T12**	**Trails B**	**Ventricles**
15 ↑ ↓	5 ↑ ↓	11 ↑ ↓	25 ↑ ↓	10 ↑ ↓

Serum albumin was found in many spots located throughout the gel, indicating the presence of modifications/fragments. Recently, Ramos-Fernandez et al, (2014) found albumin is significantly glycated and nitrated in both plasma and CSF of AD patients compared to controls[225]. These modifications resulted in changes in the physiological properties of albumin; it was more prone to aggregation, and it also was found to bind significantly more beta amyloid. The results here suggest serum albumin may be a longitudinal biomarker of preclinical AD, perhaps in a native or modified form.

Immunoglobulins; Ig alpha-1 chain C region, Ig gamma-1 chain C region, and Ig gamma-2 chain C region

Like serum albumin, immunoglobulins (IgGs) are abundantly present in human plasma, and also like albumin IgGs were found to be present in numerous 2DGE spots significantly related to AD pathology and cognitive decline. Three IgGs were consistently identified and were shown to be related to all three DVs; Ig gamma-1 chain C region, Ig gamma-2 chain C region, and Ig alpha-1 chain C region (Table 3-29). Immunoglobulins are found abundantly present in AD brains; diffusely present in brain tissue, connected to amyloid (in plaques and vessels), and in glial cells and neurons. Certain IgGs, have been reported to possess anti-amyloidogenic properties and are considered to have therapeutic potential [227]. Ig gamma-1 chain C region and Ig alpha-1 chain C region have previously been reported as a biomarker of AD diagnosis [142] and Ig gamma-1 chain C region has also been found as a predictive biomarker of amyloid load in preclinical AD[151]. These results support

the biomarker abilities of IgGs in the early stages of AD, and provide further support to claims that AD may be an autoimmune disease[228].

Table 3-29: Immunoglobulins summary; number of significant 2DGE spots in which immunoglobulins were present for each surrogate marker of AD, and their coefficient directions

	PiB PET DVR			Longitudinal measures:	
	Baseline	**T6**	**T12**	**Trails B**	**Ventricles**
Ig alpha 1 chain C region	2 ↑ ↓		1 ↓	6 ↑ ↓	3 ↑ ↓
Ig gamma 1 chain C region	4 ↑ ↓		3 ↑ ↓	3 ↑ ↓	2 ↑ ↓
Ig gamma 2 chain C region	3 ↑ ↓		1 ↑	2 ↑ ↓	2 ↑ ↓

Complement C3 & C4a

The complement is an important system in both the innate and adaptive immune system, and has been previously associated with many neurodegenerative diseases including Alzheimer's disease. The complement system is divided into three pathways; classical, alternate and the mannose-binding lectin (MBL) pathway. The classical pathway primarily acts to lyse cells and bacteria already recognised and opsonised by plasma antibodies as well as targeting these cells for immunological clearance. The alternate pathway acts independently of plasma antibodies and binds to cells and bacteria that do not express complement decay accelerating factor (DAF). The MBL pathway recognises lectins and ficolins, common bacterial surface proteins, and acts primarily to lyse bacteria and target them for immunological clearance. Complement C3 is a central component in the complement system, linking all three of these complement pathways (see Figure 3-43).

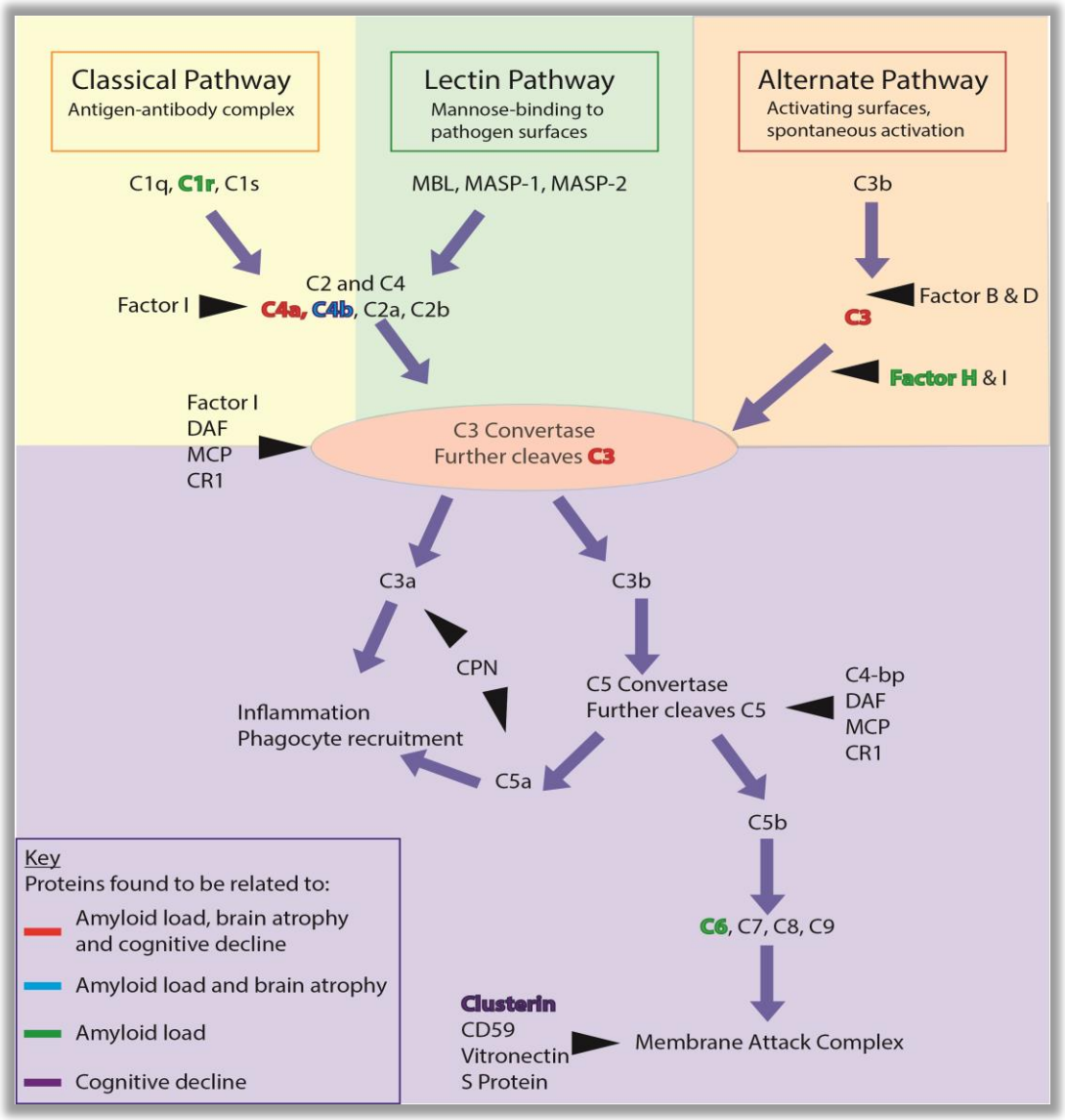

Figure 3-43: Basic illustration of proteins involved in the three complement pathways. Colour coded proteins are those found in this study to be candidate biomarkers

Here C3 was found to be significantly related to all three DVs (see Table 3-30). C3 is one of the most common proteins to be reported as an AD biomarker[188] and, like the findings shown here, both positive and negative associations of C3 and AD pathology have been reported in the literature. For example; plasma levels of C3 have been found to associate with brain amyloid burden both positively[150] and negatively[151]. Studies showing a negative relationship between C3 levels and disease severity suggest a protective role of C3[222]. Maier et al, (2008) investigated this using a complement C3-deficient amyloid precursor protein (APP) transgenic AD mouse model and found a beneficial role of C3 in plaque clearance and neuronal health, with decreased C3 levels leading to accelerated beta amyloid deposition and

neurodegeneration[229]. Other results conflict this protective hypothesis and indicate a detrimental association with increased C3; both Thambisetty et al (2011) and Zhang et al, (2004) reported elevated C3 levels in AD patients relative to controls[148, 230].

Table 3-30: Complement C3 summary; number of significant 2DGE spots in which C3 was present for each surrogate marker of AD, and their coefficient directions

PiB PET DVR			Longitudinal measures:	
Baseline	**T6**	**T12**	**Trails B**	**Ventricles**
4 ↑ ↓		3 ↓	14 ↑ ↓	2 ↓

C4a, involved in both the classical and lectin pathway, is an anaphylatoxin product of the complement cascade. Here C4a was found to be associated with all three DVs (Table 3-31). Like C3 C4a has also been reported as an AD biomarker previously. Here both positive and negative directions with DV were observed for this protein, though the literature mainly supports a positive relationship; Increased plasma levels of C4a have been found in AD patients compared to controls[231]. This increase has also been seen in CSF of AD patients compared to controls, and also compared to patients with vascular dementia[232].

Table 3-31: Complement C4a summary; number of significant 2DGE spots in which C4a was present for each surrogate marker of AD, and their coefficient directions

PiB PET DVR			Longitudinal measures:	
Baseline	**T6**	**T12**	**Trails B**	**Ventricles**
		3 ↑ ↓	4 ↑ ↓	2 ↓

Other complement proteins were found to be related to one or two DVs; C1r, Factor H, C6, C4b, and clusterin. Together these results suggest that the complement cascade in the periphery is broadly altered in AD, and effects are not limited to one specific complement pathway. These results support findings which indicate complement proteins as AD biomarkers, whilst also providing evidence of their

longitudinal utility as biomarkers in preclinical AD. In addition to the periphery, other studies reporting multiple complement proteins as AD biomarkers show that this broad complement alteration may also be occurring in the CNS[233-234]. Complement proteins show large potential to be used as early blood based biomarkers. However these proteins are known to be particularly susceptible to sample preparation and storage[188, 235], which can vary between research centres and may therefore impede further research. Additionally the study of complement proteins in relation to AD can be complicated by other inflammatory comorbidities that are commonly found in the elderly population.

Alpha-1-antitrypsin (AAT)

Alpha-1-antitrypsin (AAT) is a serine protease inhibitor involved in controlling proteases during inflammation, coagulation, and fibrinolysis[236]. It has previously been identified as an AD biomarker in a number of studies[150, 237] with higher AAT levels reported in AD plasma and CSF compared to controls[237-238]. In fact AAT is one of the most replicated plasma based AD biomarkers[188]. Unsurprisingly then in this study AAT was one of the most commonly detected proteins in significant 2DGE spots, abundantly present in 17 spots throughout the study and associating with all three DVs (Table 3-32). Increased AAT in its oxidised form has previously been found in AD plasma, showing that specific isoforms of AAT may have biomarker ability[239-240], a feature that is also supported by the varied locations of 2DGE spots in which this protein was detected. Further implicating AAT in AD immunocytochemistry has located AAT in both neurofibrillary tangles and senile plaques in AD brain tissue[241]. This suggests AAT may be functionally involved in AD pathology. Here AAT is found related to very early AD pathology (amyloid burden and brain atrophy) and cognitive decline, suggesting any AD related function of the protein occurs at an early stage.

Table 3-32: Alpha-1 antitrypsin summary; number of significant 2DGE spots in which AAT was present for each surrogate marker of AD, and their coefficient directions

PiB PET DVR			Longitudinal measures:	
Baseline	**T6**	**T12**	**Trails B**	**Ventricles**
4 ↑ ↓		7 ↑ ↓	4 ↑ ↓	2 ↑

Fibrinogen

2DGE spots significantly related to fibrinogen were found for all three DVs. This included a significant relationship at all three time points for PiB PET DVR, indicating a longitudinal relationship to all three DVs; amyloid load, cognitive decline, and brain atrophy. Fibrinogen consists of three chains; β, α, and γ. Fibrinogen β-chain was found in spots related to all three DVs, whereas fibrinogen α-chain and γ-chain were found to be related to only two DVs(Table 3-33). All three chains were related to amyloid load.

Table 3-33: Fibrinogen summary; number of significant 2DGE spots in which fibrinogen was present for each surrogate marker of AD, and their coefficient directions

	PiB PET DVR			Longitudinal measures:	
	Baseline	**T6**	**T12**	**Trails B**	**Ventricles**
Fibrinogen α-chain		1 ↑	1 ↑		1 ↓
Fibrinogen β-chain	2 ↑ ↓		2 ↑ ↓	1 ↓	3 ↑ ↓
Fibrinogen γ-chain	2 ↓		3 ↑ ↓	4 ↑ ↓	

Fibrinogen is involved in the coagulation cascade by yielding monomers that polymerise into fibrin, it also acts as a bridge between platelets to encourage aggregation, and is also a marker of inflammation. Fibrinogen contributes to plasma viscosity which may reduce cerebral blood flow[242], it is a major predictor of ischemic stroke, and may also be associated with cerebral lesions detected in stroke-free individuals using MRI[243]. Although the direction of causality is unknow, it is thought that cerebral infarcts increase the risk of dementia, and may therefore mediate any relationship with cognitive decline.

Fibrinogen has been previously identified as a potential biomarker of AD in both CSF[140, 244-245] and plasma studies[148, 150, 246]. Elevated fibrinogen has been reported in AD subjects, linked to cognitive decline[242, 247], and brain atrophy[148], and it has also been shown to increase the risk of developing AD[248]. Mouse models also support these findings with decreased fibrinogen levels appearing

beneficial; lessening cerebral amyloid angiopathy, reducing BBB permeability, reducing microglial activation, and improving cognitive performance[249]. In healthy individuals fibrinogen is normally confined to the periphery, however it has been found to pass through the BBB in the brains of individuals with AD[250-251].

AD subjects often show increased clot formation, decreased fibrinolysis, and elevated levels of coagulation factors. This may also be true in this study as antithrombin-III (AIII), a coagulation inhibitor, was found to be negatively related to AD pathology. AIII prevents excessive blood clotting and individuals with AIII deficiency have increased risk of blood clots and hypercoagulability. Here AIII was found longitudinally negatively related to Trails B score in two 2DGE spots; with reduced levels of AIII related to increased cognitive decline over time. This link between hypercoagulability and cognitive decline has been reported before, dementia patients have been seen to have increased coagulation activity compared to controls[252], and Fibrin degradation products (D-dimers), have also shown predictive ability of cognitive decline in a large elderly population[253]. Additionally correlation between senility and AIII was previously found in elderly obese individuals[254]. Further evidence to support AIIIs involvement in AD comes from immunocytochemical studies which show AIII to localize to both amyloid plaques, and neurofibrillary tangles in the brain[255-256], suggesting a potential role in AD pathogenesis.

Fibrinogen and Aβ have also been found to interact, increasing aggregation, and fibrinogen is found in Aβ deposits in the brains of AD subjects. After a review of the involvement of fibrinogen in AD Cortes-Canteli et al (2007)[257] suggest that fibrinogen-Aβ binding and altered hemostasis elevates fibrinogen levels in AD, resulting in increased Aβ deposition, decreased cerebral blood flow, increased neuroinflammation, and eventual neurodegeneration. They therefore suggest that blocking the fibrinogen-Aβ interaction may be a therapeutic target for AD. Targeting a fibrinogen-Aβ complex for intervention may allow the prevention of abnormal clotting whilst avoiding affecting other normal coagulation activity. Our findings here implicate fibrinogen in preclinical AD suggesting that such interventions may need to be implemented at a very early stage in the disease.

The evidence reported above support a detrimental effect of increased fibrinogen on cognition and AD pathology. In this study many 2DGE spots did show increased levels of fibrinogen to be detrimental. However conversely some 2DGE spots showed a negative relationship with AD surrogate markers, especially fibrinogen γ-chain for which the majority of 2DGE spots had a negative coefficient. One explanation is that another activity of fibrinogen is to act as a complement inhibitor[258-259], in fact many proteins involved in the coagulation cascade are also able to active/inhibit the complement cascade[260]. An overactive complement system is often reported in AD, and this would correspond to a reduction in complement inhibitors, including fibrinogen. Complement inhibition will be discussed in further detail later in relation to clusterin.

Apolipoprotein A-IV (ApoA-IV)

Apolipoprotein A-IV (ApoA-IV) is one of many apolipoproteins; a group of proteins related to cholesterol and lipid metabolism. Various apolipoproteins have been reported as AD biomarkers, including at a preclinical stage[261-262]. ApoA-IV has been found to bind to beta amyloid[263] and transgenic AD mice show increased AD pathology with an ApoA-IV deficit[264], indicating a potential therapeutic function ApoA-IV in AD. The results here appear to oppose this hypothesis; ApoA-IV was found to have a positive association with all three DVs (in 5/6 spots) (Table 3-34), though it is possible that in preclinical AD ApoA-IV increases as a protective mechanism.

Table 3-34: ApoA-IV summary; number of significant 2DGE spots in which ApoA-IV was present for each surrogate marker of AD, and their coefficient directions

PiB PET DVR			Longitudinal measures:	
Baseline	**T6**	**T12**	**Trails B**	**Ventricles**
1 ↑			3 ↑ ↓	2 ↑

Serum paraoxonase/arylesterase 1(PON1)

Serum paraoxonase/arylesterase (PON1) is an enzyme that associates with high density lipoproteins (HDL) and is often found associated to various apolipoproteins

(ApoA-I, ApoA-II, and ApoJ)[265]. It has also been shown that PON1 can protect low density lipoproteins (LDL) from oxidative stress, and as oxidised LDLs are present in amyloid plaques[266] PON1 may play a protective role in disease[265]. Supporting this low serum PON1 activity has been identified as a risk factor for AD[267-268]. Lower PON1 protein concentration is also associated with an increased risk for Parkinson's disease and multiple sclerosis[269]

Here PON1 was found to be positively associated with cognitive decline and amyloid load (concurrently), and both positively and negatively associated with ventricular expansion (Table 3-35). If PON1 is involved in protective mechanisms then perhaps this positive relationship with AD pathology and cognition reflects an increase in these protective mechanisms at this early preclinical stage of AD.

Table 3-35: PON1 summary; number of significant 2DGE spots in which PON1 was present for each surrogate marker of AD, and their coefficient directions

PiB PET DVR			Longitudinal measures:	
Baseline	**T6**	**T12**	**Trails B**	**Ventricles**
		1 ↑	5 ↑	1 ↑ ↓

Ceruloplasmin

Ceruloplasmin plays an important role in copper transport and metabolism, with approximately 95% of copper in human serum bound to ceruloplasmin[270]. Copper homeostasis dysfunction has been suggested to contribute to AD related neurodegeneration and predict MCI-AD conversion, with an increase in non-ceruloplasmin-copper (i.e. 'free' copper) reported in AD individuals[270-272]. However the mechanistic relationship between plasma ceruloplasmin and copper in AD is unclear.

Here ceruloplasmin was identified in 2DGE spots significantly related to all three DVs, with varying coefficient directions (Table 3-36). Most interestingly the coefficients for the two longitudinal measures disagree with a positive relationship found for Trails B decline (increase in time completing task), whereas a negative relationship was found for ventricular expansion. All bar one of the significant spots

containing ceruloplasmin were found at high molecular weights indicating that the majority of spots probably contained a form of the full length protein. One spot, longitudinally related to ventricular expansion, identified ceruloplasmin at a low molecular weight (<50kDa) indicating a fragment of the protein was identified. In CSF, increased amounts of low-molecular weight fragments of ceruloplasmin have been reported in AD patients compared to controls[270]. It was suggested that this increased fragmentation reflected impairment in the incorporation of copper into the protein. However here a negative relationship was reported between low MW ceruloplasmin and ventricular expansion, conflicting this hypothesis.

Table 3-36: Ceruloplasmin summary; number of significant 2DGE spots in which ceruloplasmin was present for each surrogate marker of AD, and their coefficient directions

PiB PET DVR			Longitudinal measures:	
Baseline	**T6**	**T12**	**Trails B**	**Ventricles**
3 ↑ ↓	1 ↑		1 ↑	1 ↓

Reduced ceruloplasmin has been previously identified in plasma samples from AD individuals[273] with a suggestion of reduced oxidative activity of this protein being a cause or consequence of the disease. Though confusingly both an increase in ceruloplasmin levels[274] and no significant difference in ceruloplasmin concentration[275] has also been found in AD serum compared to controls. A meta-analysis focusing on oxidative stress in AD concludes that a statistically significant change in serum ceruloplasmin levels are not often reported in AD, rather a reduction in activity is reported[276]. Perhaps a deeper assessment of the 2DGE spots containing ceruloplasmin would reveal that the preclinical biomarker signal detected here resulted from changing quantities of different forms of the protein, rather than quantity of ceruloplasmin as a whole.

Haptoglobin

Haptoglobin was found to be abundantly present in many 2DGE spots significantly related to all three DVs, including at all three time points for PiB PET DVR (Table 3-37). Haptoglobin is a haemoglobin binding protein, involved in the protection of

hemolysis and inhibiting oxidative activity. Decreased haptoglobin is known to indicate an increase in free plasma haemoglobin[277]. Haptoglobin has also been identified to play a role in suppressing inflammatory responses[278] with larger amount of plasma haptoglobin found in response to inflammation[279]. Additionally it has also been suggested to be a chaperone protein involved in defence mechanisms against extracellular protein aggregation such as Aβ, and has been found in amyloid plaques in vivo[278, 280]. Oxidisation of haptoglobin has been shown to increase and its expression downregulate with disease status (control-MCI-AD)[281], suggesting a progressive impairment of function throughout disease progression. Perhaps an increase in oxidisation suppresses haptoglobin's chaperone activity reducing its ability to suppress the aggregation of Aβ.

Table 3-37: Haptoglobin summary; number of significant 2DGE spots in which haptoglobin was present for each surrogate marker of AD, and their coefficient directions

PiB PET DVR			Longitudinal measures:	
Baseline	**T6**	**T12**	**Trails B**	**Ventricles**
3 ↑↓	1 ↑	2 ↓	19 ↑↓	5 ↑↓

For each DV both negative and positive relationships with haptoglobin were reported. This may be a reflection of the proteins involvement with the previously mentioned mechanisms such as inflammation and Aβ aggregation defence, which in AD would result in an increase and decrease in haptoglobin levels respectively. Different forms of haptoglobin may be related to each mechanism.

Haptoglobin has previously been reported as an AD biomarker in both plasma and CSF[151, 230, 282]. This finding supports it utility as an AD biomarker in the preclinical stage, it also provides evidence that its biomarker abilities remain stable over time.

Protein Alpha-1-microglobulin/bikunin precursor (AMBP)

The final protein found to be related to all three DV is Protein AMBP (Table 3-38). Protein AMBP is cleaved into three distinctly functioning protein chains; alpha-1-

microglobulin (α1M), bikunin, and trypstatin. The approximate molecular weight of the significant 2DGE spots containing protein AMBP (30-40kDa) indicate that the protein identified is either the full length AMBP protein (39kDa), or its largest chain α1M. Like haptoglobin, alpha-1-microglobulin is involved in hemolysis and protects against oxidative stress.

Table 3-38: Protein AMBP summary; number of significant 2DGE spots in which protein AMBP was present for each surrogate marker of AD, and their coefficient directions

PiB PET DVR			Longitudinal measures:	
Baseline	**T6**	**T12**	**Trails B**	**Ventricles**
	1 ↓	1 ↑	1 ↓	1 ↓

α1M has been shown to be involved in cell protection against oxidants, free radicals, and hemolysis[283-285], it has also shown immunoregulation properties; inhibiting interleukin-2 production of lymphocytes and inhibiting inflammatory responses[284]. This study reveals a mainly negative relationship of protein AMBP/α1M with AD pathology, indicating a reduction in the protective mechanisms of α1M may result in increased AD pathology. Plasma α1M had previously been identified as an biomarker of brain atrophy in AD[148] and a urinary α1M:ulinastatin ratio has been suggested as a biomarker to differentiate between AD and vascular dementia[286]. These results support its role as a longitudinal biomarker in preclinical AD.

3.4.5 Clusterin/ApoJ

Many other proteins were identified here as candidate biomarkers of one or two of the DVs were investigated. From these remaining candidate biomarkers clusterin is the protein for which the strongest links to Alzheimer's disease have previously been reported.

Clusterin, an inhibitor of the complement immune system and a chaperone glycoprotein, was found in two 2DGE spots shown to have a longitudinal

relationship with Trails B score. Normally chaperone proteins function to stabilise proteins and clear damaged and unfolded proteins, however the role of clusterin in AD is unclear. Here, in both spots, a decrease in clusterin over time was significantly related to increased cognitive decline.

The complement system is thought to be overactive in AD and clusterin is a known complement inhibitor (Figure 3-43). It is therefore possible that in individuals with pre-clinical AD, clusterin levels will decline overtime allowing a larger, overactive, immune response prior to clinical manifestations of the disease. This would support a reduction in plasma clusterin in the early preclinical disease stages as seen in this study. This result also indicates that increased clusterin levels may have a protective effect on cognition in healthy individuals, with higher clusterin levels correlating with less cognitive decline. Cascella et al (2013)[287] also found a protective effect of clusterin on learning and memory in rats. They injected the hippocampus of rat brains with Aβ42, when this Aβ42 was preincubated with clusterin the Aβ42-related memory impairments as well as glia inflammation and neuronal degeneration were prevented. Although a very different experimental platform from that utilised here this does support a potential mechanism of clusterin as a neuroprotective Aβ42 chaperone and complement inhibitor. Thambisetty et al (2012)'s human plasma proteomic study of plasma clusterin levels further supports this as they found higher clusterin levels were related to lower rates of brain atrophy in individuals with MCI[138]. Though in their previous cross sectional investigation Thambisetty et al (2010) reported a contrasting association; higher concentrations of plasma clusterin were associated with greater atrophy of the entorhinal cortex in AD[137]. The difference between these two studies showing conflicting results appears to be that they focus on different temporal states of the disease; MCI compared to AD. Perhaps this shows that in MCI individuals the protective mechanism of clusterin is in effect, though once AD is established this mechanism fails. The results from this study would further support this hypothesis. Increased plasma clusterin has been found to be related to disease severity in AD subjects in other studies [188, 288], Schrijvers et al (2011) hypothesized that this reflects a neuroprotective response once AD is established.

In other amyloidogenic diseases peripheral clusterin has also been shown to have a protective effect. In light chain amyloidosis (AL) an overproduction of amyloidogenic immunoglobulin light chain protein (LC) causes toxicity to blood vessels, cardiac, and other tissues. In AL clusterin has been found to co-localise with amyloid deposits in cardiac tissue and decreased levels of serum clusterin have been reported in individuals with AL[289]. Franco et al (2012)[289] report that increased clusterin has been found to prevent LC-induced cell death and arteriole endothelial dysfunction.

In inflammatory diseases such as psoriasis and rheumatoid arthritis increased levels of clusterin in plasma and synovial fluid, respectively, has also been suggested to have a positive role[290-291] suggesting reduced clusterin may be used as an indicator of systemic inflammatory activity.

As well as inhibiting the complement system, evidence also suggests that clusterin plays a protective role through Aβ clearance, reduces apoptosis and oxidative stress, induces synapse formation and increases neuronal network complexity. Interestingly, clusterin has been found to prevent deterioration and restore breakdown of the blood-retinal-barrier (BRB)[292], the BRB shares similar properties to the blood-brain-barrier which is disrupted in AD.

Results from CSF studies conflict with this neuroprotective hypothesis; Deisken et al 2014[293] reported that elevated levels of CSF clusterin correlated with larger brain atrophy in the entorhinal cortex in healthy and MCI individuals with high CSF $A\beta_{1-42}$. However it is not known whether blood and CSF results should correspond. Cellular level experiments show neuronal treatment with Aβ increases intracellular clusterin and decreases clusterin secretion[294]. It is possible that in these preclinical AD individuals where increased CSF levels of clusterin have been reported, plasma clusterin levels may be corresponding with a decrease in extracellular CSF clusterin.

The results reported here indicate that increased clusterin levels had a protective effect on cognition, with a decline in clusterin levels over time shown to be related to a decline in cognition. Together with supporting literature this backs up a hypothesis

of a neuroprotective effect of peripheral clusterin in AD, at least in the preclinical stages, and that this effect can be observed longitudinally over a period of 12 years.

3.4.6 Comparison to Thambisetty et al, (2010)

This study aimed to replicate, and expand, upon the work conducted by Thambisetty et al, (2010)[151]. They identified a panel of 18 2DGE spots that could effectively discriminate between healthy individuals who would have high and low brain amyloid burden 10 years later. In these 18 spots 6 proteins were identified, 4 of which we were able to replicate here; complement C3, Haptoglobin, serum albumin, and Ig gamma-1 chain C region (highlighted in Table 3-39).

Table 3-39: Thambisetty et al, (2010) findings: Plasma proteins identified by LC-MS/MS in 18 2DGE spots consituting the PLS-DA model for predicting brain amyloid burden 10 years later. Proteins highlighted are those successfully replicated in this discovery study.

Spot ID	Protein ID	Accession No.
370	Apolipoprotein-E precursor	P02649
1679	Apolipoprotein-E precursor	P02649
1676	Apolipoprotein-E precursor	P02649
1659	Apolipoprotein-E precursor	P02649
1669	Apolipoprotein-E precursor	P02649
1644	Apolipoprotein-E precursor	P02649
534	Plasminogen precursor	P00747
533	Plasminogen precursor	P00747
713	No ID obtained	
784	Complement C3 precursor	P01024
748	Complement C3 precursor	P01024

91	Complement C3 precursor	P01024
660	Complement C3 precursor	P01024
385	Haptoglobin precursor	P00738
1340	Serum albumin precursor	P02768
925	Serum albumin precursor	P02768
1544	Serum albumin precursor	P02768
1595	Ig gamma-1 chain C region	P01857

However their main finding was protein apolipoprotein-E (ApoE), which was present in 6 out of their 18 spots, and was previously known to be associated with AD. Using enzyme-linked immunosorbent assays (ELISA) they also validated ApoE in plasma samples concurrent to the PiB PET scan, showing that it could predict amyloid burden concurrently as well as 10 years prior. Although this study used the same cohort of healthy individuals (BLSA), and same proteomic discovery tool, ApoE was not found as a candidate biomarker of amyloid burden at any time point. This may be explained by different statistical analysis approaches; Thambisetty et al (2010) used a PLS-DA regression model to predict group classification (high and low amyloid burden), whereas this study used an elastic-net regression model and kept amyloid load as a continuous variable. Additionally, differences in protein identification from LC-MS/MS data may be responsible for the discrepancy between the studies. Here we used a novel '2 out of 3' approach to determine abundant proteins present in a 2DGE spot. ApoE was in fact present in 1 spot significantly related to amyloid load at T12 (concurrently). Abundance ranking using a 'unique peptide count' approach ranked ApoE as abundantly present in the spot, however the protein did not pass the 2 out of 3 criteria and was therefore not considered as a candidate biomarker. This highlights the importance of analysis methodology selection. More work is needed to determine the best approaches and to then standardise them across studies.

3.4.7 Conclusions

Using a well established discovery proteomic technique this investigation identifies longitudinal biomarker signatures in plasma that differ between individuals with and without neuropathological and clinical hallmarks of AD. Our findings support previous reports that plasma biomarkers have the potential to be used as a screening tool for AD. These findings also provide novel insights into the longitudinal preclinical stages of AD and suggest that we may also be able to screen for the disease at a preclinical stage. We identified numerous candidate biomarkers, many of which have been previously been reported as AD biomarkers in case v control cohorts, providing further evidence for such biomarkers and supporting their utility as biomarkers longitudinally throughout the disease. Quantitative assays are now needed to validate the proteins reported here as candidate biomarkers. Approaches to such assays also need to be standardised across studies. If validated these proteins may, independently or in combination, provide a biomarker for preclinical AD diagnosis or allow predication of disease onset.

In a lot of cases, both in the literature and in the results reported here, reports show conflicting evidence of a proteins role in AD. The 2DGE results here show that for some candidate biomarkers the protein was present in many different areas of the gel indicating that perhaps the proteins have undergone conformational or post translational changes. These changes themselves may be biomarkers of AD pathology and it would be interesting to further investigate these.

The proteins found here to be longitudinally implicated in preclinical AD are involved in a variety of systems, including; complement and inflammation, coagulation, hemostasis, fibrinolysis, and BBB integrity. Such systems may be causally related to AD onset, or be affected as a result of the disease. Additionally the involvement of these systems in AD pathology may be inter-linked or they may act independently, further work is needed to clarify these relationships. It may be possible to identify the resulting contribution of some of these pathways (e.g. chronic inflammation) as high risk factors for the development of AD in healthy individuals, comparable to that of more-established risk factors such as *APOE* ε4 status. At the

very least, the presence of these biomarkers in healthy elderly individuals indicates potential early intervention targets worthy of further investigation.

Acknowledgment

I am very grateful to Dr Emanuela Leoni for her help conducting the large number of 2DGE experiments required for this chapter.

Chapter 4. Discovering low molecular weight proteins as longitudinal biomarkers of early Alzheimer's disease pathology and cognitive decline using liquid chromatography-tandem mass spectrometry

4.1 Introduction

Low abundant proteins play important roles in major biological processes such as cell cycle control and stress response. Despite their importance they are under-represented in the current proteomic literature, most likely due to difficulty in detection compared to more abundant proteins. The plasma protein concentration range spans up to twelve orders of magnitude[295] and many current proteomic approaches are only capable of sensitively covering three or four of these. The 20 most abundant proteins account for approximately 97% of the total protein mass, these include; albumin, immunoglobulin, fibrinogen, alpha 1-antitrypsin, alpha 2-macroglobulin, transferrin and lipoproteins. Albumin on its own can represent over 50% of total plasma protein. Highly abundant proteins like these increase the protein concentration to around 80mg/ml yet there are many proteins present in the ng/ml range, or lower, which can be masked by such abundant proteins and so remain undetected. Dynamic range coverage will be a limitation of most proteomic techniques. Methods that help to access low abundance proteins by reducing the complexity of the plasma through depletion and prefractionation strategies are needed to enable the detection of less abundant and low molecular weight (LMW) proteins, especially when using complex samples such as plasma.

In Chapter 3 a discovery phase investigation into longitudinal preclinical AD biomarkers was presented using 'two dimensional gel electrophoresis' (2DGE). Although an extremely useful proteomic technique 2DGE does have limitations that need to be addressed when aiming to conduct a thorough analysis of the plasma proteome. The main limitation 2DGE places on our biomarker discovery investigation is its restricted dynamic range (~10^4)[296]. In our 2DGE experiments a 10% polyacrylamide gel was used which is able to accurately resolve proteins in a molecular weight range of approximately 20-250kDa. This study aimed to provide a complementary evaluation of the proteome and so focused on the extraction and analysis of proteins with a molecular weight of <30kDa. Together it was hoped that a

more comprehensive analysis of the plasma proteome could be achieved for the discovery of preclinical AD biomarkers.

Liquid chromatography-tandem mass spectrometry (LC-MS/MS) is an analytical technique that measures the mass-to-charge ratio of ionised particles and offers superior sensitivity and specificity for LMW analytes compared to 2DGE. LC-MS/MS also enables a clear identification of proteins whose levels change as biomarkers, unlike 2DGE where multiple proteins may be identified within a statistically significant spot. The use of complex samples such as plasma can increase the variability of the liquid chromatography separation stage, however as the majority of steps taken in LC-MS/MS are automated the technique overall is subject to less variance than 2DGE. For these reasons LC-MS/MS was chosen as the discovery tool here. LC-MS/MS methodology was firstly optimised for the discovery of LMW proteins. Following optimisation LMW proteins were targeted and analysed for the discovery of preclinical AD biomarkers.

4.2 Aims

To optimise an in-solution label free LC-MS/MS methodology to allow the detection of LMW, low abundance, plasma proteins, enabling a complementary evaluation of the proteome to that already conducted using 2DGE.

To identify LMW, low abundance proteins predictive of amyloid load using the optimised LC-MS/MS methodology. To discover the most predictive proteins at each time point (12 years prior, 6 years prior, and concurrently) using multivariate analyses of proteins against quantitative amyloid imaging measures (^{11}C-PiB PET DVR). Additionally using the same proteomic technique LMW, low abundance proteins longitudinally related to brain atrophy and cognitive decline will be identified.

4.3 Results

4.3.1 LC-MS/MS optimisation

LC-MS/MS has shown great utility in detecting LMW analytes in clinical applications such as drug and toxicology testing, biochemical genetics, and

endocrine testing of steroids (Grebe et al, (2011)[297] and Ponnayyan-Sulochana et al, (2014)[298] review some of these), However, work is still needed to optimise LC-MS/MS for the detection of LMW protein/peptides as biomarkers. In order to target and quantify LMW proteins in this study LC-MS/MS sample preparation needed to be optimised.

Firstly an in-solution based approach was chosen as it is simpler in terms of sample handling and has increased speed over gel based approaches. Secondly we considered labelled versus label-free approaches for protein quantification with mass spectrometry. Although technological advancements in mass spectrometers have dramatically enhanced their sensitivity and resolution, extracting reliable protein abundance information from either approach remains challenging. Although labelled approaches are more quantitative and require less sample runs, label free approaches are increasingly popular and were chosen for this experiment due to the quick and straightforward sample preparation, cheaper costs, and less complex data analysis compared to a labelled approach. Label free approaches also avoid the biases and reduced sensitivity that chemical derivatisation can cause in labelled approaches.

Sample preparation options considered and compared during optimisation experiments included; proteolytic digestion, abundant protein depletion, molecular weight cut off filter, and de salting. Other factors affecting the extraction of LMW proteins explored include; the duration of the chromatography separation and the gradient conditions, number of sample injections, volume and concentration of starting plasma used, and plasma loading volume for the orbitrap mass spectrometer.

For method optimisation experiments three random healthy control plasma samples were selected to be used throughout the optimisation (mean protein concentration = 66.2mg/ml). These samples had been in frozen storage since 2010 and had one previous freeze-thaw cycle. For optimisation experiments, all data was analysed in Excel. The numbers of LMW proteins detected by each method were summed and the protocol with the greatest number of LMW proteins was selected, whilst considering the time and cost taken to complete each step.

Depletion of high MW proteins, LMW cut off filter (30kDa), and desalt (ZipTip)

To enable access to LMW proteins, molecular weight (MW) cut off filters can be used to obtain a plasma filtrate containing only proteins smaller than the MW filter of choice. In addition depletion strategies aiming to remove highly abundant, high MW proteins are often successfully implemented, allowing easier access to the LMW proteome. Here a 30kDa cut off filter was considered and its performance was measured when used independently or in combination with a depletion column. In addition, buffers used during these two methods may introduce excess salt into the sample, and therefore a ZipTip desalt was also considered (Figure 4-1). 50µl of each plasma sample was analysed and all techniques were conducted as described in the methods chapter. The number of proteins identified for each approach is detailed in Table 4-1.

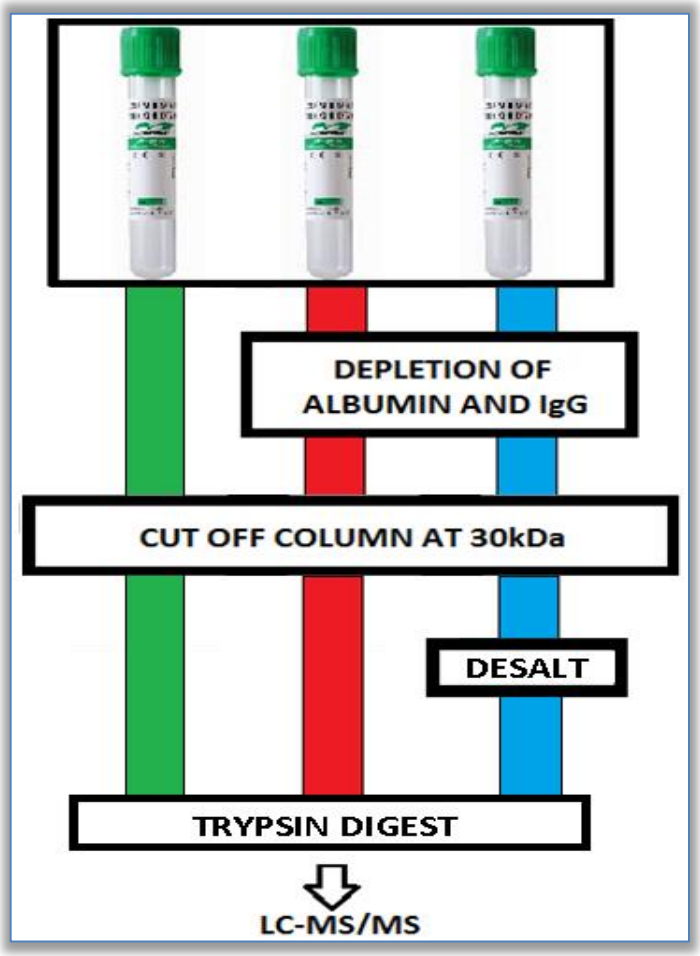

Figure 4-1: Label free LC-MS/MS optimisation for low molecular weight (MW) proteins (<30kDa). Green; 30kDa cut off filter only. Red; Depletion of albumin and IgG, followed by a 30kDa cut off filter. Blue; Depletion, 30kDa cut off filter, and ZipTip desalt. All samples were trypsin digested before analysis by LC-MS/MS.

Table 4-1: Number of proteins detected by LC-MS/MS following depletion, LMW protein cut off filter, and desalt.

Method	No. of proteins identified by LC-MS/MS
30kDa cut off filter	138
Depletion (albumin and IgG) & 30kDa cut off filter	109
Depletion (albumin and IgG), 30kDa cut off filter, & desalt	117

Although the 30kDa cut off only method identified the highest number of proteins, when looking in detail at the mass spectrometry output a lot of albumin and other high MW proteins were still being detected. As a CID top 20 search was being conducted the high MW proteins still present in the sample were preventing other less abundant, LMW, proteins from being identified. Therefore, although adding the depletion step reduced the overall number of proteins detected, it increased the detection of smaller less abundant, LMW, proteins. The ZipTip desalting step did further increase the number of proteins detected, though not dramatically. When factoring in the time taken to perform this additional step it isn't likely to be worthwhile. Therefore depletion and 30kDa cut off filter was selected as the optimal prefractionation methodology.

Proteolytic digestion (trypsin digest)

An important step in sample preparation for mass spectrometry proteomics is the conversion of proteins to peptides and in most cases trypsin is used as the proteolytic enzyme. Trypsin is a protease that specifically cleaves the proteins creating peptides in the preferred mass range for MS sequencing and with a basic residue at the carboxyl terminus of the peptide. This produces information-rich, easily interpretable peptide fragmentation mass spectra. However, due to their size, LMW proteins produce low numbers of proteolytic peptides through tryptic digestion. After plasma depletion (albumin and IgG) and MW filtering (30kDa cut off) it may be possible to detect many very small proteins via LC-MS/MS without a digestion step. Therefore

using depleted and filtered plasma a comparison between undigested and digested aliquots was performed to investigate the benefit of performing a digestion step and determine whether the time invested in this step was worthwhile for the detection of LMW proteins (Figure 4-2).

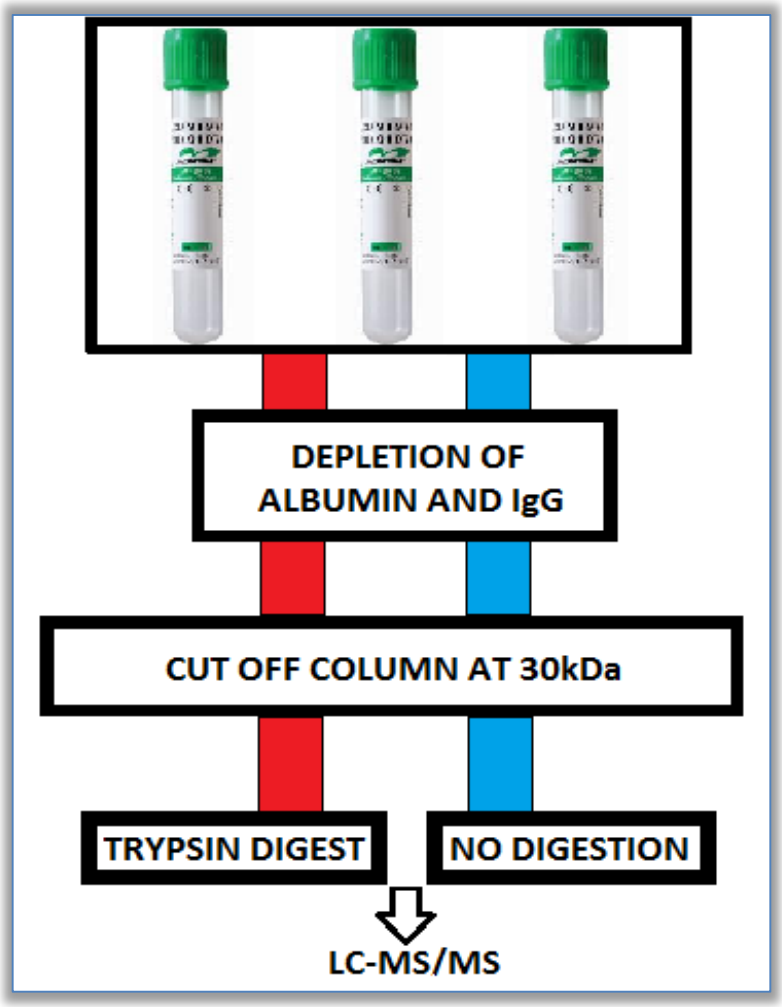

Figure 4-2: Experimental design for comparison of trypsin digest (red) versus non-digested plasma (blue).

50µl of each plasma sample was firstly depleted of albumin and IgG, the depleted sample was then passed through the 30kDa cut off filter column. Approximately 50µl of filtrate was produced (mean filtrate concentration = 0.46mg/ml), from which two 25µl aliquots were prepared. One aliquot was digested using trypsin, the other aliquot was left undigested. Table 4-2 below details the number of proteins identified via LC-MS/MS for each approach. Performing a tryptic digest enabled the identification of many more proteins.

Table 4-2: Number of proteins identified by LC-MS/MS for a trypsin digested and non-digested sample.

Method	No. of proteins identified
Endogenous	32
Trypsin	241

Run time: 35min, 1 hour, and 2 hour gradients

In a complex sample such as plasma many peptides will co-elute at any given time point during reverse-phase chromatography. Many of these co-eluting peptides will not be identified. One way in which to improve the chromatographic performance is to increase the gradient length, which in turn generally increases the number of peptides identified[299]. However this also drastically increases the sampling time of the entire analysis. Here we considered three gradients of varying lengths (35 minutes, 1 hour, and 2 hours) and compared the number of unique proteins identified by each, whilst considering the time taken to perform each option.

50ul of each depleted (albumin and IgG), filtered (30kDa cut off), and trypsin digested plasma sample was loaded onto the mass spectrometer for LC-MS/MS analysis. Each sample was injected three times with varying gradient lengths (35 minutes, 1 hour, and 2 hours) (Figure 4-3).

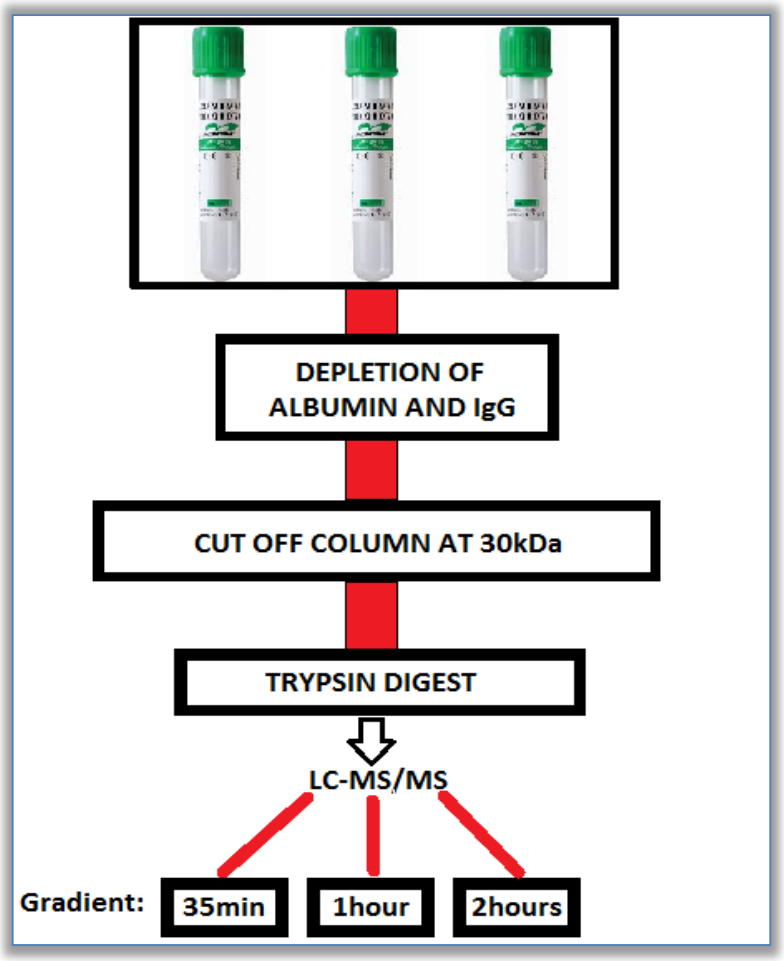

Figure 4-3: Experimental design for the comparison of gradient lengths; 35 minutes, 1 hour, and 2 hours.

Table 4-3 lists the number of proteins identified via LC-MS/MS for samples with varying liquid chromatography gradient lengths. The longer the gradient the more proteins were identified, however the 1 hour run was optimal as very few additional proteins were identified by doubling the run time to 2 hours.

Table 4-3: Number of proteins identified by LC-MS/MS for samples with varying liquid chromatography gradient lengths

Method	No. of proteins identified
35 minutes	71
1 hour	172
2 hours	179

Starting plasma volume and protein concentration

The Sigma depletion column protocol suggests that up to 50µl of plasma can be loaded onto the columns but that the column efficiency will improve with smaller volumes. The suggested range in which binding of IgG and albumin will be optimal is 25-50µl of plasma. Therefore 25µl and 50µl of starting plasma were compared for their performance when aiming to detect LMW, low abundance proteins. In addition, the effects of protein concentrations on tryptic digestion performance were considered; before digestion each sample was split into two aliquots of 15µg and 30µg total protein (Figure 4-4).

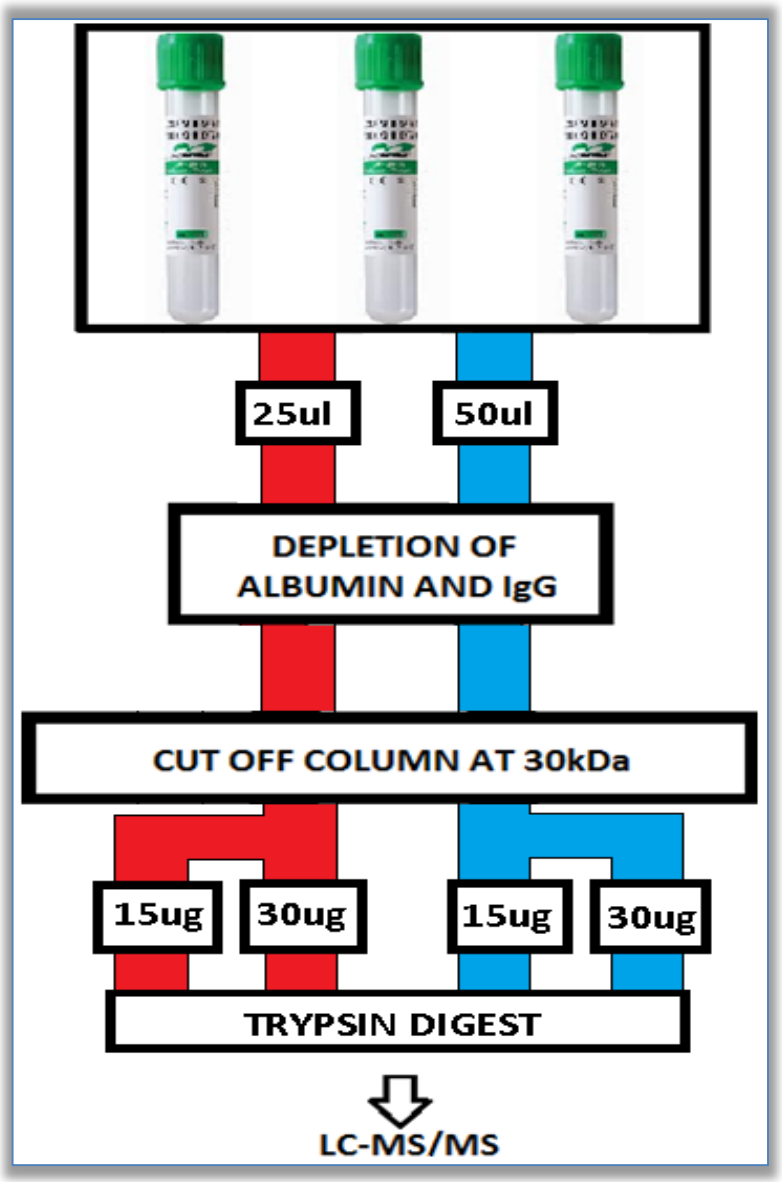

Figure 4-4: Experimental design for the comparison of 25ul (red) and 50ul (blue) starting plasma volumes, and subsequent protein concentration for trypsin digestion (15ug and 30ug).

25µl and 50µl of each plasma sample were pipetted onto depletion columns. Each depleted plasma eluate was then filtered through a 30kDa cut off column. Next, protein concentration of the resulting filtrate was determined by a nanodrop, then the sample was split into two aliquots of 15µg and 30µg of total protein. These aliquots were then trypsin digested and analysed by LC-MS/MS. The results below were obtained whilst the orbitrap was not functioning at peak level due to high analytical column pressure, and deteriorating electron multiplyer performance. This appeared to reduce the overall number of proteins detected for this experiment. Although protein detection may be higher when the orbitrap is optimally functional, the relative amount of proteins detected for each method tested should be similar allowing me to draw conclusions from these results.

Table 4-4 displays the results of these comparisons. From these results 25µl/15µg was selected as the optimal combination.

Table 4-4: Number of proteins identified by LC-MS/MS for 25µl and 50µl starting plasma 15µg and 30µg concentrations.

Plasma volume	Protein load	No. of proteins identified
25µl	15µg	45
	30µg	27
50µl	15µg	15
	30µg	42

To ensure an equal amount of protein was depleted across samples it was important to standardise the protein load onto the depletion columns. Discovery experiments would utilise samples from BLSA subjects; previous 2DGE experiments had shown the average protein concentration for these samples to be around 60mg/ml. Consequently a 25µl plasma sample aliquot would have approximately 1500µg (1.5mg) protein. Therefore 1500µg protein was selected to be loaded onto the depletion column. The first step of the depletion protocol was to dilute the plasma sample to 100ul in equilibration buffer. This ensured that equal volumes were being loaded onto the depletion columns.

Protein concentration for LC-MS/MS analysis

The suggested capacity of the orbitrap loading columns is 2µg of protein. This capacity may be flexible when using a depleted plasma sample consisting mainly of LMW proteins without the heavy presence of large abundant proteins such as albumin and IgG. To identify the optimal amount of protein to load onto the LC-MS/MS column a comparison of 1µg, 2µg, 3µg, and 4µg amounts was performed, and the number of proteins identified with each was compared.

Plasma samples were pooled together, depleted (albumin & IgG), filtered (>30kDa cut off), and then trypsin digested. Protein concentration of the resulting plasma was determined by a nanodrop, and a 15µg aliquot was prepared. This aliquot was lyophilised and re-suspended in 30µl (0.1% FA, 20% ACN, ddh$_2$0) resulting in a concentration of 0.5µg/µl. This sample was then loaded onto the mass spectrometer for LC-MS/MS analysis with three injections of 2µl, 4µl, 6µl, and 8µl (Figure 4-5).

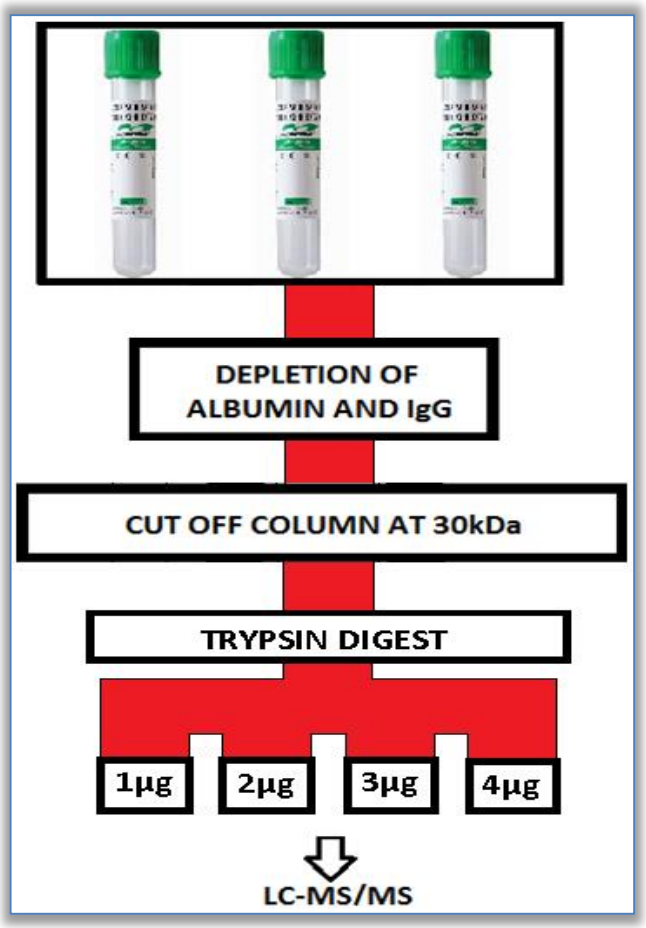

Figure 4-5: Experimental design for the comparison of protein loads for LC-MS/MS analysis

Table 4-5 lists the number of proteins identified for each protein quantity injected for LC-MS/MS analysis. As noted for the previous experiment the orbitrap was not functioning at peak level for this experiment, resulting in reduced protein detection, though relative amount of proteins detected for each method tested should be similar allowing me to draw conclusions from these results.

Overall each injection yielded comparable numbers of proteins, indicating that the column may already be saturated at 1µg. However, 8µl (4µg) did result in slightly increased protein detection and will therefore be selected as the optimal loading amount.

Table 4-5: Number of proteins identified by LC-MS/MS

Injection volume	No. of proteins identified
2ul (1µg)	46
4ul (2µg)	50
6ul (3µg)	51
8ul (4µg)	58

4.3.2 LC-MS/MS discovery study

Following optimisation experiments the resulting method selected to detect and analyse LMW proteins for preclinical AD biomarker discovery was; ~25µl starting plasma volume (1500µg protein), albumin and IgG depletion, 30kDa cut off filter column, tryptic digestion of 15µg, 8ul injection (0.5µg/µl), and a 1 hour gradient. All stages were performed as detailed in the methods chapter (chapter 2).

Tabb et al 2010[198] found that the repeatability of a label free proteomic sample was poor in that only half of the peptides discovered in an initial LC-MS/MS sample will be identified in a second replicate. This implies that the total number of peptides identified grows rapidly for the first few replicates. The authors suggest that by collecting data on a sample in triplicate is a way in which researchers can improve the sampling of complex samples. Therefore the plasma samples here were injected

in triplicate. This was also considered to aid spectral counting as larger numbers of peptides (summed data across triplicates) will enhance the ability to detect subtle changes in protein abundance. The final experimental workflow is illustrated in Figure 4-6.

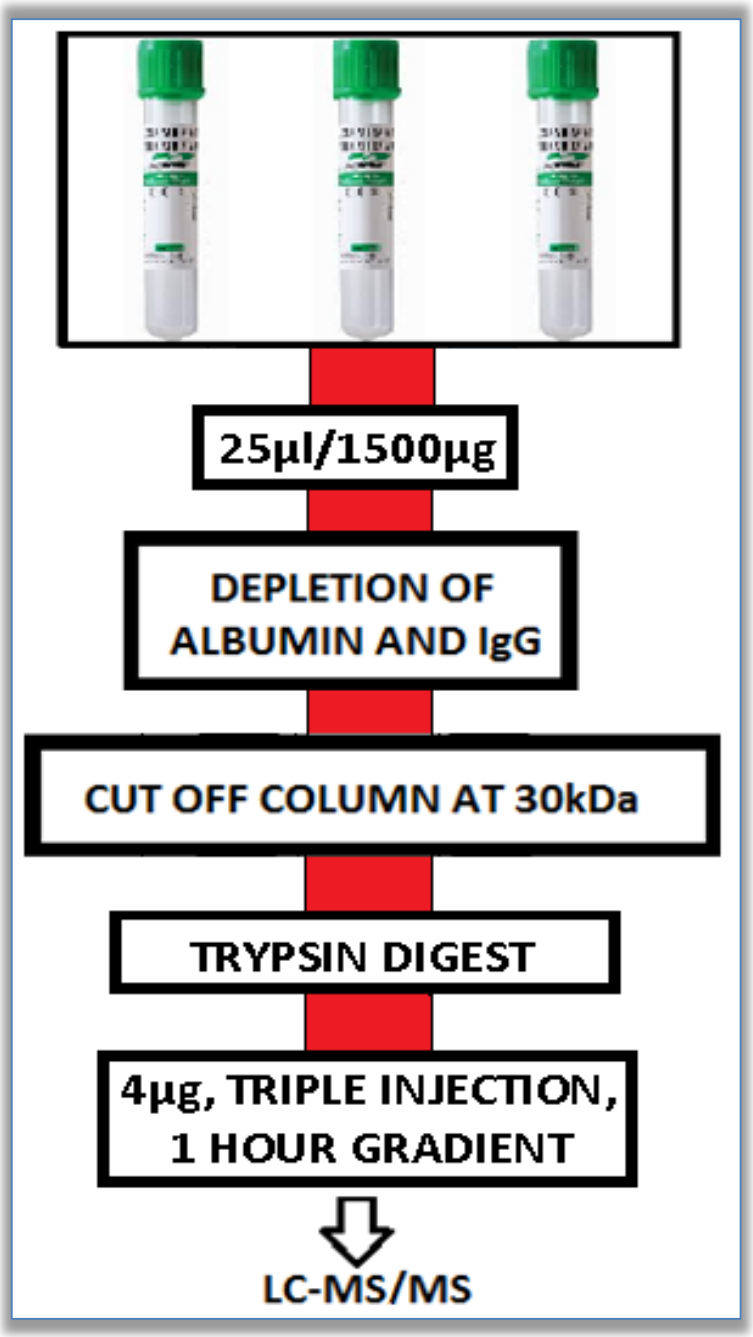

Figure 4-6: Final experimental workflow following optimisation for LMW protein discovery.

4.3.3 Demographic characteristics

Discovery phase experiments included 25 healthy individuals from the Baltimore Longitudinal Study of Aging (BLSA) neuroimaging cohort previously described (Chapter 2). These individuals all had one PiB PET scan, serial structural MRI (sMRI) scans and serial cognitive assessments. Samples from all 25 individuals had previously been included in the 2DGE discovery phase experiments.

From all 25 individuals, plasma samples were drawn from three time points (75 sample aliquots in EDTA). Time points corresponded to neuroimaging visits ~6 years apart (baseline, T6 = 6+/-2 years, and T12 = 12+/-2 years). Samples at the third time point (T12) were concurrent to the subjects PiB PET scan. Table 4-6 below summarises the demographic characteristics of the study population at baseline.

Table 4-6: Subject demographics

	N	Mean age at baseline	Std. dev
Female	13	66.31	6.25
Male	12	66.67	4.98
Total	25	66.48	5.56

Table 4-7 below displays the mean distribution volume ratios (DVR) per gender, and when the PiB PET scan was conducted (mean number of years after baseline).

Table 4-7: Subject PiB PET DVR information

	N	Mean PiB PET DVR	Mean no. years post baseline of PiB PET scan
Female	13	1.08	11.71
Male	12	1.10	11.55
Total	25	1.09	11.63

4.3.4 Protein count

To enable a full longitudinal analysis proteins must be measured at all three time points. A simple Venn diagram was constructed to illustrate the number of proteins at each time point and where they overlap. Figure 4-7 displays the number of proteins identified at each time point. 107 proteins were measured at all three time points allowing a longitudinal analysis of these proteins.

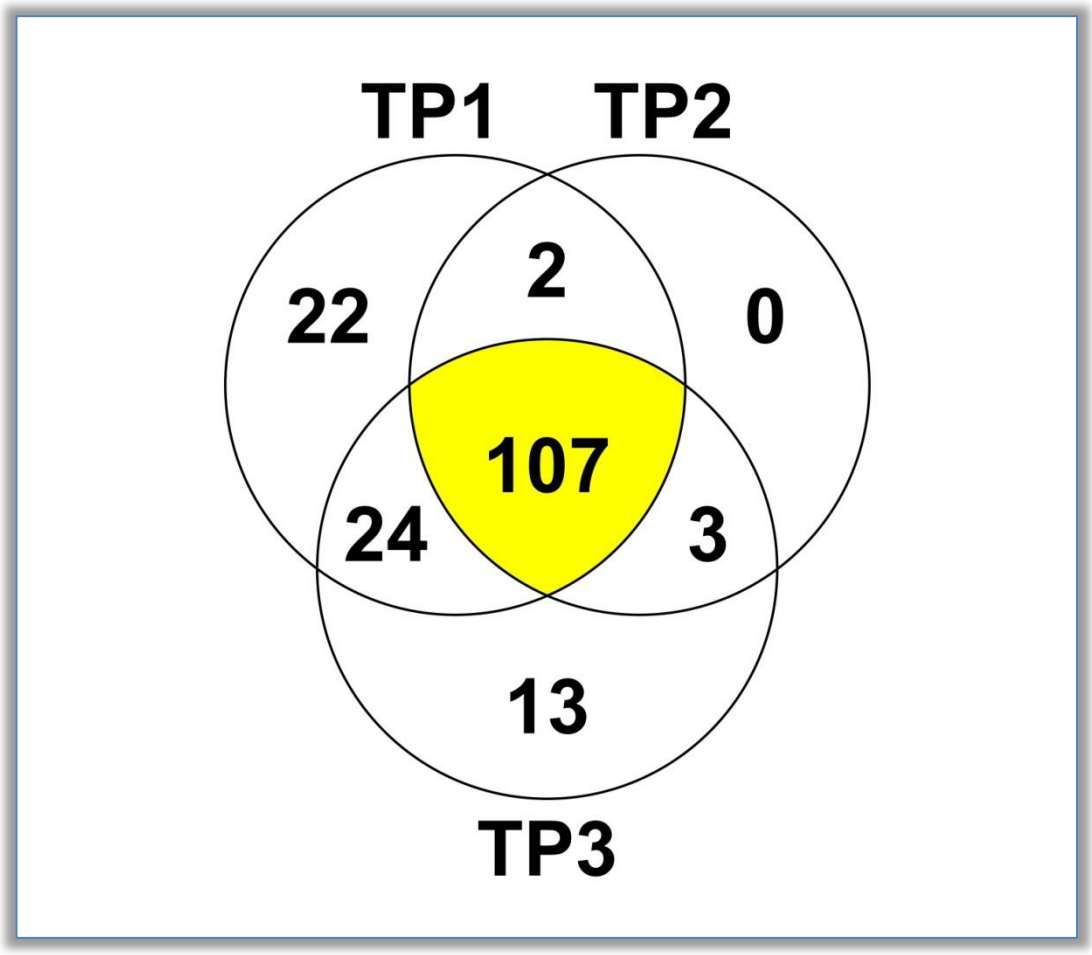

Figure 4-7: Venn diagram illustrating the number of proteins identified by LC-MS/MS at each time point, following strict filtering in Scaffold (95% protein threshold, minimum of 2 peptides matched, and 80% peptide threshold).

4.3.5 Coefficient of variation (CV)

To be able to discriminate proteomic differences between samples based upon spectral counts, the spectral count data across multiple injections of the same sample must normally be found to have low variability. Coefficients of variation (CVs),

which compare the standard deviation to the mean for these counts, were therefore computed.

CV calculations were performed on normalised total spectral counts for each run rather than absolute values as with no blank runs in between replicates slight variations in the chromatography sensitivity may be present. These normalised values were automatically calculated by Scaffold software. This normalisation entailed averaging the spectral counts for all of the samples and then multiplying the spectrum counts in each sample by this average, divided by the individual sample's sum. This normalisation procedure works when individual proteins may be up or down regulated within a sample, but the total amount of protein within each sample is approximately the same.

As proteins with >50% missing data were to be excluded from statistical analysis CVs were only calculated for proteins with <50% missing data. The overall experiment mean within-subject CV was 34.6982%. The mean CV's per time point were: baseline = 30.88%; T6 = 35.72%, and T12 = 37.47%.

It is important to consider that CVs are not ideal for this form of data as LMW proteins with very low numbers of peptides identified are more likely to have very high CVs. Additionally it is known that in complex samples such as plasma the repeatability of peptides discovered in an initial LC-MS/MS injection compared to following replicates is low, with only approximately 50% replicating [198]. Therefore the CVs achieved were considered to be acceptable for this dataset, though further statistical analysis would be conducted on summed spectral count values, rather than means.

4.3.6 Normality tests

LC-MS/MS data was pre processed using Proteome Discoverer 1.4 and Scaffold 4 (Proteome Software Inc, USA) as previously described (chapter 2). Spectral counts for triplicate injections were summed and combined into one BioSample and the Normalised Total Spectra quantitative values were calculated and exported into Excel for statistical analysis.

Normality tests were performed to determine the normality of the protein distributions. Proteins with more than 50% missing data were discarded. A Kolmogorov-Smirnov test for normality indicated that 48%, 67%, and 32% of the remaining protein distributions were normally distributed ($p>0.05$) at baseline, T6, and T12 respectively. Protein data was then logged (base 10) to minimise skewness and non-normal distributions and normality tests were repeated. Kolmogorov-Smirnov tests on logged spot data indicated that 90%, 71%, and 87% of the protein distributions were normally distributed ($p>0.05$). Logged data was therefore used for the following statistical analyses.

4.3.7 Analysis of plasma proteins associated with amyloid load as measured by PiB PET DVR

Partial correlations

Partial correlation was used to identify small proteins that have a relationship with amyloid load. Proteins correlating with ^{11}C-PiB PET DVR at each time point, whilst controlling for age, gender, education (years), body mass index (BMI), cholesterol, and *APOE* ε4 status were identified.

Partial correlations at baseline, T6, and T12 revealed 5, 2, and 2 proteins, respectively, which significantly correlated with PiB PET DVR 12 years later, 6 years later and concurrently ($p<0.05$). Additionally 3 proteins at baseline, and 1 protein at T12 tended towards significance ($p<0.1$). Significant and tending towards significance results are displayed in Table 4-8 for baseline, Table 4-9 for T6, and Table 4-10 for T12. Full results are reported in appendix 6 (baseline) appendix 7 (T6) and appendix 8 (T12).

Table 4-8: Baseline partial correlation results for proteins with PiB PET DVR. Table lists significant (red, $p<0.05$) and tending towards significance (green, $p<0.1$) proteins. Proteins ranked in order of significance based on *p* value. Full length protein MW and percentage of data available also listed.

Protein	Correlation coefficient	*P*-value	MW (kDa)	Complete data (%)
Complement C4 B	-0.498	0.022	193	96
Leucine rich alpha 2 glycoprotein 1	0.607	0.022	39	64
Zinc alpha 2 glycoprotein	0.478	0.025	34	100
Ig kappa chain C region	0.455	0.035	12	100
Fibrinogen beta chain	-0.471	0.038	56	92
Fibrinogen alpha chain	-0.429	0.050	95	100
Apolipoprotein A IV	-0.420	0.056	45	100
Beta 2 microglobulin	0.482	0.068	14	76

Table 4-9: T6 partial correlation results for proteins with PiB PET DVR. Table lists significant proteins (red, $p<0.05$). No proteins were found here to be tending towards significance ($p<0.1$). Proteins ranked in order of significance based on *p* value. Full length protein MW and percentage of data available also listed.

Protein	Correlation coefficient	*P*-value	MW (kDa)	Complete data (%)
Complement C3	-0.567	0.017	187	91
Fibrinogen alpha chain	-0.477	0.042	95	100

Table 4-10: T12 partial correlation results for proteins with PiB PET DVR. Table lists significant (red, $p<0.05$) and tending towards significance (green, $p<0.1$) proteins. Proteins ranked in order of significance based on *p* value. Full length protein MW and percentage of data available also listed.

Protein	Correlation coefficient	*P*-value	MW (kDa)	Complete data (%)
Alpha 1 acid glycoprotein 2	0.520	0.043	24	73
Beta 2 microglobulin	0.574	0.047	14	61
Complement C4 B	-0.391	0.079	193	92

4.3.8 Analysis of plasma proteins longitudinally associated with brain atrophy

Longitudinal volume data was available for 22 sMRI brain regions. Based on the ANOVAs conducted on these volumes in Chapter 3, 16 brain regions were known to display a linear change over time and were therefore suitable to be longitudinally assessed using mixed-effects regression models (MRM) as follows.

Mixed-effects regression model

Longitudinal slope comparisons between protein values and sMRI brain volumes were performed using mixed-effect regression models with age, gender, education, BMI, cholesterol and *APOE* ε4 status as covariates. Significant results ($p<0.05$) and those tending towards significance ($p<0.1$) are reported in Table 4-11 below, for full results see appendix 9.

Table 4-11: Mixed-effects regression model results for protein values with sMRI brain regions. Table lists significant (red, $p<0.05$) and tending towards significance (green, $p<0.1$) proteins. Proteins ranked in order of significance based on *p* value. Full length protein MW and the percentage of data available across subjects is also listed.

sMRI region	Protein	Coefficient	*p*-value	MW (kDa)	Complete data (%)
Cingulate Gyrus	Antithrombin III	-1674.270	0.002	53	79%
	Zinc alpha 2 glycoprotein	1022.783	0.034	34	97%
	Alpha 1 acid glycoprotein 1	1155.158	0.100	24	100%
Frontal Gray Matter	Alpha 1 acid glycoprotein 1	8162.499	0.044	24	100%
	Zinc alpha 2 glycoprotein	5446.128	0.052	34	97%
	Complement C3	-5151.136	0.053	187	89%
Grey Matter	Zinc alpha 2 glycoprotein	15675.255	0.046	34	97%
	Antithrombin III	-15127.422	0.089	53	79%
Hippocampus	Apolipoprotein E	285.516	0.034	36	68%
	Serum albumin	-209.756	0.069	69	77%
	Inter alpha trypsin inhibitor heavy chain H4	-208.944	0.080	103	100%

Inferior Occipital Gyrus	Transthyretin	786.319	0.025	16	100%
	Apolipoprotein A IV	539.710	0.087	45	94%
Medial Frontal Gyrus	Antithrombin III	-1312.703	0.027	53	79%
	Serotransferrin	-1124.889	0.063	77	100%
Middle Frontal Gyrus	Alpha 1B glycoprotein	-1750.054	0.033	54	75%
	Antithrombin III	-2063.618	0.036	53	79%
	Alpha 1 acid glycoprotein 2	-2241.501	0.078	24	74%
	Apolipoprotein E	2980.132	0.081	36	68%
Middle Occipital Gyrus	Complement C3	-833.235	0.029	187	89%
	Zinc alpha 2 glycoprotein	873.585	0.056	34	97%
	Ig kappa chain C region	1256.919	0.063	12	83%
	Alpha 1B glycoprotein	815.878	0.098	54	75%
Middle Temporal Gyrus	Zinc alpha 2 glycoprotein	1869.463	0.036	34	97%
	Ig kappa chain C region	-2493.314	0.041	12	83%
	Antithrombin III	-1672.213	0.060	53	79%
	Transthyretin	1823.895	0.097	16	100%
Superior Frontal Gyrus	Antithrombin III	-1079.660	0.077	53	79%
	Transthyretin	1146.474	0.081	16	100%

Superior Occipital Gyrus	Beta 2 microglobulin	-1331.366	0.026	14	71%
Superior Temporal Gyrus	Alpha 1 antitrypsin	2688.158	0.021	47	100%
	Zinc alpha 2 glycoprotein	1584.460	0.027	34	97%
	Apolipoprotein A I	-1502.111	0.078	31	75%
Temporal Gray	Antithrombin III	-3831.437	0.075	53	79%
	Zinc alpha 2 glycoprotein	3379.500	0.092	34	97%
	Ig kappa chain C region	-4767.157	0.099	12	83%
Ventricles	Transthyretin	-3403.640	0.053	16	100%
Whole brain	Apolipoprotein E	17064.433	0.073	36	68%
	Antithrombin III	-12999.327	0.079	53	79%

4.3.9 Analysis of plasma proteins longitudinally associated with cognitive decline

Longitudinal cognitive data was available for 12 cognitive measurements. Based on the ANOVAs conducted on these measures in Chapter 3, only one measure, Trails B, was known to show a linear change over time and was therefore suitable to be assessed using a mixed effects regression model as follows.

Mixed-effects regression model

A longitudinal slope comparison between protein values and Trails B score was performed using a mixed effects regression model with age, gender, education, BMI, cholesterol and *APOE* ε4 status as covariates. Significant results ($p<0.05$) and those tending towards significance ($p<0.1$) are reported in Table 4-12 below, for full results see appendix 10.

Table 4-12: Mixed-effects regression model results for protein values with cognitive measures. Table lists significant (red, $p<0.05$) and tending towards significance (green, $p<0.1$) proteins. Proteins ranked in order of significance based on *p* value. Full length protein MW and the percentage of data available across subjects is also listed.

Cognitive measure	Protein	Coefficient	*p*-value	MW (kDa)	Complete data (%)
Trails B	Fibrinogen alpha chain	-26.689	0.008	95	97%
	Apolipoprotein A IV	-22.119	0.025	45	94%
	Apolipoprotein E	-21.913	0.086	36	68%

4.4 Discussion

4.4.1 Optimisation of label free LC-MS/MS for the detection of LMW proteins

Optimisation experiments revealed that, from the methods considered here, the best way in which to access low abundance, LMW proteins for analysis is to utilise depletion and MW cut off filter columns in combination. It is important to remember though that potentially important biological information may be lost during depletion as certain proteins/peptides may be bound to the highly-abundant proteins removed[300]. Nevertheless it is important to access this LMW fraction of the proteome for biomarker discovery and previous studies have shown the successful use of depletion strategies for this purpose[301]. The method presented here was a simple and fast procedure to remove the most abundant proteins obscuring low abundance, LMW proteins, and hindering their detection. The removal of albumin and IgG allowed a higher load of less abundant, LMW proteins to be included in mass spectrometry analysis and increased the number of LMW proteins detected.

4.4.2 LC-MS/MS experimental performance and analysis

Many LMW proteins were identified using the optimised methodology, however they were not all consistently identified between individuals. Consequently many

LMW proteins had large amounts of missing data. Here proteins with >50% missing data were excluded from statistical analysis, and although this included many LMW proteins it was necessary to discard these as there was not sufficient data from which meaningful conclusions could be drawn. Furthermore, within-subject protein detection and quantification was not consistent between sample injections, with an overall mean CV of 37% even when proteins with >50% missing data had been removed. This is comparable to the CV the 2DGE experiments (33.52%, chapter 3). Yet for our purposes this level of replication was acceptable for two reasons. Firstly LMW proteins were expected to have high CVs, due to the low number of peptides available for detection. Secondly, it is known that only 50% of the peptides discovered in an initial LC-MS/MS injection may be replicated in a second, drastically increasing the expected CV[198]. The purpose of completing three injections for this experiment was not to accurately replicate between injections, but rather to increase the number of peptides and proteins identified for each individual so that a summation of the data obtained across injections, rather than mean values, could be used for analysis. This approach should have also reduced the amount of missing data, by allowing three attempts at detecting protein levels across individuals. However large amounts of missing data were still present, indicating the methodology needs to be further optimised, perhaps by further increasing the number of injections.

To account for poor repeatability, samples were analysed in triplicate to obtain a greater chance of detecting all peptides present. The data from the triplicate injections was then summed, and this summed value was used for analysis. However this approach causes an issue for the analysis of proteins of low abundance that should be considered: more abundant proteins are likely to be detected in all three triplicate injections and therefore a summation of all three would lead to large values of these proteins for statistical analysis. Conversely, less abundant proteins may be detected in only one or two injections, resulting in small values for statistical analysis. It would therefore be easier to detect a significant change in the proteins of larger abundance for which more data has been acquired. This is a hindrance to the aims of this study; to detect and analyse smaller, less abundant proteins. One way in which this issue could be overcome is to create a mass spectrometry rejection list for the proteins identified in a run and apply this to subsequent runs. This would ensure

that only novel proteins would be detected from each injection and all proteins would have a fair chance of obtaining equivalent amounts of data (data obtained from one injection each). However creating a rejection list after each sample run is time consuming and outside the timeframe available for this study.

Many of the highly abundant proteins detected were identified as proteins of high MW, even though all proteins had been filtered through a 30kDa cut off filter. This indicates that fragments of these high MW proteins were present that were small enough to pass through the MW filter. The detection of high MW protein fragments, as well as LMW proteins, still allowed an interesting analysis for preclinical AD biomarkers complementary to the previous 2DGE discovery study.

Normalised total spectral counts was considered here as a value indicating relative abundance, on which statistical analysis was then conducted. In the previous 2DGE discovery study three abundance approaches were considered and applied to LC-MS/MS data. However, here the focus of the analysis was different; changes in protein abundance between samples/subjects were considered, but proteins were not ranked within a sample (2DGE spot) based on abundance. This allowed a simpler approach for analysis as it was assumed that as long as the experimental setup was the same for each sample any differences in spectral counts between samples must be due to abundance changes. For example, liquid chromatography biases may influence the abundance ranking of proteins within a sample, but as long as these biases are kept constant comparisons between samples can be drawn. Spectral counting is the most commonly employed method of determining relative abundance and was therefore selected for this study. This approach uses the number of tandem spectra matched to peptides of a certain protein to determine a total spectral count. This count is considered to be positively associated with the abundance of the protein and can therefore be used as an indicator of relative abundance.

Like the previous discovery chapter, no false discovery rate (FDR) corrections were applied to the statistical results obtained here. Although this will have increased the number of false positive findings reported, an uncorrected 0.05 *p*-value was considered an acceptable significance level for this discovery stage experiment.

Subsequent validation experiments are important to confirm true positives and discard false positive findings.

4.4.3 Detection of low molecular weight proteins as preclinical AD biomarker candidates, complementary to discovery 1

This study successfully discovered LMW proteins as preclinical AD biomarkers that had not been detected in previous 2DGE experiments. These results in combination provide a greater coverage and analysis of the proteome for preclinical AD biomarker discovery. The proteins found as biomarkers, complementary to the 2DGE discovery study, are discussed below. Most of these proteins are <30kDa, though for some the full length protein is slightly larger, indicating the presence of a fragment due to the 30kDa cut off filter used during sample preparation.

Alpha 1 acid glycoprotein 1 & 2

Alpha 1 acid glycoprotein (AGP) is a known acute phase protein, with an increase in concentration found as a response to injury, inflammation, or infection[302], though the exact functional role of AGP is poorly understood. In a cohort of 17,345 individuals, AGP has recently been identified as one of four proteins which can predict short term risk of death from any cause, with AGP found as the strongest multivariate predictor of death risk[303]. This association has also been reported previously in smaller cohorts[304-305]. With an increase in AGP reported as a risk factor of death of any cause, it is unsurprising that it has also been previously reported as a biomarker for AD[230]. Here two forms of AGP were identified as candidate biomarkers of preclinical AD; alpha 1 acid glycoprotein 1 (AGP1) and alpha 1 acid glycoprotein 2 (AGP2). Interestingly the direction of relationship with AD pathology found differed between these two proteins.

AGP1 was here found to be significantly longitudinally related to brain atrophy over time; positively related to the frontal grey matter, and also tending towards a significant positive relationship with atrophy of the cingulate gyrus. These results suggest that as brain volume decreases over time, AGP1 concentration also decreases. This conflicts with the literature mentioned above. However the findings for AGP2 are in line with the previous literature; a positive relationship was found with concurrent amyloid load (at T12). Additionally a negative relationship, tending

towards significance, was reported with brain atrophy of the middle frontal gyrus. These results suggest that AGP2 concentration increases with increased amyloid burden and brain atrophy. Therefore AGP2 appears to fit the more typical findings of an increase in AGP as detrimental to health, whereas AGP1 seems to have an opposite relationship.

As much literature suggests AGP as a general risk factor of death, including cancer and vascular disease outcomes, it is therefore unlikely to perform as a specific AD biomarker, even at a preclinical stage. Instead AGP may be most useful as a marker of general decline in health, and may show its greatest utility as an AD biomarker when used in combination with other AD specific proteins in a biomarker panel. However it would be interesting to further investigate the differences between AGP1 and AGP2 and their relationship with AD pathology. Perhaps one, or a ratio of both forms, would be more specific to AD.

Transthyretin (TTR)

Like AGP, Transthyretin (TTR) has also been found as a marker of short term death of any cause, with low levels of TTR indicating increased risk[304]. However TTR has also been specifically related to AD, and even implicated in its pathogenesis. TTR has been found as an AD biomarker in CSF[133-134], serum[306], and plasma[135-136], with lower levels of TTR related to AD diagnosis and severity.

TTR was here significantly and positively related to brain atrophy over time of the superior frontal gyrus. It was also tending towards significance with three other brain regions; the middle temporal gyrus, inferior occipital gyrus, and ventricles. These findings support previous reports that TTR levels decrease with increased pathology, and provide evidence that this association occurs even at a preclinical stage.

A decrease in TTR has previously been related to protective effects of the protein on Aβ pathology. Serum and CSF TTR has been found to bind to and cleave Aβ *in vitro*, this mechanism is thought to prevent Aβ aggregation, and therefore inhibit Aβ induced neurotoxicity[307-308]. As TTR has also been found to co-localise with Aβ plaques [309-310] this suggests that *in vivo* TTR may also express proteolytic activity on Aβ deposits. This indicates a potential therapeutic role of TTR in AD

treatment. The results here suggest that TTR levels are disrupted preclinically and therefore any TTR-based interventions may need to be implemented at this early stage.

Beta 2 microglobulin (B2M)

Beta 2 microglobulin (B2M) is a component of the major histocompatibility complex (MHC) class I molecules, and is commonly used as a biomarker for some blood cell cancers, known to indicate severity and prognosis[311]. B2M is also the major constituent protein of dialysis-associated amyloidosis; B2M accumulates in the plasma of chronically uraemic patients leading to the formation and deposition of B2M-amyloid. In Alzheimer's disease B2M has been found as an biomarker in CSF and plasma, with increased levels of B2M reported in AD patients compared to controls[139, 312-313].

Here B2M was positively related to concurrent amyloid load (at T12), and was tending towards significance with amyloid load at baseline. This supports previous findings that B2M is related to amyloid accumulation, and shows this relationship exists in preclinical AD individuals. B2M was also shown here to have longitudinal biomarker utility; B2M was negatively associated with brain atrophy of the superior occipital gyrus, with increased levels of B2M related to decreasing brain volume.

Leucine rich alpha 2 glycoprotein 1 (LRG1)

The exact function of LRG1 is unknown, though it is considered an acute phase protein with an up-regulation of LRG1 found in various diseases[314-316]. LRG1 levels have been found to increase in response to acute inflammation in mice[317] indicating that it may have diagnostic or prognostic biomarker ability for inflammatory conditions. Leucine rich alpha 2 glycoprotein (LRG1) was here found significantly, and positively, related to amyloid load at baseline. LRG1 has not previously been linked to AD, although increased CSF LRG1 has been reported as a biomarker of idiopathic normal pressure hydrocephalus[318], considered a form of reversible dementia.

Alpha 1β glycoprotein (ABGP)

Relatively little is also known about alpha 1β glycoprotein (ABGP), though it has previously been shown to have AD biomarker ability, with altered levels of ABGP in CSF of AD patients compared to controls[319]. Here ABGP was significantly, negatively related to brain atrophy of the middle frontal gyrus over time. This provides support for the utility of ABGP as a longitudinal plasma biomarker for preclinical AD.

Apolipoprotein E (ApoE)

The gene encoding for Apolipoprotein E4 allele (*APOE* ε4) is a well-established genetic risk factor for sporadic AD, known to increase the risk of developing AD and decrease the age of onset[24]. There is also evidence that plasma and serum ApoE levels may have strong biomarker ability. Both total ApoE and ApoE E4 levels in plasma have been found to be reduced in AD individuals compared to controls, though the biomarker effect of total ApoE does appear to be driven by ApoE E4 levels[320]. A meta analysis of the association between peripheral levels of ApoE and AD was conducted by Wang et al (2014) [321], which concluded that lower peripheral ApoE levels is significantly associated with an AD diagnosis and may be an important risk factor for the development of AD. The results found in this discovery study support these conclusions. Here total ApoE was positively related to brain atrophy of the hippocampus, with lower levels of ApoE associated with lower hippocampal volume over time. As the hippocampus is one of the first regions effected in AD[205] this relationship is particularly interesting to preclinical AD biomarker research. ApoE was also positively, longitudinally related to two further brain regions for which the association was tending towards significance; middle frontal gyrus and whole brain volume. Also tending towards significance was a longitudinal relationship with Trails B score, where lower levels of ApoE were related to an increase in time spent completing the Trails B task, indicating cognitive decline.

Mechanisms behind the association between low ApoE protein levels and AD are unclear. Normally, plasma ApoE is known to modulate lipid metabolism and cholesterol, and it is possible that a decrease in ApoE impairs these normal physiological functions, which then in turn disrupts central nervous system functions

leading to degeneration. The results here indicate that any disruption related to decreasing levels of this protein happen at an early, preclinical AD stage. The ability of ApoE as a preclinical marker of AD was previously found in BLSA individuals by Thambisetty et al, (2010)[151] using both 2DGE and ELISA assays, these results therefore replicate their findings using a different proteomic platform.

4.4.4 Proteins replicating discovery phase 1 2DGE experiments

Although the aim of this study was to complement the findings from the 2DGE discovery experiments by exploring an additional fraction of the proteome, there are many overlapping candidate biomarkers between the two studies. Some of these proteins, and their relationship to AD, were discussed previously in chapter 3, and a comparison of results found for these proteins between the two discovery studies is summarised in Table 4-13 below. These results provide a form of replication for these proteins as preclinical AD biomarkers within the BLSA cohort using a different proteomic discovery platform. However, it is important to consider that in each study different forms of the same protein (fragments/modifications) may be producing the statistical signal observed. This is especially true for larger proteins, such as Complement C3, which due to the 30kDa cut off filter employed here must have been detected in fragment form, whereas in the previous 2DGE study C3 was detected in many 2DGE spots throughout the length of the gel indicating both full length protein and fragment detection. It is important to consider that as well as cleavage, any fragments detected may also be a result of sample degradation during storage. Detection of multiple forms of the sample protein may explain why coefficient directions found for the same protein-dependant variable relationship may differ between the two studies. In addition, the 2DGE discovery study often identified multiple proteins in each spot as candidate biomarker which will have resulted in some false positive findings. This may also explain the difference in some results reported below. However some findings do appear to correspond between studies such as Fibringogen β chain, which displayed a negative coefficient with cognitive decline in both discovery studies, and as 2DGE spots containing this protein were located at an approximate molecular weight of 30-35kDa it is possible that the same fragment is being measured in both studies.

Table 4-13: Proteins identified as biomarkers of preclinical AD in both discovery studies. +/- indicates coefficient direction.

Protein	MW	Discovery 1: 2DGE (p<0.05)	Approximate 2DGE spot MW	Discovery 2: LC-MS/MS (<30kDa) (p<0.05)
Alpha 1 antitrypsin	47kDa	+ Brain volume (ventricular expansion). +/- Cognitive decline (Trails B) +/- PiB PET DVR (Baseline & T12)	Brain volume = ~65-70kDa Cognitive decline = ~60-70kDa PiB PET DVR = ~45-60kDa (BASELINE), 25-40kDa (T12)	+ Brain volume (superior temporal gyrus volume)
Fibrinogen α chain	95kDa	+ PiB PET DVR (T6 & T12) - Brain volume (ventricular expansion)	PiB PET DVR = ~70kDa (T6) ~35kDa (T12) Brain volume = ~70-75kDa	- PiB PET DVR (baseline)
Fibrinogen β chain	56kDa	+/- PiB PET DVR (Baseline & T12) - Cognitive decline (Trails B) +/- Brain volume (ventricular expansion)	PiB PET DVR = 55-60kDa (Baseline), 30-55kDa (T12) Brain volume = ~55-60kDa (+), ~35kDa (-) Cognitive decline = ~30-35kDa	- PiB PET DVR (baseline & T6) - Cognitive decline (Trails B)
ApoA-IV	45kDa	+ PiB PET DVR (Baseline) +/- Cognitive decline (Trails B) + Brain volume (ventricular expanion)	PiB PET DVR = ~45kDa Brain volume = ~45kDa Cognitive decline = ~42-55kDa	- Cognitive decline (Trails B)

Complement C3	187kDa	+/-PiB PET DVR (Baseline) - PiB PET DVR (T12) +/- Cognitive decline (Trails B) - Brain volume (ventricular expansion)	PiB PET DVR =~150-190kDa Brain volume = ~70-115kDa Cognitive decline = 30-110kDa	- PiB PET DVR (T6) - Brain volume (middle occipital gyrus)

Proteins found as significant in both studies, but not previously discussed in Chapter 3, are discussed below.

Complement C4b

Table 4-14: Complement C4b summary; Significant relationships of C4b with surrogate markers of AD and coefficient directions (+/-). Findings from both discovery studies displayed. $p<0.05$.

MW	Discovery 1: 2DGE ($p<0.05$)	Approximate 2DGE spot MW	Discovery 2: LC-MS/MS ($p<0.05$)
193kDa	+ PiB PET DVR (T6) - PiB PET DVR (T12)	PiB PET DVR T6 = ~45kDa PiB PET DVR T12 = ~45kDa	- PiB PET DVR (baseline)

Complement C4b was found to be significantly related to amyloid load at baseline, and was also tending towards significance at T12, both with a negative coefficient direction. In the 2DGE discovery study C4b was found related to amyloid load at both T6 and T12, though with opposite coefficients at each time point. Together these results show biomarker potential of C4b over all three time points (Table 4-14), suggesting a longitudinal ability of C4b as a biomarker of amyloid load. Mainly a negative relationship of C4b was found with PiB PET DVR, indicating that as amyloid load increased the concentration of C4b decreases.

In Chapter 3 the complement cascade was discussed; C4b is involved in both the classical and lectin complement pathways (refer back to Figure 3-44). It was previously concluded that the complement system is broadly altered in preclinical AD, and the results of this study also support that.

Antithrombin-III (AIII)

Table 4-15: Antithrombin-III summary; Significant relationships of AIII with surrogate markers of AD and coefficient directions (+/-). Findings from both discovery studies displayed. $p<0.05$

MW	Discovery 1: 2DGE ($p<0.05$)	Approximate 2DGE spot MW	Discovery 2: LC-MS/MS ($p<0.05$)
53kDa	- Cognitive decline (Trails B)	Cognitive decline = ~50-65kDa	- Brain volume (cingulate gyrus, medial frontal gyrus, and middle frontal gyrus volume)

Antithrombin-III is involved in the coagulation pathway and prevents excessive blood clotting. Individuals with AIII deficiency have increased risk of blood clots and hypercoagulability which has been associated with increased incidence of myocardial infarction, cerebrovascular disease, and peripheral arterial disease. These cardiovascular problems are dementia risk factors, hinting at a link between coagulation and dementia. AIII has previously been found as an AD biomarker, as well as a marker of blood-brain-barrier integrity (BBB), and has also been found to co-localise with both amyloid plaques and neurofibrillary tangles[252-256].

Here AIII was negatively related to volumes of three brain regions (Table 4-15), and showed a tendency towards significance with five further regions, also all with a negative coefficient. This negative relationship is surprising as it conflicts previous literature in which decreased AIII has been linked to cognitive decline[254]. It also conflicts the results from chapter 3 where a longitudinal decrease in AIII was associated with cognitive decline as measured by Trails B (time taken). Significant 2DGE spots containing AIII were located between approximate molecular weights of 50-65kDa, indicating full length AIII protein. It is therefore likely that a different

form of AIII is related to cognitive decline, than that which was found related to brain atrophy in this study.

Ig kappa chain C region (IGKC)

Table 4-16: Ig kappa chain C region summary; significant relationships of IGKC with surrogate markers of AD and coefficient directions (+/-). Findings from both discovery studies displayed. $p<0.05$

MW	Discovery 1: 2DGE ($p<0.05$)	Approximate 2DGE spot MW	Discovery 2: LC-MS/MS ($p<0.05$)
12kDa	+/- PiB PET DVR (baseline & T12) - PiB PET DVR (T6) +/- Cognitive decline (Trails B)	PiB PET DVR Baseline = ~25(+) 30--40kDa(-) PiB PET DVR T6 = ~28kDa PiB PET DVR T12 = ~28-30kDa(-), ~32kDa (+) Cognitive decline = ~25-40kDa	+ PiB PET DVR (baseline) - Brain volume (middle temporal gyrus)

Immunoglobulins and their relation to AD were discussed generally in Chapter 3. Here Ig kappa chain C region (IGKC), a LMW protein of 12kDa, was found to be significantly positively associated with amyloid load 12 years later. Increased levels of IGKC also appeared detrimental to brain volume with a significant negative association found with longitudinal atrophy of the middle temporal gyrus. Additionally a longitudinal negative relationship with temporal grey matter volume was tending towards significance.

In the previous discovery study IGKC was found to be significantly related to amyloid load at all three time points, and it was also significantly longitudinally related to Trails B score, although mixed coefficient directions were found (Table 4-16). When the two discovery phases are combined IGKC was found as a candidate biomarker for all three DVs, and therefore is a very strong candidate as a preclinical

AD biomarker. The majority of findings between both studies agree that an increase in IGKC is related to increased AD pathology and cognitive decline. Further supporting IGKC as an AD biomarker Hye et al (2006) [142] reported IGKC to be present in 4 2DGE spots significantly related to AD diagnosis. All 4 spots had a positive relationship with diagnosis. Together these results suggest IGKC is related to AD both preclinically and into the clinical onset of the disease.

Zinc-alpha-2-glycoprotein (ZAG)

Table 4-17: Zinc alpha 2 glycoprotein summary; significant relationships of IGKC with surrogate markers of AD and coefficient directions (+/-). Findings from both discovery studies displayed. $p<0.05$

MW	Discovery 1: 2DGE ($p<0.05$)	Approximate 2DGE spot MW	Discovery 2: LC-MS/MS ($p<0.05$)
34kDa	+/- Brain atrophy (ventricular expansion) + Cognitive decline (Trails B)	Cognitive decline = 40-45kDa	+ PiB PET DVR (baseline) + Brain volume (cingulate gyrus, middle temporal gyrus, superior temporal gyrus, and temporal gray matter)

ZAG is a multifunctional protein, implicated in several biological processes such as lipid mobilisation, fertilisation, cell adhesion, and immunoregulation [322]. Research into ZAG to date has mainly focused on its involvement in cancer and obesity[323]. ZAG had been found over-expressed in several types of tumours, such as breast[324], prostate[325], and bladder cancer[326]. Increased serum levels of ZAG have been reported in individuals with prostate [325, 327] and cervical cancer[328] and therefore ZAG is considered a biomarker for these. As well as cancer, other conditions associated with increased serum ZAG levels include pre-eclampsia[329], chronic heart failure[330], and acute kidney disease[331]. However the most well studied property of ZAG is its involvement in the regulation of body weight; showing an inverse relationship with adiposity; being unregulated in cachexia, and reduced in obesity[332]. In adipose tissue ZAG gene expression has been found to be down-regulated with increased adiposity and circulating insulin[323], and plasma levels of ZAG in obese (ob/ob) mice are also decreased compared to lean mice[333].

In AD ZAG has previously been found as a biomarker in CSF, though the reason for a relationship with AD is unclear, as is the direction of this relationship. Increased CSF ZAG levels have been found in individuals with mild AD compared to controls suggesting ZAGs suitability as an early AD biomarker[256]. This is supported by the results of our preclinical study. However a comparison of CSF ZAG levels between autopsy confirmed AD, non-demented elderly controls, and non-AD dementias, AD subjects revealed reduced CSF ZAG levels compared to the other two groups[334]. This unclear picture of the direction of the relationship between ZAG and AD was also reflected in the results of this study.

Here ZAG was found positively associated with amyloid load at baseline; indicating that higher ZAG levels are predictive of higher amyloid burden 12 years later. However a longitudinal analysis with brain atrophy revealed that over time decreasing levels of ZAG was related to increased atrophy of four brain regions (Table 4-17). When also considering results tending towards significance ZAG was longitudinally positively related to three further brain regions: grey matter, frontal grey matter, and middle occipital gyrus. Although the associations with amyloid load and brain atrophy appear conflicting, perhaps ZAG is increased initially in preclinical AD, indicative of later increased amyloid burden, but over time ZAG levels decline which correlates with brain atrophy. More longitudinal work is needed to explore this potentially complex relationship. A significant longitudinal relationship between ZAG and brain atrophy (ventricular expansion) was also reported in the previous discovery study; though with conflicting coefficient directions. The previous discovery study also found a significant longitudinal relationship with ZAG and cognitive decline (Trails B – measured by time taken), in which all significant spots had a positive coefficient. When combining the results of both discovery studies ZAG is related to all three DVs. Although the directions of the relationships are inconclusive, these findings do highlight ZAG as a strong biomarker candidate for preclinical AD.

4.5 Conclusions

This discovery study detected LMW proteins as candidate markers of preclinical AD, adding to those found in the previous 2DGE discovery study. The additional

biomarkers discovered here shows the importance in targeting less abundant, LMW proteins for analysis as they are often masked by larger more abundant proteins. Together the two studies provide a more comprehensive analysis of the plasma proteome for the discovery of preclinical AD biomarkers. These results also provide further support that plasma biomarkers have the potential to be used as a screening tool for AD, including proteins from a LMW fraction.

However the identification of these LMW proteins varied greatly between individuals and sample injections, resulting in a vast number being discarded from analysis due to lack of data available. A more robust way to detect and quantify these proteins is needed. Isobaric labelling approaches, such as Tandem Mass Tagging (TMT), could be used to overcome the issue of missing data values and would also enable multiplexing of up to 10 samples.

Many of the candidate biomarkers found here had also been discovered in the previous 2DGE discovery study. This provides a form of replication, though it is likely that different forms of each protein (fragment or modification) were assessed by each approach; due to the prefractionation employed here and also because 2DGE had already identified many of these proteins in multiple spots, indicative of multiple forms of many proteins (modified and/or cleaved) as biomarkers.

Quantitative assays in an independent cohort are now needed to validate the proteins reported here as candidate biomarkers. If validated these proteins may, independently or in combination, provide a biomarker for preclinical AD diagnosis or allow predication of disease onset.

Chapter 5. Validation of candidate biomarkers of Alzheimer's disease pathology and cognitive decline

5.1 Introduction

In chapters 3 and 4 the discovery of biomarkers of preclinical AD pathology and cognitive decline was presented. The candidate biomarkers identified now require validation in an independent cohort using an alternative proteomic platform. This will determine whether the results are reproducible and if they can be generalised to a wider population.

The candidate biomarkers discovered are related, at a preclinical stage, to one or more DVs; amyloid load, brain atrophy, and cognitive decline. However an ideal biomarker would also enable a clear distinction between AD cases and healthy controls. This would also confirm the biomarkers involvement in AD after the clinical onset of the disease, increasing the confidence of its association to the disease preclinically, rather than acting as markers of general decline or other co-morbidities. It would additionally show their utility longitudinally throughout the disease. For these reasons the validation experiments here will be performed using cohorts of AD subjects and healthy age matched controls. Over the two discovery studies 15 proteins were identified as candidate biomarkers of all three DVs. These proteins therefore have the strongest potential as specific AD biomarkers and this validation will focus upon this subset of 15 candidate biomarkers.

Proteomic results from the discovery-phase experiments were obtained using 2DGE and LC-MS/MS proteomic techniques, both of which generate data from enzymatically digested peptides. Therefore, as an orthogonal approach, specific aptamer and antibody based techniques (SOMAlogic's SOMAscan^{TM} and enzyme-linked immunosorbent assay (ELISA)) were chosen to validate the candidates previously identified in an independent cohort of plasma samples.

Sattlecker et al (2014)[141] conducted a large scale multiplexed plasma protein study (n=691), screening for AD biomarkers using SOMAscan technology. 1,001 proteins were tested for their biomarker ability against seven outcome measurements; clinical diagnosis, MCI to AD conversion, rate of cognitive decline, and brain atrophy of the

hippocampus (left/right) and entorhinal cortex (left/right). Both previously known and novel biomarkers were identified, and a multivariate analysis identified 13 proteins which together could predict AD with an accuracy of AUC of 0.70. From this dataset SOMAscan aptamer-based assays were available for 7 of the 15 proteins chosen to be validated in our validation experiments; α1-antitrypsin (AAT), fibrinogen (α/β/γ chain), α2-macroglobulin (A2M), serum paraoxonase/arylesterase 1 (PON1), complement C3, serum albumin, and haptoglobin. Therefore to make efficient use of previously acquired assay data this dataset will here be re-analysed as a targeted validation approach for these 7 proteins. Multivariate analysis will be kept consistent with that employed by Sattlecker et al (2014), however false discovery rate corrections will be tailored specifically for the targeted protein set.

The remaining 8 proteins requiring validation are: Zinc alpha 2 glycoprotein (ZAG), Protein AMBP/alpha 1 microglobulin (A1M), Ceruloplasmin, Apolipoprotein A IV (ApoA-IV), Ig kappa chain C region, Ig gamma 1 chain C region, Ig gamma 2 chain C region, and Ig alpha 1 chain C region. Time and cost restrictions of this study meant that only two of the above proteins could be validated by ELISA. From these 8 proteins, ZAG and Protein AMBP are the two most novel AD biomarker candidates for which reliable ELISA assays could be obtained. These two proteins were therefore selected for further validation by ELISA, using a subset of subjects from the same cohorts as the SOMAscan study.

5.2 Aims

To validate previously discovered candidate biomarkers of preclinical AD pathology and cognitive decline in an independent cohort using an orthogonal proteomic platform. Specifically, to validate candidate biomarkers relationship with AD using SOMAlogic and ELISA in case versus control cohorts. To use multivariate analyses to identify proteins related to diagnosis status, brain atrophy and cognitive decline.

5.3 Results

5.3.1 Demographic characteristics

SOMAscan

SOMAscan assays were performed on plasma samples from 691 subjects recruited from AddNeuroMed (n=415), Maudsley and King's Healthcare Partners Dementia Case Register (DCR) (n=38), and Alzheimer's Research UK (ARUK) (n=238) cohorts, previously described in chapter 2. All subjects with the relevant information available were recruited from these cohorts. Table 5-1 displays the demographic characteristics for these subjects, stratified by cohort.

Table 5-1: SOMAscan assay; subject demographics, stratified by cohort

	AddNeuroMed			**ARUK**			**DCR**
	CTL N=110	**MCI N=109**	**AD N=196**	**CTL N=101**	**MCI N=40**	**AD N=97**	**AD N=38**
Age (median)	75	75.5	77.5	77	80	84	78
Gender (M/F) (missing)	48/62	47/62	64/132	54/47	11/29	22/74(1)	17/20(1)
Baseline MMSE (median)	29	27.5	21	29	27	17	21

All subjects had undergone cognitive assessment, including the Mini Mental State Examination (MMSE). Structural MRI data was obtained from 273 AddNeuromed subjects (Controls = 93, MCI = 81, AD = 99).

ELISA (A1M and ZAG)

ELISA assays were performed on a subset of the subjects included in the SOMAscan assays detailed above. Differences in ELISA plate set-up between the A1M and ZAG

assays allowed slightly different sample numbers to be tested (A1M n=140, ZAG n=144). Table 5-2 and Table 5-3 display the demographic characteristics for these subjects, stratified by cohort, for A1M and ZAG ELISAs respectively. Structural MRI data was obtained from all AddNeuromed subjects.

Table 5-2: A1M ELISA; subject demographics, stratified by cohort

	AddNeuroMed		**ARUK**	
	CTL N=61	**AD N=38**	**CTL N=8**	**AD N=33**
Age (mean)	72.0	75.7	84.5	84.0
Gender (M/F)	33/28	11/27	6/2	7/26
Baseline MMSE (mean)	29.1	20.8	29.5	17.8

Table 5-3: ZAG ELISA; subject demographics, stratified by cohort

	AddNeuroMed		**ARUK**	
	CTL N=61	**AD N=41**	**CTL N=8**	**AD N=34**
Age (mean)	72.0	75.7	84.5	83.8
Gender (M/F)	33/28	13/28	6/2	7/27
Baseline MMSE (mean)	29.1	21.3	29.5	17.9

Calculation of rate of cognitive decline

The rate of cognitive decline was calculated for AD subjects with at least three MMSE assessments over a period of up to 2 years (SOMAscan n=329, A1M n=70; ZAG n=74). This was calculated as detailed in Sattlecker et al (2014)[141]. Briefly, linear mixed effects regression models were generated, using R, with samples and test centre entered as random effects, and years of education and home environment (e.g. nursing home) included as fixed effects. The slope coefficient for MMSE score

was used as the rate of cognitive decline for further statistical analysis, defined as the change in MMSE per day.

5.3.2 SOMAscan

Candidate biomarker association with disease status (AD versus control)

For each of the 7 candidate biomarkers, logistic regression was employed to detect associations with disease status. All AD and control subjects from the combined AddNeuroMed, ARUK, and DCR cohort, described above, were included in this analysis. For each protein, False Discovery Rate (FDR) corrections were applied in order to correct for multiple testing. FDR q-values of <0.1 were considered significant, those <0.2 were considered as tending towards significance.

The single analyte logistic regression for AD cases versus controls showed that 1 protein, AAT, was associated with disease status at both a significance level of $p<0.05$ and a q-value of <0.1 (Odds Ratio (OD) =2.67, Beta = 0.98, q-value = 0.06). Full results are reported in Table 5-4.

Table 5-4: Logistic regression results for AD versus control, in order of significance

Protein	Beta	OR	*p*-Value	q-Value
α1-Antitrypsin	0.984	2.675	0.008	0.056
Fibrinogen α/β/γ chain	0.334	1.397	0.242	0.377
α2-Macroglobulin	-0.418	0.658	0.280	0.377
Serum paraoxonase/arylesterase 1	-0.799	0.450	0.286	0.377
Complement C3	-0.233	0.792	0.297	0.377
Serum albumin	-0.629	0.533	0.323	0.377
Haptoglobin, Mixed Type	0.141	1.151	0.471	0.471

Candidate biomarker association with volume of brain regions

Linear regression was used to analyse the plasma levels of the 7 proteins for their association to volumes of brain regions known to be strongly related to AD pathology (left and right entorhinal cortices, and left and right hippocampi). Age, gender, *APOE* ε4 status, and recruitment centre were all entered as covariates in the regression model.

Linear regression results revealed that AAT was the only protein found to be significantly related to brain volume. AAT was associated with left entorhinal volume and right hippocampal volume at both a significance level of $p<0.05$ and a q-value of <0.1. AAT was also associated with left hippocampal volume $p<0.05$, tending towards a significant FDR correction (q-value = 0.11). Full results are reported in Table 5-5 (left entorhinal), Table 5-6 (right entorhinal), Table 5-7 (left hippocampus), and Table 5-8 (right hippocampus).

Table 5-5: Linear regression results for candidate biomarkers with left entorhinal volume

Protein	Beta	R-squared	*p*-Value	q-Value
α1-Antitrypsin	-0.0001	0.163	0.007	0.047
Serum albumin	0.0001	0.148	0.102	0.358
Haptoglobin, Mixed Type	-0.0000	0.141	0.428	0.718
Fibrinogen α/β/γ chain	0.0000	0.141	0.431	0.718
Serum paraoxonase/arylesterase 1	0.0000	0.140	0.558	0.718
Complement C3	0.0000	0.140	0.615	0.718
α2-Macroglobulin	0.0000	0.139	0.952	0.952

Table 5-6: Linear regression results for candidate biomarkers with right entorhinal volume

Protein	Beta	R-squared	*p*-Value	q-Value
α1-Antitrypsin	-0.0001	0.108	0.104	0.665
α2-Macroglobulin	0.0001	0.103	0.318	0.665
Serum paraoxonase/arylesterase 1	0.0001	0.102	0.420	0.665
Serum albumin	0.0000	0.101	0.543	0.665
Complement C3	0.0000	0.101	0.562	0.665
Fibrinogen α/β/γ chain	0.0000	0.100	0.657	0.665
Haptoglobin, Mixed Type	0.0000	0.100	0.665	0.665

Table 5-7: Linear regression results for candidate biomarkers with left hippocampal volume

Protein	Beta	R-squared	*p*-Value	q-Value
α1-Antitrypsin	-0.0002	0.296	0.016	0.110
Haptoglobin, Mixed Type	-0.0001	0.288	0.096	0.306
Serum paraoxonase/arylesterase 1	0.0001	0.286	0.162	0.306
Serum albumin	0.0001	0.286	0.175	0.306
Fibrinogen α/β/γ chain	0.0001	0.283	0.327	0.458
Complement C3	0.0000	0.281	0.684	0.799
α2-Macroglobulin	0.0000	0.281	0.831	0.831

Table 5-8: Linear regression results for candidate biomarkers with right hippocampal volume

Protein	Beta	R-squared	*p*-Value	q-Value
α1-Antitrypsin	-0.0002	0.284	0.014	0.099
Complement C3	0.0001	0.272	0.190	0.665
Serum paraoxonase/arylesterase 1	0.0001	0.270	0.350	0.768
α2-Macroglobulin	0.0001	0.269	0.495	0.768
Haptoglobin, Mixed Type	0.0000	0.269	0.549	0.768
Fibrinogen α/β/γ chain	0.0001	0.268	0.690	0.804
Serum albumin	0.0000	0.268	0.917	0.917

Candidate biomarker association with rate of MMSE decline

The mean change in MMSE points per year for AD patients in each cohort are detailed in Table 5-9.

Table 5-9: Mean loss in MMSE points per year for AD patients within each cohort

Cohort	Mean change in MMSE (points per year)	Standard deviation
AddNeuroMed	1.5	1.5
ARUK	2.9	1.4
DCR	2.2	1.4

Linear regression was used to analyse the association between the 7 candidate biomarkers and each AD subject's rate of cognitive decline (MMSE change). Covariates were not included in this analysis as they had been adjusted for in the rate of cognitive decline slope calculation.

Both C3 and haptoglobin were significantly associated with rate of cognitive decline (p<0.05) and both proteins were tending towards significance after FDR correction (q-value = 0.116). Full results are reported in Table 5-10.

Table 5-10: Linear regression results for candidate biomarkers with rate of cognitive decline (MMSE change)

Protein	Beta	R-squared	*p*-Value	q-Value
Complement C3	0.367	0.023	0.018	0.116
Haptoglobin, Mixed Type	0.367	0.019	0.033	0.116
Serum paraoxonase/arylesterase 1	-0.996	0.007	0.184	0.429
Serum albumin	-0.326	0.002	0.490	0.857
Fibrinogen α/β/γ chain	-0.052	0.000	0.805	0.993
α1-Antitrypsin	0.053	0.000	0.855	0.993
α2-Macroglobulin	0.003	0.000	0.993	0.993

5.3.3 Enzyme linked immunosorbant assay (ELISA) for Alpha 1 microglobulin (A1M) and Zinc alpha 2 glycoprotein (ZAG)

Coefficient of variation (CV)

As every plasma sample had been run in duplicate on each ELISA plate the coefficient of variation (CV) between duplicate samples was calculated. These CVs were then averaged to obtain an overall mean within-subject CV; A1M = 6.48% and ZAG = 6.55%.

Influence of ELISA plate

For both A1M and ZAG four ELISA plates were completed in total, each on consecutive days. Although every effort is taken to ensure the procedure is standardised across plates very subtle differences in manual or environmental factors

can influence the results obtained from each plate. Although samples were randomised across plates these differences can still have an effect on the results and it is therefore important to check for and if necessary control for any changes found between plates.

The mean A1M values obtained from each plate are listed in Table 5-11 and illustrated in Figure 5-1. A one way univariate ANOVA was conducted to check for differences between these mean A1M values, whilst controlling for age, diagnosis, gender, and sample freeze-thaw. A significant main effect of ELISA plate was found, $F(3,132)=22.836$, $p<0.001$, showing that there was a significant difference between the mean A1M values between plates. It was therefore important to ensure that ELISA plate is controlled for within subsequent statistical analysis.

Table 5-11: Number of subjects, mean value, and standard deviation, for A1M ELISA plates

A1M ELISA plate	N	Mean A1M value (ng/ml)	Std. Deviation
1	23	49762.94	20295.55
2	39	50355.28	16721.01
3	39	34594.63	9702.15
4	39	60220.67	17230.34
Total	140	48615.72	18507.78

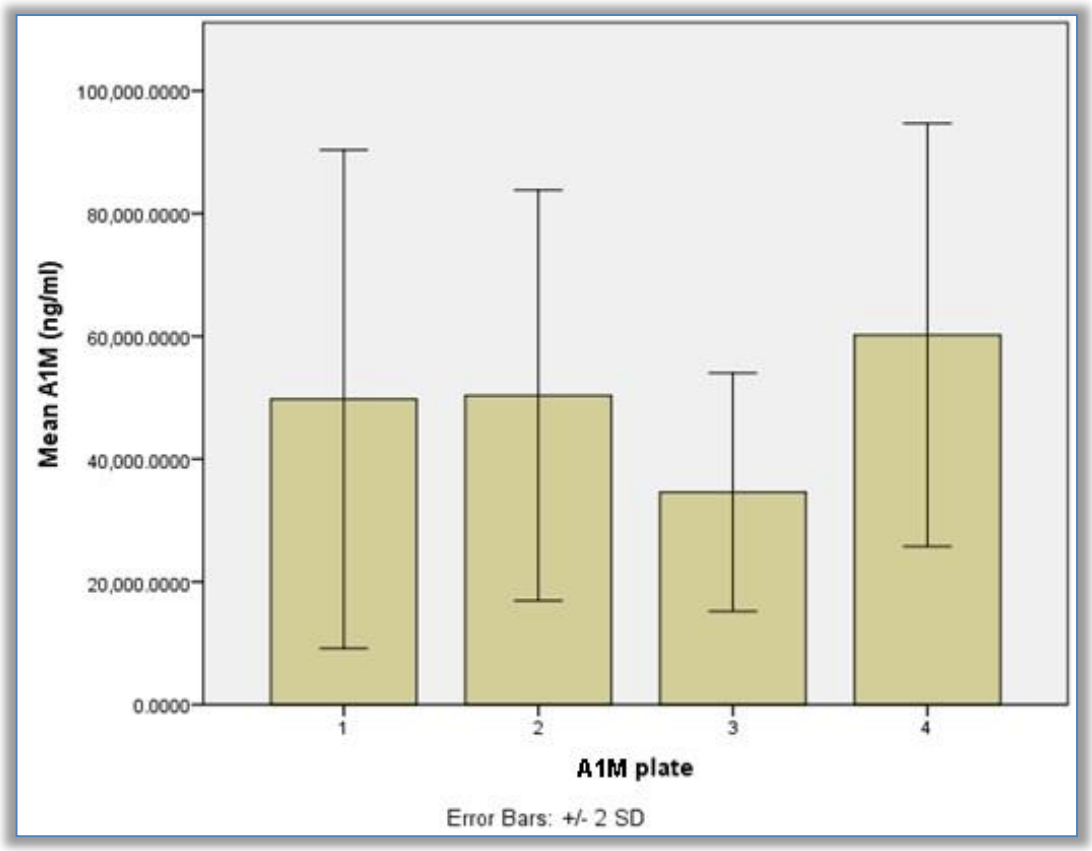

Figure 5-1: Mean A1M value for each ELISA plate.

The mean ZAG values obtained from each plate are listed in Table 5-12 and illustrated in Figure 5-2. A one way univariate ANOVA was conducted to check for differences between these mean ZAG values, whilst controlling for age, diagnosis, gender, and sample freeze-thaw. No main effect of ELISA plate was found, $p>0.05$, showing that there was no significant difference between the mean ZAG values between plates.

Table 5-12: Number of subjects, mean value, and standard deviation, for ZAG ELISA plates

ZAG ELISA Plate	N	Mean ZAG value (µg/ml)	Std. Deviation
1	25	113.29	33.64
2	41	94.80	35.01
3	38	75.51	19.53
4	33	93.32	127.28
Total	137	92.47	68.097

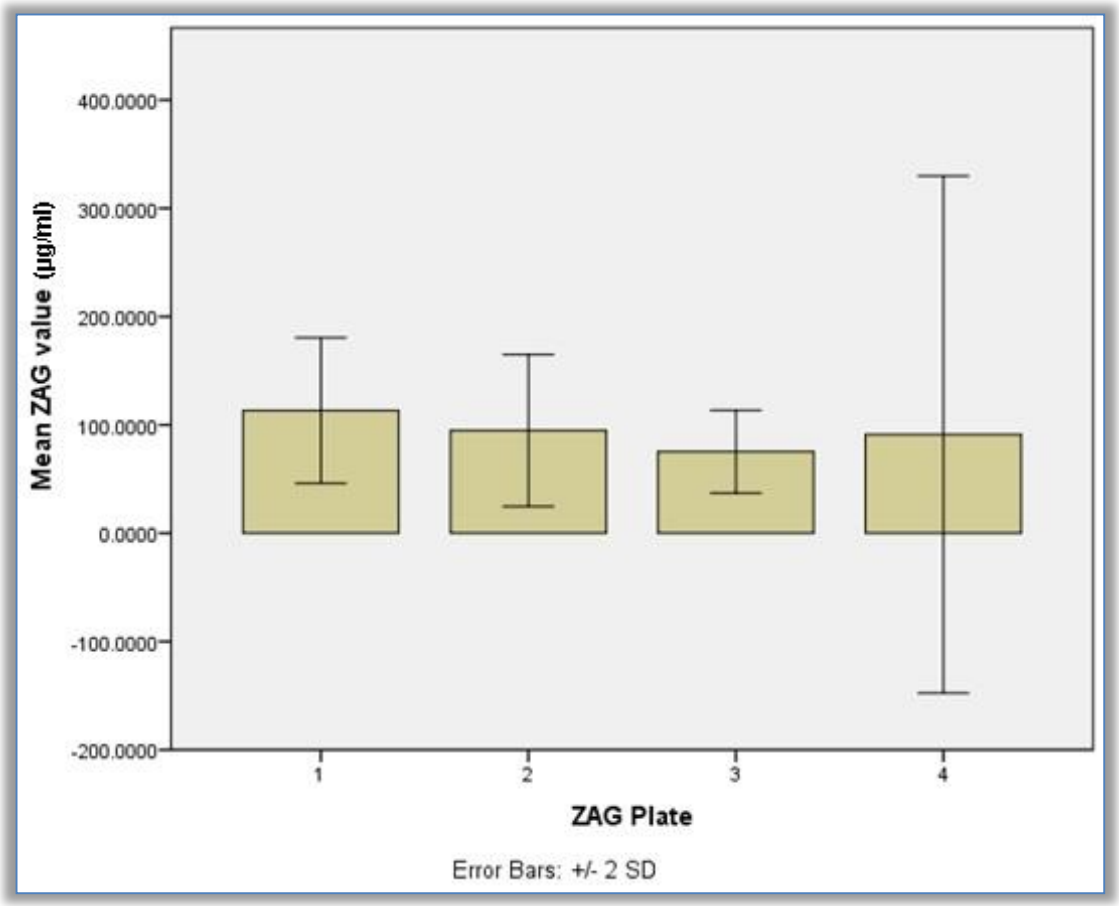

Figure 5-2: Mean ZAG value for each ELISA plate

Normality tests

Normality tests were performed to determine the normality of the A1M and ZAG data distributions. Kolmogorov-Smirnov tests for normality indicated that both A1M and ZAG datasets were non-normally distributed (p<0.05).

As skewness can affect the normality of a dataset, outliers were identified and removed so to minimize skewness. For both proteins the removal of outliers was completed in two ways, producing two separate datasets for each protein. Firstly, outliers were calculated and removed per diagnosis group (see Figure 5-3 and Figure 5-4); these datasets would be used for AD versus control comparisons. Secondly outliers were removed from the dataset as a whole (see Figure 5-5 and Figure 5-6); these datasets would be used to detect associations with brain atrophy and cognitive decline.

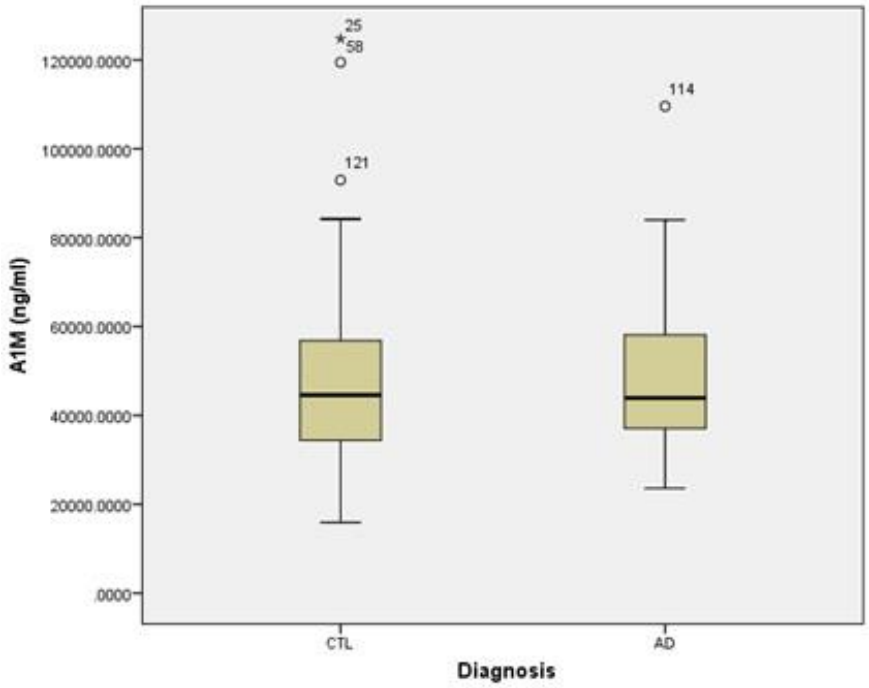

Figure 5-3: Box and whisker diagram identifying outliers (stars and circles) for each diagnosis group (AD and control), for A1M ELISA values

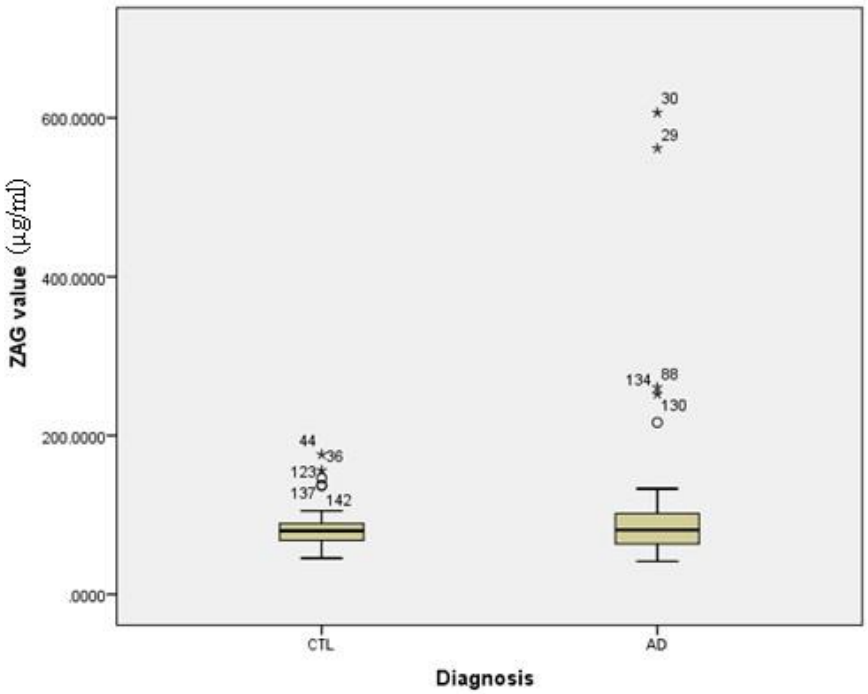

Figure 5-4: Box and whisker diagram identifying outliers (stars and circles) for each diagnosis group (AD and control), for ZAG ELISA values

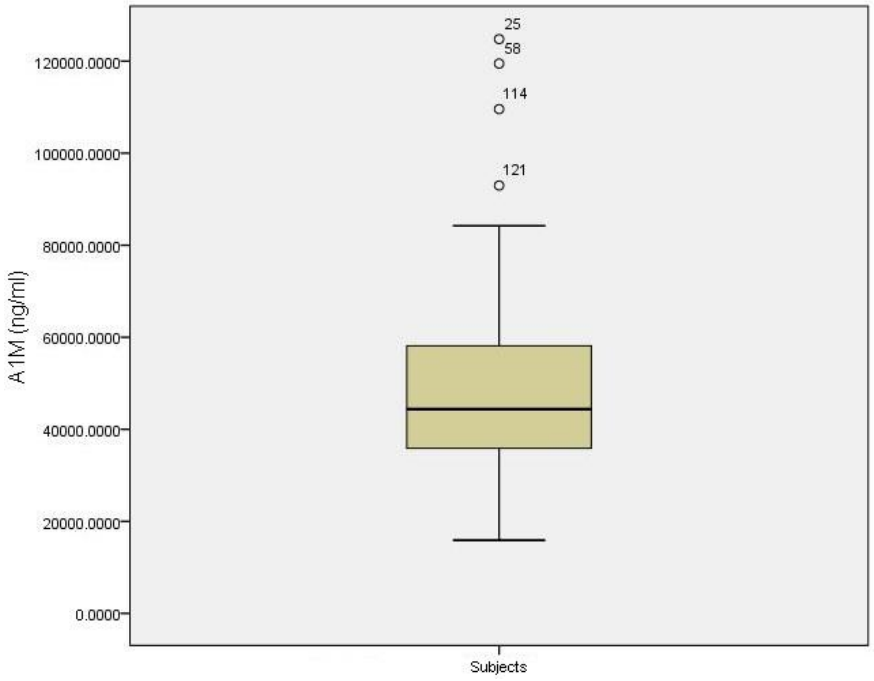

Figure 5-5: Box and whisker diagram identifying outliers (circles) for A1M ELISA values

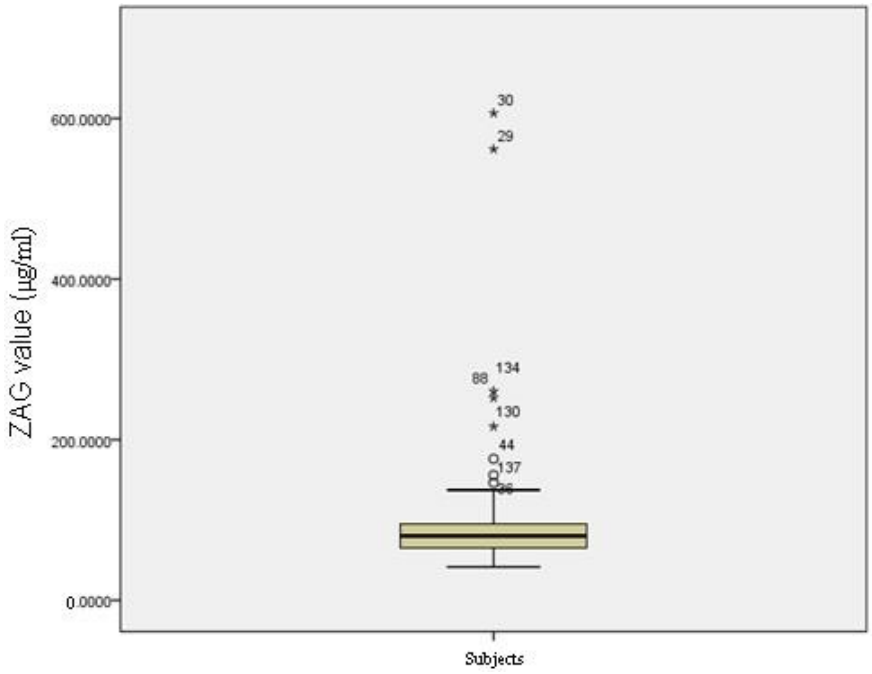

Figure 5-6: Box and whisker diagram identifying outliers (stars and circles) for ZAG ELISA values

Once outliers had been removed normality tests were repeated. Kolmogorov-Smirnov tests for normality indicated that all A1M and ZAG datasets were now normally distributed ($p>0.05$).

A1M and ZAG associations with disease status (AD versus control)

Figure 5-7 and Figure 5-8 display the mean values for A1M and ZAG for AD and control subjects.

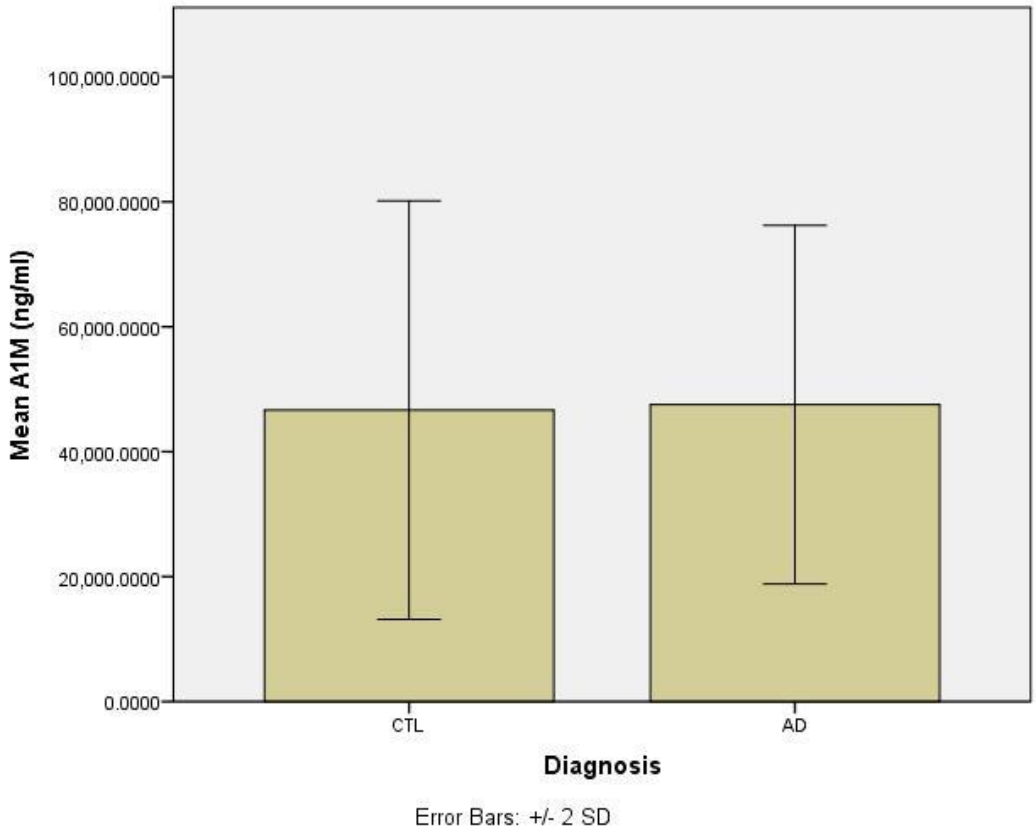

Figure 5-7: Bar chart displaying mean A1M values for AD and control subjects

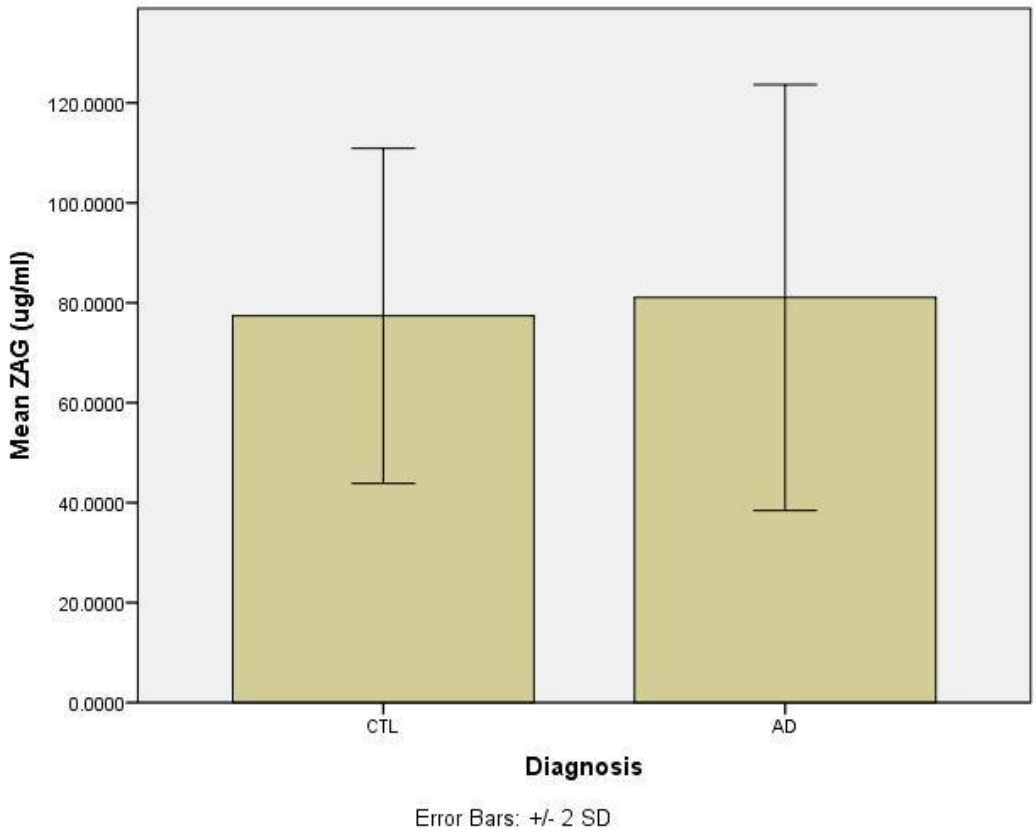

Figure 5-8: Bar chart displaying mean ZAG values for AD and control subjects

Whilst conducting these analyses it was observed that both A1M and ZAG mean values for cases and controls differed slightly between genders (see Figure 5-9 and Figure 5-10). A one-way analysis of co-variance (ANCOVA) revealed that differences between AD and control subjects within each gender were not significant for either A1M or ZAG (p>0.05), though this was an important consideration for subsequent analyses.

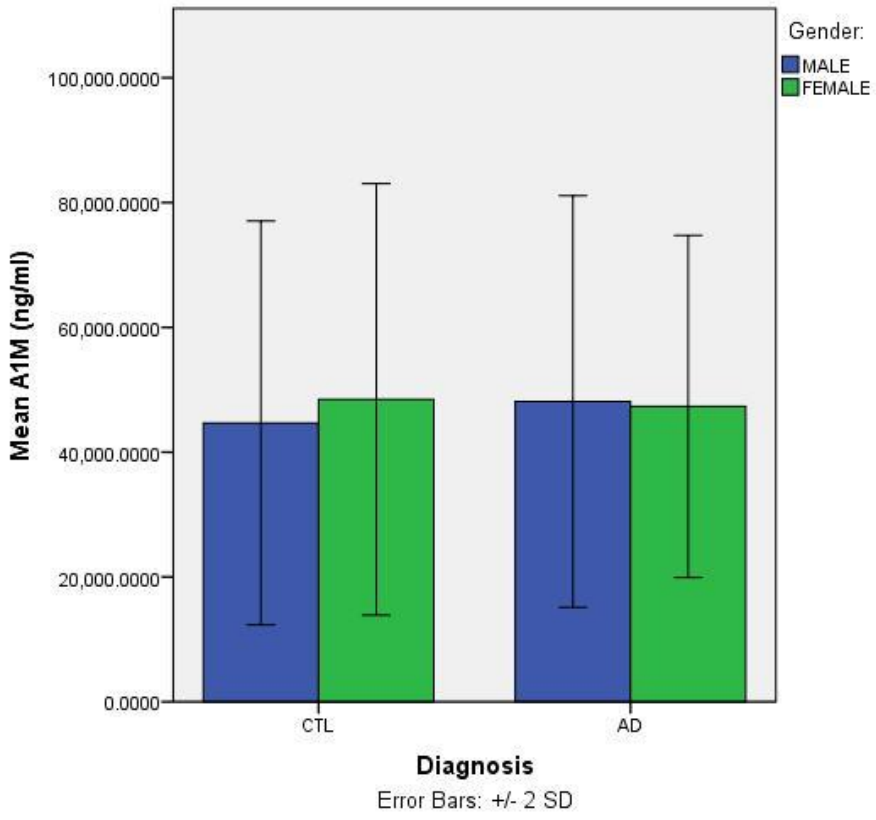

Figure 5-9: Bar chart displaying mean A1M values for AD and control subjects, split by gender

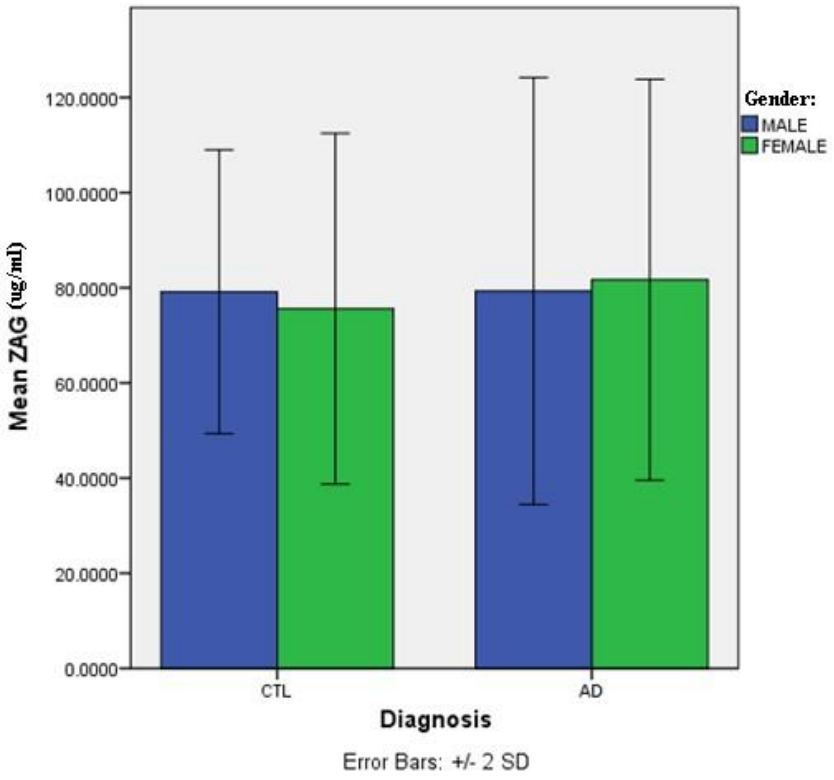

Figure 5-10: Bar chart displaying mean ZAG values for AD and control subjects, split by gender

A1M and ZAG associations with brain volume and cognitive decline

Partial correlations were performed for both A1M and ZAG to identify significant relationships with brain volumes, cognition (MMSE), and cognitive decline (MMSE change). No significant correlations were found for either A1M or ZAG ($p>0.05$), though for A1M three regions were tending towards significance; left and right entorhinal thickness, and left entorhinal volume ($p<0.1$). Full results are reported in Table 5-13 and Table 5-14 below.

Table 5-13: Partial correlation results for A1M, in order of significance

Dependant variable	Correlation coefficient	*P*-value	q-value
Left entorhinal cortical thickness	-0.200	0.057	0.302
Left entorhinal volume	-0.195	0.063	0.302
Right entorhinal cortical thickness	-0.179	0.090	0.302
Right entorhinal volume	-0.100	0.348	0.735
Whole brain	-0.096	0.367	0.735
MMSE	0.066	0.455	0.758
Left hippocampus	-0.059	0.581	0.829
Ventricles	0.045	0.673	0.842
MMSE loss per year	0.032	0.802	0.874
Right hippocampus	0.017	0.874	0.874

Table 5-14: Partial correlation results for ZAG, in order of significance

Dependant variable	Correlation coefficient	*P*-value	q-values
MMSE	-0.071	0.425	0.793
Right hippocampus	0.078	0.465	0.793
MMSE loss per year	0.092	0.468	0.793
Right entorhinal volume	0.076	0.477	0.793
Ventricles	-0.068	0.523	0.793
Whole brain	0.064	0.549	0.793
Right entorhinal cortical thickness	0.061	0.569	0.793
Left entorhinal cortical thickness	0.051	0.634	0.793
Left hippocampus	0.016	0.880	0.948
Left entorhinal volume	0.007	0.948	0.948

Previously a subtle difference in A1M and ZAG levels between males and females had been observed. Therefore partial correlations were repeated separately for each gender.

For A1M no significant correlations were found for female subjects. For male subjects significant correlations were found between A1M and both right and left entorhinal cortical thickness values ($p<0.05$), with the left entorhinal cortical thickness still remaining significant after FDR correction (q-value<0.1). Full results are reported in Table 5-15.

Table 5-15: Partial correlation results for A1M, split by gender

	Females			Males		
Dependant variable	**Correlation coefficient**	***P*-value**	**q-values**	**Correlation coefficient**	***P*-value**	**q-values**
Left entorhinal volume	-0.206	0.13	0.983	-0.222	0.220	0.620
Right entorhinal volume	-0.134	0.329	0.983	-0.210	0.248	0.620
Left hippocampus	-0.085	0.536	0.983	0.034	0.853	0.948
Ventricles	0.083	0.548	0.983	-0.084	0.650	0.929
Left entorhinal cortical thickness	-0.044	0.75	0.983	-0.457	0.006	0.060
Right hippocampus	-0.022	0.874	0.983	0.037	0.844	0.948
MMSE	-0.018	0.877	0.983	0.138	0.365	0.730
Whole brain	-0.01	0.944	0.983	-0.131	0.478	0.797
MMSE loss per year	0.004	0.981	0.983	0.007	0.981	0.981
Right entorhinal cortical thickness	-0.003	0.983	0.983	-0.354	0.041	0.205

For ZAG no significant correlations were found for male subjects. For female subjects a correlation between ZAG and left entorhinal volume was tending towards significance ($p<0.1$), though after FDR correction no relationship was found (q-value = 0.6). Full results are reported in Table 5-16.

Table 5-16: Partial correlation results for ZAG, split by gender

	Females			Males		
Dependant variable	**Correlation coefficient**	***P*-value**	**q-value**	**Correlation coefficient**	***P*-value**	**q-value**
Left entorhinal cortical thickness	-0.044	0.76	0.988	0.121	0.484	0.703
Left entorhinal volume	-0.251	0.073	0.617	0.196	0.25	0.703
Left hippocampus	0.004	0.975	0.988	0.04	0.816	0.907
MMSE	-0.065	0.576	0.988	-0.111	0.448	0.703
MMSE loss per year	0.108	0.474	0.988	-0.146	0.609	0.761
Right entorhinal cortical thickness	0.002	0.988	0.988	0.136	0.43	0.703
Right entorhinal volume	-0.207	0.143	0.617	0.256	0.127	0.703
Right Hippocampus	0.023	0.873	0.988	0.119	0.492	0.703
Ventricles	-0.053	0.714	0.988	-0.182	0.289	0.703
Whole brain	0.188	0.185	0.617	0.019	0.914	0.914

5.4 Discussion

The previous two chapters detailed the discovery of many candidate biomarkers for preclinical AD. From these, 15 proteins were found to associate with all three DVs measured (amyloid load, brain atrophy and cognitive decline). These 15 proteins

were therefore the strongest contenders to be biomarkers specific to AD and were considered for validation here.

Validation was performed using two different proteomic techniques, SOMAscan and ELISA, using a multi-centre cohort consisting of subjects from AddNeuroMed, ARUK and DCR cohorts. Biomarkers were here validated for their association to disease status, brain atrophy, and cognitive decline. Brain atrophy measurements were obtained from two brain regions; entorhinal cortex and hippocampus. These two brain regions are highly associated with AD; known as excellent imaging biomarkers of AD progression and severity[203-204, 206, 335-337]. MMSE was used as the measure of cognitive decline. MMSE is a brief test of general cognitive function and is widely used for the clinical assessment of AD; used as a screening tool as well as an indicator of disease progression[338-339]. Discovery phase experiments used Trails B as a marker of preclinical cognitive decline, and MMSE has shown utility as a predictive tool of later AD development[338, 340-341]. However MMSEs utility is mainly well-established for the assessment of clinical populations, appropriate to the cohorts used here.

SomaLogic SOMAscan validation

Using SomaLogic's SOMAscan proteomics technology 7 of these proteins were assessed for their relationship with AD status, brain atrophy and cognition. One protein, AAT, validated as an AD biomarker of disease status and brain atrophy of both the left entorhinal volume and right hippocampal volume, at the 0.1 FDR level. Increased AAT was found in AD subjects compared to controls, and higher levels of AAT correlated with decreased brain volume. This is consistent with the findings of the 2DGE discovery study where AAT was one of the most commonly detected proteins in significant 2DGE spots, with the majority of spots displaying a positive relationship with increased AD pathology and cognitive decline. Together these results provide evidence that AAT is associated with AD pathology throughout the preclinical and clinical stages. This detrimental increase in AAT has here been observed in healthy controls and AD individuals, across multiple cohorts and different proteomic techniques. These results are also consistent with previous research where increased AAT levels have been found in AD plasma and CSF compared to controls [237-238]. Although this is a very strong finding, not all of the

results found in the discovery phase experiments agree with a positive relationship between AAT and AD pathology and cognitive decline. Specifically the LC-MS/MS LMW protein discovery study identified AAT as a biomarker of brain atrophy, with decreased AAT related to increased atrophy of the superior temporal gyrus. This highlights that AAT may have a more complex relationship with AD than the previous results suggest, with, for example, AAT fragments behaving differently to the full length protein. It is important for future experiments to define which epitope of AAT the aptamers are measuring so that results can be accurately compared.

At a slightly more relaxed FDR level of 0.2 this study also validated both complement C3 and haptoglobin as biomarkers of cognitive decline. Both proteins were found to be positively related with MMSE score; with lower C3 and haptoglobin levels indicating cognitive decline. Although discovery phase experiments revealed mixed coefficient directions for these proteins with the DVs, many of the results found do agree with the findings of these validation experiments.

For all three DVs many 2DGE spots containing C3 displayed a detrimental relationship with decreased C3 levels; associating with increased amyloid deposition, larger ventricular expansion, and increased time taken to complete Trails B task. LC-MS/MS discovery experiments also revealed the same direction of relationship with increased amyloid load (at T6). Together with the validation experiments these results support a decrease in C3 as detrimental, and specifically provide evidence for its utility as a biomarker of cognitive decline, both preclinically and during the clinical stages of AD. These results also correspond with previous literature suggesting a protective role of C3[222, 229].

The 2DGE discovery experiments also reported haptoglobin as a candidate biomarker for all three DVs, with each DV showing both positive and negative relationships with haptoglobin. The results of this SOMAscan study validate the 2DGE spots showing a negative relationship with Trails B (decreased haptoglobin with increased time taken). These results suggest a longitudinal relationship between haptoglobin and cognitive decline. This is supported by literature which suggests a progressive impairment of haptoglobins functions throughout disease progression[281].

A1M and ZAG ELISA validation

8 of the 15 proteins selected for validation did not have SomaLogic SOMAscan assays available: ZAG, Protein AMBP, Ceruloplasmin, ApoA-IV, Ig kappa chain C region, Ig gamma 1 chain C region, Ig gamma 2 chain C region, and Ig alpha 1 chain C region. ELISA was selected as a targeted proteomic technique by which further validation could be conducted, though time and cost limited the number of proteins which could be validated by ELISA to two. These two proteins were selected based upon novelty to AD research and the availability of reliable ELISA assay. Ceruloplasmin, ApoA-IV and the various IgGs have a good evidence base for their involvement in AD[142, 151, 270, 273, 276, 342-343], as discussed in detail in chapters 2 and 3. ELISA availability for immunoglobulins was also relatively poor. To date comparatively less AD-related research is available for protein AMBP and ZAG, whilst many ELISA assays were available for these two proteins, therefore they were selected for validation. The coefficient of variation for these two plates was low (6.48% and 6.55%), indicating that a good level of data quality was achieved and statistical analysis was conducted with confidence.

In chapter 2 the approximate molecular weight of the significant 2DGE spots containing protein AMBP was 30-40kDa. This indicated that the protein identified was either the full length AMBP protein (39kDa), or its largest chain α1M. Therefore here an ELISA specific to the alpha-1-microglobulin (A1M) chain of protein AMBP was chosen for validation. The results here show that A1M was tending towards a significant relationship with three brain regions; right and left entorhinal cortical thickness and left entorhinal volume, with an increase in A1M found with increased brain atrophy. This relationship with right and left entorhinal cortical thickness was highly significant when considered for male subjects only. Although these results provide further support for A1M as a biomarker of AD pathology, they do not validate the 2DGE discovery phase findings where protein AMBP was found to decrease with increased brain atrophy (ventricular expansion). It is possible that a different section of protein AMBP was measured by 2DGE, not the A1M chain. It is also possible that the relationship of this protein with AD changes over time from the preclinical stage into the clinical disease onset. However discovery results did also report an increase in protein AMBP with higher amyloid load at T12, providing a form of validation for an increase in A1M with increased pathology. Although these

results are confusing, it does indicate that there is a relationship between protein AMBP/A1M and AD that needs further clarification.

ZAG was not found to be a biomarker of any of the measures tested here. Though when focusing on female subjects only it did show small potential as a marker of left entorhinal volume, tending towards significance ($p<0.1$) but not passing FDR corrections. Although this significance level renders the result doubtful, the direction of the relationship (negative) corresponds to the majority of findings in both discovery phase experiments, with all three DVs. This perhaps gives more credibility to the validation result, which with a larger cohort may have shown increased significance.

Both A1M and ZAG showed gender specific results highlighting the importance of assessing biomarker abilities for each gender separately. Gender differences in AD research are often reported; the prevalence of AD is higher in women than men, behavioural and cognitive functions are often expressed differently between genders, and brain morphology and function also differ (see [344-345] for reviews). It is therefore unsurprising that plasma biomarkers would also reflect these gender specific differences and so themselves differ between genders. Future studies should stratify and report data by gender for all aspects of the disease.

5.5 Conclusions

Proteins AAT, C3, haptoglobin, and protein AMBP showed results that validated discovery phase findings, with AAT found to be the strongest biomarker candidate. This validation provided evidence of the biomarker utility of these proteins in AD patients, indicating that their preclinical biomarker utility previously discovered is also likely to be specific for AD. Therefore these proteins can be considered as related to AD both clinically and preclinically and are able to measure disease progression from a preclinical stage throughout to a clinical diagnosis. Although the relationship with AD was tested here, the sensitivity and specificity of the biomarkers need to be further tested by assessing their relationships with other neurological diseases in future studies.

Proteins that were not found to be significant in these validation experiments may still have biomarker ability which was not tested here. Discovery phase experiments identified proteins as candidate biomarkers of amyloid load, brain atrophy and cognitive decline, therefore their strength as biomarkers may be in reflecting one of these three DVs, specifically at a preclinical stage. In addition, although brain atrophy and cognitive decline were included in this validation study, the measurements of these differed between the studies which may have hindered validation. Discovery phase experiments assessed both of these measures longitudinally over a 12 year period, whereas validation experiments measured cognitive decline over a maximum of 2 years, and brain atrophy was only measured at a single time point cross-sectionally. Furthermore information on brain amyloid load was not available for these subjects and so protein relationships with amyloid burden could not be tested. These differences were unavoidable and it is rare that cohorts match exactly on the information that they have available; another reason that comparisons between studies is difficult. For these reasons non-validating proteins should still be considered for future validation experiments.

Chapter 6. Conclusions

6.1 Overall Discussion

Recently, research has shown that it is possible to detect a peripheral signal of AD. Whilst it is unclear whether changes found in the periphery reflect direct disease mechanisms or secondary changes to disease processes in the brain, it is now clear that plasma is a rich source of biomarkers for the disease. Much research has focused upon the ability of differentially expressed proteins to classify individuals into diagnosis groups (e.g. AD versus healthy controls). Very high sensitivity and specificity has been found with these approaches, and whilst this is encouraging these approaches have their limitations. Mainly clinical heterogeneity in patients and neuropathology in controls is ignored with these approaches and so biomarkers identified may instead reflect secondary changes specific to the cohort used rather than the disease biology. Therefore using disease status as the primary outcome variable in a large scale discovery study may result in the identification of biomarkers with limited/no involvement in disease. Additionally these biomarkers may have limited clinical utility as they may lack sensitivity to disease severity or progression. Using well established surrogate markers of AD as primary outcome measurements to discover AD biomarkers can help to avoid these issues.

The main aims of this project were to discover candidate plasma biomarkers of preclinical AD pathology and cognitive decline. Increasingly research is focusing on the early preclinical stages of AD as results of clinical trials and laboratory research indicate that interventions may only be beneficial at an early stage. Biomarkers will play a crucial role in the identification and monitoring of preclinical AD individuals, and plasma based biomarkers would be most practical. In 2010 Thambisetty et al performed a retrospective preclinical AD biomarker study investigating plasma proteins reflecting brain amyloid load 10 years later[151]. This project aimed to repeat and expand upon this work. Here, plasma proteins were assessed for their relationship to amyloid load 12 years prior, 6 years prior, and concurrently to the PiB PET scan. Additionally the plasma proteome was investigated for a correlation with two more measures of Alzheimer's disease (cognitive decline and brain atrophy) over a longitudinal 12 year period.

This project used two complimentary discovery proteomic techniques for the discovery of biologically relevant plasma biomarkers of preclinical AD. 2DGE was used to discover larger proteins as biomarkers (~20-250kDa), whereas LC-MS/MS methodology was tailored to focus on the discovery of LMW proteins (<30kDa) and less abundant proteins as biomarkers. Together these two techniques provided a more comprehensive analysis of the plasma proteome for the discovery of preclinical AD biomarkers. Each technique identified unique candidate biomarkers, highlighting the importance of increasing molecular weight and dynamic range coverage in biomarker discovery; ensuring as many proteins as possible are included for analysis. In addition, many candidate proteins overlapped between the two techniques, providing a form of replication. Although it cannot be confirmed that the same forms of these proteins were being identified with each technique, these findings add confidence to the proteins ability as a preclinical AD biomarker.

Discovery stage experiments were very successful in identifying many candidate biomarkers for preclinical AD. However it was considered important to establish whether these proteins are involved in AD after clinical onset. This was to increase confidence in their relationship with AD development at the preclinical stage, rather than as markers of general decline in health or other co-morbidities. Therefore validation experiments were conducted using plasma samples from AD patients as well as healthy controls. In addition to testing biomarker ability for disease status, the proteins' relationship with cognitive decline and brain atrophy was also assessed during validation experiments.

Aptamer and antibody based techniques (SOMAlogic's SOMAscan™ and enzyme-linked immunosorbent assay (ELISA)) were chosen to validate targeted proteins. Multiple proteins had been discovered as candidate biomarkers but due to time and cost restraints only a subset could be validated. 15 proteins were considered to have the strongest likelihood of being specifically involved in AD; these were proteins which were found to be associated with all three DVs preclinically (brain amyloid burden, brain atrophy, and cognitive decline). From these 15, 7 were analysed using a pre-exisiting SOMAscan dataset, and a further 2 were selected for validation by ELISA.

Five proteins (α1-antitrypsin (AAT), complement C3, haptoglobin, protein AMBP (A1M), and zinc- α2 glycoprotein) all validated for at least one of the measures tested, though with varying significance strengths. AAT was by far the strongest biomarker candidate, showing highly significant relationships with both disease status and brain atrophy. C3 and haptoglobin both showed a relationship with cognitive decline, and A1M and ZAG displayed relationships with brain atrophy. These five proteins are therefore very interesting markers to use for these measures in preclinical individuals. These findings merit independent confirmation in future preclinical studies. If further replicated these preclinical biomarkers are likely to be examined for their utility as markers of disease in healthy individuals, being considered for clinical trials, and for treatment response at an early, preclinical stage.

As mentioned above, proteins that associated with all three DVs preclinically were considered for validation experiments. However proteins that were found to be specifically related to only one or two DVs in the discovery phase experiments are also very interesting. Although these proteins were not validated here they should still be considered for future studies. Many of these proteins already have a strong body of evidence for their biomarker ability in AD, and therefore their ability as biomarkers of preclinical AD can be considered seriously even without validation phase confirmation. For example, 2DGE experiments identified clusterin as a biomarker for cognitive decline in healthy individuals, and much previous literature has established a relationship between clusterin and AD severity, pathology, and progression[137, 288], some of which has already implicated a potentially important role for clusterin in the earliest stages of AD related neurodegeneration[261-262, 293].

Discovery phase analyses revealed unique sets of significant proteins as biomarkers for the three different DVs. Whilst all three DVs are strongly linked to AD they capture different temporal and mechanistic aspects of the disease. Brain atrophy and cognitive measures are continuous and were measured longitudinally here. Although compensatory mechanisms can delay cognitive decline, brain atrophy and cognition will be intrinsically linked. Amyloid load was only measured cross sectionally at the final time point, though this may be the most independent of the surrogate markers measured and may be capable of capturing earlier disease specific changes[70]. For

each surrogate marker it is likely that some of the proteins identified as biomarkers will correlate with each other or be involved in the same pathways or mechanisms; therefore they may be surrogates for each other. Combining proteins that capture unique aspects of AD preclinically will increase their utility as preclinical AD biomarkers. Further experiments are needed to reveal the optimal combination of these markers.

Many proteins displayed opposite coefficient directions for the significant relationships detected between studies. This highlights the complexity of the relationships some of these proteins may have with disease, and the importance of future experiments to determine exactly which parts and forms of the protein they are measuring and correlating with an outcome measure. It is not rare for different studies to report conflicting relationships of a protein with AD. Perhaps if more effort is directed towards specifying the precise protein epitope which is being measured then these conflicts would be much rarer.

The proteins found here to be implicated in preclinical AD are involved in a variety of systems, including; complement and inflammation, coagulation, hemostasis, fibrinolysis, and BBB integrity. Such systems may be causally related to AD onset, or be affected as a result of the disease. Additionally the involvement of these systems in AD pathology may be inter-linked or they may act independently, further work is needed to clarify these relationships. The involvement of these systems has also been highlighted in recent large-scale genetics studies [351], showing that results from both genetics and biology agree on the pathways of interest. It may be possible to identify the resulting contribution of some of these pathways (e.g. chronic inflammation) as high risk factors for the development of AD in healthy individuals, comparable to that of more-established risk factors such as *APOE* ε4 status. At the very least, the presence of these biomarkers in healthy elderly individuals indicates potential early intervention targets worthy of further investigation.

6.2 Summary

In conclusion, this project adds further evidence that plasma is a rich resource for AD biomarkers. Biological variation and the dynamic range of plasma complicates the discovery, but through the use of complimentary techniques these issues can be

minimised. Here we show it is also possible to detect these plasma based biomarkers at a stage long before the onset of clinical disease manifestations. Preliminary discovery studies detected many candidate biomarkers for surrogate markers of AD pathology and cognitive decline in a healthy elderly cohort. Some of these candidate biomarkers were then validated for their involvement in AD, providing support for their preclinical AD biomarker utility. As early indicators of AD these proteins may become targets of treatment or preventative healthcare measures once the mechanisms behind their involvement becomes better understood.

6.3 Future studies

Research into plasma based preclinical AD biomarkers is still an emerging field. This study provides more evidence in a growing body of literature, but more work is needed to expand upon the findings presented here and develop this research field further. Suggestions for future studies and research aims to expand upon these results are outlined below.

6.3.1 Further expand 2DGE data analysis

A limitation of 2DGE in this study is that the number of spots that can be picked for LC-MS/MS protein identification was constrained by time and cost. This restricted the amount of analysis that could be completed. Data was available for many cognitive measures and brain regions but only the measures showing the greatest linear change over time were selected for analysis. This could be expanded and would be of particular interest for brain regions, such as the entorhinal cortex and hippocampus, known to be effected early on in AD.

6.3.2 Assess post translational modifications and protein fragments for biomarker ability

2DGE experiments showed that many of the proteins identified as candidate biomarkers were found in multiple 2DGE spots located throughout the gel, this is indicative of multiple forms of the proteins (modified and/or cleaved) as biomarkers. Additionally, many of the same proteins were identified in the LC-MS/MS discovery experiments where a prefractionation stage had been completed; indicating different forms of these proteins were detected compared to those found in 2DGE spots of

high molecular weight. These results show that it would be highly interesting to assess post translational modifications and cleavage of the proteins identified as candidate biomarkers. A first approach to this could be completed through an in depth re-analysis of the mass spectrometry data generated here for proteins of interest from both discovery studies.

6.3.3 Validate candidate biomarkers of preclinical AD in an independent healthy elderly cohort.

Candidate biomarkers were here discovered in the Baltimore Longitudinal Study of Aging cohort. Validation was focused upon determining their involvement in AD, though validation is also needed for their preclinical AD biomarker ability in other healthy elderly cohorts. This will determine whether they are robust results across cohorts and studies. Reproducible results are necessary to add confidence for future clinical utility.

6.3.4 Identify a preclinical AD biomarker panel

Here proteins were individually assessed for their biomarker ability. However their true strength is likely to lie as a biomarker panel of multiple proteins, each reflecting different aspects and mechanisms involved in the development of the disease. This approach has been successfully employed in AD biomarker research several times[76, 139-141], similar approaches can be applied preclinically.

6.3.5 Determine sensitivity and specificity of preclinical biomarkers against other types of dementias and neurodegenerative diseases.

Validation of biomarkers in cohorts including patients with other types of dementias and neurodegenerative diseases would determine which biomarkers are specific for AD, helping to achieve a greater diagnostic accuracy for early AD detection.

6.3.6 Identify gender specific biomarkers for preclinical AD

Validation studies revealed gender effects on plasma biomarkers. It is likely that differences in the development of AD might also differ between genders, and such differences may be reflected in the periphery. Therefore future experiments investigating preclinical AD biomarkers should stratify based on gender.

6.4 Limitations

6.4.1 Using blood for biomarker discovery

Although blood biomarkers have significant potential in early AD detection, limitations of using blood as a source of biomarkers should be considered. Blood has a complex composition with a large dynamic range, which can pose technical difficulties for biomarker discovery. Changes within the blood are often very small and reflect a wide range of both peripheral and central processes, so pinpointing AD specific changes can be challenging. Proteomics has so far shown great success in identifying AD blood biomarkers, however detailed characterisation of these proteins including changes in quantification, location, interactions, isoforms and post-translational modifications (PTMs) is now needed to further our understanding of different biological states. The identification of these features in blood is challenging as proteins need to be identified from within a matrix of cells, tissues, fluids, and other proteins of varying concentrations. Other modalities, such as CSF, may be a simpler option to identify and characterise these biomarker candidates.

Currently some of the best AD biomarkers are CSF based (CSF tau and Aβ). Often results of blood based biomarker studies are compared to those from CSF to provide further support for their findings. However this should be done with some caution as these two modalities may not be comparable, at least not for all proteins. Differences in CSF and plasma composition (e.g. presence of cells and protein concentration) will influence the type proteins identified, protein functions may differ, and so may biomarker ability between the two modalities.

6.4.2 Aβ and tau not detected

CSF quantification of $A\beta_{1-42}$, phosphorylated tau (P-tau) and total-tau (T-tau) have shown great biomarker abilities for AD, and are thought to reflect the core pathologic features of AD; amyloid plaques, neurofibrillary tangles and neuronal loss, respectively. However in plasma the results of Aβ and tau are often contradictory, measurements are subjected to more sources of variability than CSF measurements, and increased assay sensitivity is needed to detect these proteins. Further clinical

research and assay development are needed before measures of plasma Aβ and tau can be accurately interpreted.

Throughout this study neither Aβ or tau protein was identified. Although the discovery proteomic methods used here were not expected to detect either protein without experimental optimisation it is unfortunate that the two key proteins reflecting AD neuropathology could not be detected and investigated as AD biomarkers.

6.4.3 No biomarker concentration thresholds

Threshold values for biomarkers must be determined for them to be of use as a diagnostic/screening tool. This threshold is normally calculated as the value which produces the highest test sensitivity and specificity. However in this study neither proteomic discovery technique (2DGE/LC-MS/MS) provided absolute quantification of proteins, therefore estimation of optimal thresholds could not be computed. Further testing of candidate biomarkers should be quantitative to enable this calculation.

6.4.4 Specificity of PiB PET DVR, Trails B, and ventricular expansion to Alzheimer's disease

Currently there is a lack of a 100% accurate gold standard for AD for which biomarkers can be discovered. Post mortem neuropathology analysis is considered the most accurate indicator of AD, however even this method has limitations; it is subjective, dependent upon the neuropathiologist, and is often combined with patients' clinical history to form a diagnosis. Here PiB PET DVR, Trails B and ventricular expansion were used and considered as indicators of early AD development. As previously discussed these measures have all been found to be linked to AD and change at an early, preclinical, stage. However these measurements, especially the latter two, are not specific to AD and are often altered in various other disorders including different types of dementia.

Executive dysfunction, as measured by Trails B, is a prominent feature of vascular dementia. Research has been inconclusive regarding differences in executive impairment between AD and vascular dementia, and many consider this impairment

to be similar between the two types of dementia[350]. In addition ventricular expansion is often seen in vascular dementia, due to global atrophy. The candidate biomarkers here may therefore also be useful as early markers of vascular dementia. In fact a number of the biomarkers identified here fit a profile of vascular effects, for example; AIII, fibrinogen, clusterin, and various apolipoproteins. If these markers are specific to AD then they are still likely to be reflecting the influences of cardiovascular disease in contributing to and exacerbating AD pathology.

It is also interesting to note that there was very minimal correlation between PiB PET DVR, Trails B and ventricular expansion. Only a moderate correlation was found between ventricle size and Trails B at T12, but no other correlations were reported between any DV at any time point. It was suggested that either the sensitivity of these measures differ or perhaps different forms of the same protein are related to the three DVs. However it is also possible that the subjects which show change in each of these variables are different, and therefore the lack of correlation would be unsurprising.

Further experiments are necessary to determine the biomarkers specificity to AD, and for now it is important to remember that they may not be AD specific. Instead they should be considered only as markers of amyloid deposition, executive function decline, and brain atrophy, potentially useful for multiple disorders.

6.4.5 Limitations of statistical methods

Linear data. The statistical tests used for this study could only model linear data, and therefore proteins which showed non-linear changes over time were excluded. Some of these excluded proteins may be AD biomarkers, and these dynamic changes over time may be highly biologically interesting. It is important to develop and implement more advanced statistical methods which can model dynamic changes in protein concentration over time and test these proteins for biomarker ability.

False discovery rate corrections. Throughout the discovery phase experiments false discovery rate (FDR) corrections were not applied. This was because the large number of statistical tests conducted would have resulted in an unachievable FDR threshold. Instead a *p*-value of <0.05 was considered, though this will have resulted

in many false positive findings. Future validation experiments are important to confirm true results and discard false positives. It is also important to note that *p*-values and q-values are arbitrary cut-off points. Although it is necessary to use these values, proteins on the threshold of significance which still may be interesting are ignored.

Outliers. In validation experiments extreme data outliers were excluded from analysis. It was important to remove these outliers for two reasons; firstly, so that the spread of data was normally distributed, and secondly, so that extreme values did not skew the results of the dataset. Removal of outliers therefore increases the accuracy of statistical tests and minimises their error. However there was no obvious reason here as to why these individual samples yielded extreme values and therefore it is possible that they may be legitimate data points. Though it is still unclear what should be done when a legitimate outlier is present, as removal increases statistical power but reduces validity. Further development of statistical models to include outliers is needed.

Covariates. Six covariates were included in most of the statistical tests conducted, these were; age, gender, education (years), body mass index (BMI), cholesterol, and *APOE* ε4 status. All of these factors have known impacts upon the risk of AD, and were included as covariates to remove their influence and enable any relationship between protein and AD to be identified. However 6 is a large number of covariates to include, and may have resulted in decreased efficiency of the statistical tests or over-fitting of regression models. A stepped-approach, repeating the test multiple times with different covariates added, may have clarified their effects on the statistical tests. In addition, both *APOE* ε4 status and cholesterol were included as covariates, but both of these factors may be intrinsically linked as *APOE* ε4 carriers are thought to have higher cholesterol. This may have further reduced the efficiency of the statistical tests conducted and should have been investigated.

Bibliography

1. Prince, M., R. Bryce, E. Albanese, A. Wimo, W. Ribeiro, and C.P. Ferri, *The global prevalence of dementia: A systematic review and metaanalysis.* Alzheimer's & Dementia, 2013. 9(1): p. 63-75.e2.
2. Lobo, A., L.J. Launer, L. Fratiglioni, K. Andersen, A. Di Carlo, M.M. Breteler, J.R. Copeland, J.F. Dartigues, C. Jagger, J. Martinez-Lage, H. Soininen, and A. Hofman, *Prevalence of dementia and major subtypes in Europe: A collaborative study of population-based cohorts. Neurologic Diseases in the Elderly Research Group.* Neurology, 2000. 54(11 Suppl 5): p. S4-9.
3. Wimo, A. and M. Prince, *World Alzheimer Report 2010: The Global Economic Impact of Dementia*. 2010.
4. Alzheimer, A., *Uber eine eigenartige Erkrankung der Hirnrinde.* Zeitschr Psychiatry Psychiatr-Gericht Med, 1907: p. 146-148.
5. Iliffe, S. *What is Alzheimer's disease?* 2011, Available from: http://alzheimers.org.uk/site/scripts/documents_info.php?documentID=100.
6. Association, A.P., *Diagnostic and statistical manual of mental disorders*. 2000: Washington, DC.
7. Francis, P.T., A.M. Palmer, M. Snape, and G.K. Wilcock, *The cholinergic hypothesis of Alzheimer's disease: a review of progress.* Journal of Neurology, Neurosurgery and Psychiatry, 1999. 66(2): p. 137-47.
8. Thal, L.J., K. Kantarci, E.M. Reiman, W.E. Klunk, M.W. Weiner, H. Zetterberg, D. Galasko, D. Pratico, S. Griffin, D. Schenk, and E. Siemers, *The role of biomarkers in clinical trials for Alzheimer disease.* Alzheimer Disease and Associated Disorders, 2006. 20(1): p. 6-15.
9. Goedert, M., R.A. Crowther, and C.C. Garner, *Molecular characterization of microtubule-associated proteins tau and MAP2.* Trends in Neurosciences, 1991. 14(5): p. 193-9.
10. Dickson, D.W., H.A. Crystal, C. Bevona, W. Honer, I. Vincent, and P. Davies, *Correlations of synaptic and pathological markers with cognition of the elderly.* Neurobiology of Aging, 1995. 16(3): p. 285-298.
11. Mudher, A. and S. Lovestone, *Alzheimer's disease – do tauists and baptists finally shake hands?* Trends in Neurosciences, 2002. 25(1): p. 22-26.
12. Nestor, P.J., P. Scheltens, and J.R. Hodges, *Advances in the early detection of Alzheimer's disease.* Nature Medicine, 2004. 10 Suppl: p. S34-41.
13. Wilcock, G.K. and M.M. Esiri, *Plaques, tangles and dementia. A quantitative study.* Journal of the Neurological Sciences, 1982. 56(2-3): p. 343-56.
14. Hua, X., A.D. Leow, S. Lee, A.D. Klunder, A.W. Toga, N. Lepore, Y.Y. Chou, C. Brun, M.C. Chiang, M. Barysheva, C.R. Jack, Jr., M.A. Bernstein, P.J. Britson, C.P. Ward, J.L. Whitwell, B. Borowski, A.S. Fleisher, N.C. Fox, R.G. Boyes, J. Barnes, D. Harvey, J. Kornak, N. Schuff, L. Boreta, G.E. Alexander, M.W. Weiner, P.M. Thompson, and I. Alzheimer's Disease Neuroimaging, *3D characterization of brain atrophy in Alzheimer's disease and mild cognitive impairment using tensor-based morphometry.* Neuroimage, 2008. 41(1): p. 19-34.
15. Herholz, K., S.F. Carter, and M. Jones, *Positron emission tomography imaging in dementia.* British Journal of Radiology, 2007. 80 Spec No 2: p. S160-7.

16. Weller, R.O., S.D. Preston, M. Subash, and R.O. Carare, *Cerebral amyloid angiopathy in the aetiology and immunotherapy of Alzheimer disease.* Alzheimers Res Ther, 2009. 1(2): p. 6.
17. Chartier-Harlin, M.C., F. Crawford, H. Houlden, A. Warren, D. Hughes, L. Fidani, A. Goate, M. Rossor, P. Roques, J. Hardy, and et al., *Early-onset Alzheimer's disease caused by mutations at codon 717 of the beta-amyloid precursor protein gene.* Nature, 1991. 353(6347): p. 844-6.
18. Murrell, J., M. Farlow, B. Ghetti, and M.D. Benson, *A mutation in the amyloid precursor protein associated with hereditary Alzheimer's disease.* Science, 1991. 254(5028): p. 97-9.
19. Citron, M., T. Oltersdorf, C. Haass, L. McConlogue, A.Y. Hung, P. Seubert, C. Vigo-Pelfrey, I. Lieberburg, and D.J. Selkoe, *Mutation of the beta-amyloid precursor protein in familial Alzheimer's disease increases beta-protein production.* Nature, 1992. 360(6405): p. 672-4.
20. Sherrington, R., E.I. Rogaev, Y. Liang, E.A. Rogaeva, G. Levesque, M. Ikeda, H. Chi, C. Lin, G. Li, K. Holman, T. Tsuda, L. Mar, J.F. Foncin, A.C. Bruni, M.P. Montesi, S. Sorbi, I. Rainero, L. Pinessi, L. Nee, I. Chumakov, D. Pollen, A. Brookes, P. Sanseau, R.J. Polinsky, W. Wasco, H.A. Da Silva, J.L. Haines, M.A. Perkicak-Vance, R.E. Tanzi, A.D. Roses, P.E. Fraser, J.M. Rommens, and P.H. St George-Hyslop, *Cloning of a gene bearing missense mutations in early-onset familial Alzheimer's disease.* Nature, 1995. 375(6534): p. 754-60.
21. Taddei, K., C. Fisher, S.M. Laws, G. Martins, A. Paton, R.M. Clarnette, C. Chung, W.S. Brooks, J. Hallmayer, J. Miklossy, N. Relkin, P.H. St George-Hyslop, S.E. Gandy, and R.N. Martins, *Association between presenilin-1 Glu318Gly mutation and familial Alzheimer's disease in the Australian population.* Molecular Psychiatry, 2002. 7(7): p. 776-81.
22. Gómez-Isla, T., W.B. Growdon, M.J. McNamara, D. Nochlin, T.D. Bird, J.C. Arango, F. Lopera, K.S. Kosik, P.L. Lantos, N.J. Cairns, and B.T. Hyman, *The impact of different presenilin 1 andpresenilin 2 mutations on amyloid deposition, neurofibrillary changes and neuronal loss in the familial Alzheimer's disease brain: Evidence for other phenotype-modifying factors.* Brain, 1999. 122(9): p. 1709-1719.
23. Saunders, A.M., W.J. Strittmatter, D. Schmechel, P.H. St. George-Hyslop, M.A. Pericak-Vance, S.H. Joo, B.L. Rosi, J.F. Gusella, D.R. Crapper-MacLachlan, M.J. Alberts, C. Hulette, B. Crain, D. Goldgaber, and A.D. Roses, *Association of apolipoprotein E allele ϵ4 with late-onset familial and sporadic Alzheimer's disease.* Neurology, 1993. 43(8): p. 1467.
24. Corder, E., A. Saunders, W. Strittmatter, D. Schmechel, P. Gaskell, G. Small, A. Roses, J. Haines, and M. Pericak-Vance, *Gene dose of apolipoprotein E type 4 allele and the risk of Alzheimer's disease in late onset families.* Science, 1993. 261(5123): p. 921-923.
25. Sando, S.B., S. Melquist, A. Cannon, M.L. Hutton, O. Sletvold, I. Saltvedt, L.R. White, S. Lydersen, and J.O. Aasly, *APOE epsilon 4 lowers age at onset and is a high risk factor for Alzheimer's disease; a case control study from central Norway.* BMC Neurol, 2008. 8: p. 9.
26. Henderson, A.S., S. Easteal, A.F. Jorm, A.J. Mackinnon, A.E. Korten, H. Christensen, L. Croft, and P.A. Jacomb, *Apolipoprotein E allele epsilon 4, dementia, and cognitive decline in a population sample.* Lancet, 1995. 346(8987): p. 1387-90.

27. Riley, K.P., D.A. Snowdon, A.M. Saunders, A.D. Roses, J.A. Mortimer, and N. Nanayakkara, *Cognitive function and apolipoprotein E in very old adults: findings from the Nun Study.* Journals of Gerontology. Series B, Psychological Sciences and Social Sciences, 2000. 55(2): p. S69-75.
28. Wilson, R.S., J.A. Schneider, L.L. Barnes, L.A. Beckett, N.T. Aggarwal, E.J. Cochran, E. Berry-Kravis, J. Bach, J.H. Fox, D.A. Evans, and D.A. Bennett, *The apolipoprotein E epsilon 4 allele and decline in different cognitive systems during a 6-year period.* Archives of Neurology, 2002. 59(7): p. 1154-60.
29. Altmann, A., L. Tian, V.W. Henderson, and M.D. Greicius, *Sex modifies the APOE-related risk of developing Alzheimer disease.* Annals of Neurology, 2014. 75(4): p. 563-73.
30. Guerreiro, R., A. Wojtas, J. Bras, M. Carrasquillo, E. Rogaeva, E. Majounie, C. Cruchaga, C. Sassi, J.S. Kauwe, S. Younkin, L. Hazrati, J. Collinge, J. Pocock, T. Lashley, J. Williams, J.C. Lambert, P. Amouyel, A. Goate, R. Rademakers, K. Morgan, J. Powell, P. St George-Hyslop, A. Singleton, and J. Hardy, *TREM2 variants in Alzheimer's disease.* New England Journal of Medicine, 2013. 368(2): p. 117-27.
31. Takahashi, K., C.D.P. Rochford, and H. Neumann, *Clearance of apoptotic neurons without inflammation by microglial triggering receptor expressed on myeloid cells-2.* The Journal of Experimental Medicine, 2005. 201(4): p. 647-657.
32. Harold, D., R. Abraham, P. Hollingworth, R. Sims, A. Gerrish, M.L. Hamshere, J.S. Pahwa, V. Moskvina, K. Dowzell, A. Williams, N. Jones, C. Thomas, A. Stretton, A.R. Morgan, S. Lovestone, J. Powell, P. Proitsi, M.K. Lupton, C. Brayne, D.C. Rubinsztein, M. Gill, B. Lawlor, A. Lynch, K. Morgan, K.S. Brown, P.A. Passmore, D. Craig, B. McGuinness, S. Todd, C. Holmes, D. Mann, A.D. Smith, S. Love, P.G. Kehoe, J. Hardy, S. Mead, N. Fox, M. Rossor, J. Collinge, W. Maier, F. Jessen, B. Schurmann, R. Heun, H. van den Bussche, I. Heuser, J. Kornhuber, J. Wiltfang, M. Dichgans, L. Frolich, H. Hampel, M. Hull, D. Rujescu, A.M. Goate, J.S. Kauwe, C. Cruchaga, P. Nowotny, J.C. Morris, K. Mayo, K. Sleegers, K. Bettens, S. Engelborghs, P.P. De Deyn, C. Van Broeckhoven, G. Livingston, N.J. Bass, H. Gurling, A. McQuillin, R. Gwilliam, P. Deloukas, A. Al-Chalabi, C.E. Shaw, M. Tsolaki, A.B. Singleton, R. Guerreiro, T.W. Muhleisen, M.M. Nothen, S. Moebus, K.H. Jockel, N. Klopp, H.E. Wichmann, M.M. Carrasquillo, V.S. Pankratz, S.G. Younkin, P.A. Holmans, M. O'Donovan, M.J. Owen, and J. Williams, *Genome-wide association study identifies variants at CLU and PICALM associated with Alzheimer's disease.* Nature Genetics, 2009. 41(10): p. 1088-93.
33. Naj, A.C., G. Jun, G.W. Beecham, L.S. Wang, B.N. Vardarajan, J. Buros, P.J. Gallins, J.D. Buxbaum, G.P. Jarvik, P.K. Crane, E.B. Larson, T.D. Bird, B.F. Boeve, N.R. Graff-Radford, P.L. De Jager, D. Evans, J.A. Schneider, M.M. Carrasquillo, N. Ertekin-Taner, S.G. Younkin, C. Cruchaga, J.S. Kauwe, P. Nowotny, P. Kramer, J. Hardy, M.J. Huentelman, A.J. Myers, M.M. Barmada, F.Y. Demirci, C.T. Baldwin, R.C. Green, E. Rogaeva, P. St George-Hyslop, S.E. Arnold, R. Barber, T. Beach, E.H. Bigio, J.D. Bowen, A. Boxer, J.R. Burke, N.J. Cairns, C.S. Carlson, R.M. Carney, S.L. Carroll, H.C. Chui, D.G. Clark, J. Corneveaux, C.W. Cotman, J.L. Cummings, C. DeCarli, S.T. DeKosky, R. Diaz-Arrastia, M. Dick, D.W. Dickson, W.G.

Ellis, K.M. Faber, K.B. Fallon, M.R. Farlow, S. Ferris, M.P. Frosch, D.R. Galasko, M. Ganguli, M. Gearing, D.H. Geschwind, B. Ghetti, J.R. Gilbert, S. Gilman, B. Giordani, J.D. Glass, J.H. Growdon, R.L. Hamilton, L.E. Harrell, E. Head, L.S. Honig, C.M. Hulette, B.T. Hyman, G.A. Jicha, L.W. Jin, N. Johnson, J. Karlawish, A. Karydas, J.A. Kaye, R. Kim, E.H. Koo, N.W. Kowall, J.J. Lah, A.I. Levey, A.P. Lieberman, O.L. Lopez, W.J. Mack, D.C. Marson, F. Martiniuk, D.C. Mash, E. Masliah, W.C. McCormick, S.M. McCurry, A.N. McDavid, A.C. McKee, M. Mesulam, B.L. Miller, C.A. Miller, J.W. Miller, J.E. Parisi, D.P. Perl, E. Peskind, R.C. Petersen, W.W. Poon, J.F. Quinn, R.A. Rajbhandary, M. Raskind, B. Reisberg, J.M. Ringman, E.D. Roberson, R.N. Rosenberg, M. Sano, L.S. Schneider, W. Seeley, M.L. Shelanski, M.A. Slifer, C.D. Smith, J.A. Sonnen, S. Spina, R.A. Stern, R.E. Tanzi, J.Q. Trojanowski, J.C. Troncoso, V.M. Van Deerlin, H.V. Vinters, J.P. Vonsattel, S. Weintraub, K.A. Welsh-Bohmer, J. Williamson, R.L. Woltjer, L.B. Cantwell, B.A. Dombroski, D. Beekly, K.L. Lunetta, E.R. Martin, M.I. Kamboh, A.J. Saykin, E.M. Reiman, D.A. Bennett, J.C. Morris, T.J. Montine, A.M. Goate, D. Blacker, D.W. Tsuang, H. Hakonarson, W.A. Kukull, T.M. Foroud, J.L. Haines, R. Mayeux, M.A. Pericak-Vance, L.A. Farrer and G.D. Schellenberg, *Common variants at MS4A4/MS4A6E, CD2AP, CD33 and EPHA1 are associated with late-onset Alzheimer's disease.* Nature Genetics, 2011. 43(5): p. 436-41.

34. Lambert, J.C., S. Heath, G. Even, D. Campion, K. Sleegers, M. Hiltunen, O. Combarros, D. Zelenika, M.J. Bullido, B. Tavernier, L. Letenneur, K. Bettens, C. Berr, F. Pasquier, N. Fievet, P. Barberger-Gateau, S. Engelborghs, P. De Deyn, I. Mateo, A. Franck, S. Helisalmi, E. Porcellini, O. Hanon, M.M. de Pancorbo, C. Lendon, C. Dufouil, C. Jaillard, T. Leveillard, V. Alvarez, P. Bosco, M. Mancuso, F. Panza, B. Nacmias, P. Bossu, P. Piccardi, G. Annoni, D. Seripa, D. Galimberti, D. Hannequin, F. Licastro, H. Soininen, K. Ritchie, H. Blanche, J.F. Dartigues, C. Tzourio, I. Gut, C. Van Broeckhoven, A. Alperovitch, M. Lathrop, and P. Amouyel, *Genome-wide association study identifies variants at CLU and CR1 associated with Alzheimer's disease.* Nature Genetics, 2009. 41(10): p. 1094-9.

35. Jones, L., P.A. Holmans, M.L. Hamshere, D. Harold, V. Moskvina, D. Ivanov, A. Pocklington, R. Abraham, P. Hollingworth, R. Sims, A. Gerrish, J.S. Pahwa, N. Jones, A. Stretton, A.R. Morgan, S. Lovestone, J. Powell, P. Proitsi, M.K. Lupton, C. Brayne, D.C. Rubinsztein, M. Gill, B. Lawlor, A. Lynch, K. Morgan, K.S. Brown, P.A. Passmore, D. Craig, B. McGuinness, S. Todd, C. Holmes, D. Mann, A.D. Smith, S. Love, P.G. Kehoe, S. Mead, N. Fox, M. Rossor, J. Collinge, W. Maier, F. Jessen, B. Schürmann, H. van den Bussche, I. Heuser, O. Peters, J. Kornhuber, J. Wiltfang, M. Dichgans, L. Frölich, H. Hampel, M. Hüll, D. Rujescu, A.M. Goate, J.S.K. Kauwe, C. Cruchaga, P. Nowotny, J.C. Morris, K. Mayo, G. Livingston, N.J. Bass, H. Gurling, A. McQuillin, R. Gwilliam, P. Deloukas, A. Al-Chalabi, C.E. Shaw, A.B. Singleton, R. Guerreiro, T.W. Mühleisen, M.M. Nöthen, S. Moebus, K.-H. Jöckel, N. Klopp, H.E. Wichmann, E. Rüther, M.M. Carrasquillo, V.S. Pankratz, S.G. Younkin, J. Hardy, M.C. O'Donovan, M.J. Owen, and J. Williams, *Genetic Evidence Implicates the Immune System and Cholesterol Metabolism in the Aetiology of Alzheimer's Disease.* PLoS ONE, 2010. 5(11): p. e13950.

36. Sleegers, K., J.-C. Lambert, L. Bertram, M. Cruts, P. Amouyel, and C. Van Broeckhoven, *The pursuit of susceptibility genes for Alzheimer's disease: progress and prospects.* Trends in Genetics, 2010. 26(2): p. 84-93.
37. Olivares, D., V.K. Deshpande, Y. Shi, D.K. Lahiri, N.H. Greig, J.T. Rogers, and X. Huang, *N-methyl D-aspartate (NMDA) receptor antagonists and memantine treatment for Alzheimer's disease, vascular dementia and Parkinson's disease.* Curr Alzheimer Res, 2012. 9(6): p. 746-58.
38. Woodhouse, A., T.C. Dickson, and J.C. Vickers, *Vaccination strategies for Alzheimer's disease: A new hope?* Drugs and Aging, 2007. 24(2): p. 107-19.
39. Hardy, J. and D. Allsop, *Amyloid deposition as the central event in the aetiology of Alzheimer's disease.* Trends in Pharmacological Sciences, 1991. 12(0): p. 383-388.
40. Wilcock, D. and C. Colton, *Anti-Aß immunotherapy in Alzheimer's disease; relevance of transgenic mouse studies to clinical trials.* Journal of Alzheimer's Disease, 2009. 15(4): p. 555-569.
41. Gilman, S., M. Koller, R.S. Black, L. Jenkins, S.G. Griffith, N.C. Fox, L. Eisner, L. Kirby, M.B. Rovira, F. Forette, and J.M. Orgogozo, *Clinical effects of Abeta immunization (AN1792) in patients with AD in an interrupted trial.* Neurology, 2005. 64(9): p. 1553-62.
42. Holmes, C., D. Boche, D. Wilkinson, G. Yadegarfar, V. Hopkins, A. Bayer, R.W. Jones, R. Bullock, S. Love, J.W. Neal, E. Zotova, and J.A. Nicoll, *Long-term effects of Abeta42 immunisation in Alzheimer's disease: follow-up of a randomised, placebo-controlled phase I trial.* Lancet, 2008. 372(9634): p. 216-23.
43. Yan, R. and R. Vassar, *Targeting the b-secretase BACE1 for Alzheimer's disease therapy.* The Lancet Neurology, 2014. 13(3): p. 319-329.
44. Wolfe, M., *Inhibition and modulation of γ-secretase for Alzheimer's disease.* Neurotherapeutics, 2008. 5(3): p. 391-398.
45. Chang, W.P., X. Huang, D. Downs, J.R. Cirrito, G. Koelsch, D.M. Holtzman, A.K. Ghosh, and J. Tang, *Beta-secretase inhibitor GRL-8234 rescues age-related cognitive decline in APP transgenic mice.* FASEB Journal, 2011. 25(2): p. 775-84.
46. Ghosh, A.K. and H.L. Osswald, *BACE1 ([small beta]-secretase) inhibitors for the treatment of Alzheimer's disease.* Chemical Society Reviews, 2014.
47. Ghosh, A.K., M. Brindisi, and J. Tang, *Developing beta-secretase inhibitors for treatment of Alzheimer's disease.* Journal of Neurochemistry, 2012. 120 Suppl 1: p. 71-83.
48. Doody, R.S., R. Raman, M. Farlow, T. Iwatsubo, B. Vellas, S. Joffe, K. Kieburtz, F. He, X. Sun, R.G. Thomas, P.S. Aisen, E. Siemers, G. Sethuraman, and R. Mohs, *A phase 3 trial of semagacestat for treatment of Alzheimer's disease.* New England Journal of Medicine, 2013. 369(4): p. 341-50.
49. Wischik, C.M., C.R. Harrington, and J.M. Storey, *Tau-aggregation inhibitor therapy for Alzheimer's disease.* Biochemical Pharmacology, 2014. 88(4): p. 529-39.
50. *Anti-Amyloid Treatment in Asymptomatic Alzheimer's study*. [cited 2014 13/05/14]; Available from: http://a4study.org/.
51. Jack, C.R., Jr., V.J. Lowe, M.L. Senjem, S.D. Weigand, B.J. Kemp, M.M. Shiung, D.S. Knopman, B.F. Boeve, W.E. Klunk, C.A. Mathis, and R.C. Petersen, *11C PiB and structural MRI provide complementary information in*

imaging of Alzheimer's disease and amnestic mild cognitive impairment. Brain, 2008. 131(Pt 3): p. 665-80.

52. Fagan, A.M., M.A. Mintun, A.R. Shah, P. Aldea, C.M. Roe, R.H. Mach, D. Marcus, J.C. Morris, and D.M. Holtzman, *Cerebrospinal fluid tau and ptau(181) increase with cortical amyloid deposition in cognitively normal individuals: implications for future clinical trials of Alzheimer's disease.* EMBO Mol Med, 2009. 1(8-9): p. 371-80.
53. Jack, C.R., Jr., V.J. Lowe, S.D. Weigand, H.J. Wiste, M.L. Senjem, D.S. Knopman, M.M. Shiung, J.L. Gunter, B.F. Boeve, B.J. Kemp, M. Weiner, and R.C. Petersen, *Serial PIB and MRI in normal, mild cognitive impairment and Alzheimer's disease: implications for sequence of pathological events in Alzheimer's disease.* Brain, 2009. 132(Pt 5): p. 1355-65.
54. Hunt, A., P. Schonknecht, M. Henze, P. Toro, U. Haberkorn, and J. Schroder, *CSF tau protein and FDG PET in patients with aging-associated cognitive decline and Alzheimer's disease.* Neuropsychiatr Dis Treat, 2006. 2(2): p. 207-12.
55. Schonknecht, P., J. Pantel, A. Hunt, M. Volkmann, K. Buerger, H. Hampel, and J. Schroder, *Levels of total tau and tau protein phosphorylated at threonine 181 in patients with incipient and manifest Alzheimer's disease.* Neuroscience Letters, 2003. 339(2): p. 172-4.
56. Minoshima, S., B. Giordani, S. Berent, K.A. Frey, N.L. Foster, and D.E. Kuhl, *Metabolic reduction in the posterior cingulate cortex in very early Alzheimer's disease.* Annals of Neurology, 1997. 42(1): p. 85-94.
57. de Leon, M.J., A. Convit, O.T. Wolf, C.Y. Tarshish, S. DeSanti, H. Rusinek, W. Tsui, E. Kandil, A.J. Scherer, A. Roche, A. Imossi, E. Thorn, M. Bobinski, C. Caraos, P. Lesbre, D. Schlyer, J. Poirier, B. Reisberg, and J. Fowler, *Prediction of cognitive decline in normal elderly subjects with 2-[(18)F]fluoro-2-deoxy-D-glucose/poitron-emission tomography (FDG/PET).* Proceedings of the National Academy of Sciences of the United States of America, 2001. 98(19): p. 10966-71.
58. Reiman, E.M., R.J. Caselli, L.S. Yun, K. Chen, D. Bandy, S. Minoshima, S.N. Thibodeau, and D. Osborne, *Preclinical Evidence of Alzheimer's Disease in Persons Homozygous for the ε4 Allele for Apolipoprotein E.* New England Journal of Medicine, 1996. 334(12): p. 752-758.
59. Small, G.W., J.C. Mazziotta, M.T. Collins, and et al., *APolipoprotein e type 4 allele and cerebral glucose metabolism in relatives at risk for familial alzheimer disease.* JAMA, 1995. 273(12): p. 942-947.
60. Ceravolo, R., D. Borghetti, L. Kiferle, G. Tognoni, A. Giorgetti, D. Neglia, N. Sassi, D. Frosini, C. Rossi, L. Petrozzi, G. Siciliano, and L. Murri, *CSF phosporylated TAU protein levels correlate with cerebral glucose metabolism assessed with PET in Alzheimer's disease.* Brain Research Bulletin, 2008. 76(1-2): p. 80-4.
61. Lehmann, M., P.M. Ghosh, C. Madison, R. Laforce, C. Corbetta-Rastelli, M.W. Weiner, M.D. Greicius, W.W. Seeley, M.L. Gorno-Tempini, H.J. Rosen, B.L. Miller, W.J. Jagust, and G.D. Rabinovici, *Diverging patterns of amyloid deposition and hypometabolism in clinical variants of probable Alzheimer's disease.* Brain, 2013.
62. Fagan, A.M., D. Head, A.R. Shah, D. Marcus, M. Mintun, J.C. Morris, and D.M. Holtzman, *Decreased cerebrospinal fluid Aβ42 correlates with brain*

atrophy in cognitively normal elderly. Annals of Neurology, 2009. 65(2): p. 176-183.
63. Dickerson, B.C., A. Bakkour, D.H. Salat, E. Feczko, J. Pacheco, D.N. Greve, F. Grodstein, C.I. Wright, D. Blacker, H.D. Rosas, R.A. Sperling, A. Atri, J.H. Growdon, B.T. Hyman, J.C. Morris, B. Fischl, and R.L. Buckner, *The Cortical Signature of Alzheimer's Disease: Regionally Specific Cortical Thinning Relates to Symptom Severity in Very Mild to Mild AD Dementia and is Detectable in Asymptomatic Amyloid-Positive Individuals.* Cerebral Cortex, 2009. 19(3): p. 497-510.
64. Dickerson, B.C. and D.A. Wolk, *MRI cortical thickness biomarker predicts AD-like CSF and cognitive decline in normal adults.* Neurology, 2012. 78(2): p. 84-90.
65. Vemuri, P., H.J. Wiste, S.D. Weigand, L.M. Shaw, J.Q. Trojanowski, M.W. Weiner, D.S. Knopman, R.C. Petersen, and C.R. Jack, Jr., *MRI and CSF biomarkers in normal, MCI, and AD subjects: predicting future clinical change.* Neurology, 2009. 73(4): p. 294-301.
66. Chan, D., J.C. Janssen, J.L. Whitwell, H.C. Watt, R. Jenkins, C. Frost, M.N. Rossor, and N.C. Fox, *Change in rates of cerebral atrophy over time in early-onset Alzheimer's disease: longitudinal MRI study.* The Lancet, 2003. 362(9390): p. 1121-1122.
67. Riley, K.P., G.A. Jicha, D. Davis, E.L. Abner, G.E. Cooper, N. Stiles, C.D. Smith, R.J. Kryscio, P.T. Nelson, L.J. Van Eldik, and F.A. Schmitt, *Prediction of preclinical Alzheimer's disease: longitudinal rates of change in cognition.* J Alzheimers Dis, 2011. 25(4): p. 707-17.
68. Salmon, D.P., *Neuropsychological features of mild cognitive impairment and preclinical Alzheimer's disease.* Curr Top Behav Neurosci, 2012. 10: p. 187-212.
69. Albert, M.S., M.B. Moss, R. Tanzi, and K. Jones, *Preclinical prediction of AD using neuropsychological tests.* Journal of the International Neuropsychological Society, 2001. 7(5): p. 631-9.
70. Jack, C.R., Jr., D.S. Knopman, W.J. Jagust, L.M. Shaw, P.S. Aisen, M.W. Weiner, R.C. Petersen, and J.Q. Trojanowski, *Hypothetical model of dynamic biomarkers of the Alzheimer's pathological cascade.* Lancet Neurol, 2010. 9(1): p. 119-28.
71. Jack, C.R., Jr., D.S. Knopman, W.J. Jagust, R.C. Petersen, M.W. Weiner, P.S. Aisen, L.M. Shaw, P. Vemuri, H.J. Wiste, S.D. Weigand, T.G. Lesnick, V.S. Pankratz, M.C. Donohue, and J.Q. Trojanowski, *Tracking pathophysiological processes in Alzheimer's disease: an updated hypothetical model of dynamic biomarkers.* Lancet Neurol, 2013. 12(2): p. 207-16.
72. Mitchell, A.J. and M. Shiri-Feshki, *Rate of progression of mild cognitive impairment to dementia--meta-analysis of 41 robust inception cohort studies.* Acta Psychiatrica Scandinavica, 2009. 119(4): p. 252-65.
73. Risacher, S.L., A.J. Saykin, J.D. West, L. Shen, H.A. Firpi, and B.C. McDonald, *Baseline MRI predictors of conversion from MCI to probable AD in the ADNI cohort.* Curr Alzheimer Res, 2009. 6(4): p. 347-61.
74. Dickerson, B.C. and D. Wolk, *Biomarker-based prediction of progression in MCI: Comparison of AD-signature and hippocampal volume with spinal fluid amyloid-β and tau.* Frontiers in Aging Neuroscience, 2013. 5.
75. Hye, A., J. Riddoch-Contreras, A. Baird, N. Ashton, C. Bazenet, R. Leung, E. Westman, A. Simmons, R. Dobson, M. Sattlecker, M. Lupton, K. Lunnon, A.

Keohane, M. Ward, I. Pike, H. Zucht, D. Pepin, W. Zheng, A. Tunnicliffe, J. Richardson, S. Gauthier, H. Soininen, I. Kloszewska, P. Mecocci, M. Tsolaki, V. Bruno, and S. Lovestone, *Plasma proteins predict conversion to dementia from prodromal disease.* Alzheimer's and Dementia, 2014.

76. Ray, S., M. Britschgi, C. Herbert, Y. Takeda-Uchimura, A. Boxer, K. Blennow, L.F. Friedman, D.R. Galasko, M. Jutel, A. Karydas, J.A. Kaye, J. Leszek, B.L. Miller, L. Minthon, J.F. Quinn, G.D. Rabinovici, W.H. Robinson, M.N. Sabbagh, Y.T. So, D.L. Sparks, M. Tabaton, J. Tinklenberg, J.A. Yesavage, R. Tibshirani, and T. Wyss-Coray, *Classification and prediction of clinical Alzheimer's diagnosis based on plasma signaling proteins.* Nature Medicine, 2007. 13(11): p. 1359-1362.
77. Furney, S.J., D. Kronenberg, A. Simmons, A. Guntert, R.J. Dobson, P. Proitsi, L.O. Wahlund, I. Kloszewska, P. Mecocci, H. Soininen, M. Tsolaki, B. Vellas, C. Spenger, and S. Lovestone, *Combinatorial markers of mild cognitive impairment conversion to Alzheimer's disease--cytokines and MRI measures together predict disease progression.* J Alzheimers Dis, 2011. 26 Suppl 3: p. 395-405.
78. Jack, C.R., Jr., M.S. Albert, D.S. Knopman, G.M. McKhann, R.A. Sperling, M.C. Carrillo, B. Thies, and C.H. Phelps, *Introduction to the recommendations from the National Institute on Aging-Alzheimer's Association workgroups on diagnostic guidelines for Alzheimer's disease.* Alzheimers Dement, 2011. 7(3): p. 257-62.
79. Sperling, R.A., P.S. Aisen, L.A. Beckett, D.A. Bennett, S. Craft, A.M. Fagan, T. Iwatsubo, C.R. Jack Jr, J. Kaye, T.J. Montine, D.C. Park, E.M. Reiman, C.C. Rowe, E. Siemers, Y. Stern, K. Yaffe, M.C. Carrillo, B. Thies, M. Morrison-Bogorad, M.V. Wagster, and C.H. Phelps, *Toward defining the preclinical stages of Alzheimer's disease: Recommendations from the National Institute on Aging-Alzheimer's Association workgroups on diagnostic guidelines for Alzheimer's disease.* Alzheimer's & Dementia, 2011. 7(3): p. 280-292.
80. Tabaraud, F., J.P. Leman, A.M. Milor, J.M. Roussie, G. Barrière, M. Tartary, F. Boutros-Toni, and M. Rigaud, *Alzheimer CSF biomarkers in routine clinical setting.* Acta Neurologica Scandinavica, 2011.
81. Klunk, W.E., H. Engler, A. Nordberg, Y. Wang, G. Blomqvist, D.P. Holt, M. Bergstrom, I. Savitcheva, G.F. Huang, S. Estrada, B. Ausen, M.L. Debnath, J. Barletta, J.C. Price, J. Sandell, B.J. Lopresti, A. Wall, P. Koivisto, G. Antoni, C.A. Mathis, and B. Langstrom, *Imaging brain amyloid in Alzheimer's disease with Pittsburgh Compound-B.* Annals of Neurology, 2004. 55(3): p. 306-19.
82. Edison, P., H.A. Archer, R. Hinz, A. Hammers, N. Pavese, Y.F. Tai, G. Hotton, D. Cutler, N. Fox, A. Kennedy, M. Rossor, and D.J. Brooks, *Amyloid, hypometabolism, and cognition in Alzheimer disease: an [11C]PIB and [18F]FDG PET study.* Neurology, 2007. 68(7): p. 501-8.
83. Ikonomovic, M.D., W.E. Klunk, E.E. Abrahamson, C.A. Mathis, J.C. Price, N.D. Tsopelas, B.J. Lopresti, S. Ziolko, W. Bi, W.R. Paljug, M.L. Debnath, C.E. Hope, B.A. Isanski, R.L. Hamilton, and S.T. DeKosky, *Post-mortem correlates of in vivo PiB-PET amyloid imaging in a typical case of Alzheimer's disease.* Brain, 2008. 131(6): p. 1630-1645.
84. Ng, S., V.L. Villemagne, S. Berlangieri, S.-T. Lee, M. Cherk, S.J. Gong, U. Ackermann, T. Saunder, H. Tochon-Danguy, G. Jones, C. Smith, G. O'Keefe,

C.L. Masters, and C.C. Rowe, *Visual Assessment Versus Quantitative Assessment of 11C-PIB PET and 18F-FDG PET for Detection of Alzheimer's Disease*. Journal of Nuclear Medicine, 2007. 48(4): p. 547-552.
85. Pike, K.E., G. Savage, V.L. Villemagne, S. Ng, S.A. Moss, P. Maruff, C.A. Mathis, W.E. Klunk, C.L. Masters, and C.C. Rowe, *β-amyloid imaging and memory in non-demented individuals: evidence for preclinical Alzheimer's disease*. Brain, 2007. 130(11): p. 2837-2844.
86. Rowe, C.C., S. Ng, U. Ackermann, S.J. Gong, K. Pike, G. Savage, T.F. Cowie, K.L. Dickinson, P. Maruff, D. Darby, C. Smith, M. Woodward, J. Merory, H. Tochon-Danguy, G. O'Keefe, W.E. Klunk, C.A. Mathis, J.C. Price, C.L. Masters, and V.L. Villemagne, *Imaging beta-amyloid burden in aging and dementia.* Neurology, 2007. 68(20): p. 1718-25.
87. Herholz, K. and K. Ebmeier, Clinical amyloid imaging in Alzheimer's disease. The Lancet Neurology, 2011. 10: p. 667-670.
88. Landau, S.M., B.A. Thomas, L. Thurfjell, M. Schmidt, R. Margolin, M. Mintun, M. Pontecorvo, S.L. Baker, and W.J. Jagust, *Amyloid PET imaging in Alzheimer's disease: a comparison of three radiotracers.* Eur J Nucl Med Mol Imaging, 2014.
89. Hatashita, S., H. Yamasaki, Y. Suzuki, K. Tanaka, D. Wakebe, and H. Hayakawa, *[18F]Flutemetamol amyloid-beta PET imaging compared with [11C]PIB across the spectrum of Alzheimer's disease.* Eur J Nucl Med Mol Imaging, 2014. 41(2): p. 290-300.
90. Fodero-Tavoletti, M.T., N. Okamura, S. Furumoto, R.S. Mulligan, A.R. Connor, C.A. McLean, D. Cao, A. Rigopoulos, G.A. Cartwright, G. Oâ€™Keefe, S. Gong, P.A. Adlard, K.J. Barnham, C.C. Rowe, C.L. Masters, Y. Kudo, R. Cappai, K. Yanai, and V.L. Villemagne, *18F-THK523: a novel in vivo tau imaging ligand for Alzheimer's disease.* Brain, 2011. 134(4): p. 1089-1100.
91. Fodero-Tavoletti, M.T., S. Furumoto, L. Taylor, C.A. McLean, R.S. Mulligan, I. Birchall, R. Harada, C.L. Masters, K. Yanai, Y. Kudo, C.C. Rowe, N. Okamura, and V.L. Villemagne, *Assessing THK523 selectivity for tau deposits in Alzheimer's disease and non-Alzheimer's disease tauopathies.* Alzheimers Res Ther, 2014. 6(1): p. 11.
92. Harada, R., N. Okamura, S. Furumoto, T. Tago, M. Maruyama, M. Higuchi, T. Yoshikawa, H. Arai, R. Iwata, Y. Kudo, and K. Yanai, *Comparison of the binding characteristics of [18F]THK-523 and other amyloid imaging tracers to Alzheimer's disease pathology.* Eur J Nucl Med Mol Imaging, 2013. 40(1): p. 125-32.
93. Appel, J., E. Potter, Q. Shen, G. Pantol, M.T. Greig, D. Loewenstein, and R. Duara, *A comparative analysis of structural brain MRI in the diagnosis of Alzheimer's disease.* Behav Neurol, 2009. 21(1): p. 13-9.
94. Du, A.T., N. Schuff, X.P. Zhu, W.J. Jagust, B.L. Miller, B.R. Reed, J.H. Kramer, D. Mungas, K. Yaffe, H.C. Chui, and M.W. Weiner, *Atrophy rates of entorhinal cortex in AD and normal aging.* Neurology, 2003. 60(3): p. 481-486.
95. Querbes, O., F. Aubry, J. Pariente, J.A. Lotterie, J.F. Demonet, V. Duret, M. Puel, I. Berry, J.C. Fort, and P. Celsis, *Early diagnosis of Alzheimer's disease using cortical thickness: impact of cognitive reserve.* Brain, 2009. 132(Pt 8): p. 2036-47.

96. Schott, J.M., N.C. Fox, C. Frost, R.I. Scahill, J.C. Janssen, D. Chan, R. Jenkins, and M.N. Rossor, *Assessing the onset of structural change in familial Alzheimer's disease.* Annals of Neurology, 2003. 53(2): p. 181-8.
97. Vemuri, P., J.L. Whitwell, K. Kantarci, K.A. Josephs, J.E. Parisi, M.S. Shiung, D.S. Knopman, B.F. Boeve, R.C. Petersen, D.W. Dickson, and C.R. Jack, Jr., *Antemortem MRI based STructural Abnormality iNDex (STAND)-scores correlate with postmortem Braak neurofibrillary tangle stage.* Neuroimage, 2008. 42(2): p. 559-67.
98. Braak, H. and E. Braak, *Neuropathological stageing of Alzheimer-related changes.* Acta Neuropathol, 1991. 82(4): p. 239-59.
99. Jagust, W.J., S.M. Landau, L.M. Shaw, J.Q. Trojanowski, R.A. Koeppe, E.M. Reiman, N.L. Foster, R.C. Petersen, M.W. Weiner, J.C. Price, and C.A. Mathis, *Relationships between biomarkers in aging and dementia.* Neurology, 2009. 73(15): p. 1193-9.
100. Tartaglia, M.C., H.J. Rosen, and B.L. Miller, *Neuroimaging in dementia.* Neurotherapeutics, 2011. 8(1): p. 82-92.
101. Landau, S.M., D. Harvey, C.M. Madison, E.M. Reiman, N.L. Foster, P.S. Aisen, R.C. Petersen, L.M. Shaw, J.Q. Trojanowski, C.R. Jack, Jr., M.W. Weiner, and W.J. Jagust, *Comparing predictors of conversion and decline in mild cognitive impairment.* Neurology, 2010. 75(3): p. 230-8.
102. Herholz, K., S. Westwood, C. Haense, and G. Dunn, *Evaluation of a calibrated (18)F-FDG PET score as a biomarker for progression in Alzheimer disease and mild cognitive impairment.* Journal of Nuclear Medicine, 2011. 52(8): p. 1218-26.
103. Small, G.W., S.Y. Bookheimer, P.M. Thompson, G.M. Cole, S.C. Huang, V. Kepe, and J.R. Barrio, *Current and future uses of neuroimaging for cognitively impaired patients.* Lancet Neurol, 2008. 7(2): p. 161-72.
104. Link, H. and G. Tibbling, *Principles of albumin and IgG analyses in neurological disorders. III. Evaluation of IgG synthesis within the central nervous system in multiple sclerosis.* Scandinavian Journal of Clinical and Laboratory Investigation, 1977. 37(5): p. 397-401.
105. Holsinger, R.M., C.A. McLean, S.J. Collins, C.L. Masters, and G. Evin, *Increased beta-Secretase activity in cerebrospinal fluid of Alzheimer's disease subjects.* Annals of Neurology, 2004. 55(6): p. 898-9.
106. Holsinger, R.M., J.S. Lee, A. Boyd, C.L. Masters, and S.J. Collins, *CSF BACE1 activity is increased in CJD and Alzheimer disease versus [corrected] other dementias.* Neurology, 2006. 67(4): p. 710-2.
107. Zhong, Z., M. Ewers, S. Teipel, K. Burger, A. Wallin, K. Blennow, P. He, C. McAllister, H. Hampel, and Y. Shen, *Levels of beta-secretase (BACE1) in cerebrospinal fluid as a predictor of risk in mild cognitive impairment.* Archives of General Psychiatry, 2007. 64(6): p. 718-26.
108. Mulder, S.D., W.M. van der Flier, J.H. Verheijen, C. Mulder, P. Scheltens, M.A. Blankenstein, C.E. Hack, and R. Veerhuis, *BACE1 activity in cerebrospinal fluid and its relation to markers of AD pathology.* J Alzheimers Dis, 2010. 20(1): p. 253-60.
109. Olsson, A., K. Hoglund, M. Sjogren, N. Andreasen, L. Minthon, L. Lannfelt, K. Buerger, H.J. Moller, H. Hampel, P. Davidsson, and K. Blennow, *Measurement of alpha- and beta-secretase cleaved amyloid precursor protein in cerebrospinal fluid from Alzheimer patients.* Experimental Neurology, 2003. 183(1): p. 74-80.

110. Perneczky, R., A. Tsolakidou, A. Arnold, J. Diehl-Schmid, T. Grimmer, H. Forstl, A. Kurz, and P. Alexopoulos, *CSF soluble amyloid precursor proteins in the diagnosis of incipient Alzheimer disease.* Neurology, 2011. 77(1): p. 35-8.
111. Lewczuk, P., H. Kamrowski-Kruck, O. Peters, I. Heuser, F. Jessen, J. Popp, K. Burger, H. Hampel, L. Frolich, S. Wolf, B. Prinz, H. Jahn, C. Luckhaus, R. Perneczky, M. Hull, J. Schroder, H. Kessler, J. Pantel, H.J. Gertz, H.W. Klafki, H. Kolsch, U. Reulbach, H. Esselmann, J.M. Maler, M. Bibl, J. Kornhuber, and J. Wiltfang, *Soluble amyloid precursor proteins in the cerebrospinal fluid as novel potential biomarkers of Alzheimer's disease: a multicenter study.* Molecular Psychiatry, 2010. 15(2): p. 138-45.
112. Lewczuk, P., J. Popp, N. Lelental, H. Kolsch, W. Maier, J. Kornhuber, and F. Jessen, *Cerebrospinal fluid soluble amyloid-beta protein precursor as a potential novel biomarkers of Alzheimer's disease.* J Alzheimers Dis, 2012. 28(1): p. 119-25.
113. Gao, C.M., A.Y. Yam, X. Wang, E. Magdangal, C. Salisbury, D. Peretz, R.N. Zuckermann, M.D. Connolly, O. Hansson, L. Minthon, H. Zetterberg, K. Blennow, J.P. Fedynyshyn, and S. Allauzen, *Aβ40 Oligomers Identified as a Potential Biomarker for the Diagnosis of Alzheimer's Disease.* PLoS ONE, 2010. 5(12): p. e15725.
114. Fukumoto, H., T. Tokuda, T. Kasai, N. Ishigami, H. Hidaka, M. Kondo, D. Allsop, and M. Nakagawa, *High-molecular-weight beta-amyloid oligomers are elevated in cerebrospinal fluid of Alzheimer patients.* FASEB Journal, 2010. 24(8): p. 2716-26.
115. Handoko, M., M. Grant, M. Kuskowski, K.R. Zahs, A. Wallin, K. Blennow, and K.H. Ashe, *Correlation of specific amyloid-beta oligomers with tau in cerebrospinal fluid from cognitively normal older adults.* JAMA Neurol, 2013. 70(5): p. 594-9.
116. Rosen, C., O. Hansson, K. Blennow, and H. Zetterberg, *Fluid biomarkers in Alzheimer's disease - current concepts.* Mol Neurodegener, 2013. 8: p. 20.
117. Sutphen, C.L., A.M. Fagan, and D.M. Holtzman, *Progress update: fluid and imaging biomarkers in Alzheimer's disease.* Biological Psychiatry, 2014. 75(7): p. 520-6.
118. Sui, X., J. Liu, and X. Yang, *Cerebrospinal fluid biomarkers of Alzheimer's disease.* Neurosci Bull, 2014. 30(2): p. 233-42.
119. Hampel, H., R. Frank, K. Broich, S.J. Teipel, R.G. Katz, J. Hardy, K. Herholz, A.L. Bokde, F. Jessen, Y.C. Hoessler, W.R. Sanhai, H. Zetterberg, J. Woodcock, and K. Blennow, *Biomarkers for Alzheimer's disease: academic, industry and regulatory perspectives.* Nat Rev Drug Discov, 2010. 9(7): p. 560-74.
120. Blennow, K., H. Hampel, M. Weiner, and H. Zetterberg, *Cerebrospinal fluid and plasma biomarkers in Alzheimer disease.* Nat Rev Neurol, 2010. 6(3): p. 131-44.
121. Fagan, A.M., M.A. Mintun, R.H. Mach, S.Y. Lee, C.S. Dence, A.R. Shah, G.N. LaRossa, M.L. Spinner, W.E. Klunk, C.A. Mathis, S.T. DeKosky, J.C. Morris, and D.M. Holtzman, *Inverse relation between in vivo amyloid imaging load and cerebrospinal fluid Abeta42 in humans.* Annals of Neurology, 2006. 59(3): p. 512-9.
122. Forsberg, A., H. Engler, O. Almkvist, G. Blomquist, G. Hagman, A. Wall, A. Ringheim, B. Langstrom, and A. Nordberg, *PET imaging of amyloid*

deposition in patients with mild cognitive impairment. Neurobiology of Aging, 2008. 29(10): p. 1456-65.
123. Strozyk, D., K. Blennow, L.R. White, and L.J. Launer, *CSF Abeta 42 levels correlate with amyloid-neuropathology in a population-based autopsy study.* Neurology, 2003. 60(4): p. 652-6.
124. Andreasen, N., E. Vanmechelen, H. Vanderstichele, P. Davidsson, and K. Blennow, *Cerebrospinal fluid levels of total-tau, phospho-tau and A beta 42 predicts development of Alzheimer's disease in patients with mild cognitive impairment.* Acta Neurologica Scandinavica. Supplementum, 2003. 179: p. 47-51.
125. Blennow, K., A. Wallin, H. Agren, C. Spenger, J. Siegfried, and E. Vanmechelen, *Tau protein in cerebrospinal fluid: a biochemical marker for axonal degeneration in Alzheimer disease?* Molecular and Chemical Neuropathology, 1995. 26(3): p. 231-45.
126. Vigo-Pelfrey, C., P. Seubert, R. Barbour, C. Blomquist, M. Lee, D. Lee, F. Coria, L. Chang, B. Miller, I. Lieberburg, and et al., *Elevation of microtubule-associated protein tau in the cerebrospinal fluid of patients with Alzheimer's disease.* Neurology, 1995. 45(4): p. 788-93.
127. Mori, H., K. Hosoda, E. Matsubara, T. Nakamoto, Y. Furiya, R. Endoh, M. Usami, M. Shoji, S. Maruyama, and S. Hirai, *Tau in cerebrospinal fluids: establishment of the sandwich ELISA with antibody specific to the repeat sequence in tau.* Neuroscience Letters, 1995. 186(2-3): p. 181-3.
128. Kandimalla, R.J.L., S. Prabhakar, W.Y. Wani, A. Kaushal, N. Gupta, D.R. Sharma, V.K. Grover, N. Bhardwaj, K. Jain, and K.D. Gill, *CSF p-Tau levels in the prediction of Alzheimer's disease.* Biology Open, 2013.
129. Fagan, A.M., C.M. Roe, C. Xiong, M.A. Mintun, J.C. Morris, and D.M. Holtzman, *Cerebrospinal fluid tau/beta-amyloid(42) ratio as a prediction of cognitive decline in nondemented older adults.* Archives of Neurology, 2007. 64(3): p. 343-9.
130. De Meyer, G., F. Shapiro, H. Vanderstichele, E. Vanmechelen, S. Engelborghs, P.P. De Deyn, E. Coart, O. Hansson, L. Minthon, H. Zetterberg, K. Blennow, L. Shaw, and J.Q. Trojanowski, *Diagnosis-independent Alzheimer disease biomarker signature in cognitively normal elderly people.* Archives of Neurology, 2010. 67(8): p. 949-56.
131. Li, X., T.Q. Li, N. Andreasen, M.K. Wiberg, E. Westman, and L.O. Wahlund, *Ratio of Abeta42/P-tau181p in CSF is associated with aberrant default mode network in AD.* Sci Rep, 2013. 3: p. 1339.
132. Hawkins, B.T. and T.P. Davis, *The Blood-Brain Barrier/Neurovascular Unit in Health and Disease.* Pharmacological Reviews, 2005. 57(2): p. 173-185.
133. Hansson, S.F., U. Andreasson, M. Wall, I. Skoog, N. Andreasen, A. Wallin, H. Zetterberg, and K. Blennow, *Reduced levels of amyloid-beta-binding proteins in cerebrospinal fluid from Alzheimer's disease patients.* J Alzheimers Dis, 2009. 16(2): p. 389-97.
134. Castano, E.M., A.E. Roher, C.L. Esh, T.A. Kokjohn, and T. Beach, *Comparative proteomics of cerebrospinal fluid in neuropathologically-confirmed Alzheimer's disease and non-demented elderly subjects.* Neurological Research, 2006. 28(2): p. 155-63.
135. Velayudhan, L., R. Killick, A. Hye, A. Kinsey, A. Guntert, S. Lynham, M. Ward, R. Leung, A. Lourdusamy, A.W. To, J. Powell, and S. Lovestone,

Plasma transthyretin as a candidate marker for Alzheimer's disease. J Alzheimers Dis, 2012. 28(2): p. 369-75.
136. Ribeiro, C.A., I. Santana, C. Oliveira, I. Baldeiras, J. Moreira, M.J. Saraiva, and I. Cardoso, *Transthyretin decrease in plasma of MCI and AD patients: investigation of mechanisms for disease modulation.* Curr Alzheimer Res, 2012. 9(8): p. 881-9.
137. Thambisetty, M., A. Simmons, L. Velayudhan, A. Hye, J. Campbell, Y. Zhang, L.O. Wahlund, E. Westman, A. Kinsey, A. Guntert, P. Proitsi, J. Powell, M. Causevic, R. Killick, K. Lunnon, S. Lynham, M. Broadstock, F. Choudhry, D.R. Howlett, R.J. Williams, S.I. Sharp, C. Mitchelmore, C. Tunnard, R. Leung, C. Foy, D. O'Brien, G. Breen, S.J. Furney, M. Ward, I. Kloszewska, P. Mecocci, H. Soininen, M. Tsolaki, B. Vellas, A. Hodges, D.G. Murphy, S. Parkins, J.C. Richardson, S.M. Resnick, L. Ferrucci, D.F. Wong, Y. Zhou, S. Muehlboeck, A. Evans, P.T. Francis, C. Spenger, and S. Lovestone, *Association of plasma clusterin concentration with severity, pathology, and progression in Alzheimer disease.* Archives of General Psychiatry, 2010. 67(7): p. 739-48.
138. Thambisetty, M., Y. An, A. Kinsey, D. Koka, M. Saleem, A. Guntert, M. Kraut, L. Ferrucci, C. Davatzikos, S. Lovestone, and S.M. Resnick, *Plasma clusterin concentration is associated with longitudinal brain atrophy in mild cognitive impairment.* Neuroimage, 2012. 59(1): p. 212-7.
139. Carrette, O., I. Demalte, A. Scherl, O. Yalkinoglu, G. Corthals, P. Burkhard, D.F. Hochstrasser, and J.C. Sanchez, *A panel of cerebrospinal fluid potential biomarkers for the diagnosis of Alzheimer's disease.* Proteomics, 2003. 3(8): p. 1486-94.
140. Craig-Schapiro, R., M. Kuhn, C. Xiong, E.H. Pickering, J. Liu, T.P. Misko, R.J. Perrin, K.R. Bales, H. Soares, A.M. Fagan, and D.M. Holtzman, *Multiplexed Immunoassay Panel Identifies Novel CSF Biomarkers for Alzheimer's Disease Diagnosis and Prognosis.* PLoS ONE, 2011. 6(4): p. e18850.
141. Sattlecker, M., S.J. Kiddle, S. Newhouse, P. Proitsi, S. Nelson, S. Williams, C. Johnston, R. Killick, A. Simmons, E. Westman, A. Hodges, H. Soininen, I. Kłoszewska, P. Mecocci, M. Tsolaki, B. Vellas, S. Lovestone, and R.J.B. Dobson, *Alzheimer's disease biomarker discovery using SOMAscan multiplexed protein technology.* Alzheimer's & Dementia, 2014(0).
142. Hye, A., S. Lynham, M. Thambisetty, M. Causevic, J. Campbell, H.L. Byers, C. Hooper, F. Rijsdijk, S.J. Tabrizi, S. Banner, C.E. Shaw, C. Foy, M. Poppe, N. Archer, G. Hamilton, J. Powell, R.G. Brown, P. Sham, M. Ward, and S. Lovestone, *Proteome-based plasma biomarkers for Alzheimer's disease.* Brain, 2006. 129(Pt 11): p. 3042-50.
143. Zipser, B.D., Johanson, C. E., Gonzalez, L., Berzin, T. M., Tavares, R., Hulette, C. M., Vitek, M. P., Hovanesian, V., & Stopa, E. G., *Microvascular injury and blood–brain barrier leakage in Alzheimer's disease.* Neurobiology of Aging, 2007. 28(7): p. 977-986.
144. Lewczuk P Fau - Esselmann, H., M. Esselmann H Fau - Bibl, S. Bibl M Fau - Paul, J. Paul S Fau - Svitek, J. Svitek J Fau - Miertschischk, R. Miertschischk J Fau - Meyrer, A. Meyrer R Fau - Smirnov, J.M. Smirnov A Fau - Maler, C. Maler Jm Fau - Klein, M. Klein C Fau - Otto, S. Otto M Fau - Bleich, W. Bleich S Fau - Sperling, J. Sperling W Fau - Kornhuber, E. Kornhuber J Fau -

Ruther, J. Ruther E Fau - Wiltfang, and J. Wiltfang, *Electrophoretic separation of amyloid beta peptides in plasma.* 2004(0173-0835 (Print)).
145. Anderson, N.L. and N.G. Anderson, *The Human Plasma Proteome.* Molecular & Cellular Proteomics, 2002. 1(11): p. 845-867.
146. Zeng Gq Fau - Zhang, P.F., C. Zhang Pf Fau - Li, F. Li C Fau - Peng, M.Y. Peng F Fau - Li, Y. Li My Fau - Xu, F.L. Xu Y Fau - Yu, M.J. Yu Fl Fau - Chen, H. Chen Mj Fau - Yi, G.Q. Yi H Fau - Li, Z.C. Li Gq Fau - Chen, Z.Q. Chen Zc Fau - Xiao, and Z.Q. Xiao, *Comparative Proteome Analysis of Human Lung Squamous Carcinoma using Two Different Methods: Two-Dimensional Gel Electrophoresis and iTRAQ Analysis.* 2012(1533-0338 (Electronic)).
147. Wu, W.W., G. Wang, S.J. Baek, and R.-F. Shen, *Comparative Study of Three Proteomic Quantitative Methods, DIGE, cICAT, and iTRAQ, Using 2D Gel- or LC−MALDI TOF/TOF.* Journal of Proteome Research, 2006. 5(3): p. 651-658.
148. Thambisetty, M., A. Simmons, A. Hye, J. Campbell, E. Westman, Y. Zhang, L.-O. Wahlund, A. Kinsey, M. Causevic, R. Killick, I. Kloszewska, P. Mecocci, H. Soininen, M. Tsolaki, B. Vellas, C. Spenger, S. Lovestone, and c. for the AddNeuroMed, *Plasma Biomarkers of Brain Atrophy in Alzheimer's Disease.* PLoS ONE, 2011. 6(12): p. e28527.
149. Thambisetty, M., A. Hye, C. Foy, E. Daly, A. Glover, A. Cooper, A. Simmons, D. Murphy, and S. Lovestone, *Proteome-based identification of plasma proteins associated with hippocampal metabolism in early Alzheimer's disease.* Journal of Neurology, 2008. 255(11): p. 1712-20.
150. Kiddle, S.J., M. Thambisetty, A. Simmons, J. Riddoch-Contreras, A. Hye, E. Westman, I. Pike, M. Ward, C. Johnston, M.K. Lupton, K. Lunnon, H. Soininen, I. Kloszewska, M. Tsolaki, B. Vellas, P. Mecocci, S. Lovestone, S. Newhouse, R. Dobson, and I. for the Alzheimers Disease Neuroimaging, *Plasma Based Markers of 11C PiB-PET Brain Amyloid Burden.* PLoS ONE, 2012. 7(9): p. e44260.
151. Thambisetty, M., R. Tripaldi, J. Riddoch-Contreras, A. Hye, Y. An, J. Campbell, J. Sojkova, A. Kinsey, S. Lynham, Y. Zhou, L. Ferrucci, D.F. Wong, S. Lovestone, and S.M. Resnick, *Proteome-based plasma markers of brain amyloid-beta deposition in non-demented older individuals.* J Alzheimers Dis, 2010. 22(4): p. 1099-109.
152. Ostrosky-Solis F Fau - Lopez-Arango, G., A. Lopez-Arango G Fau - Ardila, and A. Ardila, *Sensitivity and specificity of the Mini-Mental State Examination in a Spanish-speaking population.* 2000(0908-4282 (Print)).
153. Villaseñor-Cabrera, T., J. Guàrdia-Olmos, M. Jiménez-Maldonado, G. Rizo-Curiel, and M. Peró-Cebollero, *Sensitivity and specificity of the Mini-Mental State Examination in the Mexican population.* Quality & Quantity, 2010. 44(6): p. 1105-1112.
154. Robert P Fau - Ferris, S., S. Ferris S Fau - Gauthier, R. Gauthier S Fau - Ihl, B. Ihl R Fau - Winblad, F. Winblad B Fau - Tennigkeit, and F. Tennigkeit, *Review of Alzheimer's disease scales: is there a need for a new multi-domain scale for therapy evaluation in medical practice?* 2010(1758-9193 (Electronic)).
155. Stone, J.L. and A.H. Norris, *Activities and attitudes of participants in the Baltimore longitudinal study.* Journal of Gerontology, 1966. 21(4): p. 575-80.

156. Rowe, J.W., R. Andres, J.D. Tobin, A.H. Norris, and N.W. Shock, *The effect of age on creatinine clearance in men: a cross-sectional and longitudinal study.* Journal of Gerontology, 1976. 31(2): p. 155-63.
157. Schneider, E.L., *Cell replication and aging: in vitro and in vivo studies.* Federation Proceedings, 1979. 38(5): p. 1857-61.
158. Tzankoff, S.P. and A.H. Norris, *Age-related differences in lactate distribution kinetics following maximal exercise.* Eur J Appl Physiol Occup Physiol, 1979. 42(1): p. 35-40.
159. Beydoun, M.A., A.A. Gamaldo, H.A. Beydoun, T. Tanaka, K.L. Tucker, S.A. Talegawkar, L. Ferrucci, and A.B. Zonderman, *Caffeine and Alcohol Intakes and Overall Nutrient Adequacy Are Associated with Longitudinal Cognitive Performance among U.S. Adults.* Journal of Nutrition, 2014. 144(6): p. 890-901.
160. Chuang, Y.F., T. Tanaka, L.L. Beason-Held, Y. An, A. Terracciano, A.R. Sutin, M. Kraut, A.B. Singleton, S.M. Resnick, and M. Thambisetty, *FTO genotype and aging: pleiotropic longitudinal effects on adiposity, brain function, impulsivity and diet.* Molecular Psychiatry, 2014.
161. Schrager, M.A., J.A. Schrack, E.M. Simonsick, and L. Ferrucci, *Association Between Energy Availability and Physical Activity in Older Adults.* American Journal of Physical Medicine and Rehabilitation, 2014.
162. Canepa, M., P. Ameri, M. AlGhatrif, G. Pestelli, Y. Milaneschi, J.B. Strait, F. Giallauria, G. Ghigliotti, C. Brunelli, E.G. Lakatta, and L. Ferrucci, *Role of bone mineral density in the inverse relationship between body size and aortic calcification: Results from the Baltimore Longitudinal Study of Aging.* Atherosclerosis, 2014. 235(1): p. 169-175.
163. Resnick, S.M., A.F. Goldszal, C. Davatzikos, S. Golski, M.A. Kraut, E.J. Metter, R.N. Bryan, and A.B. Zonderman, *One-year Age Changes in MRI Brain Volumes in Older Adults.* Cerebral Cortex, 2000. 10(5): p. 464-472.
164. Goldszal, A.F., C. Davatzikos, D.L. Pham, M.X.H. Yan, R.N. Bryan, and S.M. Resnick, *An Image-Processing System for Qualitative and Quantitative Volumetric Analysis of Brain Images.* Journal of Computer Assisted Tomography, 1998. 22(5): p. 827-837.
165. Davatzikos, C., *Spatial normalization of 3D brain images using deformable models.* Journal of Computer Assisted Tomography, 1996. 20: p. 656-665.
166. Talairach, T. and P. Tournoux, *Co-Planar Stereotaxic Atlas of the Human Brain: 3-D Proportional System: An Approach to Cerebral Imaging* 1988, Stuttgart: Thieme Medical Publishers.
167. Sojkova, J., L. Beason-Held, Y. Zhou, Y. An, M.A. Kraut, W. Ye, L. Ferrucci, C.A. Mathis, W.E. Klunk, D.F. Wong, and S.M. Resnick, *Longitudinal Cerebral Blood Flow and Amyloid Deposition: An Emerging Pattern?* Journal of Nuclear Medicine, 2008. 49(9): p. 1465-1471.
168. Delis, D.C., Kramer, J.H., Kaplan, E., & Ober, B.A., *The California Verbal Learning Test*. 1987, New York: Psychological Organisation.
169. Benton, A.L., *Benton Visual Retention Test - Fifth Edition.* 1992, San Antonio, TX: The Psychological Corporation.
170. Ekstrom, R.B., J.W. French, H.H. Harman, and D. Dermen, *Manual for kit of factor-referenced cognitive tests.* Princeton, NJ: Educational Testing Service, 1976.

171. Spreen, O., B., A., *Neurosensory Center Comprehensive Examination for Aphasia: Manual of direction.* 1969, Victoria, BC: Neuropsychology Laboratory, University of Victoria.
172. Rosen, W., *Verbal fluency in aging and dementia.* Journal of Clinical Neuropsychology, 1980. 2: p. 135-146.
173. Wechsler, D., *WAIS-R Manual*. 1981, New York: Psychological Corporation.
174. Reitan, R.M., *Validity of the Trail Making Test as an indicator of organic brain damage.* Perceptual and Motor Skills, 1958. 8: p. 271-276.
175. Wilson, J.V., S., *In: Sex differences in cognition: Evidence from the Hawaii Family Study, in Sex and Behavior.*, ed. T. McGill, Dewsbury, D., Sachs, B., editoris. 1978, New Tork: Plenum.
176. Folstein, M.F., S.E. Folstein, and P.R. McHugh, *"Mini-mental state": A practical method for grading the cognitive state of patients for the clinician.* Journal of Psychiatric Research, 1975. 12(3): p. 189-198.
177. Radloff, L.S., *The CES-D Scale: A Self-Report Depression Scale for Research in the General Population.* Applied Psychological Measurement, 1977. 1(3): p. 385-401.
178. McKhann, G., D. Drachman, M. Folstein, R. Katzman, D. Price, and E.M. Stadlan, *Clinical diagnosis of Alzheimer's disease: Report of the NINCDS-ADRDA Work Group under the auspices of Department of Health and Human Services Task Force on Alzheimer's Disease.* Neurology, 1984. 34(7): p. 939.
179. Association, A.P., *Diagnostic and statistical manual of mental disorders: DSM-IV, ed 4, text revision.* 2000, Washington, DC: American Psychiatric Association.
180. Morris, J.C., *The Clinical Dementia Rating (CDR): current version and scoring rules.* Neurology, 1993. 43(11): p. 2412-2414.
181. *World Medical Association Declaration of Helsinki.* Journal of Law, Medicine and Ethics, 1991. 19: p. 264-265.
182. Simmons, A., E. Westman, S. Muehlboeck, P. Mecocci, B. Vellas, M. Tsolaki, I. Kłoszewska, L.-O. Wahlund, H. Soininen, S. Lovestone, A. Evans, C. Spenger, and C. for the AddNeuroMed, *MRI Measures of Alzheimer's Disease and the AddNeuroMed Study.* Annals of the New York Academy of Sciences, 2009. 1180(1): p. 47-55.
183. Moms, J.C., A. Heyman, R.C. Mohs, J.P. Hughes, G. van Belle, G. Fillenbaum, E.D. Mellits, and C. Clark, *The Consortium to Establish a Registry for Alzheimer's Disease (CERAD). Part I. Clinical and neuropsychological assesment of Alzheimer's disease.* Neurology, 1989. 39(9): p. 1159.
184. Rosen, W.G., R.C. Mohs, and K.L. Davis, *A new rating scale for Alzheimer's disease.* The American Journal of Psychiatry, 1984. 141(11): p. 1356-1364.
185. Roth, M., E. Tym, C.Q. Mountjoy, F.A. Huppert, H. Hendrie, S. Verma, and R. Goddard, *CAMDEX. A standardised instrument for the diagnosis of mental disorder in the elderly with special reference to the early detection of dementia.* British Journal of Psychiatry, 1986. 149: p. 698-709.
186. Bradford, M.M., *A rapid and sensitive method for the quantitation of microgram quantities of protein utilizing the principle of protein-dye binding.* Analytical Biochemistry, 1976. 7(72): p. 248-254.
187. Hochstrasser, D.F., A. Patchornik, and C.R. Merril, *Development of polyacrylamide gels that improve the separation of proteins and their*

detection by silver staining. Analytical Biochemistry, 1988. 173(2): p. 412-423.
188. Kiddle, S.J., M. Sattlecker, P. Proitsi, A. Simmons, E. Westman, C. Bazenet, S.K. Nelson, S. Williams, A. Hodges, C. Johnston, H. Soininen, I. Kłoszewska, P. Mecocci, M. Tsolaki, B. Vellas, S. Newhouse, S. Lovestone, and R.J.B. Dobson, *Candidate Blood Proteome Markers of Alzheimer's Disease Onset and Progression: A Systematic Review and Replication Study.* Journal of Alzheimer's Disease, 2014. 38(3): p. 515-531.
189. O'Farrell, P.H., *High resolution two-dimensional electrophoresis of proteins.* Journal of Biological Chemistry, 1975. 250(10): p. 4007-4021.
190. Klose, J., *Protein mapping by combined isoelectric focusing and electrophoresis of mouse tissues. A novel approach to testing for induced point mutations in mammals.* Humangenetik, 1975. 26(3): p. 231-43.
191. Dowsey, A.W., J.A. English, F. Lisacek, J.S. Morris, G.Z. Yang, and M.J. Dunn, *Image analysis tools and emerging algorithms for expression proteomics.* Proteomics, 2010. 10(23): p. 4226-57.
192. Burton, E.F. and W.J. Hickey, *Assessing variability in gel-based proteomic analysis of Nitrosomonas europaea.* 2011(1557-7988 (Electronic)).
193. Asirvatham, V.S., B.S. Watson, and L.W. Sumner, *Analytical and biological variances associated with proteomic studies of Medicago truncatula by two-dimensional polyacrylamide gel electrophoresis.* Proteomics, 2002. 2(8): p. 960-968.
194. Molloy, M.P., E.E. Brzezinski, J. Hang, M.T. McDowell, and R.A. VanBogelen, *Overcoming technical variation and biological variation in quantitative proteomics.* Proteomics, 2003. 3(10): p. 1912-1919.
195. Carlson, N.E., M.M. Moore, A. Dame, D. Howieson, L.C. Silbert, J.F. Quinn, and J.A. Kaye, *Trajectories of brain loss in aging and the development of cognitive impairment.* Neurology, 2008. 70(11): p. 828-833.
196. Tombaugh, T.N., *Trail Making Test A and B: Normative data stratified by age and education.* Archives of Clinical Neuropsychology, 2004. 19(2): p. 203-214.
197. Bildl, W., A. Haupt, C.S. Muller, M.L. Biniossek, J.O. Thumfart, B. Huber, B. Fakler, and U. Schulte, *Extending the dynamic range of label-free mass spectrometric quantification of affinity purifications.* Mol Cell Proteomics, 2012. 11(2): p. M111 007955.
198. Tabb, D.L., L. Vega-Montoto, P.A. Rudnick, A.M. Variyath, A.-J.L. Ham, D.M. Bunk, L.E. Kilpatrick, D.D. Billheimer, R.K. Blackman, H.L. Cardasis, S.A. Carr, K.R. Clauser, J.D. Jaffe, K.A. Kowalski, T.A. Neubert, F.E. Regnier, B. Schilling, T.J. Tegeler, M. Wang, P. Wang, J.R. Whiteaker, L.J. Zimmerman, S.J. Fisher, B.W. Gibson, C.R. Kinsinger, M. Mesri, H. Rodriguez, S.E. Stein, P. Tempst, A.G. Paulovich, D.C. Liebler, and C. Spiegelman, *Repeatability and Reproducibility in Proteomic Identifications by Liquid Chromatography−Tandem Mass Spectrometry.* Journal of Proteome Research, 2010. 9(2): p. 761-776.
199. Silva, J.C., M.V. Gorenstein, G.Z. Li, J.P. Vissers, and S.J. Geromanos, *Absolute quantification of proteins by LCMSE: a virtue of parallel MS acquisition.* Mol Cell Proteomics, 2006. 5(1): p. 144-56.
200. Grossmann, J., B. Roschitzki, C. Panse, C. Fortes, S. Barkow-Oesterreicher, D. Rutishauser, and R. Schlapbach, *Implementation and evaluation of relative*

and absolute quantification in shotgun proteomics with label-free methods. J Proteomics, 2010. 73(9): p. 1740-6.
201. Kang, Y., T. Techanukul, A. Mantalaris, and J.M. Nagy, *Comparison of three commercially available DIGE analysis software packages: minimal user intervention in gel-based proteomics.* J Proteome Res, 2009. 8(2): p. 1077-84.
202. Karp, N.A., R. Feret, D.V. Rubtsov, and K.S. Lilley, *Comparison of DIGE and post-stained gel electrophoresis with both traditional and SameSpots analysis for quantitative proteomics.* Proteomics, 2008. 8(5): p. 948-60.
203. Jack, C.R., M.M. Shiung, J.L. Gunter, P.C. O'Brien, S.D. Weigand, D.S. Knopman, B.F. Boeve, R.J. Ivnik, G.E. Smith, R.H. Cha, E.G. Tangalos, and R.C. Petersen, *Comparison of different MRI brain atrophy rate measures with clinical disease progression in AD.* Neurology, 2004. 62(4): p. 591-600.
204. Jack, C.R., Jr., M. Slomkowski, S. Gracon, T.M. Hoover, J.P. Felmlee, K. Stewart, Y. Xu, M. Shiung, P.C. O'Brien, R. Cha, D. Knopman, and R.C. Petersen, *MRI as a biomarker of disease progression in a therapeutic trial of milameline for AD.* Neurology, 2003. 60(2): p. 253-60.
205. Thompson, P.M., K.M. Hayashi, G.I. de Zubicaray, A.L. Janke, S.E. Rose, J. Semple, M.S. Hong, D.H. Herman, D. Gravano, D.M. Doddrell, and A.W. Toga, *Mapping hippocampal and ventricular change in Alzheimer disease.* Neuroimage, 2004. 22(4): p. 1754-1766.
206. Jack, C.R., M.M. Shiung, S.D. Weigand, P.C. O'Brien, J.L. Gunter, B.F. Boeve, D.S. Knopman, G.E. Smith, R.J. Ivnik, E.G. Tangalos, and R.C. Petersen, *Brain atrophy rates predict subsequent clinical conversion in normal elderly and amnestic MCI.* Neurology, 2005. 65(8): p. 1227-1231.
207. Arbuthnott, K. and J. Frank, *Trail making test, part B as a measure of executive control: validation using a set-switching paradigm.* Journal of Clinical and Experimental Neuropsychology, 2000. 22(4): p. 518-28.
208. Blacker, D., H. Lee, A. Muzikansky, and et al., *Neuropsychological measures in normal individuals that predict subsequent cognitive decline.* Archives of Neurology, 2007. 64(6): p. 862-871.
209. Lafleche, G. and M.S. Albert, *Executive function deficits in mild Alzheimer's disease.* Neuropsychology, 1995. 9(3): p. 313-320.
210. Hayden, K.M., M. Kuchibhatla, H.R. Romero, B.L. Plassman, J.R. Burke, J.N. Browndyke, and K.A. Welsh-Bohmer, *Pre-clinical Cognitive Phenotypes for Alzheimer Disease: A Latent Profile Approach.* American Journal of Geriatric Psychiatry, 2013.
211. Jack, C.R., Jr., H.J. Wiste, S.D. Weigand, D.S. Knopman, V. Lowe, P. Vemuri, M.M. Mielke, D.T. Jones, M.L. Senjem, J.L. Gunter, B.E. Gregg, V.S. Pankratz, and R.C. Petersen, *Amyloid-first and neurodegeneration-first profiles characterize incident amyloid PET positivity.* Neurology, 2013. 81(20): p. 1732-40.
212. Armstrong, P.B. and J.P. Quigley, *A role for protease inhibitors in immunity of long-lived animals.* Advances in Experimental Medicine and Biology, 2001. 484: p. 141-60.
213. Strauss, S., J. Bauer, U. Ganter, U. Jonas, M. Berger, and B. Volk, *Detection of interleukin-6 and alpha 2-macroglobulin immunoreactivity in cortex and hippocampus of Alzheimer's disease patients.* Laboratory Investigation, 1992. 66(2): p. 223-30.
214. Bauer, J., S. Strauss, U. Schreiter-Gasser, U. Ganter, P. Schlegel, I. Witt, B. Yolk, and M. Berger, *Interleukin-6 and alpha-2-macroglobulin indicate an*

acute-phase state in Alzheimer's disease cortices. FEBS Letters, 1991. 285(1): p. 111-4.
215. Du, Y., B. Ni, M. Glinn, R.C. Dodel, K.R. Bales, Z. Zhang, P.A. Hyslop, and S.M. Paul, *alpha2-Macroglobulin as a beta-amyloid peptide-binding plasma protein.* Journal of Neurochemistry, 1997. 69(1): p. 299-305.
216. Hughes, S.R., O. Khorkova, S. Goyal, J. Knaeblein, J. Heroux, N.G. Riedel, and S. Sahasrabudhe, *Alpha2-macroglobulin associates with beta-amyloid peptide and prevents fibril formation.* Proceedings of the National Academy of Sciences of the United States of America, 1998. 95(6): p. 3275-80.
217. Qiu, W.Q., W. Borth, Z. Ye, C. Haass, D.B. Teplow, and D.J. Selkoe, *Degradation of amyloid beta-protein by a serine protease-alpha2-macroglobulin complex.* Journal of Biological Chemistry, 1996. 271(14): p. 8443-51.
218. Narita, M., D.M. Holtzman, A.L. Schwartz, and G. Bu, *Alpha2-macroglobulin complexes with and mediates the endocytosis of beta-amyloid peptide via cell surface low-density lipoprotein receptor-related protein.* Journal of Neurochemistry, 1997. 69(5): p. 1904-11.
219. Blacker, D., M.A. Wilcox, N.M. Laird, L. Rodes, S.M. Horvath, R.C. Go, R. Perry, B. Watson, Jr., S.S. Bassett, M.G. McInnis, M.S. Albert, B.T. Hyman, and R.E. Tanzi, *Alpha-2 macroglobulin is genetically associated with Alzheimer disease.* Nature Genetics, 1998. 19(4): p. 357-60.
220. Flachsbart, F., A. Caliebe, M. Nothnagel, R. Kleindorp, S. Nikolaus, S. Schreiber, and A. Nebel, *Depletion of potential A2M risk haplotype for Alzheimer's disease in long-lived individuals.* European Journal of Human Genetics, 2010. 18(1): p. 59-61.
221. Yang, H., Y. Lyutvinskiy, S.K. Herukka, H. Soininen, D. Rutishauser, and R.A. Zubarev, *Prognostic Polypeptide Blood Plasma Biomarkers of Alzheimer's Disease Progression.* J Alzheimers Dis, 2014.
222. Zabel, M., M. Schrag, C. Mueller, W. Zhou, A. Crofton, F. Petersen, A. Dickson, and W.M. Kirsch, *Assessing candidate serum biomarkers for Alzheimer's disease: a longitudinal study.* J Alzheimers Dis, 2012. 30(2): p. 311-21.
223. Sui, X., X. Ren, P. Huang, S. Li, Q. Ma, M. Ying, J. Ni, J. Liu, and X. Yang, *Proteomic Analysis of Serum Proteins in Triple Transgenic Alzheimer's Disease Mice: Implications for Identifying Biomarkers for Use to Screen Potential Candidate Therapeutic Drugs for Early Alzheimer's Disease.* Journal of Alzheimer's Disease, 2014.
224. Biere, A.L., B. Ostaszewski, E.R. Stimson, B.T. Hyman, J.E. Maggio, and D.J. Selkoe, *Amyloid beta-peptide is transported on lipoproteins and albumin in human plasma.* Journal of Biological Chemistry, 1996. 271(51): p. 32916-22.
225. Ramos-Fernandez, E., M. Tajes, E. Palomer, G. Ill-Raga, M. Bosch-Morato, B. Guivernau, I. Roman-Degano, A. Eraso-Pichot, D. Alcolea, J. Fortea, L. Nunez, A. Paez, F. Alameda, X. Fernandez-Busquets, A. Lleo, R. Elosua, M. Boada, M.A. Valverde, and F.J. Munoz, *Posttranslational Nitro-Glycative Modifications of Albumin in Alzheimer's Disease: Implications in Cytotoxicity and Amyloid-beta Peptide Aggregation.* J Alzheimers Dis, 2014.
226. Thambisetty, M., A. Hye, C. Foy, E. Daly, A. Glover, A. Cooper, A. Simmons, D. Murphy, and S. Lovestone, *Proteome-based identification of*

plasma proteins associated with hippocampal metabolism in early Alzheimer's disease. Journal of Neurology, 2008. 225(11): p. 1712-1720.
227. Adekar, S.P., I. Klyubin, S. Macy, M.J. Rowan, A. Solomon, S.K. Dessain, and B. O'Nuallain, *Inherent anti-amyloidogenic activity of human immunoglobulin gamma heavy chains.* Journal of Biological Chemistry, 2010. 285(2): p. 1066-74.
228. D'Andrea, M.R., *Add Alzheimer's disease to the list of autoimmune diseases.* Medical Hypotheses, 2005. 64(3): p. 458-63.
229. Maier, M., Y. Peng, L. Jiang, T.J. Seabrook, M.C. Carroll, and C.A. Lemere, *Complement C3 deficiency leads to accelerated amyloid beta plaque deposition and neurodegeneration and modulation of the microglia/macrophage phenotype in amyloid precursor protein transgenic mice.* Journal of Neuroscience, 2008. 28(25): p. 6333-41.
230. Zhang, R., L. Barker, D. Pinchev, J. Marshall, M. Rasamoelisolo, C. Smith, P. Kupchak, I. Kireeva, L. Ingratta, and G. Jackowski, *Mining biomarkers in human sera using proteomic tools.* Proteomics, 2004. 4(1): p. 244-56.
231. Bennett, S., M. Grant, A.J. Creese, F. Mangialasche, R. Cecchetti, H.J. Cooper, P. Mecocci, and S. Aldred, *Plasma levels of complement 4a protein are increased in Alzheimer's disease.* Alzheimer Disease and Associated Disorders, 2012. 26(4): p. 329-34.
232. Simonsen, A.H., N.O. Hagnelius, G. Waldemar, T.K. Nilsson, and J. McGuire, *Protein markers for the differential diagnosis of vascular dementia and Alzheimer's disease.* Int J Proteomics, 2012. 2012: p. 824024.
233. Daborg, J., U. Andreasson, M. Pekna, R. Lautner, E. Hanse, L. Minthon, K. Blennow, O. Hansson, and H. Zetterberg, *Cerebrospinal fluid levels of complement proteins C3, C4 and CR1 in Alzheimer's disease.* Journal of Neural Transmission, 2012. 119(7): p. 789-797.
234. Wang, Y., A.M. Hancock, J. Bradner, K.A. Chung, J.F. Quinn, E.R. Peskind, D. Galasko, J. Jankovic, C.P. Zabetian, H.M. Kim, J.B. Leverenz, T.J. Montine, C. Ginghina, K.L. Edwards, K.W. Snapinn, D.S. Goldstein, M. Shi, and J. Zhang, *Complement 3 and factor h in human cerebrospinal fluid in Parkinson's disease, Alzheimer's disease, and multiple-system atrophy.* American Journal of Pathology, 2011. 178(4): p. 1509-16.
235. Demey, F., V.S. Pandey, R. Baelmans, G. Agbede, and A. Verhulst, *The effect of storage at low temperature on the haemolytic complement activity of chicken serum.* Veterinary Research Communications, 1993. 17(1): p. 37-40.
236. Potempa, J., E. Korzus, and J. Travis, *The serpin superfamily of proteinase inhibitors: Structure, function, and regulation.* Journal of Biological Chemistry, 1994. 269(23): p. 15957-15960.
237. Liao, P.-C., L. Yu, C.-C. Kuo, C. Lin, and Y.-M. Kuo, *Proteomics analysis of plasma for potential biomarkers in the diagnosis of Alzheimer's disease.* PROTEOMICS – Clinical Applications, 2007. 1(5): p. 506-512.
238. Sihlbom, C., P. Davidsson, M. Sjögren, L.-O. Wahlund, and C. Nilsson, *Structural and Quantitative Comparison of Cerebrospinal Fluid Glycoproteins in Alzheimer's Disease Patients and Healthy Individuals.* Neurochemical Research, 2008. 33(7): p. 1332-1340.
239. Yu, H.L., H.M. Chertkow, H. Bergman, and H.M. Schipper, *Aberrant profiles of native and oxidized glycoproteins in Alzheimer plasma.* Proteomics, 2003. 3(11): p. 2240-2248.

240. Choi, J., C.A. Malakowsky, J.M. Talent, C.C. Conrad, and R.W. Gracy, *Identification of oxidized plasma proteins in Alzheimer's disease.* Biochemical and Biophysical Research Communications, 2002. 293(5): p. 1566-1570.
241. Gollin, P.A., R.N. Kalaria, P. Eikelenboom, A. Rozemuller, and G. Perry, *[alpha]1-Antitrypsin and [alpha]1-antichymotrypsin are in the lesions of Alzheimer's disease.* Neuroreport, 1992. 3(2): p. 201-203.
242. Rafnsson, S.B., I.J. Deary, F.B. Smith, M.C. Whiteman, A. Rumley, G.D.O. Lowe, and F.G.R. Fowkes, *Cognitive Decline and Markers of Inflammation and Hemostasis: The Edinburgh Artery Study*. Journal of the American Geriatrics Society, 2007. 55(5): p. 700-707.
243. Knuiman, M.W., A.R. Folsom, L.E. Chambless, D. Liao, and K.K. Wu, *Association of hemostatic variables with MRI-detected cerebral abnormalities: the atherosclerosis risk in communities study.* Neuroepidemiology, 2001. 20(2): p. 96-104.
244. Vafadar-Isfahani, B., G. Ball, C. Coveney, C. Lemetre, D. Boocock, L. Minthon, O. Hansson, A.K. Miles, S.M. Janciauskiene, D. Warden, A.D. Smith, G. Wilcock, N. Kalsheker, R. Rees, B. Matharoo-Ball, and K. Morgan, *Identification of SPARC-like 1 protein as part of a biomarker panel for Alzheimer's disease in cerebrospinal fluid.* J Alzheimers Dis, 2012. 28(3): p. 625-36.
245. Lee, J., H. Namkoong, H. Kim, S. Kim, D. Hwang, H. Na, S.-A. Ha, J.-R. Kim, and J. Kim, *Fibrinogen gamma-A chain precursor in CSF: a candidate biomarker for Alzheimer's disease.* BMC Neurology, 2007. 7(1): p. 1-6.
246. Song, F., A. Poljak, N.A. Kochan, M. Raftery, H. Brodaty, G.A. Smythe, and P.S. Sachdev, *Plasma protein profiling of Mild Cognitive Impairment and Alzheimer's disease using iTRAQ quantitative proteomics.* Proteome Sci, 2014. 12(1): p. 5.
247. Xu, G., H. Zhang, S. Zhang, X. Fan, and X. Liu, *Plasma fibrinogen is associated with cognitive decline and risk for dementia in patients with mild cognitive impairment.* International Journal of Clinical Practice, 2008. 62(7): p. 1070-5.
248. van Oijen, M., J.C. Witteman, A. Hofman, P.J. Koudstaal, and M.M. Breteler, *Fibrinogen is associated with an increased risk of Alzheimer disease and vascular dementia.* Stroke, 2005. 36(12): p. 2637-41.
249. Paul, J., S. Strickland, and J.P. Melchor, *Fibrin deposition accelerates neurovascular damage and neuroinflammation in mouse models of Alzheimer's disease.* Journal of Experimental Medicine, 2007. 204(8): p. 1999-2008.
250. Lipinski, B. and E.M. Sajdel-Sulkowska, *New insight into Alzheimer disease: demonstration of fibrin(ogen)-serum albumin insoluble deposits in brain tissue.* Alzheimer Disease and Associated Disorders, 2006. 20(4): p. 323-6.
251. Ryu, J.K. and J.G. McLarnon, *A leaky blood-brain barrier, fibrinogen infiltration and microglial reactivity in inflamed Alzheimer's disease brain.* J Cell Mol Med, 2009. 13(9A): p. 2911-25.
252. Bots, M.L., M.M.B. Breteler, F. van Kooten, F. Haverkate, P. Meijer, P.J. Koudstaal, D.E. Grobbee, and C. Kluft, *Coagulation and Fibrinolysis Markers and Risk of Dementia.* Pathophysiology of Haemostasis and Thrombosis, 1998. 28(3-4): p. 216-222.

253. Wilson, C.J., H.J. Cohen, and C.F. Pieper, *Cross-Linked Fibrin Degradation Products (D-Dimer), Plasma Cytokines, and Cognitive Decline in Community-Dwelling Elderly Persons.* Journal of the American Geriatrics Society, 2003. 51(10): p. 1374-1381.
254. Ferlito, S., A. Palermo, D. Mazzone, M. Condorelli, and D. Papalia, *Fibrinogen and antithrombin III in obese subjects.* Minerva Endocrinologica, 1990. 15(2): p. 145-148.
255. Kalaria, R.N., T. Golde, S.N. Kroon, and G. Perry, *Serine protease inhibitor antithrombin III and its messenger RNA in the pathogenesis of Alzheimer's disease.* American Journal of Pathology, 1993. 143(3): p. 886-93.
256. Hu, Y., A. Hosseini, J.S.K. Kauwe, J. Gross, N.J. Cairns, A.M. Goate, A.M. Fagan, R.R. Townsend, and D.M. Holtzman, *Identification and validation of novel CSF biomarkers for early stages of Alzheimer's disease.* PROTEOMICS – Clinical Applications, 2007. 1(11): p. 1373-1384.
257. Cortes-Canteli, M., D. Zamolodchikov, H.J. Ahn, S. Strickland, and E.H. Norris, *Fibrinogen and altered hemostasis in Alzheimer's disease.* J Alzheimers Dis, 2012. 32(3): p. 599-608.
258. Carlsson, F., C. Sandin, and G. Lindahl, *Human fibrinogen bound to Streptococcus pyogenes M protein inhibits complement deposition via the classical pathway.* Molecular Microbiology, 2005. 56(1): p. 28-39.
259. Horstmann, R., Sievertsen, H., Leippe, M., Fischetti, V., *Role of fibrinogen in complement inhibition by streptococcal M protein.* Infection and Immunity, 1992. 60(12): p. 5036-5041.
260. Amara, U., D. Rittirsch, M. Flierl, U. Bruckner, A. Klos, F. Gebhard, J.D. Lambris, and M. Huber-Lang, *Interaction between the coagulation and complement system.* Advances in Experimental Medicine and Biology, 2008. 632: p. 71-9.
261. Song, F., A. Poljak, J. Crawford, N.A. Kochan, W. Wen, B. Cameron, O. Lux, H. Brodaty, K. Mather, G.A. Smythe, and P.S. Sachdev, *Plasma apolipoprotein levels are associated with cognitive status and decline in a community cohort of older individuals.* PLoS ONE, 2012. 7(6): p. e34078.
262. Thambisetty, M., Y. An, A. Kinsey, D. Koka, M. Saleem, A. Güntert, M. Kraut, L. Ferrucci, C. Davatzikos, S. Lovestone, and S.M. Resnick, *Plasma clusterin concentration is associated with longitudinal brain atrophy in mild cognitive impairment.* Neuroimage, 2012. 59(1): p. 212-217.
263. Calero, M., A. Rostagno, and J. Ghiso, *Search for amyloid-binding proteins by affinity chromatography.* Methods in Molecular Biology, 2012. 849: p. 213-23.
264. Cui, Y., M. Huang, Y. He, S. Zhang, and Y. Luo, *Genetic ablation of apolipoprotein A-IV accelerates Alzheimer's disease pathogenesis in a mouse model.* American Journal of Pathology, 2011. 178(3): p. 1298-308.
265. Sorenson, R.C., C.L. Bisgaier, M. Aviram, C. Hsu, S. Billecke, and B.N. La Du, *Human serum Paraoxonase/Arylesterase's retained hydrophobic N-terminal leader sequence associates with HDLs by binding phospholipids : apolipoprotein A-I stabilizes activity.* Arteriosclerosis, Thrombosis, and Vascular Biology, 1999. 19(9): p. 2214-25.
266. Pola, R., E. Gaetani, A. Flex, L. Gerardino, F. Aloi, R. Flore, M. Serricchio, P. Pola, and R. Bernabei, *Lack of association between Alzheimer's disease and Gln-Arg 192 Q/R polymorphism of the PON-1 gene in an Italian*

population. Dementia and Geriatric Cognitive Disorders, 2003. 15(2): p. 88-91.
267. Erlich, P.M., K.L. Lunetta, L.A. Cupples, C.R. Abraham, R.C. Green, C.T. Baldwin, and L.A. Farrer, *Serum paraoxonase activity is associated with variants in the PON gene cluster and risk of Alzheimer disease.* Neurobiology of Aging, 2012. 33(5): p. 1015 e7-23.
268. Bednarska-Makaruk, M.E., T. Krzywkowski, A. Graban, W. Lipczynska-Lojkowska, A. Bochynska, M. Rodo, H. Wehr, and D.K. Ryglewicz, *Paraoxonase 1 (PON1) gene -108C>T and p.Q192R polymorphisms and arylesterase activity of the enzyme in patients with dementia.* Folia Neuropathologica, 2013. 51(2): p. 111-9.
269. Mackness, B., Mackness, M., Aviram, M., Paragh, G, ed. *The Paraoxonases: Their Role in Disease Development and Xenobiotic Metabolism*. Proteins and Cell Regulation. Vol. 6. 2008, Springer Link. 325.
270. Squitti, R., C.C. Quattrocchi, C. Salustri, and P.M. Rossini, *Ceruloplasmin fragmentation is implicated in 'free' copper deregulation of Alzheimer's disease.* Prion, 2008. 2(1): p. 23-7.
271. Agarwal, R., S. Kushwaha, C.B. Tripathi, N. Singh, and N. Chhillar, *Serum copper in Alzheimer's disease and vascular dementia.* Indian Journal of Clinical Biochemistry, 2008. 23(4): p. 369-374.
272. Squitti, R., R. Ghidoni, M. Siotto, M. Ventriglia, L. Benussi, A. Paterlini, M. Magri, G. Binetti, E. Cassetta, D. Caprara, F. Vernieri, P.M. Rossini, and P. Pasqualetti, *Value of serum non-ceruloplasmin copper for prediction of mci conversion to ad.* Annals of Neurology, 2014.
273. Snaedal, J., J. Kristinsson, S. Gunnarsdóttir, Á. Ólafsdóttir, M. Baldvinsson, and T. Jóhannesson, *Copper, Ceruloplasmin and Superoxide Dismutase in Patients with Alzheimer's Disease.* Dementia and Geriatric Cognitive Disorders, 1998. 9(5): p. 239-242.
274. Park, J.H., D.W. Lee, and K.S. Park, *Elevated serum copper and ceruloplasmin levels in Alzheimer's disease.* Asia Pac Psychiatry, 2014. 6(1): p. 38-45.
275. Rembach, A., J.D. Doecke, B.R. Roberts, A.D. Watt, N.G. Faux, I. Volitakis, K.K. Pertile, R.L. Rumble, B.O. Trounson, C.J. Fowler, W. Wilson, K.A. Ellis, R.N. Martins, C.C. Rowe, V.L. Villemagne, D. Ames, C.L. Masters, A.r. group, and A.I. Bush, *Longitudinal analysis of serum copper and ceruloplasmin in Alzheimer's disease.* J Alzheimers Dis, 2013. 34(1): p. 171-82.
276. Schrag, M., C. Mueller, M. Zabel, A. Crofton, W.M. Kirsch, O. Ghribi, R. Squitti, and G. Perry, *Oxidative stress in blood in Alzheimer's disease and mild cognitive impairment: A meta-analysis.* Neurobiology of Disease, 2013. 59(0): p. 100-110.
277. Gupta, S., K. Ahern, F. Nakhl, and F. Forte, *Clinical Usefulness of Haptoglobin Levels to Evaluate Hemolysis in Recently Transfused Patients.* Advances in Hematology, 2011. 2011.
278. Yerbury, J.J., M.S. Rybchyn, S.B. Easterbrook-Smith, C. Henriques, and M.R. Wilson, *The acute phase protein haptoglobin is a mammalian extracellular chaperone with an action similar to clusterin.* Biochemistry, 2005. 44(32): p. 10914-25.
279. Wang, Y., E. Kinzie, F.G. Berger, S.K. Lim, and H. Baumann, *Haptoglobin, an inflammation-inducible plasma protein.* Redox Rep, 2001. 6(6): p. 379-85.

280. Powers, J.M., W.W. Schlaepfer, M.C. Willingham, and B.J. Hall, *An immunoperoxidase study of senile cerebral amyloidosis with pathogenetic considerations.* Journal of Neuropathology and Experimental Neurology, 1981. 40(6): p. 592-612.
281. Cocciolo, A., F. Di Domenico, R. Coccia, A. Fiorini, J. Cai, W.M. Pierce, P. Mecocci, D.A. Butterfield, and M. Perluigi, *Decreased expression and increased oxidation of plasma haptoglobin in Alzheimer disease: Insights from redox proteomics.* Free Radical Biology and Medicine, 2012. 53(10): p. 1868-1876.
282. Abraham, J.D., S. Calvayrac-Pawlowski, S. Cobo, N. Salvetat, G. Vicat, L. Molina, J. Touchon, B.F. Michel, F. Molina, J.M. Verdier, J. Fareh, and C. Mourton-Gilles, *Combined measurement of PEDF, haptoglobin and tau in cerebrospinal fluid improves the diagnostic discrimination between alzheimer's disease and other dementias.* Biomarkers, 2011. 16(2): p. 161-71.
283. Olsson, M.G., E.J.C. Nilsson, S. Rutardóttir, J. Paczesny, J. Pallon, and B. Åkerström, *Bystander Cell Death and Stress Response is Inhibited by the Radical Scavenger α1-Microglobulin in Irradiated Cell Cultures.* Radiation Research, 2010. 174(5): p. 590-600.
284. Olsson, M.G., M. Allhorn, L. Bulow, S.R. Hansson, D. Ley, M.L. Olsson, A. Schmidtchen, and B. Akerstrom, *Pathological conditions involving extracellular hemoglobin: molecular mechanisms, clinical significance, and novel therapeutic opportunities for alpha(1)-microglobulin.* Antioxid Redox Signal, 2012. 17(5): p. 813-46.
285. Olsson, M.G., L.W. Rosenlof, H. Kotarsky, T. Olofsson, T. Leanderson, M. Morgelin, V. Fellman, and B. Akerstrom, *The radical-binding lipocalin A1M binds to a Complex I subunit and protects mitochondrial structure and function.* Antioxid Redox Signal, 2013. 18(16): p. 2017-28.
286. Inagaki, T., T. Shikimi, H. Ishino, H. Okunishi, and S. Takaori, *Changes in the ratio of urinary alpha 1-microglobulin to ulinastatin levels in patients with Alzheimer-type dementia and vascular dementia.* Psychiatry and Clinical Neurosciences, 1995. 49(5-6): p. 287-90.
287. Cascella, R., S. Conti, F. Tatini, E. Evangelisti, T. Scartabelli, F. Casamenti, M.R. Wilson, F. Chiti, and C. Cecchi, *Extracellular chaperones prevent Aβ42-induced toxicity in rat brains.* Biochimica et Biophysica Acta (BBA) - Molecular Basis of Disease, 2013. 1832(8): p. 1217-1226.
288. Schrijvers, E.C., P.J. Koudstaal, A. Hofman, and M.B. Breteler, *PLasma clusterin and the risk of alzheimer disease.* JAMA, 2011. 305(13): p. 1322-1326.
289. Franco, S., Truran, S., Migrino, R, *Protective role of clusterin in preserving endothelial function in AL amyloidosis.* Atherosclerosis, 2012. 225(1): p. 220-223.
290. Garcia-Rodriguez, S., S. Arias-Santiago, R. Perandres-Lopez, J. Orgaz-Molina, L. Castellote, A. Buendia-Eisman, J.C. Ruiz, R. Naranjo, P. Navarro, J. Sancho, and M. Zubiaur, *Decreased plasma levels of clusterin in patients with psoriasis.* Actas Dermo-Sifiliograficas, 2013. 104(6): p. 497-503.
291. Devauchelle, V., A. Essabbani, G. De Pinieux, S. Germain, L. Tourneur, S. Mistou, F. Margottin-Goguet, P. Anract, H. Migaud, D. Le Nen, T. Lequerre, A. Saraux, M. Dougados, M. Breban, C. Fournier, and G. Chiocchia, *Characterization and functional consequences of underexpression of*

clusterin in rheumatoid arthritis. Journal of Immunology, 2006. 177(9): p. 6471-9.
292. Jeong-Hun, K., Jin, H., Young, S., Bon, H., Kyu-Won, K., *Protective Effect of Clusterin on Blood–Retinal Barrier Breakdown in Diabetic Retinopathy.* Investigative Ophthalmology and Visual Science, 2010. 51(3): p. 1659-1665.
293. Desikan, R.S., W.K. Thompson, D. Holland, and et al., *THe role of clusterin in amyloid-β–associated neurodegeneration.* JAMA Neurology, 2014. 71(2): p. 180-187.
294. Killick, R., E.M. Ribe, R. Al-Shawi, B. Malik, C. Hooper, C. Fernandes, R. Dobson, P.M. Nolan, A. Lourdusamy, S. Furney, K. Lin, G. Breen, R. Wroe, A.W. To, K. Leroy, M. Causevic, A. Usardi, M. Robinson, W. Noble, R. Williamson, K. Lunnon, S. Kellie, C.H. Reynolds, C. Bazenet, A. Hodges, J.P. Brion, J. Stephenson, J.P. Simons, and S. Lovestone, *Clusterin regulates beta-amyloid toxicity via Dickkopf-1-driven induction of the wnt-PCP-JNK pathway.* Molecular Psychiatry, 2014. 19(1): p. 88-98.
295. Anderson, N.L. and N.G. Anderson, *The human plasma proteome: history, character, and diagnostic prospects.* Mol Cell Proteomics, 2002. 1(11): p. 845-67.
296. Rabilloud, T., *Two-dimensional gel electrophoresis in proteomics: Old, old fashioned, but it still climbs up the mountains.* Proteomics, 2002. 2(1): p. 3-10.
297. Grebe, S.K. and R.J. Singh, *LC-MS/MS in the Clinical Laboratory - Where to From Here?* Clin Biochem Rev, 2011. 32(1): p. 5-31.
298. Ponnayyan Sulochana, S., K. Sharma, R. Mullangi, and S.K. Sukumaran, *Review of the validated HPLC and LC-MS/MS methods for determination of drugs used in clinical practice for Alzheimer's disease.* Biomedical Chromatography, 2014.
299. Hsieh, E.J., M.S. Bereman, S. Durand, G.A. Valaskovic, and M.J. MacCoss, *Effects of column and gradient lengths on peak capacity and peptide identification in nanoflow LC-MS/MS of complex proteomic samples.* Journal of the American Society for Mass Spectrometry, 2013. 24(1): p. 148-53.
300. Tu, C., P.A. Rudnick, M.Y. Martinez, K.L. Cheek, S.E. Stein, R.J.C. Slebos, and D.C. Liebler, *Depletion of Abundant Plasma Proteins and Limitations of Plasma Proteomics.* Journal of Proteome Research, 2010. 9(10): p. 4982-4991.
301. Polaskova, V., A. Kapur, A. Khan, M.P. Molloy, and M.S. Baker, *High-abundance protein depletion: Comparison of methods for human plasma biomarker discovery.* Electrophoresis, 2010. 31(3): p. 471-482.
302. Fournier, T., N.N. Medjoubi, and D. Porquet, *Alpha-1-acid glycoprotein.* Biochimica et Biophysica Acta, 2000. 1482(1-2): p. 157-71.
303. Fischer, K., J. Kettunen, P. Würtz, T. Haller, A.S. Havulinna, A.J. Kangas, P. Soininen, T. Esko, M.-L. Tammesoo, R. Mägi, S. Smit, A. Palotie, S. Ripatti, V. Salomaa, M. Ala-Korpela, M. Perola, and A. Metspalu, *Biomarker Profiling by Nuclear Magnetic Resonance Spectroscopy for the Prediction of All-Cause Mortality: An Observational Study of 17,345 Persons.* PLoS Med, 2014. 11(2): p. e1001606.
304. Carriere, I., A.M. Dupuy, A. Lacroux, J.P. Cristol, and C. Delcourt, *Biomarkers of inflammation and malnutrition associated with early death in healthy elderly people.* Journal of the American Geriatrics Society, 2008. 56(5): p. 840-6.

305. Bruno, R., R. Olivares, J. Berille, P. Chaikin, N. Vivier, L. Hammershaimb, G.R. Rhodes, and J.R. Rigas, *Alpha-1-acid glycoprotein as an independent predictor for treatment effects and a prognostic factor of survival in patients with non-small cell lung cancer treated with docetaxel.* Clinical Cancer Research, 2003. 9(3): p. 1077-82.
306. Han, S.H., E.S. Jung, J.H. Sohn, H.J. Hong, H.S. Hong, J.W. Kim, D.L. Na, M. Kim, H. Kim, H.J. Ha, Y.H. Kim, N. Huh, M.W. Jung, and I. Mook-Jung, *Human serum transthyretin levels correlate inversely with Alzheimer's disease.* J Alzheimers Dis, 2011. 25(1): p. 77-84.
307. Schwarzman, A.L. and D. Goldgaber, *Interaction of transthyretin with amyloid beta-protein: binding and inhibition of amyloid formation.* Ciba Foundation Symposium, 1996. 199: p. 146-60; discussion 160-4.
308. Costa, R., F. Ferreira-da-Silva, M.J. Saraiva, and I. Cardoso, *Transthyretin Protects against A-Beta Peptide Toxicity by Proteolytic Cleavage of the Peptide: A Mechanism Sensitive to the Kunitz Protease Inhibitor.* PLoS ONE, 2008. 3(8): p. e2899.
309. Shirahama, T., M. Skinner, P. Westermark, A. Rubinow, A.S. Cohen, A. Brun, and T.L. Kemper, *Senile cerebral amyloid. Prealbumin as a common constituent in the neuritic plaque, in the neurofibrillary tangle, and in the microangiopathic lesion.* American Journal of Pathology, 1982. 107(1): p. 41-50.
310. Stein, T.D., N.J. Anders, C. DeCarli, S.L. Chan, M.P. Mattson, and J.A. Johnson, *Neutralization of transthyretin reverses the neuroprotective effects of secreted amyloid precursor protein (APP) in APPSW mice resulting in tau phosphorylation and loss of hippocampal neurons: support for the amyloid hypothesis.* Journal of Neuroscience, 2004. 24(35): p. 7707-17.
311. Kantarjian, H.M., T. Smith, E. Estey, A. Polyzos, S. O'Brien, S. Pierce, M. Beran, E. Feldman, and M.J. Keating, *Prognostic significance of elevated serum beta 2-microglobulin levels in adult acute lymphocytic leukemia.* American Journal of Medicine, 1992. 93(6): p. 599-604.
312. Ward, M.A., H. Soininen, D. O'Brien, S. Lovestone, M. Hallikainen, S.-K. Herukka, E. Schofield, J. Campbell, and L. Dayon, *Evaluation of CSF cystatin C, beta-2-microglobulin, and VGF as diagnostic biomarkers of Alzheimer's disease using SRM.* Alzheimer's & dementia : the journal of the Alzheimer's Association, 2011. 7(4): p. S150-S151.
313. Doecke, J.D., S.M. Laws, N.G. Faux, W. Wilson, S.C. Burnham, C.P. Lam, A. Mondal, J. Bedo, A.I. Bush, B. Brown, K. De Ruyck, K.A. Ellis, C. Fowler, V.B. Gupta, R. Head, S.L. Macaulay, K. Pertile, C.C. Rowe, A. Rembach, M. Rodrigues, R. Rumble, C. Szoeke, K. Taddei, T. Taddei, B. Trounson, D. Ames, C.L. Masters, and R.N. Martins, *Blood-based protein biomarkers for diagnosis of Alzheimer disease.* Archives of Neurology, 2012. 69(10): p. 1318-25.
314. Kakisaka, T., T. Kondo, T. Okano, K. Fujii, K. Honda, M. Endo, A. Tsuchida, T. Aoki, T. Itoi, F. Moriyasu, T. Yamada, H. Kato, T. Nishimura, S. Todo, and S. Hirohashi, *Plasma proteomics of pancreatic cancer patients by multi-dimensional liquid chromatography and two-dimensional difference gel electrophoresis (2D-DIGE): Up-regulation of leucine-rich alpha-2-glycoprotein in pancreatic cancer.* Journal of Chromatography B: Analytical Technologies in the Biomedical and Life Sciences, 2007. 852(1-2): p. 257-267.

315. Deng, R., Z. Lu, Y. Chen, L. Zhou, and X. Lu, *Plasma proteomic analysis of pancreatic cancer by 2-dimensional gel electrophoresis.* Pancreas, 2007. 34(3): p. 310-317.
316. Shirai, R., F. Hirano, N. Ohkura, K. Ikeda, and S. Inoue, *Up-regulation of the expression of leucine-rich α2-glycoprotein in hepatocytes by the mediators of acute-phase response.* Biochemical and Biophysical Research Communications, 2009. 382(4): p. 776-779.
317. Shirai, R., F. Hirano, N. Ohkura, K. Ikeda, and S. Inoue, *Up-regulation of the expression of leucine-rich alpha(2)-glycoprotein in hepatocytes by the mediators of acute-phase response.* Biochemical and Biophysical Research Communications, 2009. 382(4): p. 776-9.
318. Li, X., M. Miyajima, R. Mineki, H. Taka, K. Murayama, and H. Arai, *Analysis of potential diagnostic biomarkers in cerebrospinal fluid of idiopathic normal pressure hydrocephalus by proteomics.* Acta Neurochirurgica, 2006. 148(8): p. 859-64; discussion 864.
319. Puchades, M., S.F. Hansson, C.L. Nilsson, N. Andreasen, K. Blennow, and P. Davidsson, *Proteomic studies of potential cerebrospinal fluid protein markers for Alzheimer's disease.* Brain Research. Molecular Brain Research, 2003. 118(1-2): p. 140-6.
320. Gupta, V.B., S.M. Laws, V.L. Villemagne, D. Ames, A.I. Bush, K.A. Ellis, J.K. Lui, C. Masters, C.C. Rowe, C. Szoeke, K. Taddei, and R.N. Martins, *Plasma apolipoprotein E and Alzheimer disease risk: the AIBL study of aging.* Neurology, 2011. 76(12): p. 1091-8.
321. Wang, C., J.-T. Yu, H.-F. Wang, T. Jiang, C.-C. Tan, X.-F. Meng, H.D. Soares, and L. Tan, *Meta-Analysis of Peripheral Blood Apolipoprotein E Levels in Alzheimer's Disease.* PLoS ONE, 2014. 9(2): p. e89041.
322. Hassan, M.I., A. Waheed, S. Yadav, T.P. Singh, and F. Ahmad, *Zinc α2-Glycoprotein: A Multidisciplinary Protein.* Molecular Cancer Research, 2008. 6(6): p. 892-906.
323. Mracek, T., Q. Ding, T. Tzanavari, K. Kos, J. Pinkney, J. Wilding, P. Trayhurn, and C. Bing, *The adipokine zinc-alpha2-glycoprotein (ZAG) is downregulated with fat mass expansion in obesity.* Clinical Endocrinology, 2010. 72(3): p. 334-41.
324. Diez-Itza, I., L.M. Sanchez, M.T. Allende, F. Vizoso, A. Ruibal, and C. Lopez-Otin, *Zn-alpha 2-glycoprotein levels in breast cancer cytosols and correlation with clinical, histological and biochemical parameters.* European Journal of Cancer, 1993. 29A(9): p. 1256-60.
325. Hale, L.P., D.T. Price, L.M. Sanchez, W. Demark-Wahnefried, and J.F. Madden, *Zinc alpha-2-glycoprotein is expressed by malignant prostatic epithelium and may serve as a potential serum marker for prostate cancer.* Clinical Cancer Research, 2001. 7(4): p. 846-53.
326. Irmak, S., D. Tilki, J. Heukeshoven, L. Oliveira-Ferrer, M. Friedrich, H. Huland, and S. Ergun, *Stage-dependent increase of orosomucoid and zinc-alpha2-glycoprotein in urinary bladder cancer.* Proteomics, 2005. 5(16): p. 4296-304.
327. Bondar, O.P., D.R. Barnidge, E.W. Klee, B.J. Davis, and G.G. Klee, *LC-MS/MS quantification of Zn-alpha2 glycoprotein: a potential serum biomarker for prostate cancer.* Clinical Chemistry, 2007. 53(4): p. 673-8.
328. Abdul-Rahman, P.S., B.K. Lim, and O.H. Hashim, *Expression of high-abundance proteins in sera of patients with endometrial and cervical*

cancers: analysis using 2-DE with silver staining and lectin detection methods. Electrophoresis, 2007. 28(12): p. 1989-96.
329. Stepan, H., A. Philipp, I. Roth, S. Kralisch, A. Jank, W. Schaarschmidt, U. Lossner, J. Kratzsch, M. Bluher, M. Stumvoll, and M. Fasshauer, *Serum levels of the adipokine zinc-alpha2-glycoprotein are increased in preeclampsia.* Journal of Endocrinological Investigation, 2012. 35(6): p. 562-5.
330. Tedeschi, S., E. Pilotti, E. Parenti, V. Vicini, P. Coghi, A. Montanari, G. Regolisti, E. Fiaccadori, and A. Cabassi, *Serum adipokine zinc alpha2-glycoprotein and lipolysis in cachectic and noncachectic heart failure patients: relationship with neurohormonal and inflammatory biomarkers.* Metabolism, 2012. 61(1): p. 37-42.
331. Sörensen-Zender, I., J. Beneke, B. Schmidt, J. Menne, H. Haller, and R. Schmitt, *Zinc-alpha2-glycoprotein in patients with acute and chronic kidney disease.* BMC Nephrology, 2013. 14(1): p. 1-6.
332. Bing, C., T. Mracek, D. Gao, and P. Trayhurn, *Zinc-alpha2-glycoprotein: an adipokine modulator of body fat mass?* Int J Obes (Lond), 2010. 34(11): p. 1559-65.
333. Mracek, T., D. Gao, T. Tzanavari, Y. Bao, X. Xiao, C. Stocker, P. Trayhurn, and C. Bing, *Downregulation of zinc-{alpha}2-glycoprotein in adipose tissue and liver of obese ob/ob mice and by tumour necrosis factor-alpha in adipocytes.* Journal of Endocrinology, 2010. 204(2): p. 165-72.
334. Roher, A.E., C.L. Maarouf, L.I. Sue, Y. Hu, J. Wilson, and T.G. Beach, *Proteomics-derived cerebrospinal fluid markers of autopsy-confirmed Alzheimer's disease.* Biomarkers, 2009. 14(7): p. 493-501.
335. Convit, A., M.J. De Leon, C. Tarshish, S. De Santi, W. Tsui, H. Rusinek, and A. George, *Specific hippocampal volume reductions in individuals at risk for Alzheimer's disease.* Neurobiology of Aging, 1997. 18(2): p. 131-8.
336. Scheff, S.W., D.A. Price, F.A. Schmitt, and E.J. Mufson, *Hippocampal synaptic loss in early Alzheimer's disease and mild cognitive impairment.* Neurobiology of Aging, 2006. 27(10): p. 1372-84.
337. Frisoni, G.B., N.C. Fox, C.R. Jack, P. Scheltens, and P.M. Thompson, *The clinical use of structural MRI in Alzheimer disease.* Nature Reviews: Neurology, 2010. 6(2): p. 1759-4758.
338. Galasko, D., M.R. Klauber, C. Hofstetter, D.P. Salmon, B. Lasker, and L.J. Thal, *THe mini-mental state examination in the early diagnosis of alzheimer's disease.* Archives of Neurology, 1990. 47(1): p. 49-52.
339. Han, L., M. Cole, F. Bellavance, J. McCusker, and F. Primeau, *Tracking Cognitive Decline in Alzheimer's Disease Using the Mini-Mental State Examination: A Meta-Analysis.* International Psychogeriatrics, 2000. 12(02): p. 231-247.
340. Small, B.J., M. Viitanen, and L. Backman, *Mini-Mental State Examination Item Scores as Predictors of Alzheimer's Disease: Incidence Data From the Kungsholmen Project, Stockholm.* The Journals of Gerontology Series A: Biological Sciences and Medical Sciences, 1997. 52A(5): p. M299-M304.
341. Benson, A.D., M.J. Slavin, T.T. Tran, J.R. Petrella, and P.M. Doraiswamy, *Screening for Early Alzheimer's Disease: Is There Still a Role for the Mini-Mental State Examination?* Prim Care Companion J Clin Psychiatry, 2005. 7(2): p. 62-69.

342. Cui, Y., M. Huang, Y. He, S. Zhang, and Y. Luo, *Genetic Ablation of Apolipoprotein A-IV Accelerates Alzheimer's Disease Pathogenesis in a Mouse Model.* The American Journal of Pathology, 2011. 178(3): p. 1298-1308.
343. Adekar, S.P., I. Klyubin, S. Macy, M.J. Rowan, A. Solomon, S.K. Dessain, and B. O'Nuallain, *Inherent Anti-amyloidogenic Activity of Human Immunoglobulin γ Heavy Chains.* Journal of Biological Chemistry, 2010. 285(2): p. 1066-1074.
344. Schmidt, R., E. Kienbacher, T. Benke, P. Dal-Bianco, M. Delazer, G. Ladurner, K. Jellinger, J. Marksteiner, G. Ransmayr, H. Schmidt, E. Stogmann, J. Friedrich, and C. Wehringer, *Sex differences in Alzheimer's disease.* Neuropsychiatrie : Klinik, Diagnostik, Therapie und Rehabilitation: Organ der Gesellschaft Osterreichischer Nervenarzte und Psychiater, 2008. 22(1): p. 1-15.
345. Mielke, M.M., P. Vemuri, and W. Rocca, *Clinical epidemiology of Alzheimer's disease: assessing sex and gender differences.* Clinical Epidemiology, 2014. 6: p. 37-48.
346. The Ronald and Nancy Reagan Research Institute of the Alzheimer's Association and the National Institute on Aging Working Group Consensus report of the Working Group on: "Molecular and Biochemical Markers of Alzheimer's Disease". Neurobiology of Aging. 1998;19:109–116. Anonymous.
347. Davis, D, S. *Alzheimer's disease and pre-emptive suicide.* Journal of Medical Ethics. 2013. Published Online First: doi:10.1136/medethics-2012-101022.
348. Kosik, K, S., Post, S., G., and Quaid, K,, A. *An Ethical Context For Presymptomatic Testing in Alzheimer's Disease*. In; Scrinto, L. and Daffner, K, Early Diagnosis of Alzheimer's Disease. 2000. (pp. 317-327). Hamana Press.
349. Ball, D. and Harper, P. *Presymptomatic testing for late-onset genetic disorders: lessons from Huntingtons's disease*. 1992. FASEB journal; 6(10): 2818-2819.
350. McGuinness, B., Barrett, S., L., Craig, D., Lawson, J., and Passmore, A., P. *Executive functioning in Alzheimer's disease and vascular dementia*. 2010. International journal of geriatric psychiatry. 25(6); 562-568.
351. Lambert, J., C., Ibrahim-Verbaas, C., A., Harold, D., Naj, A., C., Sims, R., et al. *Meta-analysis of 74,046 individuals identifies 11 new susceptibility loci for Alzheimer's disease*. 2013. Nature Genetics. 45: 1452–145

Appendices

Appendix 1

Baseline partial correlation results for 2DGE spots with PiB PET DVR. Spots ranked in order of significance based on *p* value. Spots highlighted in red are statistically significant (*p*<0.05)

Spot ID	Correlation coefficient	P-value
X1370	-0.532	0.000
X1310	-0.492	0.000
X1793	-0.484	0.000
X696	0.481	0.001
X749	-0.466	0.001
X1365	-0.451	0.001
X1554	-0.451	0.001
X2279	-0.445	0.002
X1671	-0.427	0.003
X1239	-0.423	0.003
X595	0.419	0.004
X2063	-0.416	0.004
X1258	-0.414	0.004
X632	0.409	0.005
X1295	-0.404	0.005
X529	0.401	0.006
X1331	-0.400	0.006
X1224	-0.399	0.006
X639	0.392	0.007
X716	-0.391	0.007
X758	-0.384	0.009
X1534	-0.383	0.009
X1525	-0.383	0.009
X1056	-0.380	0.009
X1029	0.378	0.010
X2245	0.374	0.011
X938	-0.374	0.011
X393	0.374	0.011
X1260	-0.371	0.012
X1583	-0.369	0.012
X1402	-0.368	0.012
X1432	-0.367	0.013
X1524	-0.365	0.013
X1292	-0.365	0.013
X1400	-0.365	0.013
X697	-0.364	0.014
X1551	0.359	0.015
X1303	-0.359	0.015
X872	0.358	0.015
X825	-0.355	0.016
X1054	-0.353	0.017
X1317	0.352	0.018
X1188	-0.352	0.018
X2026	-0.351	0.018
X1272	-0.351	0.018
X1312	-0.349	0.018
X625	0.349	0.018
X766	0.349	0.019
X1265	-0.348	0.019
X1284	0.348	0.019
X1268	-0.346	0.020
X1314	-0.343	0.021
X1732	0.342	0.021
X1155	-0.342	0.022
X1128	-0.341	0.022
X1297	0.341	0.022
X2048	0.340	0.022
X732	0.340	0.022
X1287	-0.338	0.023
X2143	-0.337	0.024
X1930	0.336	0.024
X1264	-0.336	0.024
X2031	0.335	0.024
X765	0.334	0.025
X1574	-0.333	0.026
X1332	-0.331	0.026
X1283	0.328	0.028
X991	0.328	0.028
X2187	0.328	0.028
X1561	-0.327	0.029
X1357	-0.327	0.029
X2181	-0.326	0.029
X754	-0.326	0.029
X1621	-0.326	0.029
X1313	0.325	0.030
X652	-0.325	0.030
X2105	0.323	0.031
X733	0.322	0.031
X953	0.322	0.031
X1273	0.321	0.032
X740	-0.317	0.035
X1339	-0.316	0.035
X1241	-0.316	0.035
X1237	-0.316	0.035
X1636	-0.316	0.035
X1394	0.313	0.037
X1855	-0.313	0.037
X925	-0.312	0.038
X699	-0.312	0.038
X1792	-0.312	0.038
X1052	-0.311	0.038
X746	-0.311	0.038
X1702	-0.311	0.039
X2182	-0.309	0.040
X1333	0.309	0.040
X1857	-0.308	0.040
X1315	-0.308	0.041
X2103	-0.308	0.041
X1988	0.308	0.041
X624	0.306	0.042
X2020	0.306	0.042
X1730	0.305	0.043
X1361	-0.305	0.043

X1408	-0.304	0.043
X1059	-0.304	0.044
X1110	-0.304	0.044
X1953	0.302	0.045
X653	0.302	0.045
X1410	-0.301	0.046
X680	0.301	0.046
X1508	0.301	0.046
X805	-0.301	0.046
X727	0.300	0.047
X591	0.300	0.047
X1074	-0.299	0.047
X1619	-0.299	0.048
X1966	0.298	0.048
X2157	0.298	0.048
X1189	-0.297	0.049
X2310	0.294	0.051
X2311	0.294	0.052
X1550	0.293	0.052
X2193	-0.293	0.052
X687	-0.293	0.053
X2296	0.293	0.053
X1119	-0.292	0.054
X1564	-0.291	0.054
X533	0.291	0.055
X1010	0.290	0.055
X1200	-0.290	0.055
X386	0.289	0.056
X1262	-0.289	0.057
X879	0.288	0.057
X1343	-0.288	0.057
X1324	-0.288	0.057
X698	-0.287	0.058
X2255	0.287	0.058
X2123	0.286	0.059
X1646	-0.285	0.060
X619	0.285	0.060
X2044	0.285	0.061
X1710	-0.284	0.061
X622	0.283	0.062
X1309	-0.283	0.062
X2331	0.283	0.062
X2119	0.282	0.063
X1170	0.282	0.063

X992	0.282	0.063
X2115	-0.282	0.063
X2042	0.282	0.063
X2276	-0.282	0.063
X482	0.282	0.063
X607	0.282	0.063
X2348	-0.282	0.063
X2350	0.281	0.064
X1286	-0.281	0.064
X1396	-0.280	0.065
X952	0.280	0.065
X2352	-0.279	0.066
X1482	0.279	0.067
X1593	-0.279	0.067
X1296	0.278	0.067
X1610	-0.278	0.068
X1489	-0.277	0.068
X1435	-0.276	0.070
X1066	-0.276	0.070
X1929	0.275	0.071
X2287	0.275	0.071
X1760	-0.273	0.073
X739	-0.271	0.074
X532	0.271	0.075
X2292	0.270	0.076
X657	-0.270	0.077
X1404	-0.269	0.078
X381	0.269	0.078
X1118	-0.268	0.079
X1234	-0.267	0.079
X1656	-0.267	0.079
X1424	-0.267	0.080
X627	0.267	0.080
X939	-0.266	0.081
X1592	-0.266	0.081
X1405	-0.266	0.081
X2019	0.266	0.082
X2275	-0.265	0.082
X954	0.265	0.082
X2318	0.265	0.083
X1773	-0.265	0.083
X994	0.265	0.083
X2012	0.264	0.083
X1557	0.264	0.083

X878	-0.264	0.084
X830	-0.263	0.085
X434	0.263	0.085
X1426	-0.262	0.086
X1892	-0.262	0.086
X1304	-0.262	0.086
X1412	-0.262	0.086
X1785	0.260	0.088
X689	-0.260	0.089
X1289	-0.260	0.089
X951	0.259	0.090
X741	-0.258	0.091
X2269	0.257	0.092
X1614	-0.257	0.093
X2298	-0.257	0.093
X1439	-0.256	0.093
X1597	0.256	0.094
X937	0.256	0.094
X1565	-0.255	0.095
X355	0.255	0.096
X930	-0.254	0.096
X2194	-0.254	0.096
X1664	-0.254	0.097
X1555	0.253	0.098
X1466	0.253	0.098
X1038	0.253	0.098
X255	0.252	0.099
X706	-0.252	0.100
X1762	-0.251	0.101
X986	0.251	0.101
X1377	-0.251	0.101
X1526	-0.250	0.102
X1663	-0.250	0.102
X1420	0.250	0.103
X1068	-0.249	0.104
X1267	-0.249	0.104
X1563	-0.248	0.105
X1649	-0.248	0.106
X692	-0.247	0.106
X1573	-0.247	0.107
X988	0.246	0.108
X2140	-0.245	0.111
X610	0.245	0.111
X1768	-0.245	0.111

X1527	-0.243	0.112
X631	0.243	0.113
X1560	-0.243	0.113
X850	-0.242	0.115
X1321	-0.242	0.115
X1826	-0.241	0.116
X1338	-0.241	0.116
X1513	-0.241	0.116
X1666	-0.241	0.117
X880	-0.241	0.117
X2347	-0.240	0.118
X2071	0.240	0.118
X702	-0.239	0.119
X798	0.239	0.119
X1242	-0.239	0.120
X1887	-0.238	0.121
X1926	0.238	0.121
X1235	-0.238	0.121
X1863	-0.237	0.123
X1570	-0.237	0.123
X1071	0.236	0.125
X1628	-0.236	0.125
X1544	0.236	0.125
X1057	-0.235	0.125
X806	-0.235	0.126
X1261	-0.234	0.127
X2349	-0.234	0.128
X1434	-0.234	0.128
X1774	-0.234	0.128
X705	-0.232	0.131
X1048	-0.231	0.133
X2212	0.231	0.134
X1244	-0.230	0.135
X1051	-0.229	0.136
X1263	-0.229	0.136
X1213	-0.229	0.136
X1580	0.229	0.136
X882	-0.229	0.137
X1006	0.228	0.138
X1718	-0.228	0.139
X2241	0.228	0.139
X1254	-0.228	0.139
X2114	0.228	0.139
X956	0.228	0.139
X2190	-0.227	0.140
X747	-0.227	0.140
X955	0.227	0.141
X2217	-0.227	0.141
X1772	-0.226	0.141
X1685	-0.226	0.142
X1739	0.226	0.142
X1506	0.226	0.143
X1620	0.226	0.143
X1719	0.225	0.144
X2281	-0.225	0.145
X774	0.224	0.146
X1158	-0.224	0.147
X2232	-0.224	0.147
X578	0.224	0.147
X851	0.223	0.147
X2285	-0.223	0.148
X1703	-0.223	0.148
X1198	0.223	0.149
X1756	0.222	0.149
X2032	0.222	0.149
X858	0.222	0.150
X1101	-0.222	0.150
X782	-0.221	0.152
X710	-0.220	0.153
X1747	-0.220	0.153
X717	0.220	0.154
X571	0.220	0.154
X1180	-0.220	0.154
X1487	-0.219	0.155
X1003	0.219	0.156
X633	0.219	0.156
X822	-0.218	0.157
X1819	-0.218	0.157
X983	0.218	0.158
X2188	0.218	0.159
X1062	-0.218	0.159
X725	-0.217	0.159
X1848	-0.217	0.160
X2154	-0.217	0.160
X1000	0.217	0.160
X1204	-0.217	0.160
X1226	-0.217	0.160
X1505	0.216	0.161
X738	-0.216	0.162
X1465	-0.215	0.163
X785	-0.215	0.164
X891	-0.215	0.164
X1086	0.215	0.164
X1190	-0.215	0.165
X1828	-0.214	0.166
X2072	-0.213	0.167
X605	0.213	0.168
X2085	0.212	0.169
X1085	0.212	0.170
X1326	-0.212	0.170
X1982	0.211	0.172
X1202	-0.211	0.172
X1344	-0.211	0.172
X1387	-0.211	0.173
X1207	-0.211	0.173
X1012	0.210	0.174
X1337	-0.210	0.174
X1566	-0.210	0.175
X1334	-0.210	0.175
X1902	0.210	0.175
X701	-0.209	0.176
X1043	-0.209	0.176
X609	0.209	0.177
X917	0.209	0.177
X1927	0.209	0.177
X1316	-0.208	0.178
X1890	0.208	0.179
X815	0.208	0.179
X1849	-0.206	0.182
X1538	-0.206	0.183
X2250	-0.206	0.183
X1665	-0.206	0.184
X1775	-0.205	0.184
X779	-0.205	0.185
X1192	0.205	0.185
X1854	-0.205	0.185
X1777	-0.205	0.186
X886	0.205	0.186
X752	-0.203	0.190
X1576	-0.202	0.191
X1731	-0.202	0.192
X985	0.201	0.195

X1532	-0.201	0.195
X1778	0.201	0.195
X1293	-0.200	0.196
X2045	0.200	0.196
X670	-0.200	0.197
X1063	-0.199	0.198
X1869	0.199	0.198
X1694	-0.199	0.198
X1090	0.199	0.199
X615	0.197	0.203
X2344	-0.197	0.203
X658	0.197	0.205
X1073	-0.196	0.206
X881	0.196	0.207
X722	-0.196	0.207
X1917	0.196	0.207
X281	-0.195	0.208
X1040	0.195	0.209
X626	0.194	0.210
X1359	-0.194	0.211
X1350	-0.194	0.211
X770	0.194	0.212
X2189	-0.194	0.212
X1805	0.193	0.213
X1185	-0.193	0.213
X1418	0.193	0.214
X2317	-0.193	0.214
X2301	0.193	0.214
X1154	-0.192	0.215
X1678	-0.192	0.215
X1345	-0.192	0.216
X638	0.192	0.217
X1582	-0.191	0.219
X673	-0.191	0.220
X1637	-0.190	0.220
X1657	-0.190	0.221
X1375	-0.190	0.221
X876	0.189	0.223
X902	-0.189	0.224
X1599	-0.189	0.224
X1380	0.189	0.225
X1770	-0.189	0.225
X1247	-0.188	0.226
X2304	0.188	0.226
X1925	0.188	0.227
X2239	0.187	0.228
X1042	-0.187	0.229
X726	-0.186	0.230
X1099	0.186	0.230
X1108	0.186	0.231
X593	-0.186	0.231
X1588	-0.186	0.231
X748	-0.186	0.231
X1478	-0.186	0.232
X1302	0.186	0.232
X1438	-0.186	0.232
X899	-0.185	0.233
X1236	-0.185	0.234
X1735	0.184	0.236
X1763	-0.184	0.237
X2204	0.184	0.237
X1654	0.183	0.238
X807	0.183	0.239
X2010	0.183	0.240
X1126	0.182	0.241
X2005	0.181	0.245
X1199	-0.181	0.246
X2314	-0.180	0.246
X885	-0.180	0.247
X987	0.180	0.248
X833	0.179	0.249
X1230	0.179	0.249
X1528	-0.179	0.250
X708	-0.179	0.250
X1611	-0.179	0.251
X654	-0.178	0.252
X1861	-0.178	0.252
X1618	-0.178	0.253
X2351	0.178	0.253
X682	-0.178	0.254
X1277	0.178	0.254
X2325	-0.178	0.254
X648	0.177	0.255
X690	-0.177	0.255
X2280	-0.177	0.255
X545	0.177	0.255
X1393	-0.177	0.256
X620	0.177	0.256
X1299	0.176	0.257
X2073	0.176	0.258
X1809	-0.176	0.258
X1667	-0.175	0.260
X1221	-0.175	0.261
X1109	0.175	0.262
X1616	-0.175	0.262
X1362	-0.174	0.264
X950	0.174	0.265
X866	-0.174	0.265
X1548	0.173	0.267
X907	0.172	0.268
X1205	-0.172	0.269
X831	-0.172	0.270
X1145	-0.172	0.271
X2024	-0.171	0.271
X2268	-0.171	0.271
X2271	0.171	0.272
X1462	0.171	0.273
X1500	-0.171	0.273
X1120	0.170	0.274
X757	0.170	0.276
X1256	0.168	0.280
X1436	-0.168	0.282
X834	-0.167	0.285
X895	0.166	0.286
X1113	-0.166	0.286
X1818	0.166	0.287
X608	0.166	0.287
X1516	-0.166	0.288
X2144	0.166	0.288
X1727	-0.166	0.288
X1609	-0.165	0.289
X890	-0.165	0.291
X1791	-0.165	0.291
X897	0.164	0.292
X2295	-0.164	0.293
X914	0.164	0.294
X405	0.163	0.296
X618	0.163	0.296
X1005	-0.163	0.296
X1064	-0.163	0.297
X1174	0.163	0.297
X1690	-0.163	0.297

X1644	-0.163	0.297
X484	0.163	0.297
X1376	-0.162	0.299
X1039	-0.162	0.300
X672	0.161	0.301
X2264	0.161	0.303
X2081	0.161	0.303
X1084	-0.160	0.304
X936	0.160	0.306
X1453	-0.160	0.307
X2028	0.159	0.308
X1253	-0.158	0.310
X1372	-0.158	0.310
X1369	-0.158	0.313
X918	0.157	0.314
X1577	-0.157	0.315
X2330	-0.157	0.316
X1360	-0.157	0.316
X1716	-0.157	0.316
X768	0.157	0.316
X1433	-0.156	0.317
X1821	-0.156	0.318
X1130	0.155	0.319
X422	0.155	0.321
X1807	-0.155	0.323
X296	0.154	0.323
X2082	0.154	0.323
X1429	-0.153	0.326
X1121	0.153	0.327
X1197	-0.152	0.331
X1329	-0.152	0.331
X1575	-0.152	0.332
X761	-0.151	0.333
X1562	-0.151	0.333
X1423	0.151	0.333
X1641	-0.151	0.333
X2152	0.151	0.334
X1419	0.151	0.335
X1959	0.151	0.336
X1032	0.150	0.336
X1368	0.150	0.336
X649	-0.150	0.337
X2303	-0.150	0.337
X1401	-0.150	0.337
X957	0.150	0.337
X1802	-0.150	0.338
X432	0.149	0.339
X1585	-0.149	0.339
X778	-0.149	0.339
X1411	-0.149	0.340
X628	0.149	0.341
X2253	0.149	0.341
X999	0.148	0.343
X1708	0.148	0.343
X1431	-0.148	0.343
X2237	-0.148	0.343
X1787	-0.147	0.348
X1125	0.146	0.351
X1786	-0.146	0.352
X903	0.146	0.352
X2308	0.145	0.353
X1374	-0.145	0.354
X1755	0.145	0.354
X2104	-0.145	0.355
X2174	-0.145	0.355
X1201	-0.144	0.356
X1906	0.144	0.356
X1008	-0.144	0.358
X1990	0.144	0.359
X642	-0.143	0.360
X1050	-0.142	0.364
X1355	-0.142	0.365
X1030	0.142	0.365
X2041	-0.142	0.366
X824	-0.141	0.366
X1680	-0.141	0.368
X1746	0.141	0.368
X2098	0.140	0.370
X1255	-0.140	0.371
X606	0.140	0.371
X1353	0.140	0.372
X2315	-0.140	0.372
X1501	-0.139	0.374
X1713	0.139	0.375
X744	-0.139	0.375
X1650	-0.139	0.376
X1464	0.139	0.376
X1617	-0.138	0.377
X1962	-0.138	0.378
X685	-0.138	0.379
X1479	-0.137	0.380
X1813	-0.137	0.381
X1162	-0.137	0.382
X1106	0.137	0.383
X1875	0.137	0.383
X1645	-0.137	0.383
X2049	0.136	0.384
X1034	0.136	0.384
X2231	0.136	0.385
X1218	-0.136	0.386
X961	0.135	0.387
X958	0.135	0.387
X1146	-0.135	0.387
X1228	-0.135	0.388
X617	0.135	0.388
X1311	-0.135	0.389
X2106	0.135	0.390
X894	0.135	0.390
X1789	-0.135	0.390
X1542	-0.135	0.391
X1123	0.134	0.393
X2141	-0.134	0.393
X2218	-0.133	0.395
X1450	-0.133	0.395
X1076	0.133	0.396
X1552	0.133	0.396
X1356	-0.132	0.398
X855	0.132	0.398
X1602	-0.132	0.398
X840	0.132	0.399
X921	0.132	0.399
X2210	-0.132	0.399
X1195	-0.132	0.399
X525	-0.132	0.401
X1749	0.131	0.402
X1225	-0.131	0.404
X2036	0.130	0.406
X1728	0.130	0.406
X2087	-0.130	0.406
X1386	-0.130	0.407
X2109	-0.130	0.407
X1721	-0.129	0.409

X1173	-0.129	0.410
X788	-0.129	0.411
X1015	0.129	0.412
X707	-0.129	0.412
X1459	0.128	0.414
X2095	0.128	0.414
X1812	-0.128	0.414
X1836	-0.128	0.414
X1622	-0.128	0.414
X1652	-0.128	0.414
X1127	0.128	0.415
X1837	-0.127	0.416
X1648	-0.127	0.417
X1307	0.127	0.417
X1553	-0.127	0.417
X1795	0.127	0.418
X266	-0.127	0.418
X1194	-0.127	0.418
X2240	0.127	0.419
X1078	-0.127	0.419
X970	0.126	0.420
X1709	-0.126	0.420
X2023	-0.126	0.421
X2179	-0.126	0.421
X2155	-0.126	0.423
X1067	-0.126	0.423
X2326	-0.126	0.423
X1167	0.126	0.423
X1416	0.125	0.424
X1944	0.125	0.425
X1767	-0.125	0.426
X1219	-0.125	0.427
X1148	0.125	0.427
X909	0.124	0.428
X1163	-0.124	0.428
X1330	-0.124	0.429
X1613	-0.124	0.429
X977	0.124	0.431
X1817	0.124	0.431
X681	0.123	0.434
X1227	-0.123	0.434
X387	0.123	0.434
X667	0.122	0.436
X1540	-0.122	0.437
X2116	-0.122	0.438
X1724	-0.122	0.438
X1676	0.122	0.438
X734	0.121	0.440
X594	0.121	0.441
X1251	-0.121	0.441
X839	0.121	0.442
X721	-0.121	0.442
X1660	-0.121	0.442
X2130	0.120	0.444
X821	-0.120	0.444
X808	-0.120	0.445
X1515	-0.120	0.445
X1417	-0.120	0.446
X621	0.120	0.446
X2086	0.119	0.448
X995	0.119	0.448
X1021	-0.119	0.449
X644	-0.119	0.449
X1725	0.119	0.450
X1495	-0.118	0.451
X2328	-0.118	0.451
X1662	-0.118	0.452
X2333	0.118	0.453
X453	0.118	0.454
X1392	-0.118	0.454
X669	-0.118	0.454
X1862	-0.117	0.455
X1406	-0.117	0.457
X396	0.117	0.458
X1829	-0.117	0.458
X1233	-0.116	0.460
X802	-0.116	0.461
X1488	-0.116	0.462
X1203	0.116	0.462
X998	0.116	0.462
X2184	0.115	0.463
X459	0.115	0.466
X2138	-0.114	0.466
X1391	0.114	0.466
X1864	0.114	0.466
X1695	-0.114	0.467
X311	0.114	0.467
X1191	-0.114	0.467
X2294	-0.114	0.467
X2313	-0.114	0.467
X1252	0.114	0.469
X1832	0.114	0.469
X2198	0.113	0.471
X892	-0.113	0.472
X1347	-0.113	0.472
X1594	-0.113	0.472
X596	-0.113	0.472
X908	0.112	0.474
X2108	0.112	0.474
X1936	0.112	0.474
X1060	0.112	0.475
X1699	0.112	0.477
X884	-0.112	0.477
X1245	-0.112	0.477
X1915	0.111	0.478
X1684	-0.111	0.479
X1147	0.111	0.479
X2283	0.111	0.480
X1468	-0.111	0.480
X906	0.111	0.480
X826	-0.111	0.481
X2332	0.110	0.483
X863	0.110	0.483
X1133	0.110	0.485
X2353	0.110	0.486
X1275	0.110	0.486
X1989	-0.109	0.486
X781	-0.109	0.487
X1291	-0.109	0.487
X1661	-0.109	0.488
X1546	-0.109	0.488
X2159	0.109	0.490
X1631	-0.108	0.491
X1122	0.108	0.491
X1876	0.108	0.491
X2341	-0.108	0.492
X601	0.108	0.492
X2177	-0.108	0.493
X715	-0.108	0.493
X893	-0.107	0.496
X718	-0.107	0.496
X712	0.107	0.498

X1342	-0.107	0.498
X1103	-0.106	0.499
X616	0.106	0.500
X375	0.106	0.501
X584	-0.106	0.502
X2169	0.106	0.502
X1117	-0.106	0.502
X845	0.105	0.502
X1741	0.105	0.503
X773	0.105	0.505
X1065	-0.105	0.505
X1399	0.105	0.506
X2244	0.104	0.506
X587	-0.104	0.507
X1521	0.104	0.508
X742	-0.104	0.509
X799	-0.104	0.510
X1124	0.104	0.510
X1901	0.103	0.511
X2088	0.103	0.514
X1510	0.102	0.515
X2335	0.102	0.516
X1222	-0.102	0.517
X1094	-0.101	0.521
X978	0.101	0.522
X1514	-0.101	0.522
X1390	0.101	0.522
X1696	0.101	0.522
X1075	0.100	0.523
X2128	0.100	0.524
X963	-0.100	0.525
X965	-0.100	0.525
X1161	-0.100	0.526
X873	-0.100	0.526
X1833	0.100	0.527
X1874	0.100	0.527
X1504	-0.099	0.528
X1141	0.099	0.528
X1373	0.099	0.529
X1700	-0.099	0.529
X1427	-0.099	0.530
X1835	-0.099	0.531
X1098	0.098	0.532
X794	0.098	0.532
X2007	0.098	0.532
X2238	0.098	0.532
X1742	-0.098	0.532
X2091	0.098	0.533
X1159	-0.098	0.533
X2168	-0.098	0.534
X836	-0.098	0.534
X1822	0.098	0.534
X1298	-0.098	0.535
X1220	-0.097	0.536
X2209	0.097	0.537
X820	-0.097	0.538
X2180	-0.097	0.538
X656	0.097	0.539
X2096	0.097	0.539
X1381	0.096	0.540
X928	0.096	0.540
X1729	-0.096	0.543
X637	0.096	0.543
X527	0.096	0.543
X1451	-0.096	0.543
X1751	-0.096	0.544
X2277	-0.095	0.545
X1748	0.095	0.545
X1831	-0.095	0.547
X735	0.095	0.548
X2256	-0.094	0.549
X1079	-0.094	0.549
X1186	-0.094	0.550
X2278	0.094	0.550
X1856	-0.093	0.553
X743	0.093	0.553
X911	-0.093	0.554
X1469	-0.093	0.554
X1367	-0.093	0.555
X1320	-0.093	0.555
X1698	-0.093	0.556
X1781	0.093	0.556
X1740	0.093	0.557
X1677	-0.093	0.557
X645	0.092	0.557
X1140	0.092	0.557
X2097	0.092	0.557
X811	0.092	0.558
X2171	0.092	0.558
X501	0.092	0.558
X2267	-0.092	0.559
X1151	0.092	0.559
X2125	-0.092	0.559
X379	0.092	0.560
X1846	0.092	0.560
X1651	-0.092	0.560
X1091	0.092	0.561
X1246	-0.092	0.561
X1590	-0.091	0.562
X2185	0.091	0.563
X1053	-0.091	0.563
X1409	-0.091	0.563
X1627	-0.090	0.566
X1674	0.090	0.567
X1278	-0.090	0.569
X1274	0.089	0.571
X1486	0.089	0.572
X1383	-0.089	0.572
X1045	-0.089	0.573
X753	0.089	0.574
X1968	-0.089	0.574
X1572	-0.088	0.575
X242	0.088	0.575
X643	0.088	0.575
X1752	0.088	0.576
X1496	-0.087	0.579
X1586	-0.087	0.579
X655	-0.087	0.580
X324	-0.087	0.580
X1788	-0.087	0.580
X1547	-0.087	0.581
X719	-0.087	0.582
X1290	-0.087	0.582
X804	-0.086	0.583
X2050	-0.086	0.583
X1471	-0.086	0.583
X916	0.086	0.585
X943	0.086	0.585
X1964	0.086	0.585
X585	0.086	0.586
X912	0.085	0.589
X869	0.085	0.589

X1037	0.085	0.590
X634	-0.085	0.591
X1413	-0.085	0.591
X1279	-0.084	0.592
X829	0.084	0.594
X1519	0.084	0.595
X665	-0.083	0.597
X603	0.083	0.597
X786	-0.083	0.597
X1414	0.083	0.598
X933	0.083	0.599
X1825	-0.083	0.599
X2054	-0.083	0.600
X1717	0.082	0.601
X2124	-0.082	0.602
X659	-0.082	0.602
X1900	0.082	0.602
X2242	-0.082	0.603
X861	0.082	0.603
X795	-0.082	0.605
X1149	-0.082	0.605
X1160	0.082	0.605
X558	-0.081	0.605
X1026	-0.081	0.606
X1397	-0.081	0.606
X1535	-0.081	0.607
X1531	-0.081	0.608
X1608	-0.081	0.609
X2021	-0.081	0.609
X817	0.080	0.610
X2254	0.080	0.610
X1830	0.080	0.611
X1270	-0.080	0.611
X1215	-0.080	0.611
X2043	0.080	0.614
X745	-0.079	0.615
X2053	0.079	0.615
X901	-0.079	0.617
X1536	-0.079	0.618
X1046	-0.079	0.618
X750	0.078	0.619
X1948	0.078	0.621
X724	-0.078	0.622
X1259	0.078	0.622
X2235	0.077	0.623
X1232	-0.077	0.624
X1134	0.077	0.625
X1257	-0.077	0.625
X1047	0.077	0.626
X491	0.076	0.629
X694	-0.076	0.629
X322	-0.076	0.630
X1607	0.076	0.630
X972	0.076	0.631
X2214	0.076	0.631
X1758	-0.075	0.632
X1736	0.075	0.632
X1385	-0.075	0.633
X842	-0.075	0.633
X1675	-0.075	0.634
X860	-0.075	0.635
X1483	-0.075	0.636
X1679	-0.074	0.639
X2120	-0.074	0.639
X1541	-0.074	0.640
X1757	-0.073	0.641
X1061	-0.073	0.642
X286	0.073	0.642
X1697	-0.073	0.642
X1689	-0.073	0.643
X1640	-0.073	0.644
X2037	0.073	0.644
X1726	-0.073	0.644
X989	0.073	0.645
X769	-0.072	0.646
X865	-0.072	0.647
X1058	0.072	0.648
X2203	-0.072	0.649
X1092	-0.072	0.649
X1182	0.071	0.651
X664	0.071	0.651
X589	-0.071	0.651
X1745	0.071	0.651
X1181	0.071	0.652
X1288	-0.071	0.653
X1480	-0.071	0.653
X1102	0.071	0.654
X2222	0.071	0.655
X206	-0.071	0.655
X1759	-0.070	0.655
X2101	-0.070	0.655
X1211	-0.070	0.655
X661	-0.070	0.656
X471	0.070	0.658
X2016	-0.070	0.659
X1881	0.069	0.660
X1511	0.069	0.660
X1587	0.069	0.661
X1013	0.069	0.663
X1169	0.069	0.663
X2221	-0.069	0.664
X1629	-0.068	0.665
X1152	0.068	0.666
X728	0.068	0.668
X1269	-0.068	0.668
X1137	-0.068	0.668
X310	-0.068	0.668
X1815	0.067	0.670
X1112	-0.067	0.671
X1081	0.067	0.671
X2156	0.067	0.673
X1351	-0.066	0.674
X1737	-0.066	0.674
X574	0.066	0.675
X874	0.066	0.676
X974	-0.066	0.677
X777	0.066	0.677
X1509	0.066	0.678
X1771	-0.065	0.679
X755	-0.064	0.685
X2164	-0.064	0.686
X848	0.063	0.688
X2215	-0.063	0.689
X2201	0.063	0.691
X599	-0.063	0.691
X969	-0.063	0.692
X997	-0.062	0.693
X713	-0.061	0.697
X1939	0.061	0.698
X810	0.061	0.698
X1971	-0.061	0.699
X996	0.061	0.700

X1623	-0.061	0.701
X2118	-0.061	0.701
X1543	0.060	0.702
X867	0.060	0.702
X1794	0.060	0.703
X272	0.060	0.704
X1490	-0.060	0.705
X1457	-0.060	0.706
X1715	-0.059	0.707
X1579	0.059	0.707
X1897	-0.059	0.709
X2202	0.059	0.710
X1176	-0.058	0.712
X397	-0.058	0.712
X480	0.058	0.713
X1903	-0.058	0.713
X1041	0.058	0.714
X910	0.058	0.714
X1156	-0.058	0.714
X818	0.058	0.715
X1705	0.058	0.716
X1584	-0.057	0.717
X1282	0.057	0.718
X1379	-0.057	0.718
X1135	0.057	0.720
X2196	-0.056	0.721
X305	0.056	0.722
X1965	0.056	0.722
X371	0.056	0.722
X1129	-0.056	0.723
X813	0.056	0.723
X1157	0.056	0.724
X590	0.055	0.726
X2022	-0.055	0.726
X2040	0.055	0.727
X671	-0.055	0.728
X2339	-0.055	0.728
X2307	-0.055	0.729
X1093	0.054	0.731
X790	0.054	0.731
X1635	0.054	0.732
X966	-0.054	0.732
X1879	0.053	0.736
X675	-0.053	0.737
X1503	0.053	0.738
X1518	0.053	0.739
X1766	-0.053	0.739
X1281	-0.053	0.740
X1407	0.052	0.740
X887	0.052	0.741
X809	-0.052	0.743
X1308	-0.052	0.743
X841	0.052	0.743
X1783	-0.052	0.744
X2293	-0.052	0.744
X1801	-0.051	0.745
X2199	-0.051	0.746
X2013	0.051	0.747
X2226	0.050	0.754
X1733	0.049	0.754
X1070	-0.049	0.755
X875	0.049	0.755
X635	0.049	0.757
X1810	-0.049	0.758
X1765	0.049	0.759
X827	-0.048	0.760
X1941	-0.048	0.760
X668	-0.048	0.761
X1422	-0.048	0.762
X1481	0.048	0.763
X662	0.047	0.764
X946	0.047	0.765
X2111	0.047	0.765
X2146	0.047	0.766
X2297	-0.047	0.766
X1779	0.047	0.767
X935	0.046	0.769
X1138	-0.046	0.769
X2273	0.046	0.769
X1556	0.045	0.774
X2014	0.045	0.775
X767	-0.045	0.776
X1089	-0.045	0.776
X1744	-0.045	0.776
X1738	-0.045	0.776
X412	-0.045	0.777
X378	0.044	0.778
X1033	0.044	0.780
X1077	-0.044	0.780
X688	-0.044	0.780
X1658	-0.044	0.782
X731	0.044	0.783
X1780	-0.043	0.785
X1707	-0.043	0.785
X792	0.043	0.786
X1882	-0.043	0.786
X1023	0.043	0.786
X1398	0.042	0.788
X1706	-0.042	0.788
X1659	-0.042	0.789
X904	0.042	0.790
X789	-0.042	0.792
X1981	0.041	0.796
X2006	-0.041	0.797
X2099	0.041	0.797
X1229	0.040	0.798
X793	-0.040	0.798
X1216	-0.040	0.801
X944	0.040	0.803
X1430	0.039	0.803
X1642	-0.039	0.805
X684	-0.039	0.805
X1492	0.039	0.805
X1036	-0.039	0.806
X604	0.038	0.810
X1624	-0.038	0.811
X576	0.038	0.812
X947	-0.038	0.812
X1512	-0.037	0.813
X1522	0.037	0.814
X973	0.037	0.816
X2136	0.037	0.816
X676	0.036	0.817
X1581	-0.036	0.819
X677	-0.036	0.819
X1769	0.036	0.820
X1210	0.036	0.821
X666	-0.036	0.821
X2337	0.036	0.821
X2345	0.036	0.821
X1714	-0.036	0.822
X1083	0.035	0.822

X2147	0.035	0.823
X771	0.035	0.823
X1600	0.035	0.824
X1183	-0.035	0.824
X1606	0.035	0.825
X403	0.035	0.826
X400	0.035	0.826
X857	-0.035	0.827
X1165	-0.034	0.827
X1212	0.034	0.829
X828	-0.034	0.829
X1463	0.034	0.832
X1734	-0.033	0.832
X222	-0.033	0.833
X2213	0.033	0.833
X1997	0.033	0.836
X1643	-0.032	0.838
X1598	-0.032	0.839
X1743	-0.032	0.840
X812	-0.032	0.840
X2343	0.032	0.840
X1816	-0.032	0.840
X814	0.032	0.841
X791	-0.032	0.842
X1806	-0.031	0.843
X2274	-0.031	0.844
X1491	-0.031	0.844
X1440	-0.031	0.845
X1808	0.031	0.845
X783	-0.031	0.846
X926	0.030	0.847
X1007	0.030	0.849
X1958	0.030	0.849
X2137	0.030	0.849
X184	0.030	0.850
X1688	0.030	0.852
X2151	0.030	0.852
X1018	-0.029	0.853
X1104	0.029	0.856
X2216	-0.028	0.858
X1341	-0.028	0.858
X1111	-0.028	0.858
X1537	-0.028	0.858
X1595	0.028	0.861
X915	-0.028	0.862
X2284	-0.027	0.863
X1485	-0.027	0.863
X1639	0.027	0.863
X1153	-0.027	0.865
X686	-0.027	0.865
X1470	-0.027	0.865
X1022	0.027	0.866
X1171	-0.027	0.866
X1150	0.027	0.866
X2354	-0.027	0.866
X896	0.026	0.868
X1088	0.026	0.870
X1507	0.026	0.872
X816	0.026	0.872
X2070	-0.025	0.872
X1442	0.025	0.874
X1208	0.025	0.874
X1811	-0.025	0.875
X1352	-0.024	0.877
X1476	0.024	0.877
X1940	0.024	0.878
X636	-0.024	0.878
X1223	0.024	0.879
X1184	-0.024	0.879
X1474	0.024	0.880
X678	0.024	0.881
X2299	0.023	0.882
X1069	-0.023	0.883
X1028	0.023	0.883
X2102	-0.023	0.885
X1782	-0.023	0.885
X1589	-0.023	0.886
X2126	0.022	0.887
X800	-0.022	0.888
X1668	-0.022	0.889
X870	-0.022	0.889
X1784	-0.022	0.890
X2236	0.022	0.890
X1530	0.022	0.890
X1087	0.022	0.891
X2211	-0.022	0.891
X971	0.021	0.893
X803	-0.021	0.894
X990	0.021	0.894
X1686	-0.021	0.896
X993	0.020	0.899
X1425	-0.020	0.899
X598	-0.020	0.900
X1704	-0.020	0.900
X1131	0.020	0.900
X1701	-0.019	0.902
X1761	0.019	0.902
X945	-0.019	0.903
X1669	-0.019	0.904
X948	0.019	0.905
X679	0.019	0.905
X640	-0.019	0.905
X1016	0.019	0.905
X942	-0.019	0.905
X2172	-0.019	0.906
X868	-0.018	0.908
X1499	-0.018	0.908
X709	0.018	0.909
X646	-0.018	0.909
X1549	0.018	0.910
X898	-0.018	0.912
X1193	-0.018	0.912
X1865	0.018	0.912
X1692	0.017	0.912
X2246	0.017	0.912
X629	-0.017	0.913
X976	0.017	0.913
X1166	-0.017	0.913
X1294	0.017	0.913
X1001	0.017	0.913
X2025	-0.017	0.914
X1754	-0.017	0.915
X580	-0.017	0.915
X1354	0.017	0.916
X1172	0.017	0.916
X1973	-0.016	0.917
X1523	0.016	0.918
X1545	-0.016	0.918
X1456	-0.016	0.921
X1612	-0.015	0.922
X905	0.015	0.922
X2336	-0.015	0.923

X871	0.015	0.924
X849	-0.015	0.924
X900	0.015	0.925
X1691	0.015	0.926
X1132	0.015	0.926
X934	0.015	0.926
X1720	0.015	0.927
X1823	0.015	0.927
X389	0.014	0.927
X1753	-0.014	0.927
X1963	0.014	0.929
X913	-0.014	0.930
X1803	-0.014	0.930
X852	-0.014	0.931
X2219	0.014	0.931
X775	-0.013	0.932
X1520	-0.013	0.932
X1493	0.013	0.932
X2033	0.013	0.935
X1838	0.013	0.936
X660	0.012	0.937
X823	0.012	0.938
X1014	-0.012	0.938
X630	-0.012	0.939
X1604	0.012	0.939
X1473	0.012	0.940
X1009	-0.012	0.940
X2135	0.012	0.941
X1723	0.012	0.941
X663	-0.011	0.943
X1638	-0.011	0.944
X1494	-0.011	0.944
X1972	0.011	0.944
X1421	-0.011	0.946
X602	-0.011	0.946
X763	-0.010	0.948
X1017	-0.010	0.948
X1318	-0.010	0.949
X1164	-0.010	0.950
X797	-0.010	0.950
X1095	-0.010	0.951
X853	0.010	0.951
X1115	0.010	0.952
X772	0.010	0.952
X1633	0.009	0.952
X1072	0.009	0.953
X1116	0.009	0.954
X1175	-0.009	0.955
X2127	0.009	0.956
X1790	0.008	0.957
X229	0.008	0.961
X2148	-0.008	0.961
X1428	0.008	0.961
X1168	-0.008	0.962
X1049	0.007	0.962
X1187	0.007	0.963
X1196	-0.007	0.964
X2233	-0.007	0.965
X2142	0.007	0.967
X1814	-0.006	0.967
X1605	-0.006	0.968
X714	-0.006	0.970
X931	-0.006	0.971
X2230	0.006	0.971
X1687	-0.006	0.972
X597	0.006	0.972
X1139	0.006	0.972
X1305	-0.005	0.973
X968	0.005	0.974
X844	-0.005	0.974
X1591	-0.005	0.975
X1371	-0.005	0.976
X846	-0.005	0.976
X949	0.005	0.976
X1800	0.005	0.977
X1693	-0.004	0.977
X1950	0.004	0.978
X1107	0.004	0.979
X1615	-0.003	0.983
X2161	0.003	0.983
X641	0.003	0.984
X1415	-0.003	0.984
X2338	-0.003	0.986
X1363	0.002	0.988
X1558	0.002	0.988
X819	-0.002	0.988
X1942	0.002	0.988
X1454	0.001	0.994
X1238	-0.001	0.994
X1517	-0.001	0.996
X1448	0.000	0.998
X1601	0.000	0.999
X1019	0.000	0.999
X1323	0.000	1.000
X1271	0.000	1.000

Appendix 2

T6 partial correlation results for 2DGE spots with PiB PET DVR. Spots ranked in order of significance based on *p* value. Results highlighted in red are statistically significant ($p<0.05$).

Spot ID	Correlation coefficient	P-value
X558	0.524	0.000
X527	0.494	0.000
X1699	-0.461	0.001
X842	-0.454	0.001
X808	-0.445	0.001
X2063	-0.444	0.001
X1309	-0.422	0.003
X2267	0.383	0.007
X1648	-0.383	0.007
X831	-0.369	0.010
X1054	-0.363	0.012
X2177	0.360	0.012
X1245	-0.360	0.012
X1833	0.356	0.014
X1787	0.353	0.014
X869	-0.351	0.015
X2209	0.348	0.016
X815	0.342	0.018
X875	-0.339	0.019
X2344	-0.335	0.021
X2345	-0.332	0.022
X797	-0.332	0.022
X1770	-0.331	0.023
X1660	-0.330	0.024
X1527	0.327	0.025
X822	-0.324	0.027
X1267	-0.322	0.027
X1941	-0.318	0.029
X1694	-0.314	0.032
X1406	0.314	0.032
X2271	0.312	0.033
X802	-0.312	0.033
X1394	0.311	0.034
X949	0.311	0.034
X1197	-0.311	0.034
X1544	-0.310	0.035
X1917	0.310	0.035
X1334	-0.309	0.035
X1619	-0.306	0.038
X1695	-0.303	0.039
X1409	-0.303	0.039
X1763	-0.302	0.040
X1298	0.300	0.041
X1257	-0.300	0.042
X819	0.298	0.043
X1261	0.298	0.043
X255	0.297	0.044
X1615	0.294	0.046
X1556	-0.294	0.046
X1365	-0.293	0.047
X1015	-0.293	0.047
X791	-0.293	0.047
X1696	0.291	0.049
X1495	-0.290	0.050
X1555	-0.289	0.050
X1665	-0.289	0.051
X1051	-0.288	0.051
X716	-0.285	0.054
X2348	-0.285	0.054
X829	-0.285	0.054
X2212	0.284	0.055
X1661	-0.283	0.056
X817	0.281	0.058
X1528	0.280	0.059
X890	0.280	0.059
X2264	0.279	0.059
X1165	-0.279	0.059
X1792	-0.278	0.061
X761	0.277	0.061
X1966	0.277	0.062
X1062	-0.276	0.063
X1864	-0.275	0.064
X2214	0.274	0.065
X1343	-0.274	0.065
X1790	0.273	0.066
X830	-0.273	0.066
X1607	-0.272	0.067
X2308	0.271	0.069
X948	0.270	0.069
X355	0.270	0.070
X717	-0.269	0.071
X2141	-0.268	0.072
X1408	-0.267	0.072
X1202	-0.264	0.076
X1253	-0.264	0.076
X848	-0.264	0.076
X781	-0.264	0.077
X785	-0.263	0.077
X1421	0.263	0.078
X2246	-0.262	0.078
X1631	0.260	0.081
X1402	-0.259	0.083
X1642	-0.255	0.087
X1767	-0.255	0.087
X1940	0.254	0.088
X747	-0.254	0.089
X1225	-0.254	0.089
X902	-0.254	0.089
X1608	0.253	0.090
X2285	-0.252	0.092
X1018	-0.252	0.092
X1014	-0.251	0.093
X1646	-0.250	0.094
X1400	-0.250	0.095
X1342	-0.249	0.095
X480	0.249	0.096
X758	-0.248	0.096
X1482	-0.248	0.097
X1710	0.246	0.099
X1589	-0.245	0.101

X1224	0.244	0.102
X874	-0.244	0.103
X1418	0.244	0.103
X793	-0.243	0.104
X1846	-0.243	0.104
X1769	-0.242	0.105
X576	0.242	0.106
X1875	-0.242	0.106
X1318	-0.242	0.106
X935	0.242	0.107
X701	-0.241	0.107
X533	-0.241	0.107
X2187	0.240	0.109
X951	0.240	0.109
X2213	0.240	0.109
X893	-0.240	0.109
X1721	-0.240	0.110
X742	0.240	0.110
X783	-0.239	0.110
X754	-0.239	0.111
X1925	0.239	0.111
X1017	-0.238	0.112
X1601	0.238	0.113
X2114	0.237	0.113
X812	0.236	0.116
X722	-0.235	0.117
X1067	-0.235	0.117
X825	-0.235	0.117
X1666	-0.235	0.118
X1182	-0.234	0.118
X1356	-0.233	0.121
X1295	-0.231	0.124
X1396	-0.231	0.124
X689	-0.231	0.124
X811	0.230	0.126
X1310	-0.230	0.126
X1199	-0.229	0.127
X698	-0.229	0.128
X719	-0.227	0.130
X434	0.227	0.130
X1810	-0.227	0.131
X1391	-0.226	0.132
X1359	-0.226	0.133
X1193	-0.225	0.134
X1690	-0.225	0.135
X1545	0.225	0.135
X2255	-0.225	0.135
X1649	-0.223	0.139
X870	-0.223	0.139
X1173	-0.222	0.140
X1101	0.222	0.140
X491	0.222	0.141
X735	0.221	0.141
X955	0.221	0.141
X1713	0.221	0.142
X1760	0.221	0.142
X1069	-0.220	0.143
X1579	0.220	0.144
X1520	-0.219	0.146
X1222	-0.218	0.147
X757	-0.217	0.150
X2137	-0.215	0.153
X2025	-0.215	0.153
X1788	0.215	0.154
X2161	-0.215	0.154
X1463	0.214	0.156
X699	-0.214	0.156
X2277	-0.214	0.156
X1641	0.214	0.156
X1610	0.213	0.158
X1541	-0.212	0.160
X1075	-0.211	0.162
X1507	0.211	0.162
X1061	-0.210	0.163
X1747	-0.210	0.163
X709	-0.210	0.163
X1232	-0.210	0.164
X790	-0.210	0.165
X322	0.209	0.165
X1404	-0.208	0.168
X1324	-0.206	0.172
X834	0.205	0.174
X1606	-0.205	0.174
X1855	-0.205	0.175
X1200	-0.205	0.175
X673	-0.205	0.176
X850	-0.204	0.177
X1008	0.204	0.177
X891	0.204	0.177
X884	0.203	0.179
X2181	-0.203	0.180
X1068	-0.203	0.180
X1973	0.202	0.181
X1585	0.202	0.182
X2037	0.202	0.182
X1742	-0.202	0.182
X618	-0.201	0.183
X777	-0.201	0.183
X2236	-0.201	0.184
X1926	0.201	0.184
X2217	-0.201	0.184
X1663	-0.201	0.185
X656	-0.200	0.186
X672	-0.200	0.187
X1429	0.199	0.187
X482	0.199	0.188
X1453	0.199	0.189
X2143	-0.199	0.189
X2188	0.199	0.189
X644	-0.198	0.190
X882	-0.198	0.190
X1262	-0.198	0.191
X2036	0.197	0.192
X1474	0.197	0.193
X1637	-0.197	0.194
X1263	-0.196	0.196
X1398	-0.196	0.196
X1338	0.195	0.197
X956	0.195	0.198
X688	-0.195	0.198
X1740	-0.194	0.201
X1715	0.193	0.202
X1128	0.193	0.204
X2006	0.192	0.205
X1329	-0.192	0.205
X1375	-0.192	0.206
X1244	-0.191	0.208
X1013	-0.191	0.208
X1496	0.190	0.209
X818	0.190	0.209
X1252	0.189	0.211
X953	0.189	0.211

X412	0.189	0.213
X1761	-0.188	0.214
X1234	-0.188	0.215
X2124	0.187	0.217
X828	-0.187	0.218
X1815	-0.187	0.218
X1605	0.187	0.218
X912	0.187	0.218
X1604	0.187	0.218
X296	-0.186	0.219
X1573	-0.186	0.220
X403	-0.186	0.220
X1755	0.186	0.221
X1684	0.185	0.222
X1550	-0.185	0.222
X898	-0.185	0.223
X1417	-0.185	0.224
X986	0.184	0.224
X2154	0.184	0.225
X484	0.183	0.227
X1486	0.183	0.228
X799	-0.183	0.228
X652	-0.182	0.229
X2332	0.181	0.233
X1828	-0.181	0.234
X2157	0.180	0.235
X206	0.180	0.236
X806	-0.180	0.236
X1854	-0.180	0.236
X1219	-0.180	0.237
X2125	0.179	0.238
X957	0.179	0.239
X899	-0.179	0.239
X1113	-0.178	0.242
X1094	-0.178	0.242
X1320	-0.178	0.242
X1617	-0.177	0.244
X1353	-0.177	0.244
X1040	0.177	0.245
X1513	0.176	0.245
X732	0.176	0.246
X710	-0.176	0.246
X868	0.176	0.247
X2168	-0.176	0.247

X1056	-0.176	0.248
X1289	0.175	0.249
X2352	-0.175	0.249
X952	0.175	0.249
X844	0.175	0.250
X788	0.175	0.250
X807	-0.175	0.250
X2310	0.174	0.251
X1137	-0.174	0.252
X907	-0.174	0.252
X1953	0.174	0.252
X748	-0.174	0.253
X813	0.174	0.253
X1493	-0.173	0.255
X823	0.173	0.256
X1237	-0.172	0.258
X2218	-0.172	0.258
X658	-0.172	0.259
X1508	0.171	0.262
X1574	0.171	0.262
X1399	0.170	0.264
X792	0.170	0.264
X1242	-0.170	0.265
X1233	-0.170	0.265
X1612	-0.169	0.267
X1600	0.169	0.268
X1145	-0.168	0.269
X734	0.168	0.270
X1370	-0.168	0.270
X1609	0.168	0.271
X1583	0.167	0.271
X1337	-0.167	0.271
X2201	-0.167	0.272
X1241	0.167	0.274
X671	-0.166	0.274
X779	-0.166	0.275
X1693	-0.166	0.275
X1156	-0.166	0.276
X1633	-0.166	0.276
X1772	0.166	0.277
X1519	-0.165	0.278
X1771	-0.165	0.278
X820	-0.165	0.279
X728	0.165	0.279

X616	-0.164	0.280
X1768	-0.164	0.280
X2204	0.164	0.281
X1726	-0.164	0.281
X2108	0.164	0.282
X1038	0.164	0.283
X1801	0.163	0.283
X1662	-0.163	0.284
X2202	0.163	0.285
X1292	-0.163	0.285
X1168	-0.163	0.285
X1112	0.162	0.286
X1230	0.162	0.287
X2333	0.161	0.289
X886	-0.161	0.289
X1021	0.161	0.290
X1638	-0.161	0.292
X1001	-0.160	0.292
X2328	0.160	0.294
X585	0.160	0.294
X2099	0.160	0.294
X1215	-0.160	0.294
X1258	-0.159	0.296
X1354	-0.159	0.296
X1773	-0.159	0.296
X1959	0.159	0.296
X1084	0.159	0.298
X1119	-0.158	0.300
X2331	-0.158	0.300
X222	0.158	0.300
X1194	-0.158	0.300
X1536	0.158	0.301
X1490	-0.158	0.301
X816	-0.158	0.301
X794	0.157	0.302
X663	0.157	0.302
X678	-0.157	0.304
X1563	-0.157	0.304
X1149	-0.157	0.304
X885	0.157	0.304
X389	0.156	0.305
X827	0.156	0.305
X1065	-0.156	0.305
X910	0.156	0.306

X2189	-0.156	0.306
X2102	0.156	0.307
X696	0.156	0.307
X1159	-0.155	0.308
X1118	-0.155	0.308
X2033	0.155	0.309
X1736	-0.155	0.310
X1675	-0.154	0.313
X670	-0.154	0.314
X810	0.153	0.314
X2297	-0.153	0.315
X1865	-0.153	0.315
X1540	0.153	0.316
X880	-0.153	0.317
X1277	-0.152	0.319
X1181	-0.152	0.320
X1129	0.151	0.321
X997	0.151	0.322
X1582	0.151	0.322
X1034	0.151	0.322
X2278	-0.150	0.324
X2233	-0.150	0.326
X1286	-0.150	0.326
X1698	0.150	0.326
X662	-0.150	0.326
X1835	-0.150	0.326
X892	0.150	0.327
X1900	0.149	0.330
X1950	0.149	0.330
X1517	-0.148	0.331
X1107	0.148	0.331
X1534	-0.148	0.333
X2118	-0.147	0.336
X805	-0.147	0.336
X1125	0.147	0.336
X966	-0.146	0.338
X690	-0.146	0.338
X750	0.146	0.338
X1819	0.146	0.338
X2054	-0.146	0.338
X2180	-0.146	0.339
X706	-0.146	0.339
X1597	0.145	0.341
X2082	0.145	0.341
X1110	0.145	0.341
X1115	-0.145	0.343
X1187	-0.145	0.344
X1807	-0.144	0.346
X1708	0.144	0.346
X2172	0.144	0.347
X1278	0.143	0.348
X1892	-0.143	0.348
X1134	0.143	0.349
X2041	0.143	0.349
X1132	0.143	0.349
X1754	-0.143	0.349
X2022	-0.143	0.350
X1723	0.143	0.351
X769	0.142	0.351
X1564	-0.142	0.351
X1192	-0.142	0.353
X841	0.142	0.353
X1751	-0.142	0.353
X1198	-0.142	0.354
X628	-0.141	0.354
X2109	-0.141	0.355
X2269	0.140	0.358
X677	-0.140	0.358
X184	0.140	0.358
X1628	-0.140	0.361
X707	-0.140	0.361
X590	0.139	0.362
X1584	0.139	0.362
X1111	0.139	0.363
X1915	-0.139	0.364
X665	-0.139	0.364
X1139	-0.139	0.364
X824	0.138	0.365
X1078	-0.138	0.366
X525	-0.138	0.366
X836	0.138	0.368
X1613	-0.138	0.368
X1813	-0.137	0.368
X1862	0.137	0.370
X1716	0.137	0.371
X789	0.136	0.372
X1148	-0.136	0.373
X1333	0.136	0.373
X2343	0.136	0.373
X601	-0.136	0.373
X1706	0.136	0.373
X1235	0.136	0.373
X1332	-0.136	0.374
X1102	0.136	0.374
X2190	-0.136	0.374
X1411	-0.136	0.375
X1312	-0.136	0.375
X708	-0.135	0.378
X1727	-0.134	0.382
X1901	0.134	0.382
X471	0.134	0.382
X944	0.133	0.383
X1016	-0.133	0.383
X1023	0.133	0.383
X1368	-0.133	0.384
X1669	0.133	0.385
X1557	0.133	0.385
X1074	-0.133	0.385
X1958	0.133	0.385
X606	0.133	0.385
X1019	-0.133	0.385
X1509	0.133	0.385
X1383	0.133	0.386
X1104	0.132	0.386
X804	-0.132	0.387
X1210	-0.132	0.387
X970	-0.132	0.387
X743	0.132	0.388
X958	0.132	0.388
X1906	-0.132	0.388
X814	0.132	0.388
X1451	-0.132	0.389
X913	-0.131	0.390
X2235	0.131	0.391
X1457	-0.131	0.392
X2182	-0.131	0.392
X2274	-0.131	0.392
X1414	0.131	0.392
X928	0.131	0.392
X1551	0.131	0.392
X1195	-0.131	0.392
X1308	-0.131	0.392

X998	0.131	0.393
X1037	-0.131	0.393
X2155	-0.131	0.393
X911	-0.130	0.394
X375	0.130	0.396
X1028	-0.130	0.396
X1752	0.130	0.396
X1775	0.130	0.397
X849	-0.129	0.400
X1420	-0.128	0.402
X2072	0.128	0.403
X715	-0.128	0.403
X731	-0.128	0.403
X2028	0.128	0.404
X697	-0.128	0.405
X773	-0.127	0.405
X1416	0.127	0.407
X422	0.127	0.408
X989	-0.127	0.408
X2104	-0.126	0.411
X1323	-0.126	0.411
X1504	0.126	0.411
X1729	0.125	0.413
X1652	-0.125	0.413
X1227	-0.125	0.414
X1476	0.125	0.415
X1714	-0.125	0.415
X1777	-0.125	0.416
X914	-0.125	0.416
X529	-0.125	0.416
X1939	-0.125	0.416
X2179	-0.124	0.418
X1758	-0.124	0.419
X727	0.124	0.419
X1090	0.123	0.421
X1737	0.123	0.421
X1236	-0.123	0.421
X1307	0.123	0.422
X2299	0.123	0.422
X2253	0.123	0.423
X2105	0.123	0.423
X1562	-0.123	0.423
X2304	0.123	0.424
X702	-0.122	0.424
X615	-0.122	0.424
X1426	-0.122	0.425
X1639	-0.122	0.426
X1592	-0.122	0.426
X655	-0.122	0.426
X2216	-0.122	0.426
X1271	0.122	0.426
X1223	-0.121	0.429
X1831	-0.121	0.430
X988	0.121	0.430
X2130	0.120	0.431
X931	0.120	0.432
X2279	0.120	0.432
X1313	-0.120	0.432
X1532	0.120	0.433
X1989	0.120	0.434
X1352	-0.120	0.434
X1733	0.119	0.436
X936	0.119	0.437
X2242	-0.119	0.437
X1531	0.119	0.437
X961	0.119	0.438
X1656	-0.119	0.438
X858	0.119	0.439
X1141	-0.118	0.440
X1048	-0.118	0.441
X1066	-0.118	0.442
X926	0.118	0.442
X1355	-0.118	0.443
X1255	0.118	0.443
X946	0.118	0.443
X1734	0.117	0.443
X879	-0.117	0.445
X1739	-0.117	0.446
X1704	0.117	0.446
X1576	-0.117	0.446
X2293	-0.116	0.449
X726	-0.116	0.449
X1288	-0.116	0.449
X2010	0.116	0.449
X2071	0.116	0.450
X1602	0.116	0.450
X925	0.115	0.452
X1553	-0.115	0.452
X921	0.115	0.452
X1468	0.115	0.452
X1594	0.115	0.453
X1133	0.115	0.453
X1103	0.114	0.456
X619	-0.114	0.456
X1700	-0.114	0.456
X605	0.114	0.457
X1554	0.114	0.457
X1618	-0.114	0.458
X2023	-0.114	0.458
X1887	-0.114	0.458
X1154	-0.114	0.458
X934	0.114	0.458
X2012	0.113	0.459
X1357	-0.113	0.459
X2250	0.113	0.462
X2325	-0.113	0.462
X1515	-0.113	0.462
X881	0.112	0.464
X1279	0.112	0.465
X1724	0.112	0.465
X1369	0.112	0.465
X2042	0.112	0.467
X846	0.111	0.467
X845	0.111	0.468
X1861	-0.111	0.469
X1284	-0.111	0.469
X840	0.111	0.470
X972	-0.110	0.472
X909	0.110	0.473
X1470	0.110	0.473
X1439	-0.110	0.474
X2144	0.110	0.475
X1083	-0.110	0.475
X1135	-0.110	0.475
X1560	-0.109	0.476
X1522	0.109	0.476
X2276	0.109	0.476
X915	0.109	0.477
X2164	0.108	0.482
X1774	-0.108	0.482
X772	-0.107	0.484
X1902	0.107	0.485

X2318	0.107	0.486
X649	-0.107	0.486
X1351	-0.107	0.486
X453	0.107	0.487
X1003	0.107	0.487
X1026	-0.106	0.489
X1454	-0.106	0.489
X1272	-0.106	0.490
X2031	0.106	0.490
X1057	-0.106	0.491
X2219	-0.106	0.491
X578	-0.105	0.493
X2005	0.105	0.493
X1172	-0.105	0.494
X1176	-0.105	0.494
X2268	-0.105	0.496
X917	-0.105	0.496
X1254	-0.104	0.496
X2095	0.104	0.496
X1524	-0.104	0.499
X2147	-0.103	0.501
X1869	-0.103	0.501
X2106	0.103	0.501
X733	0.103	0.504
X1190	-0.102	0.505
X1546	0.102	0.507
X660	-0.102	0.507
X950	0.102	0.508
X1811	-0.101	0.509
X1874	0.101	0.509
X668	0.101	0.511
X1108	0.101	0.511
X1372	0.101	0.511
X2349	0.101	0.511
X766	0.101	0.512
X852	0.101	0.512
X1379	-0.100	0.513
X1086	0.100	0.514
X1741	-0.100	0.517
X1623	-0.099	0.519
X937	0.098	0.522
X1085	0.098	0.524
X1376	0.098	0.524
X1936	-0.098	0.525
X1410	-0.097	0.526
X1071	0.097	0.528
X896	0.097	0.529
X1188	0.097	0.529
X860	0.097	0.529
X1373	-0.097	0.530
X1791	-0.096	0.531
X855	0.096	0.532
X2053	0.096	0.532
X1614	-0.096	0.533
X1196	-0.096	0.533
X324	0.096	0.534
X1785	-0.096	0.534
X861	0.095	0.535
X1095	-0.095	0.537
X1473	0.095	0.537
X1800	0.095	0.537
X661	-0.095	0.538
X974	0.095	0.538
X2240	0.095	0.538
X1049	-0.094	0.539
X2239	-0.094	0.539
X1762	-0.094	0.539
X1526	0.094	0.539
X1302	-0.094	0.540
X1256	0.094	0.540
X310	0.094	0.540
X1203	0.094	0.540
X2295	-0.094	0.540
X1371	0.094	0.541
X2151	-0.094	0.542
X459	-0.094	0.542
X604	0.093	0.544
X587	0.093	0.544
X2044	0.093	0.545
X992	-0.093	0.546
X2016	0.093	0.547
X1330	-0.092	0.548
X633	-0.092	0.549
X1480	0.092	0.551
X1709	0.091	0.552
X1432	-0.091	0.554
X1131	-0.091	0.554
X1651	-0.090	0.557
X2231	0.090	0.558
X978	0.090	0.558
X2301	0.090	0.559
X1109	0.090	0.559
X985	0.089	0.560
X903	0.089	0.561
X2292	0.089	0.561
X908	-0.089	0.561
X2120	-0.089	0.564
X1423	0.089	0.564
X1643	-0.088	0.567
X1464	0.088	0.569
X1005	-0.087	0.570
X627	0.087	0.571
X1435	-0.087	0.572
X1268	-0.087	0.572
X887	0.087	0.572
X1314	-0.087	0.573
X2317	-0.086	0.574
X1766	-0.086	0.575
X371	0.086	0.576
X1022	-0.086	0.576
X636	-0.086	0.577
X1166	0.085	0.578
X2339	-0.085	0.579
X1283	-0.085	0.580
X1664	-0.085	0.580
X872	-0.085	0.580
X1466	-0.085	0.581
X1304	-0.085	0.582
X2014	0.085	0.582
X621	-0.085	0.582
X1367	0.084	0.584
X642	-0.084	0.587
X1780	0.083	0.589
X2073	0.083	0.589
X1150	-0.083	0.590
X753	0.083	0.590
X1228	-0.083	0.591
X1184	-0.083	0.591
X1072	-0.082	0.592
X809	0.082	0.593
X1138	-0.082	0.594
X833	0.082	0.594

X1676	-0.082	0.595
X1503	0.081	0.597
X1561	0.081	0.598
X775	0.081	0.598
X991	-0.081	0.598
X1593	-0.081	0.598
X1438	-0.081	0.598
X1765	-0.081	0.598
X2222	-0.081	0.599
X1042	0.081	0.600
X990	-0.081	0.601
X943	0.080	0.601
X1730	0.080	0.601
X1220	-0.080	0.603
X1401	0.079	0.606
X1155	-0.079	0.606
X1041	-0.079	0.607
X400	-0.079	0.608
X229	-0.079	0.609
X1462	-0.078	0.610
X686	-0.078	0.610
X1595	0.078	0.611
X2351	-0.078	0.611
X1965	0.078	0.612
X378	0.078	0.613
X1812	0.077	0.617
X1208	-0.077	0.617
X1419	0.077	0.618
X632	-0.077	0.618
X1047	0.076	0.620
X1667	0.076	0.620
X1759	0.076	0.620
X617	0.076	0.622
X272	0.076	0.622
X2174	-0.075	0.624
X2238	-0.075	0.625
X1778	0.075	0.625
X1692	-0.075	0.626
X1525	-0.075	0.627
X1030	-0.075	0.627
X1046	-0.075	0.627
X694	-0.075	0.628
X1678	0.074	0.629
X2050	-0.074	0.629
X1806	-0.074	0.632
X1735	-0.074	0.633
X1492	-0.074	0.633
X798	-0.074	0.633
X2354	0.073	0.633
X1347	-0.073	0.634
X821	0.073	0.635
X826	0.073	0.637
X1882	-0.073	0.637
X1838	-0.072	0.638
X2287	0.072	0.638
X597	-0.072	0.639
X1291	0.072	0.640
X1581	-0.072	0.640
X1657	0.072	0.641
X1407	0.072	0.642
X712	-0.072	0.642
X1611	0.071	0.643
X1036	0.071	0.643
X1413	-0.071	0.644
X1817	0.071	0.645
X1674	-0.071	0.646
X1374	-0.071	0.647
X2226	-0.071	0.647
X1757	0.071	0.647
X2256	0.070	0.647
X1629	-0.070	0.648
X2128	0.070	0.648
X1990	0.070	0.648
X1162	-0.070	0.649
X705	-0.070	0.649
X1362	-0.070	0.649
X1793	-0.070	0.650
X1944	-0.070	0.650
X995	0.070	0.651
X1281	-0.069	0.652
X2007	0.069	0.652
X795	0.069	0.652
X714	-0.069	0.653
X1516	-0.069	0.654
X2115	-0.069	0.654
X681	0.069	0.655
X2284	0.069	0.655
X1728	-0.069	0.656
X954	0.068	0.656
X971	-0.068	0.656
X1823	-0.068	0.660
X1590	-0.068	0.660
X1988	0.068	0.660
X608	-0.067	0.662
X1805	0.067	0.662
X1007	-0.067	0.662
X2123	0.067	0.662
X1591	0.067	0.663
X1063	-0.067	0.664
X1073	-0.067	0.664
X2203	-0.067	0.666
X1538	0.067	0.666
X2350	0.066	0.668
X1160	0.066	0.668
X1701	-0.066	0.669
X1599	0.065	0.671
X1081	0.065	0.672
X1000	-0.065	0.672
X963	0.065	0.673
X669	0.065	0.674
X1822	-0.065	0.674
X1826	-0.064	0.676
X1120	0.064	0.676
X1523	0.064	0.677
X1381	0.064	0.678
X1321	-0.063	0.680
X2159	0.063	0.681
X2298	-0.063	0.682
X432	0.063	0.682
X1749	-0.063	0.682
X1586	-0.063	0.682
X1385	-0.063	0.682
X1361	-0.063	0.683
X1130	0.063	0.684
X1717	0.063	0.684
X1677	-0.063	0.684
X1161	-0.062	0.685
X1543	-0.062	0.685
X778	-0.062	0.685
X1942	-0.062	0.686
X638	-0.062	0.686
X1705	-0.062	0.687

X266	0.062	0.688
X2210	-0.062	0.688
X744	-0.062	0.688
X1265	-0.062	0.688
X999	0.062	0.689
X2019	0.061	0.690
X1045	0.061	0.692
X1786	-0.061	0.692
X2116	0.061	0.692
X1186	0.061	0.693
X1341	0.060	0.695
X1485	-0.060	0.695
X679	0.060	0.696
X1180	-0.060	0.696
X1033	-0.060	0.696
X1448	-0.060	0.697
X1738	-0.060	0.697
X1659	-0.060	0.698
X1282	0.060	0.698
X1434	-0.060	0.698
X574	0.060	0.699
X945	0.059	0.700
X1587	0.059	0.700
X2032	0.059	0.701
X1598	0.059	0.702
X771	-0.059	0.703
X1424	-0.059	0.703
X2169	0.058	0.704
X1164	0.058	0.704
X851	0.058	0.708
X1211	0.057	0.710
X1566	-0.057	0.711
X878	-0.057	0.711
X1363	-0.057	0.712
X1487	-0.057	0.713
X1903	-0.057	0.714
X1972	0.056	0.714
X1092	0.056	0.715
X1491	-0.056	0.716
X305	0.056	0.716
X1814	0.056	0.716
X782	-0.056	0.717
X774	-0.056	0.718
X1547	0.056	0.718
X2111	-0.056	0.718
X906	-0.056	0.718
X768	0.056	0.719
X996	0.055	0.719
X2070	-0.055	0.719
X1856	0.055	0.719
X1226	0.055	0.720
X1879	0.055	0.720
X1802	-0.055	0.721
X1616	0.055	0.721
X724	0.055	0.721
X1012	0.055	0.722
X1089	0.055	0.722
X682	-0.055	0.722
X1500	0.055	0.723
X2341	0.055	0.723
X1221	0.055	0.723
X1331	-0.055	0.723
X1392	0.054	0.724
X591	-0.054	0.726
X2098	0.054	0.728
X1783	-0.054	0.728
X2126	0.054	0.728
X1218	-0.053	0.728
X1305	-0.053	0.730
X1275	-0.053	0.731
X1687	0.053	0.732
X968	-0.053	0.732
X1140	-0.053	0.732
X2021	0.053	0.733
X1450	0.052	0.734
X721	-0.052	0.735
X1671	0.052	0.735
X1622	0.052	0.736
X635	-0.052	0.736
X2185	0.052	0.737
X2245	-0.052	0.738
X2020	0.051	0.740
X1377	0.051	0.740
X646	-0.051	0.740
X676	0.051	0.741
X2024	-0.051	0.741
X1422	-0.051	0.743
X1273	-0.050	0.743
X1440	-0.050	0.743
X1997	0.050	0.743
X648	0.050	0.744
X1794	-0.050	0.745
X594	-0.050	0.746
X2087	-0.050	0.746
X397	-0.050	0.747
X1174	-0.049	0.748
X1303	-0.049	0.749
X1163	0.049	0.749
X1152	-0.049	0.750
X1818	-0.049	0.750
X1481	0.049	0.751
X1380	-0.049	0.751
X1627	-0.049	0.752
X1703	-0.049	0.752
X1530	0.049	0.752
X871	-0.048	0.753
X1654	-0.048	0.754
X657	0.048	0.755
X1264	-0.048	0.755
X1658	0.048	0.756
X1857	-0.048	0.758
X1825	0.048	0.758
X1580	-0.047	0.759
X2101	-0.047	0.761
X2184	-0.046	0.765
X2254	0.046	0.766
X976	-0.046	0.766
X2353	-0.046	0.767
X1436	-0.046	0.767
X1009	-0.046	0.768
X2336	0.045	0.768
X867	0.045	0.769
X897	-0.045	0.770
X1465	-0.045	0.771
X965	0.045	0.772
X675	-0.045	0.772
X741	-0.045	0.772
X918	0.045	0.773
X1205	0.044	0.773
X1624	0.044	0.773
X599	-0.044	0.773
X2049	-0.044	0.775

X1405	-0.044	0.775
X2194	0.044	0.776
X1010	-0.044	0.777
X746	-0.044	0.778
X1552	0.043	0.778
X637	-0.043	0.779
X2091	0.043	0.779
X1691	0.043	0.780
X1315	-0.043	0.780
X281	0.043	0.781
X1326	0.043	0.782
X1170	-0.043	0.782
X1229	0.042	0.783
X1981	-0.042	0.784
X740	0.042	0.785
X738	-0.042	0.786
X1968	0.042	0.786
X387	0.042	0.787
X2241	-0.042	0.788
X2127	0.041	0.788
X1830	-0.041	0.789
X1171	-0.041	0.789
X1478	0.041	0.790
X1433	0.041	0.790
X1191	-0.041	0.790
X2138	0.041	0.791
X1098	0.041	0.791
X1299	-0.041	0.791
X1549	-0.041	0.792
X1126	0.041	0.792
X1962	0.041	0.792
X938	-0.041	0.792
X2303	-0.040	0.794
X1147	-0.040	0.794
X602	0.040	0.794
X654	0.040	0.794
X1317	-0.040	0.795
X873	-0.040	0.796
X1270	0.040	0.796
X1821	0.040	0.796
X1506	0.040	0.797
X1058	-0.040	0.798
X1535	-0.039	0.798
X2198	0.039	0.798
X1204	0.039	0.799
X1339	-0.039	0.800
X620	0.039	0.801
X2081	-0.039	0.801
X1060	-0.039	0.801
X993	0.039	0.802
X1397	-0.039	0.802
X2313	0.039	0.802
X2347	0.039	0.803
X755	0.038	0.804
X2314	-0.038	0.805
X718	-0.038	0.805
X1668	0.038	0.806
X625	0.037	0.809
X1521	0.037	0.809
X2013	-0.037	0.810
X1123	-0.037	0.812
X1964	-0.037	0.813
X607	-0.036	0.814
X2281	-0.036	0.814
X1963	0.036	0.816
X603	-0.036	0.816
X659	-0.036	0.817
X1360	0.036	0.817
X1588	-0.036	0.818
X969	-0.035	0.818
X2330	-0.035	0.819
X1293	-0.035	0.819
X947	-0.035	0.820
X1269	0.035	0.820
X1006	0.035	0.821
X386	0.035	0.822
X786	-0.035	0.823
X905	-0.034	0.823
X1702	-0.034	0.824
X2221	-0.033	0.829
X684	-0.033	0.830
X1296	-0.033	0.832
X1685	-0.032	0.833
X2337	-0.032	0.834
X1719	0.032	0.834
X1816	-0.032	0.836
X857	0.032	0.836
X501	0.032	0.837
X2326	0.032	0.837
X2237	0.032	0.837
X598	-0.032	0.837
X405	-0.032	0.838
X994	0.031	0.839
X1029	-0.031	0.840
X1753	0.031	0.840
X1789	0.031	0.841
X1345	0.031	0.841
X1471	0.031	0.841
X571	0.031	0.841
X2097	-0.031	0.841
X1499	-0.031	0.843
X930	-0.030	0.844
X1124	-0.030	0.844
X876	0.030	0.845
X2103	0.030	0.846
X1848	-0.030	0.846
X942	0.030	0.848
X1548	0.029	0.850
X1442	0.029	0.852
X2140	0.029	0.852
X639	0.029	0.853
X1829	-0.029	0.853
X1621	0.028	0.854
X393	0.028	0.854
X1146	0.028	0.855
X1425	0.028	0.856
X1505	-0.028	0.857
X916	-0.028	0.857
X1808	-0.028	0.858
X2085	0.027	0.859
X987	0.027	0.859
X1350	-0.027	0.859
X2045	0.027	0.860
X1679	0.027	0.861
X1494	-0.027	0.861
X2040	0.027	0.863
X1427	-0.026	0.864
X680	-0.026	0.866
X745	-0.026	0.866
X1897	-0.026	0.866
X2244	-0.025	0.869
X1043	-0.025	0.869

X1837	-0.025	0.870
X1849	0.025	0.870
X643	-0.025	0.871
X2215	-0.025	0.872
X1558	0.025	0.872
X1294	-0.025	0.873
X900	0.025	0.873
X1640	-0.025	0.874
X626	0.024	0.874
X1744	0.024	0.876
X2335	0.024	0.876
X1344	0.024	0.877
X2152	-0.023	0.879
X1577	-0.023	0.879
X1743	0.023	0.879
X894	-0.023	0.880
X1121	0.023	0.880
X396	0.023	0.880
X2199	-0.023	0.881
X739	0.023	0.882
X933	0.023	0.883
X1686	-0.023	0.883
X800	-0.023	0.884
X1756	0.022	0.884
X1106	-0.022	0.885
X1175	-0.022	0.885
X1032	-0.022	0.885
X973	-0.022	0.886
X1537	-0.022	0.887
X1053	0.022	0.887
X1050	0.022	0.887
X1510	0.022	0.887
X2048	-0.022	0.888
X1620	0.022	0.889
X1431	0.021	0.890
X1311	-0.021	0.890
X1246	-0.021	0.891
X1836	0.021	0.891
X1079	0.021	0.891
X1731	0.021	0.891
X1153	-0.021	0.892
X379	0.021	0.892
X1212	0.021	0.894
X1881	-0.021	0.894
X1876	-0.020	0.895
X983	0.020	0.896
X1239	0.020	0.896
X1732	0.020	0.897
X687	0.020	0.897
X2026	0.020	0.898
X2196	0.019	0.899
X2193	-0.019	0.900
X2283	-0.019	0.900
X1274	-0.019	0.901
X1169	0.019	0.901
X1216	-0.019	0.901
X311	-0.019	0.901
X1650	-0.019	0.903
X664	-0.019	0.903
X2338	0.019	0.903
X1488	-0.018	0.905
X595	0.018	0.905
X630	-0.018	0.906
X763	0.018	0.907
X1784	0.018	0.907
X1287	0.018	0.907
X2086	0.018	0.907
X1803	-0.018	0.907
X1929	-0.018	0.907
X1127	0.018	0.908
X1122	-0.018	0.909
X1412	-0.018	0.909
X2296	-0.017	0.910
X1746	-0.017	0.910
X713	0.017	0.910
X1077	-0.017	0.911
X1697	0.017	0.911
X2119	-0.017	0.912
X634	0.017	0.912
X641	0.017	0.912
X1718	-0.017	0.912
X1512	-0.017	0.913
X1259	0.017	0.914
X1635	0.016	0.915
X767	-0.016	0.915
X1483	-0.016	0.916
X1725	-0.016	0.916
X752	0.016	0.917
X1689	0.016	0.918
X1518	-0.016	0.918
X685	-0.016	0.919
X596	-0.016	0.920
X645	-0.015	0.921
X593	0.015	0.921
X1213	0.015	0.921
X2211	-0.015	0.921
X1948	0.015	0.921
X1779	0.015	0.922
X1459	-0.015	0.922
X2136	0.015	0.922
X1645	-0.015	0.922
X1088	-0.015	0.922
X580	0.015	0.924
X629	0.015	0.924
X1064	0.015	0.924
X1039	0.015	0.925
X2096	-0.014	0.926
X1456	0.014	0.926
X2232	0.014	0.926
X1390	0.014	0.926
X1565	0.014	0.927
X2088	0.014	0.928
X1720	0.014	0.928
X1781	-0.014	0.928
X895	-0.014	0.930
X765	0.013	0.932
X1238	-0.013	0.933
X1093	0.013	0.933
X1099	-0.013	0.934
X1247	-0.013	0.934
X1386	-0.013	0.935
X839	-0.013	0.935
X1087	0.012	0.936
X2156	-0.012	0.937
X863	-0.012	0.937
X725	0.012	0.937
X1070	-0.012	0.939
X589	-0.012	0.939
X2171	0.012	0.940
X1189	0.012	0.940
X1387	0.012	0.940
X904	0.011	0.942

X1863	0.011	0.942
X1151	-0.011	0.943
X584	0.011	0.943
X1542	0.011	0.943
X1167	-0.011	0.944
X1428	-0.011	0.945
X1251	0.010	0.946
X2294	0.010	0.946
X2148	0.010	0.947
X1076	-0.010	0.947
X1748	-0.010	0.947
X770	0.010	0.948
X667	0.010	0.949
X1890	0.010	0.949
X1782	0.010	0.951
X653	0.010	0.951
X1183	-0.009	0.951
X2146	0.009	0.952
X1688	-0.009	0.952
X381	0.009	0.953
X1052	0.009	0.954
X1091	0.009	0.955
X1745	-0.009	0.955
X1290	-0.009	0.955
X853	0.009	0.956
X1971	0.008	0.956
X1927	-0.008	0.957
X1707	0.008	0.958
X2315	-0.008	0.958
X1415	-0.008	0.959
X622	-0.008	0.959
X1185	0.008	0.960
X609	0.008	0.960
X624	-0.008	0.960
X2142	-0.008	0.960
X2273	0.008	0.960
X1982	0.007	0.962
X2043	-0.007	0.963
X532	0.007	0.964
X866	0.007	0.965
X1575	-0.007	0.966
X1316	0.007	0.966
X2307	-0.006	0.966
X1157	-0.006	0.968
X749	0.006	0.969
X1572	0.006	0.970
X1809	0.006	0.971
X803	0.006	0.971
X977	-0.005	0.972
X1207	-0.005	0.973
X1297	0.005	0.974
X1644	-0.005	0.976
X1795	-0.005	0.976
X2135	-0.005	0.976
X2311	-0.004	0.977
X1260	0.004	0.977
X1930	-0.004	0.978
X939	0.004	0.978
X865	0.004	0.979
X2275	0.004	0.980
X1511	-0.004	0.981
X1393	-0.004	0.982
X1117	-0.003	0.983
X1570	-0.003	0.983
X286	-0.003	0.984
X1430	0.003	0.984
X1680	-0.002	0.989
X640	-0.002	0.989
X545	-0.002	0.990
X692	-0.002	0.991
X610	0.002	0.991
X1158	-0.002	0.991
X1479	0.002	0.991
X1201	-0.002	0.992
X1514	-0.001	0.993
X631	0.001	0.993
X242	0.001	0.994
X2280	-0.001	0.994
X2230	-0.001	0.995
X1501	-0.001	0.995
X666	-0.001	0.995
X901	0.001	0.996
X1469	-0.001	0.996
X1636	0.001	0.997
X1832	0.001	0.997
X1489	0.000	0.999
X1116	0.000	1.000
X1059	0.000	1.000

Appendix 3

T12 partial correlation results for 2DGE spots with PiB PET DVR. Spots ranked in order of significance based on p value. Results highlighted in red are statistically significant ($p<0.05$).

Spot ID	Correlation coefficient	P-value
X2143	-0.533	0.000
X1309	-0.500	0.000
X630	-0.468	0.000
X635	-0.439	0.001
X1110	0.428	0.002
X598	-0.424	0.002
X1496	0.424	0.002
X966	-0.423	0.002
X1780	0.415	0.002
X899	-0.410	0.003
X381	-0.406	0.003
X1171	-0.398	0.004
X1500	0.392	0.004
X589	-0.391	0.004
X1718	0.390	0.004
X969	-0.389	0.005
X2141	-0.388	0.005
X996	-0.385	0.005
X1549	0.382	0.006
X593	-0.380	0.006
X911	-0.377	0.006
X584	-0.369	0.008
X2177	0.366	0.008
X1015	-0.365	0.009
X596	-0.364	0.009
X1377	0.360	0.010
X1597	0.359	0.010
X1593	0.359	0.010
X1557	0.356	0.011
X386	-0.353	0.011
X641	-0.353	0.011
X642	-0.350	0.012
X1112	0.349	0.012
X1710	-0.342	0.015
X1662	-0.340	0.015
X1303	-0.339	0.015
X587	-0.337	0.016
X685	-0.335	0.017
X629	-0.334	0.017
X272	-0.331	0.019
X1399	0.329	0.019
X2024	-0.329	0.020
X1929	0.328	0.020
X2040	-0.327	0.020
X993	-0.327	0.020
X2235	0.325	0.021
X1129	0.322	0.022
X585	0.321	0.023
X1170	-0.318	0.024
X1580	0.317	0.025
X1738	-0.317	0.025
X705	-0.315	0.026
X1172	-0.312	0.027
X634	-0.311	0.028
X1963	0.310	0.029
X1617	0.309	0.029
X1017	-0.309	0.029
X1299	0.308	0.030
X1078	-0.307	0.031
X1067	-0.303	0.033
X1402	-0.302	0.034
X640	-0.299	0.035
X2214	0.296	0.038
X1966	0.295	0.038
X525	-0.293	0.040
X1762	-0.293	0.040
X971	-0.292	0.041
X905	-0.290	0.042
X1362	0.289	0.043
X906	-0.289	0.043
X1367	0.288	0.044
X1474	0.286	0.045
X669	-0.286	0.045
X1071	0.285	0.046
X654	-0.283	0.047
X281	-0.283	0.048
X826	-0.279	0.051
X2111	-0.279	0.052
X631	-0.278	0.052
X910	-0.278	0.052
X1814	0.276	0.054
X1404	-0.275	0.055
X766	0.275	0.055
X1741	-0.275	0.055
X1018	-0.271	0.059
X1290	-0.270	0.060
X913	-0.270	0.060
X707	-0.269	0.061
X874	-0.269	0.061
X633	-0.268	0.062
X1111	-0.268	0.062
X1010	0.268	0.062
X597	-0.268	0.062
X1724	0.267	0.063
X1339	-0.267	0.063
X1277	-0.266	0.064
X1521	-0.266	0.064
X1548	0.265	0.065
X643	-0.265	0.065
X904	-0.263	0.067
X686	-0.263	0.068
X626	-0.262	0.068
X1400	-0.262	0.069
X1588	0.261	0.070
X590	0.260	0.070
X1063	-0.260	0.071
X1748	0.260	0.071
X1777	0.255	0.076
X1408	-0.254	0.078
X1463	-0.253	0.080

X1374	0.252	0.080
X1903	0.252	0.081
X2147	-0.252	0.081
X754	-0.252	0.081
X2268	-0.251	0.081
X710	-0.251	0.081
X1679	0.251	0.082
X1723	0.251	0.082
X1394	0.251	0.083
X2049	-0.250	0.083
X1486	0.250	0.083
X2125	-0.250	0.084
X1466	0.250	0.084
X1590	-0.249	0.084
X680	0.249	0.084
X1070	-0.249	0.085
X2275	-0.247	0.087
X2010	-0.247	0.087
X1379	-0.247	0.087
X816	-0.247	0.087
X1258	-0.247	0.087
X379	-0.247	0.088
X266	-0.246	0.089
X625	-0.245	0.090
X480	0.245	0.090
X1621	0.245	0.090
X1968	0.245	0.090
X690	-0.245	0.091
X1057	-0.244	0.091
X1396	-0.244	0.092
X2045	-0.243	0.093
X1094	-0.243	0.093
X1139	-0.241	0.096
X1692	0.241	0.096
X1816	0.240	0.098
X2023	-0.240	0.098
X972	-0.239	0.098
X999	-0.239	0.099
X968	-0.239	0.099
X1657	0.238	0.100
X1612	-0.238	0.100
X2142	-0.238	0.100
X925	-0.237	0.101
X1192	0.236	0.103

X791	-0.235	0.105
X2317	-0.235	0.105
X2044	-0.235	0.105
X2053	-0.235	0.106
X1598	0.235	0.106
X936	0.234	0.106
X1169	-0.234	0.106
X1014	-0.234	0.107
X1068	-0.233	0.107
X2281	-0.233	0.108
X1691	0.233	0.108
X1828	-0.233	0.108
X1528	0.232	0.109
X2341	-0.232	0.110
X1524	-0.231	0.111
X1906	-0.231	0.111
X1997	-0.231	0.111
X2211	-0.231	0.112
X891	-0.230	0.113
X985	-0.229	0.114
X1613	-0.229	0.115
X1508	0.228	0.115
X753	0.228	0.116
X1161	-0.228	0.116
X2120	-0.228	0.117
X1392	0.227	0.117
X2250	0.227	0.119
X2226	0.227	0.119
X2081	0.226	0.119
X2155	0.226	0.119
X1331	-0.226	0.120
X2209	0.224	0.122
X1054	-0.224	0.123
X2273	-0.224	0.124
X1902	0.223	0.125
X1049	-0.222	0.126
X712	-0.222	0.127
X610	-0.221	0.128
X628	-0.221	0.128
X1393	-0.220	0.131
X772	-0.220	0.131
X1238	0.219	0.131
X1390	-0.219	0.132
X1153	-0.219	0.132

X2315	-0.219	0.132
X2063	-0.218	0.134
X656	-0.218	0.134
X708	-0.218	0.135
X1047	-0.217	0.135
X1013	-0.217	0.136
X2271	-0.217	0.136
X855	-0.216	0.137
X1246	-0.216	0.137
X657	0.216	0.138
X998	-0.215	0.140
X668	-0.215	0.141
X1023	-0.215	0.141
X1618	0.214	0.141
X2140	-0.214	0.142
X1022	-0.214	0.142
X1809	0.213	0.144
X2087	-0.213	0.144
X1737	-0.212	0.145
X1499	-0.212	0.146
X580	-0.212	0.146
X679	-0.212	0.146
X1312	-0.212	0.146
X951	0.210	0.149
X1247	-0.210	0.149
X1084	-0.210	0.149
X696	0.210	0.150
X1163	-0.209	0.151
X702	-0.209	0.152
X2109	-0.209	0.152
X2244	0.208	0.153
X638	-0.208	0.153
X2054	-0.208	0.154
X621	-0.207	0.156
X1782	0.206	0.158
X665	-0.206	0.158
X1310	-0.206	0.159
X939	0.205	0.159
X1099	-0.205	0.159
X2007	-0.205	0.159
X1507	0.205	0.161
X1195	-0.205	0.161
X1821	0.205	0.161
X2159	0.204	0.163

X1510	0.204	0.163
X594	-0.204	0.163
X822	0.204	0.163
X2082	0.203	0.165
X1646	-0.202	0.166
X1648	-0.202	0.167
X1685	-0.202	0.167
X1716	0.202	0.167
X1818	0.202	0.168
X1518	0.201	0.168
X1397	-0.201	0.169
X1135	-0.201	0.169
X1775	-0.200	0.170
X2025	-0.200	0.171
X2184	0.200	0.171
X2102	0.200	0.172
X765	0.200	0.172
X1637	-0.199	0.172
X1244	-0.199	0.173
X1043	-0.199	0.173
X1196	-0.199	0.174
X706	-0.198	0.176
X1337	-0.197	0.178
X1227	-0.197	0.178
X602	0.196	0.179
X1551	0.196	0.179
X1357	-0.196	0.180
X2348	-0.196	0.180
X676	0.196	0.180
X1092	-0.196	0.180
X2126	-0.196	0.180
X659	-0.195	0.181
X2036	-0.195	0.181
X1271	0.195	0.182
X1639	-0.195	0.182
X1052	-0.195	0.183
X2190	-0.194	0.184
X533	0.194	0.184
X1773	-0.194	0.184
X976	-0.194	0.184
X1470	0.194	0.185
X1376	0.194	0.185
X1283	0.193	0.186
X574	-0.193	0.186
X1803	0.193	0.187
X886	-0.193	0.188
X763	-0.192	0.189
X1958	0.192	0.190
X928	0.191	0.192
X601	0.190	0.194
X2085	0.190	0.194
X1927	0.190	0.195
X1579	0.189	0.196
X1587	0.189	0.197
X2043	-0.189	0.197
X1687	-0.189	0.198
X1167	-0.189	0.198
X1808	0.188	0.198
X1645	-0.188	0.200
X1915	0.187	0.200
X1926	0.187	0.201
X902	-0.187	0.202
X848	-0.187	0.202
X471	0.187	0.202
X1128	0.187	0.203
X1465	0.187	0.203
X1026	-0.187	0.203
X844	0.186	0.204
X678	-0.186	0.205
X1489	-0.186	0.205
X2137	-0.185	0.206
X1823	0.185	0.206
X1633	-0.185	0.206
X1771	0.185	0.206
X2240	0.185	0.207
X1278	-0.185	0.207
X1623	-0.185	0.208
X1046	-0.184	0.208
X1222	-0.184	0.209
X403	-0.183	0.211
X2203	0.183	0.212
X748	-0.183	0.212
X1781	0.183	0.212
X1787	0.183	0.212
X758	-0.183	0.213
X305	-0.182	0.214
X1756	0.181	0.216
X1338	-0.181	0.216
X2095	0.181	0.217
X921	-0.181	0.218
X1059	-0.180	0.218
X1134	0.180	0.218
X1757	0.180	0.218
X2218	-0.179	0.221
X2231	0.179	0.222
X947	-0.179	0.223
X1573	-0.179	0.223
X1695	-0.179	0.223
X637	-0.179	0.223
X746	-0.178	0.224
X1454	-0.178	0.224
X898	-0.177	0.226
X2156	-0.177	0.229
X1190	-0.177	0.229
X2339	-0.176	0.230
X1785	0.176	0.231
X1053	-0.175	0.232
X852	0.174	0.235
X2331	0.173	0.238
X1353	-0.173	0.239
X1950	0.172	0.242
X558	0.172	0.243
X595	0.171	0.243
X722	-0.170	0.246
X1168	-0.170	0.246
X645	-0.170	0.247
X2096	-0.170	0.247
X1426	-0.170	0.247
X1173	-0.168	0.252
X2313	-0.168	0.252
X963	-0.168	0.252
X694	-0.168	0.253
X1314	-0.168	0.254
X1650	0.166	0.258
X1805	0.166	0.258
X1356	-0.166	0.258
X2304	0.166	0.258
X184	-0.166	0.259
X1925	0.165	0.261
X725	-0.165	0.261
X885	-0.165	0.262
X1715	0.165	0.263

X1421	-0.164	0.264
X1538	0.164	0.264
X1727	0.163	0.267
X741	-0.163	0.267
X1422	0.163	0.268
X1036	-0.163	0.269
X974	-0.162	0.270
X1802	0.162	0.271
X1042	-0.162	0.271
X2237	-0.162	0.271
X1825	0.162	0.271
X944	-0.161	0.273
X1523	-0.161	0.273
X887	0.161	0.274
X1604	0.161	0.275
X973	-0.161	0.275
X1959	0.160	0.276
X1930	0.160	0.278
X2144	-0.160	0.278
X1032	0.160	0.278
X1619	0.159	0.279
X2239	0.159	0.279
X2198	-0.159	0.280
X1581	0.159	0.280
X779	-0.159	0.280
X1610	0.159	0.280
X757	0.159	0.281
X1678	0.158	0.282
X2115	-0.158	0.282
X1713	0.158	0.283
X1154	0.158	0.284
X733	0.157	0.286
X661	-0.156	0.289
X2194	0.156	0.289
X1255	-0.156	0.291
X1698	0.155	0.291
X627	-0.155	0.292
X1663	-0.155	0.292
X1520	-0.154	0.296
X1572	-0.153	0.298
X1668	0.153	0.299
X1158	-0.153	0.299
X484	0.153	0.300
X1401	0.153	0.300

X1832	-0.153	0.300
X2298	-0.152	0.302
X1073	-0.152	0.302
X1942	-0.152	0.303
X1819	0.151	0.304
X2345	-0.151	0.304
X1307	0.151	0.305
X609	-0.150	0.307
X945	-0.150	0.308
X1189	0.150	0.309
X2246	0.150	0.309
X649	0.150	0.310
X1810	0.149	0.311
X387	-0.149	0.311
X1029	-0.149	0.312
X1725	-0.148	0.314
X2292	-0.148	0.314
X938	-0.148	0.315
X1794	-0.148	0.315
X2086	0.148	0.315
X798	-0.148	0.317
X1811	0.147	0.318
X1410	-0.147	0.318
X1223	0.147	0.319
X1273	0.147	0.320
X1462	0.147	0.320
X1917	0.147	0.320
X1892	0.146	0.321
X1973	0.146	0.321
X1175	-0.146	0.321
X2104	0.146	0.322
X1690	-0.146	0.323
X1552	0.146	0.323
X1448	0.146	0.323
X1341	-0.145	0.325
X845	-0.145	0.326
X1141	-0.145	0.326
X1768	-0.145	0.327
X1743	0.143	0.331
X1450	0.143	0.331
X2245	-0.143	0.331
X1611	-0.143	0.332
X692	-0.143	0.332
X1990	-0.143	0.332

X2187	0.143	0.333
X1439	-0.143	0.333
X1245	-0.143	0.333
X2014	-0.143	0.334
X2118	0.143	0.334
X1405	-0.143	0.334
X2127	-0.143	0.334
X1730	-0.142	0.335
X950	0.142	0.335
X1480	-0.142	0.336
X1076	-0.142	0.336
X1531	0.142	0.337
X667	-0.141	0.338
X1159	0.141	0.339
X1412	-0.141	0.339
X2274	0.141	0.339
X1411	-0.141	0.339
X1676	-0.141	0.341
X670	-0.141	0.341
X1564	0.140	0.341
X2221	0.140	0.342
X1108	0.140	0.344
X2037	-0.139	0.347
X2006	-0.139	0.347
X2026	-0.139	0.348
X2091	-0.138	0.350
X400	-0.138	0.351
X1471	0.137	0.353
X740	-0.137	0.355
X1409	-0.137	0.355
X1642	-0.136	0.356
X991	-0.136	0.356
X942	-0.136	0.356
X1848	0.136	0.357
X786	-0.136	0.358
X663	-0.136	0.359
X1033	-0.135	0.359
X1624	-0.135	0.360
X2352	0.135	0.361
X624	-0.135	0.361
X988	0.135	0.362
X1491	-0.135	0.362
X2215	0.134	0.363
X1039	-0.134	0.363

X422	-0.134	0.364
X1304	0.133	0.366
X2204	0.133	0.367
X1191	-0.133	0.369
X1609	-0.132	0.370
X1282	-0.132	0.370
X1758	-0.132	0.371
X1887	0.132	0.371
X1289	-0.132	0.372
X1296	0.132	0.372
X1430	-0.132	0.373
X983	-0.132	0.373
X895	-0.131	0.374
X1016	-0.131	0.374
X432	-0.131	0.374
X2335	-0.131	0.375
X1438	-0.131	0.377
X1440	-0.131	0.377
X773	-0.130	0.377
X2311	0.130	0.378
X1759	-0.129	0.381
X788	-0.129	0.382
X1087	-0.129	0.383
X1599	0.129	0.384
X2088	-0.129	0.384
X1106	0.129	0.385
X2332	-0.128	0.385
X749	-0.128	0.385
X1215	-0.128	0.386
X389	-0.128	0.386
X1156	0.128	0.386
X946	-0.128	0.388
X778	-0.127	0.389
X1562	0.127	0.390
X545	-0.127	0.390
X603	-0.127	0.390
X1308	0.127	0.391
X1103	-0.126	0.393
X1849	0.126	0.393
X1806	0.126	0.393
X687	0.126	0.395
X1941	0.126	0.395
X615	-0.126	0.396
X1614	0.125	0.397
X2168	0.125	0.397
X1117	-0.125	0.398
X1152	-0.125	0.398
X1414	0.125	0.398
X1251	0.125	0.400
X1817	0.124	0.400
X884	0.124	0.401
X1464	0.124	0.401
X1684	0.124	0.401
X1856	-0.124	0.402
X2349	0.124	0.402
X2276	0.124	0.403
X795	0.124	0.403
X738	-0.124	0.403
X1005	0.123	0.405
X1066	0.123	0.405
X1494	0.123	0.405
X1352	-0.123	0.405
X1813	0.123	0.405
X1607	0.123	0.405
X664	-0.123	0.405
X1347	0.123	0.406
X242	0.123	0.406
X858	0.123	0.406
X1506	0.123	0.407
X396	-0.123	0.407
X1600	0.122	0.408
X1212	0.122	0.408
X1631	0.122	0.409
X1561	-0.122	0.409
X1779	0.122	0.409
X1131	-0.122	0.409
X1890	0.122	0.409
X970	-0.122	0.410
X2217	-0.122	0.411
X1391	0.121	0.412
X2280	-0.121	0.412
X809	0.121	0.412
X861	0.121	0.413
X1260	-0.121	0.415
X591	-0.121	0.415
X1732	-0.121	0.415
X1121	-0.120	0.418
X658	0.120	0.418
X1345	-0.120	0.419
X1210	-0.120	0.419
X1504	0.119	0.420
X1133	0.119	0.421
X744	0.119	0.423
X397	-0.118	0.424
X860	0.118	0.425
X2050	0.118	0.425
X718	-0.118	0.426
X2071	0.118	0.427
X607	0.117	0.428
X869	-0.117	0.429
X701	0.117	0.430
X1228	-0.117	0.431
X1774	-0.117	0.431
X1224	0.116	0.432
X1233	0.116	0.433
X371	-0.116	0.433
X617	-0.115	0.436
X1040	0.115	0.437
X770	0.115	0.437
X1317	0.115	0.437
X1962	0.115	0.439
X1742	-0.114	0.440
X311	-0.114	0.440
X1264	-0.114	0.440
X662	-0.114	0.440
X1323	-0.114	0.442
X1398	-0.114	0.442
X2135	0.114	0.442
X2283	0.114	0.443
X953	0.113	0.445
X1125	0.113	0.446
X1666	-0.113	0.446
X833	-0.113	0.447
X1833	0.113	0.447
X2242	-0.113	0.448
X2285	0.112	0.448
X1665	-0.112	0.448
X817	0.112	0.448
X618	-0.112	0.448
X1822	0.112	0.448
X1298	0.112	0.450
X616	-0.112	0.450

X1093	-0.112	0.451
X1755	0.111	0.452
X1407	0.111	0.453
X1418	-0.111	0.453
X1675	0.111	0.453
X1359	0.111	0.454
X1262	-0.111	0.454
X1536	0.110	0.456
X994	-0.110	0.458
X599	0.110	0.458
X1428	-0.109	0.460
X1778	0.109	0.460
X1001	-0.109	0.463
X1527	0.109	0.464
X1265	-0.108	0.465
X727	-0.108	0.466
X2172	-0.108	0.466
X1537	-0.108	0.468
X688	-0.107	0.469
X605	-0.107	0.469
X1582	0.107	0.471
X2016	-0.107	0.472
X1021	-0.107	0.472
X1736	-0.106	0.473
X1981	-0.106	0.473
X1638	-0.106	0.473
X1555	0.106	0.474
X2116	-0.106	0.475
X1791	0.106	0.475
X1788	-0.106	0.476
X2238	0.105	0.478
X1261	0.105	0.478
X434	-0.105	0.480
X799	-0.105	0.480
X2151	-0.105	0.480
X620	-0.105	0.481
X324	-0.104	0.481
X606	-0.104	0.481
X1763	-0.104	0.481
X2048	-0.104	0.482
X1707	-0.104	0.482
X1211	0.104	0.483
X1651	0.104	0.484
X1160	-0.103	0.486
X745	0.103	0.486
X1372	0.103	0.486
X1515	0.103	0.487
X1831	0.103	0.487
X1095	-0.103	0.488
X810	0.103	0.489
X1635	-0.103	0.489
X1767	-0.103	0.489
X1659	-0.103	0.489
X1104	0.103	0.489
X1369	0.102	0.489
X1162	-0.102	0.490
X1468	0.102	0.490
X1749	0.102	0.491
X2032	-0.102	0.491
X1869	0.102	0.491
X797	-0.102	0.491
X825	0.102	0.492
X2232	0.102	0.493
X1313	-0.101	0.495
X937	0.101	0.496
X1293	0.101	0.497
X2295	0.100	0.498
X774	0.100	0.499
X1699	-0.100	0.499
X1269	0.100	0.499
X2219	-0.100	0.501
X1380	0.100	0.501
X1180	0.099	0.502
X1286	-0.099	0.503
X689	-0.099	0.503
X2351	-0.099	0.503
X1835	0.099	0.505
X2161	0.099	0.505
X892	-0.099	0.506
X1234	-0.099	0.506
X1164	-0.099	0.506
X1451	0.099	0.507
X646	-0.097	0.511
X1622	-0.097	0.512
X1288	-0.097	0.512
X255	-0.097	0.515
X1575	0.096	0.516
X721	-0.096	0.517
X1115	-0.096	0.517
X820	-0.095	0.521
X652	0.095	0.521
X907	-0.095	0.521
X2114	0.095	0.521
X1140	-0.095	0.521
X2123	0.095	0.522
X1708	-0.095	0.523
X1252	-0.095	0.524
X824	-0.095	0.524
X1492	-0.094	0.525
X1545	-0.094	0.525
X1865	-0.094	0.525
X1360	-0.094	0.527
X1065	0.094	0.527
X1605	0.094	0.528
X2269	-0.094	0.528
X807	-0.094	0.529
X1761	-0.093	0.530
X2333	-0.093	0.532
X1200	0.093	0.533
X1584	0.092	0.534
X1769	0.092	0.535
X872	-0.092	0.535
X2344	0.092	0.535
X1045	-0.092	0.536
X1009	-0.091	0.539
X808	0.091	0.539
X841	0.091	0.539
X728	-0.091	0.540
X453	-0.091	0.541
X990	-0.091	0.541
X1363	-0.091	0.542
X1406	0.090	0.544
X943	-0.090	0.544
X1553	0.090	0.544
X1514	0.090	0.544
X2296	-0.090	0.545
X1721	0.090	0.546
X1383	0.090	0.546
X1606	0.090	0.546
X1733	-0.089	0.548
X805	-0.089	0.548
X1720	-0.089	0.549

X2181	-0.089	0.550
X1731	0.089	0.550
X783	-0.088	0.551
X915	-0.088	0.553
X1424	0.088	0.554
X1294	-0.088	0.554
X1953	0.088	0.555
X1062	-0.088	0.555
X673	-0.087	0.556
X1085	-0.087	0.556
X926	0.087	0.558
X684	0.087	0.559
X1790	0.087	0.559
X955	-0.087	0.560
X1595	-0.086	0.560
X2307	0.086	0.561
X1686	0.086	0.561
X286	0.086	0.561
X726	-0.086	0.563
X1413	0.086	0.563
X1268	-0.086	0.564
X1315	-0.086	0.564
X2031	-0.085	0.565
X1517	0.085	0.566
X653	0.085	0.566
X1881	0.085	0.566
X1284	0.085	0.567
X750	0.085	0.567
X1116	-0.085	0.568
X1700	0.085	0.569
X2189	-0.085	0.569
X849	-0.084	0.570
X1473	0.084	0.571
X1344	0.084	0.571
X1661	-0.084	0.571
X1481	0.084	0.572
X1387	0.084	0.574
X1735	-0.083	0.576
X789	-0.083	0.576
X699	0.083	0.576
X1652	-0.083	0.577
X2325	-0.083	0.577
X739	-0.083	0.577
X1783	0.083	0.578

X2005	-0.083	0.578
X578	0.083	0.578
X2353	-0.082	0.579
X1236	-0.082	0.579
X1148	-0.082	0.580
X1760	0.082	0.582
X1863	-0.081	0.584
X1479	0.081	0.584
X1354	0.081	0.585
X1577	-0.081	0.585
X1124	-0.081	0.585
X1751	0.081	0.586
X2310	0.081	0.587
X965	-0.081	0.587
X1846	0.081	0.587
X2347	0.081	0.588
X2293	0.080	0.588
X1677	0.080	0.588
X1229	0.080	0.589
X1482	0.080	0.589
X806	-0.080	0.591
X755	-0.080	0.592
X1503	-0.080	0.592
X576	-0.080	0.592
X767	0.080	0.593
X412	-0.079	0.594
X1201	-0.079	0.594
X1207	0.078	0.598
X814	0.078	0.599
X1259	0.078	0.600
X2328	-0.078	0.601
X1242	-0.078	0.601
X842	0.078	0.601
X1051	-0.078	0.602
X1525	0.077	0.603
X1151	-0.077	0.605
X747	-0.077	0.605
X1864	-0.076	0.608
X1792	0.076	0.608
X1197	0.076	0.608
X2337	-0.076	0.609
X777	-0.076	0.609
X1534	-0.076	0.610
X682	-0.076	0.610

X1585	0.076	0.611
X782	-0.076	0.611
X1205	0.075	0.612
X1789	0.075	0.613
X752	-0.075	0.614
X1183	-0.075	0.615
X977	-0.075	0.615
X1122	-0.075	0.615
X1836	0.074	0.616
X2185	0.074	0.616
X2222	-0.074	0.618
X1939	0.074	0.619
X1649	-0.074	0.620
X1267	-0.074	0.621
X1589	-0.073	0.622
X1370	-0.073	0.622
X781	-0.073	0.623
X1838	0.073	0.623
X2013	-0.073	0.623
X1056	-0.073	0.625
X900	-0.072	0.626
X2287	0.072	0.626
X802	-0.072	0.628
X1640	-0.072	0.629
X1726	-0.072	0.630
X296	0.072	0.630
X1829	-0.071	0.632
X863	0.071	0.632
X622	-0.071	0.632
X1253	0.071	0.632
X1081	-0.071	0.633
X1532	0.071	0.634
X1547	-0.071	0.635
X375	-0.071	0.635
X1427	0.070	0.636
X1541	-0.070	0.637
X957	-0.070	0.637
X1385	-0.070	0.638
X1861	0.070	0.638
X871	-0.070	0.638
X935	0.070	0.638
X2033	-0.070	0.639
X222	0.070	0.639
X1187	0.070	0.639

X677	0.070	0.640
X2279	0.070	0.640
X1801	-0.070	0.640
X785	0.070	0.640
X1086	0.069	0.640
X2216	-0.069	0.641
X1897	0.069	0.641
X1554	0.069	0.642
X1060	0.069	0.643
X2099	0.069	0.644
X1034	0.069	0.644
X2318	-0.069	0.644
X2022	-0.069	0.645
X878	0.068	0.646
X2236	0.068	0.646
X604	-0.068	0.647
X1000	-0.068	0.648
X2297	-0.068	0.648
X1113	-0.068	0.648
X1038	-0.068	0.649
X1429	-0.068	0.649
X800	-0.068	0.649
X1982	0.068	0.649
X1373	0.068	0.649
X1270	0.068	0.650
X672	-0.067	0.650
X2108	0.067	0.651
X666	0.067	0.651
X1765	0.067	0.653
X803	-0.067	0.653
X697	-0.067	0.653
X1628	-0.067	0.654
X1807	0.067	0.655
X1436	0.066	0.655
X1072	-0.066	0.655
X1433	0.066	0.656
X1717	0.066	0.658
X709	-0.066	0.659
X1188	0.066	0.659
X1165	0.065	0.660
X2196	-0.065	0.660
X931	0.065	0.662
X698	-0.065	0.662
X1964	0.065	0.662

X1664	0.064	0.666
X2106	0.064	0.667
X1218	-0.064	0.667
X819	0.064	0.667
X1166	-0.064	0.667
X714	-0.064	0.667
X1365	-0.064	0.668
X890	-0.064	0.668
X1291	0.064	0.669
X952	0.063	0.670
X1900	0.063	0.671
X1815	0.063	0.672
X1204	0.063	0.672
X1375	0.063	0.673
X1442	0.063	0.673
X834	0.062	0.676
X879	-0.062	0.676
X1570	0.062	0.677
X2350	0.062	0.679
X1118	-0.061	0.681
X840	-0.061	0.682
X715	-0.061	0.683
X1127	-0.061	0.683
X1048	-0.061	0.684
X1766	-0.061	0.684
X2199	-0.061	0.684
X793	-0.061	0.684
X1459	-0.060	0.685
X830	0.060	0.685
X1012	0.060	0.685
X2098	0.060	0.685
X2028	-0.059	0.689
X1944	0.059	0.690
X2299	-0.059	0.691
X1857	-0.059	0.693
X1830	-0.059	0.693
X1971	-0.059	0.693
X1297	-0.058	0.695
X1058	-0.058	0.696
X1542	-0.058	0.696
X1457	-0.058	0.698
X2254	-0.058	0.698
X608	-0.058	0.698
X1434	0.058	0.699

X948	0.058	0.699
X846	-0.057	0.700
X1126	-0.057	0.701
X1279	0.057	0.703
X1221	-0.056	0.709
X405	0.055	0.710
X1318	-0.055	0.710
X1090	-0.055	0.711
X2255	0.055	0.712
X868	0.055	0.712
X1729	-0.055	0.712
X1627	0.055	0.713
X1295	0.055	0.713
X1371	-0.054	0.714
X655	-0.054	0.715
X1030	-0.054	0.717
X1198	-0.054	0.718
X1311	-0.053	0.720
X529	-0.053	0.721
X1381	-0.053	0.722
X1316	-0.053	0.724
X1419	0.052	0.728
X527	0.052	0.729
X2019	0.051	0.730
X894	-0.051	0.730
X571	0.051	0.731
X1879	0.051	0.731
X2148	-0.051	0.733
X2343	-0.051	0.733
X1940	0.051	0.733
X1793	0.051	0.734
X1703	-0.051	0.734
X2174	0.051	0.734
X1719	0.050	0.735
X1123	-0.050	0.735
X1671	-0.050	0.736
X1705	0.050	0.736
X1263	-0.050	0.737
X893	0.050	0.737
X2354	-0.050	0.737
X829	0.050	0.739
X870	-0.050	0.739
X1697	0.050	0.739
X918	0.050	0.739

X2338	-0.050	0.740
X1469	0.049	0.741
X1656	-0.049	0.742
X1689	-0.049	0.742
X1137	-0.049	0.743
X681	0.049	0.744
X1770	0.048	0.745
X1333	0.048	0.746
X1693	-0.048	0.746
X1669	0.048	0.747
X853	-0.048	0.748
X1305	-0.048	0.748
X1543	0.048	0.748
X1254	0.048	0.749
X632	-0.048	0.749
X2230	0.048	0.749
X491	0.047	0.750
X828	-0.047	0.750
X821	0.047	0.751
X1837	0.047	0.751
X1202	-0.047	0.752
X229	-0.047	0.752
X1176	0.046	0.756
X1592	0.046	0.756
X1007	0.046	0.757
X1425	0.046	0.759
X2136	-0.046	0.759
X378	-0.046	0.760
X1754	-0.045	0.761
X1688	-0.045	0.762
X1431	-0.045	0.762
X1006	-0.045	0.762
X1563	-0.045	0.763
X1574	-0.045	0.763
X1530	-0.045	0.764
X1146	0.045	0.764
X1526	0.045	0.764
X934	-0.045	0.764
X811	-0.045	0.764
X2241	-0.045	0.765
X1077	0.045	0.765
X768	-0.044	0.765
X1752	0.044	0.767
X671	-0.044	0.769
X719	0.044	0.769
X2154	-0.044	0.769
X1088	0.044	0.770
X1747	-0.043	0.770
X1453	0.043	0.771
X880	-0.043	0.772
X1216	-0.043	0.773
X827	0.043	0.774
X310	-0.043	0.775
X1423	-0.043	0.775
X735	-0.043	0.775
X1643	-0.042	0.777
X2193	0.042	0.778
X393	0.042	0.779
X1098	0.042	0.779
X1182	0.042	0.779
X909	-0.042	0.780
X1199	-0.042	0.780
X792	-0.041	0.782
X908	-0.041	0.785
X732	0.041	0.785
X2179	-0.041	0.785
X1003	0.041	0.785
X903	0.041	0.786
X1948	0.040	0.787
X1826	0.040	0.789
X2138	-0.040	0.789
X1456	0.040	0.789
X501	-0.040	0.790
X459	0.039	0.791
X2072	-0.039	0.793
X2180	-0.039	0.794
X1132	0.039	0.794
X873	-0.038	0.797
X1658	0.038	0.797
X2326	-0.038	0.797
X1435	0.038	0.798
X1037	-0.038	0.799
X1784	0.038	0.799
X989	-0.038	0.799
X2041	-0.038	0.799
X997	0.038	0.800
X1493	-0.038	0.801
X1544	0.037	0.801
X2277	0.037	0.801
X2267	0.037	0.802
X1208	0.037	0.803
X639	0.037	0.804
X1566	0.037	0.804
X713	-0.037	0.804
X1241	0.037	0.806
X1326	-0.036	0.806
X644	-0.036	0.807
X1147	-0.036	0.807
X769	-0.036	0.807
X1602	-0.036	0.810
X1150	0.036	0.811
X956	-0.035	0.812
X1654	0.035	0.814
X995	-0.035	0.816
X804	0.035	0.816
X1432	-0.034	0.817
X2253	0.034	0.818
X2097	-0.034	0.818
X1329	0.034	0.818
X916	-0.034	0.819
X1415	-0.034	0.819
X1667	0.034	0.819
X1734	0.034	0.820
X1257	0.034	0.821
X1875	-0.034	0.822
X857	-0.034	0.822
X1594	-0.034	0.822
X1714	0.033	0.822
X818	0.033	0.823
X1583	-0.033	0.824
X2021	0.033	0.825
X1629	-0.033	0.826
X1074	-0.032	0.828
X866	0.032	0.829
X1420	0.032	0.829
X1186	-0.032	0.830
X1119	-0.032	0.832
X2210	0.031	0.833
X1772	-0.031	0.834
X1230	0.031	0.834
X1495	-0.031	0.835
X1616	0.031	0.836

X1368	-0.031	0.836
X1620	0.030	0.838
X1226	0.030	0.840
X1522	-0.030	0.840
X1239	-0.030	0.840
X1145	-0.030	0.840
X1519	-0.030	0.842
X660	-0.030	0.842
X1237	-0.030	0.842
X914	0.030	0.842
X724	-0.030	0.843
X1386	-0.029	0.844
X1292	-0.029	0.844
X2213	0.029	0.845
X775	-0.029	0.845
X1079	-0.029	0.845
X1704	0.029	0.847
X2105	-0.029	0.848
X1615	0.028	0.849
X1194	-0.028	0.849
X2128	0.028	0.849
X1728	0.028	0.849
X2130	-0.028	0.851
X2264	-0.028	0.852
X1795	0.028	0.852
X2256	0.028	0.853
X2201	-0.028	0.854
X1694	0.027	0.855
X930	-0.027	0.856
X978	0.027	0.856
X1560	-0.027	0.857
X2212	-0.027	0.858
X1483	-0.027	0.859
X1028	0.026	0.859
X961	-0.026	0.859
X1185	0.026	0.861
X2182	-0.026	0.863
X1321	-0.026	0.863
X1485	0.026	0.863
X1812	0.026	0.863
X901	-0.026	0.864
X619	0.026	0.864
X1355	-0.026	0.864
X206	-0.025	0.865
X1334	0.025	0.867
X1089	0.025	0.868
X717	-0.025	0.869
X1275	-0.025	0.869
X2169	0.025	0.869
X1862	0.024	0.870
X815	-0.024	0.872
X1193	0.024	0.872
X1050	-0.024	0.873
X731	-0.023	0.875
X322	-0.023	0.875
X1256	-0.023	0.877
X532	-0.023	0.877
X1608	0.023	0.877
X1696	-0.023	0.878
X851	-0.023	0.879
X1342	-0.023	0.880
X1901	-0.022	0.880
X1102	-0.022	0.881
X1512	-0.022	0.881
X881	-0.022	0.881
X2336	-0.022	0.885
X933	0.022	0.885
X1184	-0.022	0.885
X2202	0.022	0.885
X734	0.021	0.886
X1157	-0.021	0.886
X917	0.021	0.887
X1350	-0.021	0.888
X1565	0.021	0.888
X1509	-0.020	0.891
X1636	-0.020	0.892
X1478	-0.020	0.892
X865	0.020	0.895
X2314	0.020	0.895
X1740	-0.020	0.895
X1235	-0.020	0.896
X1680	-0.019	0.896
X1320	-0.019	0.898
X2188	0.019	0.898
X1709	0.019	0.899
X1272	0.019	0.899
X1109	-0.019	0.899
X958	-0.019	0.900
X1155	-0.019	0.901
X2070	-0.018	0.902
X850	-0.018	0.903
X1488	-0.018	0.903
X2152	-0.018	0.906
X813	0.018	0.906
X1416	-0.017	0.907
X2294	0.017	0.909
X742	-0.017	0.909
X2308	-0.017	0.910
X790	0.017	0.910
X2012	-0.017	0.911
X1075	0.017	0.911
X912	-0.017	0.911
X1558	-0.016	0.912
X1745	0.016	0.914
X2278	0.016	0.914
X1008	0.016	0.915
X1855	0.016	0.917
X1225	0.015	0.918
X1324	-0.015	0.919
X2171	-0.015	0.920
X1302	0.015	0.920
X1701	-0.015	0.921
X1130	0.015	0.921
X2284	0.015	0.921
X1203	0.015	0.922
X2233	0.014	0.925
X1476	0.014	0.925
X1120	0.014	0.927
X1535	-0.014	0.927
X1882	0.013	0.928
X823	-0.013	0.929
X897	-0.013	0.930
X716	0.013	0.932
X1644	-0.013	0.933
X882	-0.012	0.933
X1213	-0.012	0.934
X675	-0.012	0.934
X743	-0.012	0.935
X1988	0.012	0.938
X1674	0.012	0.938
X1936	0.011	0.939
X1487	-0.011	0.940

X1511	-0.011	0.940
X1219	0.011	0.941
X1972	-0.011	0.941
X2073	-0.011	0.944
X2303	0.010	0.944
X1744	0.010	0.944
X794	0.010	0.944
X831	-0.010	0.945
X1232	0.010	0.945
X986	-0.010	0.946
X867	0.010	0.947
X648	-0.010	0.948
X1591	0.010	0.948
X1516	0.010	0.949
X2020	0.009	0.950
X1041	-0.009	0.953
X1220	-0.009	0.953
X1061	-0.008	0.955
X2042	0.008	0.955
X2119	-0.008	0.955
X1546	-0.008	0.958
X1702	0.008	0.958
X1330	0.008	0.958
X1149	-0.008	0.958
X1351	0.008	0.959
X1019	-0.008	0.960
X1505	-0.007	0.960
X2157	-0.007	0.962
X482	0.007	0.962
X1138	0.007	0.962
X954	0.007	0.962
X2146	-0.007	0.963
X1287	-0.007	0.963
X1854	0.007	0.964
X1786	0.007	0.964
X1107	-0.007	0.965
X992	0.006	0.966
X987	-0.006	0.966
X1739	-0.006	0.967
X1501	0.006	0.967
X896	0.006	0.968
X1490	0.006	0.970
X771	-0.005	0.971
X1281	0.005	0.973
X1361	-0.005	0.973
X875	0.005	0.973
X1556	-0.005	0.973
X355	0.005	0.973
X1513	-0.005	0.974
X836	0.005	0.975
X1069	-0.004	0.976
X812	0.004	0.976
X1746	0.004	0.976
X1586	0.004	0.977
X1101	-0.004	0.977
X1181	-0.004	0.978
X1706	-0.004	0.979
X2164	0.004	0.979
X2301	-0.004	0.981
X1091	0.003	0.982
X1550	0.003	0.982
X1641	0.003	0.982
X876	0.003	0.982
X1753	0.003	0.986
X1064	-0.003	0.986
X1601	0.002	0.987
X1083	0.002	0.988
X636	-0.002	0.989
X2101	-0.002	0.990
X1965	-0.002	0.990
X1274	-0.002	0.990
X1989	-0.002	0.991
X2330	0.002	0.991
X1332	0.002	0.991
X839	0.002	0.991
X949	0.002	0.991
X1874	0.001	0.993
X761	-0.001	0.994
X1540	0.001	0.994
X1660	-0.001	0.994
X1174	0.001	0.995
X2103	0.001	0.996
X1876	0.001	0.996
X2124	-0.001	0.997
X1343	0.000	0.998
X1417	0.000	0.999
X1800	0.000	0.999
X1576	0.000	1.000

Appendix 4

Mixed effects regression model results for 2DGE protein spots with ventricular expansion whilst controlling for age, gender, education, BMI, cholesterol, and *APOE* ε4 status. Results highlighted in red are statistically significant ($p<0.05$)

Spot ID	Coefficient	*p* value
X1595	-5622.09	0.000543
X1948	-10591.9	0.001269
X1406	-6316.04	0.003753
X767	-4875.01	0.004717
X1068	6049.642	0.00568
X1586	-4200.86	0.006049
X1643	5407.359	0.009337
X1470	-4813.45	0.015904
X1351	4521.493	0.021022
X1412	-3934.76	0.021512
X1590	-3594.51	0.025876
X865	-5258.35	0.025906
X2174	4028.063	0.026012
X988	-4212.2	0.026781
X471	4921.971	0.027109
X2292	4607.122	0.028906
X1435	-3311.15	0.032718
X1837	4719.904	0.033362
X1495	-4054.4	0.033829
X2157	7679.915	0.034074
X1297	5368.935	0.036631
X1284	3836.693	0.038436
X1165	5265.663	0.041349
X993	-4304.7	0.041744
X1624	4594.943	0.044159
X1694	-3550.88	0.045329
X432	4430.796	0.045723
X1550	-6216.19	0.046278
X1689	-3310.46	0.046992
X1050	6968.624	0.047168
X1156	4743.363	0.047843
X1085	7165.327	0.04795
X1501	-3377.37	0.048327
X594	-3201.58	0.049544
X1022	5436.878	0.049806
X2273	-3992.37	0.050451
X1076	5985.901	0.053714
X1094	6383.062	0.054898
X1383	4246.399	0.056165
X1157	4739.194	0.056975
X675	3515.251	0.05819
X974	-2931.14	0.058468
X1072	-3797.68	0.058818
X1953	-5191.78	0.058825
X1098	8977.226	0.063296
X655	-2911.18	0.063617
X1393	-4428.25	0.063666
X871	-4058.53	0.064081
X1185	4359.69	0.064508
X857	-3756.79	0.064711
X707	-3565.94	0.0648
X2271	-3281.74	0.065169
X1138	-2827.22	0.06519
X2041	3378.931	0.066164
X1183	4461.255	0.066275
X1659	-3287.81	0.066621
X1211	3773.424	0.066699
X873	-4842.2	0.067062
X899	5354.945	0.067491
X1623	-3985.04	0.068188
X1218	-2835.35	0.0683
X2239	3928.585	0.068727
X1735	-4612.22	0.069243
X1729	6673.395	0.069594
X599	-4935.04	0.070069
X1392	-3829.12	0.071827
X2141	-4465.62	0.07234
X1450	-3333.22	0.072773
X1585	-5107.03	0.07397
X936	-2528.91	0.075443
X1180	3802.491	0.075855
X602	-3920.61	0.076899
X1621	-4451.58	0.077248
X1525	-3161.23	0.078128

X1215	2990.882	0.078762
X1790	3104.454	0.078937
X952	-2193.71	0.079183
X2328	-3105.4	0.081037
X1635	-4043.76	0.081694
X1617	-4767.63	0.082
X1229	-4595.71	0.083981
X1019	5080.788	0.086018
X2256	3708.893	0.086186
X1756	5591.949	0.086814
X1135	8381.993	0.088321
X1075	-3150.21	0.088725
X1439	-3042.39	0.09082
X1414	3735.296	0.091499
X1212	3618.714	0.091817
X1442	-4734.79	0.09221
X657	-2759.94	0.094686
X1765	-5172.27	0.094989
X911	4231.903	0.097169
X823	-2970.18	0.097611
X1147	6903.477	0.098462
X1549	5091.182	0.098489
X1090	6058.121	0.100084
X690	-3417.51	0.101038
X1714	-5532.08	0.102309
X1615	-3300.13	0.102452
X1739	6618.229	0.102475
X1201	-2721.57	0.102508
X1315	-2240.35	0.103523
X1691	-3562.1	0.104178
X1003	-2118.79	0.104183
X1184	3787.602	0.104398
X2196	-3485.41	0.104554
X1732	4893.654	0.105406
X2338	3175.738	0.10627
X2171	4218.307	0.106934
X879	-3462.87	0.107372
X1930	3537.058	0.107707
X1010	-2437.41	0.108848
X1687	-3229.52	0.109378
X393	-3156.24	0.110197
X1034	4056.637	0.110681
X1309	3197.237	0.111774
X2188	6251.088	0.112486
X2161	-3144.95	0.113426
X1664	-4195.7	0.114741
X1620	-3118.13	0.115314
X1216	-2479.18	0.115822
X891	-2414.09	0.119582
X1344	2243.964	0.120368
X1343	2378.565	0.120973
X1152	3892.141	0.121918
X712	2724.017	0.123447
X673	-3050.23	0.125584
X2213	-4598.99	0.125859
X1115	-2443.74	0.126276
X1294	-4071.24	0.126503
X622	2220.947	0.126755
X1418	-2841.41	0.127352
X2147	5830.636	0.129884
X1166	5533.744	0.130048
X1761	3647	0.132524
X1341	5236.845	0.133771
X1690	-4462.8	0.135347
X2214	4881.636	0.135456
X1355	2556.09	0.137334
X2049	2282.706	0.137501
X878	-3864.59	0.138908
X1198	-3355.1	0.139836
X839	-5687.82	0.142806
X2217	4357.275	0.142866
X1140	5220.295	0.143259
X1704	4457.621	0.145279
X1703	4668.424	0.146002
X1553	-2596.94	0.147118
X2102	2000.333	0.147341
X1759	-3034.48	0.147876
X2287	2940.228	0.148426
X1537	-3015.06	0.148558
X779	-3219.45	0.148576
X714	3239.88	0.149491
X772	-4290.46	0.150705
X1715	4688.973	0.152586
X626	2085.236	0.155937
X1244	-3302.1	0.157835
X1777	2892.195	0.158515
X2025	2268.061	0.15894
X1752	5050.394	0.15916

X783	-2117.5	0.159955
X2245	3940.864	0.160611
X1151	5991.582	0.161403
X1028	4430.791	0.162016
X750	-2260	0.162309
X2119	4020.342	0.162854
X1728	5240.548	0.163316
X2177	3281.673	0.16359
X670	-2514.18	0.163691
X2098	6309.752	0.165729
X973	-3634.06	0.166031
X1317	2841.523	0.166322
X1260	-2780.7	0.167895
X1519	-2104.38	0.168784
X709	2962.913	0.169861
X968	-3746.68	0.170181
X1042	-3305.25	0.170873
X1774	2628.187	0.171658
X1817	2778.795	0.173151
X652	-2183.73	0.173919
X2114	1819.101	0.174896
X2111	3933.008	0.176926
X1496	4147.424	0.177281
X1111	-1931.33	0.178214
X667	-2645.53	0.181959
X1356	1943.803	0.182025
X1512	3385.594	0.182443
X681	3333.105	0.183536
X1959	2587.052	0.183989
X953	-1530.89	0.184953
X1262	-3179.47	0.185071
X2347	-2783.41	0.185134
X2043	1995.551	0.185336
X644	-2189.23	0.185527
X1073	3130.145	0.186706
X1368	-1839.67	0.186884
X1391	2767.842	0.189369
X1645	2996.761	0.189879
X1304	-1588.44	0.190136
X1246	2367.352	0.190324
X597	-2907.46	0.19048
X1754	4977.321	0.190815
X1126	4846.904	0.191177
X2198	-2790.82	0.192694
X965	-3848.85	0.19396
X1614	-3225.18	0.194225
X576	-2422.78	0.194312
X1273	3810.71	0.195524
X1302	3957.764	0.195898
X1552	-3969.05	0.19718
X403	-2716.05	0.198386
X2330	3129.598	0.200209
X1503	-2593.51	0.200527
X2233	2380.648	0.201066
X634	1707.635	0.201649
X1706	3901.194	0.202139
X2128	-2507.83	0.202885
X641	1615.871	0.203661
X620	1685.886	0.204359
X676	3286.244	0.204477
X1307	4746.029	0.205224
X890	-2650.5	0.205906
X1828	-3301.98	0.206215
X2005	2791.939	0.206259
X1818	2642.95	0.207156
X2203	-2618.2	0.207166
X1741	4644.845	0.207518
X2040	1718.39	0.208774
X1527	-2980.28	0.20901
X824	-3285.47	0.209484
X2344	2556.709	0.209777
X1482	-2392.38	0.209793
X1117	-1824.61	0.209878
X976	-3011.43	0.210141
X1091	5148.262	0.210364
X904	3431.283	0.21038
X2140	-2765.06	0.210397
X578	-2730.13	0.210698
X1854	2563.808	0.212484
X1811	3947.106	0.213811
X829	-2252.98	0.214408
X1489	-2386.42	0.215011
X1705	3619.708	0.21708
X721	1948.564	0.21814
X2024	1907.046	0.218679
X1397	-2243.29	0.219651
X731	3296.137	0.220045
X1815	2433.939	0.220086

X2072	-2983.48	0.220309
X868	-2911.91	0.221686
X1106	4105.781	0.222282
X808	-2266.86	0.222285
X913	4115.099	0.222356
X2033	3384.864	0.222885
X1131	6203.287	0.223098
X1679	-2741	0.223594
X2216	4489.522	0.224022
X1121	4075.36	0.224388
X1148	5461.285	0.225078
X1139	5576.388	0.228878
X791	-2235.21	0.229318
X812	1859.643	0.230902
X624	1517.513	0.230925
X1971	2837.168	0.231424
X1485	2933.773	0.231859
X825	-2112.03	0.233064
X734	3656.823	0.233106
X2044	1482.433	0.233311
X1026	-4303.54	0.233866
X738	-2347.22	0.235203
X621	1877.696	0.235367
X1637	-2506.26	0.236275
X918	4061.227	0.236512
X2028	2651.976	0.236521
X1897	-3205.91	0.237236
X2318	2410.364	0.237398
X1825	2214.846	0.238777
X807	-2286.37	0.239244
X1644	-2570.81	0.240565
X1657	2754.885	0.241079
X1518	-3769.15	0.24244
X1582	-2810.02	0.242526
X1251	3020.872	0.243252
X1232	2108.589	0.243666
X909	-1741.75	0.245045
X2181	-1707.52	0.2459
X1227	2116.013	0.246048
X1141	4712.193	0.246418
X1675	3021.092	0.2466
X1462	-2297.61	0.246809
X2048	1164.905	0.250424
X378	2134.121	0.251358
X1398	-1971.66	0.252123
X1434	-2475.89	0.25225
X589	-2313.85	0.254831
X1310	2059.026	0.255658
X1326	1990.56	0.255953
X1807	2026.4	0.256626
X1247	-2148.69	0.257735
X2332	1589.762	0.258571
X1848	-3387.82	0.25904
X2045	1587.976	0.259707
X2333	1929.163	0.260781
X1018	3519.352	0.26136
X1401	-2019.42	0.261366
X1048	3965.868	0.261431
X558	-2514.03	0.261521
X1127	4227.179	0.26207
X977	-2411.34	0.262662
X1431	-1945.58	0.263217
X1014	2837.694	0.263552
X1371	-2811.18	0.264371
X1861	2201.678	0.265099
X1556	-1754.37	0.267103
X1070	2350.805	0.267324
X2152	1934.529	0.268231
X845	-1930.33	0.268653
X1083	3024.441	0.268757
X1782	2820.086	0.26894
X1661	1987.346	0.270477
X994	-3030.76	0.272199
X1958	2345.55	0.272378
X1583	-2295.94	0.273913
X1755	3435.717	0.274082
X1680	-2207.14	0.275013
X970	-2591.94	0.275186
X939	1282.338	0.275577
X1012	-1524.62	0.275604
X802	-1795.66	0.276402
X1720	-2697.12	0.279758
X755	-2752.18	0.281395
X1733	-2634.27	0.282059
X1222	-1819.39	0.282687
X688	-2238.12	0.283638
X2351	1748.033	0.28425
X2297	-1478.94	0.284687

X1594	2650.387	0.28708
X1122	4010.704	0.287114
X910	-2936.52	0.287613
X1267	-2059.29	0.288705
X2185	2733.821	0.290591
X1008	-1965.68	0.291142
X1059	-1730.23	0.29115
X1093	3718.866	0.292715
X1064	-2460.43	0.293461
X1033	2439.563	0.293508
X682	-2103.55	0.295472
X2210	-2628.32	0.295611
X1054	2321.932	0.296475
X1678	-2228	0.299486
X1255	2675.541	0.299632
X811	1647.571	0.300528
X892	-1708.94	0.300646
X1515	2391.69	0.302889
X1086	4694.336	0.303107
X692	-1873.04	0.303848
X1275	-2745.56	0.304391
X1256	2410.575	0.304409
X713	-1641.57	0.304547
X1669	2624.171	0.305801
X1036	1013.304	0.306422
X1652	1693.032	0.306515
X1405	-2689.41	0.306901
X803	-2742.9	0.308252
X648	2434.186	0.309354
X2118	3064.384	0.30995
X2281	-1721.16	0.310973
X1089	2338.095	0.311284
X1517	-2770.12	0.311355
X1555	-2345.13	0.312946
X1736	3541.375	0.314804
X1196	-1519.91	0.315811
X659	-2350.2	0.316473
X1303	2294.154	0.317093
X603	-1833.79	0.317502
X1570	2256.143	0.31768
X1598	2432.448	0.317847
X2226	-1175.71	0.31838
X1713	-2080.11	0.318408
X1763	2938.645	0.318428
X861	-2104.2	0.318824
X1605	2800.42	0.319685
X1333	3120.585	0.321209
X1023	2335.373	0.321714
X1557	-3112.95	0.321752
X2190	2148.547	0.322648
X972	-2546.65	0.325638
X2063	-2033.53	0.326213
X680	1429.118	0.326228
X1700	2654.658	0.327334
X1130	3359.859	0.328021
X1037	2783.79	0.328776
X1390	-1911.99	0.329814
X1658	-2263.7	0.33265
X1174	2236.075	0.332701
X1528	-2184.29	0.332921
X687	-2004.23	0.333611
X2276	-2731.22	0.333784
X1562	-1938.86	0.334453
X2199	1474.933	0.335653
X636	-1580.78	0.335712
X587	-1744.02	0.336703
X609	1854.642	0.33703
X491	-2629.73	0.338093
X954	-1295.03	0.338135
X1381	-1245.56	0.338715
X2336	2215.33	0.339835
X951	-1301.63	0.339838
X1874	-1883.17	0.340397
X1981	-1641.47	0.341088
X1463	-1697.86	0.342929
X387	1328.371	0.343008
X1771	-1868.91	0.343486
X1753	4320.955	0.343608
X2104	2311.911	0.344329
X1407	-2264.33	0.344468
X453	2215.699	0.346032
X1474	-2541.74	0.347765
X1619	-2225.94	0.350342
X1723	1994.852	0.350348
X1654	-2033.36	0.352999
X635	1243.48	0.353633
X836	-1745.31	0.355307
X617	1390.475	0.355469

X1879	-1764.67	0.357497
X666	-1345.93	0.357897
X1436	-2068.32	0.358963
X1254	-2057.39	0.35947
X797	-1632.22	0.35965
X874	-1977.67	0.359971
X1150	-2367.91	0.360092
X1107	4231.851	0.360249
X1599	-2643.43	0.361301
X646	-1908.73	0.363838
X1701	2367.159	0.364366
X2350	2494.914	0.364553
X1149	2207.843	0.366759
X2343	3334.459	0.368704
X2106	3110.583	0.369211
X1065	1810.386	0.369253
X745	-1523.34	0.370128
X1129	-2558.5	0.372134
X855	-1604.14	0.372268
X1481	2016.209	0.373223
X1650	-2018.91	0.37391
X1925	1913.625	0.373929
X2120	2567.99	0.374135
X1261	-2389.41	0.375547
X629	1570.573	0.375859
X989	-1777.12	0.377841
X2103	942.3249	0.378033
X1088	3111.193	0.378836
X1788	2000.973	0.379048
X724	2763.2	0.379112
X1514	1837.818	0.379418
X1566	-1662.69	0.380194
X1305	2036.075	0.380301
X2285	1396.131	0.380337
X1543	-1734.21	0.380413
X2169	3019.316	0.380893
X1787	1410.774	0.381077
X1573	-1504.78	0.382489
X2218	-2714.31	0.383226
X1271	1976.409	0.383581
X1521	-1592.92	0.384597
X1780	-2249.08	0.385232
X1544	-1632.63	0.385923
X1363	-1767.26	0.387094
X2314	1843.46	0.387332
X1146	-1913.29	0.388643
X778	2467.935	0.390233
X931	-1156.58	0.390848
X2310	-1970.33	0.390913
X1584	-1915.48	0.391041
X2242	-2608.25	0.391211
X2124	2354.928	0.393026
X867	-1729.64	0.39308
X1274	2282.306	0.393643
X1001	-2002.65	0.393926
X1466	-1890.56	0.39407
X1361	-1794.11	0.394328
X1419	2265.739	0.395077
X1006	1355	0.396512
X625	1272.748	0.396737
X653	-1477.91	0.398074
X1917	-2511.91	0.39818
X1057	1458.044	0.398808
X2295	1764.272	0.399916
X2082	-2098.94	0.400699
X826	-2334.6	0.400972
X885	1607.467	0.401925
X785	-1281.86	0.401989
X1375	-1617.92	0.402442
X640	967.6473	0.403499
X1950	-1913.11	0.403939
X1021	2235.492	0.405046
X1170	-1661.87	0.407887
X1548	2516.47	0.408226
X1791	1233.3	0.408232
X1926	1881.972	0.408525
X2215	2638.144	0.411293
X580	-1257.63	0.411352
X1269	-2017	0.412946
X1745	-1394.72	0.414317
X2222	1194.647	0.414588
X719	-1207.65	0.414844
X1189	1937.234	0.414944
X1642	-1674.07	0.416223
X2230	-1938.53	0.416534
X1499	-1157.43	0.416829
X963	-2065.26	0.41696
X1766	2393.811	0.417722

X905	2523.432	0.419092
X1591	1636.899	0.419337
X950	-1079.49	0.420294
X2202	1731.96	0.420732
X769	-1745.53	0.421011
X1677	-1560.8	0.423062
X1627	-1949.47	0.423313
X1719	2212.736	0.423718
X598	-1617.25	0.423752
X434	1775.134	0.423831
X985	-1554.35	0.423941
X2274	1315.876	0.423959
X545	-1975.08	0.424893
X1287	1334.882	0.426113
X1823	1395.764	0.426855
X1708	-1988.57	0.426991
X1671	-1475.42	0.427194
X998	-1821.56	0.429141
X2136	-1345.51	0.429646
X2275	-1663.74	0.429987
X1321	-1713.4	0.430884
X619	-1325.35	0.430975
X860	-1769.77	0.431293
X1427	-2342.54	0.431656
X2313	1873.622	0.43211
X804	-1535.16	0.432298
X948	1296.677	0.434165
X1056	1161.465	0.434533
X1760	1727.837	0.436599
X1030	1871.6	0.437176
X311	1414.386	0.437957
X1693	-2053.4	0.438361
X1505	-1234.72	0.438871
X2354	1559.797	0.439229
X1535	-1433.62	0.43943
X1069	-1429.07	0.44026
X2151	1277.627	0.440325
X229	-1792.72	0.440852
X2036	-1834.91	0.440921
X1123	3028.259	0.440969
X1296	-2515.44	0.441318
X1604	1840.282	0.441441
X672	-1629.34	0.442072
X2264	1689.427	0.4421
X1810	1099.415	0.442203
X2023	1407.94	0.442716
X1281	1219.172	0.442813
X774	2133.067	0.443189
X2088	-1746.97	0.44544
X2137	1648.772	0.445984
X1716	-1541.13	0.446406
X2231	4348.562	0.447478
X1830	1709.266	0.44793
X697	-1447.66	0.448887
X1592	1553.432	0.449408
X1540	1504.683	0.451369
X1334	1609.571	0.453004
X1724	-1826.02	0.455687
X532	1313.359	0.456171
X2085	3809.256	0.456365
X2335	1176.412	0.457177
X1589	-1197.43	0.458569
X917	1199.631	0.460294
X1510	-1924.32	0.460725
X1289	1466.479	0.462204
X886	-2655.52	0.46271
X1268	1035.881	0.462971
X322	-1266.24	0.463544
X2337	-1154.31	0.464705
X1649	-1570.69	0.465306
X992	-1432.99	0.465881
X1009	-2775.3	0.466182
X1725	-1727.67	0.466188
X1409	-1617.29	0.466574
X1454	-1887.69	0.467417
X1338	1302.039	0.468616
X184	1537.25	0.468771
X1270	-1265.32	0.468794
X1053	1500.555	0.46929
X1377	1246.774	0.469581
X765	1816.816	0.470961
X1041	1823.204	0.472277
X484	-1967.27	0.47481
X1345	1034.248	0.476525
X1038	1093.806	0.476984
X1520	-1212.37	0.477694
X1767	1459.326	0.478122
X1613	-1136.29	0.478547

X1095	1642.981	0.478582
X604	1250.685	0.479915
X1113	1344.215	0.480037
X1362	-2007.63	0.481212
X1990	1279.086	0.481247
X830	-1278.41	0.481561
X2204	2096.268	0.481638
X661	1420.437	0.482522
X1744	2045.438	0.483153
X1440	1243.574	0.484341
X1283	1983.75	0.486281
X1846	1281.473	0.486774
X1234	-1583.06	0.487036
X1162	-1845.78	0.489079
X1597	1890.091	0.489146
X2209	1954.969	0.49018
X844	1290.253	0.490991
X1581	1524.04	0.491219
X1738	2202.317	0.492521
X1692	-1789.37	0.492618
X851	3463.658	0.493121
X753	1487.426	0.493684
X1964	1524.685	0.494475
X627	1092.562	0.494695
X1628	-1938.53	0.495054
X1182	1446.399	0.49625
X908	-1654.51	0.497586
X725	-1334.98	0.497646
X527	-1377.63	0.498474
X606	1013.217	0.49878
X2254	-1000.34	0.499435
X1108	2064.669	0.50032
X1674	-1884.57	0.500457
X2235	1686.591	0.50181
X781	-1155.63	0.501866
X1029	1165.948	0.502202
X1773	-1303.72	0.502561
X615	-1120.64	0.503893
X2127	-1353.25	0.504552
X978	-1547.16	0.504595
X1331	1400.015	0.505853
X1421	-1257.95	0.506138
X422	1029.689	0.506413
X1191	2001.159	0.507937
X501	1647.844	0.508544
X2006	1231.243	0.50916
X2125	1440.022	0.510562
X1015	1358.479	0.510936
X2053	-1244.96	0.51095
X645	-1018.11	0.512714
X699	-1321.36	0.516477
X810	1257.016	0.517199
X272	-1223.94	0.518775
X1052	1855.541	0.520083
X1277	-1510.61	0.522512
X1109	-1062.89	0.522674
X2278	1254.863	0.523433
X1963	1608.644	0.525146
X590	1649.602	0.526499
X1299	1226.062	0.526686
X893	-1392.21	0.527986
X2155	-1081.82	0.530141
X809	1069.837	0.530228
X1648	1311.852	0.530417
X1045	-1339.48	0.531077
X848	1210.675	0.531129
X815	-951.612	0.531674
X1785	1227.722	0.53423
X907	1822.977	0.534816
X1793	-1035.06	0.535486
X255	-1567.27	0.535608
X1779	1452.691	0.535766
X1369	-1252.41	0.535845
X1717	1434.516	0.536071
X1058	1366.088	0.537934
X818	-1162.02	0.538208
X902	-1050.76	0.538912
X1831	863.6649	0.540632
X628	-1030.98	0.540903
X2311	1500.799	0.541523
X1832	-1687.17	0.542742
X766	1377.015	0.543067
X1686	-1552.56	0.543129
X1486	1619.487	0.543814
X1430	1202.737	0.544245
X1875	-1220.36	0.546018
X1278	1412.453	0.546437
X286	-994.124	0.546524

X584	-1117.19	0.546801
X706	-1346.83	0.548248
X1423	-949.085	0.549758
X679	-1244.61	0.549819
X1688	-952.851	0.550473
X938	-605.48	0.550531
X770	-2322.34	0.550856
X1805	1617.422	0.553519
X961	792.2874	0.554234
X1813	1042.975	0.554595
X991	-1487.58	0.555069
X1792	-1635.97	0.555288
X1078	-1090	0.555999
X1410	-1376.4	0.556847
X1360	-1528.7	0.558874
X805	-1215.06	0.559617
X757	-1238.03	0.560801
X1168	943.1871	0.561169
X1663	-1037.32	0.563063
X684	-1061.64	0.563331
X2353	-931.064	0.563504
X1795	3144.77	0.565205
X1972	1583.82	0.565756
X1007	-1162.54	0.566433
X1538	1391.058	0.567028
X642	818.269	0.567205
X788	-1427.38	0.567401
X1855	1040.453	0.56873
X2232	-1072.29	0.569492
X1318	-1109.87	0.569788
X2317	-1277.94	0.569801
X1292	-1178.32	0.570159
X1936	-1769.45	0.570277
X1892	-1631.56	0.570444
X2071	-1470.78	0.570832
X820	-1012.75	0.572702
X1154	1636.585	0.572912
X840	2963.836	0.573422
X966	-1708.06	0.573823
X916	909.326	0.573938
X1451	-1078.25	0.574382
X2031	1200.163	0.575942
X1746	1866.932	0.575945
X1087	1927.132	0.576358
X1220	955.9944	0.576776
X1982	-1048.71	0.576899
X1856	-916.438	0.577023
X1312	-1158.87	0.577159
X771	1202.803	0.577353
X1286	1185.08	0.578167
X2109	1272.387	0.579317
X1968	1473.698	0.580409
X1208	-1313.7	0.581246
X1457	1099.863	0.581487
X638	-916.616	0.582978
X1380	-865.312	0.584313
X1429	-1033.05	0.584759
X1379	-1069.59	0.585287
X662	1200.699	0.585735
X1241	1056.489	0.586317
X1602	1200.394	0.586386
X799	-1089.85	0.586651
X735	1873.619	0.586684
X1228	710.8075	0.587333
X1651	-1710.82	0.587467
X1636	1208.567	0.587576
X1480	-989.603	0.587802
X733	1065.167	0.587952
X1579	2001.115	0.588716
X1298	-1068.5	0.588924
X1017	1432.03	0.589235
X798	900.3707	0.589911
X1547	-1079.97	0.590008
X1159	1291.902	0.590717
X1145	-945.171	0.590839
X1016	1624.586	0.591117
X1339	1048.35	0.593095
X903	1421.102	0.594997
X858	2908.416	0.595491
X2081	3301.727	0.595729
X2095	1348.009	0.596085
X1600	1527.408	0.596478
X2299	-1186.8	0.598192
X1727	1388.707	0.598722
X958	-705.94	0.599351
X671	-934.895	0.599793
X752	-972.594	0.600062
X242	-1291.69	0.601516

X895	847.3783	0.603377
X1133	1546.497	0.604384
X2026	831.9059	0.604968
X1350	1525.214	0.606011
X1506	1667.715	0.606233
X896	810.8058	0.606812
X2250	-867.452	0.606848
X1560	-976.279	0.60895
X643	709.9129	0.609127
X206	-1203.19	0.610851
X1032	421.4112	0.611672
X1320	1126.393	0.612402
X1459	-837.418	0.612607
X631	716.1765	0.613489
X389	685.0028	0.6138
X1631	-1433.28	0.613952
X1770	1033.101	0.614006
X716	-1024.29	0.61415
X660	-932.575	0.614914
X1901	1168.37	0.615027
X1769	-1078.72	0.615159
X2130	-1105.66	0.615908
X1660	-857.775	0.615912
X1370	870.9328	0.616835
X2164	-1799.32	0.617981
X947	1098.657	0.618229
X900	-914.493	0.618348
X841	2133.809	0.61907
X949	734.5422	0.619145
X1902	837.5229	0.620363
X1942	-1664.33	0.620461
X1611	-1390.33	0.62083
X2283	-1145.06	0.621719
X1778	1153.759	0.622169
X1490	-909.745	0.623143
X2219	-1613.48	0.62343
X1656	-874.28	0.624496
X1432	-764.503	0.626035
X914	-811.081	0.627435
X793	-1071.19	0.627548
X381	947.33	0.629766
X1399	1174.139	0.631676
X2240	945.9727	0.631742
X1530	-989.889	0.631895
X1522	-1258.76	0.632156
X744	-910.235	0.633866
X1929	-1065.1	0.634056
X754	1031.422	0.634408
X983	1060.56	0.634737
X1365	-876.047	0.634875
X749	947.4549	0.635427
X1386	980.2302	0.635789
X884	1124.962	0.636377
X875	-901.38	0.637746
X2349	955.1688	0.638104
X1966	-1411.57	0.638374
X1245	926.4108	0.640764
X782	-703.546	0.641528
X324	-832.354	0.64172
X2194	1221.456	0.642698
X1789	673.246	0.644296
X1092	1181.57	0.645068
X850	-806.484	0.645412
X1415	1018.432	0.647347
X1313	1209.55	0.648494
X708	-1000.08	0.649077
X1775	947.4218	0.649381
X2091	658.1428	0.649798
X1665	789.8999	0.650149
X2179	599.8795	0.65056
X1067	995.2769	0.651495
X1709	-1524.45	0.651656
X1181	1140.124	0.651819
X933	757.3331	0.652876
X656	-764.15	0.653121
X1468	-1369.45	0.653709
X1783	-757.118	0.654482
X1200	-773.168	0.654616
X1838	-763.007	0.655376
X2241	988.3398	0.656717
X849	-712.253	0.657398
X1158	1272.247	0.658686
X1469	-789.056	0.660315
X1806	-1108.39	0.661582
X1536	-1089.86	0.663577
X937	-538.29	0.664412
X1821	1115.718	0.665084
X678	-840.287	0.66617

X1385	-640.953	0.666418
X1532	-941.892	0.667448
X2019	676.0631	0.668402
X1575	777.0948	0.669609
X822	815.6328	0.670223
X1164	1483.58	0.670507
X926	1695.411	0.670509
X1438	748.2073	0.671625
X2126	-1299.89	0.671835
X1668	984.1185	0.672591
X632	721.9627	0.673342
X2180	696.8975	0.676002
X1864	-891.841	0.676319
X2221	720.0273	0.676432
X2168	-879.813	0.677612
X853	1133.11	0.6777
X1387	-753.032	0.678088
X1563	-749.126	0.678943
X1137	-885.787	0.679152
X1308	879.6785	0.680461
X1062	-754.064	0.681379
X1523	-647.185	0.682155
X722	1018.705	0.683508
X710	734.66	0.684656
X901	-740.167	0.684898
X2148	696.9545	0.685197
X1941	1227.995	0.685834
X1263	-756.056	0.68595
X1927	850.0864	0.688592
X665	-626.497	0.689357
X1063	786.3148	0.691701
X1802	-691.476	0.691752
X1962	-1047.69	0.692147
X1546	835.9572	0.693171
X1721	937.5299	0.693458
X1233	867.5647	0.694173
X668	-599.147	0.696709
X1258	637.4382	0.697761
X828	-613.597	0.698698
X2086	-1050.26	0.699172
X794	-1187.15	0.699845
X1316	-614.28	0.701258
X789	-1068.38	0.701425
X1881	-629.875	0.701847
X1695	-849.696	0.701881
X618	-609.17	0.702897
X1702	1042.883	0.703086
X1534	798.022	0.703124
X1622	-934.14	0.703435
X1476	-645.668	0.705213
X1836	784.8502	0.705213
X1186	921.5429	0.705662
X1819	727.1167	0.705778
X894	630.0571	0.70633
X897	950.6775	0.706901
X1915	-732.756	0.707607
X1857	748.4208	0.707701
X2050	-723.261	0.709131
X1887	-1011.97	0.710713
X1167	630.6129	0.71233
X1545	-908.219	0.712688
X1748	-1079.62	0.713676
X396	639.7294	0.714089
X1606	-941.636	0.714877
X1803	571.2752	0.714891
X1758	1019.905	0.715138
X1816	763.9177	0.715448
X689	-911.612	0.716222
X2308	-801.028	0.716831
X705	-777.423	0.716889
X1047	-818.435	0.717244
X1265	-484.898	0.717469
X987	-698.376	0.717825
X1311	930.6467	0.717977
X1359	-575.567	0.718035
X2184	977.5964	0.718204
X2182	-554.393	0.719
X1046	-838.254	0.721623
X1944	-1151.18	0.722021
X1593	-836.253	0.722112
X1125	931.4654	0.722518
X571	-908.069	0.72261
X1493	667.2954	0.722971
X1749	-848.086	0.72396
X995	-819.932	0.724411
X882	-827.056	0.726
X1509	-647.878	0.726101
X1188	777.6244	0.726104

X1124	1511.015	0.726483
X880	-573.545	0.727318
X1473	-777.758	0.727738
X942	858.9673	0.727951
X1587	668.6679	0.728513
X1743	-603.717	0.728655
X1194	569.8091	0.729642
X1574	-652.115	0.730318
X1751	-719.597	0.730736
X1483	-598.053	0.731979
X2253	-410.131	0.73285
X717	642.7127	0.733982
X2010	-551.315	0.734517
X1453	725.8983	0.735302
X1640	649.6549	0.735712
X1203	769.033	0.736835
X1876	-756.589	0.737106
X2246	-640.927	0.737194
X1110	858.9159	0.737397
X1155	1002.084	0.737723
X739	570.6472	0.737849
X2255	-635.661	0.738491
X2172	619.8744	0.738504
X1040	-1094.07	0.738935
X1066	742.5681	0.739555
X310	714.4787	0.739637
X2016	626.4131	0.739793
X1676	755.0548	0.741914
X1013	874.7625	0.741996
X1965	-921.113	0.74249
X616	-525.813	0.742987
X1531	805.3223	0.743053
X792	-1047.08	0.743782
X1734	-789.712	0.745326
X1112	-863.293	0.747766
X2042	-456.884	0.748471
X1757	-814.275	0.748668
X412	-711.472	0.750962
X1259	764.5473	0.751177
X1610	-741.374	0.751736
X1408	-658.165	0.752472
X1288	567.1613	0.753483
X355	-649.366	0.75609
X827	-522.04	0.756484
X482	854.3272	0.757194
X608	-550.515	0.758367
X1524	-625.064	0.758458
X1160	847.8006	0.75924
X1696	583.9559	0.760129
X1081	672.8428	0.760448
X1376	565.3247	0.760522
X1829	-687.419	0.760545
X2007	-674.387	0.760824
X768	723.8149	0.761122
X1718	746.8532	0.762276
X1332	526.667	0.763682
X1809	-437.973	0.765869
X986	-662.618	0.7662
X1781	550.2846	0.766934
X630	438.8665	0.766999
X2277	-641.559	0.76702
X1195	418.7065	0.76935
X813	450.8554	0.769352
X1071	866.1299	0.769565
X1132	737.3277	0.769631
X649	-457.66	0.773432
X1000	598.6635	0.773614
X1051	1016.543	0.773848
X1373	-543.988	0.774427
X593	-577.382	0.775106
X1118	-435.23	0.775337
X1225	-661.249	0.775806
X2096	927.1608	0.777099
X1253	-475.371	0.777301
X1707	878.7675	0.778205
X1210	742.436	0.779359
X574	405.5547	0.779875
X1865	-502.643	0.780901
X2108	632.4652	0.781123
X816	694.5971	0.781197
X2339	-590.18	0.783536
X1616	-614.115	0.78419
X1239	560.4086	0.784216
X1726	-703.903	0.785484
X726	528.6894	0.786879
X296	-671.129	0.787048
X1367	-699.571	0.787473
X777	-720.857	0.787775

X1882	385.5282	0.789878
X1731	731.2014	0.790994
X1102	-1008.89	0.791699
X1465	-719.174	0.792414
X1236	593.0837	0.792763
X969	-719.839	0.792847
X281	-465.397	0.793361
X1190	708.9608	0.794278
X806	-491.548	0.794636
X585	694.7104	0.79567
X1128	-672.397	0.797704
X1084	580.0307	0.79805
X1005	-320.776	0.798524
X1662	584.1716	0.798673
X1192	-377.56	0.799946
X1742	549.9151	0.800825
X846	-482.109	0.801238
X935	354.5893	0.80195
X2280	-580.891	0.802078
X1413	-507.516	0.803206
X1667	533.5605	0.803215
X1900	441.1272	0.804141
X1456	-529.344	0.805225
X1272	501.4238	0.8055
X1511	557.3315	0.805823
X1554	472.5376	0.805869
X2159	862.8925	0.806682
X1542	-588.596	0.806946
X2143	713.2341	0.807358
X2146	556.6245	0.807656
X790	-522.619	0.809162
X921	-798.754	0.809231
X1784	-746.844	0.809257
X747	427.6633	0.809776
X1426	-463.729	0.809832
X833	-1011.45	0.809956
X2341	-377.561	0.810116
X1417	-638.366	0.810821
X2144	653.4941	0.812121
X1282	-662.507	0.81299
X728	648.0082	0.813553
X1492	249.9134	0.814169
X637	316.5608	0.814259
X2326	-396.152	0.814487
X1641	-490.28	0.814551
X887	-363.37	0.814639
X740	-411.91	0.815109
X1786	410.6249	0.815419
X633	-315.129	0.815883
X1049	-521.949	0.816007
X718	-438.147	0.817011
X2142	-667.06	0.817163
X2116	1015.573	0.817256
X2345	594.3198	0.817885
X1153	561.6793	0.818098
X800	-619.599	0.819025
X397	289.2743	0.819126
X996	-477.816	0.81945
X1491	-433.948	0.819925
X2101	559.697	0.820815
X1347	518.3837	0.821538
X459	411.8932	0.822775
X842	481.4205	0.822985
X1372	-460.378	0.824553
X1576	-412.573	0.825327
X1290	-407.021	0.825557
X2303	471.8941	0.825873
X763	-448.317	0.828308
X1448	-410.846	0.828434
X529	-358.089	0.829073
X925	223.135	0.830129
X1171	372.7849	0.830288
X1890	373.2281	0.830838
X1187	638.7854	0.831074
X819	350.9119	0.83221
X1226	-428.629	0.833992
X1516	442.0169	0.834651
X1526	-549.008	0.834966
X2123	281.6916	0.835406
X2212	-448.231	0.835766
X1997	-407.907	0.836457
X1464	-463.343	0.836482
X2244	514.2093	0.836675
X1940	-585.813	0.838003
X1354	383.4628	0.839655
X1342	259.9921	0.839865
X1580	719.6204	0.839879
X601	-434.523	0.841337

X1939	-454.422	0.84147
X1116	-292.329	0.841846
X2021	-382.405	0.841888
X997	313.0383	0.84222
X2193	-436.996	0.843409
X814	-379.982	0.843815
X1822	389.6095	0.844558
X715	-330.675	0.844835
X1478	352.7233	0.848121
X1103	453.9119	0.848234
X1176	-294.466	0.848555
X1043	-495.61	0.849323
X1404	-531.643	0.849707
X1488	-298.184	0.850501
X1849	467.4207	0.850568
X1541	-291.495	0.850621
X999	-450.068	0.850782
X1629	396.3771	0.850799
X1684	428.7705	0.852202
X1242	300.7376	0.852294
X1808	-311.87	0.852363
X1119	277.654	0.85296
X664	-287.769	0.853245
X610	-319.799	0.853549
X944	442.9916	0.854659
X1747	513.2768	0.855811
X1202	268.975	0.856462
X405	280.0812	0.85786
X2293	388.3732	0.85829
X1134	520.0504	0.858592
X2097	-769.382	0.858833
X2013	324.178	0.858873
X727	-328.549	0.860184
X2352	260.8484	0.861508
X1323	-310.165	0.861805
X1175	260.4311	0.861961
X1104	442.1519	0.864059
X1835	-304.679	0.864587
X1199	225.7633	0.865072
X990	-389.963	0.865307
X1291	334.1842	0.865836
X1060	751.4761	0.866242
X930	163.0172	0.86697
X2156	469.6325	0.868285

X1101	319.7788	0.869556
X746	-245.943	0.873832
X605	279.2275	0.873986
X677	-255.373	0.875004
X2020	240.5219	0.875177
X2105	413.4809	0.875393
X1577	-301.693	0.876378
X1504	-323.8	0.876569
X2268	-357.907	0.876885
X1213	329.5876	0.877413
X2238	-495.105	0.877862
X2135	-299.616	0.877888
X1906	-338.255	0.878923
X1433	-390.989	0.879218
X1221	-310.563	0.879436
X1801	303.3999	0.87953
X1646	-269.194	0.879547
X928	-193.281	0.87992
X1337	262.6798	0.880057
X1487	258.6499	0.88057
X1163	362.2223	0.881195
X1794	-630.488	0.882554
X696	-253.856	0.882902
X971	-378.947	0.883325
X1772	287.4712	0.8834
X758	-348.893	0.885137
X946	-313.978	0.88596
X1989	241.9845	0.886721
X955	174.0794	0.887098
X2070	445.5092	0.887681
X741	214.8608	0.888848
X1161	-329.489	0.88929
X1988	-265.457	0.890066
X1197	257.9715	0.890654
X386	267.2063	0.891653
X1400	356.8474	0.891695
X1558	-268.653	0.89196
X525	-242.475	0.892553
X2296	310.5414	0.893273
X2348	-269.751	0.893655
X869	216.8056	0.895543
X876	-321.209	0.895676
X1357	260.2563	0.895735
X2014	239.4571	0.896575

X1508	-373.181	0.897175
X1869	256.1749	0.897229
X934	250.6152	0.897702
X1561	-251.112	0.899179
X2189	-262.005	0.899997
X2331	-390.54	0.900122
X654	-186.485	0.901394
X1394	-247.296	0.901921
X1238	272.1593	0.902944
X371	-217.388	0.903143
X1697	398.8772	0.903371
X2032	-254.517	0.903484
X698	-243.591	0.904232
X1471	212.6994	0.904242
X2301	261.2752	0.904262
X1295	202.5706	0.905105
X1264	232.8579	0.905924
X866	-304.335	0.906461
X480	-282.631	0.906612
X2294	-220.753	0.906897
X1500	-269.328	0.908095
X732	220.0932	0.908513
X1737	413.3015	0.908765
X2211	268.9537	0.908801
X863	177.3955	0.910759
X1077	-342.974	0.911013
X1862	239.9313	0.911361
X1219	-253.696	0.911591
X2298	-247.391	0.912046
X775	-193.63	0.912548
X1572	-246.198	0.912939
X748	186.863	0.913233
X1638	-221.253	0.913252
X2138	-251.066	0.913471
X1565	243.1627	0.914844
X1329	172.1257	0.915939
X686	-197.706	0.916366
X1551	-235.976	0.916924
X1173	149.2174	0.91735
X1402	-255.056	0.917974
X1416	156.0833	0.921064
X222	220.9175	0.922509
X1863	-206.449	0.92487
X912	208.5125	0.925754
X742	152.3477	0.926445
X1588	230.7858	0.926936
X831	142.4797	0.929703
X1973	-247.291	0.930661
X2201	153.4555	0.931565
X663	138.1163	0.93177
X1235	148.0633	0.931821
X834	145.4414	0.932131
X2307	-173.76	0.932451
X1074	168.1899	0.932789
X1374	156.5623	0.93301
X533	134.5933	0.93348
X685	148.5927	0.934475
X2236	-266.149	0.934573
X1833	-219.769	0.935211
X702	-171.116	0.935677
X1633	-173.966	0.93581
X1120	242.9958	0.93594
X1762	186.4948	0.936335
X1710	158.4841	0.936669
X1279	-155.156	0.936872
X1237	163.1091	0.938465
X2099	254.3287	0.938867
X1699	-157.669	0.939568
X1257	-140.486	0.939618
X1507	219.3428	0.940495
X945	168.3976	0.940827
X1618	-188.121	0.940916
X2073	309.217	0.940961
X773	204.5357	0.942077
X817	-136.521	0.943082
X1172	-138.569	0.944462
X821	-122.329	0.944499
X1330	113.6929	0.945655
X305	124.8999	0.947056
X1424	105.2995	0.947172
X1204	161.0859	0.947306
X1698	-190.333	0.948653
X956	94.58924	0.949267
X658	-118.097	0.950955
X1730	-201.012	0.952555
X1826	104.9896	0.955357
X400	73.99089	0.955391
X881	155.3812	0.955722

X639	89.77402	0.956119
X1768	-103.532	0.956388
X872	120.4217	0.95663
X596	79.10773	0.956679
X2325	-105.062	0.957136
X1513	107.2435	0.957371
X1353	75.24139	0.957544
X1740	226.9389	0.958974
X1612	92.31631	0.959325
X2187	-166.303	0.959818
X2284	150.4963	0.95992
X701	-91.356	0.961051
X1411	-97.4383	0.961614
X1422	122.9423	0.961626
X1564	-100.979	0.962706
X1814	-99.2122	0.96376
X1061	-85.3552	0.963807
X595	-78.6051	0.964703
X1903	95.04678	0.965934
X1099	119.4821	0.966934
X795	108.9447	0.967173
X2115	103.4144	0.968703
X1608	77.61087	0.969044
X898	-62.2222	0.969845
X1609	80.20866	0.970574
X1252	66.97674	0.971056
X1039	-116.623	0.97155
X607	-64.5055	0.972171
X1800	88.18686	0.972887
X1425	93.63283	0.972943
X1428	74.8305	0.973496
X1230	76.78729	0.97449
X943	-59.7876	0.976053
X915	44.15613	0.977083
X1169	61.25235	0.97846
X957	33.70035	0.978823
X1601	66.55009	0.978981
X591	41.28908	0.979331
X1352	-64.8627	0.979951
X743	45.76671	0.979995
X1324	-36.3951	0.98008
X1812	-45.5168	0.980278
X2237	-39.5564	0.981069
X852	47.16845	0.981171
X2154	75.13063	0.981758
X1193	38.41487	0.981771
X1205	-50.8706	0.982337
X1666	68.7371	0.982504
X2279	-34.5333	0.982615
X2269	29.32353	0.98452
X906	57.25713	0.985525
X1396	50.26508	0.986303
X669	-26.8968	0.98654
X2267	35.4187	0.986965
X2022	-31.9668	0.987501
X1685	40.88756	0.98824
X2037	-35.5344	0.989372
X379	-28.0324	0.989543
X1293	-19.1071	0.989966
X870	28.3704	0.990247
X2054	-25.1596	0.99029
X1224	-26.0106	0.99039
X1607	-27.8701	0.991313
X1494	17.28814	0.991697
X375	17.17769	0.99244
X786	-22.4411	0.992746
X761	-20.9905	0.992807
X1479	-18.8593	0.99351
X1314	-12.5083	0.993961
X1420	12.06012	0.99571
X266	-7.38643	0.996352
X2087	15.09858	0.99698
X2304	7.114496	0.997404
X1207	4.405727	0.998574
X1639	-2.56442	0.998826
X2012	-2.6815	0.998996
X694	3.0466	0.999068
X1223	1.925792	0.999159
X1079	1.258233	0.999667
X2315	0.892933	0.999683

Appendix 5

Mixed effects regression model results for 2DGE protein spots with Trails B decline whilst controlling for age, gender, education, BMI, cholesterol, and *APOE* ε4 status. Results highlighted in red are statistically significant ($p<0.05$)

Spot ID	Coefficient	*p*-value
X779	-38.8492329	0.000129
X1138	-22.6147243	0.001265
X2187	44.18654861	0.0014
X767	-25.8127413	0.001442
X1543	-24.764491	0.002762
X849	-21.3638027	0.00312
X1307	39.64948297	0.003603
X1302	35.67988648	0.004902
X1644	-25.9229164	0.005499
X2184	30.82080343	0.005551
X1656	-23.4113819	0.005726
X1492	-13.7809576	0.006758
X1368	-16.3115874	0.007011
X1228	-15.2270665	0.007089
X1758	34.06306507	0.00758
X1595	-19.2328974	0.008156
X2256	26.91087468	0.008471
X324	21.46611472	0.010289
X865	-29.0653696	0.011975
X1639	-19.9488006	0.012429
X2188	33.83091186	0.01316
X1538	-26.5877435	0.013985
X2142	30.02389939	0.014312
X2111	32.17498689	0.014767
X1879	21.76259571	0.015948
X688	-22.5864682	0.016207
X1095	-25.6577157	0.01682
X1401	-20.7567029	0.016832
X1134	29.60979672	0.01701
X2232	19.88615869	0.017103
X1037	30.89805589	0.017657
X1036	10.48178108	0.017812
X2031	23.28869105	0.017885
X782	-16.1362958	0.01847
X2091	15.10258622	0.018686
X1694	-19.6434596	0.019307
X682	21.61107032	0.020827
X1427	-27.5135054	0.022179
X1755	32.18365359	0.023301
X1297	25.36407848	0.024246
X1359	-16.9147605	0.024872
X1693	-25.2178795	0.024905
X1057	-17.2591557	0.025338
X887	-16.0460346	0.0256
X2274	-16.9932297	0.026973
X1590	-15.6650304	0.027109
X1296	30.42412166	0.027331
X763	-20.2976746	0.027794
X2341	16.15078578	0.028154
X1495	-19.4584054	0.029494
X1347	-22.9767284	0.029749
X1511	-22.0383665	0.029792
X1499	-14.3737404	0.030476
X804	-19.2768316	0.030818
X1431	-16.0895998	0.031042
X1743	16.75944942	0.031338
X661	19.48381126	0.031421
X1785	-20.2840052	0.032761
X1990	16.74274954	0.032982
X1283	25.48531274	0.034231
X1640	-17.5831067	0.034311
X1671	-18.6216857	0.035148
X1463	-17.197246	0.036268
X1196	-12.9554852	0.037104
X1649	-19.6685034	0.037119
X663	15.35375583	0.038327
X758	-20.7793545	0.039644
X1732	27.0881448	0.040093
X1163	-23.3349569	0.040317
X1631	-24.5003442	0.041297
X1153	-22.6541249	0.042028
X931	12.40310856	0.042028
X1271	21.49938078	0.042199
X813	14.51678027	0.042937

X1459	-15.3047626	0.043009
X1367	22.66852487	0.044395
X1022	23.26224815	0.044732
X2255	-18.3771034	0.044869
X2202	-19.0059032	0.046178
X1516	-19.4738434	0.046449
X793	-20.0510331	0.047364
X2210	-21.0433851	0.047386
X1513	-18.3121775	0.047616
X2250	-16.7490082	0.048107
X811	14.1477596	0.049033
X799	-18.3947516	0.049093
X1058	-19.7344176	0.049152
X815	13.96285968	0.049244
X839	-31.5325736	0.049551
X2216	30.87618328	0.050843
X928	11.52143845	0.051728
X1846	16.38286773	0.053083
X719	-13.6649045	0.053213
X1989	15.43901732	0.053644
X1294	-21.2881567	0.05453
X2141	-20.7835935	0.055151
X803	23.59822883	0.056316
X1172	-17.1847256	0.056601
X1778	19.79563049	0.057367
X1034	21.59019667	0.058733
X628	14.79059366	0.058836
X1706	26.29756272	0.060223
X806	-16.4849148	0.060351
X1754	32.54747624	0.061658
X1501	-14.6766732	0.061925
X626	13.07010337	0.06194
X1195	-11.4496826	0.062108
X2097	32.07763767	0.062631
X1361	-17.9785541	0.064456
X1321	-18.8440379	0.064981
X2281	-14.1022067	0.065435
X1793	-13.4827742	0.066424
X1638	-16.1393269	0.066684
X1279	-15.6692222	0.067428
X810	15.78082565	0.068012
X1116	-11.9213865	0.068812
X1230	19.8045132	0.069065
X1718	21.73640013	0.069245

X935	12.09259595	0.069292
X1068	18.23925214	0.069969
X2072	-20.2265139	0.070912
X903	20.69093145	0.071509
X1642	-16.5411967	0.071558
X311	-15.8321965	0.072042
X1173	-12.0331718	0.072242
X880	-13.1682389	0.073637
X1586	-12.6936145	0.076131
X222	-19.0348038	0.076482
X1665	-13.6752597	0.0776
X802	-14.048936	0.078663
X1313	21.56313842	0.07955
X1251	19.61495406	0.079598
X1223	-14.8176963	0.081568
X1197	-13.6458325	0.084717
X2294	14.62388346	0.084901
X669	12.85074435	0.085086
X1534	-16.5454477	0.085513
X1802	12.88100848	0.086545
X1812	15.17448516	0.086613
X1926	15.88872753	0.087354
X1652	-12.8705725	0.087832
X1731	20.72787895	0.087885
X934	15.6387975	0.088586
X809	13.26978638	0.089993
X1468	-23.9341146	0.090028
X1663	-13.7376669	0.090955
X990	16.73134178	0.091398
X2299	-17.6621613	0.091608
X2179	-9.45203611	0.092367
X2028	15.57403795	0.092982
X1115	-11.8269199	0.09336
X1541	-12.3203364	0.095346
X2106	26.11147112	0.095772
X1083	-20.0608041	0.096447
X1950	-17.9097486	0.096867
X1432	-12.0852781	0.097935
:X875	-14.7582921	0.098502
X1816	16.18626741	0.098963
:X925	7.94272415	0.09936
X1661	-13.6919237	0.099417
X1462	-14.4604783	0.099654
X1637	-14.7903927	0.099978

X532	-13.0789761	0.101123
X819	12.38665101	0.102802
X1618	-17.3981789	0.103456
X2278	-14.6566801	0.1037
X1315	-10.1113831	0.104959
X1331	-14.8512555	0.10529
X1341	21.15867166	0.107124
X1692	-18.1862673	0.107603
X1691	-15.719558	0.107799
X1746	23.15264803	0.109265
X1019	18.73529152	0.109268
X1733	-17.6241556	0.109602
X1064	-16.7243011	0.111764
X1487	12.86397286	0.112851
:X668	11.41903747	0.113192
X1407	-17.2226875	0.113195
X1316	-11.4292991	0.113492
X1528	-16.9535813	0.113623
:X869	-12.0286365	0.11486
X1436	-15.6432746	0.115439
:X654	11.139853	0.115798
X1277	16.51290604	0.116433
:X814	12.6656376	0.116609
:X911	17.05836143	0.116846
:X873	-18.9090463	0.117069
:X685	13.39151691	0.117571
:X917	11.5279635	0.119718
:X808	-12.8975393	0.120858
:X658	-13.579753	0.12121
X1393	-16.5683286	0.122631
X1390	-13.8755888	0.122753
:X769	15.22494131	0.122753
X2103	7.802328818	0.123086
:X608	13.18733559	0.123159
X1081	-15.2959794	0.123748
X1148	28.16524932	0.124139
X2345	-18.3041135	0.126535
:X375	12.56933698	0.128298
:X371	12.39425129	0.128501
X2310	16.13316298	0.129527
X2138	16.06246909	0.130293
X1581	-16.1125853	0.130313
X2303	-14.6625017	0.131082
:X666	-9.46527577	0.131905
X2348	-12.9291925	0.132021
:X893	-15.5072437	0.13253
X1212	14.7466763	0.133042
X1236	-15.1213434	0.133139
X1675	17.18799639	0.133146
:X798	-12.1608759	0.133881
X2180	-10.2629314	0.134543
X1290	13.01124538	0.134961
X1420	-15.885986	0.135112
X2185	16.15005141	0.135425
:X715	-11.3957978	0.136325
X1448	13.22640673	0.137568
:X827	11.44033516	0.139141
X1014	15.38329778	0.139187
X1317	12.93820808	0.140345
X1862	14.14569728	0.14078
:X948	11.4031606	0.140917
:X772	-18.6540721	0.141358
X1267	-12.741541	0.141891
X1749	-15.9625809	0.14204
X2098	27.82251625	0.142801
X1781	12.47867895	0.145177
X1857	12.12925872	0.145913
X1355	-11.4697404	0.148983
X1252	12.47533176	0.149596
:X949	9.637173595	0.149994
X1520	11.6520741	0.151431
X1023	15.07632597	0.151848
X2048	6.933909537	0.151884
:X255	-14.8368226	0.153616
X2014	12.03381778	0.153651
X2022	-13.2408077	0.153939
X1966	-18.9821463	0.154372
X1763	18.63723998	0.154385
X1270	-11.880342	0.155609
X1659	-11.2023511	0.156603
X1194	-9.78505131	0.156663
:X850	-11.2816477	0.157304
X1045	13.30795149	0.158255
:X930	6.415151121	0.162462
:X812	10.4323152	0.162677
:X480	-15.8397629	0.165749
X1253	-10.4961975	0.165802
X1729	22.84954491	0.16607

X2213	-18.6904251	0.166094
X1861	13.20301212	0.166422
:X643	-8.81407461	0.167452
X1863	13.72867626	0.167785
X1069	-11.2736985	0.169355
X1333	16.78634275	0.169687
X1363	-12.084194	0.169697
X1330	-10.6617251	0.169776
X1295	-9.78767259	0.169827
X1369	-12.5501285	0.170169
X2301	14.18848901	0.17113
X2236	-18.8628264	0.172133
X1187	18.78862649	0.172782
X2199	9.428193338	0.17297
X1222	-10.5159269	0.173756
X1544	-12.4398437	0.173932
X1744	18.27639986	0.175735
X1056	-9.15329106	0.176492
X1201	-10.2863845	0.17676
X1397	-12.5986891	0.177719
X2293	12.75178395	0.178489
X2279	-10.1705815	0.178594
X2221	10.83861056	0.178805
X1810	8.879460103	0.179074
X1738	17.59987687	0.179697
X1193	-9.40221197	0.180163
X2238	-20.2767103	0.180579
:X726	12.27475093	0.180995
:X777	-17.0732447	0.181626
X1737	21.61842072	0.18175
:X627	10.13593803	0.182003
X1573	-10.1869455	0.182317
:X971	-14.88485	0.182484
X2135	11.28756091	0.182642
X1623	-12.4849799	0.184334
:X620	8.101896801	0.184792
X1973	17.75182476	0.185417
X1566	-11.9330395	0.185567
X1813	10.77274005	0.1856
X1809	8.958296458	0.185913
X1418	-11.4714006	0.186912
X1128	-15.9806057	0.187236
:X860	-12.8040402	0.188358
:X597	12.11186736	0.189386

X1556	-9.85961247	0.189578
X1204	14.50771342	0.190711
X1848	-16.8172647	0.191297
:X622	8.805085732	0.191903
:X184	-13.0060613	0.193732
:X630	-8.7020248	0.193969
:X665	-7.85152633	0.194291
X1766	-16.5075902	0.195665
X1117	-8.39156349	0.196078
X2043	9.209855506	0.196274
:X296	16.04148711	0.196577
X1434	-12.7150024	0.196688
X1257	-10.463082	0.196875
:X754	-12.1684473	0.197237
X1186	14.35723945	0.197265
X2032	11.66944227	0.197892
:X831	-9.6120284	0.199129
:X969	-15.7688202	0.199447
X1900	-9.65068873	0.199765
:X946	12.89120664	0.200118
X1309	11.79987399	0.200278
:X926	22.28398302	0.200358
X1075	-10.6971107	0.201676
X1505	-9.33938459	0.203167
X1724	13.66845425	0.204911
:X879	-13.0750763	0.20553
X2156	-15.703727	0.206478
X2099	19.07467278	0.207767
X1561	11.43928784	0.208218
:X355	12.54585849	0.20977
X1735	-13.4774259	0.211192
X1379	-10.8460871	0.211406
X2218	17.09035673	0.211572
:X713	-8.85827659	0.212829
X1376	-10.3116164	0.212892
X1021	13.79677795	0.213706
:X739	9.613352896	0.215693
X1503	-11.5162849	0.215809
:X618	-9.07054627	0.216313
X1417	-13.6931978	0.218697
:X885	-10.8865922	0.219727
X2157	18.62867879	0.219826
:X966	-16.8385043	0.221003
X2168	-11.7111521	0.222963

:X621	8.719148375	0.222976
X1042	12.74201178	0.223005
:X712	9.766261899	0.223049
X2026	-9.30261821	0.223586
X2330	14.73413843	0.223755
X1789	8.202305498	0.224026
X1775	11.26243004	0.226048
X1767	10.95435501	0.226169
X1372	-11.8342808	0.226236
:X396	9.67060785	0.227429
X1012	7.95583722	0.228199
X1719	14.83531854	0.228305
:X942	13.13246882	0.228494
X2254	-7.30285323	0.229663
:X989	11.46353341	0.230742
X2071	-14.4870267	0.232719
:X727	10.53616366	0.234252
:X788	-13.3294803	0.234922
X1284	10.28905504	0.235625
X2353	-8.73772509	0.236267
:X578	-12.6783581	0.236645
X1514	-11.0792415	0.237193
X1373	9.24784233	0.238322
:X659	12.14106217	0.238682
:X866	-13.7310924	0.238932
X1739	18.69911878	0.239347
X2244	13.32876038	0.239377
X2337	8.54437793	0.242851
X2118	15.08216153	0.242969
X1709	18.05526347	0.243795
X1207	12.36103698	0.244529
X2233	-9.85124386	0.24511
:X606	7.858704796	0.245563
X2005	12.27190867	0.246043
X1704	14.70895044	0.246043
X2070	16.2117565	0.24717
X1494	-8.75271763	0.248975
X1352	-13.0565553	0.249225
:X624	6.826444993	0.249855
X1890	-8.98828045	0.249908
X1028	14.92586072	0.249983
X1202	-7.40327869	0.250191
X1504	-11.1740886	0.251488
X1756	15.06430707	0.25171
X1784	15.45596741	0.251886
X1059	-8.77290518	0.251919
X1540	-10.2404981	0.252049
X1688	-8.49009145	0.252139
:X745	9.085413744	0.253252
:X820	9.119203983	0.253581
X2307	10.28466074	0.254484
:X794	-15.5350724	0.254808
X2217	14.82449578	0.256638
X2331	16.56894804	0.257843
X1473	11.17842141	0.257992
:X434	-11.2978123	0.258495
:X867	-11.0951342	0.258564
X1577	-10.4914	0.259236
X1375	9.199328181	0.262716
X2212	11.60956151	0.263048
X1832	13.80743697	0.263275
X1874	-10.1489492	0.264511
X1753	21.64702712	0.264797
:X938	5.296130309	0.265696
X1159	-12.041106	0.26621
X1051	16.42904919	0.266416
X1438	-9.25117162	0.266468
X1046	11.37834068	0.26672
:X740	9.358152084	0.267059
X1343	-7.93574652	0.268311
:X617	7.521187991	0.268802
:X821	8.938662625	0.26936
X1189	-11.5334921	0.269422
:X797	-9.26687935	0.269728
:X824	13.35750485	0.269837
X1171	-9.18267101	0.269973
X1535	-8.03382863	0.270341
:X892	8.25460421	0.271572
X1822	9.560881148	0.271661
X1293	-7.51541037	0.271775
:X681	12.43221012	0.271815
X1450	-9.37454088	0.272311
:X671	-8.74013157	0.27292
:X714	11.29557189	0.272984
X1169	-10.8659594	0.273428
X2146	11.00401437	0.273709
X1609	-11.1451148	0.274722
X2333	8.258981974	0.275491

:X453	10.67243339	0.275792
:X852	9.221678566	0.276004
X1237	-10.4708192	0.276531
X1168	7.938011629	0.277267
:X933	8.723227999	0.277283
:X995	11.42508993	0.277401
X1170	-9.93111222	0.279174
X1818	10.22136989	0.280439
X1770	10.14024676	0.280762
X1429	-8.48240927	0.281195
X1864	10.03618684	0.281937
:X898	-8.13709503	0.282259
X1901	-10.8996281	0.28242
X1635	-11.0040518	0.282462
X1013	-11.4420229	0.284831
X1150	-12.8848012	0.287248
X1664	-12.9566804	0.287853
X1017	11.99977705	0.288502
X1524	-10.0282728	0.288639
X1613	-7.4506635	0.289162
X1350	11.57717011	0.29191
X1854	9.073772273	0.292115
X1385	-7.10893456	0.292403
X1600	13.2386042	0.292962
X1771	-9.57458485	0.293389
:X604	8.449755991	0.293625
X1344	-6.80070917	0.293641
:X387	6.799220171	0.294276
X1112	-11.9738996	0.296223
:X851	21.16977183	0.296378
X1679	-10.5524694	0.296972
X1953	-12.7106779	0.297033
X2194	-12.1360181	0.297132
X1092	-11.8913582	0.297275
X2021	-9.68092127	0.297492
X2087	18.02264282	0.298277
X1362	13.06049132	0.301328
:X783	-7.00763095	0.301811
X1542	-10.9241076	0.30251
X1175	7.281007774	0.303344
X1090	15.42421382	0.303706
:X825	8.424019247	0.305743
X1715	14.66343733	0.30577
X1485	11.15448805	0.305935
X1787	-7.56617129	0.305975
X1147	17.79414108	0.306539
X1107	18.79582988	0.306647
:X721	-7.46352023	0.30707
X1218	-6.55762843	0.30811
X1823	8.301265903	0.308774
X1587	-9.71235944	0.309094
X1564	9.542965946	0.309096
X1483	8.067277303	0.309195
X1412	-8.79190098	0.309412
X1416	-7.69114233	0.310233
X1968	-11.3698035	0.31094
X1332	-8.13908005	0.311123
X2298	-9.14577288	0.312051
X1982	8.369540241	0.312785
:X242	-11.7446478	0.313486
X1936	-14.1200781	0.313857
:X805	-9.64686615	0.317001
X1658	-10.021347	0.317953
X2215	-13.3392262	0.318116
X2285	-7.50910555	0.318598
:X963	11.3206921	0.319221
:X863	-7.59393654	0.319585
X1646	-7.76341325	0.320386
:X636	7.781295069	0.320459
X2041	8.434062273	0.320541
X1435	-7.25686044	0.320578
X1451	-8.88156375	0.320805
X1256	10.09654129	0.322637
X1356	-6.44095529	0.323154
:X725	9.464806232	0.323421
X1769	9.43354002	0.32425
X1902	-7.3142972	0.324536
X1167	-7.77349304	0.325268
X1676	-10.0447961	0.32551
X1726	-10.7946667	0.326446
X1768	8.088695409	0.327266
X1305	10.46942598	0.327407
X1788	9.324813399	0.327919
:X591	7.737648079	0.329039
X1118	-6.67129657	0.331263
:X834	7.596155229	0.332459
X2332	6.074840392	0.333771
X1174	-10.0919228	0.334299

:X733	8.903627732	0.335468
X1723	-8.77782861	0.336992
X1377	-7.30726387	0.339361
X2352	-6.68253668	0.339486
:X896	5.931991775	0.339843
:X752	8.657098488	0.340305
:X881	11.70560423	0.341073
X1660	-7.03806928	0.343692
X2016	7.991717444	0.343779
X2086	-11.1908455	0.344555
:X728	11.41584276	0.345695
X2088	-9.58577581	0.346609
:X574	6.073100209	0.348255
X1415	-8.93670489	0.348326
X1563	7.937615952	0.348733
:X709	-9.64436716	0.348772
:X998	9.185819585	0.350969
X1811	12.58682761	0.351008
:X653	7.972739677	0.351078
X1826	7.689854939	0.351138
:X732	8.42017528	0.35158
:X987	8.419863538	0.352267
:X861	-8.33766989	0.353666
X1184	-9.81107896	0.354297
X1552	11.82374769	0.354341
X1192	-6.49859266	0.354407
X1762	-9.52068404	0.355767
X1425	-11.1346182	0.355801
X2050	8.698833958	0.356436
X1108	-12.2599779	0.357987
X1779	9.376229543	0.358207
:X598	8.08406429	0.358708
X1589	-6.29398025	0.359026
:X673	8.721364026	0.359354
X2126	-12.498157	0.360603
X2174	-7.29429933	0.360759
X1146	-8.73397964	0.36122
X1667	9.239101857	0.361227
X1030	10.34180482	0.361485
X1748	-10.917731	0.361836
X1807	7.045574885	0.362093
X1131	17.69230346	0.364001
X1835	-6.9703175	0.365966
X1016	10.60437408	0.367557

X1648	-7.8043041	0.368313
X2343	14.45616743	0.368748
X1849	-10.1033571	0.369847
:X937	5.05633065	0.37045
:X642	-5.46180343	0.37063
X2144	11.02141319	0.371581
X1716	-8.38518231	0.371649
X2169	14.33118935	0.372991
X1281	-6.3952814	0.373223
X2245	-12.5631948	0.37405
X1546	7.847228406	0.374556
:X978	-8.44447099	0.374619
X1728	14.66362205	0.376677
X2189	-8.17724636	0.377157
X1181	-10.6311748	0.377668
X2338	7.836266987	0.377851
X2033	10.091285	0.378503
X1814	8.720979436	0.379014
:X816	-10.0795982	0.380449
X1392	-7.55996878	0.380976
X1032	3.380871143	0.381457
X2120	10.37739904	0.381607
:X655	-5.98104627	0.382748
X1282	-12.2257524	0.382879
X1527	-9.195213	0.382991
X1091	14.32563297	0.383073
:X874	-8.84729402	0.383597
X1026	13.40624386	0.383728
X1734	-9.29776455	0.383939
:X633	5.450870899	0.384341
X1156	9.190776486	0.385739
X1005	-5.11798374	0.386259
X2140	-8.72923109	0.386968
X1304	-5.02459	0.387
X2143	-11.2500253	0.38798
X1430	7.741470886	0.389071
:X842	-8.74235599	0.389213
X1292	8.219899936	0.389596
:X882	-9.34930368	0.389855
X1491	7.097762163	0.389894
X1759	-8.28218629	0.39138
:X954	5.338081065	0.391641
X2085	19.20174419	0.391685
:X593	7.767347406	0.391967

X2161	-7.58161316	0.39197
X2044	4.885374424	0.392108
:X599	-10.9797623	0.393949
X1584	-8.92550798	0.395914
X2328	-6.93520011	0.396697
:X731	10.10467629	0.396955
X1015	7.454960907	0.397357
X2347	8.122084687	0.398399
X1125	9.243024337	0.399788
X2109	-9.00874178	0.3999
X1703	11.57706117	0.40044
:X601	-8.77520735	0.400845
X1777	7.234672948	0.40377
X1740	13.91833191	0.404109
:X310	7.997642999	0.405632
X1892	11.72116011	0.405888
X1765	-11.0723899	0.408188
X1033	8.869715418	0.40829
X1641	-8.10826816	0.40868
:X944	9.199411655	0.408888
X1599	10.54856728	0.409074
X1575	-6.66634159	0.409338
X1752	13.07690918	0.409408
:X895	5.570781925	0.409537
:X890	-8.07032773	0.41048
X1698	-9.64544076	0.412321
X1374	-7.25158648	0.414645
X1060	15.04399865	0.41486
X1585	-10.3946221	0.415334
:X977	-7.7080325	0.416581
X2276	-9.87443117	0.417427
:X936	5.327347377	0.418188
:X991	9.070867425	0.418431
X2148	5.691986119	0.418452
X1925	7.318387393	0.41967
:X999	8.23601801	0.42028
X1530	7.995279622	0.421207
X1594	-8.45126819	0.422238
X1160	9.849175064	0.422335
:X602	8.88119447	0.423061
X1612	-6.01090822	0.423309
:X945	8.349266109	0.424333
X1774	7.124403399	0.424898
X1423	-5.87695941	0.425265

X1157	-9.25319952	0.425881
X1620	-7.22197156	0.425886
X1224	-7.35527482	0.426923
X1588	-9.06425178	0.428026
X1003	-4.90126606	0.429184
X1085	11.80504308	0.429646
X2264	-7.68581977	0.432168
:X716	-7.36544468	0.432646
:X757	-7.62281075	0.433552
:X710	-6.40248625	0.434067
X1205	7.759854412	0.435648
X1939	7.78586367	0.436127
X1554	-6.87043729	0.436271
X1825	6.657540284	0.436398
X1457	-7.11529063	0.436569
X2242	10.97857472	0.436917
:X648	8.319972739	0.436942
X1512	-8.70443408	0.437928
:X894	5.625898308	0.438325
X1439	-6.66947396	0.439092
X1428	-7.26361018	0.439114
:X786	-9.33840527	0.439204
:X734	10.31495941	0.441101
X1410	-7.53374501	0.443982
X1419	8.80856774	0.444822
X2012	-7.70675372	0.446037
X1856	-5.87653772	0.446346
:X625	5.250333176	0.446945
X1286	7.402883304	0.448479
X1310	6.178863832	0.448622
X1180	-7.54689697	0.44947
:X679	-6.8195847	0.449514
X1971	-8.12389937	0.450469
X1109	5.620035923	0.45103
X2297	-4.90038776	0.452443
X1829	-7.48621777	0.454175
X1615	-7.14732898	0.454463
X1137	-7.13589562	0.454831
X1948	-11.0370923	0.455491
X1668	7.603688393	0.455707
X1381	-4.23929898	0.456164
:X952	4.416906234	0.457574
X1133	9.022473821	0.457716
X1697	10.49850342	0.457977

X1326	-5.8279481	0.458523
X1717	7.184866623	0.459295
X2154	-10.5125023	0.459463
X1828	-8.29730891	0.461524
X2246	-7.17357497	0.46154
X2209	10.02485519	0.461558
X2007	7.713478867	0.462175
X2271	-6.18774681	0.462484
X2171	8.592057962	0.464542
X1471	-5.7509709	0.465471
X2006	5.992860541	0.465961
X1940	-9.89116261	0.466147
:X857	-6.71052893	0.46666
:X501	8.348611961	0.468494
X1324	4.911626923	0.468609
X1351	-6.52111208	0.468781
X1093	11.98700559	0.468828
:X605	5.618285093	0.470051
:X943	6.827700446	0.470669
:X432	-7.25406794	0.471063
:X698	6.200505524	0.472456
X1702	8.421489727	0.473353
X1509	-6.18010612	0.473433
X1139	14.03234669	0.473598
X2287	-6.79266493	0.473922
X1705	8.896597009	0.474187
:X724	9.81844927	0.47566
:X792	10.02245737	0.475678
X2253	-3.27848562	0.475828
X1466	-7.21518845	0.476821
X1246	-5.92965182	0.478078
X1120	-8.07125305	0.480489
X2211	7.4359613	0.48052
X1135	13.78181061	0.480862
:X974	-4.95498065	0.481957
X1010	5.028220668	0.482724
:X953	3.823040446	0.482894
X1773	6.184840254	0.484838
:X901	5.844112565	0.485181
X1424	-5.98415756	0.485551
X1191	-10.109796	0.486342
X1551	7.383247003	0.486824
X2049	4.837984903	0.486859
X1040	-10.3402538	0.488512

:X902	5.520620167	0.490232
:X848	-6.2821061	0.490337
:X778	-9.10590618	0.490924
X1233	-6.61086538	0.491272
:X631	4.500186682	0.492043
X1636	-7.06061759	0.492058
X2313	7.017082879	0.492598
X2137	6.860014074	0.493398
:X596	-4.34770138	0.493447
X1103	-7.4729758	0.493574
X2268	-7.3668853	0.493892
X1098	13.98506047	0.494144
X1383	6.389933609	0.494678
:X826	8.95943428	0.495081
X1707	8.902520584	0.4958
:X823	-5.44010155	0.496425
X1353	-4.57157381	0.497253
:X701	5.556994395	0.49792
X1405	-7.33416669	0.498229
X2269	4.574467132	0.498369
:X706	6.776752089	0.498831
X1342	4.028272089	0.499088
:X525	-5.79035566	0.499434
:X910	-8.17746458	0.499498
X1149	7.237316837	0.500004
X1018	8.203172647	0.500528
:X997	-4.87031369	0.500744
:X853	-8.6605903	0.501165
:X909	4.503413921	0.502504
X1220	-4.69945844	0.502944
:X589	6.085706747	0.503498
X1803	-4.83169433	0.503905
X1624	7.099060974	0.505044
X1476	-5.55763873	0.505221
X1482	-6.1867572	0.50537
X1602	6.922688565	0.50573
X1760	6.851975537	0.50654
X1245	-5.75220677	0.506686
X1255	8.255909254	0.506747
X1084	-6.66358766	0.506749
X1929	7.091614706	0.507527
:X635	-4.01611115	0.50769
X1782	-7.8514408	0.509611
X1110	-7.59220418	0.51038

X1102	10.40553468	0.511765
:X422	-4.85787422	0.512007
X1287	-4.7273869	0.512624
X1275	-8.23791997	0.514244
X1227	-5.62293172	0.514316
:X908	-6.63641783	0.514975
X2025	-4.82934456	0.516414
X2152	4.419601731	0.516554
X1786	5.364287436	0.51722
:X634	-3.89456273	0.51914
X1474	-8.309346	0.519189
:X676	7.206795448	0.521685
X2102	4.053464838	0.521992
:X836	5.273783204	0.522189
X1708	7.471443831	0.523349
X1269	6.687634288	0.525499
:X637	3.946276798	0.525886
X1244	-6.69208591	0.526173
X1291	-6.07166408	0.527848
X1101	-5.88935236	0.527937
X1815	5.799584592	0.528063
X1387	-5.08636441	0.528098
:X717	5.519741183	0.529042
X2119	8.616753124	0.529136
:X755	-7.2048056	0.529161
:X947	6.555568476	0.529176
:X672	-7.32122463	0.529742
X1622	-7.19877276	0.530906
X1360	-7.13483244	0.53285
X1221	6.347152203	0.534335
X1232	5.292528009	0.535521
X1008	-5.30351135	0.535578
:X748	-4.92760048	0.535817
X1188	-6.02284424	0.536454
X1545	-7.09398667	0.536745
X1710	-5.99047222	0.536976
X2230	-6.49804551	0.538028
:X484	-7.90941925	0.538486
:X871	-6.64874346	0.539565
:X707	5.197575741	0.540341
:X771	6.04158859	0.540358
X1962	7.729882496	0.54121
X1855	4.747454502	0.542326
X1453	-6.1744263	0.54336

X1456	-6.04312278	0.543631
X2226	3.404808728	0.544408
:X807	-5.3999229	0.544425
X1817	5.635013604	0.544867
X1329	-4.65433894	0.545903
X1736	9.024747084	0.546726
X1657	5.756332707	0.546801
:X696	-4.57433754	0.549271
X2237	4.704956414	0.549316
X1525	-5.13291315	0.549897
X1727	7.236115644	0.551112
X1522	7.201884431	0.551744
X1721	6.313640621	0.55212
:X576	5.438777871	0.552299
:X968	6.988699767	0.553033
:X789	-7.13301215	0.553671
X1289	5.127132425	0.553762
X1548	8.007680441	0.553763
X1617	7.325511386	0.554792
:X914	4.494629539	0.555057
X2317	5.423680366	0.556292
X1536	6.436905106	0.557322
X2023	4.791164876	0.557544
X2296	6.284056269	0.558461
X1099	-7.3332762	0.55871
X2284	8.378675712	0.559148
X1700	6.794942996	0.559226
X1299	-5.3069858	0.560513
:X785	-4.15476636	0.560783
:X840	11.84917369	0.561087
:X738	5.11315704	0.561487
X1821	6.689793019	0.561549
X2241	-6.26726401	0.562304
:X904	6.72718101	0.562648
:X616	-4.3449428	0.562739
X1071	-7.72070247	0.563919
X1690	-7.36746227	0.563927
X2267	-6.21426889	0.564019
X1887	7.283672564	0.564564
X1650	-5.93646024	0.564813
X2204	7.175542202	0.565057
:X381	5.068007715	0.565281
X1337	-4.53629119	0.567955
X2196	-5.87507875	0.568652

X2053	4.80473937	0.568748
:X386	5.327772599	0.574085
X1550	-7.85176273	0.575394
X1235	4.107385751	0.576244
X1713	5.474857407	0.576823
:X742	-4.13443857	0.57782
:X891	-4.19392372	0.57792
:X844	4.880518007	0.577996
X1009	9.180287313	0.579123
:X610	4.285627967	0.57955
X1610	-6.14045715	0.582018
:X818	4.982928208	0.583016
X1104	-6.52125149	0.583382
:X670	4.651376683	0.58537
X1006	-4.06443733	0.585403
:X690	5.195796125	0.586637
X1394	4.902475436	0.587789
X1234	5.435541824	0.588391
:X662	5.295375604	0.588671
X1203	-5.66408901	0.589976
:X702	5.232907921	0.589991
X1154	6.664323961	0.590816
X2190	4.527232485	0.592317
X2037	6.118096309	0.5957
X2350	-6.90378979	0.596606
:X378	-4.60912595	0.598073
X2013	4.450111447	0.599685
X1129	-6.41517884	0.600228
X1897	6.74768186	0.601203
:X993	5.29029931	0.603262
X1547	-4.46324451	0.604353
:X459	4.441197878	0.604627
X2235	-6.09336845	0.604772
X1616	-5.21398299	0.604801
X2292	-5.09786038	0.605032
X1686	5.837323159	0.606263
:X743	4.434551608	0.606463
X1515	-5.55915609	0.608307
X1278	-5.49672554	0.608855
X1318	-4.45487014	0.609138
:X921	7.310446547	0.609141
:X393	-4.96635885	0.609931
X1274	6.022228466	0.610995
X1791	3.407089704	0.613926

X1413	-4.82851552	0.615361
X2128	4.514616227	0.61784
:X878	-6.00100984	0.618567
X1470	-4.71950837	0.619371
X1666	-6.72594348	0.620098
X1145	4.167315891	0.620579
X1065	-4.38416445	0.622771
X1422	-5.73869911	0.62344
X1066	-4.62575803	0.624546
X1238	-4.89859978	0.625449
:X686	4.176084525	0.627422
X1837	4.575903686	0.627453
:X913	6.986156767	0.628861
X1433	-5.02573767	0.629481
X1696	-4.43531254	0.629501
X1553	-4.11797019	0.629512
X1532	-4.69586863	0.629562
X1576	-4.00245817	0.629658
X1478	-4.13590964	0.629697
:X649	-3.6069247	0.63064
X1073	-4.95173772	0.631855
:X822	-4.19852826	0.632355
:X684	4.142392942	0.632951
X2219	6.656110279	0.633399
X1094	6.003634434	0.634185
:X678	-4.45585399	0.635029
:X765	5.391002692	0.635801
:X545	5.17757244	0.63643
X1054	-4.97455345	0.636825
X1216	-3.1708406	0.638476
:X405	3.429669168	0.63872
:X961	2.858325437	0.638734
X1320	-4.96778471	0.640086
X1311	5.095416874	0.640299
X1741	7.722039932	0.641665
X1507	-5.6893437	0.642412
X1906	5.080283985	0.6428
:X886	7.378477387	0.642919
X1720	4.831085654	0.642969
:X718	3.989406453	0.643133
X1465	-5.87169041	0.644099
:X533	-3.44147192	0.64481
X1067	4.76394587	0.645321
X1508	-5.76485973	0.645366

X1761	-5.26242351	0.645933
:X379	-4.34981482	0.647572
:X645	3.33931619	0.64961
X2335	3.228649068	0.651005
X1865	3.783967622	0.651096
X1190	-5.31575721	0.65198
:X677	-3.33389207	0.652201
X1496	6.445643079	0.653627
X1598	-5.19603803	0.653771
X2336	4.789225109	0.653883
:X992	4.113681424	0.653965
:X965	-6.13764335	0.655045
X1680	-4.07570571	0.655284
X1062	-3.68258428	0.65606
:X689	-5.07019454	0.657369
X1651	-6.69929277	0.657443
X1480	-3.52019138	0.658639
:X639	-3.52386563	0.658912
:X986	4.00536822	0.658912
X1493	-3.63610085	0.659224
X1629	4.297713192	0.660217
X1549	-6.08135191	0.660578
X1570	-4.47641948	0.660869
X1215	-3.46449053	0.661
:X305	3.991723013	0.662891
:X705	4.103785761	0.665476
X1339	-3.96824715	0.666653
X1126	6.292266521	0.667173
:X845	3.247011227	0.667384
X2081	-11.3130399	0.667731
X1633	4.563952506	0.667996
X1007	3.967898986	0.66886
:X988	-3.99470245	0.668886
:X994	5.133030312	0.669239
X2182	-2.84681285	0.670057
:X870	4.594996103	0.670361
X1479	4.589134071	0.671299
X1176	-3.05244688	0.671375
X1162	5.342443545	0.671557
:X899	4.777187173	0.67237
X1518	6.608147927	0.673205
:X491	5.31450369	0.673291
:X206	-4.64043369	0.673759
X1489	-3.52980868	0.674031
X1783	3.190598993	0.674459
X1526	-4.97141329	0.674647
:X594	-3.23127595	0.674991
X1882	-2.96638346	0.67563
:X585	-5.26709674	0.675933
X1272	-3.8863379	0.677102
:X580	2.984631402	0.677865
X1800	-5.25765216	0.679546
X1127	6.150416269	0.681024
X1608	-3.89529495	0.683592
X1039	5.661220353	0.684172
X1454	-5.00190358	0.684299
X1972	-5.03970492	0.68436
X1614	-4.55186237	0.684484
X1357	3.533211848	0.686014
X1225	4.33631724	0.68745
X1684	4.256513331	0.688144
:X958	2.511565902	0.68898
X1677	-3.69803739	0.689976
X1942	-5.82547058	0.690347
X2214	-5.31323084	0.691354
:X897	4.482906957	0.691441
X2172	3.193256927	0.692998
:X587	3.278387922	0.693784
X1323	3.267639126	0.694372
X1654	-3.82493005	0.694516
X2136	3.120043299	0.694714
X1038	2.710997908	0.695366
X2222	2.693072381	0.697199
X1687	-3.59798235	0.697476
:X603	3.409664984	0.697596
X1265	-2.37725938	0.698072
X1808	2.943523673	0.699435
:X403	-3.76691938	0.700106
:X773	-4.89239394	0.700224
X1560	3.294616622	0.702429
:X746	2.798015021	0.702816
X2198	-3.81370407	0.70302
X1831	-2.41076364	0.705584
X1111	-2.56849876	0.706416
X1838	-3.05532538	0.706697
:X699	3.402548121	0.706871
X2177	4.305227554	0.707139
X1089	-3.96651473	0.707334

:X389	2.302160209	0.709467
X1000	3.537094268	0.710973
:X697	3.188670403	0.713714
:X972	4.268962448	0.713803
X1772	3.224121081	0.713929
X1200	2.906859644	0.714356
X1264	-3.01396189	0.714544
X1048	5.275654862	0.714928
X2045	2.33199386	0.715274
:X983	3.519083922	0.715855
X1254	-3.60398487	0.716578
:X817	-3.17286962	0.717661
:X708	3.524478696	0.719988
X1669	-3.59144547	0.720288
X2125	3.663891352	0.720633
X1442	-4.48545299	0.720676
X1881	-2.76849389	0.721148
X1365	-2.93204036	0.721361
X1386	-3.08356053	0.721746
X1338	-2.93999796	0.724263
X1132	-3.71768836	0.724268
:X766	3.86785376	0.725978
:X955	2.036619104	0.725994
X1555	3.681543066	0.726172
:X656	-2.77667946	0.72674
:X747	2.804995563	0.727585
X2010	-2.8106044	0.728835
X2201	-2.81026881	0.72985
:X876	-3.87367512	0.730186
:X800	4.073313991	0.730533
X1619	3.783444948	0.730859
:X906	4.555463899	0.732237
X2063	3.26485579	0.733225
:X770	5.65208752	0.733573
X1521	-2.78165291	0.733659
X1113	2.988810265	0.734293
X1063	3.159131981	0.734673
X1414	-3.62331274	0.734942
X2318	3.233950515	0.735743
X1151	5.901648616	0.736777
X2314	3.232538954	0.73774
X2354	3.19408687	0.740971
X1408	3.025998018	0.741772
X1915	3.148737987	0.74231

:X976	3.600117341	0.742427
X1562	-2.97903664	0.745419
X1312	-3.01065187	0.745582
X1510	-3.88489411	0.745731
X1490	2.739109066	0.747222
:X400	1.998479056	0.747853
X1592	-3.14071061	0.748903
:X768	-3.39576153	0.74891
:X675	-2.58634307	0.750272
X1579	4.824030383	0.751437
:X970	3.360707546	0.752763
X1226	-2.84017345	0.75458
:X858	7.148879003	0.755422
X1165	3.639367588	0.755435
:X286	-2.39716504	0.755463
X2082	3.519809153	0.755601
X1699	3.038069359	0.755969
X2073	-5.10435775	0.755988
X1523	2.13545379	0.756447
X1833	3.944568045	0.756754
X1695	3.159677213	0.75722
X1199	1.890336244	0.758408
:X652	2.383432753	0.758537
:X629	-2.51540573	0.758602
X2024	2.211578312	0.75917
X1643	-2.74507375	0.759866
X1519	2.097009755	0.760348
X2155	2.370442071	0.760376
X2295	2.87374609	0.761434
X1959	2.589435648	0.761575
X1166	4.759358048	0.762298
X1053	-2.53581216	0.76373
:X529	-2.18702092	0.764755
:X722	3.327159132	0.766128
:X322	-2.34806021	0.769348
:X939	1.553634059	0.772658
:X781	-2.21928154	0.773548
X1298	-2.49691522	0.774246
X1198	2.902177073	0.774884
X2315	2.91147661	0.775348
X2344	2.70130971	0.775989
:X775	-2.38261563	0.776331
X1792	-3.21100937	0.777638
X1106	-3.93855622	0.778209

X1273	3.64765298	0.778678
X1152	-3.16266698	0.778822
X1757	3.420708381	0.779625
X1380	2.082137888	0.780302
X1869	2.563546184	0.781879
X2151	-1.88736354	0.78395
X2036	2.90897108	0.784074
X1029	-2.25114833	0.784317
X1041	3.153905569	0.784915
X1079	-3.85614466	0.785482
:X482	3.372244351	0.786055
X1464	2.732384929	0.7866
:X753	-2.68881812	0.787712
:X571	3.191084686	0.788025
X1819	-2.42308165	0.789352
X1122	4.088087963	0.790082
X1930	2.681590668	0.790213
X1730	3.90197308	0.792072
X2181	-1.76640345	0.792854
X2277	-2.50570242	0.793234
X2164	-4.22466568	0.794494
X1161	2.701331177	0.794669
:X833	-4.35804949	0.795196
X1396	-3.07245853	0.796468
:X657	2.030337985	0.799722
:X687	-2.24968281	0.799999
:X619	1.908726482	0.802378
X1488	1.869642984	0.80322
X1506	-3.34944202	0.803277
:X915	-1.83463476	0.803586
X1262	-2.71240684	0.806021
X1580	-3.98902629	0.80645
:X916	1.840135799	0.806539
X1801	-2.08109433	0.807529
X1674	3.064911745	0.808194
X1121	3.216496797	0.810549
X1795	4.991942929	0.810623
X1354	-2.07244956	0.810776
:X749	2.201790715	0.812644
X2054	-2.26981219	0.81268
:X907	3.053542469	0.813271
X1409	-2.38251329	0.813875
:X615	1.760723362	0.813978
X1486	2.482707269	0.814101
X1558	-1.99282161	0.814288
X1565	2.319486508	0.8143
X2020	-1.67467183	0.814729
:X471	-2.44775373	0.815454
X2095	-2.69432676	0.815577
X1593	2.458931519	0.817258
X1074	-2.26673008	0.817772
:X527	-2.27147558	0.819235
:X791	-1.9597071	0.821393
:X956	1.492207849	0.823393
X1628	-2.84657925	0.823761
:X632	1.815902957	0.824489
X1260	1.997387935	0.825597
X1751	2.140876066	0.826295
:X640	1.182117959	0.826397
:X951	1.329736639	0.828036
:X829	-1.77797737	0.828236
X1219	2.186341627	0.828939
X2115	2.551216406	0.830346
X2325	-1.96031699	0.830484
X2101	-2.47191876	0.834183
X2193	-2.1788478	0.834407
:X584	-1.80878929	0.835048
X2040	1.251978019	0.835314
X1406	2.135338251	0.835703
:X905	-2.74701825	0.835925
:X607	-1.78539147	0.835992
X1078	-1.77581453	0.836503
:X985	1.831422935	0.837527
X2104	2.359822195	0.837869
X1790	-1.54687476	0.838158
X1958	1.863059212	0.838301
X1794	-3.16693254	0.839708
X1605	2.689055116	0.840137
X2147	3.212336798	0.840573
X1689	1.61658793	0.841166
:X830	-1.68294486	0.841832
X2123	1.263459077	0.842605
X1061	1.701241034	0.842964
:X761	-2.18006119	0.843604
:X660	1.594955999	0.845197
X1678	-1.87215564	0.846348
X1208	-2.01992988	0.846854
:X855	-1.49580869	0.847826

:X266	1.425864483	0.85168
:X272	1.668025866	0.851909
X1621	-2.24156557	0.852179
X1645	1.840712805	0.852913
X2304	1.763478334	0.855141
:X912	1.897879632	0.85615
X1997	-1.59703678	0.859966
X2108	1.942834883	0.86035
X1119	1.21157513	0.861526
:X957	1.008447112	0.861678
X1001	1.846706506	0.863614
X1241	-1.4145228	0.863979
X1399	-1.91001854	0.864576
X2124	1.941914023	0.865935
X1404	1.858366517	0.867226
X1402	1.743988747	0.868188
X1263	1.385116095	0.868238
:X397	-0.98498935	0.868387
X1591	-1.58760518	0.869673
:X412	-1.74663926	0.870086
X1261	1.838189354	0.870279
X1050	2.501268029	0.870662
X1745	-1.28955037	0.871295
X2275	1.534090003	0.871712
:X609	-1.40623077	0.871726
X1574	-1.3458884	0.873886
X1742	-1.58343853	0.874782
:X641	-0.88220019	0.876486
X1411	1.422762059	0.878354
:X558	-1.69739333	0.878996
X1088	-2.22113749	0.8812
:X664	1.055671892	0.881355
X2105	1.779912994	0.88149
X2042	0.986163381	0.881618
X1141	-2.60216748	0.882937
X1944	-2.24414064	0.883466
X2130	-1.46153069	0.886363
X2339	-1.38155629	0.886401
X1239	-1.18304899	0.888771
X1805	-1.75113369	0.889992
X1247	-1.11689051	0.890523
X1685	1.774314934	0.890618
:X667	-1.21887673	0.890633
:X900	1.141721417	0.890829

X1398	1.131358202	0.890861
X1164	2.132378436	0.891581
X1076	1.714368339	0.89209
X2116	2.556244652	0.892176
:X741	0.986392924	0.892224
X1087	1.729953342	0.893433
X1314	1.004904711	0.894561
X1268	0.793863034	0.895193
X2240	-1.23506164	0.895231
X2239	-1.29093699	0.896452
X1981	-1.00020461	0.898227
:X646	-1.16988891	0.89959
X2351	0.93687806	0.901388
X1806	-1.3904802	0.902441
X2096	-1.52979689	0.904915
X1421	1.084348294	0.905324
X1124	1.989221381	0.907937
X1070	-1.02822571	0.91151
X2019	0.826705602	0.911647
X1043	1.257405171	0.912113
X1400	1.188928205	0.912369
X1714	1.471355317	0.913716
X1229	1.242043943	0.913896
X1391	1.051396884	0.91466
X1965	1.385364526	0.915852
X1963	-1.27351164	0.917067
:X692	-0.85091142	0.918734
X1371	-1.10641011	0.919281
X1611	1.217021606	0.919498
X2308	-1.04839258	0.920981
X1517	1.247196031	0.922517
X1537	-0.85114293	0.924237
X1780	1.024575731	0.924393
X1288	-0.69309995	0.925306
X1875	0.817902973	0.926347
X1481	-0.98232202	0.926702
X1662	-0.9191046	0.927111
X2280	0.882590187	0.928921
X1242	0.645481451	0.929327
X1701	-0.98377216	0.929803
X1072	0.776588714	0.931304
:X680	0.619746722	0.931478
:X774	1.063145463	0.932316
X1182	-0.84958457	0.933864

X1183	-0.96786185	0.934006
X2159	1.257269275	0.93592
X1426	-0.67176363	0.93596
:X735	1.168369664	0.937554
:X694	-0.78906418	0.937752
:X790	0.77489208	0.937782
:X828	0.592260043	0.939113
X1259	-0.78429488	0.93925
:X918	-0.99959685	0.941539
:X950	0.441295275	0.942657
X1185	0.758272694	0.944101
X1210	0.803822827	0.944182
X2326	0.551143429	0.945301
X1964	-0.72567239	0.947262
X1049	0.582599945	0.947765
:X846	0.548044224	0.94879
X1572	0.665288467	0.94919
X1531	-0.67423805	0.951505
X2203	0.589790967	0.95171
X1927	0.561072008	0.952418
X1747	-0.71094554	0.952876
:X644	-0.46152078	0.954708
X2127	0.508734807	0.954735
X1052	-0.70614063	0.955492
X1988	-0.4757422	0.956873
X1582	-0.60008274	0.957752
X2283	-0.54342619	0.958987
X1941	-0.71548807	0.959175
X1158	-0.63310969	0.959268
:X872	0.510706337	0.959882
X1830	-0.52515111	0.96055
X2273	-0.46077589	0.960734
X1606	-0.55330566	0.961244
X1876	0.552048935	0.961385
X1334	0.445990402	0.961477
X2231	1.083704745	0.961591
X1130	0.678010784	0.962331
:X973	0.544172521	0.963574
X1077	-0.62901434	0.963629
:X590	0.515756009	0.965429
:X638	-0.32180622	0.966621

:X281	-0.3460116	0.967237
X1500	0.436303737	0.968755
X1903	-0.38313915	0.969383
X1345	-0.23909499	0.972355
X1440	0.268213686	0.97348
:X868	0.35978437	0.974024
X1469	0.258245702	0.974431
X1047	0.275230398	0.975191
X1627	-0.35036184	0.975441
:X841	-0.56396341	0.976778
X1601	0.302515039	0.978571
X1308	0.218800032	0.981764
X2349	0.221921725	0.981876
:X750	-0.16723165	0.982602
X2114	-0.11368621	0.984563
X1597	-0.23636679	0.984697
X1583	0.188039938	0.985001
X1140	0.257955273	0.986546
X1213	0.171094851	0.98683
X1607	0.196039278	0.987103
:X996	0.137927873	0.987851
:X795	0.186615876	0.987895
X1836	-0.12347142	0.988948
X1557	-0.17692707	0.990048
X1211	0.111519939	0.990465
X2311	-0.13052645	0.990634
:X744	0.102703129	0.990813
X1155	0.122546884	0.99257
:X229	0.082056012	0.993504
X1604	0.08497529	0.994035
:X595	-0.06087833	0.994152
X1725	-0.07640855	0.994159
:X884	0.074676101	0.994764
X1258	-0.04427388	0.995062
X1086	0.07826602	0.996419
X1917	0.031965091	0.998167
X1370	-0.01784706	0.998191
X1123	-0.02741152	0.998622
X1303	-0.00535596	0.999583

Appendix 6

Baseline partial correlation results for proteins with PiB PET DVR. Proteins ranked in order of significance based on *p* value. Proteins highlighted in red are statistically significant ($p<0.05$), those highlighted in green are tending towards significance ($p<0.1$).

Protein	Correlation coefficient	*P*-value
Complement C4 B	-0.498	0.022
Leucine rich alpha 2 glycoprotein	0.607	0.022
Zinc alpha 2 glycoprotein.	0.478	0.025
Ig kappa chain C region	0.455	0.035
Fibrinogen beta chain	-0.471	0.038
Fibrinogen alpha chain	-0.429	0.050
Apolipoprotein A IV	-0.420	0.056
Beta 2 microglobulin	0.482	0.068
Hemopexin.	0.364	0.107
Alpha 1 antitrypsin	0.362	0.109
Ig alpha 1 chain C region	0.457	0.123
Immunoglobulin lambda like polypeptide 5	-0.454	0.127
Angiotensinogen	-0.407	0.140
Serotransferrin	0.321	0.162
Serum.albumin	-0.376	0.179

Vitamin D binding protein	-0.342	0.227
Protein AMBP	0.250	0.288
Alpha 1 acid glycoprotein 1	0.226	0.338
Complement C3	-0.164	0.519
Kininogen 1	0.142	0.555
Alpha 1B glycoprotein	0.159	0.576
Antithrombin III	0.129	0.626
Apolipoprotein E	0.108	0.717
Transthyretin	0.072	0.765
Alpha 2 HS glycoprotein	0.068	0.868
Apolipoprotein A I	0.033	0.912
Inter alpha trypsin inhibitor heavy chain H4	-0.025	0.917
Alpha 1 acid glycoprotein 2	0.026	0.932
Retinol binding protein 4	-0.020	0.947

Appendix 7

T6 partial correlation results for proteins with PiB PET DVR. Proteins ranked in order of significance based on *p* value. Proteins highlighted in red are statistically significant ($p<0.05$), those highlighted in green are tending towards significance ($p<0.1$).

Protein	Correlation coefficient	*P*-value
Complement.C3	-0.567	0.017
Fibrinogen alpha chain	-0.477	0.042
Leucine rich alpha 2 glycoprotein	-0.503	0.100
Complement C4 B	-0.410	0.119
Alpha 1 acid glycoprotein 1	-0.382	0.122
Fibrinogen beta chain	-0.364	0.158
Platelet basic protein	0.572	0.163
Apolipoprotein L1	-0.452	0.310
Carbonic anhydrase 1	0.348	0.327
Inter alpha trypsin inhibitor heavy chain H4	-0.214	0.413
Angiotensinogen	-0.290	0.423
Alpha 1 antitrypsin	-0.208	0.426
Transthyretin	-0.206	0.431
Serum albumin	-0.249	0.467
Zinc alpha 2 glycoprotein	-0.181	0.506

Hemopexin	-0.164	0.534
Apolipoprotein A I	0.211	0.542
Ig kappa chain C region	0.210	0.544
Beta 2 microglobulin	-0.190	0.562
Retinol binding protein 4	0.195	0.575
Kininogen 1	-0.142	0.591
Antithrombin III	-0.152	0.627
Apolipoprotein A IV	-0.127	0.658
Alpha 1B glycoprotein	0.123	0.726
Vitamin D binding protein	0.121	0.731
Ig alpha 1 chain C region	0.110	0.769
Apolipoprotein E	-0.129	0.771
Alpha 1 acid glycoprotein 2	0.096	0.785
Immunoglobulin lambda like polypeptide 5	0.074	0.845
Protein AMBP	0.008	0.977
Serotransferrin	0.006	0.981

Appendix 8

T12 partial correlation results for proteins with PiB PET DVR. Proteins ranked in order of significance based on *p* value. Proteins highlighted in red are statistically significant ($p<0.05$), those highlighted in green are tending towards significance ($p<0.1$).

Protein	Correlation coefficient	*P*-value
Alpha 1 acid glycoprotein 2	0.520	0.043
Beta 2 microglobulin	0.574	0.047
Complement C4 B	-0.391	0.079
Ig lambda 2 chain C regions	-0.548	0.142
Apolipoprotein A I	-0.349	0.196
Apolipoprotein E	-0.373	0.203
Alpha 1 acid glycoprotein 1	0.275	0.225
Protein AMBP	-0.277	0.235
Complement C3	-0.294	0.251
Leucine rich alpha 2 glycoprotein	0.315	0.271
Serum albumin	-0.292	0.271
Angiotensinogen	0.354	0.285
Carbonic anhydrase 1	-0.337	0.312
Immunoglobulin lambda like polypeptide 5	-0.287	0.369
Fibrinogen alpha chain	-0.194	0.428

Retinol binding protein 4	0.286	0.504
Ig alpha 1 chain C region	-0.195	0.575
Transthyretin	-0.104	0.657
Fibrinogen beta chain	-0.102	0.663
Alpha 1 antitrypsin	-0.098	0.676
Kininogen 1	-0.096	0.682
Serotransferrin	-0.096	0.683
Ig kappa chain C region	-0.111	0.698
Hemopexin	-0.053	0.822
Vitamin D binding protein	-0.047	0.860
Alpha 1B glycoprotein	0.048	0.869
Inter alpha trypsin inhibitor heavy chain H4	0.034	0.885
Zinc alpha 2 glycoprotein	-0.030	0.901
Apolipoprotein A IV	-0.026	0.917
Antithrombin III	0.013	0.964

Appendix 9

Mixed-effects regression model results for protein values with sMRI brain regions. Proteins ranked in order of significance based on *p* value. Proteins highlighted in red are statistically significant ($p<0.05$), those highlighted in green are tending towards significance ($p<0.1$).

sMRI region	Protein	Coefficient	*p*-value
Cingulate gyrus	Antithrombin III	-1674.270	0.002
	Zinc alpha 2 glycoprotein	1022.783	0.034
	Alpha 1 acid glycoprotein 1	1155.158	0.100
	Apolipoprotein A IV	754.236	0.123
	Serum albumin	-842.335	0.183
	Alpha 1B glycoprotein	-696.896	0.185
	Hemopexin	992.420	0.215
	Inter alpha trypsin inhibitor heavy chain H4	-745.905	0.243
	Apolipoprotein E	704.077	0.337
	Retinol binding protein	-607.918	0.378
	Immunoglobulin lambda like polypeptide 5	-1015.044	0.379
	Carbonic anhydrase 1	-714.182	0.462
	Beta 2 microglobulin	-567.921	0.472
	Serotransferrin	387.691	0.491
	Complement C4 B	-280.900	0.572

	Angiotensinogen	-348.233	0.643
	Vitamin D binding protein	-377.917	0.647
	Complement C3	-154.896	0.708
	Kininogen 1	-161.744	0.711
	Ig kappa chain C region	-200.456	0.747
	Transthyretin	183.803	0.768
	Ig alpha 1 chain C region	-277.887	0.779
	Protein AMBP	172.022	0.827
	Fibrinogen alpha chain	81.552	0.883
	Fibrinogen beta chain	-77.361	0.913
	Leucine rich apha 2 glycoprotein	75.268	0.920
	Alpha 1 acid glycoprotein	-47.026	0.959
	Alpha 1 antitrypsin	-30.093	0.970
	Apolipoprotein A I	-5.310	0.992
Entorhinal cortex	Retinol binding protein	-294.493	0.138
	Carbonic anhydrase 1	-388.814	0.144
	Hemopexin	-270.117	0.150
	Beta 2 microglobulin	-221.820	0.222
	Protein AMBP	-187.763	0.315
	Apolipoprotein A IV	120.353	0.337

	Alpha 1 acid glycoprotein	-162.265	0.436
	Fibrinogen alpha chain	94.967	0.446
	Zinc alpha 2 glycoprotein	-84.956	0.474
	Angiotensinogen	-122.007	0.523
	Fibrinogen beta chain	97.195	0.548
	Vitamin D binding protein	-94.479	0.556
	Immunoglobulin lambda like polypeptide 5	134.057	0.563
	Serotransferrin	-74.784	0.564
	Serum albumin	78.278	0.565
	Antithrombin III	52.168	0.651
	Alpha 1B glycoprotein	-53.058	0.674
	Ig alpha 1 chain C region	69.891	0.678
	Transthyretin	55.985	0.694
	Alpha 1 acid glycoprotein 1	34.998	0.829
	Apolipoprotein A I	23.754	0.859
	Complement C3	-16.957	0.877
	Complement C4 B	12.694	0.903
	Ig kappa chain C region	14.095	0.924
	Apolipoprotein E	11.218	0.933
	Inter alpha trypsin inhibitor heavy chain H4	12.459	0.933

	Kininogen 1	7.504	0.940
	Alpha 1 antitrypsin	-9.582	0.959
	Leucine rich apha 2 glycoprotein	3.043	0.984
Frontal Grey	Alpha 1 acid glycoprotein 1	8162.499	0.044
	Zinc alpha 2 glycoprotein	5446.128	0.052
	Complement C3	-5151.136	0.053
	Antithrombin III	-5367.144	0.106
	Apolipoprotein A I	-4968.396	0.144
	Carbonic anhydrase 1	-7007.675	0.186
	Fibrinogen alpha chain	-3804.693	0.217
	Protein AMBP	5056.038	0.278
	Transthyretin	3324.963	0.351
	Alpha 1 antitrypsin	4004.326	0.390
	Leucine rich apha 2 glycoprotein	3212.731	0.410
	Vitamin D binding protein	3398.218	0.415
	Serotransferrin	-2083.871	0.520
	Fibrinogen beta chain	-2507.811	0.530
	Serum albumin	-1814.472	0.584
	Alpha 1B glycoprotein	1677.655	0.593
	Kininogen 1	1225.610	0.625

	Apolipoprotein E	2270.769	0.634
	Apolipoprotein A IV	1445.794	0.649
	Hemopexin	1827.956	0.694
	Inter alpha trypsin inhibitor heavy chain H4	-1023.951	0.782
	Alpha 1 acid glycoprotein	1324.076	0.797
	Complement C4 B	-603.843	0.826
	Beta 2 microglobulin	1051.266	0.836
	Ig kappa chain C region	-833.660	0.842
	Retinol binding protein	-626.144	0.894
	Ig alpha 1 chain C region	597.817	0.916
	Angiotensinogen	456.199	0.920
	Immunoglobulin lambda like polypeptide 5	-76.176	0.990
Grey matter	Zinc alpha 2 glycoprotein	15675.255	0.046
	Antithrombin III	-15127.422	0.089
	Alpha 1 acid glycoprotein 1	15315.969	0.177
	Apolipoprotein A IV	9779.601	0.266
	Alpha 1 antitrypsin	13312.343	0.305

	Carbonic anhydrase 1	-14939.678	0.340
	Transthyretin	9382.220	0.345
	Leucine rich apha 2 glycoprotein	9775.410	0.400
	Fibrinogen alpha chain	-7005.888	0.424
	Apolipoprotein A I	-7399.148	0.428
	Serotransferrin	-6735.623	0.453
	Complement C3	-4496.194	0.547
	Retinol binding protein	-7994.273	0.556
	Beta 2 microglobulin	-7459.334	0.607
	Immunoglobulin lambda like polypeptide 5	-8176.370	0.615
	Alpha 1B glycoprotein	4177.441	0.629
	Kininogen 1	-2868.078	0.682
	Protein AMBP	5188.974	0.691
	Ig kappa chain C region	-4125.730	0.725
	Complement C4 B	-2466.340	0.749
	Fibrinogen beta chain	-3438.829	0.761
	Hemopexin	3756.727	0.770
	Apolipoprotein E	3368.329	0.804
	Serum albumin	-1872.537	0.842

	Ig alpha 1 chain C region	3023.688	0.847
	Angiotensinogen	-1719.328	0.893
	Inter alpha trypsin inhibitor heavy chain H4	1272.129	0.901
	Vitamin D binding protein	-396.520	0.975
	Alpha 1 acid glycoprotein	-240.615	0.987
Hippocampus	Apolipoprotein E	285.516	0.034
	Serum albumin	-209.756	0.069
	Inter alpha trypsin inhibitor heavy chain H4	-208.944	0.080
	Leucine rich apha 2 glycoprotein	-212.601	0.138
	Beta 2 microglobulin	-204.808	0.166
	Kininogen 1	106.461	0.192
	Complement C4 B	115.753	0.222
	Vitamin D binding protein	-158.752	0.268
	Alpha 1B glycoprotein	-136.935	0.269
	Apolipoprotein A IV	-118.836	0.270
	Apolipoprotein A I	111.146	0.301
	Immunoglobulin lambda like polypeptide 5	-203.815	0.312
	Protein AMBP	145.816	0.338
	Serotransferrin	73.568	0.484
	Retinol binding protein	118.755	0.513

	Alpha 1 acid glycoprotein 1	82.165	0.532
	Complement C3	50.243	0.566
	Fibrinogen alpha chain	-55.886	0.582
	Antithrombin III	-34.112	0.701
	Fibrinogen beta chain	-47.047	0.703
	Ig alpha 1 chain C region	-54.914	0.771
	Ig kappa chain C region	39.446	0.789
	Zinc alpha 2 glycoprotein	18.494	0.844
	Alpha 1 acid glycoprotein	33.676	0.853
	Transthyretin	20.926	0.858
	Angiotensinogen	-24.583	0.865
	Alpha 1 antitrypsin	12.708	0.933
	Carbonic anhydrase 1	-6.971	0.972
	Hemopexin	1.225	0.994
Inferior occipital gyrus	Transthyretin	786.319	0.025
	Apolipoprotein A IV	539.710	0.087
	Alpha 1 antitrypsin	681.389	0.144
	Antithrombin III	-408.261	0.214
	Alpha 1B glycoprotein	-360.329	0.255
	Protein AMBP	522.973	0.269

	Leucine rich apha 2 glycoprotein	436.640	0.280
	Retinol binding protein	-480.713	0.281
	Serotransferrin	-345.560	0.286
	Zinc alpha 2 glycoprotein	280.151	0.335
	Apolipoprotein E	454.122	0.377
	Inter alpha trypsin inhibitor heavy chain H4	299.692	0.417
	Serum albumin	-259.967	0.423
	Immunoglobulin lambda like polypeptide 5	-417.429	0.479
	Ig kappa chain C region	-235.349	0.590
	Complement C3	136.680	0.611
	Beta 2 microglobulin	-242.656	0.635
	Fibrinogen beta chain	-190.035	0.643
	Ig alpha 1 chain C region	-231.953	0.653
	Complement C4 B	124.832	0.669
	Apolipoprotein A I	-135.695	0.692
	Carbonic anhydrase 1	-188.641	0.723
	Angiotensinogen	152.864	0.744
	Hemopexin	140.732	0.767
	Vitamin D binding protein	-113.691	0.800
	Fibrinogen alpha chain	71.724	0.822

	Alpha 1 acid glycoprotein 1	77.279	0.850
	Alpha 1 acid glycoprotein	-62.994	0.907
	Kininogen 1	-16.186	0.949
Insula	Apolipoprotein A IV	1086.778	0.039
	Kininogen 1	-787.277	0.055
	Retinol binding protein	-1026.712	0.185
	Antithrombin III	-591.128	0.228
	Beta 2 microglobulin	-844.844	0.314
	Immunoglobulin lambda like polypeptide 5	-955.488	0.322
	Apolipoprotein A I	567.214	0.358
	Leucine rich apha 2 glycoprotein	606.041	0.384
	Alpha 1B glycoprotein	445.584	0.416
	Zinc alpha 2 glycoprotein	365.126	0.445
	Complement C3	333.027	0.449
	Alpha 1 acid glycoprotein	-663.555	0.452
	Protein AMBP	-569.412	0.471
	Inter alpha trypsin inhibitor heavy chain H4	427.392	0.488
	Serotransferrin	-344.973	0.524
	Alpha 1 antitrypsin	449.056	0.560
	Ig alpha 1 chain C region	505.060	0.583

	Apolipoprotein E	343.769	0.596
	Transthyretin	278.950	0.638
	Carbonic anhydrase 1	-394.927	0.650
	Serum albumin	234.687	0.687
	Fibrinogen alpha chain	195.339	0.698
	Fibrinogen beta chain	-203.714	0.763
	Vitamin D binding protein	212.866	0.776
	Complement C4 B	96.248	0.837
	Hemopexin	-160.298	0.840
	Ig kappa chain C region	86.031	0.898
	Angiotensinogen	-19.506	0.980
	Alpha 1 acid glycoprotein 1	15.628	0.982
Medial frontal gyrus	Antithrombin III	-1312.703	0.027
	Serotransferrin	-1124.889	0.063
	Transthyretin	1037.397	0.120
	Apolipoprotein A I	-699.521	0.273
	Complement C3	-505.150	0.311
	Ig kappa chain C region	-680.593	0.370
	Alpha 1 acid glycoprotein	-929.914	0.400
	Zinc alpha 2 glycoprotein	454.694	0.402

	Hemopexin	-726.993	0.405
	Vitamin D binding protein	649.475	0.443
	Serum albumin	-475.280	0.499
	Protein AMBP	593.878	0.504
	Apolipoprotein E	472.361	0.513
	Complement C4 B	339.882	0.520
	Carbonic anhydrase 1	-405.442	0.686
	Apolipoprotein A IV	190.120	0.754
	Angiotensinogen	261.523	0.775
	Alpha 1B glycoprotein	-144.151	0.826
	Leucine rich apha 2 glycoprotein	-154.386	0.840
	Fibrinogen alpha chain	-105.515	0.852
	Beta 2 microglobulin	-175.217	0.854
	Alpha 1 antitrypsin	161.163	0.855
	Immunoglobulin lambda like polypeptide 5	-216.071	0.863
	Ig alpha 1 chain C region	165.393	0.882
	Fibrinogen beta chain	-105.006	0.888
	Kininogen 1	61.372	0.897
	Alpha 1 acid glycoprotein 1	32.629	0.966
	Inter alpha trypsin inhibitor heavy chain H4	-27.974	0.968

	Retinol binding protein	23.802	0.978
Middle frontal gyrus	Alpha 1B glycoprotein	-1750.054	0.033
	Antithrombin III	-2063.618	0.036
	Alpha 1 acid glycoprotein	-2241.501	0.078
	Apolipoprotein E	2980.132	0.081
	Complement C4 B	1088.344	0.193
	Serum albumin	-977.810	0.207
	Ig alpha 1 chain C region	-1734.727	0.212
	Leucine rich apha 2 glycoprotein	-1095.689	0.257
	Carbonic anhydrase 1	1024.451	0.335
	Inter alpha trypsin inhibitor heavy chain H4	-985.275	0.357
	Fibrinogen beta chain	-989.972	0.395
	Angiotensinogen	-922.676	0.395
	Zinc alpha 2 glycoprotein	652.253	0.423
	Immunoglobulin lambda like polypeptide 5	-1104.741	0.485
	Ig kappa chain C region	-891.026	0.486
	Vitamin D binding protein	-712.462	0.498
	Protein AMBP	835.977	0.540
	Serotransferrin	-509.982	0.588
	Complement C3	429.430	0.608

	Transthyretin	478.932	0.645
	Apolipoprotein A IV	-396.374	0.667
	Apolipoprotein A I	-266.011	0.800
	Kininogen 1	165.021	0.821
	Alpha 1 acid glycoprotein 1	243.918	0.836
	Retinol binding protein	-170.043	0.886
	Alpha 1 antitrypsin	175.235	0.897
	Fibrinogen alpha chain	120.116	0.898
	Hemopexin	157.235	0.907
	Beta 2 microglobulin	-8.248	0.995
Middle occipital gyrus	Complement C3	-833.235	0.029
	Zinc alpha 2 glycoprotein	873.585	0.056
	Ig kappa chain C region	1256.919	0.063
	Alpha 1B glycoprotein	815.878	0.098
	Fibrinogen alpha chain	-643.438	0.162
	Hemopexin	1020.627	0.168
	Ig alpha 1 chain C region	903.454	0.273
	Apolipoprotein A I	-479.990	0.354
	Inter alpha trypsin inhibitor heavy chain H4	491.474	0.388
	Serotransferrin	427.795	0.394

	Complement C4 B	-365.833	0.396
	Retinol binding protein	659.040	0.403
	Leucine rich apha 2 glycoprotein	512.528	0.418
	Serum albumin	431.057	0.420
	Alpha 1 acid glycoprotein 1	458.229	0.466
	Alpha 1 antitrypsin	488.504	0.492
	Carbonic anhydrase 1	639.370	0.494
	Transthyretin	-371.671	0.498
	Protein AMBP	461.900	0.532
	Apolipoprotein E	438.687	0.546
	Apolipoprotein A IV	297.537	0.549
	Fibrinogen beta chain	-322.429	0.600
	Immunoglobulin lambda like polypeptide 5	390.510	0.667
	Beta 2 microglobulin	-268.248	0.733
	Alpha 1 acid glycoprotein	237.052	0.759
	Antithrombin III	-118.881	0.799
	Angiotensinogen	130.456	0.869
	Vitamin D binding protein	92.754	0.900
	Kininogen 1	12.165	0.975
Middle temporal	Zinc alpha 2 glycoprotein	1869.463	0.036

gyrus	Ig kappa chain C region	-2493.314	0.041
	Antithrombin III	-1672.213	0.060
	Transthyretin	1823.895	0.097
	Alpha 1 acid glycoprotein 1	1824.746	0.150
	Alpha 1 antitrypsin	1766.816	0.221
	Alpha 1B glycoprotein	-1188.874	0.275
	Leucine rich apha 2 glycoprotein	1411.602	0.302
	Kininogen 1	773.697	0.316
	Complement C4 B	860.946	0.334
	Apolipoprotein E	1150.840	0.379
	Hemopexin	1254.299	0.383
	Protein AMBP	1184.561	0.412
	Serotransferrin	-814.375	0.415
	Complement C3	621.849	0.431
	Immunoglobulin lambda like polypeptide 5	1261.304	0.499
	Ig alpha 1 chain C region	-1113.430	0.514
	Angiotensinogen	-737.001	0.557
	Alpha 1 acid glycoprotein	970.468	0.562
	Fibrinogen beta chain	-610.032	0.624
	Serum albumin	-343.188	0.758

	Apolipoprotein A I	-313.398	0.763
	Inter alpha trypsin inhibitor heavy chain H4	336.041	0.768
	Beta 2 microglobulin	264.130	0.848
	Retinol binding protein	243.064	0.877
	Vitamin D binding protein	-75.927	0.958
	Apolipoprotein A IV	-51.763	0.958
	Carbonic anhydrase 1	23.307	0.990
	Fibrinogen alpha chain	9.779	0.992
Orbito frontal gyrus	Carbonic anhydrase 1	-3932.504	0.006
	Alpha 1 acid glycoprotein 1	2431.306	0.013
	Zinc alpha 2 glycoprotein	1487.389	0.035
	Leucine rich apha 2 glycoprotein	1746.057	0.079
	Complement C3	-1120.828	0.083
	Apolipoprotein A I	-1105.925	0.149
	Alpha 1B glycoprotein	954.225	0.210
	Apolipoprotein A IV	723.421	0.353
	Retinol binding protein	-1083.733	0.363
	Alpha 1 antitrypsin	1023.450	0.365
	Transthyretin	783.153	0.368
	Serum albumin	-746.732	0.377

	Fibrinogen alpha chain	-666.611	0.385
	Hemopexin	984.197	0.394
	Beta 2 microglobulin	-1057.282	0.410
	Vitamin D binding protein	854.167	0.433
	Complement C4 B	-478.093	0.453
	Alpha 1 acid glycoprotein	902.352	0.460
	Angiotensinogen	-782.863	0.545
	Ig alpha 1 chain C region	-657.545	0.616
	Antithrombin III	-320.411	0.694
	Inter alpha trypsin inhibitor heavy chain H4	-344.071	0.703
	Immunoglobulin lambda like polypeptide 5	-428.562	0.776
	Protein AMBP	288.964	0.805
	Fibrinogen beta chain	-176.382	0.858
	Ig kappa chain C region	-145.919	0.888
	Serotransferrin	-108.322	0.892
	Apolipoprotein E	-55.949	0.961
	Kininogen 1	-11.311	0.985
Parahippocampal gyrus	Alpha 1 acid glycoprotein 1	231.366	0.035
	Apolipoprotein A IV	-172.073	0.036
	Carbonic anhydrase 1	-181.096	0.141

	Fibrinogen alpha chain	-121.331	0.155
	Vitamin D binding protein	-145.056	0.180
	Zinc alpha 2 glycoprotein	90.858	0.252
	Alpha 1B glycoprotein	78.700	0.324
	Immunoglobulin lambda like polypeptide 5	-130.159	0.379
	Kininogen 1	48.346	0.474
	Apolipoprotein A I	58.277	0.484
	Antithrombin III	59.335	0.486
	Inter alpha trypsin inhibitor heavy chain H4	-66.317	0.509
	Transthyretin	-62.453	0.519
	Alpha 1 acid glycoprotein	80.419	0.529
	Serotransferrin	51.875	0.558
	Protein AMBP	63.044	0.625
	Angiotensinogen	42.529	0.649
	Leucine rich apha 2 glycoprotein	-44.662	0.651
	Hemopexin	57.799	0.655
	Complement C4 B	34.589	0.656
	Ig kappa chain C region	49.957	0.660
	Retinol binding protein	27.747	0.746
	Serum albumin	19.246	0.812

	Alpha 1 antitrypsin	24.908	0.843
	Ig alpha 1 chain C region	-12.851	0.913
	Apolipoprotein E	12.332	0.925
	Complement C3	7.066	0.925
	Beta 2 microglobulin	-8.820	0.939
	Fibrinogen beta chain	2.822	0.979
Superior frontal gyrus	Antithrombin III	-1079.660	0.077
	Transthyretin	1146.474	0.081
	Fibrinogen beta chain	-1200.061	0.101
	Zinc alpha 2 glycoprotein	807.779	0.135
	Alpha 1 antitrypsin	1170.160	0.176
	Complement C3	-583.246	0.181
	Leucine rich apha 2 glycoprotein	1125.198	0.182
	Angiotensinogen	1076.367	0.219
	Vitamin D binding protein	865.695	0.328
	Protein AMBP	835.587	0.344
	Alpha 1 acid glycoprotein 1	609.656	0.427
	Serum albumin	-543.510	0.443
	Serotransferrin	-460.125	0.452
	Apolipoprotein A I	-447.985	0.484

	Fibrinogen alpha chain	-409.532	0.495
	Immunoglobulin lambda like polypeptide 5	-654.442	0.535
	Ig kappa chain C region	-374.687	0.602
	Beta 2 microglobulin	-452.766	0.624
	Kininogen 1	-220.870	0.641
	Retinol binding protein	-346.343	0.684
	Inter alpha trypsin inhibitor heavy chain H4	229.895	0.741
	Apolipoprotein E	181.062	0.753
	Carbonic anhydrase 1	-325.654	0.780
	Complement C4 B	118.805	0.824
	Ig alpha 1 chain C region	164.488	0.850
	Hemopexin	124.896	0.887
	Apolipoprotein A IV	86.017	0.888
	Alpha 1 acid glycoprotein	109.605	0.916
	Alpha 1B glycoprotein	-49.030	0.943
Superior occipital gyrus	Beta 2 microglobulin	-1331.366	0.026
	Zinc alpha 2 glycoprotein	631.023	0.152
	Alpha 1 antitrypsin	922.986	0.180
	Leucine rich apha 2 glycoprotein	684.812	0.191
	Vitamin D binding protein	-638.090	0.259

	Immunoglobulin lambda like polypeptide 5	-849.349	0.293
	Alpha 1 acid glycoprotein 1	628.388	0.301
	Ig alpha 1 chain C region	-638.796	0.369
	Hemopexin	610.406	0.387
	Apolipoprotein A I	379.366	0.408
	Antithrombin III	339.027	0.423
	Fibrinogen alpha chain	-377.602	0.425
	Apolipoprotein A IV	-362.028	0.440
	Ig kappa chain C region	-491.130	0.453
	Protein AMBP	-520.949	0.455
	Angiotensinogen	-423.926	0.479
	Retinol binding protein	-488.201	0.495
	Serotransferrin	286.538	0.552
	Alpha 1B glycoprotein	274.825	0.594
	Transthyretin	269.619	0.611
	Complement C4 B	154.428	0.713
	Carbonic anhydrase 1	-292.201	0.721
	Alpha 1 acid glycoprotein	226.948	0.751
	Complement C3	114.462	0.780
	Serum albumin	-111.469	0.815

	Apolipoprotein E	148.571	0.821
	Fibrinogen beta chain	100.136	0.867
	Kininogen 1	47.004	0.899
	Inter alpha trypsin inhibitor heavy chain H4	43.660	0.937
Superior parietal lobule	Alpha 1 acid glycoprotein 1	2192.198	0.113
	Retinol binding protein	-2310.716	0.166
	Alpha 1 antitrypsin	2022.199	0.197
	Serum albumin	1416.545	0.224
	Carbonic anhydrase 1	-2153.369	0.291
	Serotransferrin	-1142.365	0.294
	Alpha 1B glycoprotein	1136.205	0.297
	Ig alpha 1 chain C region	1626.940	0.304
	Inter alpha trypsin inhibitor heavy chain H4	1256.625	0.310
	Leucine rich apha 2 glycoprotein	1104.245	0.333
	Apolipoprotein A IV	1006.405	0.345
	Fibrinogen alpha chain	-977.430	0.346
	Zinc alpha 2 glycoprotein	869.623	0.374
	Apolipoprotein A I	-997.339	0.379
	Apolipoprotein E	-1144.884	0.434
	Ig kappa chain C region	1018.482	0.493

	Angiotensinogen	1040.589	0.494
	Hemopexin	-1047.350	0.506
	Complement C4 B	-606.765	0.517
	Transthyretin	733.268	0.544
	Vitamin D binding protein	-529.796	0.692
	Beta 2 microglobulin	546.913	0.730
	Complement C3	-265.293	0.764
	Alpha 1 acid glycoprotein	531.605	0.773
	Kininogen 1	-231.612	0.785
	Protein AMBP	-279.257	0.859
	Fibrinogen beta chain	-180.945	0.895
	Antithrombin III	46.455	0.961
	Immunoglobulin lambda like polypeptide 5	-18.822	0.991
Superior temporal gyrus	Alpha 1 antitrypsin	2688.158	0.021
	Zinc alpha 2 glycoprotein	1584.460	0.027
	Apolipoprotein A I	-1502.111	0.078
	Protein AMBP	1856.802	0.114
	Alpha 1 acid glycoprotein 1	1580.022	0.129
	Transthyretin	1239.329	0.169
	Leucine rich apha 2 glycoprotein	1016.667	0.372

	Antithrombin III	-675.444	0.379
	Hemopexin	1021.150	0.391
	Fibrinogen alpha chain	-630.790	0.427
	Apolipoprotein E	-791.521	0.475
	Complement C3	-412.470	0.544
	Beta 2 microglobulin	739.197	0.556
	Fibrinogen beta chain	574.072	0.571
	Apolipoprotein A IV	445.775	0.586
	Serotransferrin	-448.328	0.587
	Kininogen 1	240.290	0.707
	Immunoglobulin lambda like polypeptide 5	613.570	0.713
	Alpha 1B glycoprotein	250.394	0.761
	Inter alpha trypsin inhibitor heavy chain H4	280.299	0.765
	Retinol binding protein	-375.275	0.775
	Complement C4 B	-206.962	0.782
	Alpha 1 acid glycoprotein	385.531	0.782
	Serum albumin	-197.062	0.832
	Ig kappa chain C region	151.536	0.880
	Ig alpha 1 chain C region	66.002	0.966
	Vitamin D binding protein	49.465	0.968

	Carbonic anhydrase 1	-33.599	0.982
	Angiotensinogen	-18.330	0.987
Temporal white matter	Complement C4 B	6407.603	0.024
	Complement C3	5502.655	0.054
	Apolipoprotein A IV	-6250.117	0.063
	Apolipoprotein E	7557.176	0.107
	Vitamin D binding protein	-6314.692	0.184
	Carbonic anhydrase 1	6842.000	0.210
	Kininogen 1	3317.437	0.211
	Alpha 1B glycoprotein	-4342.025	0.217
	Zinc alpha 2 glycoprotein	-3169.034	0.307
	Fibrinogen alpha chain	2478.934	0.458
	Apolipoprotein A I	2690.749	0.463
	Serotransferrin	-2494.448	0.473
	Ig alpha 1 chain C region	-3867.088	0.488
	Alpha 1 acid glycoprotein	3613.592	0.512
	Immunoglobulin lambda like polypeptide 5	-4169.684	0.516
	Serum albumin	-1663.811	0.635
	Leucine rich apha 2 glycoprotein	-1996.579	0.652
	Alpha 1 acid glycoprotein 1	1496.980	0.729

	Fibrinogen beta chain	1346.796	0.753
	Beta 2 microglobulin	1122.373	0.835
	Angiotensinogen	-956.758	0.863
	Antithrombin III	530.447	0.876
	Alpha 1 antitrypsin	724.316	0.883
	Retinol binding protein	-691.507	0.893
	Ig kappa chain C region	474.355	0.914
	Protein AMBP	-516.268	0.918
	Hemopexin	-390.881	0.938
	Inter alpha trypsin inhibitor heavy chain H4	-293.132	0.941
	Transthyretin	55.015	0.988
Temporal grey matter	Antithrombin III	-3831.437	0.075
	Zinc alpha 2 glycoprotein	3379.500	0.092
	Ig kappa chain C region	-4767.157	0.099
	Serotransferrin	-3558.946	0.112
	Transthyretin	3893.704	0.116
	Alpha 1 antitrypsin	4125.468	0.205
	Angiotensinogen	-3077.365	0.321
	Alpha 1 acid glycoprotein 1	2763.282	0.333
	Apolipoprotein A I	-2176.729	0.353

	Alpha 1B glycoprotein	-2077.850	0.361
	Serum albumin	-1968.453	0.430
	Retinol binding protein	-2679.767	0.458
	Complement C4 B	1218.093	0.538
	Ig alpha 1 chain C region	-2491.813	0.538
	Carbonic anhydrase 1	-2444.430	0.548
	Beta 2 microglobulin	-1965.678	0.555
	Apolipoprotein A IV	1302.199	0.564
	Apolipoprotein E	1724.021	0.595
	Protein AMBP	1739.249	0.598
	Leucine rich apha 2 glycoprotein	1164.202	0.704
	Fibrinogen beta chain	-960.126	0.731
	Alpha 1 acid glycoprotein	-1228.701	0.735
	Vitamin D binding protein	-982.117	0.762
	Immunoglobulin lambda like polypeptide 5	1241.549	0.774
	Fibrinogen alpha chain	-624.911	0.779
	Complement C3	314.042	0.867
	Hemopexin	-411.010	0.899
	Kininogen 1	109.804	0.950
	Inter alpha trypsin inhibitor heavy chain H4	68.062	0.979

Ventricles	Transthyretin	-3403.640	0.053
	Immunoglobulin lambda like polypeptide 5	-5204.793	0.123
	Vitamin D binding protein	-3336.643	0.177
	Inter alpha trypsin inhibitor heavy chain H4	-2322.304	0.199
	Carbonic anhydrase 1	-3337.188	0.207
	Angiotensinogen	-2317.640	0.230
	Kininogen 1	-1361.551	0.274
	Protein AMBP	-2485.887	0.283
	Fibrinogen beta chain	-1977.789	0.301
	Ig alpha 1 chain C region	-2834.357	0.330
	Alpha 1 antitrypsin	-2150.634	0.352
	Retinol binding protein	-2042.170	0.410
	Zinc alpha 2 glycoprotein	-1105.050	0.435
	Beta 2 microglobulin	-1714.765	0.462
	Complement C4 B	-920.346	0.533
	Alpha 1B glycoprotein	-794.486	0.540
	Serotransferrin	954.139	0.552
	Leucine rich apha 2 glycoprotein	1209.070	0.558
	Apolipoprotein A I	765.805	0.627
	Serum albumin	-614.895	0.722

	Hemopexin	667.929	0.770
	Alpha 1 acid glycoprotein 1	-423.763	0.833
	Apolipoprotein E	-443.797	0.862
	Alpha 1 acid glycoprotein	-308.140	0.909
	Apolipoprotein A IV	83.792	0.958
	Ig kappa chain C region	96.788	0.965
	Complement C3	50.679	0.971
	Antithrombin III	28.504	0.985
	Fibrinogen alpha chain	24.335	0.987
White matter	Complement C4 B	19633.829	0.047
	Apolipoprotein A IV	-22090.706	0.056
	Apolipoprotein E	25308.778	0.121
	Complement C3	13674.825	0.172
	Zinc alpha 2 glycoprotein	-12511.283	0.238
	Alpha 1B glycoprotein	-12007.310	0.316

	Carbonic anhydrase 1	17892.858	0.325
	Kininogen 1	8446.239	0.355
	Apolipoprotein A I	9396.433	0.452
	Serum albumin	-8600.830	0.455
	Vitamin D binding protein	-11919.862	0.478
	Leucine rich apha 2 glycoprotein	-10093.135	0.515
	Alpha 1 acid glycoprotein	12263.925	0.521
	Fibrinogen alpha chain	7024.067	0.541
	Alpha 1 acid glycoprotein 1	7892.272	0.596
	Immunoglobulin lambda like polypeptide 5	-10912.669	0.605
	Ig alpha 1 chain C region	-10178.479	0.610
	Transthyretin	-5242.456	0.689
	Ig kappa chain C region	5872.217	0.711
	Protein AMBP	-4938.887	0.774

	Antithrombin III	3294.428	0.779
	Beta 2 microglobulin	5319.824	0.789
	Serotransferrin	-2968.155	0.803
	Inter alpha trypsin inhibitor heavy chain H4	-3247.519	0.810
	Fibrinogen beta chain	2645.114	0.858
	Retinol binding protein	-2944.127	0.869
	Alpha 1 antitrypsin	-2653.073	0.876
	Angiotensinogen	2801.078	0.882
	Hemopexin	2477.836	0.885
Wholebrain	Apolipoprotein E	17064.433	0.073
	Antithrombin III	-12999.327	0.079
	Complement C4 B	11173.490	0.134
	Transthyretin	8667.316	0.342
	Kininogen 1	5590.794	0.378
	Apolipoprotein A IV	-7044.113	0.382
	Alpha 1B glycoprotein	-7270.308	0.421
	Complement C3	5395.289	0.426
	Serotransferrin	-6053.175	0.458

	Immunoglobulin lambda like polypeptide 5	-12417.029	0.484
	Alpha 1 acid glycoprotein 1	6937.563	0.499
	Protein AMBP	7782.606	0.503
	Zinc alpha 2 glycoprotein	4342.417	0.539
	Serum albumin	-5359.814	0.565
	Angiotensinogen	7264.572	0.578
	Alpha 1 acid glycoprotein	7481.937	0.630
	Retinol binding protein	5838.821	0.650
	Ig kappa chain C region	-4341.216	0.667
	Fibrinogen alpha chain	-3213.537	0.684
	Vitamin D binding protein	-4057.288	0.757
	Carbonic anhydrase 1	4741.474	0.776
	Ig alpha 1 chain C region	-3606.615	0.812
	Apolipoprotein A I	-2157.080	0.812
	Hemopexin	2001.291	0.862
	Leucine rich apha 2 glycoprotein	1898.549	0.872
	Alpha 1 antitrypsin	1746.116	0.883
	Fibrinogen beta chain	284.483	0.978
	Inter alpha trypsin inhibitor heavy chain H4	260.735	0.978

	Beta 2 microglobulin	185.455	0.989

Appendix 10

Mixed-effects regression model results for protein values with cognitive measures. Proteins ranked in order of significance based on *p* value. Proteins highlighted in red are statistically significant ($p<0.05$), those highlighted in green are tending towards significance ($p<0.1$).

Cognitive Measure	Protein	Coefficient	*p*-value
Benton visual retention total	Fibrinogen alpha chain	-3.049	0.020
	Inter alpha trypsin inhibitor heavy chain H4	-2.628	0.073
	Zinc alpha 2 glycoprotein	1.592	0.182
	Apolipoprotein A IV	-1.403	0.185
	Apolipoprotein E	-1.722	0.259
	Complement C4 B	1.202	0.280
	Alpha 1 antitrypsin	1.702	0.346
	Vitamin D binding protein	-1.132	0.359
	Angiotensinogen	-1.018	0.384
	Serum albumin	-1.216	0.387
	Transthyretin	1.177	0.409
	Complement C3	-0.905	0.420
	Fibrinogen beta chain	-0.921	0.452
	Retinol binding protein	1.590	0.452

	Alpha 1acid glycoprotein 1	-1.157	0.481
	Carbonic anhydrase 1	-1.001	0.509
	Alpha 1 acid glycoprotein	0.914	0.540
	Ig kappa chain C region	-1.058	0.552
	Apolipoprotein A I	0.499	0.579
	Antithrombin III	-0.386	0.682
	Ig alpha 1 chain C region	-0.780	0.738
	Beta 2 microglobulin	-0.411	0.738
	Leucine rich alpha 2 glycoprotein	0.384	0.767
	Serotransferrin	-0.348	0.802
	Kininogen 1	0.219	0.825
	Alpha 1B glycoprotein	0.266	0.844
	Hemopexin	-0.287	0.883
	Immunoglobulin lambda like polypeptide 5	0.359	0.885
	Protein AMBP	0.077	0.968
Card Rotation Total	Alpha 1B glycoprotein	17.800	0.018
	Ig alpha 1 chain C region	31.781	0.024
	Inter alpha trypsin inhibitor heavy chain H4	22.418	0.051
	Ig kappa chain C region	26.584	0.060
	Apolipoprotein A IV	19.940	0.066

	Vitamin D binding protein	22.162	0.103
	Angiotensinogen	16.004	0.136
	Beta 2 microglobulin	14.873	0.148
	Alpha 1 acid glycoprotein	17.693	0.173
	Leucine rich alpha 2 glycoprotein	12.042	0.181
	Alpha 1acid glycoprotein 1	14.334	0.244
	Serum albumin	8.027	0.273
	Fibrinogen beta chain	13.322	0.287
	Antithrombin III	9.986	0.311
	Protein AMBP	12.862	0.368
	Carbonic anhydrase 1	9.110	0.387
	Fibrinogen alpha chain	9.300	0.391
	Immunoglobulin lambda like polypeptide 5	12.366	0.433
	Alpha 1 antitrypsin	10.271	0.461
	Apolipoprotein A I	4.672	0.511
	Hemopexin	8.511	0.543
	Zinc alpha 2 glycoprotein	5.186	0.555
	Retinol binding protein	-6.012	0.560
	Apolipoprotein E	9.304	0.599
	Complement C3	4.130	0.639

	Transthyretin	3.892	0.721
	Complement C4 B	1.752	0.851
	Kininogen 1	-1.221	0.876
	Serotransferrin	1.354	0.897
CESD	Immunoglobulin lambda like polypeptide 5	-5.123	0.067
	Leucine rich alpha 2 glycoprotein	1.856	0.243
	Kininogen 1	1.552	0.302
	Vitamin D binding protein	-1.845	0.338
	Carbonic anhydrase 1	-1.993	0.341
	Alpha 1acid glycoprotein 1	-2.020	0.392
	Serum albumin	-1.249	0.416
	Angiotensinogen	-1.246	0.456
	Inter alpha trypsin inhibitor heavy chain H4	1.513	0.482
	Alpha 1 antitrypsin	2.003	0.487
	Antithrombin III	1.162	0.501
	Ig alpha 1 chain C region	1.794	0.504
	Apolipoprotein A I	0.808	0.554
	Alpha 1 acid glycoprotein	1.085	0.560
	Apolipoprotein E	-1.687	0.580
	Beta 2 microglobulin	-0.926	0.638

	Apolipoprotein A IV	-0.856	0.666
	Retinol binding protein	1.026	0.670
	Protein AMBP	-1.050	0.708
	Transthyretin	0.750	0.718
	Fibrinogen alpha chain	0.654	0.747
	Hemopexin	-0.754	0.785
	Zinc alpha 2 glycoprotein	-0.436	0.801
	Fibrinogen beta chain	-0.475	0.836
	Ig kappa chain C region	0.407	0.881
	Serotransferrin	-0.166	0.935
	Complement C3	-0.120	0.939
	Complement C4 B	0.067	0.968
	Alpha 1B glycoprotein	-0.009	0.996
California verbal learning test	Inter alpha trypsin inhibitor heavy chain H4	12.382	0.048
	Alpha 1 acid glycoprotein	-17.320	0.053
	Fibrinogen alpha chain	8.839	0.058
	Apolipoprotein E	12.611	0.060
	Zinc alpha 2 glycoprotein	-8.749	0.063
	Complement C3	5.766	0.083
	Protein AMBP	-	0.132

		11.642	
	Serotransferrin	-8.128	0.159
	Alpha 1 antitrypsin	-9.833	0.180
	Angiotensinogen	11.244	0.189
	Fibrinogen beta chain	-7.367	0.253
	Immunoglobulin lambda like polypeptide 5	-11.451	0.263
	Carbonic anhydrase 1	10.350	0.301
	Alpha 1acid glycoprotein 1	-6.745	0.330
	Ig alpha 1 chain C region	9.292	0.333
	Apolipoprotein A IV	4.738	0.347
	Antithrombin III	-3.686	0.384
	Apolipoprotein A I	3.822	0.476
	Hemopexin	-5.356	0.499
	Serum albumin	-3.819	0.533
	Leucine rich alpha 2 glycoprotein	-4.281	0.569
	Retinol binding protein	-3.850	0.633
	Complement C4 B	1.467	0.755
	Ig kappa chain C region	1.736	0.811
	Vitamin D binding protein	-1.594	0.829
	Kininogen 1	-0.476	0.909

	Beta 2 microglobulin	-0.744	0.935
	Transthyretin	0.325	0.956
	Alpha 1B glycoprotein	-0.219	0.964
Digit span backwards	Transthyretin	-2.034	0.032
	Serum albumin	1.874	0.037
	Apolipoprotein A IV	-1.688	0.038
	Beta 2 microglobulin	-1.855	0.145
	Fibrinogen beta chain	-1.510	0.152
	Vitamin D binding protein	1.417	0.161
	Carbonic anhydrase 1	1.907	0.186
	Serotransferrin	1.136	0.189
	Alpha 1 antitrypsin	-1.551	0.201
	Alpha 1B glycoprotein	0.991	0.243
	Inter alpha trypsin inhibitor heavy chain H4	-1.075	0.271
	Protein AMBP	-1.322	0.291
	Alpha 1 acid glycoprotein	-1.388	0.304
	Zinc alpha 2 glycoprotein	-0.729	0.305
	Ig kappa chain C region	-0.757	0.411
	Apolipoprotein E	0.954	0.412
	Fibrinogen alpha chain	-0.603	0.466

	Ig alpha 1 chain C region	1.098	0.474
	Hemopexin	0.659	0.607
	Apolipoprotein A I	-0.455	0.611
	Leucine rich alpha 2 glycoprotein	-0.507	0.641
	Angiotensinogen	-0.409	0.712
	Alpha 1acid glycoprotein 1	0.385	0.720
	Antithrombin III	0.190	0.777
	Complement C4 B	-0.143	0.850
	Complement C3	-0.132	0.854
	Retinol binding protein	0.198	0.880
	Kininogen 1	0.096	0.883
	Immunoglobulin lambda like polypeptide 5	0.158	0.911
Digit span forwards	Serotransferrin	1.574	0.101
	Beta 2 microglobulin	-2.254	0.134
	Apolipoprotein A IV	-1.388	0.142
	Hemopexin	2.090	0.149
	Carbonic anhydrase 1	1.794	0.199
	Inter alpha trypsin inhibitor heavy chain H4	-1.189	0.265
	Alpha 1acid glycoprotein 1	1.278	0.290
	Serum albumin	1.044	0.291

	Fibrinogen beta chain	-1.141	0.325
	Alpha 1B glycoprotein	0.844	0.362
	Transthyretin	-0.900	0.376
	Complement C4 B	0.580	0.483
	Apolipoprotein E	0.900	0.491
	Immunoglobulin lambda like polypeptide 5	0.947	0.534
	Vitamin D binding protein	0.638	0.542
	Ig alpha 1 chain C region	1.005	0.548
	Retinol binding protein	0.898	0.563
	Antithrombin III	0.399	0.567
	Ig kappa chain C region	-0.520	0.610
	Apolipoprotein A I	-0.437	0.683
	Kininogen 1	0.284	0.684
	Fibrinogen alpha chain	-0.243	0.788
	Angiotensinogen	0.220	0.857
	Alpha 1 acid glycoprotein	0.219	0.886
	Leucine rich alpha 2 glycoprotein	0.098	0.935
	Alpha 1 antitrypsin	-0.076	0.953
	Protein AMBP	0.068	0.962
	Zinc alpha 2 glycoprotein	0.015	0.986

	Complement C3	-0.002	0.998
Fluency categories	Retinol binding protein	-3.460	0.021
	Zinc alpha 2 glycoprotein	-1.574	0.043
	Apolipoprotein A IV	1.637	0.098
	Hemopexin	-2.122	0.100
	Carbonic anhydrase 1	-3.400	0.106
	Ig kappa chain C region	1.400	0.159
	Serotransferrin	-1.312	0.188
	Alpha 1 acid glycoprotein	-1.711	0.283
	Antithrombin III	0.829	0.331
	Kininogen 1	-0.526	0.506
	Beta 2 microglobulin	-0.663	0.561
	Angiotensinogen	0.551	0.565
	Apolipoprotein E	0.641	0.629
	Ig alpha 1 chain C region	0.352	0.690
	Alpha 1B glycoprotein	0.404	0.701
	Fibrinogen beta chain	-0.445	0.720
	Complement C4 B	-0.224	0.763
	Serum albumin	0.289	0.771
	Immunoglobulin lambda like polypeptide 5	-0.410	0.797

	Leucine rich alpha 2 glycoprotein	0.156	0.817
	Apolipoprotein A I	0.201	0.825
	Fibrinogen alpha chain	0.223	0.827
	Vitamin D binding protein	0.215	0.849
	Transthyretin	0.191	0.852
	Complement C3	0.138	0.868
	Inter alpha trypsin inhibitor heavy chain H4	-0.146	0.888
	Alpha 1acid glycoprotein 1	0.161	0.893
	Protein AMBP	-0.064	0.962
	Alpha 1 antitrypsin	0.046	0.973
Fluency letters	Ig kappa chain C region	3.378	0.001
	Serum albumin	2.010	0.058
	Leucine rich alpha 2 glycoprotein	2.140	0.062
	Kininogen 1	1.319	0.093
	Antithrombin III	1.546	0.104
	Immunoglobulin lambda like polypeptide 5	3.032	0.119
	Angiotensinogen	1.913	0.126
	Alpha 1acid glycoprotein 1	1.545	0.189
	Alpha 1B glycoprotein	1.430	0.190
	Retinol binding protein	-1.328	0.290

	Protein AMBP	1.371	0.300
	Alpha 1 antitrypsin	1.340	0.320
	Apolipoprotein A I	-0.787	0.402
	Ig alpha 1 chain C region	1.011	0.476
	Inter alpha trypsin inhibitor heavy chain H4	0.731	0.477
	Fibrinogen alpha chain	-0.600	0.538
	Transthyretin	0.616	0.541
	Apolipoprotein E	0.714	0.561
	Fibrinogen beta chain	0.634	0.598
	Complement C4 B	-0.409	0.610
	Alpha 1 acid glycoprotein	0.651	0.691
	Vitamin D binding protein	-0.509	0.696
	Hemopexin	0.425	0.746
	Serotransferrin	0.303	0.761
	Beta 2 microglobulin	0.369	0.781
	Complement C3	-0.160	0.828
	Carbonic anhydrase 1	0.278	0.898
	Apolipoprotein A IV	-0.031	0.976
	Zinc alpha 2 glycoprotein	0.015	0.985
MMSE	Leucine rich alpha 2 glycoprotein	-1.110	0.010

	Fibrinogen alpha chain	1.010	0.065
	Zinc alpha 2 glycoprotein	-0.846	0.070
	Complement C3	0.797	0.073
	Apolipoprotein E	1.480	0.080
	Immunoglobulin lambda like polypeptide 5	-1.123	0.136
	Apolipoprotein A I	0.404	0.175
	Vitamin D binding protein	0.827	0.226
	Inter alpha trypsin inhibitor heavy chain H4	0.712	0.226
	Angiotensinogen	0.564	0.227
	Alpha 1 antitrypsin	-0.720	0.334
	Kininogen 1	-0.402	0.335
	Carbonic anhydrase 1	0.497	0.353
	Protein AMBP	-0.701	0.359
	Alpha 1acid glycoprotein 1	-0.603	0.375
	Alpha 1 acid glycoprotein	-0.474	0.453
	Hemopexin	-0.526	0.498
	Apolipoprotein A IV	0.357	0.499
	Ig alpha 1 chain C region	-0.480	0.539
	Ig kappa chain C region	0.378	0.613
	Antithrombin III	-0.203	0.654

	Serotransferrin	-0.117	0.836
	Transthyretin	-0.111	0.849
	Serum albumin	0.078	0.855
	Fibrinogen beta chain	0.113	0.858
	Retinol binding protein	-0.063	0.910
	Beta 2 microglobulin	0.057	0.927
	Complement C4 B	0.024	0.958
	Alpha 1B glycoprotein	0.023	0.958
Primary mental abilities vocabulary 3	Vitamin D binding protein	4.997	0.007
	Serum albumin	2.562	0.118
	Zinc alpha 2 glycoprotein	-2.131	0.129
	Apolipoprotein E	-3.672	0.132
	Immunoglobulin lambda like polypeptide 5	4.357	0.136
	Protein AMBP	-3.394	0.140
	Alpha 1 antitrypsin	-2.863	0.207
	Kininogen 1	-1.589	0.218
	Transthyretin	-2.188	0.220
	Fibrinogen alpha chain	1.866	0.299
	Alpha 1B glycoprotein	1.545	0.335
	Alpha 1 acid glycoprotein	-2.386	0.368

	Ig alpha 1 chain C region	1.801	0.385
	Fibrinogen beta chain	-1.643	0.405
	Beta 2 microglobulin	1.373	0.464
	Retinol binding protein	-1.367	0.532
	Complement C3	-0.848	0.544
	Carbonic anhydrase 1	1.382	0.584
	Apolipoprotein A I	-0.738	0.587
	Complement C4 B	-0.764	0.599
	Inter alpha trypsin inhibitor heavy chain H4	-0.850	0.653
	Antithrombin III	-0.590	0.694
	Hemopexin	-0.721	0.752
	Leucine rich alpha 2 glycoprotein	0.380	0.825
	Alpha 1acid glycoprotein 1	-0.435	0.829
	Apolipoprotein A IV	0.332	0.843
	Serotransferrin	-0.279	0.871
	Ig kappa chain C region	0.299	0.885
	Angiotensinogen	0.142	0.941
Trails A	Alpha 1B glycoprotein	-3.077	0.189
	Complement C4 B	2.793	0.193
	Ig alpha 1 chain C region	-4.689	0.235

	Alpha 1acid glycoprotein 1	-3.597	0.244
	Ig kappa chain C region	-3.508	0.267
	Leucine rich alpha 2 glycoprotein	-2.477	0.338
	Hemopexin	-3.031	0.401
	Apolipoprotein A IV	-2.176	0.410
	Beta 2 microglobulin	-2.647	0.441
	Fibrinogen beta chain	2.314	0.454
	Apolipoprotein A I	-1.990	0.457
	Antithrombin III	1.802	0.459
	Complement C3	-1.498	0.488
	Transthyretin	1.783	0.508
	Kininogen 1	1.033	0.590
	Alpha 1 antitrypsin	1.798	0.598
	Angiotensinogen	1.683	0.617
	Protein AMBP	1.773	0.624
	Retinol binding protein	1.847	0.643
	Inter alpha trypsin inhibitor heavy chain H4	1.230	0.670
	Serum albumin	-0.865	0.712
	Immunoglobulin lambda like polypeptide 5	-1.465	0.725
	Carbonic anhydrase 1	-1.006	0.743

	Alpha 1 acid glycoprotein	-1.103	0.763
	Serotransferrin	-0.700	0.789
	Zinc alpha 2 glycoprotein	0.230	0.914
	Apolipoprotein E	0.429	0.915
	Vitamin D binding protein	-0.248	0.938
	Fibrinogen alpha chain	0.077	0.977
Trails B	Fibrinogen alpha chain	-26.689	0.008
	Apolipoprotein A IV	-22.119	0.025
	Apolipoprotein E	-21.913	0.086
	Ig alpha 1 chain C region	-22.102	0.117
	Alpha 1 antitrypsin	19.303	0.119
	Fibrinogen beta chain	-13.911	0.174
	Leucine rich alpha 2 glycoprotein	12.127	0.294
	Inter alpha trypsin inhibitor heavy chain H4	-10.547	0.314
	Angiotensinogen	-10.336	0.329
	Alpha 1B glycoprotein	-7.034	0.435

	Carbonic anhydrase 1	9.067	0.464
	Apolipoprotein A I	-6.267	0.485
	Alpha 1acid glycoprotein 1	-7.641	0.494
	Beta 2 microglobulin	-6.944	0.527
	Serum albumin	-4.931	0.561
	Protein AMBP	6.857	0.597
	Ig kappa chain C region	-5.477	0.618
	Vitamin D binding protein	-5.212	0.618
	Zinc alpha 2 glycoprotein	3.640	0.640
	Hemopexin	5.536	0.666
	Complement C3	-2.887	0.690
	Transthyretin	2.634	0.788
	Complement C4 B	2.066	0.798
	Retinol binding protein	3.038	0.816
	Alpha 1 acid glycoprotein	2.550	0.840
	Antithrombin III	1.517	0.853
	Immunoglobulin lambda like polypeptide 5	-1.677	0.912
	Serotransferrin	0.715	0.940
	Kininogen 1	0.008	0.999